frontiers | Research Topics

Identification of therapeutic targets and novel biomarkers in prostate cancer

Edited by
Shashwat Sharad, Hua Li, Alagarsamy Srinivasan and Suman Kapur

Published in
Frontiers in Oncology

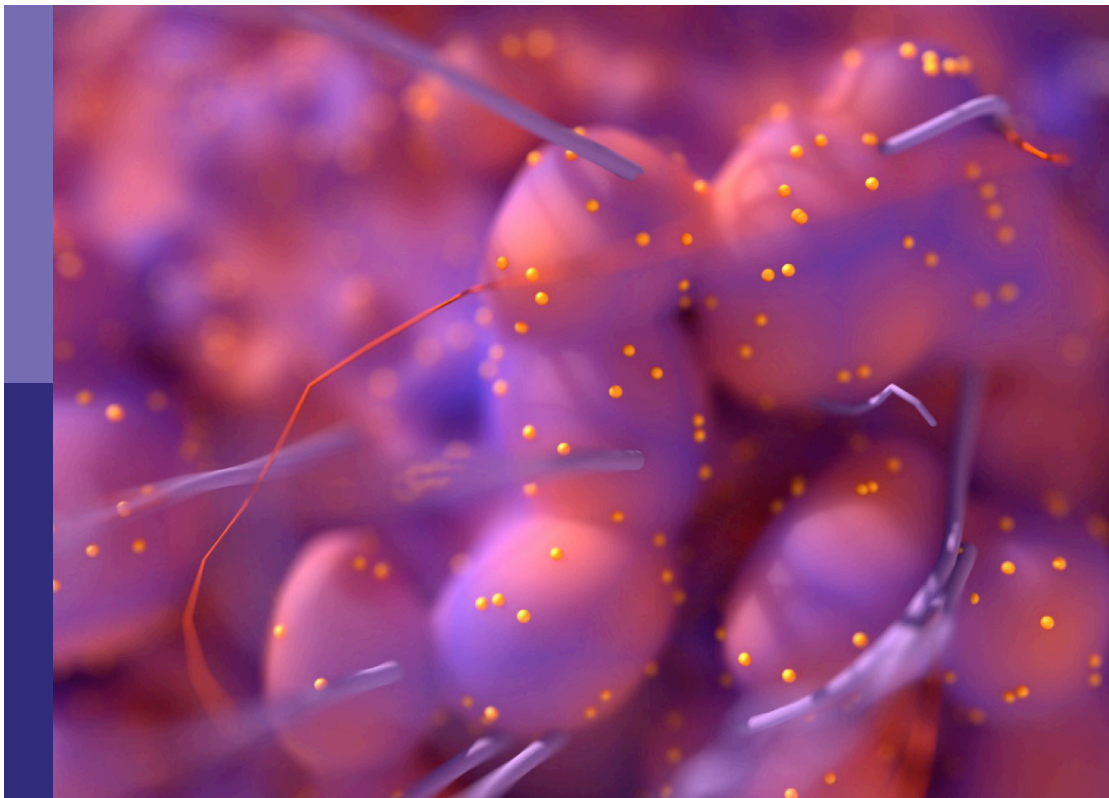

ISSN 1664-8714
ISBN 978-2-83251-409-2
DOI 10.3389/978-2-83251-409-2

About Frontiers

Frontiers is more than just an open access publisher of scholarly articles: it is a pioneering approach to the world of academia, radically improving the way scholarly research is managed. The grand vision of Frontiers is a world where all people have an equal opportunity to seek, share and generate knowledge. Frontiers provides immediate and permanent online open access to all its publications, but this alone is not enough to realize our grand goals.

Frontiers journal series

The Frontiers journal series is a multi-tier and interdisciplinary set of open-access, online journals, promising a paradigm shift from the current review, selection and dissemination processes in academic publishing. All Frontiers journals are driven by researchers for researchers; therefore, they constitute a service to the scholarly community. At the same time, the *Frontiers journal series* operates on a revolutionary invention, the tiered publishing system, initially addressing specific communities of scholars, and gradually climbing up to broader public understanding, thus serving the interests of the lay society, too.

Dedication to quality

Each Frontiers article is a landmark of the highest quality, thanks to genuinely collaborative interactions between authors and review editors, who include some of the world's best academicians. Research must be certified by peers before entering a stream of knowledge that may eventually reach the public - and shape society; therefore, Frontiers only applies the most rigorous and unbiased reviews. Frontiers revolutionizes research publishing by freely delivering the most outstanding research, evaluated with no bias from both the academic and social point of view. By applying the most advanced information technologies, Frontiers is catapulting scholarly publishing into a new generation.

What are Frontiers Research Topics?

Frontiers Research Topics are very popular trademarks of the *Frontiers journals series*: they are collections of at least ten articles, all centered on a particular subject. With their unique mix of varied contributions from Original Research to Review Articles, Frontiers Research Topics unify the most influential researchers, the latest key findings and historical advances in a hot research area.

Find out more on how to host your own Frontiers Research Topic or contribute to one as an author by contacting the Frontiers editorial office: frontiersin.org/about/contact

Identification of therapeutic targets and novel biomarkers in prostate cancer

Topic editors

Shashwat Sharad — Center for Prostate Disease Research (CPDR), United States
Hua Li — Henry M Jackson Foundation for the Advancement of Military Medicine (HJF), United States
Alagarsamy Srinivasan — NanoBio Diagnostics, United States
Suman Kapur — Birla Institute of Technology and Science, India

Citation

Sharad, S., Li, H., Srinivasan, A., Kapur, S., eds. (2023). *Identification of therapeutic targets and novel biomarkers in prostate cancer*. Lausanne: Frontiers Media SA. doi: 10.3389/978-2-83251-409-2

Table of contents

frontiers in Oncology

ORIGINAL RESEARCH
published: 15 October 2021
doi: 10.3389/fonc.2021.754353

MiR-629-5p Promotes Prostate Cancer Development and Metastasis by Targeting AKAP13

Yangzhou Liu[1†], Shankun Zhao[2†], Jiamin Wang[1†], Zhiguo Zhu[3], Lianmin Luo[1], Qian Xiang[1], Mingda Zhou[1], Yuxiang Ma[1], Zuomin Wang[1] and Zhigang Zhao[1]*

[1] Department of Urology & Andrology, Minimally Invasive Surgery Center, Guangdong Provincial Key Laboratory of Urology, The First Affiliated Hospital of GuangZhou Medical University, Guangzhou, China, [2] Department of Urology, Taizhou Central Hospital (Taizhou University Hospital), Taizhou, China, [3] Department of Urology, Affiliated Hospital of Jining Medical University, Jining, China

Prostate cancer (PCa) has become the most frequently occurring cancer among western men according to the latest report, and patients' prognosis is often poor in the event of tumor progression, therefore, many researches are devoted to exploring the molecular mechanism of PCa metastasis. MicroRNAs (miRNA) have proved to play an important role in this process. In present study, by combining clinical samples with public databases, we found that miR-629-5p increased to varying degrees in primary localized PCa tissues and metastatic PCa tissues compared with adjacent normal tissues, and bioinformatics analysis suggested that high level of miR-629-5p was related to poor prognosis. Functionally, miR-629-5p drove PCa cell proliferation, migration and invasion *in vitro*, and promoted growth of PCa cells *in vivo*. Moreover, A-kinase Anchor Protein 13 (AKAP13) was screened as a direct target of miR-629-5p, that expression was negatively correlated with the malignant phenotype of tumor cells. In the end, through verification in clinical specimens, we found that AKAP13 could be independently used as a clinical prognostic indicator. Overall, the present study indicates that miR-629-5p plays an oncogenic role in PCa by targeting AKAP13, which provides a new idea for clinical diagnosis and treatment of complex refractory PCa.

Keywords: prostate cancer, miR-629-5p, AKAP13, phenotype, prognosis

OPEN ACCESS

Edited by:
Alagarsamy Srinivasan, NanoBio Diagnostics, United States

Reviewed by:
Maolake Aerken, University at Buffalo, United States
Nagaraja Sethuraman Balakathiresan, Division of Neuroscience and Behavior (NIAAA), United States

****Correspondence:***
Zhigang Zhao
zgzhaodr@126.com

[†]These authors have contributed equally to this work

Specialty section:
This article was submitted to Genitourinary Oncology, a section of the journal Frontiers in Oncology

Received: *06 August 2021*
Accepted: *28 September 2021*
Published: *15 October 2021*

Citation:
Liu Y, Zhao S, Wang J, Zhu Z, Luo L, Xiang Q, Zhou M, Ma Y, Wang Z and Zhao Z (2021) MiR-629-5p Promotes Prostate Cancer Development and Metastasis by Targeting AKAP13. Front. Oncol. 11:754353. doi: 10.3389/fonc.2021.754353

INTRODUCTION

According to the latest research report, prostate cancer (PCa) has become the most frequently occurring cancer among western men, it accounts for about a quarter of all types of tumors (1). The incidence and mortality of PCa are also getting higher in China (2). Although clinical treatments such as surgery and endocrine therapy can effectively intervene the progression of PCa, patients' prognosis is often poor in the event of tumor metastasis or castration resistance (3). Therefore, in the background of limited treatment, a better understanding of the molecular mechanism of PCa metastasis will contribute to the early diagnosis and intervention of patients with refractory PCa.

MicroRNAs (miRNAs) belong to endogenous small noncoding RNAs that post-transcriptionally regulate the gene expression by binding to the 3'-untranslated region (3'-UTR) of target mRNA, thereby inducing downstream mRNA degradation or protein synthesis repression (4). Accumulating researches have suggested that miRNAs play important roles in human cancer biological progression as novel types of tumor suppressors or oncogenes (5). A group of miRNAs, such as miR-146b, miR-210-3p, miR-636, miR-491-5p, have proved to play the driving role in the growth and metastasis of PCa (6–8). In addition, our previous studies have confirmed that miR-199b-5p and miR-671-5p can influence the metastasis of PCa by affecting epithelial-mesenchymal transition and transcriptional regulation, respectively (9, 10). Therefore, on this basis, we will further study the regulatory mechanism of miRNAs in the process of tumor metastasis.

By combining clinical samples with public databases, we found that miR-629-5p increased to varying degrees in primary localized PCa tissues (PPCa) and metastatic PCa tissues (MPCa) compared with adjacent normal tissues (ANT), and bioinformatics analysis suggested that high level of miR-629-5p was related to poor prognosis. Although miR-629-5p has proved to play a role in promoting tumor growth and metastasis in different types of tumors such as colorectal cancer, hepatocellular carcinoma, lung adenocarcinoma and osteosarcoma (11–14). However, the exact mechanism of its role in PCa metastasis remains unknown. In the present study, in addition to exploring the biological function of miR-629-5p as a key miRNA, we further confirmed that its mechanism is to promote the growth and metastasis of PCa by targeting inhibition of AKAP13, a tumor suppressor. These findings provide a clearer understanding of the mechanism of miRNA promoting PCa.

MATERIAL AND METHODS

Human Tissue Samples and Cell Lines

A total of 53 prostate clinicopathological samples were collected, including ANT (n = 13), PPCa tissue (n = 25) and MPCa tissue (n = 15), as reported in our previous research (10). This study was approved by the Ethics Committee of the First Affiliated Hospital for Guangzhou Medical University, and all patients have signed informed consents.

The normal human prostate epithelial cell line RWPE-1 and human PCa cell lines LNCaP, PC3, DU145 and VCaP were purchased from the Type Culture Collection of the Chinese Academy of Sciences (Shanghai, China). Human PCa cell line C4-2 and human embryonic kidney cell 293 T were obtained from the American Type Culture Collection (Manassas, VA, USA). All cell lines have been authenticated and were cultured as described previously (9).

Public Database Analysis

The TCGA prostate adenocarcinoma (PRAD) database was acquired from the UCSC Xena database platform (http://xena.ucsc.edu/). The GSE21032 human PCa datasets were acquired from the GEO database (https://www.ncbi.nlm.nih.gov/geo/), which included two subsets: GSE21034 (mRNA sequencing data) and GSE21036 (miRNA sequencing data). The basic information of included datasets was presented in **Supplementary Table S1**. Overall, samples with complete clinical information and comprehensive matching gene expression were selected for subsequent analysis, and in order to ensure the validity of sufficient data, we chose biochemical recurrence (BCR, the amount of prostate-specific antigen in the blood has risen again after cancer treatment) as the endpoint event of prognosis index.

RNA Transfection and Construction of Stable Cell Lines

In order to study the biological function of miRNA, we constructed a cell line stably transfected with lentivirus, including miR-629-5p overexpression cell line (named as miR-629-5p mimic: 5'-TGGGTTTACGTTGGGAGAACT-3'), miR-629-5p inhibition cell line (named as miR-629-5p inhibitor: 5'-AGTTCTCCCAACGTAAACCCA-3') and the corresponding miRNA negative control (named as NC). Reagents used are all designed and constructed by GenePharma (Jiangsu, China). In addition, stable knockdown or knockout of AKAP13 expression PCa cells were established to further study the downstream target mRNA of miR-629-5p. The knockdown lentiviral vectors, which contain a specific shRNA (named as sh-AKAP13: target-1, 5'-GCAGCTCA ATTCCTAGCAACC-3'; target-2, 5'-GCTTCT AACCGAGGAGAATGC-3'; target-3, 5'-GCCAGTTCCCT GGATGGTAAC-3'; negative control named as sh-NC) against AKAP13 were synthesized by GenePharma (Jiangsu, China). The CRISPR/Cas9 knockout lentivirus (named as KO-AKAP13: target-1, 5'-CCAGAAGAGATGCTGCATCA-3'; target-2, 5'-ACTGGATCCGGTGATATCAC-3'; target-3, 5'-GTCCAGT GAAGCCGTGTCAT-3'; negative control named as KO-NC) was purchased from Guangzhou huiyuanyuan Co.ltd. (Guangzhou, China) (15), and the constructs were verified by DNA sequencing. Stable cell lines were selected for 10 days with Puromycin (PC-3, 2 μg/mL; LNCaP and C4-2, 4 μg/mL) or G418 (500 μg/mL). The transfection efficiency was identified by quantitative real-time polymerase chain reaction (qRT-PCR) and/or western blotting, and the most efficient virus was used in the following experiments.

RNA Extraction and qRT-PCR

Total RNA was isolated using TRIzol (Invitrogen; Thermo Fisher Scientific, CA, USA). For miRNA quantification, TaqMan MicroRNA Reverse Transcription kit (Thermo Fisher Scientific Inc, MA, USA) and specific primers (RIBOBIO, Guangzhou, China) were used. For mRNA quantification, All-in-One First-Strand cDNA Synthesis kit (GeneCopoeia, Guangzhou, China) was used to prepare cDNA. qPCR for quantification of miRNA or gene expression was performed with SYBR green Premix Ex Taq II (Takara) on a CFX-96 system (Bio-Rad, Hercules, CA).

The miRNA PCR thermal cycling conditions consisted of an initial denaturation at 95°C for 10 min, followed by 40 cycles of denaturation at 95°C for 10 s, annealing at 60°C for 20 s, and a 10 s extension at 72°C. The mRNA PCR protocol consisted of an initial denaturation at 95 °C for 15 min, followed by 40 cycles of denaturation at 95°C for 10 s, annealing at 58°C for 20 s, and a 30 s extension at 72°C. U6 and GAPDH were used as internal controls for miRNA and genes, respectively. Relative expression was determined by $2^{-\triangle\triangle Ct}$ method. Primer information was listed in **Supplementary Table S2**.

Protein Extraction and Western Blotting

Total proteins were firstly extracted from cells, which were washed by cold PBS and treated with RIPA lysis buffer (KeyGEN, KGP703) (supplemented with protease inhibitors 1 mmol/L phenylmethylsulfonylfluoride, 10 mg/L pepstatin, 10 mg/L aprotinin and 5 mg/L leupeptin). Protein concentrations were determined using the BCA protein assay regents (#23225, Thermo Pierce, Rockford, IL, USA). The procedure of western blot was conducted as previously described (9). Primary antibodies used in the study include anti-AKAP13 (Immunoway, YT0161; Abcam, ab99377), anti-HEG1 (Biorbyt, orb157480), anti-caspase 3 (Immunoway, YT6113), anti-caspase 3 p17 (Immunoway, YT6161). Anti-β-tubulin (Abcam, ab210797) was used as internal standard. Detection was achieved in Odyssey CLX Two-color infrared laser imaging system (LI-COR Biosciences, Nebraska, USA). Densitometric analysis of the bands was performed using ImageJ software.

Cell Proliferation Assays

The proliferation ability of PCa cells was measured by colony formation assay and 5-ethynyl-2′-deoxyuridine (EdU) assay. For colony formation assay, 500 cells were seeded in 6-well plate and incubated in media containing 10% FBS for 2 weeks to allow colony formation. Then, colonies were fixed with 4% paraformaldehyde and stained with 0.1% crystal violet, and the results were recorded and counted (colony >50 cells). For EdU assay, cells were inoculated into a 24-well plate, and the EdU kit (C10310-1, RIBOBIO, Guangzhou, China) was used to assess cell proliferations. The results were acquired using the fluorescent microscope (AX80, Olympus, Tokyo, Japan).

Cell Migration and Invasion Assays

The migration and invasion ability of PCa cells were measured by wound-healing assays and transwell assay, respectively. The detailed procedure was conducted as described in our previous research (9, 16). For wound-healing assays, cells were plated into 6-well culture plates and cultured until 100% confluence, then the growth medium was removed, cells were washed and cultured with fresh serum-free medium, and the wound was produced by a 10μL sterile pipette tip. The transwell assay was using a transwell permeable support chamber (Corning Incorporated, Corning, NY, USA), which were coated with Matrigel (BD Biosciences), and was carried out according to the manufacturer's instructions. Then, we observe cell migration/invasion and film the images under the optical microscope (CKX41, Olympus) at the indicated time points.

Cell Apoptosis Assays

In order to study the effect of downstream gene expression changes on cell apoptosis, we first treated the KO-NC/KO-AKAP13 cell with 10μM Carbonyl cyanide 3-chlorophenylhydrazone (CCCP, solarbio) for 12 h to induce apoptosis, and then cells were harvested to detect apoptosis rate by Annexin V-FITC/propidium iodide (PI) Apoptosis Detection kit (Key Gen Biotech, Jiangsu, China). The experimental procedure was carried out according to the manufacturer's protocol. Cytofluorimetric analysis was performed by the flow cytometer (Millipore, MA, USA).

Target Gene Prediction and Dual-Luciferase Reporter Assays

Prediction of miR-629-5p target genes was accomplished by using miRWalk (http://mirwalk.umm.uni-heidelberg.de/), TarBase (http://carolina.imis.athena-innovation.gr/diana_tools/web/index.php?r=site%2Ftools), TargetScan (http://www.targetscan.org/vert_72/) and MicroT-CDS (http://diana.imis.athena-innovation.gr/DianaTools/index.php?r=microT_CDS/index) online tools. To further verify the target sites of miR-629-5p, dual-luciferase reporter assay was carried out. HK293T were plated in 96-well plates and transfected with pLUC-AKAP13-3'UTR-wild type (WT) or pLUC-AKAP13-3'UTR-mutant type (MUT) luciferase plasmids (GenePharma, Jiangsu, China) by lipofectamine 3000 (Invitrogen, Thermo Fisher Scientific, Inc.). After 48 h, Luciferase and Renilla signals were measured using Dual-Luciferase Reporter Assay System (Promega, Madison, WI, USA).

Animal Experiments

Thirty 5 weeks old male BALB/c nude mice were purchased from the Experimental Animal Center of Guangdong Province (Guangzhou, China). The animals were fed as described previously (9). All procedures related to the experimental animals were approved by the Animal Care and Use Committee of the First Affiliated Hospital of Guangzhou Medical University.

To evaluate the effects of miR-629-5p on tumor growth, mice were randomly divided into six groups (NC/mimic/inhibitor group, n=5/group) and each mouse was subcutaneously injected with concentrated tumor cells 2×10^6 to establish xenograft tumors. The tumor sizes were monitored weekly. After 4 weeks, the mice were sacrificed by cervical dislocation, and the tumors were dissected and weighed. The tissue was fixed and embedded in paraffin wax for histological examination and immunohistochemical (IHC) assay.

Histological and Immunohistochemical Assessment

Histological and IHC analysis were performed in mice xenografts and clinical PCa samples. The tissue morphology was observed by haematoxylin and eosin (H&E) staining, and the expression of target protein in different tissues was evaluated by IHC.

The procedure of H&E and IHC were carried out as described previously (17). For IHC, primary antibodies used in the study include anti-AKAP13 (Novus, NBP1-89163) and anti-KI67 (Servicebio, GB111499). When the experiment was complete, the results were observed and recorded under the optical microscope (CKX41, Olympus), and the expression intensity of target protein was quantified according to the previous protocol (17).

Statistical Analyses

The SPSS V24.0 software (SPSS Inc., Chicago, IL, USA) and GraphPad Prism 7.0 (San Diego, CA, USA) were used to perform statistical analyses. For continuous variables, data were presented as the means ± SD. Comparison between groups was carried out using the Student's t test, paired t-test or one way ANOVA. The Fisher's exact test was used for 2 × 2 tables. Spearman's correlations were calculated for the expression levels between miR-629-5p and target gene. Survival curves were plotted using Kaplan-Meier's method and compared between groups by the log-rank test. X-tile program was used to determine the cut-off values which optimized the significance of the split between Kaplan-Meier survival curves (18). $P < 0.05$ was considered statistically significant.

RESULTS

Identify and Verify miRNA Associated With PCa Progression by Bioinformatics Analysis

By combining the miRNA sequencing result of clinical samples in our previous research (9) (**Figure 1A** and **Supplementary Table S3**, 102 upregulated differential expression miRNA/160 downregulated differential expression miRNA related to PCa metastasis) with it in the TCGA-PRAD database (**Figure 1B**, **Supplementary Table S4**, 50 upregulated differential expression miRNA/13 downregulated differential expression miRNA related to PCa formation), we have identified four key differential expression miRNA related to the progression of PCa (**Figure 1C**, 3 upregulated: miR-629-5p, miR-146b-3p, miR-210-3p; 1 downregulated: miR-221-3p). By consulting relevant literature, we found that the mechanism of miR-146b-3p, miR-210-3p and miR-221-3p in PCa has been reported (6, 7, 19), which further confirmed the reliability of our screening results from the side. Therefore, we chose miR-629-5p for verification in the follow-up study.

First, we found that miR-629-5p expression increased to varying degrees in primary localized PCa tissues and metastatic PCa tissues compared with adjacent normal tissues, and it had a consistent trend between TCGA tumor and adjacent normal tissues paired samples (**Figures 1D, E**). The same result was also verified in GSE21036 dataset (**Figure 1H**). At the same time, we found that miR-629-5p expression was upregulated in most other tumors by using dbDEMC 3.0 (**Supplementary Table S5**) (20). Subsequently, in order to test whether miR-629-5p can be used as a potential clinical prognostic indicator, we explored the association between miR-629-5p expression and patients' BCR and whether it has survival prognostic value. The results in GSE21036 dataset show that the expression of miR-629-5p and patients' BCR were related, and high miR-629-5p expression associated with shorter BCR-free survival, which suggested that high expression of miR-629-5p predicted poor prognosis (**Figures 1I, J**). However, the same result was not found in TCGA-PRAD database (**Figures 1F, G**). Finally, we examined miR-629-5p expression in prostate related cell line, and found it was significantly high expression in PCa cells compared with normal prostate epithelial cell line RWPE-1, especially in higher malignant degree PC3 cell lines. (**Figure 1K**).

MiR-629-5p Facilitates PCa Cells Proliferation, Migration, and Invasion *In Vitro*

In order to investigate the biological functions of miR-629-5p in PCa, we selected PCa cell lines with the lowest (LNCaP) and highest (PC3) miRNA expression levels as the research objects, and manipulated the expression level of miRNA by stably transfecting lentivirus. First, qPCR was conducted to confirm the transfection efficiency (**Figure 2A**). Colony formation and EdU assays were performed to assess the influence of miR-629-5p on the proliferation ability of PCa cells. The Colony formation assay revealed that the cell viability was prominently enhanced by miR-629-5p mimics, while miR-629-5p inhibitors inhibited the viability (**Figure 2B**). The corresponding change in the percentage of positive cells in EDU assay also supports this result (**Figure 2C**). Then, the migration and invasion ability of PCa cells were measured by wound-healing assays and transwell assays, respectively. To put it simply, over-expressing miR-629-5p dramatically facilitated the migratory and invasive capacities of cell, while inhibit miR-629-5p significantly suppressed these capacities (**Figures 2D, E**). These results suggested that miR-629-5p acts as an oncogenic miRNA in PCa cells *in vitro*.

MiR-629-5p Promotes Tumor Growth *In Vivo*

To investigate the effect of miR-629-5p on PCa cell proliferation *in vivo*, we established a subcutaneous xenograft tumor model in nude mice (**Figure 3A**). The results show that, compared with NC group, the cell lines overexpressing miRNA had faster tumor growth rate and larger weight, while the cell lines silencing miRNA showed the opposite trend (**Figures 3B, C**). H&E staining showed the histopathological features of the tumor tissues (**Figure 3D**). Furthermore, we further verified the change of tumor growth ability by cell proliferation marker KI67 immunostaining (**Figure 3E**). Taken together, *in vivo* study also confirmed the correlation between miR-629-5p and tumor malignancy.

AKAP13 Is a Direct Function Target of miR-629-5p

MiRNA has proved to play a biological function by regulating the expression of target genes. In order to clarify its mechanism, we screened out three candidate genes (HEG1, AKAP13 and TNRC6B) through the tool of target gene prediction (**Figure 4A**). Among them, HEG1 and AKAP13 were found in GSE21032 database and have better correlation with miR-629-5p (Pearson's rho = -0.4457 and -0.4346, **Figure 4B**). However, merely AKAP13 could be

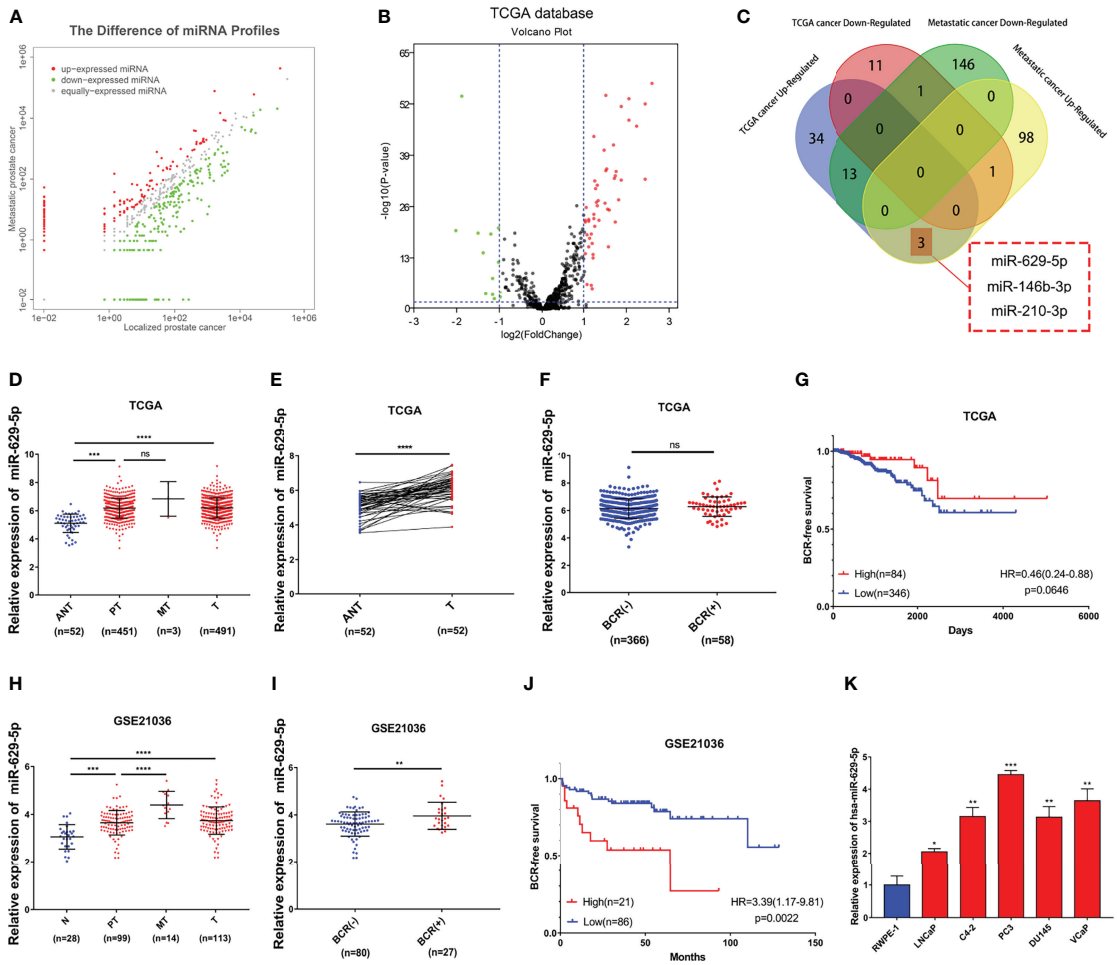

FIGURE 1 | Identify and verify miRNA associated with PCa progression by bioinformatics analysis. **(A)** The differential expression miRNA of clinical samples (102 upregulated/160 downregulated miRNAs related to PCa metastasis, threshold set as |log2(Fold Change)|≥1, P < 0.05). **(B)** The differential expression miRNA of TCGA-PRAD database (50 upregulated/13 downregulated miRNAs related to PCa formation, threshold set as |log2(Fold Change)|≥1, P < 0.05). **(C)** Identify key miRNAs related to PCa progression by combining clinical samples with TCGA database. **(D)** miR-629-5p expression increased in primary localized PCa tissues and metastatic PCa tissues compared with adjacent normal tissues in TCGA. **(E)** miR-629-5p expression levels was upregulated in 52 paired PCa tissues compared with that in the matching adjacent normal tissues in TCGA. **(F)** Correlations between miR-629-5p expression and patients' BCR status in TCGA. **(G)** The Kaplan-Meier survival analysis of BCR-free survival about miR-629-5p expression in TCGA. **(H)** miR-629-5p expression increased in primary localized PCa tissues and metastatic PCa tissues compared with normal tissues in GSE21036. **(I)** Correlations between miR-629-5p expression and patients' BCR status in GSE21036. **(J)** The Kaplan-Meier survival analysis of BCR-free survival about miR-629-5p expression in GSE21036. **(K)** Real-time PCR analysis of miR-629-5p expression in normal prostate epithelial cell (RWPE-1) and PCa cells. The data were presented as means ± SD from three biological replicates. $^{ns}P > 0.05$; $^{*}P < 0.05$; $^{**}P < 0.01$; $^{***}P < 0.001$; $^{****}P < 0.0001$; Student's t-test **(D, F, H, I, K)**; paired t-test **(E)**. ANT, adjacent normal tissues; N, normal tissues; PT, primary localized PCa tissues; MT, metastatic PCa tissues; T, tumor tissues; BCR, biochemical recurrence; HR, hazard ratio.

significantly regulated by miR-629-5p at the protein level (**Figure 4C**). To further verify the regulatory relationship, we analyzed the existence of miR-629-5p binding sites in the 3'UTR region of AKAP13, and based on this, we designed dual-luciferase reporter assays. The overexpression of miR-629-5p significantly reduced the luciferase activity of binding site of AKAP13, and the mutation of binding site blocked the interaction (**Figure 4D**). Which proved that AKAP13 is a direct target of miR-629-5p. IHC staining of xenografts also revealed that AKAP13 expression was regulated by miR-629-5p (**Figure 4E**).

AKAP13 Is Essential for miR-629-5p Enhanced Cell Proliferation and Motility in PCa

Through the detection of AKAP13 protein in prostate related cell lines, high-level expression in RWPE-1 indicates that it might be a potential tumor suppressor gene (**Figure 5A**). In order to validate whether AKAP13 is the downstream effector of miR-629-5p in PCa, the expression was downregulated by transfecting knockdown/knockout lentivirus (**Figure 5B**). Particularly, in order to make the effect of gene down-regulation more

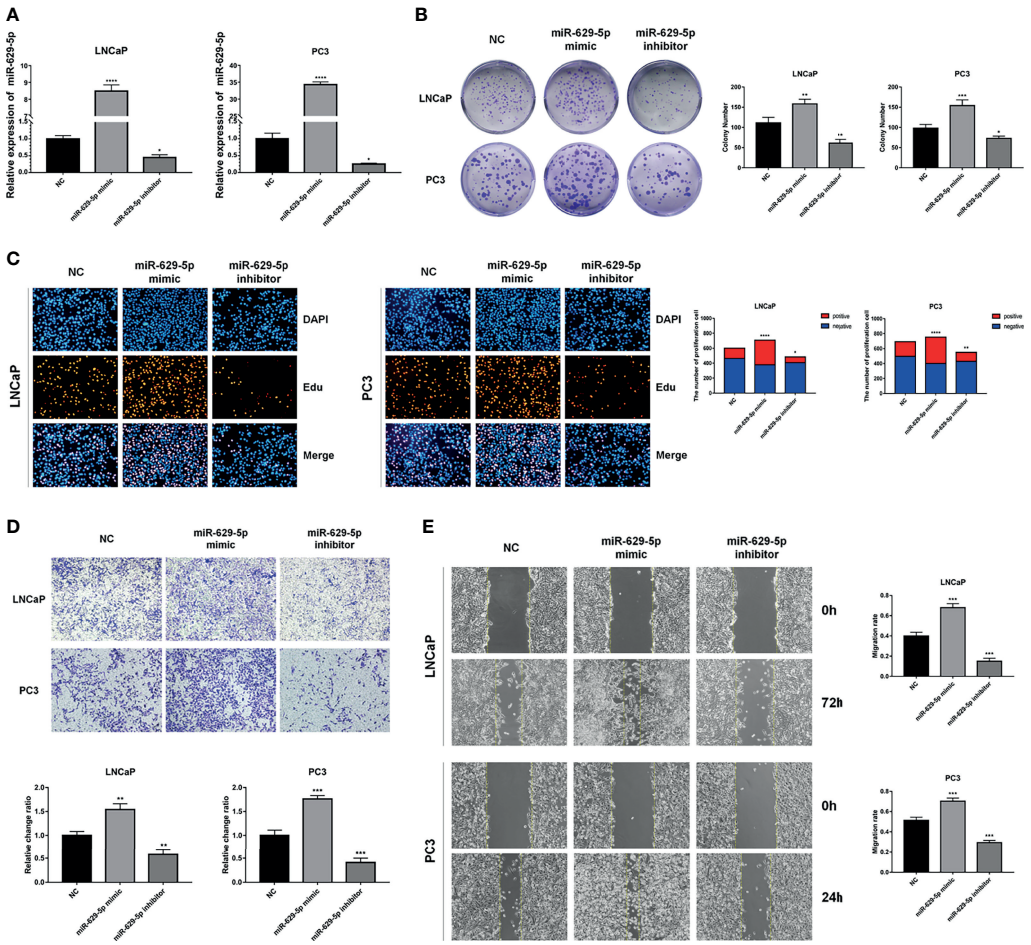

FIGURE 2 | MiR-629-5p facilitates PCa cells proliferation, migration, and invasion *in vitro*. **(A)** Stable miR-629-5p overexpression or inhibition PCa cell lines were established and confirmed by qRT-PCR. **(B)** Colony formation assays and **(C)** EdU assays were performed to assess the proliferation ability changes in miR-629-5p overexpressing or inhibitory cell lines. **(D)** Transwell assays and **(E)** Wound-healing assays were performed to assess the invasion and migration ability changes in miR-629-5p overexpressing or inhibitory cell lines. The data were presented as means ± SD from three biological replicates. *P < 0.05; **P < 0.01; ***P < 0.001; ****P < 0.0001; Student's t-test.

obvious, we selected LNCaP and C4-2 cell line as the follow-up research objects. Subsequently, the increase of cell proliferation and metastasis ability in different degrees demonstrated the negative regulation effect of AKAP13 on cell malignant phenotype (**Figures 5C–E**). In addition, compared with the control group, gene knockout can increase the tolerance of cells to apoptosis induction (**Figure 5F**). The corresponding changes of apoptosis-related proteins expression also verified this finding (**Figure 5B**).

To further confirm whether miR-629-5p promoted PCa development through AKAP13, we performed rescue experiment of AKAP13 knockdown in corresponding cells with stable miRNA inhibited (**Figure 6A**). As shown in **Figures 6B, C**, after gene double knockdown, the proliferation and metastasis ability of PCa cells partially recovered, the anticancer effect of miR-629-5p inhibitor could be reversed. Our results suggested that AKAP13 is essential for miR-629-5p takes effect in PCa progress.

AKAP13 Expression Is Negatively Correlated With PCa Malignant Degree and Correlate With Clinical Outcomes of PCa Patients

Immunohistochemical staining was performed on enrolled 53 clinical samples. By evaluating and counting the staining results, we get the number of AKAP13 different expression (-: negative expression; +: weak expression; ++: moderate expression; +++: strong expression) in three groups of patients (ANT, PPCa and MPCa) (**Figure 7A**). As shown in **Table 1**, combined with the clinicopathological characteristics of patients, we found that the expression level of AKAP13 has a significant correlation with the patients' part clinical indicators, such as gleason score (P=0.006) and distant metastasis (P=0.029). At the same time, by analyzing the survival data of patients, we found that AKAP13 negative patients had shorter overall survival time (**Figure 7B**), which suggested that AKAP13 expression is negatively correlated with

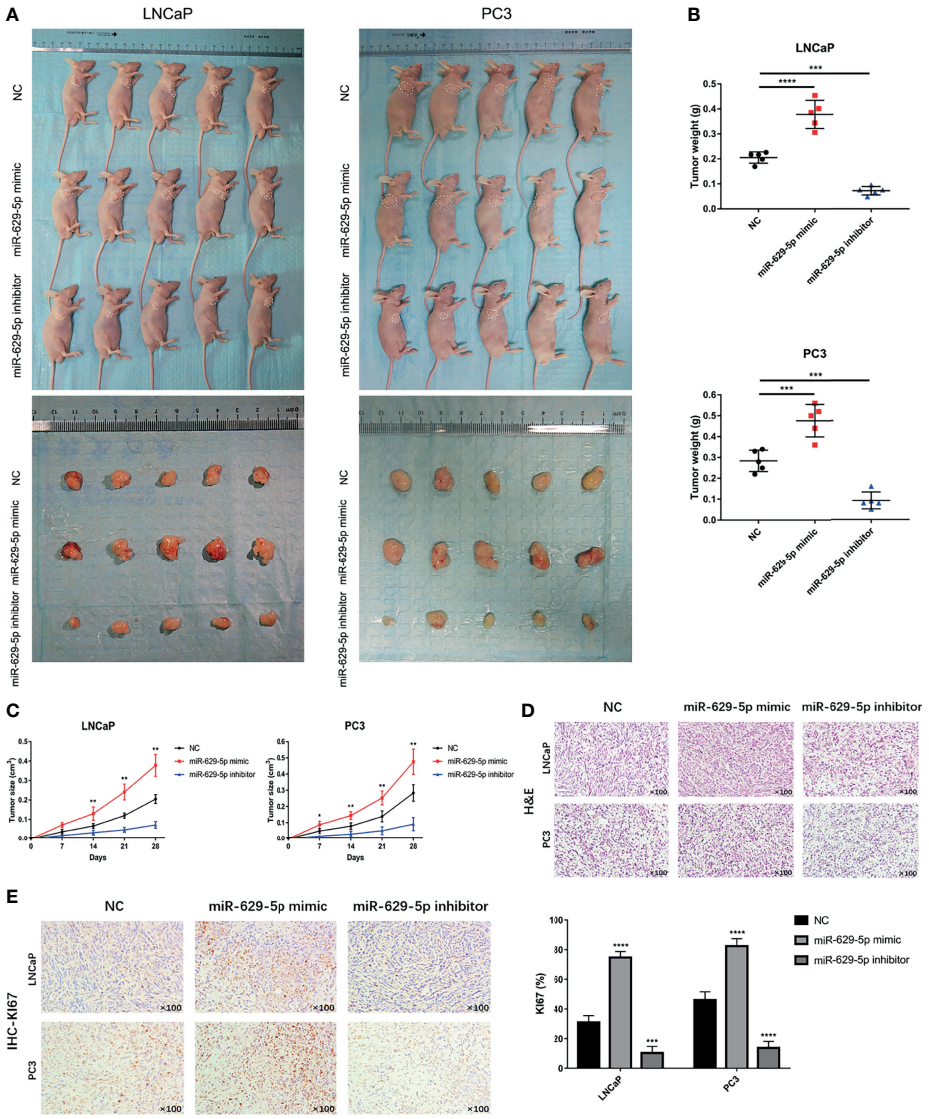

FIGURE 3 | MiR-629-5p promotes tumor growth *in vivo*. **(A)** The subcutaneous xenograft tumor model in nude mice was established, and the representative appearance of tumor mass resected from each group of mice. **(B)** Final tumor weights were measured at autopsy on day 28 after subcutaneous injection stable transfected PCa cells. **(C)** The tumor growth curves were measured with a calliper at the indicated days after cell injecting. **(D)** The xenograft tumor tissues were stained with H&E. **(E)** KI67 IHC staining was performed in xenograft tumor tissues to assess tumor proliferation. Magnification, ×100. The data were presented as means ± SD from three biological replicates. *P < 0.05; **P < 0.01; ***P < 0.001; ****P < 0.0001; Student's t-test.

PCa malignant degree and could be used as a potential clinical prognostic indicator. Finally, we verify this result by analyzing the public database (TCGA-PRAD database and GSE21034 dataset) (**Figures 7C–F**).

DISCUSSION

Because of the complexity of mechanism, tumor metastasis often means higher medical expenses and worse quality of life for patients. Therefore, many researches are devoted to exploring the molecular mechanism of PCa metastasis. More and more miRNAs have been shown to participate in various tumor processes, including tumor initiation, progression, and metastasis. In this research, by combining clinical samples with public databases, we found a novel miRNA (miR-629-5p) related to the occurrence and development of PCa, and proved that its expression is closely associated with the malignant phenotype of tumor on cell and animal models. On this basis, we searched for the downstream target gene (AKAP13) of miR-629-5p, and confirmed that it played biological function through this key gene. Finally, the potential value of AKAP13 as a tumor suppressor gene was verified in clinical data.

The miR-629-5p has been reported to play an oncogenic in many types of cancer. In renal cell carcinoma, Kentaro et al. have

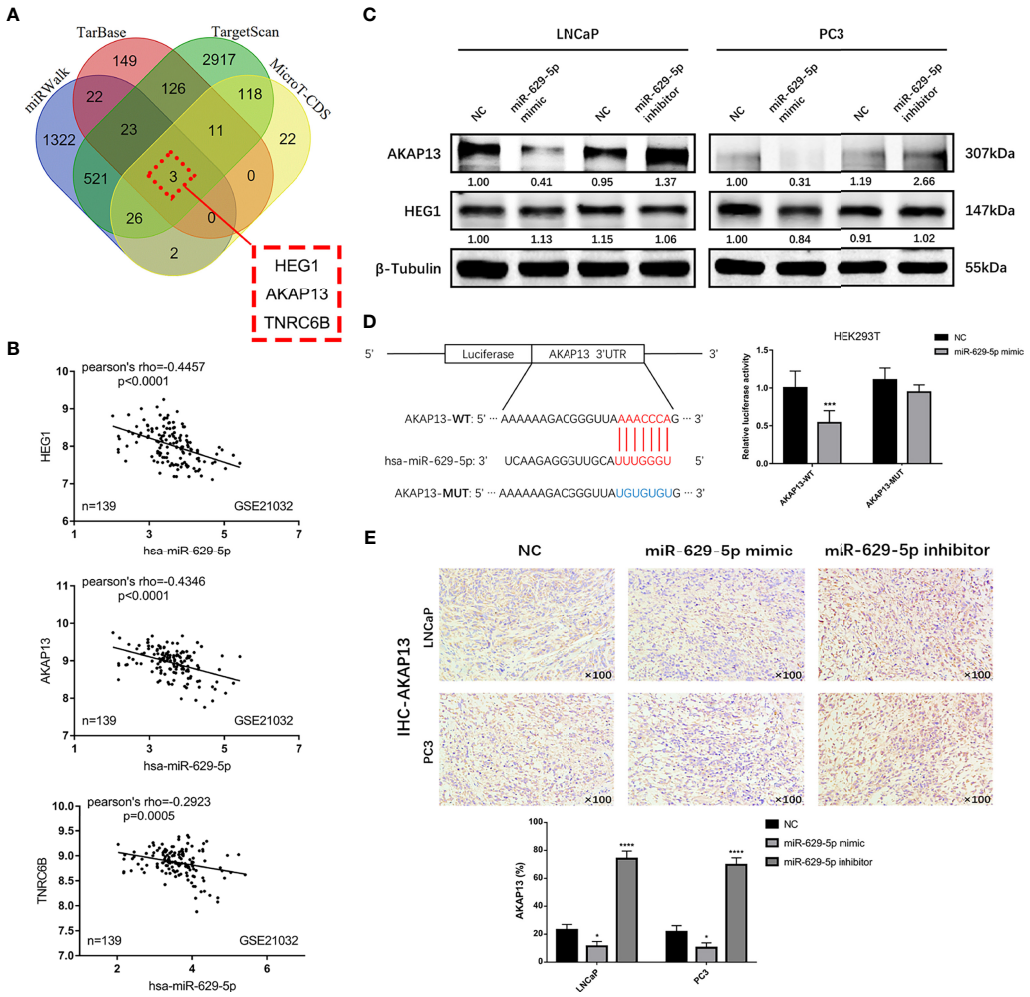

FIGURE 4 | AKAP13 is a direct function target of miR-629-5p. **(A)** Identify potential miR-629-5p target genes by four common miRNA prediction tools. **(B)** The correlations between miR-629-5p expression and HEG1, AKAP13 and TNRC6B expression in GSE21032. **(C)** Western blotting was carried out to verify the expression of HEG1 and AKAP13 at protein level in stable transfected PCa cells, merely AKAP13 could be significantly regulated by miR-629-5p, but not HEG1. **(D)** Left: potential miR-629-5p binding sites in the 3'UTR of AKAP13 mRNAs. Right: the dual-luciferase reporter assays showed that miR-629-5p overexpression significantly reduced the luciferase activity of binding site of AKAP13, and the mutation of binding site blocked the interaction. **(E)** AKAP13 IHC staining was performed in xenograft tumor tissues. Magnification, ×100. The data were presented as means ± SD from three biological replicates. *P < 0.05; ***P < 0.001; ****P < 0.0001; Student's t-test. WT, wide type; MUT, mutant type.

proved that miR-629 could promote TGFβ/Smad Signaling and tumor metastatic phenotypes by targeting TRIM33 (21). A recent study by Li et al. reported that miR-629-5p could increase the invasiveness of tumor cells while increasing the permeability of endothelial cells, thereby promoting the invasion of lung adenocarcinoma (13). Zhu et al. found that miR-629 promotes the tumorigenesis of non-small-cell lung cancer by targeting FOXO1 and activating PI3K/AKT pathway (22). In addition, the study by Cheng et al. showed that the overexpression of miR-629-5p has immunosuppressive effect on the anti-tumor $CD8^+$ T cells, which demonstrates its role in promoting cancer from a new perspective (23). However, it remains unclear whether miR-629-5p is involved in the regulation of PCa progression. In this study, we started with clinical data, and a series of functional experiments were preformed, whose results showed that miR-629-5p facilitated PCa cell malignant phenotype *in vitro* and vivo. Overall, these present results suggest that miR-629-5p works as an oncogene in PCa.

Downstream target genes, such as FOXO3, CXXC, PDCD4, SFRP2 and LRP6, which are directly affected by miR-629-5p, have been reported and verified by previous studies (11, 12, 24–26). In our study, however, a novel target gene of miR-629-5p was identified in PCa by dual-luciferase reporter assay. The A-Kinase Anchoring Protein (AKAPs) are a family of multivalent scaffolds that constrain signaling enzymes and effectors at subcellular locations to drive essential physiological events (27). Among them, AKAP4 and AKAP9 have been widely studied as cancer-promoting factors, while AKAP12 have proved to play the opposite

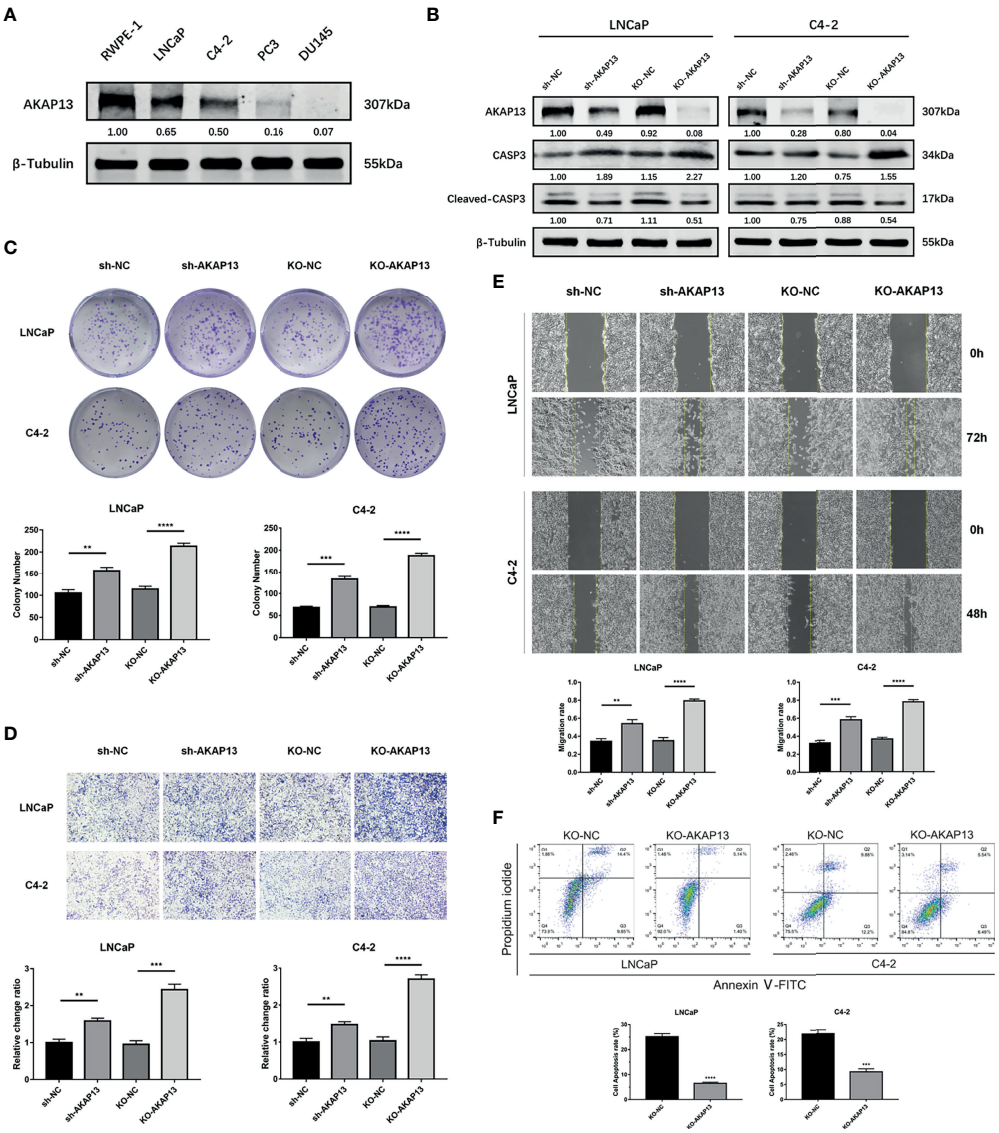

FIGURE 5 | AKAP13 expression changes can affect the malignant phenotype of PCa cells. **(A)** Western blotting analysis of AKAP13 protein expression in RWPE-1 and PCa cells. **(B)** Stable AKAP13 knockdown or knockout PCa cell lines were established, and the sequence with the highest inhibitory efficiency was verified by Western blotting. After adding CCCP to stably transfected cell lines to induce apoptosis, the expression of apoptosis-related proteins changed. **(C)** Colony formation assays were performed to assess the proliferation ability changes in AKAP13 inhibitory cell lines. **(D)** Transwell assays and **(E)** Wound-healing assays were performed to assess the invasion and migration ability changes in AKAP13 inhibitory cell lines. **(F)** After adding CCCP to stably AKAP13 knockout cell lines to induce apoptosis, then cell apoptosis rate was determined by Annexin V-FITC/PI staining. The data were presented as means ± SD from three biological replicates. $^{**}P < 0.01$; $^{***}P < 0.001$; $^{****}P < 0.0001$; Student's t-test. CCCP, Carbonyl cyanide 3-chlorophenylhydrazone.

role (28–30). AKAP13 serves as a scaffold protein for PKA and other transduction enzymes, and functions as a guanine nucleotide exchange factor for the small molecular weight GTPases RhoA and RhoC (31). Although it has been shown to be overexpressed in several cancers including esophageal cancers, breast cancer and hepatocellular carcinoma (32–34). According to a recent study, AKAP13 was regarded as a new tumor suppressor in PCa, which could prevent tumor invasion in collaboration with PTEN (35). However, its mechanism of action has not been deeply studied. In the present study, we confirmed this finding by knocking out AKAP13 in PCa cells and observed the phenotypic changes, and then verified its prognostic value in clinical data. More importantly, the silence of AKAP13 expression could reverse the tumor suppressor function of miR-629-5p inhibitor in PCa cells. Interestingly, we observed that its anti-cancer effect might be through promoting apoptosis.

To our knowledge, this study is the first research that provided the comprehensive evaluation of the role of miR-629-5p in PCa. There are still limitations in our current study that need to be taken into account. Firstly, we have verified the role of

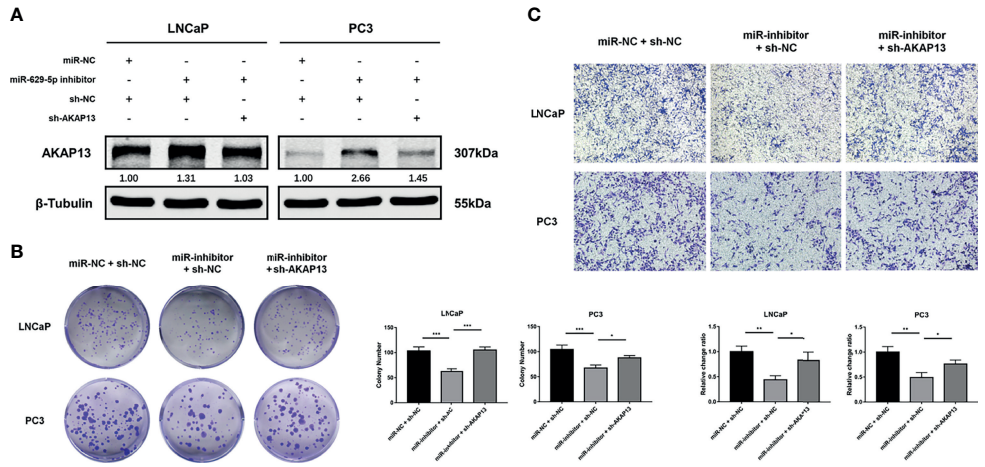

FIGURE 6 | AKAP13 knockdown rescues the miR-629-5p inhibition-attenuated PCa cell proliferation and motility. **(A)** AKAP13 was knocked down by the shRNA in PCa cells with miR-629-5p inhibition, and the transfection efficiency was confirmed by western blotting. **(B)** Colony formation assays and **(C)** Transwell assays were performed to assess the proliferation and invasion abilities of PCa cells transfected with the corresponding vectors. The data were presented as means ± SD from three biological replicates. *P < 0.05; **P < 0.01; ***P < 0.001. Student's t-test.

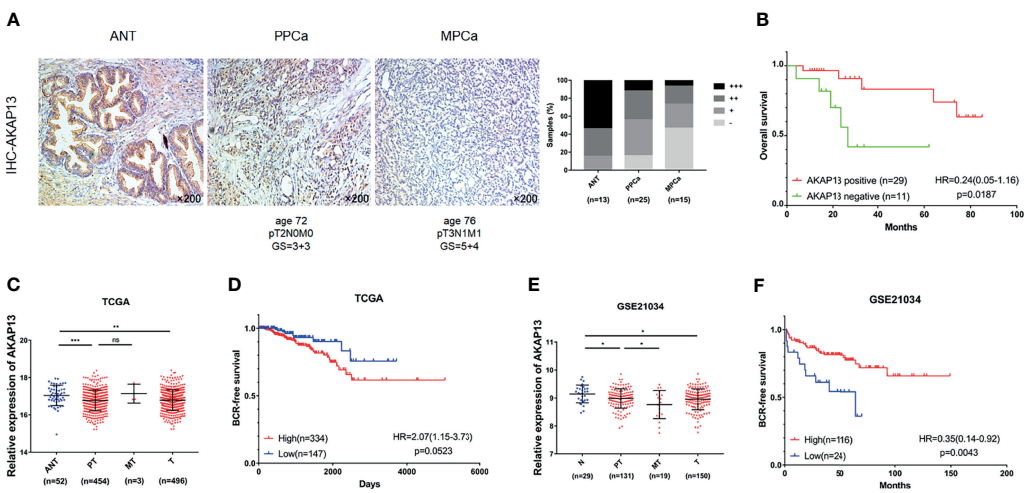

FIGURE 7 | AKAP13 expression is negatively correlated with PCa malignant degree and correlate with clinical outcomes of PCa patients. **(A)** AKAP13 IHC staining was performed in clinical adjacent normal tissues (n = 13) and PCa tissue samples (n = 40). Left: representative IHC photographs of ANT and tumor tissue samples (PPCa, MPCa) were shown as indicated. Right: the composition of AKAP13 different expression degree (-: negative expression; +: weak expression; ++: moderate expression; +++: strong expression) in each group of tissue samples was counted. **(B)** The Kaplan-Meier survival analysis of overall survival of PCa patients with different AKAP13 expression levels. **(C)** AKAP13 expression decreased in PCa tumor tissues compared with adjacent normal tissues in TCGA. **(D)** The Kaplan-Meier survival analysis of BCR-free survival about AKAP13 expression in TCGA. **(E)** AKAP13 expression decreased in primary localized PCa tissues and metastatic PCa tissues compared with normal tissues in GSE21034. **(F)** The Kaplan-Meier survival analysis of BCR-free survival about AKAP13 expression in GSE21034. Magnification, ×200. The data were presented as means ± SD. ^{ns}P > 0.05; *P < 0.05; **P < 0.01; ***P < 0.001; Student's t-test. ANT, adjacent normal tissues; N, normal tissues; PPCa/PT, primary localized PCa tissues; MPCa/MT, metastatic PCa tissues; T, tumor tissues; BCR, biochemical recurrence; HR, hazard ratio.

miR-629-5p in promoting tumor growth in animal models, but its role in promoting metastasis needs to be further confirmed. Secondly, some of the results in the public database do not support our conclusions, so it needs to be further verified by increasing the number of clinical samples. Finally, although it has been found that AKAP13 may be related to the apoptosis pathway, the specific mechanism of its function still needs further study.

In conclusion, our results demonstrated that high miR-629-5p expression is associated with the increase of malignant degree

TABLE 1 | Correlation between AKAP13 expression with clinicopathological characteristics in PCa.

Variables	n	AKAP13		p[a]
		Positive (%)	Negative (%)	
Patients	40	29 (72.5)	11 (27.5)	
Age (year)				
≤72	19	15 (78.9)	4 (21.1)	0.488
>72	21	14 (66.7)	7 (33.3)	
GS				
<7	22	20 (90.9)	2 (9.1)	0.006
≥7	18	9 (50.0)	9 (50.0)	
pT				
≤T2	20	12 (60.0)	8 (40.0)	0.155
T3–T4	20	17 (85.0)	3 (15.0)	
pN				
N0	28	21 (75.0)	7 (25.0)	0.704
N1	12	8 (66.7)	4 (33.3)	
M				
M0	26	22 (84.6)	4 (15.4)	0.029
M1	14	7 (50.0)	7 (50.0)	

AKAP13 expression was determined by IHC.
GS, gleason score; pT, pathologic tumor stage; pN, pathologic lymph node metastasis; M, distant metastasis.
[a]*Chi-square test.*

of PCa, and suggests a worse clinical prognosis. More precisely, the function of miR-629-5p tumor-promoting effect is realized by targeting AKAP13, which provides a new idea for clinical diagnosis and treatment of complex refractory PCa.

DATA AVAILABILITY STATEMENT

The original contributions presented in the study are included in the article/**Supplementary Material**. Further inquiries can be directed to the corresponding author.

ETHICS STATEMENT

The studies involving human participants were reviewed and approved by the Ethics Committee of the First Affiliated Hospital for Guangzhou Medical University. The patients/participants provided their written informed consent to participate in this study. The animal study was reviewed and approved by the Animal Care and Use Committee of the First Affiliated Hospital of Guangzhou Medical University.

AUTHOR CONTRIBUTIONS

YL: project development, data analysis and manuscript writing. SZ and JW: experiment model establishment and data analysis. ZZhu and LL: cell culture and data collection. QX and MZ: histology examination and data collection. YM and ZW: data analysis. ZZhao: project development and manuscript editing. All authors contributed to the article and approved the submitted version.

FUNDING

This work was supported by the grants from National Natural Science Foundation of China (No. 81572537 for ZZhao).

SUPPLEMENTARY MATERIAL

The Supplementary Material for this article can be found online at: https://www.frontiersin.org/articles/10.3389/fonc.2021.754353/full#supplementary-material

REFERENCES

1. Siegel RL, Miller KD, Fuchs HE, Jemal A. Cancer Statistics, 2021. *CA: A Cancer J Clin* (2021) 71(1):7–33. doi: 10.3322/caac.21654
2. Chen W, Zheng R, Baade PD, Zhang S, Zeng H, Bray F, et al. Cancer Statistics in China, 2015. *CA: A Cancer J Clin* (2016) 66(2):115–32. doi: 10.3322/caac.21338
3. Bubendorf L, Schöpfer A, Wagner U, Sauter G, Moch H, Willi N, et al. Metastatic Patterns of Prostate Cancer: An Autopsy Study of 1,589 Patients. *Hum Pathol* (2000) 31(5):578–83. doi: 10.1053/hp.2000.6698
4. Bartel DP. MicroRNAs: Target Recognition and Regulatory Functions. *Cell* (2009) 136(2):215–33. doi: 10.1016/j.cell.2009.01.002
5. Calin GA, Croce CM. MicroRNA Signatures in Human Cancers. *Nat Rev Cancer* (2006) 6(11):857–66. doi: 10.1038/nrc1997
6. Gao S, Zhao Z, Wu R, Wu L, Tian X, Zhang Z. MiR-146b Inhibits Autophagy in Prostate Cancer by Targeting the PTEN/Akt/mTOR Signaling Pathway. *Aging* (2018) 10(8):2113–21. doi: 10.18632/aging.101534
7. Ren D, Yang Q, Dai Y, Guo W, Du H, Song L, et al. Oncogenic miR-210-3p Promotes Prostate Cancer Cell EMT and Bone Metastasis *via* NF-κb Signaling Pathway. *Mol Cancer* (2017) 16(1):117. doi: 10.1186/s12943-017-0688-6
8. Zhu Z, Wen Y, Xuan C, Chen Q, Xiang Q, Wang J, et al. Identifying the Key Genes and microRNAs in Prostate Cancer Bone Metastasis by Bioinformatics Analysis. *FEBS Open Bio* (2020) 10(4):674–88. doi: 10.1002/2211-5463.12805
9. Zhao Z, Zhao S, Luo L, Xiang Q, Zhu Z, Wang J, et al. miR-199b-5p-DDR1-ERK Signalling Axis Suppresses Prostate Cancer Metastasis *via* Inhibiting Epithelial-Mesenchymal Transition. *Brit J Cancer* (2021) 124(5):982–94. doi: 10.1038/s41416-020-01187-8
10. Zhu Z, Luo L, Xiang Q, Wang J, Liu Y, Deng Y, et al. MiRNA-671-5p Promotes Prostate Cancer Development and Metastasis by Targeting NFIA/CRYAB Axis. *Cell Death Dis* (2020) 11(11):949. doi: 10.1038/s41419-020-03138-w
11. Lu J, Lu S, Li J, Yu Q, Liu L, Li Q. MiR-629-5p Promotes Colorectal Cancer Progression Through Targetting CXXC Finger Protein 4. *Biosci Rep* (2018) 38 (4):BSR20180613. doi: 10.1042/BSR20180613
12. Tao X, Yang X, Wu K, Yang L, Huang Y, Jin Q, et al. miR-629–5p Promotes Growth and Metastasis of Hepatocellular Carcinoma by Activating β-Catenin. *Exp Cell Res* (2019) 380(2):124–30. doi: 10.1016/j.yexcr.2019.03.042
13. Li Y, Zhang H, Fan L, Mou J, Yin Y, Peng C, et al. MiR-629-5p Promotes the Invasion of Lung Adenocarcinoma *via* Increasing Both Tumor Cell Invasion and Endothelial Cell Permeability. *Oncogene* (2020) 39(17):3473–88. doi: 10.1038/s41388-020-1228-1
14. Gao C, Gao J, Zeng G, Yan H, Zheng J, Guo W. MicroRNA-629-5p Promotes Osteosarcoma Proliferation and Migration by Targeting Caveolin 1. *Braz J Med Biol Res* (2021) 54(6):e10474. doi: 10.1590/1414-431X202010474
15. Cao J, Wei J, Yang P, Zhang T, Chen Z, He F, et al. Genome-Scale CRISPR-Cas9 Knockout Screening in Gastrointestinal Stromal Tumor With Imatinib Resistance. *Mol Cancer* (2018) 17(1):121. doi: 10.1186/s12943-018-0865-2

16. Liu L, Li E, Luo L, Zhao S, Li F, Wang J, et al. PSCA Regulates IL-6 Expression Through P38/NF-κb Signaling in Prostate Cancer. *Prostate* (2017) 77 (14):1389–400. doi: 10.1002/pros.23399
17. Li E, Liu L, Li F, Luo L, Zhao S, Wang J, et al. PSCA Promotes Prostate Cancer Proliferation and Cell-Cycle Progression by Up-Regulating C-Myc. *Prostate* (2017) 77(16):1563–72. doi: 10.1002/pros.23432
18. Camp RL, Dolled-Filhart M, Rimm DL. X-Tile. *Clin Cancer Res* (2004) 10 (21):7252–9. doi: 10.1158/1078-0432.CCR-04-0713
19. Krebs M, Solimando AG, Kalogirou C, Marquardt A, Frank T, Sokolakis I, et al. miR-221-3p Regulates VEGFR2 Expression in High-Risk Prostate Cancer and Represents an Escape Mechanism From Sunitinib *In Vitro*. *J Clin Med* (2020) 9(3):670. doi: 10.3390/jcm9030670
20. Yang Z, Wu L, Wang A, Tang W, Zhao Y, Zhao H, et al. dbDEMC 2.0: Updated Database of Differentially Expressed miRNAs in Human Cancers. *Nucleic Acids Res* (2017) 45(D1):D812–8. doi: 10.1093/nar/gkw1079
21. Jingushi K, Ueda Y, Kitae K, Hase H, Egawa H, Ohshio I, et al. miR-629 Targets TRIM33 to Promote Tgfβ/Smad Signaling and Metastatic Phenotypes in ccRCC. *Mol Cancer Res* (2015) 13(3):565–74. doi: 10.1158/1541-7786.MCR-14-0300
22. Zhu L, Chen Y, Liu J, Nie K, Xiao Y, Yu H. MicroRNA-629 Promotes the Tumorigenesis of non-Small-Cell Lung Cancer by Targeting FOXO1 and Activating PI3K/AKT Pathway. *Cancer Biomark* (2020) 29(3):347–57. doi: 10.3233/CBM-201685
23. Cheng C, Lin H, Chiang Y, Chang J, Sie Z, Yang B, et al. Nicotine Exhausts CD8+ T Cells Against Tumor Cells Through Increasing miR-629-5p to Repress IL2RB-Mediated Granzyme B Expression. *Cancer Immunol Immunother* (2021) 70(5):1351–64. doi: 10.1007/s00262-020-02770-x
24. Yan H, Li Q, Wu J, Hu W, Jiang J, Shi L, et al. MiR-629 Promotes Human Pancreatic Cancer Progression by Targeting FOXO3. *Cell Death Dis* (2017) 8 (10):e3154–4. doi: 10.1038/cddis.2017.525
25. Zheng Y, Bai Y, Yang S, Cui Y, Wang Y, Hu W. MircoRNA-629 Promotes Proliferation, Invasion and Migration of Nasopharyngeal Carcinoma Through Targeting PDCD4. *Eur Rev Med Pharmaco* (2019) 23(1):207–16. doi: 10.26355/eurrev_201901_16766
26. Yan G, Li C, Zhao Y, Yue M, Wang L. Downregulation of microRNA−629−5p in Colorectal Cancer and Prevention of the Malignant Phenotype by Direct Targeting of Low−Density Lipoprotein Receptor−Related Protein 6. *Int J Mol Med* (2019) 44(3):1139–50. doi: 10.3892/ijmm.2019.4245
27. Bucko PJ, Scott JD. Drugs That Regulate Local Cell Signaling: AKAP Targeting as a Therapeutic Option. *Annu Rev Pharmacol* (2021) 61(1):361–79. doi: 10.1146/annurev-pharmtox-022420-112134
28. Li S, Qin X, Li Y, Guo A, Ma L, Jiao F, et al. AKAP4 Mediated Tumor Malignancy in Esophageal Cancer. *Am J Transl Res* (2016) 8(2):597–605.
29. Hu Z, Liu Y, Xie L, Wang X, Yang F, Chen S, et al. AKAP-9 Promotes Colorectal Cancer Development by Regulating Cdc42 Interacting Protein 4. *Biochim Biophys Acta (BBA) - Mol Basis Dis* (2016) 1862(6):1172–81. doi: 10.1016/j.bbadis.2016.03.012
30. Choi M, Jong H, Kim TY, Song S, Lee DS, Lee JW, et al. AKAP12/Gravin is Inactivated by Epigenetic Mechanism in Human Gastric Carcinoma and Shows Growth Suppressor Activity. *Oncogene* (2004) 23(42):7095–103. doi: 10.1038/sj.onc.1207932
31. Diviani D, Soderling J, Scott JD. AKAP-Lbc Anchors Protein Kinase A and Nucleates Gα12-Selective Rho-Mediated Stress Fiber Formation. *J Biol Chem* (2001) 276(47):44247–57. doi: 10.1074/jbc.M106629200
32. Kumar A, Chatopadhyay T, Raziuddin M, Ralhan R. Discovery of Deregulation of Zinc Homeostasis and its Associated Genes in Esophageal Squamous Cell Carcinoma Using cDNA Microarray. *Int J Cancer* (2007) 120 (2):230–42. doi: 10.1002/ijc.22246
33. Wirtenberger M, Tchatchou S, Hemminki K, Klaes R, Schmutzler RK, Bermejo JL, et al. Association of Genetic Variants in the Rho Guanine Nucleotide Exchange Factor AKAP13 With Familial Breast Cancer. *Carcinogenesis* (2006) 27(3):593–8. doi: 10.1093/carcin/bgi245
34. Molee P, Adisakwattana P, Reamtong O, Petmitr S, Sricharunrat T, Suwandittakul N, et al. Up-Regulation of AKAP13 and MAGT1 on Cytoplasmic Membrane in Progressive Hepatocellular Carcinoma: A Novel Target for Prognosis. *Int J Clin Exp Pathol* (2015) 8(9):9796–811.
35. de la Rosa J, Weber J, Friedrich MJ, Li Y, Rad L, Ponstingl H, et al. A Single-Copy Sleeping Beauty Transposon Mutagenesis Screen Identifies New PTEN-Cooperating Tumor Suppressor Genes. *Nat Genet* (2017) 49(5):730–41. doi: 10.1038/ng.3817

Conflict of Interest: The authors declare that the research was conducted in the absence of any commercial or financial relationships that could be construed as a potential conflict of interest.

frontiers in Oncology

ORIGINAL RESEARCH
published: 05 November 2021
doi: 10.3389/fonc.2021.761643

Screening to Identify an Immune Landscape-Based Prognostic Predictor and Therapeutic Target for Prostate Cancer

Yanting Shen[1†], Huan Xu[1†], Manmei Long[2†], Miaomiao Guo[3], Peizhang Li[1], Ming Zhan[1,3] and Zhong Wang[1*]*

[1] Department of Urology, Shanghai Ninth People's Hospital, Shanghai Jiaotong University School of Medicine, Shanghai, China, [2] Department of Pathology, Shanghai Ninth People's Hospital, Shanghai Jiaotong University School of Medicine, Shanghai, China, [3] The Core Laboratory in Medical Center of Clinical Research, Department of Endocrinology, Shanghai Ninth People's Hospital, State Key Laboratory of Medical Genomics, Shanghai Jiao Tong University School of Medicine, Shanghai, China

OPEN ACCESS

Edited by:
Alagarsamy Srinivasan, NanoBio Diagnostics, United States

Reviewed by:
Baijun Dong, Shanghai JiaoTong University, China
Tan Shyh-Han, Uniformed Services University of the Health Sciences, United States

***Correspondence:**
Zhong Wang
zhongwang2000@sina.com
Ming Zhan
zhanming@shsmu.edu.cn

[†]These authors have contributed equally to this work and share first authorship

Specialty section:
This article was submitted to Genitourinary Oncology, a section of the journal Frontiers in Oncology

Received: *20 August 2021*
Accepted: *18 October 2021*
Published: *05 November 2021*

Citation:
Shen Y, Xu H, Long M, Guo M, Li P, Zhan M and Wang Z (2021) Screening to Identify an Immune Landscape-Based Prognostic Predictor and Therapeutic Target for Prostate Cancer. Front. Oncol. 11:761643. doi: 10.3389/fonc.2021.761643

Objectives: Existing prognostic risk assessment strategies for prostate cancer (PCa) remain unsatisfactory. Similar treatments for patients at the same disease stage can lead to different survival outcomes. Thus, we aimed to explore a novel immune landscape-based prognostic predictor and therapeutic target for PCa patients.

Methods: A total of 490 PCa patients from The Cancer Genome Atlas Project (TCGA) cohort were analyzed to obtain immune landscape-based prognostic features. Then, analyses at different levels were performed to explore the relevant survival mechanisms, prognostic predictors, and therapeutic targets. Finally, experimental verification was performed using a tissue microarray (TMA) from 310 PCa patients. Furthermore, a nomogram was constructed to provide a quantitative approach for predicting the prognosis of patients with PCa.

Results: The immune landscape-based risk score (ILBRS) was obtained. Then, VAV1, which presented a significant positive correlation with Treg infiltration and ILBRS, was screened and identified to be significantly related to the prognosis of PCa. Finally, experimental verification confirmed the prognostic value of VAV1 for PCa prognosis at the protein level.

Conclusions: VAV1 has the potential to be developed as an immune landscape-based PCa prognostic predictor and therapeutic target and will help improve prognosis by enabling the selection of individualized, targeted therapy.

Keywords: prognostic predictor, immune infiltration, progression-free survival (PFS), overall survival (OS), prostate cancer

Abbreviations: ILBRS, immune landscape based risk score; IL-DEGs, immune landscape based DEGs.

INTRODUCTION

Prostate cancer (PCa) is the most common malignancy of the male reproductive system. Its incidence ranks second only to lung cancer among male malignancies worldwide (1). Although there are some curable therapeutic methods, such as radical prostatectomy (RP), a high recurrence rate still exists due to the biological characteristics of malignant tumors, distant micrometastases, and focal residuals (2). Salvage therapy performed in the early stage of recurrence can reduce the distant metastatic rate, prolong survival, and even cure tumors (3). Therefore, identifying PCa recurrences early greatly reduces mortality and improves patient prognosis.

In clinical practice, serum prostate-specific antigen (PSA), Gleason scores (GS), and pathological TNM (pTNM) staging are commonly used to evaluate recurrence and predict the prognosis of PCa patients. However, they have some limitations. The rising serum PSA level after curable treatment, defined as biochemical recurrence (BCR), is unreliable for predicting PCa patient prognoses because some benign conditions can mimic BCR (4). For many men, BCR does not mean that they are at a high risk of death from PCa (4). GS and pTNM staging are limited by the subjective nature of their assessment, distant micrometastasis, and variations among patients with the same tumor stage or GS. Recently, immune infiltration has become a rapidly growing field of research to identify special immune cells and their relevant molecules for evaluating the prognosis of various cancers, such as gastric cancer, ovarian cancer, and melanoma (5–9). Some studies have reported PCa by estimating immune cell infiltration patterns (5, 9, 10). However, most of these studies focused on BCR (5, 10), which could limit the prediction power to identify PCa patients with poorer prognoses (4). These studies have provided the motivation and goal for further research exploring credible immune landscape-based prognostic predictors for patients with a high risk of death from PCa.

Progression-free survival (PFS) events were the recommended clinical outcome endpoints of The Cancer Genome Atlas Project (TCGA) database for PCa survival studies (11). It was defined as a new tumor event or death without new tumor events. Therefore, the prognostic predictor constructed using the PFS event would present higher predicted accuracy for identifying patients with an increased risk of death from PCa than those constructed using BCR. In view of this, we chose PFS as a clinical outcome endpoint to establish an immune landscape-based prognostic predictor and therapeutic target for PCa. By identifying patients with a high risk of death from PCa at an early stage, our outcomes would help reduce the mortality of PCa and improve the prognosis of patients.

METHODS

PCa Gene Expression Dataset

The gene expression data [counts and fragments per kilobase per million (FPKM)] of PCa tissues were downloaded from the TCGA database. FPKM data were transformed into transcripts per million (TPM) values following $\log_2 (x + 1)$ normalization. Count data were used for differentially expressed gene (DEG) analysis. The clinical data for PFS analysis were downloaded from TCGA Pan-Cancer Clinical Data Resource (TCGA-CDR) (11). The PFS analysis integrated TCGA pan-cancer clinical data resources and could drive high-quality survival outcome analytics. Finally, a total of 490 PCa patients from the TCGA cohort were included in the present study. Their clinical features are presented in **Table 1**. Patients with a PFS event were defined as those who had a new tumor event after RP, whether it was a progression of the disease, local recurrence, distant metastasis, new primary tumors at all sites, or died of cancer without a new tumor event, including cases with a new tumor event whose type was N/A (11).

Establishment of Immune Landscape-Based Risk Score

First, the immune score was calculated for each PCa tissue in the TCGA cohort using ESTIMATE (12). Then, PCa tissue samples were classified into two groups, the low immune score group and the high immune score group, according to the optimal cutoff value determined by X-tile 3.6.1 software (Yale University, New Haven, CT, USA). DEG analysis between these two groups was performed using the "EdgeR" package (13) using R software 4.0.5, and genes with $|\log_2$ fold change$| > 1$ and Benjamini–Hochberg-adjusted $p < 0.01$ were considered immune landscape-based DEGs (IL-DEGs). Subsequently, PFS analyses for these IL-DEGs *via* univariate Cox regression were performed using the Kaplan–Meier function in the R software 4.0.5 survival package. Statistical significance was set at $p < 0.05$. Finally, stepwise Cox regression was used to establish the immune landscape-based risk score (ILBRS) for PFS in patients with PCa. Moreover, a Kaplan–Meier curve was drawn to assess its predictive ability.

Identification of ILBRS-Relevant Cellular and Molecular Signatures

For the ILBRS-relevant cellular signature, CIBERSORT (14) was used to estimate the proportions of 22 immune cell types in each PCa tissue sample of patients in the TCGA-PRAD cohort. Then, PFS analysis, *t*-test, and Pearson correlation analysis were performed to evaluate the relationship between immune infiltration and ILBRS. For the ILBRS-relevant molecular signature, PCa tissue samples were reclassified into low ILBRS and high ILBRS groups according to the optimal cutoff value of ILBRS determined by X-tile 3.6.1 software (Yale University, New Haven, CT, USA) (15). Then, gene set enrichment analysis (GSEA) was performed between these two groups to identify the significantly enriched immune-relevant KEGG pathways (normal p (NP) < 0.01 and false discovery rate (FDR) < 0.05). Finally, single-sample GSEA (ssGSEA) was performed to estimate the enrichment score (ES) of KEGG pathways for each PCa tissue sample. Gene set variation analysis (GSVA), PFS analysis, and Pearson correlation analyses were performed to identify ILBRS-relevant molecular mechanisms and therapeutic targets.

Immunohistochemical Analysis

Samples of tissue microarray (TMA) were obtained from patients with PCa who underwent RP between January 2008 and

TABLE 1 | Clinical features for 490 PCa patients from the TCGA cohort.

Clinical features	Value
Age	Mean +/- standard error (SE): 60.99 +/- 0.309
Gleason score (6/7/8/9/10)	45/244/63/135/3 patients
Distant metastasis	6 patients
Death	4 patients
Death from PCa	2 patients
Patients with PFS event	89 patients
Prior treatment	Not mentioned
Radiation therapy (follow-up)	23 patients
Pharmaceutical therapy (follow-up)	23 patients
Radiation therapy (new tumor event)	24 patients
Pharmaceutical therapy (new tumor event)	22 patients

December 2018 at the Department of Urology of Shanghai Ninth People's Hospital, Shanghai Jiaotong University School of Medicine. All patients were informed of the importance of follow-up and were regularly followed up. Overall survival was defined as the time interval between surgery and the last follow-up (December 31, 2019) or death. Clinical information is shown in **Table S1**. All paraffin tissue sections obtained from the TMA were dewaxed and rehydrated. After antigen retrieval and blocking with bovine serum albumin (Sango Biotech, Shanghai, China), the slides were incubated with anti-VAV1 (1:50, Cat. #HPA001864, Sigma-Aldrich, St. Louis, MO, USA) overnight at 4°C. Then, they were incubated with a goat anti-rabbit horseradish peroxidase-conjugated secondary antibody (Cell Signaling Technology, Beverly, MA, USA) for 1 h at 25°C. DAB solution was used for brown color development. Quantification of immunohistochemical (IHC) staining was based on the staining intensity (I score: negative, 0; weak, 1; moderate, 2; and intense, 3) and the percentage of positively stained cells (P score: 0%–5%, a score of 0; 6%–35%, a score of 1; 36%–70%, a score of 2; and >70%, a score of 3). The final score was obtained by using the formula Q score = I score × P score. Samples with Q scores of ≥ 4 were considered highly expressed, while those with Q scores < 4 were considered to have low expression. IHC staining results were independently evaluated by at least two senior pathologists.

Nomogram Construction and Evaluation

We further used the coefficients of the multivariable Cox regression model to formulate a nomogram using the "rms" package (16) in R software 4.0.5. The 5-year calibration curves were assessed graphically by plotting the observed rates against the nomogram-predicted probabilities. A concordance index (C-index) was calculated using a bootstrap method with 1,000 resamples to determine the discrimination of the nomogram.

Statistical Analysis

Statistical analyses were performed using R software (version 4.0.5). The χ^2-test was used for risk assessment. Pearson's correlation analysis was performed to determine the correlation between the two variables. PFS analysis *via* the Kaplan–Meier method was performed using Log Rank (Mantel–Cox) to evaluate long-term PFS and Breslow (Generalized Wilcoxon) to evaluate short-term PFS. Statistical significance was set at $p < 0.05$.

RESULTS

Patients With High Immune Scores Had a Poorer PFS, Suggesting That Immune Landscape Affected PCa Prognosis

In this study, three major steps were performed to uncover the immune landscape-based prognostic signature for PCa: establishing ILBRS, determining the ILBRS-relevant underlying survival mechanism, and conducting the experimental verification of the ILBRS-relevant key molecule. A detailed strategy is shown in **Figure 1**. A total of 800 PCa data points were included in the present study. Expression data of genes were from the TCGA-PRAD cohort, and those of proteins were obtained from our cohort.

First, the immune score representing the immune landscape was calculated for 490 PCa tissues in the TCGA-PRAD cohort by ESTIMATE. This method used gene expression signatures to infer the fraction of immune cells and determined the immune score *via* ssGSEA (**Table S2**) (11). Then, X-tile software was used to choose the best cutoff value to divide these 490 PCa tissues into high and low immune score groups. As expected, the results of risk assessment and PFS analysis *via* the Kaplan–Meier method showed that patients with high immune scores had a higher risk for PFS events ($\chi^2 = 10.826$, $p = 0.001$, OR = 2.190, 95% CI = (1.364–3.518)) and poorer short-term and long-term PFS than patients with low immune scores (Log Rank [Mantel–Cox]: $\chi^2 = 10.461$, $p = 0.001$; Breslow (Generalized Wilcoxon): $\chi^2 = 12.199$, $p < 0.0001$; **Figure 2A**), indicating that immune score was a risk factor for PFS events and significantly affected the prognosis of PCa patients.

ILBRS, the Prognostic Signature for PFS of PCa Patients, Was Obtained

In order to establish the ILBRS to describe the immune landscape-based prognostic signature for PCa, four major steps were performed: identification of IL-DEGs, PFS analysis of IL-DEGs *via* the Kaplan–Meier method and univariate Cox regression, establishment of ILBRS *via* stepwise Cox regression multivariate analysis, and preliminary evaluation of ILBRS and the variables in its formula.

Gene expression differences were compared between the groups with high immune and low immune scores, and 1,907 IL-DEGs were identified. Of these, 934 were coding genes

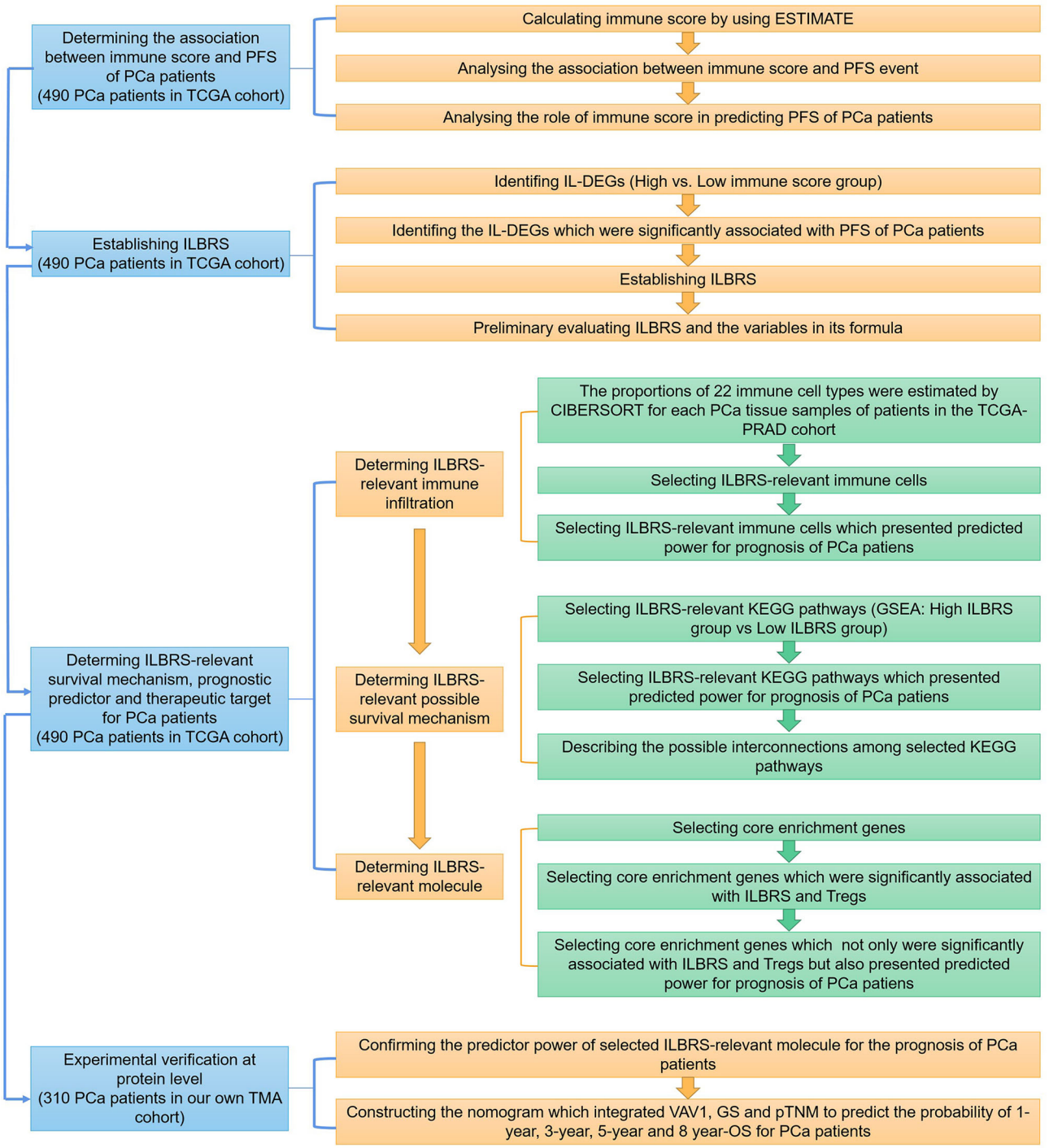

FIGURE 1 | The detailed strategy of discovering the immune landscape-based prognostic predictor and therapeutic target for prostate cancer.

(**Figure 2B**). After filtering low-abundance genes, the average expression level was lower than 0.01, and 415 IL-DEGs were selected for subsequent PFS analyses. The results of PFS analysis *via* univariate Cox regression showed that 137 IL-DEGs played a significant role in predicting PFS in PCa patients (**Table S3**). Among them, 135 IL-DEGs were chosen for further stepwise Cox regression multivariate analysis, which was used to screen the optimal combination and establish ILBRS (two IL-DEGs (*ALB* and *LCN2*) were excluded because of the opposite results of their DEGs analysis and PFS analysis). The results are presented in **Table 2**. ILBRS was established using five IL-DEGs including RELT TNF receptor (*RELT*), matrix metallopeptidase 11

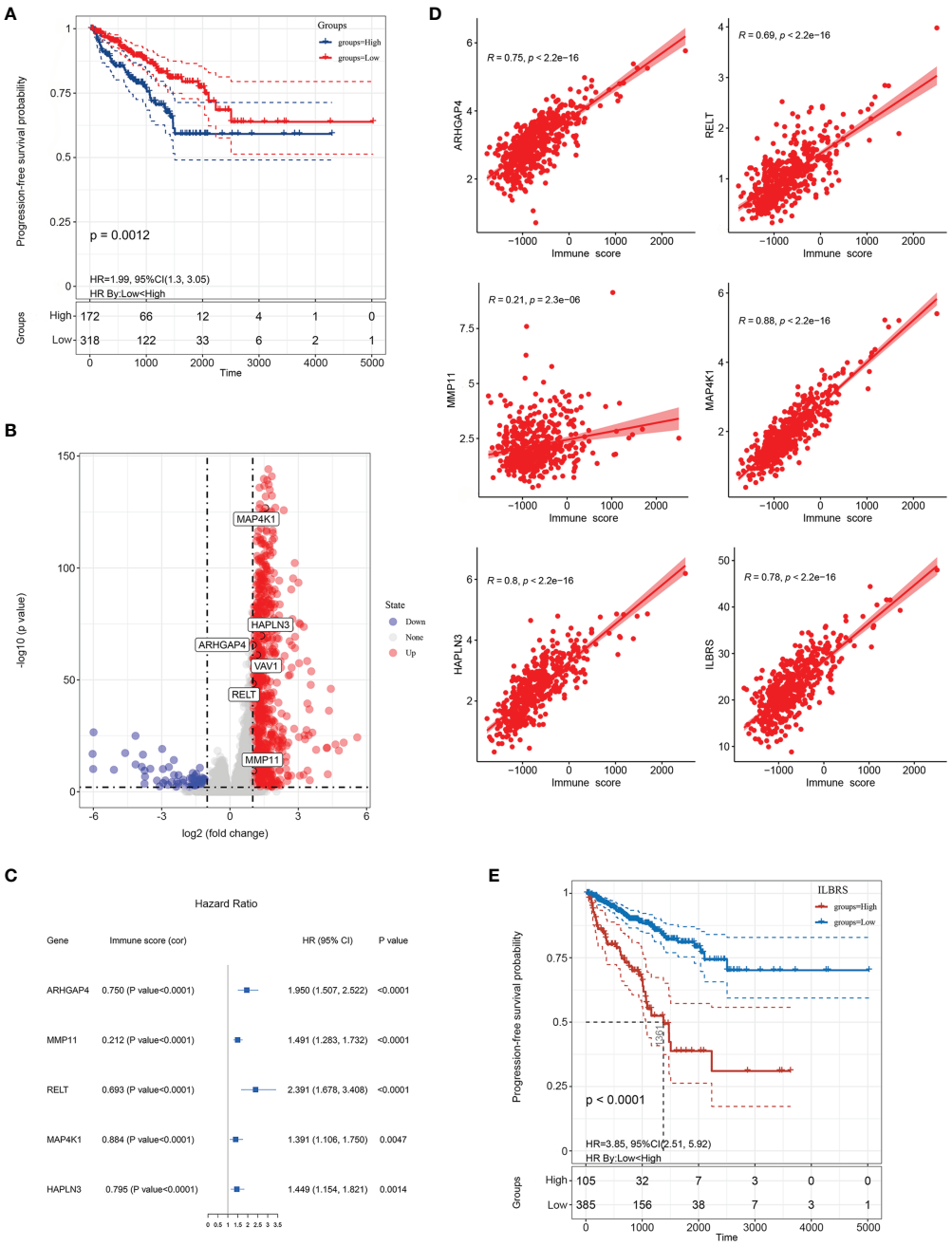

FIGURE 2 | Establishment of immune landscape-based risk score (ILBRS). **(A)** Kaplan–Meier curves for high and low immune score patient groups in TCGA-PRAD data. **(B)** Volcano plot of immune landscape-based DEGs (IL-DEGs). **(C)** Forest plot of the results of univariate Cox regression analyses of IL-DEGs included in the ILBRS formula. The square data markers indicate the estimated hazard ratios (HRs). Error bars represent 95% confidence intervals (CIs). "cor" indicates the coefficient gained through Pearson correlation analysis. **(D)** Pearson correlation analysis of ILBRS and its variables with immune scores. **(E)** Kaplan–Meier curves for high and low ILBRS patient groups in TCGA-PRAD data.

(*MMP11*), Rho GTPase activating protein 4 (*ARHGAP4*), mitogen-activated protein kinase 1 (*MAP4K1*), and hyaluronan and proteoglycan link protein 3 (*HAPLN3*) (Omnibus test: $p < 0.0001$). The formula for calculating ILBRS for each patient was as follows: ILBRS = (2.816 * expression level of *RELT*) + (1.318 * expression level of *MMP11*) + (4.774 * expression level of *ARHGAP4*) + (0.393 * expression level of *MAP4K1*) + (0.613 * expression level of *HAPLN3*). Preliminary evaluation of ILBRS and IL-DEGs in its formula was performed. As shown in **Figure 2C**, the expression of five IL-DEGs was upregulated significantly, increasing the immune score. Except for *MMP11*, all IL-DEGs and ILBRS exhibited a strong positive correlation

TABLE 2 | Immune landscape-based DEGs (IL-DEGs) included in the formula of the immune landscape-based risk score (ILBRS).

IL-DEGs	B	Standard deviation (SD)	*p*-value	Coefficient	95% Confidence interval (CI)	
					Upper limits	Lower limits
RELT	1.035	0.340	0.002	2.816	1.445	5.489
MMP11	0.276	0.090	0.002	1.318	1.105	1.573
ARHGAP4	1.563	0.335	0.000	4.774	2.475	9.209
MAP4K1	-0.934	0.283	0.001	0.393	0.226	0.685
HAPLN3	-0.490	0.220	0.026	0.613	0.398	0.944

with the immune score (**Figure 2D**). Then, the optimal cutoff value (26.9) chosen by the x-tile software was used to regroup the 490 patients in the TCGA-PRAD cohort into high and low ILBRS groups. As shown in **Figure 2E**, the patients with high ILBRS had poorer short-term and long-term PFS than those with low ILBRS (Log Rank [Mantel–Cox]: $\chi^2 = 44.085$, $p < 0.0001$; Breslow (Generalized Wilcoxon): $\chi^2 = 37.901$, $p < 0.0001$). These results suggest that ILBRS and the variables in its formula are robust immune landscape-based prognostic signatures for PFS in PCa patients.

VAV1, ILBRS-Relevant Predictor and Therapy Target for PFS of PCa Patients, Was Identified

The underlying ILBRS-relevant survival mechanisms and therapeutic targets were further explored at different levels. For analyses at the cellular level, the proportions of 22 immune cell types in each PCa tissue sample of patients in the TCGA-PRAD cohort were estimated by CIBERSORT. The results showed that 21 immune cell types were found in PCa tissues (**Table S4**). Naive B-cells, $CD8^+$ T cells, activated $CD4^+$ T cells (memory), Tregs, eosinophils, and mast cells significantly differed in their proportions in PCa tissues from patients with high ILBRS and low ILBRS. Infiltrations of naive B cells ($p < 0.0001$), $CD8^+$ T cells ($p = 0.002$), activated $CD4^+$ T cells (memory) ($p = 0.012$), and Tregs ($p < 0.0001$) in patients with high ILBRS were much higher than those in patients with low ILBRS, while infiltration of eosinophils ($p = 0.037$) and mast cells (resting) ($p < 0.0001$) in patients with high ILBRS were less than those in patients with low ILBRS (**Figure 3A**). B-cell-naive, $CD8^+$ T-cells, activated $CD4^+$ T-cells (memory), Tregs, eosinophils, and mast cells were also significantly correlated with ILBRS based on the results of Pearson correlation analyses (**Table S5**). Among them, naive B cells, $CD8^+$ T-cells, activated $CD4^+$ T-cells (memory), and eosinophils were shown to be significantly weakly correlated with ILBRS; Tregs (**Figure 3B**) and mast cells (resting) presented significant moderate correlations with ILBRS. Furthermore, the results of univariate Cox regression and Kaplan–Meier analysis showed that only Tregs were well predicted for PFS of PCa patients (**Table S5**); patients with a high proportion of Tregs had poorer short-term and long-term PFS than patients with a low proportion of Tregs (Log Rank [Mantel–Cox]: $\chi^2 = 8.092$, $p = 0.004$; Breslow (Generalized Wilcoxon): $\chi^2 = 12.079$, $p = 0.001$; **Figure 3C**). Above all, we speculated that Treg infiltration could be a key event in the ILBRS-relevant survival mechanism of PCa.

For analyses at the molecular level, two steps were performed. First, GSEA analysis was used to explore the ILBRS-relevant molecular mechanisms. The results showed that six immune-relevant KEGG pathways, including the B cell receptor signaling pathway, the chemokine signaling pathway, the FC epsilon RI signaling pathway, FC gamma R-mediated phagocytosis, natural killer cell-mediated cytotoxicity, and the cytosolic DNA sensing pathway, were significantly enriched between the high ILBRS group and the low ILBRS group (**Table S6**). All of them were upregulated in the tissues of PCa patients with high ILBRS (**Figure 3D**). The KEGG natural killer cell-mediated cytotoxicity was not included in the subsequent analyses because there was no difference in activated NK cell infiltration between the high and low ILBRS groups (**Figure 3A**). Analyses were performed based on ssGSEA, GSVA, and PFS to evaluate the association between the five immune-relevant KEGG pathways and PFS events. As shown in **Figures 3E–G**, the ES of FC gamma R-mediated phagocytosis was significantly increased not only in patients with PFS events but also in patients with poorer prognoses (Kaplan–Meier method: Log Rank (Mantel–Cox) $\chi^2 = 8.563$, $p = 0.003$; Breslow (Generalized Wilcoxon): $\chi^2 = 8.275$, $p = 0.004$). Although the five immune-relevant KEGG pathways were significantly associated with ILBRS, FC gamma R-mediated phagocytosis might contribute more to PCa survival.

Furthermore, KEGG and Venn plots were drawn to describe the possible interconnections among these five immune-relevant KEGG pathways. As shown in **Figures 3H, I**, not all of them were directly connected. Overlapping enrichment genes were common, which were proposed as the link among these five immune-relevant KEGG pathways and had the potential to be developed into ILBRS-relevant prognostic predictors and therapeutic targets for PCa patients. Therefore, a series of analyses focusing on overlapping core enrichment genes were performed. Based on the results of GSEA, 97 core enrichment genes from five immune-relevant KEGG pathways were selected for subsequent analyses (**Table S7**). Univariate Cox regression analysis revealed that 33 core enrichment genes, none of which belonged to the cytosolic DNA sensing pathway, were found to be significantly associated with PFS in PCa patients (**Table S8** and **Figure 4A**). Except for the cytosolic DNA sensing pathway, three core enrichment genes, including *VAV1*, *PIK3R5*, and *PIK3CD*, overlapped among four immune-relevant KEGG pathways (**Figure 4B**). Among them, *VAV1* was identified as the key molecule involved in the ILBRS-relevant survival mechanism due to its significant association with an immune score, ILBRS, Tregs, PFS event, and five immune-relevant KEGG pathways (**Figures 4C–E**). In addition, the results of Kaplan–Meier analysis showed that patients with high *VAV1* expression

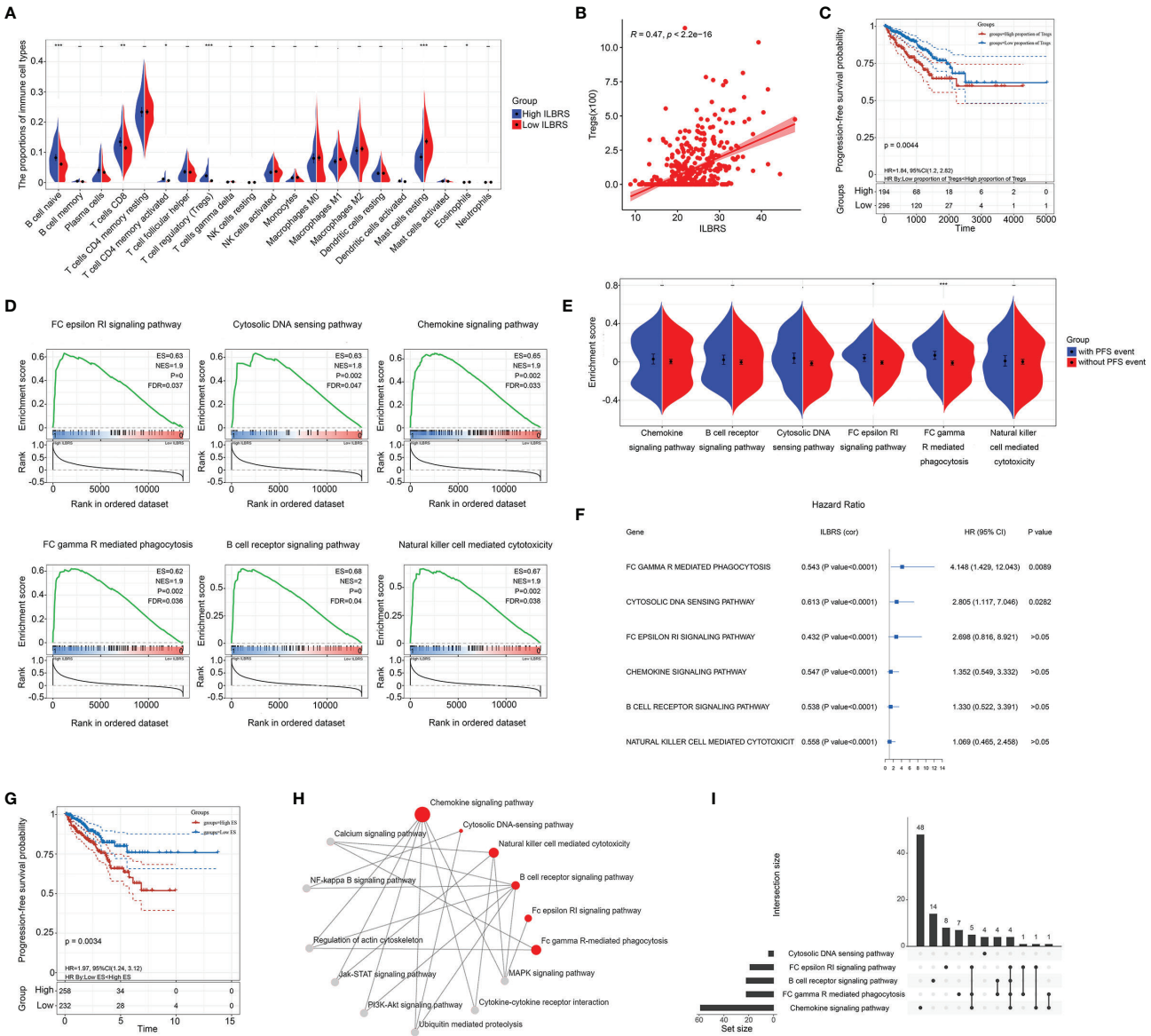

FIGURE 3 | ILBRS-relevant immune cell infiltration and immune-relevant KEGG pathways. **(A)** The proportions of 22 immune cell types in high and low ILBRS patient groups in TCGA-PRAD data. **(B)** Pearson correlation analysis of ILBRS and Tregs infiltration. **(C)** Kaplan–Meier curves for the PCa tissues from patients with high and low Tregs infiltration in TCGA-PRAD data. **(D)** KEGG pathway analyses show a notable pathway of the gene signature. **(E)** PFS event risk assessment for the ES of the immune-relevant KEGG pathways. **(F)** Forest plot of the results of univariate Cox regression analyses of the ES of the immune-relevant KEGG pathways. The square data markers indicate estimated hazard ratios (HR). The error bars represent 95% CIs. "cor" shows the coefficient gained through Pearson correlation analysis. **(G)** Kaplan–Meier curves for the PCa tissues from patients with high and low ES of FC gamma R-mediated phagocytosis in TCGA-PRAD data. **(H)** The immune-relevant KEGG pathway network. The red dots represent the six pathways. The gray dots are the intermediate pathways between two of the immune-relevant KEGG pathways. **(I)** Venn plot presenting overlapped genes among the immune-relevant KEGG pathways. *$p < 0.05$; **$p < 0.01$; ***$p < 0.0001$.

had poorer short-term and long-term PFS than those with low expression of *VAV1* (log-rank (Mantel–Cox): $\chi^2 = 6.685$, $p = 0.001$; Breslow (Generalized Wilcoxon): $\chi^2 = 6.67$, $p = 0.01$; **Figure 4F**). Taken together, due to the strong positive correlation with ILBRS, we proposed that *VAV1* could be used instead of ILBRS. Thus, we demonstrated an economical, convenient, and suitable prognostic predictor and therapy target for PCa patients.

Experimental Verification of VAV1 in PCa TMA

VAV1 is a member of the VAV family of genes. Its coded protein plays an important role in T-cell and B-cell development and activation. Therefore, further experimental verification at the protein level for VAV1 was performed using TMA, including 310 PCa tissue samples. The results showed that a higher expression of

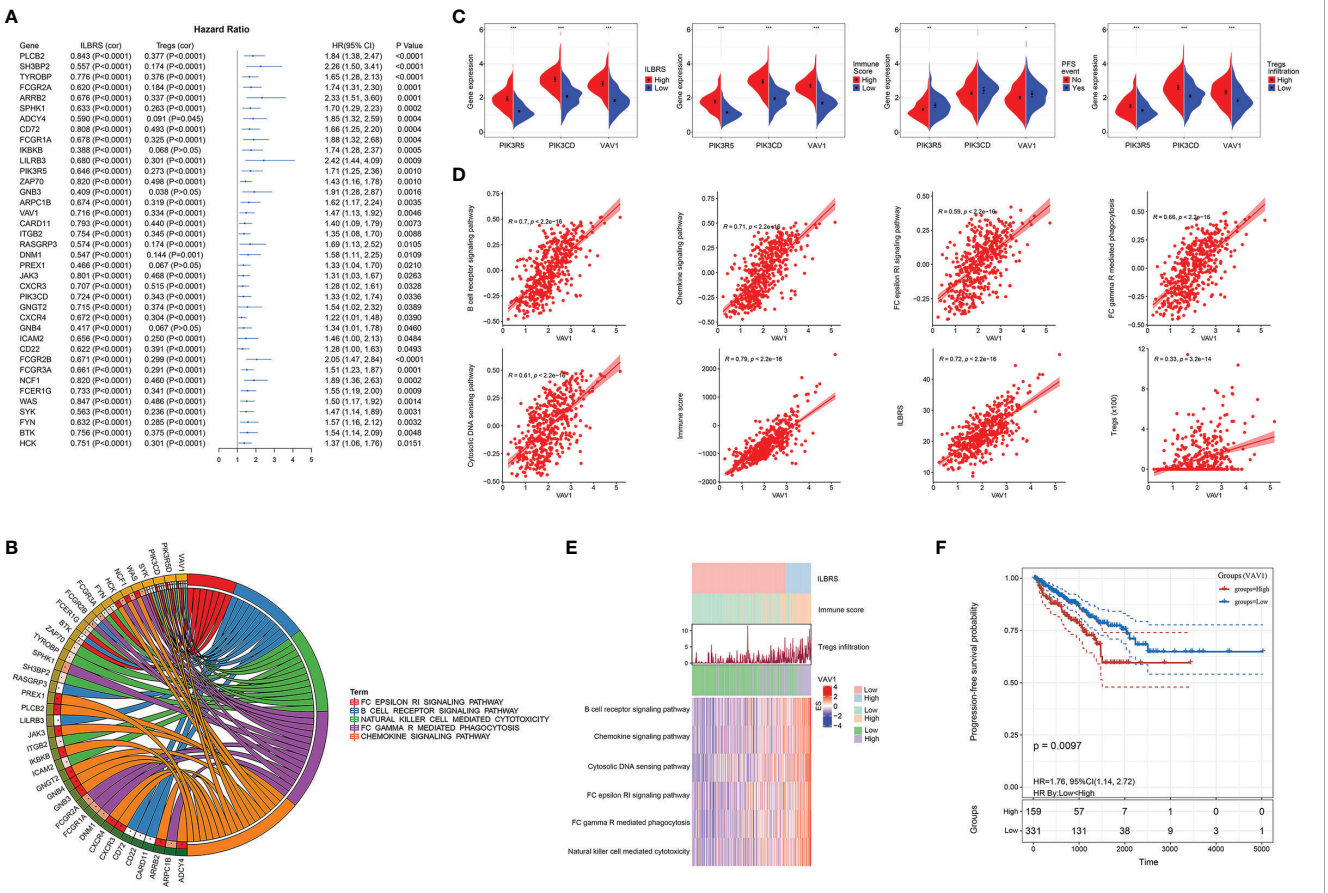

FIGURE 4 | Identification of *VAV1*, an ILBRS-relevant predictor and therapy target for PFS of PCa patients. **(A)** Forest plot of the results of univariate Cox regression analyses of the core enrichment genes of the immune-relevant KEGG pathways. The square data markers indicate estimated hazard ratios (HR). The error bars represented 95% CIs. "cor" indicates the coefficient gained through Pearson correlation analysis. **(B)** The core enrichment genes are associated with PFS of PCa patients in immune-relevant KEGG pathways. **(C)** Different expressions of *VAV1*, *PIK3CD*, and *PIK3R5* between PCa patients with high and low ILBRS, Tregs infiltration, and immune score, and between PCa patients with and without PFS event. **(D)** Pearson correlation analyses of *VAV1* with Tregs infiltration, ILBRS, immune score, and the immune-relevant KEGG pathways. **(E)** Heat map of the immune-relevant KEGG pathways. **(F)** Kaplan–Meier curves for the PCa tissues from patients with high and low expression of *VAV1* in TCGA-PRAD data. $^{*}p < 0.05$; $^{**}p < 0.01$; $^{***}p < 0.0001$.

VAV1 was significantly associated with GS ≥ 7 ($\chi^2 = 10.419, p = 0.001$, OR = 2.315, 95% CI = (1.382–3.887)), pT3–pT4 ($\chi^2 = 6.281, p = 0.012$, OR = 1.996, 95% CI = (1.157–3.444)), lymph node invasion (N1) ($\chi^2 = 8.536$, $p = 0.003$, OR = 11.607, 95% CI = (1.480–91.038)), and nerve invasion ($\chi^2 = 13.929, p < 0.0001$, OR = 2.446, 95% CI = (1.522–3.932)) (**Figure 5A**), indicating that VAV1 expression might affect cell invasiveness. Furthermore, Kaplan–Meier analysis was performed, and the results showed that patients with high VAV1 expression had poorer short-term and long-term overall survival (OS) than those with low VAV1 expression (log rank (Mantel–Cox): $\chi^2 = 17.328, p < 0.0001$; Breslow (Generalized Wilcoxon): $\chi^2 = 13.227$, $p < 0.0001$; **Figure 5B**). Together, these results verified the stability and reliability of VAV1 for predicting the prognosis of PCa patients, which further suggested that it may be developed as a potential therapeutic target for PCa patients with poor prognoses.

In addition, based on multivariate Cox analysis, the 310 samples were also used to construct a nomogram that integrated VAV1, GS, and pTNM to predict the probability of 3- and 5-year OS for PCa patients (**Figure 5C**). The C-index of the predicted model was 0.829. The predictive power of the nomogram model was evaluated and quantified by measuring the degree of fit between the C-index and baseline time predicted by the nomogram in the standard curve. As shown in the calibration curve shown in **Figure 5D**, the nomogram model presented well the predicting value of the 5-year OS of PCa patients.

DISCUSSION

In recent years, the incidence of PCa has increased. Although there are some curative therapeutic methods, the recurrence rate remains high. However, salvage at an early stage of recurrence can improve PCa prognoses. Therefore, the prediction of recurrence has attracted increasing attention. There are some prediction methods in clinical practice, such as the serum PSA test, GS, and pTNM staging, but limitations exist. After curative

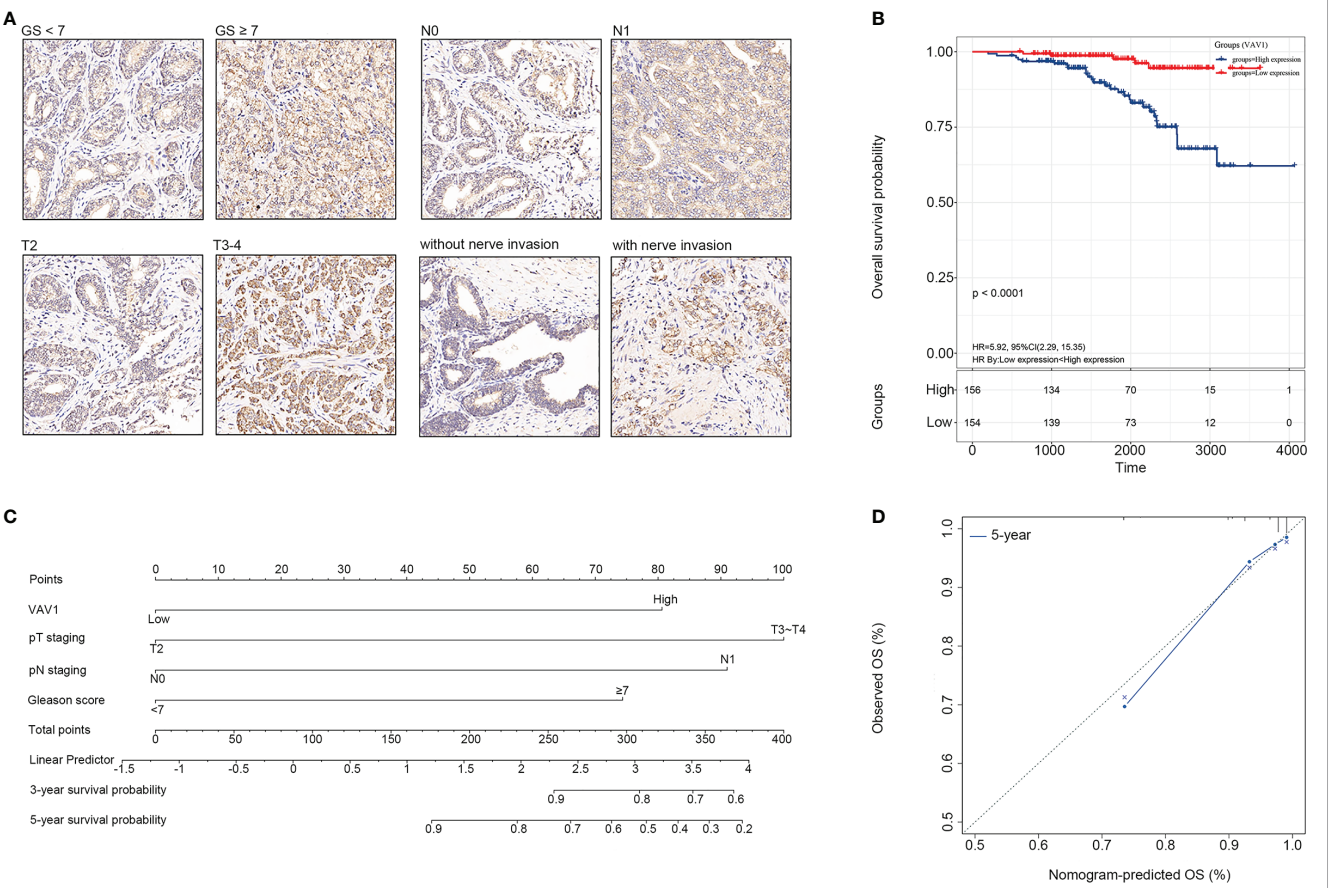

FIGURE 5 | Experimental verification of VAV1 in PCa tissue microarray (TMA). **(A)** The protein expression and localization of VAV1 in PCa TMA. **(B)** Kaplan–Meier curves for the PCa tissues from patients with high and low expression of VAV1 in TMA data. **(C)** Nomogram integrating VAV1, GS, and pTNM to predict the probability of 3- and 5-year OS for PCa patients in TMA data. **(D)** The calibration curve shows that the nomogram model has a better predictive effect on the 5-year OS of PCa patients in TMA data.

treatment, BCR is diagnosed when the serum PSA level rises. However, this does not mean that patients with elevated PSA are at a high risk of death from PCa in the longer term because BCR can be mimicked by some benign conditions (4).

In contrast, GS and pTNM staging are deemed more credible for prognostic risk assessment. However, they depend on pathological examinations, are subjected to subjective judgment, and cannot identify distant micro-metastases. In addition, given the heterogeneous nature of PCa, patients with the same GS and pTNM staging may have different prognoses after receiving the same treatment (17, 18). Thus, a satisfactory prognostic predictor beyond the current risk assessment system is desired to accurately identify patients likely to have poor prognoses, followed by better guide management after curative therapy such as RP (19–21). Recently, some studies indicated that the role of immune cell infiltration and their relevant molecules in evaluating the prognosis of PCa could not be ignored (5, 9, 10). However, the study by Rui lacked experimental validation at the protein level and dismissed patients with recurrences caused by focal residual (9); the studies by Shao (5) and Liu (10) focused on BCR, by which the constructed predictor models would have limited predictive power to identify PCa patients with poorer prognoses (4). Therefore, in the present study, we used well-established TCGA-PRAD cohort data to delineate the immune landscape-based prognostic signature for PCa patients and explore its relevant underlying survival mechanism, predictors, and therapeutic targets through analyses at the cellular and molecular levels. Furthermore, experimental verification was performed to prove our outcome's stability and reliability at the protein level using TMA data from 310 PCa patients.

Immune scores were calculated for each sample in the TCGA-PRAD cohort, based on which ILBRS was established as the prognostic signature for PFS in PCa patients. The formula contained five genes, *RELT*, *MMP11*, *ARHGAP4*, *MAP4K1*, and *HAPLN3*. Except for *MMP11*, all of them presented a strong positive correlation with the immune score. To our knowledge, only MMP11 and HAPLN3 have been reported as possible diagnostic biomarkers or prognostic predictors for PCa (22–25). There is no research on the roles of ARHGAP4 and HAOPLN3 in PCa, but the existing evidence indicates that their functions in tumor recurrence and metastases should not be ignored. ARHGAP4 has been reported to play an important role in regulating cell migration and invasion in pancreatic

cancer (26). MAP4K1 could inhibit T cell function and has been proposed as a promising target for cancer immunotherapy (27, 28). RELT is a member of the TNFR superfamily and is primarily expressed in immune cells and lymphoid tissues. Its immunological function is not well defined, and no relevant study describes its association with malignancy. However, Choi et al. proposed that RELT could act as a negative regulator that controls the early phase of T-cell activation, probably by promoting T-cell apoptosis (29). Therefore, we speculated that RELT might play a role in tumor immunosuppression in PCa. Considered together, ILBSR reflects the immune features of cellular migration, invasion, and tumor immunosuppression.

Cellular and molecular analyses were performed to explore the ILBSR-relevant underlying survival mechanism, prognostic predictor, and therapeutic target for PCa patients. Tregs are immunosuppressive cells that play an important role in tumor immune escape (30). As expected, we noticed that high infiltration was significantly associated with poor prognosis in PCa patients, consistent with Liu et al. (10). In addition, five immune-relevant KEGG pathways and their common core enrichment gene *VAV1* were identified. *VAV1* is a member of the VAV family of genes. Previous studies have shown that VAV1 could promote T cell transformation into Tregs, while Tregs could also indirectly induce macrophage VAV1 which enhances the efferocytosis of macrophages, leading to tumor immune escape (31). Our study found that *VAV1* was a key link connecting Tregs and five immune-relevant KEGG pathways and revealed the features of tumor invasion and immunosuppression. *VAV1* was positively correlated with immune scores, ILBRS, Treg infiltration, and five immune-relevant KEGG pathways, and both it and its coded protein presented significant predictive power for the prognosis of PCa patients. Moreover, VAV1 was significantly associated with GS, pathological T staging, lymph node invasion (pathological N staging), and nerve invasion at the protein level, indicating its effect on tumor cell invasiveness. Taken together, we propose that by combining with Tregs, VAV1 might play an important immunosuppressive role in ILBRS-related survival mechanisms and could be more economical, convenient, and suitable as a prognostic predictor and therapy target for PCa patients.

Finally, to provide clinicians with a quantitative approach for predicting PCa patients' prognosis, a nomogram that integrated VAV1, GS, pathological T staging, and pathological N staging was constructed. The nomogram was more accurate for predicting short-term and long-term survival in PCa patients than individual prognostic factors.

Although VAV1 has been reported as a predictor for the prognosis of some malignancies (32), its role in PCa survival remains unclear. To our knowledge, our study is the first to report the feasibility and accuracy of VAV1 for determining PCa prognosis. Moreover, given the immune landscape, we propose that VAV1 is the key molecule involved in ILBRS-relevant survival mechanisms, indicating its potential as an immune therapeutic target for PCa patients with poor prognoses. However, this study has several limitations. First, OS is an important clinical outcome endpoint for survival studies, with the advantage that there is minimal ambiguity in defining an OS event. At the same time, it is not recommended for PCa survival studies using the TCGA cohort, where there are only 10 OS events out of 500 cases (11). Therefore, in this study using the TCGA database, PFS was chosen as a substitute for OS to establish ILBRS and identify its relevant key molecule. Although the results of experimental verification using our TMA cohort confirmed the predictive power of VAV1 at the protein level for OS of PCa patients, unpredictable biases may still exist. Second, the biological mechanisms of VAV1 and Tregs involved in the survival mechanism of PCa remain elusive. Further in-depth investigations into their functions should be performed in the future.

In conclusion, VAV1 was identified as a key molecule involved in the underlying immune-relevant survival mechanism in this study. This finding indicates that VAV1 could be an immune landscape-based prognostic predictor and therapeutic target for PCa patients in the future.

DATA AVAILABILITY STATEMENT

The original contributions presented in the study are included in the article/**Supplementary Material**. Further inquiries can be directed to the corresponding authors.

ETHICS STATEMENT

The studies involving human participants were reviewed and approved by the Ethics Committee of Shanghai Ninth People's Hospital. The patients/participants provided their written informed consent to participate in this study.

AUTHOR CONTRIBUTIONS

ZW and MZ had full access to all of the data in the study and take responsibility for the integrity of the data, the accuracy of the data analysis, and the critical revision of the manuscript for important intellectual content. YS and HX took responsibility for the concept, design, data analysis, and paper written. ML took responsibility for the sample collection, TMA preparation, and pathological diagnosis. ML, MG, and PL took responsibility for the immunohistochemistry and evaluation of immunostaining. All authors contributed to the article and approved the submitted version.

FUNDING

This work was supported by the National Science Foundation of China (Nos. 81970656 and 62101319).

SUPPLEMENTARY MATERIAL

The Supplementary Material for this article can be found online at: https://www.frontiersin.org/articles/10.3389/fonc.2021.761643/full#supplementary-material.

REFERENCES

1. Carlsson SV, Vickers AJ. Screening for Prostate Cancer. *Med Clin North Am* (2020) 104:1051–62. doi: 10.1016/j.mcna.2020.08.007
2. McCammack KC, Raman SS, Margolis DJ. Imaging of Local Recurrence in Prostate Cancer. *Future Oncol* (2016) 12:2401–15. doi: 10.2217/fon-2016-0122
3. Rans K, Berghen C, Joniau S, De Meerleer G. Salvage Radiotherapy for Prostate Cancer. *Clin Oncol (R Coll Radiol)* (2020) 32:156–62. doi: 10.1016/j.clon.2020.01.003
4. Van den Broeck T, van den Bergh RCN, Arfi N, Gross T, Moris L, Briers E, et al. Prognostic Value of Biochemical Recurrence Following Treatment With Curative Intent for Prostate Cancer: A Systematic Review. *Eur Urol* (2019) 75:967–87. doi: 10.1016/j.eururo.2018.10.011
5. Shao N, Tang H, Mi Y, Zhu Y, Wan F, Ye D. A Novel Gene Signature to Predict Immune Infiltration and Outcome in Patients With Prostate Cancer. *Oncoimmunology* (2020) 9:1762473. doi: 10.1080/2162402X.2020.1762473
6. Cai WY, Dong ZN, Fu XT, Lin LY, Wang L, Ye GD, et al. Identification of a Tumor Microenvironment-Relevant Gene Set-Based Prognostic Signature and Related Therapy Targets in Gastric Cancer. *Theranostics* (2020) 10:8633–47. doi: 10.7150/thno.47938
7. Shen S, Wang G, Zhang R, Zhao Y, Yu H, Wei Y, et al. Development and Validation of an Immune Gene-Set Based Prognostic Signature in Ovarian Cancer. *EBioMedicine* (2019) 40:318–26. doi: 10.1016/j.ebiom.2018.12.054
8. Huang R, Mao M, Lu Y. A Novel Immune-Related Genes Prognosis Biomarker for Melanoma: Associated With Tumor Microenvironment. *Aging (Albany NY)* (2020) 12:6966–80. doi: 10.18632/aging.103054
9. Rui X, Shao S, Wang L, Leng J. Identification of Recurrence Marker Associated With Immune Infiltration in Prostate Cancer With Radical Resection and Build Prognostic Nomogram. *BMC Cancer* (2019) 19:1179. doi: 10.1186/s12885-019-6391-9
10. Liu Z, Zhong J, Cai C, Lu J, Wu W, Zeng G. Immune-Related Biomarker Risk Score Predicts Prognosis in Prostate Cancer. *Aging (Albany NY)* (2020) 12 (22):22776–93. doi: 10.18632/aging.103921
11. Liu J, Lichtenberg T, Hoadley KA, Poisson LM, Lazar AJ, Cherniack AD, et al. An Integrated TCGA Pan-Cancer Clinical Data Resource to Drive High-Quality Survival Outcome Analytics. *Cell* (2018) 173:400–16. doi: 10.1016/j.cell.2018.02.052
12. Yoshihara K, Shahmoradgoli M, Martínez E, Vegesna R, Kim H, Torres-Garcia W. Inferring Tumour Purity and Stromal and Immune Cell Admixture From Expression Data. *Nat Commun* (2013) 4:2612. doi: 10.1038/ncomms3612
13. Robinson MD, McCarthy DJ, Smyth GK. Edger: A Bioconductor Package for Differential Expression Analysis of Digital Gene Expression Data. *Bioinformatics* (2010) 26:139–40. doi: 10.1093/bioinformatics/btp616
14. Newman AM, Liu CL, Green MR, Gentles AJ, Feng W, Xu Y, et al. Robust Enumeration of Cell Subsets From Tissue Expression Profiles. *Nat Methods* (2015) 12(5):453–7. doi: 10.1038/nmeth.3337
15. Camp RL, Dolled-Filhart M, Rimm DL. X-Tile: A New Bio-Informatics Tool for Biomarker Assessment and Outcome-Based Cut-Point Optimization. *Clin Cancer Res* (2004) 10:7252–9. doi: 10.1158/1078-0432.CCR-04-0713
16. Jiang W, Guo Q, Wang C, Zhu Y. A Nomogram Based on 9-lncRNAs Signature for Improving Prognostic Prediction of Clear Cell Renal Cell Carcinoma. *Cancer Cell Int* (2019) 19:208. doi: 10.1186/s12935-019-0928-5
17. Scher HI, Fizazi K, Saad F, Taplin ME, Sternberg CN, Miller K, et al. Increased Survival With Enzalutamide in Prostate Cancer After Chemotherapy. *N Engl J Med* (2012) 367:1187–97. doi: 10.1056/NEJMoa1207506
18. Hansen J, Bianchi M, Sun M, Rink M, Castiglione F, Abdollah F, et al. Percentage of High-Grade Tumour Volume Does Not Meaningfully Improve Prediction of Early Biochemical Recurrence After Radical Prostatectomy Compared With Gleason Score. *BJU Int* (2014) 113:399–407. doi: 10.1111/bju.12424
19. Intasqui P, Bertolla RP, Sadi MV. Prostate Cancer Proteomics: Clinically Useful Protein Biomarkers and Future Perspectives. *Expert Rev Proteomics* (2018) 15:65–79. doi: 10.1080/14789450.2018.1417846
20. Kruck S, Bedke J, Kuczyk MA, Merseburger AS. Second-Line Systemic Therapy for the Treatment of Metastatic Renal Cell Cancer. *Expert Rev Anticancer Ther* (2012) 12:777–85. doi: 10.1586/era.12.43
21. Roobol MJ, Carlsson SV. Risk Stratification in Prostate Cancer Screening. *Nat Rev Urol* (2013) 10:38–48. doi: 10.1038/nrurol.2012.225
22. Eiro N, Fernandez-Gomez J, Sacristán R, Fernandez-Garcia B, Lobo B, Gonzalez-Suarez J, et al. Stromal Factors Involved in Human Prostate Cancer Development, Progression and Castration Resistance. *J Cancer Res Clin Oncol* (2017) 143:351–9. doi: 10.1007/s00432-016-2284-3
23. Wu X, Lv D, Eftekhar M, Khan A, Cai C, Zhao Z, et al. A New Risk Stratification System of Prostate Cancer to Identify High-Risk Biochemical Recurrence Patients. *Transl Androl Urol* (2020) 296:2572–86. doi: 10.21037/tau-20-1019
24. Patel PG, Wessel T, Kawashima A, Okello JBA, Jamaspishvili T, Guérard KP, et al. A Three-Gene DNA Methylation Biomarker Accurately Classifies Early Stage Prostate Cancer. *Prostate* (2019) 79:1705–14. doi: 10.1002/pros.23895
25. Strand SH, Orntoft TF, Sorensen KD. Prognostic DNA Methylation Markers for Prostate Cancer. *Int J Mol Sci* (2014) 15:16544–76. doi: 10.3390/ijms150916544
26. Shen Y, Xu L, Ning Z, Liu L, Lin J, Chen H, et al. ARHGAP4 Regulates the Cell Migration and Invasion of Pancreatic Cancer by the HDAC2/β-Catenin Signaling Pathway. *Carcinogenesis* (2019) 40:1405–14. doi: 10.1093/carcin/bgz067
27. Si J, Shi X, Sun S, Zou B, Li Y, An D, et al. Hematopoietic Progenitor Kinase1 (HPK1) Mediates T Cell Dysfunction and Is a Druggable Target for T Cell-Based Immunotherapies. *Cancer Cell* (2020) 38:551–66.e11. doi: 10.1016/j.ccell.2020.08.001
28. You D, Hillerman S, Locke G, Chaudhry C, Stromko C, Murtaza A, et al. Enhanced Antitumor Immunity by a Novel Small Molecule HPK1 Inhibitor. *J Immunother Cancer* (2021) 9:e001402. doi: 10.1136/jitc-2020-001402
29. Choi BK, Kim SH, Kim YH, Lee DG, Oh HS, Han C, et al. RELT Negatively Regulates the Early Phase of the T-Cell Response in Mice. *Eur J Immunol* (2018) 48:1739–49. doi: 10.1002/eji.201847633
30. Zheng Y, Chen Z, Han Y, Han L, Zou X, Zhou B, et al. Immune Suppressive Landscape in the Human Esophageal Squamous Cell Carcinoma Microenvironment. *Nat Commun* (2020) 11(1):6268. doi: 10.1038/s41467-020-20019-0
31. Proto JD, Doran AC, Gusarova G, Yurdagul AJ, Sozen E, Subramanian M, et al. Regulatory T Cells Promote Macrophage Efferocytosis During Inflammation Resolution. *Immunity* (2018) 49:666–677.e6. doi: 10.1016/j.immuni.2018.07.015
32. Kang L, Hao X, Tang Y, Zhao Z, Zhang H, Gong Y. Elevated Level of Vav1 was Correlated With Advanced Biological Behavior and Poor Prognosis in Patients With Gastric Cancer. *Int J Clin Exp Pathol* (2018) 11:391–8.

Conflict of Interest: The authors declare that the research was conducted in the absence of any commercial or financial relationships that could be construed as a potential conflict of interest.

The reviewer BD declared a shared affiliation, with no collaboration, with the authors to the handling editor at the time of review.

frontiers in Oncology

ORIGINAL RESEARCH
published: 19 November 2021
doi: 10.3389/fonc.2021.778989

Development of Siglec-9 Blocking Antibody to Enhance Anti-Tumor Immunity

Hyeree Choi‡, Michelle Ho‡, Opeyemi S. Adeniji, Leila Giron, Devivasha Bordoloi, Abhijeet J. Kulkarni, Alfredo Perales Puchalt, Mohamed Abdel-Mohsen and Kar Muthumani*†*

Vaccine & Immunotherapy Center, The Wistar Institute, Philadelphia, PA, United States

OPEN ACCESS

Edited by:
Shashwat Sharad, Center for Prostate Disease Research (CPDR), United States

Reviewed by:
Maria Helena Ornellas, Universidade Estadual do Rio de Janeiro, Brazil
Aleksandr Shulyak, National Academy of Medical Sciences of Ukraine, Ukraine

***Correspondence:**
Mohamed Abdel-Mohsen
mmohsen@wistar.org
Kar Muthumani
kmuthumani@gmail.com

†Present address:
Kar Muthumani, Research and Development, GeneOne Life Science Inc, Seoul, South Korea

‡*These authors have contributed equally to this work*

Specialty section:
This article was submitted to Genitourinary Oncology, a section of the journal Frontiers in Oncology

Received: *17 September 2021*
Accepted: *18 October 2021*
Published: *19 November 2021*

Citation:
Choi H, Ho M, Adeniji OS, Giron L, Bordoloi D, Kulkarni AJ, Puchalt AP, Abdel-Mohsen M and Muthumani K (2021) Development of Siglec-9 Blocking Antibody to Enhance Anti-Tumor Immunity. Front. Oncol. 11:778989. doi: 10.3389/fonc.2021.778989

Sialic acid-binding Immunoglobulin-like lectin-9 (Siglec-9) is a glyco-immune negative checkpoint expressed on several immune cells. Siglec-9 exerts its inhibitory effects by binding to sialoglycan ligands expressed on cancer cells, enabling them to evade immunosurveillance. We developed a panel of human anti-Siglec-9 hybridoma clones by immunizing mice with Siglec-9-encoding DNA and Siglec-9 protein. The lead antibodies, with high specificity and functionality against Siglec-9, were identified through screening of clones. The *in vitro* cytotoxicity assays showed that our lead antibody enhances anti-tumor immune activity. Further, *in vivo* testing utilizing ovarian cancer humanized mouse model showed a drastic reduction in tumor volume. Together, we developed novel antibodies that augment anti-tumor immunity through interference with Siglec-9-mediated immunosuppression.

Keywords: human Siglec 9, NK cell, monoclonal antibodies, ovarian cancer, immunotherapy

INTRODUCTION

Immune checkpoints are conventionally responsible for preventing unregulated immune responses to ensure limited collateral damage to surrounding cells (1–5). However, cancer cells can engage these immune checkpoints on immune cells to render them inactive/anergic, ensuring self-survival and growth (4). Thus, one important approach of cancer immunotherapy is the usage of immune checkpoint inhibitors [including monoclonal antibodies (mAbs)] with the ability to block the immuno-regulatory interactions between tumor and immune cells (4, 6, 7).

One emerging class of immune checkpoints is Sialic acid-binding Immunoglobulin-like lectin (Siglec) receptors, which are single-pass transmembrane I-type lectins present on hematopoietic cells (5, 8–10). Siglecs are key immunomodulatory receptors expressed by several types of immune cells, such as eosinophils, neutrophils, macrophages, natural killer (NK) cells, dendritic cells, B cells, and T lymphocytes (11). Siglecs facilitate activation and inhibition of immune responses through immunoreceptor tyrosine-based inhibitory motifs by interactions with sialogylcans on cancer cells (5, 11). The expression of sialoglycans on tumor cells surfaces facilitates tumor survival as well as growth by preventing recognition during immunosurveillance (12, 13).

Among Siglecs, Siglec-9 is expressed on myeloid cells, NK cells, and a subset of T cells (7, 14–23) and can bind to sialoglycans (on cancer cells), resulting in inhibiting anti-tumor immune responses (7, 17, 24). For instance, Siglec-9 expression on NK cells can inhibit anti-tumor immunity (17).

Siglec-9 is also expressed on a subset of CD8+ T cells in the tumor microenvironment (7), and its interactions with sialic acid inhibit CD8+ T cell functionality (7). Finally, Siglec-E (the mice homolog of Siglec-9) on mice neutrophils and tumor-associated macrophages promotes cancer cell metastasis, induces apoptosis of neutrophils, and aids in the formation of a pro-tumorigenic phenotype of macrophages (25).

Owing to the important immunomodulatory roles of Siglec-9 in the tumor microenvironment, it has gained attention as a target to achieve enhanced anti-tumor immunity. Siglec-sialic acid interactions are important immune negative checkpoints against autoimmunity (26–29), and several Siglec members share high homology (9). Therefore, the success of targeting Siglec-9 as a potential immunotherapy approach hinges on the availability of highly specific antibodies to Siglec-9. In this study, we generated and characterized monoclonal blocking antibodies against human Siglec-9 with anti-tumor activities *in vitro* and *in vivo*.

RESULTS

Generation, Expansion, and Binding Characterization of Human Siglec-9 mAbs

Mice were immunized with human Siglec-9 to generate a humoral immune response. Spleen from the immunized mice was harvested and used for the development of hybridomas expressing anti-human Siglec-9 antibodies. Following the intramuscular injection of mice with an expression vector containing DNA for human Siglec-9, a strong humoral immune response was noted, and antibodies to human Siglec-9 were observed in the sera of all mice. The antibody reaction became more substantial, and the polyclonal antibody titer against human Siglec-9 remained high after subsequent injections. Hybridomas were incubated for 2-3 weeks after fusion with 2P2/0 mouse myeloma cells. A total of 1152 mAb clones (hybridoma supernatants) were screened for anti-human Siglec-9 binding activity by ELISA (data not shown). An additional flow cytometry-based screening test called IntelliCyt FACS analysis was performed on the top 50 candidates from the ELISA screening. Briefly, Siglec-9-GFP overexpressing K562 cells were stained with primary test hybridoma supernatants followed by secondary APC-conjugated anti-mouse antibodies and analyzed by IntelliCyt iQue screener PLUS based FACS analysis. Gating was done for double-positive cells (GFP^+ and APC^+ staining) and top 20 candidates that conferred high hits, 17 intermediate from Intellicyte screenings high % double positive hybridoma clones (**Figure 1A**). We again performed an ELISA assay for the top 20 anti-Siglec 9 mAbs from the IntelliCyt iQue screener PLUS-based FACS analysis at 1:50 dilution to further confirmed binding (strong binding = OD>0.6 at 450nM) (**Figure 1B**). **Figure 1C** shows tertiary hybridoma screening for the best ten clones, which were analyzed by serial dilutions of hybridoma supernatant by ELISA with recombinant human Siglec 9 protein. We included negative and positive control wells to confirm the results of primary and secondary screening and rule out the cross-reactivity and specificity. A high level of binding was achieved for the 8A1E9 clone, and we expanded further characterization of this clone. Based on this analysis of high binding capacity to human siglec-9, the selected 8A1E9 clone was moved onto the large-scale amplification/expansion for further characterization.

Recombinant Antibody Expression in HEK293 Cells and Functional Characterization

We adopted the HEK293 mammalian cell line grown at high densities in suspension and was used for recombinant antibody expression. The antibody cloning method represents a simple two-step protocol with complete design flexibility. Antibody sequence (VH and VL) encoding clone 8A1E9 nucleotide sequences were optimized for humans and then was cloned into optimized human IgG1 and then constructed in pCDNA3.4 expression vector for recombinant production. The purity and apparent molecular weight of purified antibodies were assessed by SDS-PAGE analysis. The molecular sizes corresponding to the heavy chains (HC) (50-60 kDa) and light chains (LC) (25 kDa) suggested that the secreted antibodies are properly folded (**Figure 2A**). **Figure 2B** depicts recombinant expressed antibody (clone-8A1E9) binding to recombinant human Siglec-9 protein as measured by ELISA. Further, ELISA analysis was carried out to determine the specificity of recombinant anti-Siglec-9 against recombinant human Siglec-3, Siglec-7, and Siglec-9 antigens. Anti-Siglec 9 only exhibited significant binding and showed specificity to recombinant human Siglec-9 protein, whereas no binding was detected with recombinant Siglec-3 or Siglec-7 proteins (**Figure 2C**).

Next, we assessed the functional characteristics of the recombinantly expressed anti-Siglec-9 (8A1E9) antibody. Indirect ELISA was used to determine potential epitope(s) for anti-Siglec-9 antibody binding. In this assay, 20-mer peptides were generated against human Siglec 9 protein, and commercially available anti-Siglec-9 antibody was used as antigens to identify the epitope. Data from the analysis show that the recombinantly expressed antibody (clone-8A1E9) binds strongly to peptide # 5 and moderately to peptide # 7 (**Figure 2D**). No overlap between epitopes for the antibody (clone-8A1E9) and commercial anti-human Siglec-9 antibody was observed.

Anti-Siglec-9 Antibody Enhances Human NK Degranulation

To evaluate the effects of the anti-Siglec-9 (clone -8A1E9) on NK cell degranulation, Siglec-9 ligands expression on the tumor cell lines were used in the study was tested to mitigate the validity of the specificity of anti-Siglec-9 mAb generated. Therefore, cell surface Siglec-9 ligand expression was characterized on ovarian cancer cell line SKOV3 and human leukemia cell line K562 cells. SKOV3 or K562 cells were incubated with varying amounts of recombinant human Siglec-9 Fc protein. The binding of Siglec-9 Fc to cells was measured using an anti-human Fc fluorescent secondary antibody (**Figure 3A**). Removing these ligands using

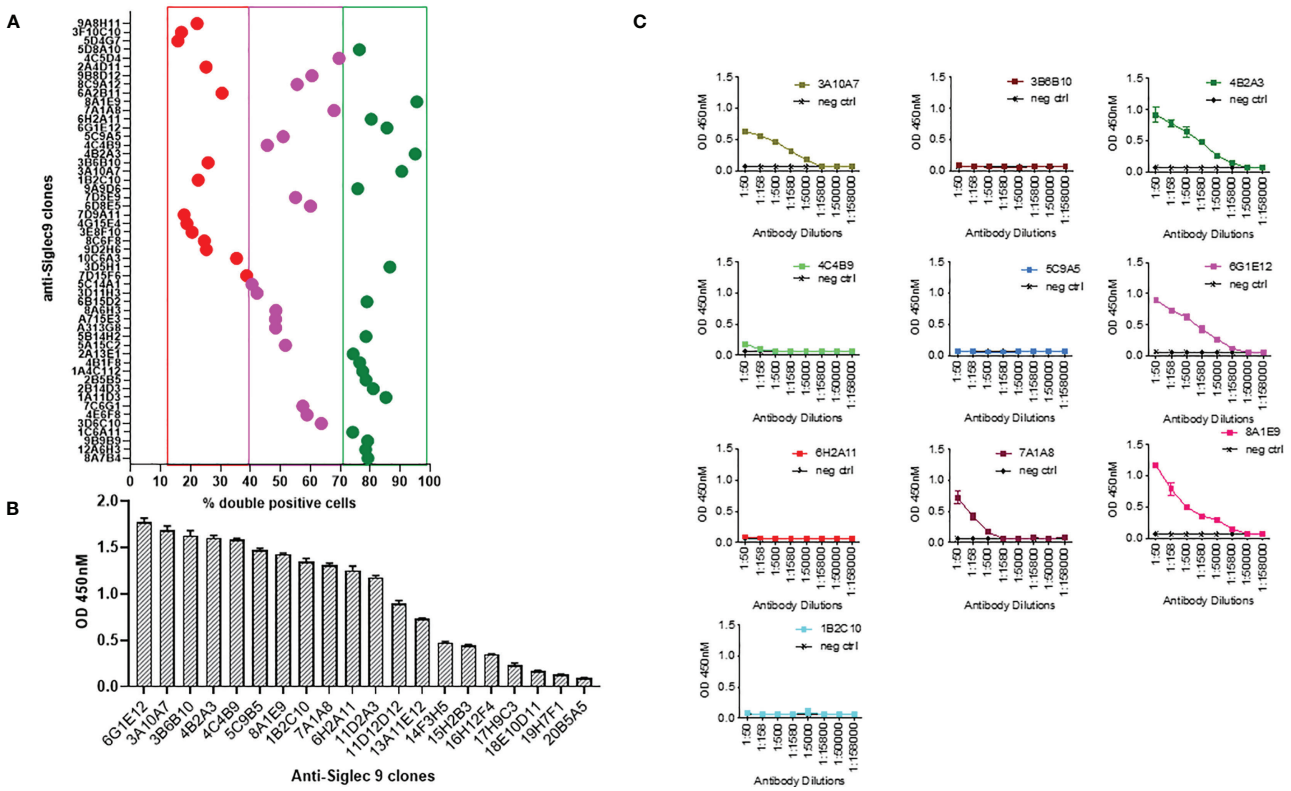

FIGURE 1 | Generation of monoclonal antibodies against human Siglec-9. **(A)** Mice were first immunized with human Siglec-9 DNA (2x), then boosted with recombinant human Siglec-9 protein to generate a humoral immune response and tested for antibody levels. Spleens from the mice were harvested, fused with 2P2/0 mouse Myeloma cells. Developed hybridomas were exhibiting anti-human Siglec-9 expression confirmed by ELISA and IntelliCyt FACS assay. Analysis of top 50 candidates: flow cytometry-based screening to evaluate anti-human Siglec-9 binding; Siglec-9 overexpressing K562 cells were first stained with hybridoma supernatants primary test and subsequently with APC-conjugated anti-mouse secondary antibodies followed by analysis using Intellicyt iQue screener PLUS system. GFP+ and APC+ cells were gated using IntelliCyt iQue screened PLUS system, where high % double-positive cells were identified. **(B)** Binding ELISA of top 20 GFP+ and APC+ %double positive anti-human Siglec-9 mAb candidates by ELISA. Recombinant human Siglec-9 protein was used in ELISA to assess the antigen-specific binding. **(C)** Screening and titration of serially diluted mAb candidates. Recombinant human Siglec-9 protein was used as a coating antigen for binding ELISA. The positive control shows responses, and the negative control (recombinant HIV-1 gp120 protein) shows no response with anti-human Siglec 9 hybridomas. Each point represents the OD value with the mean ± standard deviation from three determinations.

sialidase (**Figure 3B**) enhances PBMCs-mediated Cytotoxicity against these cells (**Figure 3C**).

We then examined the effects of anti-Siglec 9 antibody (8A1E9 clone) on NK cytotoxicity against K562 cells. K562 cells were incubated with primary NK cells in the presence of anti-Siglec 9 antibody or control IgG. Following incubation, NK cells were stained with antibodies against CD16, CD56, and CD107a and evaluated by flow cytometry. The expression of CD107a corresponds to the degree of degranulation of NK cells. The plot of % $CD107a^+$ *vs.* effector: target (NK cells: K562 tumor cells ratio, where NK cells were fixed at 200,000 cells, shows that the anti-Siglec 9 antibody (8A1E9 clone) induced higher degranulation of NK cells compared to control IgG (**Figure 3D**).

Anti-Siglec-9 Monoclonal Antibody Enhances Human PBMCs Toxicity Towards Cancer Cells

To test for the 8A1E9 antibody's ability to enhance immune cytotoxicity, PBMCs were co-cultured with K562 cells, with and without anti-Siglec-9 antibodies (at 100:1 effector: target ratio). In the presence of anti-Siglec-9 antibody, % cytotoxicity was increased, as measured by the amount of LDH released from these cells (normalized to the background as described in the methods section), suggesting the involvement of Siglec-9 antibodies in the restoration of immune functions against cancer cells (**Figure 3E**).

Anti-Siglec-9 Antibody Reduces Tumor Volume in a Humanized Mouse Model of Ovarian Cancer

Wild-type mice do not express human immune cells. Hu-mice is a humanized mouse model that harbors functional human immune cells that respond to tumor challenges (30). Hu-mice were reconstituted from immunodeficient NSG (NOD.Cg-Prkdcscid IL2rgtm1 Wjl/SzJ) mice with HLA-A allele matched $CD34^+$ hematopoietic cells and thymic cells (placed under renal capsule) and customized cytokine cocktails delivered by DNA (30). The reconstituted hu-mice showed strong repopulation of a

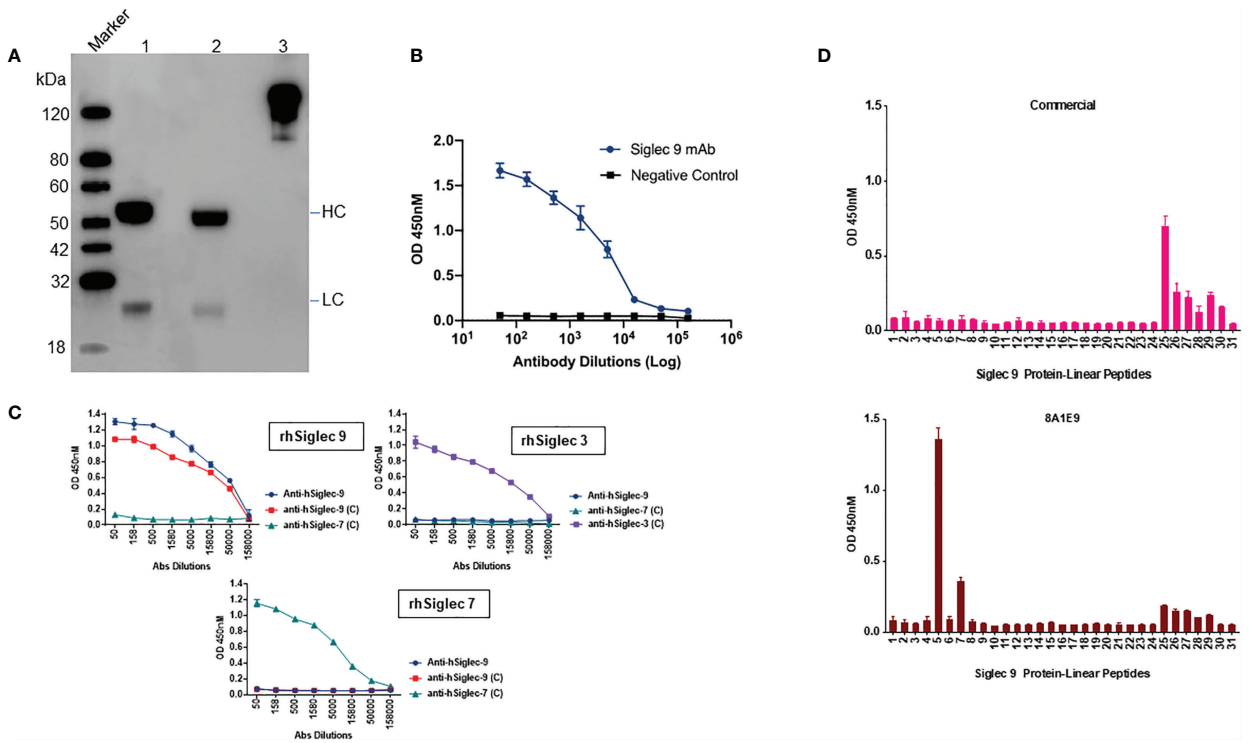

FIGURE 2 | Characterization of recombinantly expressed human Siglec-9. **(A)** Western blot analysis of recombinantly expressed anti-Siglec-9. Recombinant antibodies are expressed monoclonal antibodies that are generated *in vitro* using synthetic genes. The purified recombinant antibody was analyzed by SDS-PAGE, Western blot analysis to determine the molecular weight and purity under non-reducing (lane 2) alongside isotype control human IgG1, Kappa antibody (lane 1). Reducing and non-reducing loading buffer was added to protein sample respectively, and the final concentration of protein was 0.5 mg/ml. HC, Heavy Chain; LC, Light Chain. **(B)** Siglec-9 antigen binding of recombinantly expressed Siglec-9 antibodies was measured by ELISA. Assay plates were coated with recombinant Siglec-9, and recombinantly expressed mAbs were used. The binding was determined by ELISA. **(C)** Recombinantly expressed monoclonal antibodies were tested by ELISA to determine the binding specificity of anti-hSiglec-9. Assay plates were coated with recombinant human Siglec 3, 7, and 9 and then probed with recombinantly expressed anti-hSiglec-9 as well commercial antibodies (labeled as C) against each other to test immune cross reactivity. Anti-hSiglec-9 showed binding specificity to only recombinant hSiglec-9 and did not exhibit any binding to hSiglec-3 or hSiglec-7. **(D)** To determine potential epitope(s) regions for anti-Siglec-9 antibody binding, an indirect ELISA was performed. Peptide-based ELISA was performed using 100 µL/well of peptide at 2 µg/mL. ELISA plates were coated with 20mer peptides of human Siglec 9 protein as indicated, and recombinant anti-Siglec 9 and commercial antibodies samples were diluted 1:50 and analysed by ELISA as indicated in the Materials and Methods. Data are mean ± SDs for three wells (representative of two independent experiments).

diverse human immune repertoire (**Figures 4A, B**). To test *in vivo* the efficacy of the anti-Siglec-9 8A1E9 antibody, we implanted SKOV3 ovarian cancer cells (a cell line expressing high levels of Siglec-9 ligands; **Figure 3A**) subcutaneously in 2 groups of hu-mice. Seven days post tumor implantation; we treated one group with 100µg of 8A1E9 antibody and the other group with control antibody on days 7 and 14. Siglec-9 blockade by 8A1E9 was able to significantly reduce tumor burden in this hu-mice (**Figure 4C**).

DISCUSSION

Siglec-9 (expressed on the surface of several immune cells) can bind to its sialic acid-containing ligands (overexpressed on cancer cells). This binding exerts a negative signaling cascade that eventually inhibits the functions of these immune cells. Notably, the Siglec-9-mediated inhibition of immune functions is MHC-independent; therefore, cancer cells can utilize this mechanism to evade host immune surveillance (31). Indeed, emerging evidence suggests that Siglec-9 is an important glyco-immune negative checkpoint that can be targeted to enhance immune functions against cancer and virally infected cells (5, 20, 22, 24). However, the success of such an approach hinges on the availability of specific monoclonal antibodies that can block Siglec-9 and induce immune functions. In this short report, we developed such an efficient antibody and tested it *in vitro* and *in vivo*.

Siglec-9 shares around 84% sequence homology with Siglec-7 (21). However, our lead antibody showed no binding to Siglec-7 (or to Siglec-3) and a high binding to Siglec-9. This data suggest that our novel antibody can be used, in the future, to selectively target Siglec-9 without impacting the functions of other Siglecs. This is important as many of these Siglec interactions are important against autoimmunity (26–29). This high selectivity of our lead antibody was coupled with its ability to significantly

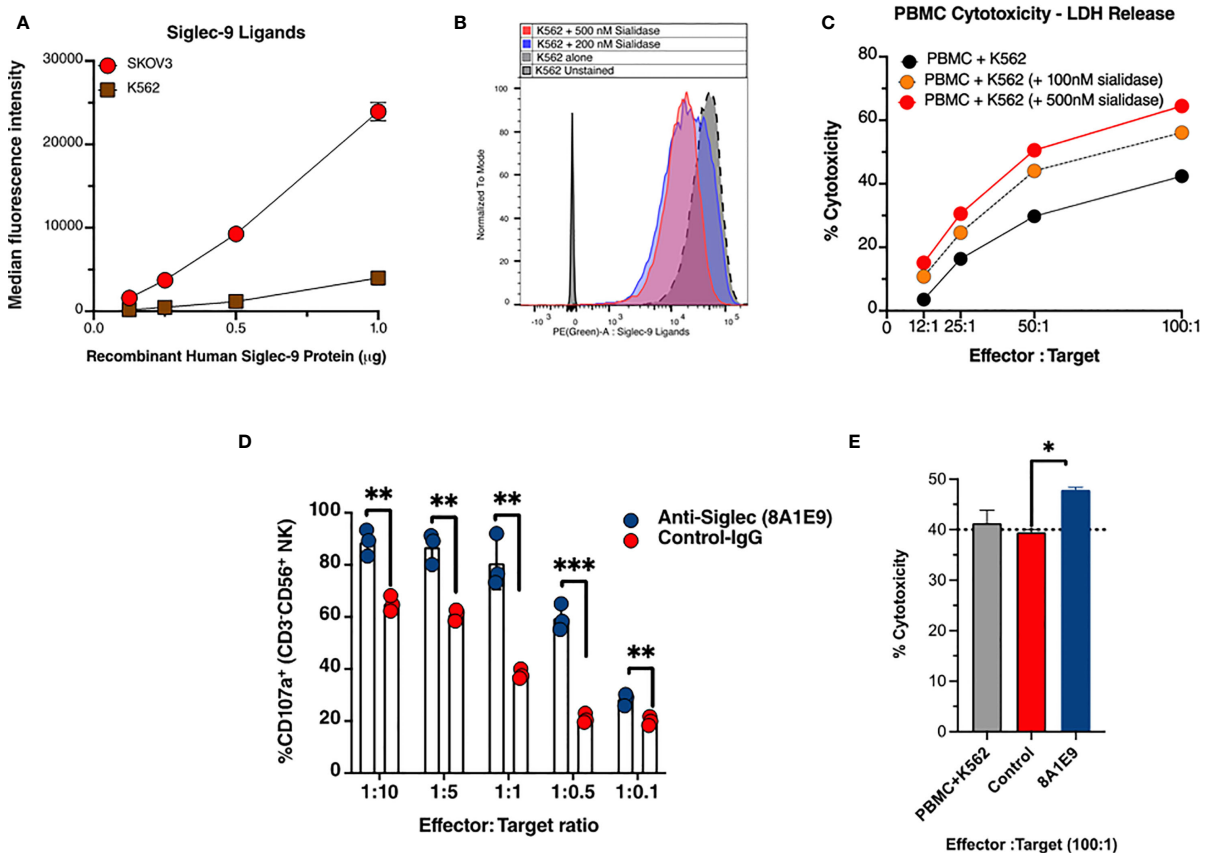

FIGURE 3 | Anti-Siglec-9 mAb is functional and enhances anti-tumor immune activities in vitro. **(A)** Cell surface Siglec-9 ligand expression on K562 and SKOV3 cells. An equal number of indicated cells were incubated with varying amounts of recombinant human Siglec-9 Fc protein. The binding of Siglec-9-Fc to cells was measured using PE anti-human Fc fluorescent secondary antibody. **(B)** K562 cells were treated with 200nM or 500nM sialidase for 1 h at 37°C and then were incubated with 1μg recombinant human Siglec-9 Fc protein. The binding of Siglec-9 Fc to cells was revealed using PE anti-human Fc fluorescent secondary antibody. **(C)** K562 (desialylated or not) cells were co-incubated with PBMCs from a healthy donor at different effector to target ratios. Cytotoxicity was determined by the LDH assay. **(D)** Measurement of NK cells activity against K562 target tumor cells with and with anti-Siglec-9 recombinant mAb (8A1E9 clone). Effectors are NK cells fixed at 200,000 cells. **(E)** Evaluation of antibody-dependent cell cytotoxicity using lactate dehydrogenase (LDH) measurement. The cytolytic activity of human Peripheral Blood Monolayer Cells (PBMCs) against K562 (NK-sensitive tumor cells) targets in the presence of anti-siglec-9 antibodies (1:10 dilution). Cytotoxicity was determined by measuring the amount of endogenous lactate dehydrogenase (LDH) released into the media. The assay was performed at ~100:1 effector-to-target ratio per well; triplicate. PBMC+K562 is the baseline cytotoxicity with no antibody. * = p<0.05, ** = p<0.01, and *** = p<0.001.

enhance immune functions against cancer cells *in vitro* as well as to reduce ovarian cancer progression *in vivo* in a humanized mouse model. Together, these data suggest that this antibody represents a promising opportunity to target Siglec-9 interactions in a selective and efficient manner.

Siglec-9 is expressed on myeloid cells, NK cells, and a subset of T cells (7, 14–23). It will be important, in future studies, to examine the contribution of each of these cell types in our observed *in vivo* anti-tumor effects. This can be achieved by depleting each of these cell types before the cancer challenge. Also, it will be important to determine the potentially additive effect of combining these antibodies with other cancer therapeutic approaches. Finally, in addition to Ovarian cancer, Siglec-9 interactions have been described to be important for the progression of Melanoma (7) and Pancreatic cancer (20). Beyond cancer, these interactions have also been shown to play a role in modulating viral infections (22). Testing our lead antibodies in other cancer models and models of infectious diseases should be the subject of future studies.

In summary, we used a novel approach to create a DNA plasmid that encodes the Siglec-9 antibody sequence with the codon and mRNA optimized for improved selectivity and *in vivo* expression. Immunological and molecular characterization assays were used to down select clones with the highest affinity for Siglec-9 using recombinant Siglec-9 protein. Binding ELISAs and Western blot showed Siglec-9 mAb clone to bind to only Siglec-9 protein. We have also tested our Siglec-9 antibody's ability to enhance anti-tumor functions *in vitro* and its ability to generate anti-tumor immunity in tumor-bearing mice. Indeed, anti-Siglec-9 antibodies reduced tumor burden *in vivo*. The findings observed from this investigation support the importance of this

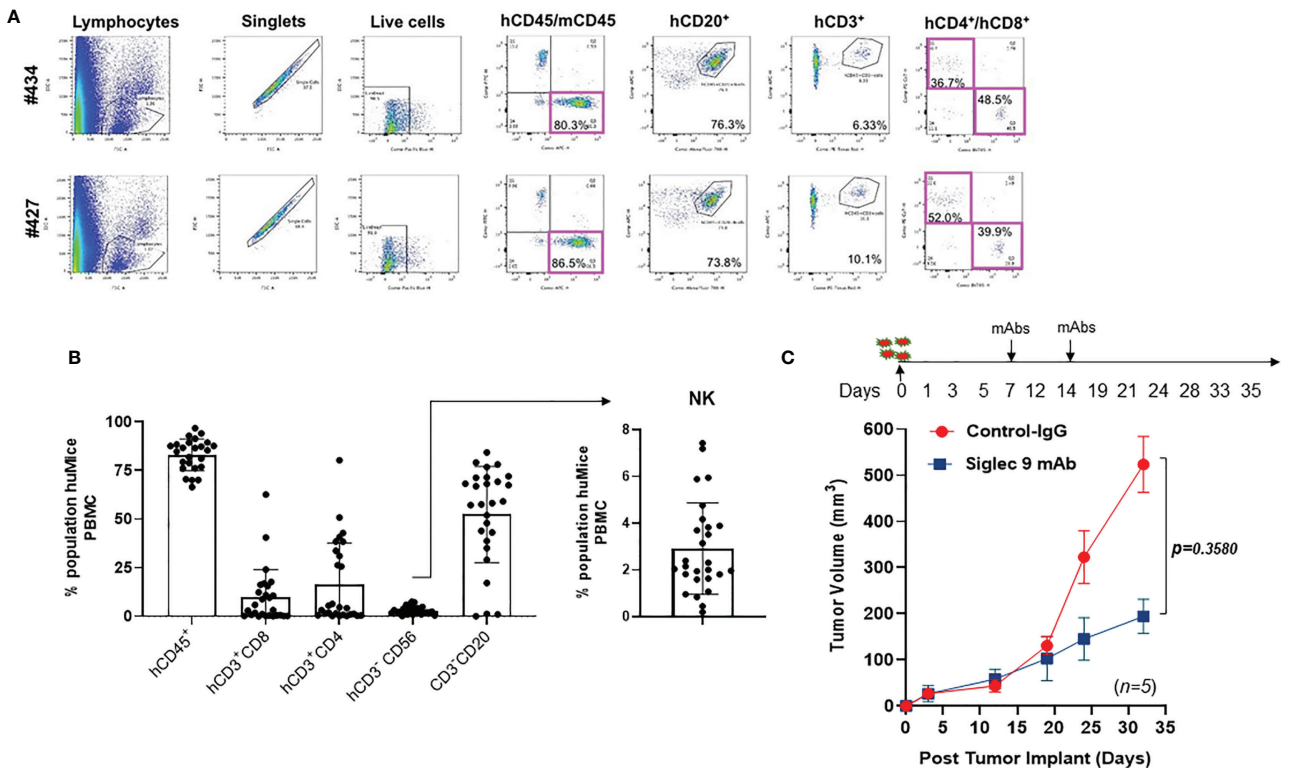

FIGURE 4 | Anti-Siglec-9 mAb reduces tumor volume in vivo in a humanized mouse model of ovarian cancer. **(A)** Dot plots showing selected windows and gating strategy as applied to the identification of major immune cell populations in the hu-mice. Percentage represents the means of values obtained in 2 independent experiments. **(B)** Representative flow cytometry histograms of FACS analysis immune cell populations in the hu-Mice. Each marker was tested on at least three independent experiments and created from a batch of 27 mice; hCD45+ show n=25 dots, CD20 show n=27 dots, CD56 show n=27 dots. Data were calculated as average % of expressing cell ± SD. All panels are representative of 3 independent experiments. **(C)** Effects of anti-human Siglec-9 antibody on tumor growth in hu-mice. On day 0, humanized mice (n=5) were injected with 5x105 SKOV3 cells. 100µg of anti-hSiglec-9 antibody or control IgG was administered to each mouse on days 7 and 14. Tumor volume was measured on days 3, 12, 19, 24, and 33. After tumors became detectable, tumor masses were measured with a manual caliper, and tumor volumes were calculated, approximating the tumor mass to a sphere, according to the following equation: tumor volume = ½ (length x width2).

novel Siglec-9 immune-checkpoint and the potential for targeting it as effective cancer immunotherapy.

MATERIAL AND METHODS

Cell Culture

Cell lines K562, A549, SKOV3, HEK293, and Phoenix AMPHO were used. Phoenix AMPHO, A549, HEK293, and SKOV3 were maintained in Dulbecco's Modification of Eagle's Medium (DMEM) (Corning Cellgro) with 4.5g/L glucose, L-glutamine, sodium pyruvate, supplemented with 10% heat-inactivated FBS (Atlas Biologicals). K562 cells were maintained in RPMI 1640 Medium (ThermoFisher) supplemented with 10% heat-inactivated FBS. All cell types were maintained at 37°C in humidified 95% air and 5% CO_2 atmosphere. All cell lines were mycoplasma negative. Primary PBMC and NK cells, isolated from healthy donors, were purchased from the Human Immunology Core at the University of Pennsylvania. All primary cells were collected under a protocol approved by a University Institutional Review Board, and written informed consent was obtained from each healthy, normal donor.

MOUSE IMMUNIZATION, HYBRIDOMA GENERATION, AND DNA-ENCODED mAb GENERATION

Female BALB/c mice (5-7 weeks of age) were purchased from the Jackson Laboratory. Animals were housed under a pathogen-free barrier facility in accordance with NIH guidelines. All animal procedures were approved by the Institutional Animal Care and Use Committee at The Wistar Institute (protocol #112763). The mice were immunized intramuscularly (hind limbs) three times at 2-week intervals (in weeks 0, 2 and 4) with 50µg (50µl in saline) of plasmid encoding human Siglec-9 and adjuvant was mixed 1:1 (volume/volume) with CFA (Sigma-Aldrich) or IFA (Sigma-Aldrich) in a total volume of 100µl mixed by syringe. The animals then received two booster injections at two-week intervals, the first booster containing Siglec-9 DNA of identical method and the second

booster containing 50μg of purified human Siglec-9 recombinant protein. Three days after the protein boost, mice were sacrificed. Their spleens were removed and fused with SP2/0 mouse myeloma cells using the HY Hybridoma Cloning Kit according to the manufacturer's protocol using method A (Stem Cell Technologies). Hybridomas of 1152 mAb candidates were generated and screened using the ELISA method (> 0.6 O.D. 450nm in a binding assay as described below), then top 50 hits were selected for further screening using IntelliCyt-FACS analysis as described below. After characterization and sequencing the best clones, recombinant antibodies heavy and light chain sequences were assembled into the human IgG1 framework and cloned into pcDNA3.4 antibody expression vectors, as previously described (32). Plasmids were then transfected into Expi293F cells using the Expifectamine 293 Expression Kit (Thermo Fisher Scientific), and recombinant Abs have purified with protein A agarose (Invitrogen) (32).

ENZYME-LINKED IMMUNOSORBENT ASSAY FOR HYBRIDOMAS SCREENING

ELISA was carried out using 96-well MaxiSorp plates (Nunc) (Thermo Fisher Scientific) coated with 1μg/mL of recombinant hSiglec-9, hSiglec 7, or hSiglec 3 proteins (R&D Systems) in PBS and incubated overnight at 4°C. For the binding characterization ELISA, anti-Siglec 3 (Mouse IgG1 Clone # 6C5/2), anti-Siglec 7 (Mouse IgG2B Clone # 194212), and anti-Sigelc 9 (Mouse IgG2A Clone # 191240) were acquired from R& D systems and used as described below. Following incubation, plates were washed with PBS-T (PBS with 0.05% Tween 20) and blocked using PBS containing 10% FBS for 1 hour at room temperature (RT). Subsequently, the plates were washed with PBS-T and incubated with hybridoma, serially diluted in PBS with 1% FBS and 0.1% Tween 20 for 30 minutes on a shaker and 90 minutes at room temperature. After another wash, the plates were treated with goat-anti-mouse IgG H+L conjugated to Horse Radish Peroxidase (Bethyl Laboratories) at a dilution of 1:10000 for 1 hour at room temperature. After post-final wash, the plates were developed with SigmaFast OPD substrate (Sigma-Aldrich) for 5-10 min in the dark, and the reaction was stopped using 1N H_2SO_4. The plates were read using a Synergy2 plate reader (BioTek Instruments) at an optical density of 450nm (32).

For the avidity test, an in-house avidity assay was standardized using a commercial ELISA kit for detecting specific IgG antibodies modified to incorporate an elution step with urea to remove low-avidity antibodies from the target antigen. For the assay, 100μl of each diluted serum was added to wells of polystyrene plates coated with human Siglec-9 protein. All serum samples were run twice in duplicate, as described before (32).

PRODUCTION OF SIGLEC-9-GFP OVEREXPRESSING K562 STABLE CELL LINES

Human Siglec-9 was encoded in DNA using synthetic oligonucleotides. The final sequence was cloned into a mammalian expression vector (pBMN-I-GFP) followed by subsequent large-scale production (Genscript, Piscataway, NJ). Phoenix AMPHO cells cultured in a T-182 flask (Fisher) were allowed to attain 60-80% confluency and transfected with DNA using GeneJammer Transfection Reagent (Agilent Technologies) as per manufacturer's instructions. To the transfection mixture consisting of serum-free DMEM and GeneJammer reagent (Agilent Technologies), 10μg of the plasmid (pBMN-I-GFP-hSiglec-9) was added and incubated for 30 minutes at room temperature. The transfection mixture was then added to cultured Phoenix AMPHO cells and incubated for 24-72 hours at standard growth conditions. Successful transfection was confirmed using fluorescence microscopy for the expression of GFP. The culture media-rich with lentivirus was collected 72 hours following transfection and stored at -80°C for further use (33). For cell transduction, six-well plates were coated with 10μg/mL of RetroNectin reagent (Takara Bio) and incubated overnight at 4°C. The coated plates were washed with PBS-T and blocked for 2 hours using PBS with 10% FBS at RT. Following another wash, 1mL of generated lentivirus was added to the coated wells and centrifuged for 120 min at 2000g. The supernatant from the wells was discarded, and 1 million K562 cells were added to the wells. The plates were again centrifuged for 10 minutes at 1500rpm and incubated at standard growth conditions. Successful transduction into Sigle-9-GFP overexpressing K562 cells was confirmed using fluorescence microscopy for GFP expression; cells were pooled and cultured at appropriate growth conditions for further analysis (33).

HYBRIDOMA SCREENING USING INTELLICYTE FACS ANALYSIS

$1x10^5$ of Siglec-9-GFP-overexpressing K562 cells co-cultured with an equal number of K562 cells in 96 healthy U-bottom plates (Fisher brand). These cells were probed with antibodies (Siglec-9 hybridoma supernatants) from clones designated positive from screening ELISA. Rat-anti-mouse IgG antibody conjugated with APC (BioLegend) at 1:200 dilution was added and incubated for 30 min at 4°C. Following incubation and washing with PBS and 1% FBS, cells were analyzed using the Intellicyt iQue screener PLUS system to identify double-positive cells (GFP and APC). Cells and beads were gated on a dot plot of side-scattered *versus* forward-scattered light intensity (33, 34).

CLONING AND EXPRESSION OF A VECTOR SYSTEM FOR RECOMBINANT ANTIBODY EXPRESSION IN HEK293 CELLS

We adopted the HEK293 mammalian cell line, grown at high densities in suspension, for the recombinant antibody expression. The antibody cloning method represents a simple two-step protocol with complete design flexibility. Sequence

analysis was performed, and a recombinant anti-Siglec-9 mAb plasmid was constructed. Variable- or constant-region domains for human IgG1 designed within the pcDNA3.4 antibody expression cassette develop a large-scale antibody production for subsequent use in cell culture and animal model studies.

WESTERN BLOT ANALYSIS

Human recombinant Siglec-9, Siglec-3, and Siglec-7 proteins (R&D Systems) were reduced using NuPAGE Sample Reducing Agent (10x) (Thermo Fisher Scientific) and heated at 70°C for 10 min, then loaded onto sample lanes with Odyssey Protein Molecule Weight (LI-COR). The gel electrophoresis was carried out using sodium dodecyl sulfate-12% polyacrylamide gel for 50 min at 200V. Following electrophoresis, samples were transferred onto polyvinylidene fluoride (PVDF) membranes *via* an iBlot-2 system (Thermo Fisher Scientific) and blocked using Odyssey Blocking Buffer (35) (LI-COR) for 1-2 hours on a rocker. Membranes were treated with antibody culture supernatant (1:500) in OBB containing 0.1% Tween 20 overnight at 4°C. Following incubation, the membranes were washed four times at 5 min intervals with PBS-T. Subsequently, washed membranes were treated with goat anti-mouse secondary antibody (IRDye 800 CW) in OBB containing 0.1% Tween 20 and 0.01% SDS at a dilution of 1:10000 and incubated for 60 minutes in the dark on the rocker at room temperature. Following incubation, the membranes were rewashed four times and scanned using Odyssey CLx Imager (LI-COR).

ANTIBODY PEPTIDE MAPPING

Human Siglec-9 derived 20-mer peptides (GenScript) were coated on 96-well MaxiSorp plates (Nunc) (Thermo Fisher Scientific) at a concentration of 1μg/mL and incubated overnight at 4°C. After four washes with PBS-T, the plates were blocked using 10% FBS containing PBS for 2 hours at room temperature. 100μL of anti-Siglec 9 or anti-Sigelc 9 (Mouse IgG2A Clone # 191240) at 1μg/mL were added to the washed plates, and this setup was incubated for 2 hours at room temperature. Post incubation and washing, 100 μL of Goat-anti-mouse antibody conjugated with Horse Radish Peroxidase (Bethyl Laboratories) at a dilution of 1:10000 were added and incubated for 60 min at room temperature. After a final series of washing, plates were developed using SigmaFast OPD substrate (Sigma-Aldrich) for 15 min in the dark, and the reaction was stopped using 1N H2SO4. Finally, the plates were read using a Synergy2 plate reader (BioTek Instruments) at an optical density of 450nm. Each clone was screened in duplicate.

EVALUATION OF NK CELL DEGRANULATION

NK cells (effector) and K562 cells (target) at multiple effector: target ratios (ranging from 1:10, 1:5, 1:1, 1:0.5, and 1:0.1) were co-cultured. The number of effector cells was fixed at 2x105 cells per well. 10μg/mL of anti-Siglec-9 mAb was added to wells consisting of co-cultured cells, and plates were incubated for 20 hours at 37°C. Post incubation and wash, cells were stained for markers CD16 using APC Mouse Anti-human antibody (BD biosciences), CD56 using PE anti-human antibody (Bio Legend), and CD107a (a marker for NK cell activity derived from peripheral blood) using AF700 Mouse Anti-human CD107a antibody (BD Biosciences) and analyzed by Flow Cytometry using LSRII flow cytometer (BD Biosciences) (36). The analysis was done using FlowJo software (Tree Star).

EVALUATION OF PBMCs CYTOTOXICITY USING LACTATE DEHYDROGENASE MEASUREMENT

The cytolytic activity of human Peripheral Blood Monolayer Cells (PBMCs) against K562 targets was determined using the LDH method. The setup involved co-incubation of human PBMCs and K562 cells at an effector to target ratio of 100:1 with or without Siglec-9 mAb (1:10 dilution) for 4 hours at 37°C. Quantification of the release of endogenous LDH into the media was used as a measure for cytolytic activity. The assay was performed in triplicate, wherein PBMC+K562 is the baseline cytotoxicity with no antibody (37). The following formula was applied for calculating Cytotoxicity in this assay: % Cytotoxicity = Experimental value-Effector cell spontaneous control-Target cell spontaneous control divided by target cell maximum control-Target cell spontaneous Control.

DETECTION OF CELL SURFACE SIGLEC-9 LIGANDS

2 x 10^5 cells were resuspended in 100μl PBS supplemented with 0.5% bovine serum albumin 0.1% sodium azide. Different amounts (beginning at 1 μg) of recombinant human Siglec-9-Fc (R&D Systems) were added and incubated for 1 h at room temperature. Following incubation, cells were washed twice and incubated with PE Fc-specific goat anti-human IgG (eBiosceince); 1:250 dilution, for 20 min at room temperature. Cells were further washed, fixed (BD Cytofix/Cytoperm), and acquired by flow cytometry (LSR II, BD). Flow cytometry data were analyzed using FlowJo software.

SIGLEC-9 LIGAND DETECTION AFTER DESIALYLATING CELLS

5 x 105 cells were resuspended in 100 μl PBS supplemented with 0.5% bovine serum albumin 0.1% sodium azide. Sialidase (200nM or 500nM) was added and incubated for 1 h at 37°C. To remove residual sialidase, cells were washed twice by centrifugation 400g for 5 min. Next, cells were evaluated for cell surface Siglec-9 ligand content following protocol to detect cell surface siglec-9 ligands as described. Desialylated cells were also used in LDH cytotoxicity

assays, as described above. Sialidase was prepared in-house using Vibrio cholerae nanH gene cloned into pCVD364 vector, which was generously provided to us by Dr. Eric R. Vimr at the University of Illinois Urbana (38).

OVARIAN CANCER TUMOR CHALLENGE IN NSG AND HU-MICE MICE

For our *in vivo* examination of the potency of our blocking antibodies, we used a recently developed advanced humanized mice (hu-mice) model (30). This model harbors functional human immune cells that respond to tumor challenges (30). Immunodeficient NSG (NOD.Cg-Prkdcscid IL2rgtm1 Wjl/SzJ) mice were used to generate hu-mice by injecting $CD34^+$ hematopoietic cells (i.v.) and autologous thymus (placed under renal capsule) and sequential delivery of cytokines as described before (30). Hu-mice (n=5) were then injected subcutaneously with $5x10^5$ cells of SKOV3 on day 0. Anti-human Siglec-9 (100μg) or control IgG was administered to each mouse on days 7 and 14. Tumor dimensions were measured by manual caliper on days 3, 12, 19, 24, and 33 following tumor injection. Tumor volume was calculated using the formula [tumor volume = ½ (length x width2)] (39). All mice were maintained inappropriate environmental conditions. All animal protocols were approved by Wistar Institutional Animal Care and Use Committee.

STATISTICAL ANALYSIS

Differences between the means of experimental groups were calculated using two-tailed unpaired t-tests. Error bars represent the standard error of the mean. Survival rates were compared using the log-rank test. All statistical analyses were done using Graph Pad Prism 8. $p < 0.05$ was considered statistically significant.

DATA AVAILABILITY STATEMENT

The raw data supporting the conclusions of this article will be made available by the authors, without undue reservation.

ETHICS STATEMENT

All animal procedures were approved by the Institutional Animal Care and Use Committee at The Wistar Institute (protocol #112763).

AUTHOR CONTRIBUTIONS

MA-M and KM conceived and designed the experiments for this study. HC, MH, LG, AK, OA, and AP performed the experiments. MA-M and KM wrote the original concept and manuscript, and HC, MH, and DB reviewed and edited it. MA-M and KM acquired funding; APP provided resources. MA-M and KM provided supervision. All authors contributed to the article and approved the submitted version.

FUNDING

This work was part of a Wistar-Sponsored Research Agreement entitled "Targeting Siglec-9/Mucin Interaction for Cancer Immunotherapy" to MA-M and KM. Support for Shared Resources utilized in this study was provided by Cancer Center Support Grant (CCSG) P30CA010815 to The Wistar Institute.

ACKNOWLEDGMENTS

This paper is dedicated to the memory of Dr. Rajasekharan Somasundaram, whose devotion to characterization and establishment of Wistar-huMice was unsurpassed. SKOV3 cells were provided by J.R. Conejo-Garcia (Department of Immunology, Moffitt Cancer Center, Tampa, Florida). We would like to thank the Animal Facility staff at the Wistar Institute for providing house and care to the animals. We thank the Wistar Flow Core for assistance with the flow/sorting experiments and for their technical assistance. We also thank Dr. Pamela Nakajima at the Fox Chase Cancer Center for developing hybridomas.

REFERENCES

1. Pesce S, Greppi M, Grossi F, Del Zotto G, Moretta L, Sivori S, et al. PD/1-PD-Ls Checkpoint: Insight on the Potential Role of NK Cells. *Front Immunol* (2019) 10:1242. doi: 10.3389/fimmu.2019.01242
2. Sivori S, Della Chiesa M, Carlomagno S, Quatrini L, Munari E, Vacca P, et al. Inhibitory Receptors and Checkpoints in Human NK Cells, Implications for the Immunotherapy of Cancer. *Front Immunol* (2020) 11:2156. doi: 10.3389/fimmu.2020.02156
3. Patel SA, Minn AJ. Combination Cancer Therapy With Immune Checkpoint Blockade: Mechanisms and Strategies. *Immunity* (2018) 48(3):417–33. doi: 10.1016/j.immuni.2018.03.007
4. Pardoll DM. The Blockade of Immune Checkpoints in Cancer Immunotherapy. *Nat Rev Cancer* (2012) 12(4):252–64. doi: 10.1038/nrc3239
5. Stanczak MA, Siddiqui SS, Trefny MP, Thommen DS, Boligan KF, von Gunten S, et al. Self-Associated Molecular Patterns Mediate Cancer Immune Evasion by Engaging Siglecs on T Cells. *J Clin Invest* (2018) 128(11):4912–23. doi: 10.1172/JCI120612
6. Grywalska EPasiarski M, Gozdz S, Rolinski J. Immune-Checkpoint Inhibitors for Combating T-Cell Dysfunction in Cancer. *Onco Targets Ther* (2018) 11:6505–24. doi: 10.2147/OTT.S150817
7. Haas Q, Boligan KF, Jandus C, Schneider C, Simillion C, Stanczak MA, et al. Siglec-9 Regulates an Effector Memory CD8+ T-Cell Subset That Congregates in the Melanoma Tumor Microenvironment. *Cancer Immunol Res* (2019) 7 (5):707–18. doi: 10.1158/2326-6066.CIR-18-0505
8. Angata T, Nycholat CM, Macauley MS. Therapeutic Targeting of Siglecs Using Antibody- and Glycan-Based Approaches. *Trends Pharmacol Sci* (2015) 36(10):645–60. doi: 10.1016/j.tips.2015.06.008
9. Bornhofft KF, Goldammer T, Rebl A, Galuska SP. Siglecs: A Journey Through the Evolution of Sialic Acid-Binding Immunoglobulin-Type Lectins. *Dev Comp Immunol* (2018) 86:219–31. doi: 10.1016/j.dci.2018.05.008

10. O'Reilly MK, Paulson JC. Siglecs as Targets for Therapy in Immune-Cell-Mediated Disease. *Trends Pharmacol Sci* (2009) 30(5):240–8. doi: 10.1016/j.tips.2009.02.005
11. Pillai S, Netravali IA, Cariappa A, Mattoo H. Siglecs and Immune Regulation. *Annu Rev Immunol* (2012) 30:357–92. doi: 10.1146/annurev-immunol-020711-075018
12. Pearce OM, Laubli H. Sialic Acids in Cancer Biology and Immunity. *Glycobiology* (2016) 26(2):111–28. doi: 10.1093/glycob/cwv097
13. Rodrigues E, Macauley MS. Hypersialylation in Cancer: Modulation of Inflammation and Therapeutic Opportunities. *Cancers (Basel)* (2018) 10 (6):207. doi: 10.3390/cancers10060207
14. Ando M, Tu W, Nishijima K, Iijima S. Siglec-9 Enhances IL-10 Production in Macrophages *via* Tyrosine-Based Motifs. *Biochem Biophys Res Commun* (2008) 369(3):878–83. doi: 10.1016/j.bbrc.2008.02.111
15. Belisle JA, Horibata S, Jennifer GA, Petrie S, Kapur A, Andre S, et al. Identification of Siglec-9 as the Receptor for MUC16 on Human NK Cells, B Cells, and Monocytes. *Mol Cancer* (2010) 9:118. doi: 10.1186/1476-4598-9-118
16. Chu S, Zhu X, You N, Zhang W, Zheng F, Cai B, et al. The Fab Fragment of a Human Anti-Siglec-9 Monoclonal Antibody Suppresses LPS-Induced Inflammatory Responses in Human Macrophages. *Front Immunol* (2016) 7:649. doi: 10.3389/fimmu.2016.00649
17. Jandus C, Boligan KF, Chijioke O, Liu H, Dahlhaus M, Démoulins T, et al. Interactions Between Siglec-7/9 Receptors and Ligands Influence NK Cell-Dependent Tumor Immunosurveillance. *J Clin Invest* (2014) 124(4):1810–20. doi: 10.1172/JCI65899
18. Khatua B, Bhattacharya K, Mandal C. Sialoglycoproteins Adsorbed by Pseudomonas Aeruginosa Facilitate Their Survival by Impeding Neutrophil Extracellular Trap Through Siglec-9. *J Leukoc Biol* (2012) 91(4):641–55. doi: 10.1189/jlb.0511260
19. Kiser ZM, Lizcano A, Nguyen J, Becker GL, Belcher JD, Varki AP, et al. Decreased Erythrocyte Binding of Siglec-9 Increases Neutrophil Activation in Sickle Cell Disease. *Blood Cells Mol Dis* (2020) 81:102399. doi: 10.1016/j.bcmd.2019.102399
20. Rodriguez E, Boelaars K, Brown K, Eveline Li RJ, Kruijssen L, Bruijns SCM, et al. Sialic Acids in Pancreatic Cancer Cells Drive Tumour-Associated Macrophage Differentiation *via* the Siglec Receptors Siglec-7 and Siglec-9. *Nat Commun* (2021) 12(1):1270. doi: 10.1016/j.bcmd.2019.102399
21. Zhang JQ, Nicoll G, Jones C, Crocker PR. Siglec-9, a Novel Sialic Acid Binding Member of the Immunoglobulin Superfamily Expressed Broadly on Human Blood Leukocytes. *J Biol Chem* (2000) 275(29):22121–6. doi: 10.1074/jbc.M002788200
22. Zhao D, Jiang X, Xu Y, Yang H, Gao D, Li X, et al. Decreased Siglec-9 Expression on Natural Killer Cell Subset Associated With Persistent HBV Replication. *Front Immunol* (2018) 9:1124. doi: 10.3389/fimmu.2018.01124
23. Rosenstock P, Kaufmann T. Sialic Acids and Their Influence on Human NK Cell Function. *Cells* (2021) 10(2). doi: 10.3390/cells10020263
24. Beatson R, Tajadura-Ortega V, Achkova D, Picco G, Tsourouktsoglou T-D, Klausing S, et al. The Mucin MUC1 Modulates the Tumor Immunological Microenvironment Through Engagement of the Lectin Siglec-9. *Nat Immunol* (2016) 17(11):1273–81. doi: 10.1038/ni.3552
25. Agrawal B, Gupta N, Konowalchuk JD. MUC1 Mucin: A Putative Regulatory (Checkpoint) Molecule of T Cells. *Front Immunol* (2018) 9:2391. doi: 10.3389/fimmu.2018.02391
26. Dharmadhikari G, Stolz K, Hauke M, Morgan NG, Varki A, de Koning E, et al. Siglec-7 Restores Beta-Cell Function and Survival and Reduces Inflammation in Pancreatic Islets From Patients With Diabetes. *Sci Rep* (2017) 7:45319. doi: 10.1038/srep45319
27. Laubli H, Varki A. Sialic Acid-Binding Immunoglobulin-Like Lectins (Siglecs) Detect Self-Associated Molecular Patterns to Regulate Immune Responses. *Cell Mol Life Sci* (2020) 77(4):593–605. doi: 10.1007/s00018-019-03288-x
28. Schwarz F, Pearce OMT, Wang X, Samraj AN, Läubli H, Garcia JO, et al. Siglec Receptors Impact Mammalian Lifespan by Modulating Oxidative Stress. *Elife* (2015) 4. doi: 10.7554/eLife.06184
29. Varki A, Gagneux P. Multifarious Roles of Sialic Acids in Immunity. *Ann N Y Acad Sci* (2012) 1253(1):16–36. doi: 10.1111/j.1749-6632.2012.06517.x
30. Somasundaram R, Connelly T, Choi R, Choi H, Samarkina A, Li L, et al. Tumor-Infiltrating Mast Cells Are Associated With Resistance to Anti-PD-1 Therapy. *Nat Commun* (2021) 12(1):346. doi: 10.1111/j.1749-6632.2012.06517.x
31. Daly J, Carlsten M, O'Dwyer M. Sugar Free: Novel Immunotherapeutic Approaches Targeting Siglecs and Sialic Acids to Enhance Natural Killer Cell Cytotoxicity Against Cancer. *Front Immunol* (2019) 10:1047. doi: 10.3389/fimmu.2019.01047
32. Choi H, Kudchodkar SB, Reuschel EL, Asija K, Borole P, Agarwal S, et al. Synthetic Nucleic Acid Antibody Prophylaxis Confers Rapid and Durable Protective Immunity Against Zika Virus Challenge. *Hum Vaccin Immunother* (2020) 16(4):907–18. doi: 10.1080/21645515.2019.1688038
33. Perales-Puchalt A, Duperret EK, Yang X, Hernandez P, Wojtak K, Zhu X, et al. DNA-Encoded Bispecific T Cell Engagers and Antibodies Present Long-Term Antitumor Activity. *JCI Insight* (2019) 4(8). doi: 10.1172/jci.insight.126086
34. Perales-Puchalt A, Wojtak K, Duperret EK, Yang X, Slager AM, Yan J, et al. Engineered DNA Vaccination Against Follicle-Stimulating Hormone Receptor Delays Ovarian Cancer Progression in Animal Models. *Mol Ther* (2019) 27 (2):314–25. doi: 10.1016/j.ymthe.2018.11.014
35. Modjarrad K, Roberts CC, Mills KT, Castellano AR, Paolino K, Muthumani K, et al. Safety and Immunogenicity of an Anti-Middle East Respiratory Syndrome Coronavirus DNA Vaccine: A Phase 1, Open-Label, Single-Arm, Dose-Escalation Trial. *Lancet Infect Dis* (2019) 19(9):1013–22. doi: 10.1016/S1473-3099(19)30266-X
36. Veluchamy JP, Delso-Vallejo M, Kok N, Bohme F, Seggewiss-Bernhardt R, van der Vliet HJ, et al. Standardized and Flexible Eight Colour Flow Cytometry Panels Harmonized Between Different Laboratories to Study Human NK Cell Phenotype and Function. *Sci Rep* (2017) 7(1):43873. doi: 10.1038/srep43873
37. Broussas M, Broyer L, Goetsch L. Evaluation of Antibody-Dependent Cell Cytotoxicity Using Lactate Dehydrogenase (LDH) Measurement. *Methods Mol Biol* (2013) 988:305–17. doi: 10.1007/978-1-62703-327-5_19
38. Taylor G, Vimr E, Garman E, Laver G. Purification, Crystallization and Preliminary Crystallographic Study of Neuraminidase From Vibrio Cholerae and Salmonella Typhimurium LT2. *J Mol Biol* (1992) 226(4):1287–90. doi: 10.1016/0022-2836(92)91069-2
39. Duperret EK, Trautz A, Stoltz R, Patel A, Wise MC, Perales-Puchalt A, et al. Synthetic DNA-Encoded Monoclonal Antibody Delivery of Anti-CTLA-4 Antibodies Induces Tumor Shrinkage In Vivo. *Cancer Res* (2018) 78 (22):6363–70. doi: 10.1158/0008-5472.CAN-18-1429

Conflict of Interest: MA-M and KM are named inventors of the 206193-0040-P1US patent application titled "Monoclonal Antibody Against Human Siglec-9 and Use for Cancer Immunotherapy".

The remaining authors declare that the research was conducted in the absence of any commercial or financial relationships that could be construed as a potential conflict of interest.

Publisher's Note: All claims expressed in this article are solely those of the authors and do not necessarily represent those of their affiliated organizations, or those of the publisher, the editors and the reviewers. Any product that may be evaluated in this article, or claim that may be made by its manufacturer, is not guaranteed or endorsed by the publisher.

frontiers in Oncology

SYSTEMATIC REVIEW
published: 22 November 2021
doi: 10.3389/fonc.2021.771864

The Quantitative Assessment of Using Multiparametric MRI for Prediction of Extraprostatic Extension in Patients Undergoing Radical Prostatectomy: A *Systematic Review and Meta-Analysis*

Wei Li[1], *Yuan Sun*[2], *Yiman Wu*[1], *Feng Lu*[3] *and Hongtao Xu*[1]*

[1] Department of Medical Imaging, Jiangsu Vocational College of Medicine, Yancheng, China, [2] Department of Burn and Plastic Surgery, 71st Group Army Hospital of People's Liberation Army of China, Xuzhou, China, [3] Department of Radiology, Wuxi No. 2 People's Hospital, Wuxi, China

OPEN ACCESS

Edited by:
Shashwat Sharad, Center for Prostate Disease Research (CPDR), United States

Reviewed by:
Arie Carneiro, Albert Einstein Israelite Hospital, Brazil
Cedric Poyet, University Hospital Zürich, Switzerland

***Correspondence:**
Hongtao Xu
hfjs2000@outlook.com

Specialty section:
This article was submitted to Genitourinary Oncology, a section of the journal Frontiers in Oncology

Received: *07 September 2021*
Accepted: *28 October 2021*
Published: *22 November 2021*

Citation:
Li W, Sun Y, Wu Y, Lu F and Xu H (2021) The Quantitative Assessment of Using Multiparametric MRI for Prediction of Extraprostatic Extension in Patients Undergoing Radical Prostatectomy: A Systematic Review and Meta-Analysis. Front. Oncol. 11:771864. doi: 10.3389/fonc.2021.771864

Purpose: To investigate the diagnostic performance of using quantitative assessment with multiparametric MRI (mpMRI) for prediction of extraprostatic extension (EPE) in patients with prostate cancer (PCa).

Methods: We performed a computerized search of MEDLINE, Embase, Cochrane Library, Web of Science, and Google Scholar from inception until July 31, 2021. Summary estimates of sensitivity and specificity were pooled with the bivariate model, and quality assessment of included studies was performed with the Quality Assessment of Diagnostic Accuracy Studies-2. We plotted forest plots to graphically present the results. Multiple subgroup analyses and meta-regression were performed to explore the variate clinical settings and heterogeneity.

Results: A total of 23 studies with 3,931 participants were included. The pooled sensitivity and specificity for length of capsular contact (LCC) were 0.79 (95% CI 0.75–0.83) and 0.77 (95% CI 0.73–0.80), for apparent diffusion coefficient (ADC) were 0.71 (95% CI 0.50–0.86) and 0.71 (95% CI 059–0.81), for tumor size were 0.62 (95% CI 0.57–0.67) and 0.75 (95% CI 0.67–0.82), and for tumor volume were 0.77 (95% CI 0.68–0.84) and 0.72 (95% CI 0.56–0.83), respectively. Substantial heterogeneity was presented among included studies, and meta-regression showed that publication year (≤2017 *vs.* >2017) was the significant factor in studies using LCC as the quantitative assessment (P=0.02).

Conclusion: Four quantitative assessments of LCC, ADC, tumor size, and tumor volume showed moderate to high diagnostic performance of predicting EPE. However, the optimal cutoff threshold varied widely among studies and needs further investigation to establish.

Keywords: magnetic resonance imaging, prostate neoplasms, quantitative, meta-analysis, tumor size

INTRODUCTION

Extraprostatic extension (T3a and T3b) in PCa is associated with a higher risk of biochemical recurrence and metastatic disease after radical prostatectomy (RP) or radiotherapy (1, 2). Although patients who undergo RP have shown high cancer-specific survival, they have a risk of suffering from postoperative erectile dysfunction and urinary incontinence (3). Preservation of the neurovascular bundles (NVB) can improve postoperative potency rate, however, which may increase the risk of positive surgical margins, bringing about biochemical recurrence and treatment failure (4, 5). Therefore, comprehensive risk assessment and staging is of great importance, which will influence the treatment planning and management. To overcome this problem, various nomograms and guidelines were proposed to improve the preoperative risk evaluation, including Partin tables, Memorial Sloan Kettering Cancer Center nomograms, and the cancer of the prostate risk assessment score (6–8). However, these well-established measures are roughly correlated with the final pathologic stage and lacking accuracy in clinical practice (9, 10).

In recent years, mpMRI has been widely applied in detection, staging, and localization of prostate cancer (PCa). In 2012, the European Society of Urogenital Radiology (ESUR) introduced Prostate Imaging Reporting and Data System (PI-RADS) for performing, interpreting, and reporting the PCa with mpMRI (11–13), which was validated and widely used in clinical practice (14, 15). Nevertheless, for localized advantage PCa of EPE, the ESUR PI-RADS demonstrated moderate diagnostic accuracy, and mainly depended on radiologists' own experience then short of reproducibility and inter-reader agreement (16, 17). At present, quantitative assessments of EPE with mpMRI have been intensively studied and demonstrated the potential of improving accuracy, inter-reader agreement, and pathology correlation (18, 19). In PI-RADS version 2.1, quantitative metrics such as length of capsular contact (LCC), apparent diffusion coefficient (ADC), tumor size, and tumor volume were included for assisting in prediction of EPE (13). However, these parameters have not been evaluated systematically up to date. Thus, the purpose of our study was to assess the diagnostic accuracy of using quantitative metrics for the prediction of EPE.

METHODS AND MATERIALS

This systematic review and meta-analysis was performed in accordance with the preferred reporting items for systematic reviews and meta-analyses (PRISMA) guidelines (20). The primary outcome was the diagnostic performance of using mpMRI quantitative metrics of LCC, ADC, tumor size, and tumor volume as independent predictors for prediction of EPE in PCa.

Search Strategy and Selection Criteria

For this systematic review, we carried out an electronic database search of MEDLINE, Embase, Cochrane Library, Web of Science, and Google Scholar from inception until July 31, 2021, with language restricted to English. The searches were supplemented by screening references from the most recent reviews and eligible studies. The search terms combined acronyms used for MRI, PCa, EPE, and quantitative assessments as follows: ([MR] or [MRI] or [mpMRI] or [magnetic resonance] or [magnetic resonance imaging]) and ([prostate cancer] or [PCa] or [prostate carcinoma]) and ([EPE] or [extraprostatic extension] or [ECE] or [extracapsular extension]) and ([tumor size] or [tumor volume] or [tumor dimension] or [ADC] or [apparent diffusion coefficient] or [LCC] or [TCL] or [length of tumor capsular contact] or [capsule contact length] or [tumor contact length]).

Inclusion Criteria

We included studies that met all criteria as follows: (1) patients underwent mpMRI for assessment of suspected EPE; (2) with quantitative metric of LCC, ADC, tumor size, and tumor volume as independent predictors; (3) reported the true positive (TP), false positive (FP), false negative (FN), and true negative (TN), or other details for the reconstruction of 2×2 tables to evaluate the diagnostic performance; and (4) with pathological results after radical prostatectomy as the reference standard.

Exclusion Criteria

We excluded studies that satisfied any of the following criteria: (1) studies involving less than 10 participants, (2) did not use the quantitative metrics as an independent predictor but combined with other scoring system or guidelines, (3) not reported sufficient for assessing the diagnostic performance, and (4) review articles, guidelines, consensus statements, letters, editorials, and conference abstracts. The literature selection was performed by two investigators (LW and SY, with 8 and 11 years of experience in performing systematic reviews and meta-analyses) independently. All disagreements were resolved by discussion and consultation with a third investigator (WM) until consensus was reached.

Data Extraction and Quality Assessment

We used a standardized form to extract information from individual studies as follows: (1) demographic and clinical characteristics, including sample size, patient age, PSA level, and Gleason score, number of patients diagnosed with EPE; (2) study characteristics, including authors, year of publication, affiliation, country of origin, duration of patient recruitment, study design, quantitative metrics used and corresponding cutoff thresholds, number of readers and their experience, blinding; and (3) technical characteristics of mpMRI, including magnetic field strength, $\boldsymbol{b}$ values, and coil type. We used the Quality Assessment of Diagnostic Accuracy Studies-2 to evaluate the quality of studies and likelihood of bias (21), in which four domains were scored for individual study: patient selection, method of the index test (parameter measurement and use of appropriate threshold to classify lesions), using pathological results as a reference standard, and flow and timing. Data extraction was performed by one investigator (LW) and confirmed by a second investigator (SY).

Data Synthesis and Analysis

The degree of heterogeneity between studies was measured using the inconsistency index (I^2): 0–40%, might or have no heterogeneity; 30–60%, moderate heterogeneity; 50–90%, substantial heterogeneity; and 75–100%, considerable heterogeneity (22). The summary estimates of sensitivity and specificity were calculated with the bivariate model and hierarchical summary receiver operating characteristic (HSROC) model (23, 24). The forest plots were used to graphically present the 95% confidence interval (95% CI) of sensitivity and specificity for each study. In addition, an HSROC curve with a 95% confidence region and prediction region was constructed to demonstrate the results. The Deeks' funnel plot was used to estimate the publication bias, and statistical significance was determined by the Deeks' asymmetry test (25).

In the light of varied cutoff values reported across included studies, multiple subgroup analyses were performed to assess the following various clinical settings: (1) use of tumor size ≥15 mm as the cutoff threshold, (2) use of the value of ADC mean, (3) use of LCC ≤10 mm as the cutoff threshold, (4) use of LCC ≤12 mm as the cutoff threshold, (5) use of LCC >10 mm as the cutoff threshold, (6) use of LCC >12 mm as the cutoff threshold. We performed meta-regression to explore the sources of heterogeneity. For studies using LCC as the quantitative metric, the following covariates were added to the bivariate model: (1) study design (prospective *vs.* retrospective), (2) patient number (≤150 *vs.* >150), (3) magnetic field strength (1.5 T *vs.* 3.0 T), (4) malignant rate (≤30 *vs.* >30%), (5) LCC length (≤10 *vs.* >10 mm, and ≤12 *vs.* >12 mm), (6) reader number (<2 *vs.* ≥2), (7) blinded to the final results (blinded *vs.* aware partial patient information), (8) publication year (≤2017 *vs.* >2017), and (9) length of tumor size (15 *vs.* >15 mm). All analyses were conducted using STATA 16.0, and statistical significance was set at ***P*** values less than 0.05.

RESULTS

Literature Search

A flow chart summarizing the publication selection process is presented in **Figure 1**. Our literature search initially yielded 438 results, of which 251 were excluded owing to duplicates. After screening of titles and abstracts, a total of 125 results were excluded. Full-text analysis was performed among the remaining 62 potentially eligible articles, and 39 were excluded for reasons as follows: with insufficient data to reconstruct 2×2 tables (*n*=27), not in the field of interest (*n*=8), and partially overlapping patient cohort (*n*=4). Finally, a total of 23 studies with 3,931 participants assessing diagnostic performance of mpMRI quantitative metrics for detection of EPE were included in this study (26–48).

Characteristics of the Included Studies

The detailed demographic characteristics are summarized in **Table 1**. The sample size of the study population ranged from 25 to 553 patients, with a mean age of 60–68 years. Based on pathological results after RP, EPE was found in 23–67% percent of participants. The PSA levels of participants ranged from 2.1 to 58.7, with a Gleason score of 5–10. In 16 studies, LCC was used

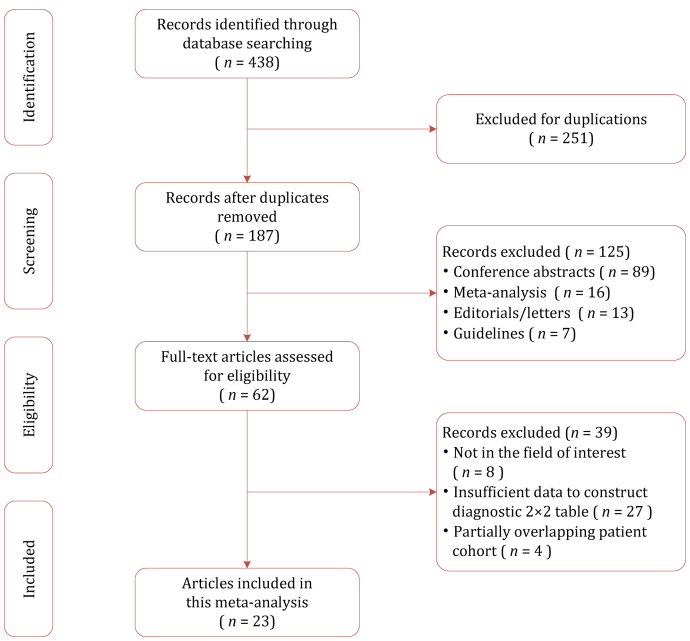

FIGURE 1 | Study selection process for this systematic review and meta-analysis.

TABLE 1 | Demographic characteristics of the included studies.

First Author	Country	Year	Period	Patients number	Malignant	Age (year, mean ± SD/median, range)	PSA (ng/ml, mean ± SD)	GS (Range)
Abreu-Gomez et al. (26)	Canada	2020	2012/2018	267	223	63 ± 6	11.7 ± 10.8	≥6
Ahn et al. (27)	Korea	2019	Jan. 2011/Dec. 2016	221	69	<75	16.7 ± 17.4	6–9
Baco et al. (28)	Norway	2014	Jan. 2010/Jul. 2013	111	40	64 (45–75)	8.9 (2.5–44.0)	6–9
Bakir et al. (30)	Turkey	2020	2012/2018	86	24	62.5 ± 6.2	7.52 (2.1–40.0)	NA
Caglic et al. (48)	UK	2019	Sep. 2014/Jan. 2017	75	48	64.5 (57.2–67)	8.5 (5.7–10.4)	6–9
Costa et al. (29)	USA	2018	Nov. 2015/Jul. 2016	80	46	64 ± 8	8.0 ± 6.1	≥6
Dominguez et al. (32)	Colombia	2018	May. 2011/Dec. 2013	79	33	61.1 ± 7.5	7.0 ± 7.25	6–9
Kim et al. (40)	Korea	2014	Feb. 2006/Apr. 2008	167	23	66.5 (52–78) *	8.5 (1.1–37.3) *	6–9
Kim et al. (41)	Korea	2016	Dec. 2013/Jan. 2015	292	111	64.5 (42–79) *	10.4 (0.13–58.7) *	6–10
Krishna et al. (35)	Canada	2017	Nov. 2012/May. 2015	149	92	62.8 ± 6.1	7.8 ± 7.0	6–9
Lim et al. (42)	Canada	2015	Jan. 2012/Jun. 2014	73	38	62.8 ± 5.7	10.7 ± 10.6	6–9
Lim et al. (43)	Canada	2016	May. 2012/May. 2015	113	76	63 ± 5.8	8.8 ± 9.3	6–9
Matsuoka et al. (36)	Japan	2017	Aug. 2007/Mar. 2015	210	56	67 (50–81)	7.0 (2.9–30.0)	5–10
Mehralivand et al. (38)	USA	2019	Jun. 2007/Mar. 2017	553	125	60 ± 8	6.3 (0.2–170)	6–10
Rud et al. (39)	Norway	2018	Dec. 2009/Jun. 2012	183	103	65 (60–68)	7.9 (5.8–11.5)	6–9
Kongnyuy et al. (34)	USA	2016	May. 2017/Dec. 2015	397	87	60.0 (38–76)	5.5 (0.1–55.7)	≥6
Park et al. (46)	Korea	2020	Jul. 2016/Mar. 2017	301	129	65 ± 7	7.6 ± 5.6	6–10
Woo et al. (45)	Korea	2015	Jan. 2013/Dec. 2013	117	50	68.0 ± 6.8	12.2 ± 13.1	6–10
Woo et al. (44)	Korea	2016	Jan. 2012/Dec. 2012	185	51	66.7 ± 7.0	10.2 ± 13.6	6–9
Schieda et al. (37)	Canada	2016	Jan. 2012/Dec. 2015	25	13	65.0 ± 5.9	9.9 ± 7.7	6–9
Giganti et al. (33)	Italy	2016	NA	70	23	64 (58.9–70.5)	6.8 (5.0–9.9)	6–10
Onay et al. (31)	Turkey	2019	2012/2017	105	24	62 (40–77) *	7.95 (2.1–46.0) *	NA
Rosenkrantz et al. (47)	USA	2015	NA	90	23	64 ± 8	9.0 ± 11.4	6–9

NA, not available; SD, standard deviation; PSA, prostate serum antigen; GS, Gleason score.
**mean, range.*

for independent predictor of EPE, with cutoff values ranging from 6 to 20 mm (27–29, 31, 32, 34–36, 38, 39, 43, 44, 46–48). In three studies, tumor size was used for independent predictor, with a cutoff value of 0.9–2.1 (33, 39, 42). The diagnostic accuracy of using ADC value as independent predictor was reported by seven studies (32, 33, 35, 39–41, 45). In five studies, tumor volume was used as independent predictor, with cutoff thresholds ranging from 15 to 19 mm (26, 27, 35, 37, 46). Regarding study design, only four studies (34, 36, 38, 39) were prospective, and all of the remaining 19 studies were retrospective in nature. In 18 studies, the MRI was performed with 3.0 T scanners, whereas in the remaining five studies, MRI was performed with 1.5 T scanners (28, 32, 33, 36, 39). The MRI images were interpreted by one to three radiologists, with experience of 2–23 years. Most studies reported that radiologists were blinded to final pathological results; however, in seven studies, the readers were aware that patients had PCa (30–32, 40, 41, 45, 46). The study characteristics are summarized in **Table 2**.

Quality Assessment

The overall quality of the included studies was not substantially high. Concerning the patient selection domain, there was generally high risk of bias because the majority of included studies were retrospective in design (34, 36, 38, 39). In four studies, patients who classified as PI-RADS score 1–3 were excluded (26, 27, 43, 48), and in two studies, the location was restricted to the anterior prostate cancer (27, 37). Regarding the index test domain, in seven studies the radiologists were aware that patients had biopsy-proven PCa but did not know the final

TABLE 2 | Study Characteristics of Included Studies.

First Author	Design	Readers	Experience (Year)	Magnet field strength	*b* Values (mm/s^2)	Coil	Blinded	Assessment metric	Cutoff threshold[†]
Abreu-Gomezet al. (26)	Retrospective	2	13/17	3.0 T	0/500/1,000	Surface	Yes	Size	15/19
Ahnet al. (27)	Retrospective	2	23/19	3.0 T	0/100/1,000	Cardiac	Yes	LLC/Size	10–16/18
Baco et al. (28)	Retrospective	1	>700 cases	1.5 T	0/500/2,000	Surface	NA	LLC	20
Bakir et al. (30)	Retrospective	3	3/6	3.0 T	0–800	Surface	Yes*	LLC	15.2/16.1
Caglic et al. (48)	Retrospective	1	8	3.0 T	150/750/1,400/ 2,000	PAC	Yes	LLC	10.5/13.5
Costa et al. (29)	Retrospective	3	NA	3.0 T	0–2,000	ERC	Yes	LLC	10
Dominguez et al. (32)	Retrospective	2	8/14	1.5 T	NA	None	Yes*	LLC/ADC	12/0.87
Kim et al. (40)	Retrospective	2	7/9	3.0 T	1,000	PAC	Yes*	ADC	1.09
Kim et al. (41)	Retrospective	2	2/9	3.0 T	NA	PAC	Yes*	ADC	0.785
Krishna et al. (35)	Retrospective	2	11/15	3.0 T	0/500/1,000	Surface	Yes	ADC/LLC/Size	6.991/11/15
Lim et al. (42)	Retrospective	2	9/14	3.0 T	0/500/1,000	Surface	Yes	Volume	2.1
Lim et al. (43)	Retrospective	2	11/15	3.0 T	0/500/1,000	Surface	Yes	LLC	15
Matsuoka et al. (36)	Prospective	2	5/10	1.5 T	0/1,000/2,000	Surface	Yes	LLC	10
Mehralivand et al. (38)	Prospective	2	9/15	3.0 T	1,500/2,000	Cardiac	Yes	LLC	15
Rud et al. (39)	Prospective	1	2	1.5 T	50–1,000	Surface	Yes	LLC/Volume/ADC	13/0.9/0.89
Kongnyuy et al. (34)	Prospective	2	8/16	3.0 T	NA	Surface	Yes	LLC	12.5
Park et al. (46)	Retrospective	2	3/15	3.0 T	0/50/500/1,000	Surface	Yes*	LLC/Size	10/15
Woo et al. (45)	Retrospective	2	21/9	3.0 T	0/1,000	None	Yes*	ADC	0.893
Woo et al. (44)	Retrospective	1	22	3.0 T	0/1,000	NA	Yes	LLC	12/13/14
Schieda et al. (37)	Retrospective	2	11/16	3.0 T	0/500/1,000/ 1,500	PAC	Yes	Size	16
Giganti et al. (33)	Retrospective	3	NA	1.5 T	0/800/1,600	ERC	Yes	ADC/Volume	0.84/0.88
Onay et al. (31)	Retrospective	2	5/12	3.0 T	0–800	Surface	Yes*	LLC	13/13.5
Rosenkrantz et al. (47)	Retrospective	2	1/4	3.0 T	50 and 1,000	PAC	Yes	LLC	6

ADC, apparent diffusion coefficient; ERC, endorectal coil; LCC, length of capsular contact; NA, not available; PAC, phase-array coil; RP, radical prostatectomy; SD, standard deviation.
**Aware that all patients had prostate cancer.*
[†]For length of capsular contact and tumor size, mm; for tumor volume, ml.

pathological results (30–32, 40, 41, 45, 46). One study had a concern of applicability because the blinding was not reported explicitly (28). Concerning the flow and timing domain, all studies were scored as low risk of bias as patients received the same reference standard. **Figure 2** shows the detailed quality assessment of included studies.

Diagnostic Performance of Different Quantitative Methods

The pooled diagnostic performance of LCC, ADC, and tumor size for detection of EPE is demonstrated in **Figure 3**, and the HSROC curve is presented in **Figure 4**. Regarding LCC, the pooled sensitivity and specificity were 0.79 (95% CI 0.75–0.83,

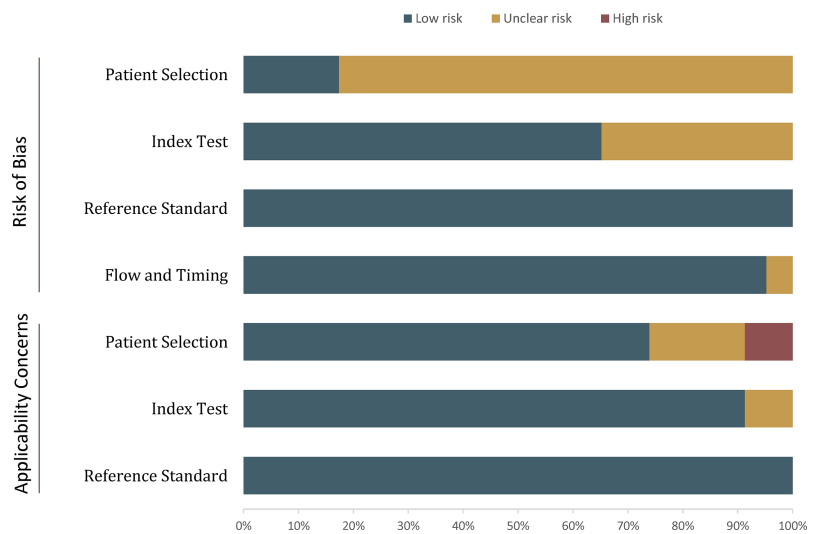

FIGURE 2 | Grouped bar charts show the risk of bias and concerns for applicability of included studies.

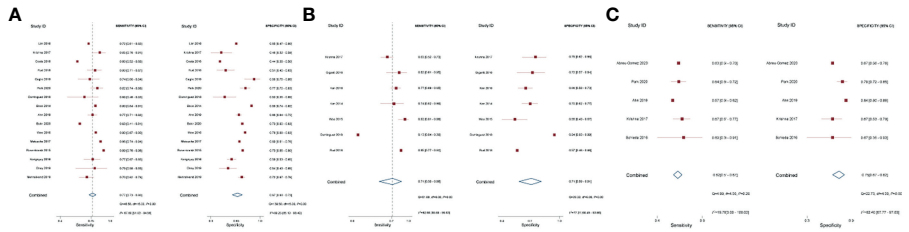

FIGURE 3 | Coupled forest plot of pooled sensitivity and specificity. Numbers are pooled estimates with 95% CI in parentheses. Corresponding heterogeneity statistics are provided at bottom right corners. Horizontal lines indicate 95% confidence intervals. **(A)** Length of capsular contact; **(B)** apparent diffusion coefficient; **(C)** tumor size.

I^2 = 67.8%) and 0.77 (95% CI 0.73–0.80, I^2 = 89.3%), with area under HSROC curve of 0.67 (95% CI 0.60–0.73). For ADC, the pooled sensitivity and specificity were 0.71 (95% CI 0.50–0.86, I^2 = 92.7%) and 0.71 (95% CI 059–0.81, I^2 = 77.2%), with area under HSROC curve of 0.77 (95% CI 0.73–0.80). Regarding tumor size, the pooled sensitivity and specificity were 0.62 (95% CI 0.57–0.67, I^2 = 19.8%) and 0.75 (95% CI 0.67–0.82, I^2 = 82.4%), with area under HSROC curve of 0.70 (95% CI 0.66–0.74). As for tumor volume, the pooled sensitivity and specificity were 0.77 (95% CI 0.68–0.84) and 0.72 (95% CI 0.56–0.83), with area under HSROC curve of 0.78 (95% CI 0.73–0.97). The Deeks' funnel plot and asymmetry test demonstrated that there was no significant probability of publication bias regarding the four quantitative metrics, with ***P*** values ranging from 0.34 to 0.93 (**Figure 5**).

We performed direct comparisons between different quantitative metrics in studies providing head-to-head comparisons. Concerning LCC *vs.* ADC, the pooled summary estimates based on three studies revealed that LCC yielded significantly higher specificity as compared to ADC (0.49 *vs.* 0.79, P=0.047); however, there was no significant difference in sensitivity (0.79 *vs.* 0.55, P=0.22) (32, 35, 39). As for LCC *vs.* tumor size, the pooled summary estimates based on three studies indicated that LCC yielded significantly higher sensitivity as compared to tumor size (0.80 *vs.* 0.60, P=0.003), but at the cost of decreased specificity (0.65 *vs.* 0.78, P=0.13) (27, 35, 46). In indirect comparisons, we noted that the pooled sensitivity of LCC and tumor volume was significantly higher than tumor size, with P values of 0.002 and 0.013, respectively. Additionally, the pooled specificity for tumor volume was significantly higher than tumor size (P=0.04). Otherwise, the indirect comparisons did not identify any statistically significant differences between these four quantitative metrics (**Supplementary Table 1**).

Subgroup Analysis and Meta-Regression

In view of different cutoff thresholds were used, we performed multiple subgroup analyses to evaluate various clinical settings. Regarding the tumor size, the pooled sensitivity and specificity were 0.72 (95% CI 0.47–0.89) and 0.70 (95% CI 0.56–0.82) for four studies using 15 mm as the cutoff threshold (26, 27, 35, 46). Regarding the ADC, the pooled sensitivity and specificity were 0.67 (95% CI 0.62–0.72) and 0.70 (95% CI 0.63–0.76) for six studies using ADC mean value (32, 33, 39–41). Regarding the LCC, the pooled sensitivity and specificity for six studies using a cutoff threshold ≤10 mm were 0.78 (95% CI 0.71–0.84) and 0.67 (95% CI 0.59–0.75), for 11 studies using a cutoff threshold ≤12 mm were 0.78 (95% CI 0.73–0.83) and 0.67 (95% CI 0.60–0.74), for 20 studies using a cutoff threshold >10 mm were 0.74

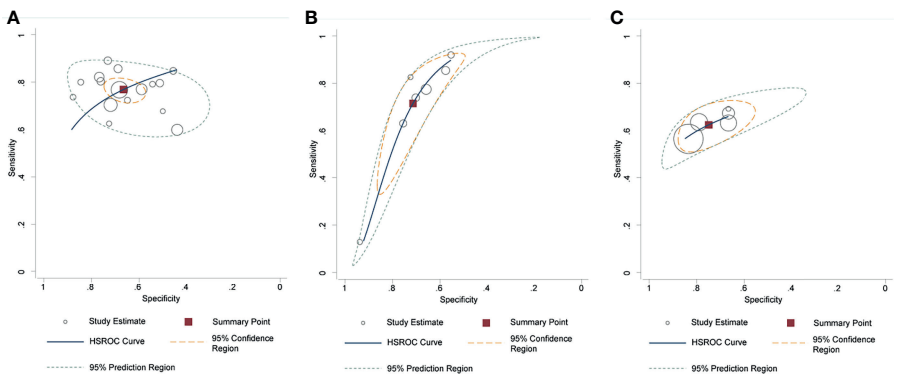

FIGURE 4 | Hierarchic summary receiver operating characteristic plots with summary point and 95% confidence area for the overall. **(A)** length of capsular contact; **(B)** apparent diffusion coefficient; **(C)** tumor size.

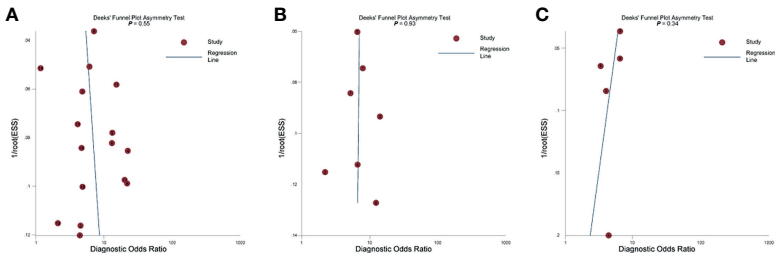

FIGURE 5 | The Deeks' funnel plot. **(A)** Length of capsular contact; **(B)** apparent diffusion coefficient; **(C)** tumor size.

(95% CI 0.70–0.78) and 0.68 (95% CI 0.62–0.74), for 15 studies using a cutoff threshold >12 mm were 0.73 (95% CI 0.68–0.77) and 0.69 (95% CI 0.61–0.75).

As considerable heterogeneity existed among included studies, we performed meta-regression to investigate the sources. Concerning studies using LCC, only publication year (≤2017 *vs.* >2017, P=0.02) was significantly associated with heterogeneity. Other factors such as length of LCC (≤10 *vs.* >10 mm and ≤12 *vs.* >12 mm), malignant rate (≤30 *vs.* >30%), study design (prospective *vs.* retrospective), magnet field strength (1.5 *vs.* 3.0 T), number of readers (<2 *vs.* ≥2), number of patients (≤150 *vs.* >150), and the publication year (≤2017 *vs.* >2017) were not significant factors contributing to heterogeneity, with ***P*** ranging from 0.11 to 0.96. For studies using other quantitative metrics, no significant factor was found substantially associated with heterogeneity, which are demonstrated in **Supplementary Table 2**.

DISCUSSION

In this meta-analysis, we investigated the diagnostic performance of several quantitative metrics with mpMRI for prediction of EPE at radical prostatectomy. The summary estimates of sensitivity and specificity for 16 studies using LCC were 0.79 (95% CI 0.75–0.83) and 0.77 (95% CI 0.73–0.80), for seven studies using ADC were 0.71 (95% CI 0.50–0.86) and 0.71 (95% CI 059–0.81), for five studies using tumor size were 0.62 (95% CI 0.57–0.67) and 0.75 (95% CI 0.67–0.82), and for three studies using tumor volume were 0.77 (95% CI 0.68–0.84) and 0.72 (95% CI 0.56–0.83), respectively. As considerable heterogeneity was observed between studies, we performed meta-regression to explore the sources. Among the several potential factors, we found that only publication year (≤2017 *vs.* >2017) was the significant factor responsible for heterogeneity (P=0.02). As several studies provided head-to-head comparison between LCC and ADC, as well as between LCC and tumor size, we performed direct comparison in available studies. According to our analyses, LCC was significantly inferior to ADC in specificity but was superior to tumor size in sensitivity; nevertheless, both comparisons were based on merely three studies and need more large-sample studies to validate in future.

LLC is defined as the length of prostate tumor in contact with the capsule, and the rationale behind which is that greater LCC on histopathology correlates with higher probability of EPE (49). A prior meta-analysis investigated the diagnostic accuracy of using LCC as independent predictor for detection of EPE, in which the pooled sensitivity and specificity were 0.79 and 0.67 (50). As for ADC, studies revealed that as tumor grade increases, a trend of increasing cellular density, with loss of the normal glandular structures and a decrease in the extracellular space, limiting water diffusivity and yielding lower ADC values (51, 52). ADC value has been shown to inversely correlate with pathological stage (42, 53), and a previous study demonstrated that when combining ADC value with other clinical information, the pooled sensitivity and specificity were 0.85 and 0.71 (54). The rationale of using tumor volume as predictor of EPE is based on findings that the diameter of the index lesion has a strong correlation with tumor volume at radical prostatectomy (42, 55). We performed indirect comparisons between these quantitative metrics, and the results demonstrated that the pooled sensitivity from tumor size was significantly lower than LCC (P=0.002) and tumor volume (P=0.013). Moreover, our analyses showed that the pooled specificity in tumor size was substantially lower than tumor size (P=0.04). However, these results were obtained from indirect comparisons thus should be interpreted with caution.

Considering that different cutoff thresholds were used with respect to LCC and tumor size, multiple subgroup analyses were performed to account for various outcomes. When restricted subgroup analysis to six studies using a cutoff value ≤10 mm, the pooled sensitivity and specificity were 0.78 and 0.67. In contrast, a cutoff value >10 mm yielded slightly lower sensitivity (0.74) and equivalent specificity (0.68). Likewise, a cutoff threshold ≤12 mm yielded an equivalent diagnostic performance as compared with >12 mm, with sensitivity of 0.78 *vs.* 0.73 and specificity of 0.67 *vs.* 0.69. As for the tumor size, subgroup analysis suggested that using a tumor size of 15 mm yield a moderate diagnostic performance, with sensitivity of 0.67 and specificity of 0.70. When compared with the subjective assessment that mainly depends on radiologists' personal pattern and experience, the quantitative analysis offers several potential advantages of improving accuracy, interobserver agreement, and histopathology correlation. However, different

measurement methods and tools, as well as MRI techniques and sequences, all may affect the final results, then lead to widely varied optimal cutoff values (18, 19). Regarding LCC, the reported optimal cutoff values ranged from 6 to 20 mm, with corresponding sensitivity of 0.60–0.89 and specificity of 0.44–0.88. Nevertheless, no significant difference between these cutoff thresholds. As for tumor size, although the PI-RADS recommends 15 mm for prediction of EPE, two studies demonstrated that a cutoff value of 16–18 mm yielded the best diagnostic performance (27, 37). With regard to ADC, despite that most studies included used the mean value as the assessment, two studies reported that results from ADC ratio or ADC entropy were superior to ADC mean value for distinguishing malignant from benign (33, 35). Using tumor volume as assessment for prediction of EPE was reported by merely three studies, which may be that it is often time-consuming and may require postprocessing on an independent workstation (33, 39, 43).

Our study has some limitations. First, most studies included were retrospective in study design, which resulted in a high risk regarding patient selection domain. Nevertheless, considering that nearly all studies available were retrospective, it was unfeasible to calculate summary estimates from the merely four prospective studies. Second, the heterogeneity was substantial among studies, which affected the general applicability of our study. We performed meta-regression and multiple subgroup analyses to explore the sources of heterogeneity; however, we found that most clinical covariates were not associated with the heterogeneity, thus a large proportion of which remains unexplained. Nonetheless, we applied a solid and robust methodology for this meta-analysis using the guidelines published by the Cochrane Collaboration. Third, the diagnostic results were extracted from the most accurate results; moreover, the size or length was measured using different MRI sequences or techniques. Last, the comparisons were based on indirect or merely several studies; thus, the results should be interpreted with caution.

CONCLUSION

The mpMRI quantitative assessments of LCC, ADC, tumor size, and tumor volume showed moderate to high diagnostic performance in the prediction of EPE, of them LCC and tumor volume demonstrated higher accuracy than other assessments. However, the optimal cutoff threshold varied widely and should be established to apply them in clinical practice.

DATA AVAILABILITY STATEMENT

The original contributions presented in the study are included in the article/**Supplementary Material**. Further inquiries can be directed to the corresponding author.

AUTHOR CONTRIBUTIONS

Guarantor of the article: HTX. Conception and design: WL and YS. Collection and assembly of data: YMW and FL. Data analysis and interpretation: WL, YMW, and FL. All authors contributed to the article and approved the submitted version.

FUNDING

This study was supported by the Natural Science Foundation of Jiangsu Vocational College of Medicine (No. 20204112).

SUPPLEMENTARY MATERIAL

The Supplementary Material for this article can be found online at: https://www.frontiersin.org/articles/10.3389/fonc.2021.771864/full#supplementary-material

REFERENCES

1. Tollefson MK, Karnes RJ, Rangel LJ, Bergstralh EJ, Boorjian SA. The Impact of Clinical Stage on Prostate Cancer Survival Following Radical Prostatectomy. *J Urol* (2013) 189:1707–12. doi: 10.1016/j.juro.2012.11.065
2. Mikel Hubanks J, Boorjian SA, Frank I, Gettman MT, Houston Thompson R, Rangel LJ, et al. The Presence of Extracapsular Extension Is Associated With an Increased Risk of Death From Prostate Cancer After Radical Prostatectomy for Patients With Seminal Vesicle Invasion and Negative Lymph Nodes. *Urol Oncol* (2014) 32:26.e1–7. doi: 10.1016/j.urolonc.2012.09.002
3. Quinlan DM, Epstein JI, Carter BS, Walsh PC. Sexual Function Following Radical Prostatectomy: Influence of Preservation of Neurovascular Bundles. *J Urol* (1991) 145:998–1002. doi: 10.1016/s0022-5347(17)38512-9
4. Swindle P, Eastham JA, Ohori M, Kattan MW, Wheeler T, Maru N, et al. Do Margins Matter? The Prognostic Significance of Positive Surgical Margins in Radical Prostatectomy Specimens. *J Urol* (2008) 179:S47–51. doi: 10.1016/j.juro.2008.03.137
5. Avulova S, Zhao Z, Lee D, Huang L-C, Koyama T, Hoffman KE, et al. The Effect of Nerve Sparing Status on Sexual and Urinary Function: 3-Year Results From the CEASAR Study. *J Urol* (2018) 199:1202–9. doi: 10.1016/j.juro.2017.12.037
6. Eifler JB, Feng Z, Lin BM, Partin MT, Humphreys EB, Han M, et al. An Updated Prostate Cancer Staging Nomogram (Partin Tables) Based on Cases From 2006 to 2011. *BJU Int* (2013) 111:22–9. doi: 10.1111/j.1464-410X.2012.11324.x
7. Brajtbord JS, Leapman MS, Cooperberg MR. The CAPRA Score at 10 Years: Contemporary Perspectives and Analysis of Supporting Studies. *Eur Urol* (2017) 71:705–9. doi: 10.1016/j.eururo.2016.08.065
8. Ohori M, Kattan MW, Koh H, Maru N, Slawin KM, Shariat S, et al. Predicting the Presence and Side of Extracapsular Extension: A Nomogram for Staging Prostate Cancer. *J Urol* (2004) 171:1844–9. doi: 10.1097/01.ju.0000121693.05077.3d
9. Augustin H, Fritz GA, Ehammer T, Auprich M, Pummer K. Accuracy of 3-Tesla Magnetic Resonance Imaging for the Staging of Prostate Cancer in Comparison to the Partin Tables. *Acta Radiol* (2009) 50:562–9. doi: 10.1080/02841850902889846
10. Gupta RT, Faridi KF, Singh AA, Passoni NM, Garcia-Reyes K, Madden JF, et al. Comparing 3-T Multiparametric MRI and the Partin Tables to Predict Organ-Confined Prostate Cancer After Radical Prostatectomy. *Urol Oncol Semin Orig Investig* (2014) 32:1292–9. doi: 10.1016/j.urolonc.2014.04.017
11. Barentsz JO, Richenberg J, Clements R, Choyke P, Verma S, Villeirs G, et al. ESUR Prostate MR Guidelines 2012. *Eur Radiol* (2012) 22:746–57. doi: 10.1007/s00330-011-2377-y

12. Weinreb JC, Barentsz JO, Choyke PL, Cornud F, Haider MA, Macura KJ, et al. PI-RADS Prostate Imaging – Reporting and Data System: 2015, Version 2. *Eur Urol* (2016) 69:16–40. doi: 10.1016/j.eururo.2015.08.052
13. Turkbey B, Rosenkrantz AB, Haider MA, Padhani AR, Villeirs G, Macura KJ, et al. Prostate Imaging Reporting and Data System Version 2.1: 2019 Update of Prostate Imaging Reporting and Data System Version 2. *Eur Urol* (2019) 76:340–51. doi: 10.1016/j.eururo.2019.02.033
14. Hamoen EHJ, Rooij M, Witjes JA, Barentsz JO, Rovers MM. Use of the Prostate Imaging Reporting and Data System (PI-RADS) for Prostate Cancer Detection With Multiparametric Magnetic Resonance Imaging: A Diagnostic Meta-Analysis. *Eur Urol* (2015) 67:1112–21. doi: 10.1016/j.eururo.2014.10.033
15. Woo S, Suh CH, Kim SY, Cho JY, Kim SH. Diagnostic Performance of Prostate Imaging Reporting and Data System Version 2 for Detection of Prostate Cancer: A Systematic Review and Diagnostic Meta-Analysis. *Eur Urol* (2017) 72:177–88. doi: 10.1016/j.eururo.2017.01.042
16. Kayat Bittencourt L, Litjens G, Hulsbergen-van de Kaa CA, Turkbey B, Gasparetto EL, Barentsz JO. Prostate Cancer: The European Society of Urogenital Radiology Prostate Imaging Reporting and Data System Criteria for Predicting Extraprostatic Extension by Using 3-T Multiparametric MR Imaging. *Radiology* (2015) 276:479–89. doi: 10.1148/radiol.15141412
17. Schieda N, Quon JS, Lim C, El-Khodary M, Shabana W, Singh V, et al. Evaluation of the European Society of Urogenital Radiology (ESUR) PI-RADS Scoring System for Assessment of Extra-Prostatic Extension in Prostatic Carcinoma. *Eur J Radiol* (2015) 84:1843–8. doi: 10.1016/j.ejrad.2015.06.016
18. Schieda N, Lim CS, Zabihollahy F, Abreu-Gomez J, Krishna S, Woo S, et al. Quantitative Prostate MRI. *J Magn Reson Imaging* (2020) 53:1632–45. doi: 10.1002/jmri.27191
19. Shieh AC, Guler E, Ojili V, Paspulati RM, Elliott R, Ramaiya NH, et al. Extraprostatic Extension in Prostate Cancer: Primer for Radiologists. *Abdom Radiol N Y* (2020) 45:4040–51. doi: 10.1007/s00261-020-02555-x
20. Liberati A, Altman DG, Tetzlaff J, Mulrow C, Gøtzsche PC, Ioannidis JPA, et al. The PRISMA Statement for Reporting Systematic Reviews and Meta-Analyses of Studies That Evaluate Healthcare Interventions: Explanation and Elaboration. *Epidemiol Biostat Public Health* (2009) 6:e1–34. doi: 10.1136/bmj.b2700
21. Whiting PF. QUADAS-2: A Revised Tool for the Quality Assessment of Diagnostic Accuracy Studies. *Ann Intern Med* (2011) 155:529. doi: 10.7326/0003-4819-155-8-201110180-00009
22. Higgins JPT, Altman DG, Gøtzsche PC, Jüni P, Moher D, Oxman AD, et al. The Cochrane Collaboration's Tool for Assessing Risk of Bias in Randomised Trials. *BMJ* (2011) 343:889–93. doi: 10.1136/bmj.d5928
23. Reitsma JB, Glas AS, Rutjes AWS, Scholten RJPM, Bossuyt PM, Zwinderman AH. Bivariate Analysis of Sensitivity and Specificity Produces Informative Summary Measures in Diagnostic Reviews. *J Clin Epidemiol* (2005) 58:982–90. doi: 10.1016/j.jclinepi.2005.02.022
24. Rutter CM, Gatsonis CA. A Hierarchical Regression Approach to Meta-Analysis of Diagnostic Test Accuracy Evaluations. *Stat Med* (2001) 20:2865–84. doi: 10.1002/sim.942
25. Deeks JJ. Systematic Reviews of Evaluations of Diagnostic and Screening Tests. *BMJ* (2001) 323:157–62. doi: 10.1136/bmj.323.7305.157
26. Abreu-Gomez J, Walker D, Alotaibi T, McInnes MDF, Flood TA, Schieda N. Effect of Observation Size and Apparent Diffusion Coefficient (ADC) Value in PI-RADS V2.1 Assessment Category 4 and 5 Observations Compared to Adverse Pathological Outcomes. *Eur Radiol* (2020) 30:4251–61. doi: 10.1007/s00330-020-06725-9
27. Ahn H, Hwang SI, Lee HJ, Suh HS, Choe G, Byun S-S, et al. Prediction of Extraprostatic Extension on Multi-Parametric Magnetic Resonance Imaging in Patients With Anterior Prostate Cancer. *Eur Radiol* (2020) 30:26–37. doi: 10.1007/s00330-019-06340-3
28. Baco E, Rud E, Vlatkovic L, Svindland A, Eggesbø HB, Hung AJ, et al. Predictive Value of Magnetic Resonance Imaging Determined Tumor Contact Length for Extracapsular Extension of Prostate Cancer. *J Urol* (2015) 193:466–72. doi: 10.1016/j.juro.2014.08.084
29. Costa DN, Passoni NM, Leyendecker JR, de Leon AD, Lotan Y, Roehrborn CG, et al. Diagnostic Utility of a Likert Scale Versus Qualitative Descriptors and Length of Capsular Contact for Determining Extraprostatic Tumor Extension at Multiparametric Prostate MRI. *Am J Roentgenol* (2018) 210:1066–72. doi: 10.2214/AJR.17.18849
30. Bakir B, Onay A, Vural M, Armutlu A, Yıldız SÖ, Esen T. Can Extraprostatic Extension Be Predicted by Tumor-Capsule Contact Length in Prostate Cancer? Relationship With International Society of Urological Pathology Grade Groups. *AJR Am J Roentgenol* (2020) 214:588–96. doi: 10.2214/AJR.19.21828
31. Onay A, Vural M, Armutlu A, Ozel Yıldız S, Kiremit MC, Esen T, et al. Evaluation of the Most Optimal Multiparametric Magnetic Resonance Imaging Sequence for Determining Pathological Length of Capsular Contact. *Eur J Radiol* (2019) 112:192–9. doi: 10.1016/j.ejrad.2019.01.020
32. Dominguez C, Plata M, Cataño J, Palau M, Aguirre D, Narvaez J, et al. Diagnostic Accuracy of Multiparametric Magnetic Resonance Imaging in Detecting Extracapsular Extension in Intermediate and High - Risk Prostate Cancer. *Int Braz J Urol* (2018) 44:688–96. doi: 10.1590/S1677-5538.IBJU.2016.0485
33. Giganti F, Coppola A, Ambrosi A, Ravelli S, Esposito A, Freschi M, et al. Apparent Diffusion Coefficient in the Evaluation of Side-Specific Extracapsular Extension in Prostate Cancer: Development and External Validation of a Nomogram of Clinical Use. *Urol Oncol* (2016) 34:291.e9–291.e17. doi: 10.1016/j.urolonc.2016.02.015
34. Kongnyuy M, Sidana A, George AK, Muthigi A, Iyer A, Ho R, et al. Tumor Contact With Prostate Capsule on Magnetic Resonance Imaging: A Potential Biomarker for Staging and Prognosis. *Urol Oncol Semin Orig Investig* (2016) 35:30.e1–30.e8. doi: 10.1016/j.urolonc.2016.07.013
35. Krishna S, Lim CS, Mcinnes MDF, Flood TA, Shabana WM, Lim RS, et al. Evaluation of MRI for Diagnosis of Extraprostatic Extension in Prostate Cancer. *J Magn Reson Imaging* (2017) 47:176–85. doi: 10.1002/jmri.25729/pdf
36. Matsuoka Y, Ishioka J, Tanaka H, Kimura T, Yoshida S, Saito K, et al. Impact of the Prostate Imaging Reporting and Data System, Version 2, on MRI Diagnosis for Extracapsular Extension of Prostate Cancer. *Am J Roentgenol* (2017) 209:W76–84. doi: 10.2214/AJR.16.17163
37. Schieda N, Lim CS, Idris M, Lim RS, Morash C, Breau RH, et al. MRI Assessment of Pathological Stage and Surgical Margins in Anterior Prostate Cancer (APC) Using Subjective and Quantitative Analysis. *J Magn Reson Imaging* (2017) 45:1296–303. doi: 10.1002/jmri.25510
38. Mehralivand S, Shih JH, Harmon S, Smith C, Bloom J, Czarniecki M, et al. A Grading System for the Assessment of Risk of Extraprostatic Extension of Prostate Cancer at Multiparametric MRI. *Radiology* (2019) 290:709–19. doi: 10.1148/radiol.2018181278
39. Rud E, Diep L, Baco E. A Prospective Study Evaluating Indirect MRI-Signs for the Prediction of Extraprostatic Disease in Patients With Prostate Cancer: Tumor Volume, Tumor Contact Length and Tumor Apparent Diffusion Coefficient. *World J Urol* (2018) 36:629–37. doi: 10.1007/s00345-018-2171-4
40. Kim CK, Park SY, Park JJ, Park BK. Diffusion-Weighted MRI as a Predictor of Extracapsular Extension in Prostate Cancer. *AJR Am J Roentgenol* (2014) 202:W270. doi: 10.2214/AJR.13.11333
41. Kim W, Kim CK, Park JJ, Kim M, Kim J-H. Evaluation of Extracapsular Extension in Prostate Cancer Using Qualitative and Quantitative Multiparametric MRI. *J Magn Reson Imaging* (2017) 45:1760–70. doi: 10.1002/jmri.25515
42. Lim C, Flood TA, Hakim SW, Shabana WM, Quon JS, Elkhodary M, et al. Evaluation of Apparent Diffusion Coefficient and MR Volumetry as Independent Associative Factors for Extra-Prostatic Extension (EPE) in Prostatic Carcinoma. *J Magn Reson Imaging* (2016) 43:726–36. doi: 10.1002/jmri.25033
43. Lim CS, McInnes MDF, Lim RS, Breau RH, Flood TA, Krishna S, et al. Prognostic Value of Prostate Imaging and Data Reporting System (PI-RADS) V. 2 Assessment Categories 4 and 5 Compared to Histopathological Outcomes After Radical Prostatectomy. *J Magn Reson Imaging* (2016) 46:257–66. doi: 10.1002/jmri.25539
44. Woo S, Kim SY, Cho JY, Kim SH. Length of Capsular Contact on Prostate MRI as a Predictor of Extracapsular Extension: Which Is the Most Optimal Sequence? *Acta Radiol* (2017) 58:489–97. doi: 10.1177/0284185116658684
45. Woo S, Cho JY, Kim SY, Kim SH. Extracapsular Extension in Prostate Cancer: Added Value of Diffusion-Weighted MRI in Patients With Equivocal Findings on T2-Weighted Imaging. *AJR Am J Roentgenol* (2015) 204:W168–175. doi: 10.2214/AJR.14.12939
46. Park KJ, Kim M, Kim JK. Extraprostatic Tumor Extension: Comparison of Preoperative Multiparametric MRI Criteria and Histopathologic Correlation

After Radical Prostatectomy. *Radiology* (2020) 296:192133. doi: 10.1148/radiol.2020192133
47. Rosenkrantz AB, Shanbhogue AK, Wang A, Kong MX, Babb JS, Taneja SS. Length of Capsular Contact for Diagnosing Extraprostatic Extension on Prostate MRI: Assessment at an Optimal Threshold. *J Magn Reson Imaging* (2016) 43:990–7. doi: 10.1002/jmri.25040
48. Caglic I, Povalej Brzan P, Warren AY, Bratt O, Shah N, Barrett T. Defining the Incremental Value of 3D T2-Weighted Imaging in the Assessment of Prostate Cancer Extracapsular Extension. *Eur Radiol* (2019) 29:5488–97. doi: 10.1007/s00330-019-06070-6
49. Ukimura O, Troncoso P, Ramirez EI, Babaian RJ. Prostate Cancer Staging: Correlation Between Ultrasound Determined Tumor Contact Length and Pathologically Confirmed Extraprostatic Extension. *J Urol* (1998) 159:1251–9. doi: 10.1016/S0022-5347(01)63575-4
50. Kim T-H, Woo S, Han S, Suh CH, Ghafoor S, Hricak H, et al. The Diagnostic Performance of the Length of Tumor Capsular Contact on MRI for Detecting Prostate Cancer Extraprostatic Extension: A Systematic Review and Meta-Analysis. *Korean J Radiol* (2020) 21:684–94. doi: 10.3348/kjr.2019.0842
51. Surov A, Meyer HJ, Wienke A. Correlations Between Apparent Diffusion Coefficient and Gleason Score in Prostate Cancer: A Systematic Review. *Eur Urol Oncol* (2020) 3:489–97. doi: 10.1016/j.euo.2018.12.006
52. Langer DL, van der Kwast TH, Evans AJ, Plotkin A, Trachtenberg J, Wilson BC, et al. Prostate Tissue Composition and MR Measurements: Investigating the Relationships Between ADC, T2, K(trans), V(E), and Corresponding Histologic Features. *Radiology* (2010) 255:485–94. doi: 10.1148/radiol.10091343
53. Lawrence EM, Gallagher FA, Barrett T, Warren AY, Priest AN, Goldman DA, et al. Preoperative 3-T Diffusion-Weighted MRI for the Qualitative and Quantitative Assessment of Extracapsular Extension in Patients With Intermediate- or High-Risk Prostate Cancer. *Am J Roentgenol* (2014) 203:W280–6. doi: 10.2214/AJR.13.11754
54. Bai K, Sun Y, Li W, Zhang L. Apparent Diffusion Coefficient in Extraprostatic Extension of Prostate Cancer: A Systematic Review and Diagnostic Meta-Analysis. *Cancer Manag Res* (2019) 11:3125–37. doi: 10.2147/CMAR.S191738
55. Knoedler JJ, Karnes RJ, Thompson RH, Rangel LJ, Bergstralh EJ, Boorjian SA. The Association of Tumor Volume With Mortality Following Radical Prostatectomy. *Prostate Cancer Prostatic Dis* (2014) 17:144–8. doi: 10.1038/pcan.2013.61

Conflict of Interest: The authors declare that the research was conducted in the absence of any commercial or financial relationships that could be construed as a potential conflict of interest.

Publisher's Note: All claims expressed in this article are solely those of the authors and do not necessarily represent those of their affiliated organizations, or those of the publisher, the editors and the reviewers. Any product that may be evaluated in this article, or claim that may be made by its manufacturer, is not guaranteed or endorsed by the publisher.

frontiers in Oncology

ORIGINAL RESEARCH
published: 07 March 2022
doi: 10.3389/fonc.2022.791365

BK002 Induces miR-192-5p-Mediated Apoptosis in Castration-Resistant Prostate Cancer Cells *via* Modulation of PI3K/CHOP

Moon Nyeo Park[1,2†], Hyunmin Park[1†], Md. Ataur Rahman[1,2], Jeong Woo Kim[1], Se Sun Park[1], Yongmin Cho[1,2], Jinwon Choi[1], So-Ri Son[3], Dae Sik Jang[3], Bum-Sang Shim[1], Sung-Hoon Kim[1], Seong-Gyu Ko[2], Chunhoo Cheon[2] and Bonglee Kim[1,2]*

[1] Department of Pathology, College of Korean Medicine, Kyung Hee University, Seoul, Republic of Korea, [2] Korean Medicine-Based Drug Repositioning Cancer Research Center, College of Korean Medicine, Kyung Hee University, Seoul, Republic of Korea, [3] Collage of Science in Pharmacy, Kyung Hee University, Seoul, Republic of Korea

OPEN ACCESS

Edited by:
Alagarsamy Srinivasan, NanoBio Diagnostics, United States

Reviewed by:
Nagaraja Sethuraman Balakathiresan, Division of Neuroscience and Behavior (NIAAA), United States
Pothana Saikumar, The University of Texas Health Science Center at San Antonio, United States

***Correspondence:**
Bonglee Kim
bongleekim@khu.ac.kr

[†]*These authors have equally contributed to this work*

Specialty section:
This article was submitted to Genitourinary Oncology, a section of the journal Frontiers in Oncology

Received: *08 October 2021*
Accepted: *25 January 2022*
Published: *07 March 2022*

Citation:
Park MN, Park H, Rahman MA, Kim JW, Park SS, Cho Y, Choi J, Son S-R, Jang DS, Shim B-S, Kim S-H, Ko S-G, Cheon C and Kim B (2022) BK002 Induces miR-192-5p-Mediated Apoptosis in Castration-Resistant Prostate Cancer Cells via Modulation of PI3K/CHOP. Front. Oncol. 12:791365. doi: 10.3389/fonc.2022.791365

BK002 consists of *Achyranthes japonica* Nakai (AJN) and *Melandrium firmum* Rohrbach (MFR) that have been used as herbal medicines in China and Korea. AJN and MFR have been reported to have anti-inflammatory, anti-oxidative, and anti-cancer activities, although the synergistic targeting multiple anti-cancer mechanism in castration-resistant prostate cancer (CRPC) has not been well reported. However, the drug resistance and transition to the androgen-independent state of prostate cancer contributing to CRPC is not well studied. Here, we reported that BK002 exerted cytotoxicity and apoptosis in CRPC PC3 cell lines and prostate cancer DU145 cell lines examined by cytotoxicity, western blot, a LIVE/DEAD cell imaging assay, reactive oxygen species (ROS) detection, quantitative real-time polymerase chain reaction (RT-PCR), and transfection assays. The results from our investigation found that BK002 showed more cellular cytotoxicity than AJN and MFR alone, suggesting that BK002 exhibited potential cytotoxic properties. Consistently, BK002 increased DNA damage, and activated p-γH2A.X and depletion of survivin-activated ubiquitination of pro-PARP, caspase9, and caspase3. Notably, live cell imaging using confocal microscopy found that BK002 effectively increased DNA-binding red fluorescent intensity in PC3 and DU145 cells. Also, BK002 increased the anti-proliferative effect with activation of the C/EBP homologous protein (CHOP) and significantly attenuated PI3K/AKT expression. Notably, BK002-treated cells increased ROS generation and co-treatment of N-Acetyl-L-cysteine (NAC), an ROS inhibitor, significantly preventing ROS production and cellular cytotoxicity, suggesting that ROS production is essential for initiating apoptosis in PC3 and DU145 cells. In addition, we found that BK002 significantly enhanced miR-192-5p expression, and co-treatment with BK002 and miR-192-5p inhibitor significantly reduced miR-192-5p expression and cellular viability in PC3 and DU145 cells, indicating modulation of miR-192-5p mediated apoptosis. Finally, we found that BK002-mediated CHOP upregulation and PI3K downregulation were significantly reduced and restrained by miR-192-5p inhibitor

respectively, suggesting that the anti-cancer effect of BK002 is associated with the miR-192-5p/PI3K/CHOP pathway. Therefore, our study reveals that a combination of AJN and MFR might be more effective than single treatment against apoptotic activities of both CRPC cells and prostate cancer cells.

Keywords: BK002, *Achyranthes japonica* Nakai, *Melandryum firmum* Rohrbach, castration-resistant prostate cancer, miR-192-5p

INTRODUCTION

Prostate cancer (PC) is a malignant cancer that represents the second highest death rate of male cancer worldwide, with 1.3 million new cases and 359,000 mortalities in 2018 (3.8% of cancer deaths) (1, 2). Prostate cancer can become castration-resistant prostate cancer (CRPC) after recurrence due to hormone deprivation therapy (3). CRPC is classified by intracrine/paracrine androgen secretion due to resistance acquired after testosterone deprivation therapy (4). The incidence of CRPC was estimated at 42,970 in 2020 and with annual progression in the US (5). However, the mortality rate rapidly progressed to a 50% rise in CRPC (6). After being diagnosed with CRPC, the survival rate is 9 to 13 months (7). Despite novel drugs, the mortality rate of CRPC is still high (8). The androgen receptor (AR) is stimulated by androgen binding including testosterone and dihydro testosterone which are responsible for development or reproductive function. However, 90% of the early stage of prostate cancer are AR-dependent. Many researchers had conducted studies for novel therapies for CRPC by 2020 (5). To date, abiraterone acetate (AA, Zytiga) and enzalutamide (Xtandi) are hormone inhibitors that have been approved by the Food and Drug Administration (FDA) for treatment of CRPC. Additionally, AA is an inhibitor that plays a role in inhibition of cytochrome P450 enzymatic activation associated with testosterone synthesis. Consistently, enzalutamide is responsible for the agonistic effect related to inhibiting by interfering with the translocation to the nucleus by competitively binding to AR. That is why the necessity of discovering a new biomarker has increased for CRPC (6).

Among the most three most well-known genes of prostate cancer, PI3K, RB, and RAS/RAF, here we investigated PI3K which is known to induce PTEN alteration and exert malignant progression in prostate cancer (9). Notably, PI3K is a major mediator of resistance to therapy in a wide range of alterations such as aggressive oncogene amplification as well as tumor suppressor deletion which lead to CRPC (10–13). Additionally, the endoplasmic reticulum (ER) plays a major role in protein synthesis and maturation which is known to be associated with disease and cancer due to its unfolded protein response (UPR) (14–17). Therefore, ER stress induced by cancer obviously promotes resistance to chemotherapy (18), and ER stress can reduce the apoptotic pathway by elevating the level of proliferation signaling activator PI3K (19, 20). Thus, in our study, we analyzed whether the BK002 contains ecdysterone related to drug resistance in cancer via modulation of PI3K and ER stress-induced ROS generation.

Currently, herbal medicine is known to cure the imbalance of the human body which causes diverse diseases including diabetes, neurodegenerative disease, and cancer (21, 22). To emphasize these, Korean traditional medicine are used as a complementary and alternative medicine (CAM) to modulate cancer (23, 24). Advantages of herbal medicine include less cytotoxicity, a reduction of side effects, and an increase in the effect of chemotherapy (24). Recently, ecdysteroids derived from plants have been reported to inhibit drug resistance in multidrug resistance (MDR) cancer cells (25–29). Recently, numerous researchers have investigated whether the anti-cancer mechanisms of traditional herbal medicines are related to the regulation between miRNA and cancer (30). In malignant hematological cancer, Spatholobus suberectus Dunn, Salvia miltiorrhiza, and Cnidium officinale Makino showed an anti-cancer effect via regulation of miR-657/ATF-2, miR-216b/c-Jun, and miR-211/CHOP, respectively (16a) (31, 32). MiR-192-5p has been found to have a potential anti-cancerous effect in lung cancer cells (33). *Achyranthes japonica* Nakai (AJN) was used for urinary problems including dysuria. *Melandrium firmum* Rohrbach (MFR) was also used as a traditional medicine for urinary problems, and tumor and blood stasis. This combination of AJN and MFR (known as BK002) is designed to increase the effect and reduce the side effects by using the two drugs at a low dose. Thus, in our study, the anti-cancer mechanism of BK002 treatment is investigated in androgen-independent prostate cancer cells through enhancing pro-apoptotic protein CHOP *via* downregulation of PI3K, AKT, and PARP. Additionally, we investigate whether BK002 anti-cancer and apoptosis effects are related to the miR-192-5p-mediated pathway in PC3 and DU145 prostate cancer cells.

MATERIALS AND METHODS

Materials

MFR and AJN (200 g) each were harvested in Hongchungun, Gangwondo, Korea. We prepared the extracts as previously defined (34, 35). In brief, MFR, and AJN were filtered and extracted twice in 99% ethanol for 3 days each. The solution was extracted by an evaporator (EYELA, Yamato, Tokyo, Japan) and dried under a vacuum in freezing conditions (EYELA, Yamato, Tokyo, Japan). After extraction, the powder was dissolved in DMSO.

High-Performance Liquid Chromatography Analysis for β-Ecdysterone

The ethanol extracts of MFR (50 mg) and AJN (20 mg) were dissolved in 1.0 and 2.0 ml of methanol, respectively, and

sonicated for 1 h at room temperature. The standard solution of β-ecdysterone (SigmaAldrich, St. Louis, MO, USA) was prepared in methanol (0.5 mg/ml). To prepare the calibration standards, the standard solution was serially diluted and finally adjusted to 15.125, 31.25, 62.5, 125, and 250 μg/ml. Prior to HPLC analysis, samples and standard solutions were filtered with 0.2 μm PTFE filter (Whatman Inc., Maidstone, UK). The analysis was performed by Waters HPLC systems (Waters, Milford, MA, USA) equipped with the W1525 binary pump, W717 plus auto-sampler, and W996 PDA detector. The column was a Gemini NX C-18 110A column (5 μm, 250 x 4.6 mm I.D., Phenomenex International, USA). The flow rate was 0.7 ml/min with the mobile phase for aqueous 0.1% (v/v) trifluoroacetic acid (solvent A) and acetonitrile (solvent B). The linear gradient elution was as follows: 0–2 min, 10% B; 2–10 min 15% B; 10–40 min 25% B; 40–48 min 100% B; 48–49 min 5% B, and then 6 min to stabilize in the initial condition. The injection volume was 10.0 μL and the detection was conducted at 260 nm. All analysis was repeated three times to check its reproducibility.

Cell Culture

PC3 (castration-resistant prostate cancer cell line) and DU145 (castration-resistant prostate cancer cell line) were purchased from ATCC. MDBK (normal kidney cell line) was obtained from Korean Cell Line Bank (KCLB, Seoul, Republic of Korea). The DU145 or PC3 cells, and MDBK cells were cultured with RPMI 1640 medium containing 10% fetal bovine serum (FBS), 2 μM of L-glutamine, and 10,000 U/ml of penicillin/streptomycin (Gibco, Grand Island, NY, USA). The medium was changed every 2-3 days.

Cytotoxicity Assay

PC3, DU145, and MDBK cells were subjected to a cytotoxicity assay using an EZ-Cytox cell viability assay kit (Daeil Lab Service, Seoul, Republic of Korea) according to the manufacturer's protocol. Cells were seeded in a 96-well plate in which various concentrations (12.5, 25, 50, 100, 200 μg/ml) of AJN and MFR were added for 24 h. The combination concentrations were determined as AJN (100 μg/ml) and MFR (50 μg/ml) in PC3 cells or AJN (50 μg/ml) and MFR (25 μg/ml) in DU145 cells for 24 h. The highest concentrations (0.035, 0.07, 0.15, 0.3, 0.6 μg/ml) of β-ecdysterone were determined in 200 μg/ml of AJN compared to MFR in PC3, DU145, and MDBK cells for 24 h. The absorbance values of cell viability were measured at 450 nm using a micro plate reader (Bio-Rad, Hercules, CA, USA).

Western Blot Analysis

The protein was isolated from cells with lysis buffer (pH=7.4, 1% NP-40, 1 mM Na_3VO_4, 1 M EDTA, 1 mM NaF, 50 mM Tris-Hcl, 0.25% sodium deoxycholic acid, 150 mM NaCl) containing protease inhibitor cocktail (Amresco, Scolon, OH, USA). Protein quantification was normalized with β-actin using a Bio-Rad DC protein assay kit II (Bio-Rad, Hercules, CA, USA). The differences of protein expression were determined by Western blotting using SDS-PAGE 8% and 10% gel by electrophoresis. After blocking in 3% skim milk, the membrane with protein was probed with various primary antibodies for p-AKT, pro-PARP, CHOP (Cell signaling, Beverly, MA, USA), PI3K, and β-actin (Santa Cruz Biotechnologies, Santa Cruz, CA, USA) for 24 h followed by exposure to horseradish peroxidase (HRP)-conjugated secondary anti-mouse or rabbit antibodies for 1 h. Protein expression levels were identified by the chemiluminescence (ECL) system (Amersham Pharmacia, Piscataway, NJ, USA).

Live and Dead Cell Imaging Assay

PC3 and DU145 (2×10^5 a 6-well plate at 1 ml/well. At 24 h after seeding, the culture medium was treated with BK002 for 24 h. Cells were washed with DPBS and then loaded for 30 min with Calcein-AM green (LIVE/DEAD® Viability/Cytotoxicity kit, Thermo Fisherscientific, Waltham, MA, USA) or ethidium homodimer-1 (LIVE/DEAD® Cell imaging kit, Thermo Fisherscientific, USA) and added to each slide according to the manufacturer's protocol. The images were obtained by confocal microscopy using FV10i (OLYMPUS Fluoview USA. Green: live cell; Red: dead cells; 50×, scale bar; 100 μm).

Measurement of ROS

The Reactive Oxygen Species Detection Assay (Abcam, Cambridge, United Kingdom) was used to detect hydroxyl, peroxyl, and to analyze other ROS of cellular cytosolic hydrogen peroxide (H_2O_2). PC3 cells and DU145 cells were seeded into a 96-well plate and pretreated with N-Acetyl-L-cysteine (NAC, Sigma Aldrich Co., St. Louis, MO, USA) for 30 min; untreated NAC cells were also added. After being stained with 20 μM of DCFDA for 2 h in the dark at room temperature (RT), PC3 cells were treated with AJN (100 μg/ml) and MFR (50 μg/ml) and DU145 cells were treated with AJN (50 μg/ml) and MFR (25 μg/ml) for 2 h. Then the 96-well plate was measured using an ELISA reader (Bio-Rad, Hercules, CA, USA) (Ex/Em= 485/535 nm).

Quantitative Real-Time PCR Analysis

RNA was isolated using the RNeasy mini kit (EZ™ Total RNA Mini prep Kit, Enzynomics, Korea). The total RNA was reversed transcribed using the HB miRNA Multi Assay kit ™ System I (HeimBiotek, Seoul, Republic of Korea) according to the manufacturer's protocol. PCR started at 95°C for 15 min, followed by 40 cycles at 95°C for 10 s, 60°C for 40 s, and finished by 40 s at 60°C in the last cycle. The relative miRNA fold change was normalized using standard C_t values of RNU6B (U6) (HeimBiotek, Korea). The miR-specific primer Hsa-miR-192-5p was designed and synthesized by HeimBiotek Company. Three experiments were performed and analyzed by means of the $2^{-\Delta CT}$ method. RT-PCR was performed using the Light Cyber™ instrument (Roche Applied Science, Indianapolis, IN, USA).

Transfection Assay

PC3 cells and DU145 cells were transfected with the miR192-5p inhibitor using ViaFect™ Transfection Reagent according to the protocol. After transfection for 48 h, in DU145, AJN (50 μg/ml) and MFR (25 μg/ml) and in PC3, AJN (100 μg/ml) and MFR (50 μg/ml) were treated for 24 h. The inhibitor oligo base type with the following 2' O-Methyl RNA base was applied by HeimBiotek (Seoul, Repulbic of Korea).

Statistical Analysis

Data were presented as means ± standard deviation (SD). Statistically significant differences between the control and BK002-treated group were calculated by Student's t-test using Sigma plot version 12 software (SysTest Software Inc., San Jose, CA, USA). All experiments were performed in triplicate. The value of $p < 0.05$ was considered to represent a statistically significant difference.

RESULTS

Identification and Quantification of β-Ecdysterone in MFR and AJN by HPLC

To check whether MFR and AJN contain β-ecdysterone, we measured β-ecdysterone level by HPLC methods. β-ecdysterone and phytoestrogen derived from the root of *A. bidentata* have been reported to be anti-oxidative in a concentration-dependent manner (36, 37). The HPLC chromatograms showed the existence of β-ecdysterone (R_t = 28.36 min) in BK002 by comparison with retention time (R_t) and photodiode array (PDA) spectrum of the standard solution (**Figure 1**). To quantify the content of β-ecdysterone, the calibration curve of the standard was obtained with serially diluted solutions (15–250 μg/ml). Here, we found that the MFR and AJN β-ecdysterone peak was very small (**Figures 1B–D**), additionally, β-ecdysterone exhibited more cellular cytotoxicity in normal MDBK cells than prostate cancer PC and DU145 cells (**Figure 1E**), suggesting that β-ecdysterone has no toxic effects on cancer cells. The regression equation was $y = 16421x - 36509$ ($r^2 = 0.9993$, n = 5). The contents of β-ecdysterone in MFR and AJN were determined to be 66.43 ± 2.82 and 307.59 ± 4.18 mg/100g, respectively (**Table 1**).

AJN and MFR Exerts Cytotoxicity in PC3 and DU145 Prostate Cancer Cells

To investigate the potency of BK002 against prostate cancer cells, the different concentrations of AJN, MFR, and BK002 were exposed to PC3 and DU145 cells for 24 h, and the numbers of viable cells were determined by an EZ-Cytox cell viability assay. In the results from our study, we found that AJN and MFR concentration dependently reduced cellular viability in PC3 prostate cancer cells (**Figure 2A**). On the other hand, combination of AJN (100 μg/ml) and MFR (50 μg/ml), called BK002, significantly reduced more cellular viability than AJN and MFR single treatment in PC3 cells (**Figure 2B**). However, in DU145 cells, AJN and MFR concentration dependently reduced cell viability and combination of AJN (50 μg/ml) and MFR (25 μg/ml) significantly decreased more cellular viability than AJN and MFR single treatment (**Figures 2C, D**). On the other hand, AJN, MFR, and BK002 did not show any cytotoxic effect on normal MDBK cells (**Figures 2E, F**). Taken together, these results indicate that BK002 was more effective and cytotoxic in prostate cancer cells rather than normal cells which suggests the combined use of AJN and MFR for more cytotoxic activities than single AJN and MFR in our further investigations.

AJN and MFR Exhibit Anti-Proliferative Effects in PC3 and DU145 Cells

To further determine the cytotoxic effect of BK002 on PC3 and DU145 cells, we were interested to know whether these cytotoxic effects might be caused by induction of apoptotic mechanisms determined by western blot in addition to a live and dead cell assay. It has been found that dysregulation of anti-apoptotic proteins PI3K and AKT are known to be associated with CRPC progression as well as drug resistance (38, 39). Here, we found that single treatment of AJN and MFR exhibited lower PI3K and phosphor-AKT expression, on the other hand, combined AJN and MFR (BK002)-treated cells showed a significant reduction of PI3K and phosphor-AKT on PC3 and DU145 cells (**Figures 3A–D**). It has been implicated that pro-apoptotic protein CHOP, belonging to the family of CCAAT/enhancer binding proteins (C/EBPs), is involved in gene regulation of cellular proliferation, differentiation, and energy metabolism which plays a crucial role to induce apoptosis (40). Moreover, anti-apoptotic poly (ADP-ribosyl)ation of nuclear proteins (PARPs) has been shown to be required for apoptosis induction in various cell lines (41). In our investigation, we found that BK002-treated cells significantly attenuated the full length of pro-PARP and increased CHOP expression in DU145 cells better than in PC3 cells, indicating that cytotoxicity was enabled by an apoptosis-mediated pathway in both prostate cells (**Figures 3A–D**)

BK002 Exhibits Apoptosis in PC3 and DU145 Cells

To further investigate whether the anti-cancer effects of BK002 possibly lead to apoptosis, western blotting and a live and dead cell assay were performed in PC3 and DU145 cells. It is well known that drug resistance in association with the poor survival rate of the patient and apoptosis inhibition are modulated by survivin (42). To determine whether BK002 inhibited drug resistance and anti-apoptotic factors, western blotting was adopted in PC3 and DU145 cells. As shown in **Figures 4A, D**, the expression of survivin was suppressed compared to untreated groups. Consistently, activation of caspase was confirmed in BK002-treated PC3 and DU145 cells. Pro-PARP, pro-caspase 9, and pro-caspase 3 were depleted in PC3 and DU145 cells, compared to untreated groups (**Figures 4A, D**). In addition, BK002 increased DNA damage marker p- γH2A.X in PC3 and DU145 cells (**Figures 4A, D**). Similarly, it was confirmed that the red fluorescence probe was significantly increased due to dead cells in BK002-treated cells compared to the untreated group by confocal microscopy (**Figures 4C, F**).

BK002 Promotes ROS Generation and ROS Scavenger Attenuates Cytotoxicity of BK002-Treated Prostate Cancer Cells

ROS has a critical role in cell death-related pathways due to severe ER stress (27). To evaluate the effect on ROS generation of BK002-mediated apoptosis, a ROS measurement was performed by a fluorescent-based 2', 7'-dichlorofluorescein diacetate (DCFDA) assay. Here, we found that AJN and MFR treatment significantly increased ROS generation in both PC3 and DU145 cells (**Figures 5A, B**). In addition, combined treatment of AJN

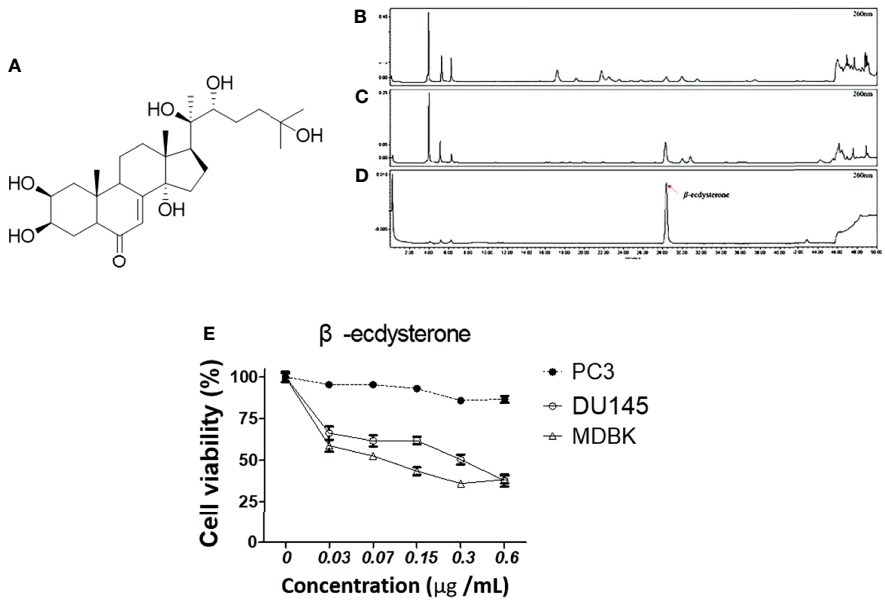

FIGURE 1 | The HPLC chromatograms of **(A)** a diagram of the structure of β-ecdysterone **(B)** MFR, **(C)** AJN, and **(D)** β-ecdysterone detected at 260 nm. The presence of β-ecdysterone was confirmed according to the retention time and PDA spectrum. β-ecdysterone was observed at R_t 28.36 min. **(E)** Cytotoxic effects of β-ecdysterone in PC3, DU145, and MDBK cells were determined in a concentration-dependent manner by an EZ-cytox cell viability assay. Data represent means ± SD; *p < 0.05, **p < 0.01, ***p < 0.001 compared to untreated control.

and MFR (BK002) significantly promoted more ROS generation compared to single AJN and MFR treatment in both PC3 and DU145 cells (**Figures 5A, B**). Thus, the results indicate that BK002-mediated apoptosis has an important role in generating ROS production in prostate cancer cells. To confirm the role of ROS production in BK002-induced apoptosis, we further used a ROS inhibitor, N-acetyl-L-cysteine (NAC) (43), and examined ROS generation by an ROS detection assay. Here, we found that BK002-treated cells significantly increased ROS generation, and co-treatment with NAC and BK002 significantly decreased ROS production in both PC3 and DU145 cells (**Figures 5C, D**). Concomitantly, the cytotoxic effect of BK002 was significantly restrained when pre-treated by NAC on both PC3 and DU145 cells (**Figures 5E, F**). Because of an error, there was a difference between the cytotoxicity value in **Figures 2D** and **Figure 5F**. Therefore, these observations suggest that BK002-mediated apoptosis might contribute to ROS generation in prostate cancer cells.

BK002 Increases MicroRNA-192-5p Expression in Prostate Cancer Cells

Recently, it has been found that miR-192-5p, a member of the miR-192 family, plays a crucial role in vital biological processes and regulates oxidative stress, proliferation, apoptosis, inflammatory responses, and various cancers such as lung, liver, and breast (44). To check the effect of BK002 on the expression of miR-192-5p, qRT-PCR was performed. We found that combined treatment of AJN and MFR significantly upregulated the expression of miR-192-5p compared to single AJN and MFR treatment in both PC3 and DU145 cells (**Figures 6A, B**). Additionally, co-treatment of BK002 and miR-192-5p inhibitor significantly decreased miR-192-5p

TABLE 1 | Calibration curve of β-ecdysterone.

Standard solutions		Regression equations		R^2 [8]	Stability (RSD%)			Inter-day		Intra-dav	
β-ecdysterone		y = 16421x + 36509		0.9993	0.155053			RT[3] (mm)	RSD[4]	RT[3] (mm)	RSD[4]
							β-ecdysterone	28.38083	0.155053	28.41133	0.389274
	Area.	ppm[6]	Sample conc.	*β* -ecdysterone						*β*-ecdysterone	
				Conc. (%)[7]	Conc.(mg/100g)[7]		Area.	ppm[6]	Sample conc.	Conc. (%)[7]	Conc.(mg/100g)
MFR[1]	584.765	33.213	50 mg ml	0.0664260	66.43	AJN[2]	1.301,194	76.898	25 mg/ml	0.3075933	307.59
SD[5]	23.098	1.408		0.003	2.817	SD[5]	17.122	1.044		0.004	4.178

All the results were shown as the mean n = 3.

[1]MFR, Melandrium firmum Rohrbach; [2]AJN, Achyranthes japonica Nakai; [3]RT, Retention time;[4] RSD, relative standard deviations; [5] SD, standard deviation; [6]ppm, parts per million; [7]Con., concentration; [8]R^2, R-squared.

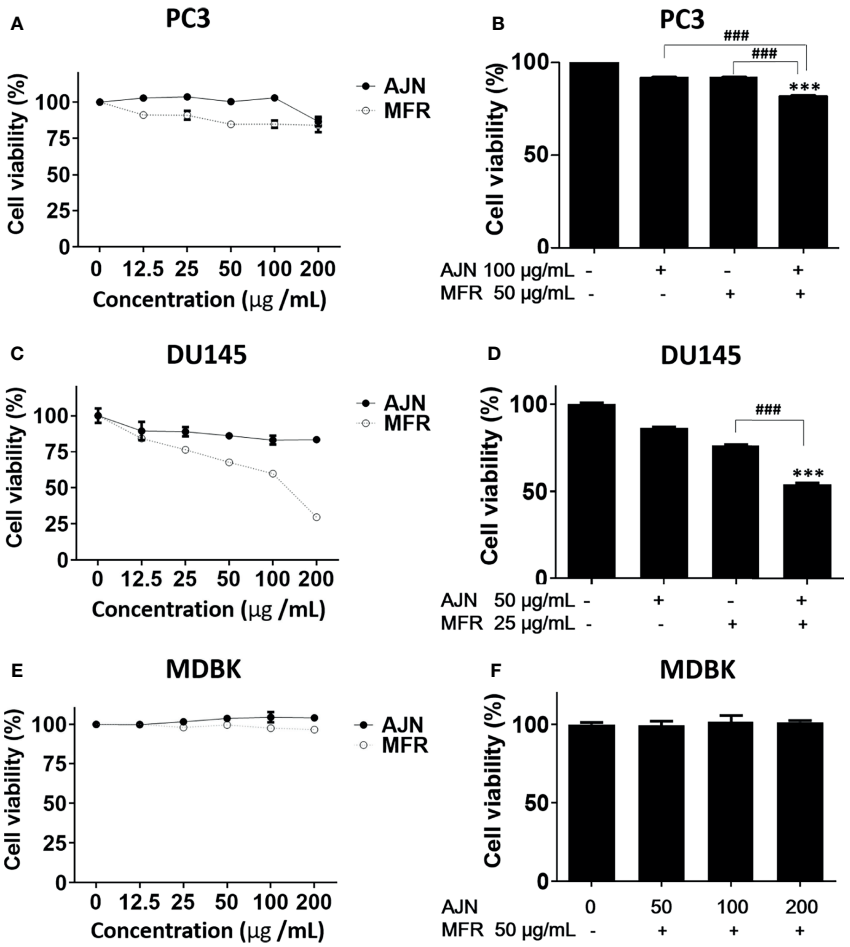

FIGURE 2 | Cytotoxic effects of AJN and MFR in PC3 and DU145 cells. The indicated concentrations of AJN and MFR were added to **(A)** PC3, **(C)** DU145, and **(E)** MDBK for 24 h. **(B, D, F)** A cell viability assay was performed in AJN and MFR-treated cells using an EZ-cytox cell viability assay. The values above represent the means of three experiments. Means ± SD; $^{***}p<0.001$ compared to untreated control, $^{###}p<0.001$ between two groups.

expression in both PC3 and DU145 cells determined by a transfection assay (**Figures 6C, D**). However, cellular viability was significantly increased with co-treatment of BK002 and miR-192-5p inhibitor in both prostate cancer cells (**Figures 6E, F**). All together these investigations suggest that BK002-induced cytotoxicity is also dependent on a miR-192-5p-mediated pathway.

BK002 Regulates Apoptosis-Related Protein *via* Modulation of miR-192-5p in Prostate Cells

We investigated whether the role of miR-192-5p in an apoptosis pathway and CHOP and PI3K expressions are closely related with cancer progression (45). Here, we found that co-treatment with BK002 and miR-192-5p inhibitor significantly reduced pro-apoptotic protein CHOP expression in both cells when miR-192-5p was suppressed by the transfection of miR-192-5p inhibitor (**Figures 7A–C**). Conversely, PI3K expression was significantly restrained with co-treatment of BK002 and miR-192-5p inhibitor in PC3 cells and DU145 cells examined by suppression of miR-192-5p *via* transfection of miR-192-5p inhibitor (**Figures 7D–F**). Taken together our results demonstrate that BK002-mediated apoptosis was regulated by miR-192-5p in prostate cancer cells.

DISCUSSION

Prostate cancer has the third highest mortality rate of middle and older aged men characterized by malignant progression due to frequently recurrence and resistance (46, 47). Approximately, 90% of cases have an increased survival rate with early treatment such as local radiotherapy, prostatectomy, and chemotherapy (47). Notably, over 30% of patients diagnosed with disease progression depend on androgen, at this state, androgen deprivation is a very effective treatment including single and combination administration of gonadotropin-releasing hormone (GnRH). Despite such a prognosis, most patients commonly experience recurrence within 3 years and the disease state progresses toward prostate cancer (48). In the present study,

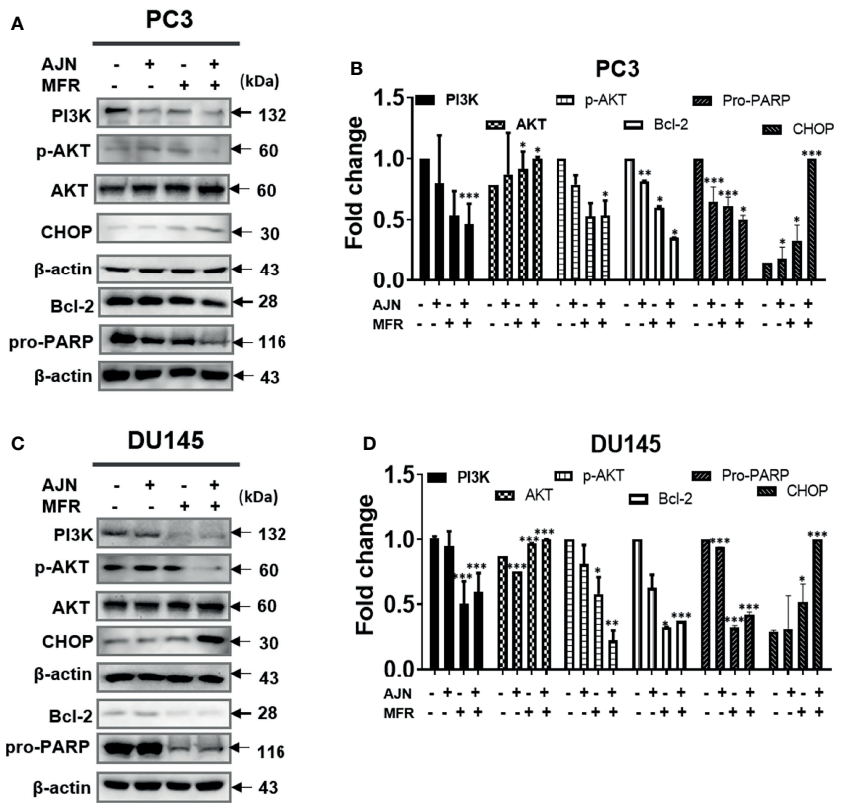

FIGURE 3 | Treatment of BK002 induced apoptosis in PC3 and DU145 cells. Cells were treated with AJN (100 mg/ml) and MFR (50 mg/ml) in **(A)** PC3 cells or AJN (50 mg/ml) and MFR (25 mg/ml) in **(C)** DU145 cells for 24 h. The proteins isolated from both PC3 and DU145 cells were subjected to western blot for PI3K, p-AKT pro-PARP, and CHOP. β-actin was exploited as a loading control. **(B, D)** The graph shows the quantification of western blot replicates. Data represent means ± SD; *p<0.05, **p<0.01, ***p<0.001 compared to untreated control.

we investigated the anti-cancer effect of natural plant extracts on CRPC PC3 and DU145 prostate cancer cells and focused our mechanistic investigations on cancer treatment resistance as well as micro-RNA-192-5p modulation.

Prostate cancer is treated by androgen deprivation therapy (ADT), referred to as endocrine therapy, that leads to 80% symptomatic improvement, temporarily. Then, most patients experience a hormone-independent state. In such a condition, we should change the terminology from hormone-independent cancer to CRPC (49). CRPC was identified as the major cause of morbidity in prostate cancer (50). The treatment selection of the CRPC patient is restricted to docetaxel and prednisone (DP) which was approved by the United States' FDA in 2004. The benefit of DP is not for improving the survival rate but consolidation of bone pain due to palliative quality of life, of which tolerability is still debatable due to the burden to older patients. During a 3-week trial, DP was replaced by mitoxantrone and prednisone (MP) as the standard guideline of care for CRPC (50). The median progression-free survival (PFS) of MP was about 6 months and overall survival (OS) was less than 2 years (50). Despite chemotherapy and consolidation treatment, patients had an unfavorable response due to acquired heterogenous mutations and different side effects (51). Recently, it has been found that natural products have been used as a complement to cancer chemotherapy *via* pharmacological modulation of the apoptosis pathway (52). Of note, natural products have been known to have antitumor, antioxidative, antibacterial, and anti-inflammatory capabilities as they contain bioactive components (53). Therefore, natural products might be required for further consideration of apoptosis induction which could lead to treatment for castration-resistant prostate cancer. Herein, a natural product is required for accurate analysis due to the diversity of bioactive components which lead to toxicity by accumulative doses containing components not yet identified (54). Recently, it was found that a combination of β-ecdysterone (250~750 μM) and doxorubicin (0.15 or 0.25 μM) enhanced the anticancer effect in drug-resistant breast cancer cells (55). Based on the above, to find the potential pharmacological effect of BK002 in CRPC, qualitative and quantitative analysis of bioactive compound β-ecdysterone in BK002 was investigated by HPLC (**Figure 1**). Thus, the underlying anticancer effect of BK002 was investigated in association with multiple targeting mechanisms for possible applications in CRPC.

Of note, we elucidated that combined treatment of *Achyranthes japonica* Nakai and *Melandrium firmum* Rohrbach (BK002) increased significant cytotoxicity in prostate

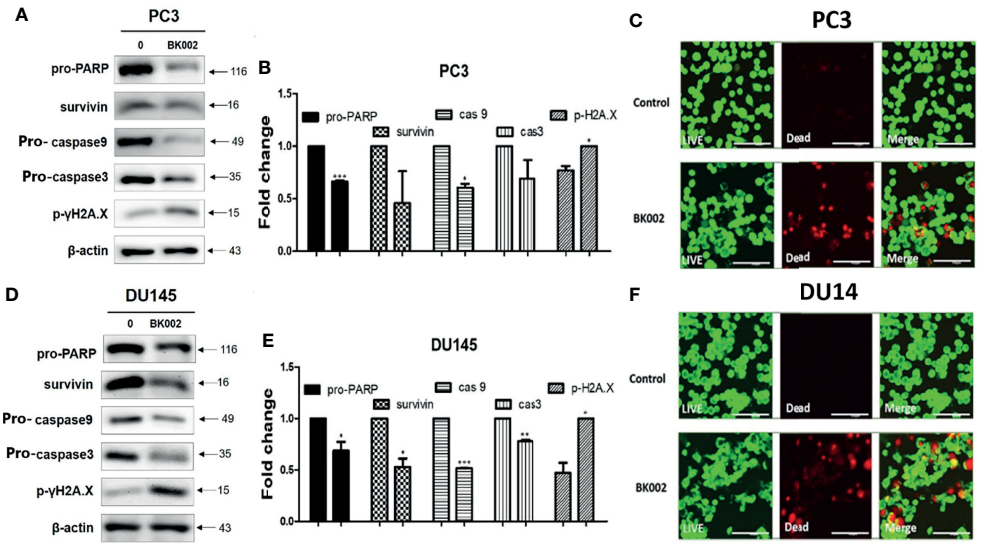

FIGURE 4 | Treatment of BK002 induced apoptosis in PC3 and DU145 cells. Cells were treated with AJN (100 μg/ml) and MFR (50 μg/ml) in **(A–C)** PC3 cells or AJN (50 μg/ml) and MFR (25 μg/ml) in **(D–F)** DU145 cells for 24 h. **(A, D)** Effect of BK002 on pro-PARP, survivin, pro-caspase-9, pro-caspase-3, and p-γH2A.X in PC3 and DU145 cells. Both PC3 and DU145 cells were subjected to western blot analysis. **(B, E)** The bar graph represents the results from the western blot analysis. **(C, F)** Cells were stained with calcein AM and ethidium homodimer-1 for the live and dead assay. The green fluorescent indicates the live cells and red fluorescent indicates dead cells. Live and dead results were visualized with a fluorescent optical filter (485 ± 10 nm) and rhodamine optical filter (530 ± 12.5 nm). Magnification × 50. (Scale bar, 100 μm). The graph shows the quantification of western blot replicates. Data represent means ± SD; *p<0.05, **p<0.01, ***p<0.001 compared to untreated control.

cancer cells without killing normal cells, implying selective damage to cancer in association with a reduction of side effects (56, 57) (**Figure 2**). Additionally, for the possibility of a synergistic anti-cancer effect, single treatment compared to the combination of BK002 was investigated. Notably, the effect of BK002 was significant in PC3 and DU145 in prostate cancer cells without affecting MDBK normal cells. PC3 cells have a high aggressive metastatic potential and DU145 cells have a moderate aggressive potential that is consistent with the fact that DU145 cells are more susceptible to BK002 than PC3 cells. In addition, both PC3 and DU145 cells are similar to androgen hormone-independent cells.

Recently, analysis of accumulation of AS in CRPC has been reported, which is controlled by interconnection between the truncated isoform of AR activation and the PI3K pathway (58, 59). Accordingly, the PI3K pathway has been highlighted as a prognostic and clinical biomarker of CRPC (60, 61). Nevertheless, the underlying anticancer effect of BK002 has not been revealed in relation to regulation of PI3K in CRPC. To date, BK002 has been mostly used for anti-diabetic, anti-inflammatory, anti-microbial, anti-oxidative, and osteoprotective effect (62). In the present investigation, we found that BK002-induced apoptosis was associated with PI3K regulation in CRPC (**Figure 3**). Additionally, the ER implement retained the homeostasis of posttranslational modification for protein activity and structure (63). Whereas, the ER stress condition might be generated by a cancer-derived abnormal state including hypoxia and malnutrition, resulting in accumulations of unfolded proteins. Under severe ER stress, the ER-induced CHOP-mediated apoptosis pathway was associated with degradation of pro-PARP (50, 57). Besides, BK002 significantly reduced PI3K and phospho-AKT, a castration-resistant progression biomarker, and this apoptosis increased ER-related apoptotic proteins such as CHOP and pro-PARP (**Figure 3**). Therefore, in this study, the role of PI3K and CHOP has been elucidated in association with BK002-induced anti-cancer effect in CHOP-sensitive and hormone-independent PC3 cells and DU145 prostate cancer cells.

Moreover, DNA damage-induced apoptosis signaling is the critical target for cancer treatment (64). So far, survivin has been known as a poor prognostic factor in various malignant cancers due to chemoresistance and inhibition of caspase activation (42, 65). Herein, BK002-treated PC3 and DU145 cells significantly suppressed survivin leading to caspase activation. BK002 stimulated the inactive zymogenic form of caspase such as caspase 9 or caspase 3 or pro-PARP and was modified posttranslationally by ubiquitination (66) (**Figure 4**). It is well known that p-γH2A.X is a critical marker for double strand breaks (DSBs) due to ionizing radiation or chemotherapy (67). Herein, BK002 significantly induced the expression of p-γH2A.X, demonstrating potential pro-apoptotic properties in resistant prostate cancer cells and prostate cancer cells as well. Notably, this was confirmed by the LIVE/DEAD™ Cell imaging kit using dying cell DNA-binding dyes in BK002-treated PC3 cells or DU145 cells (**Figure 4**). Of note, fluorescein diacetate (FDA) is a very sensitive and selective probe that is associated with live cells, where green fluorescence is produced by cytoplasmic esterase, and in dying and dead cells, a bright red fluorescence is generated

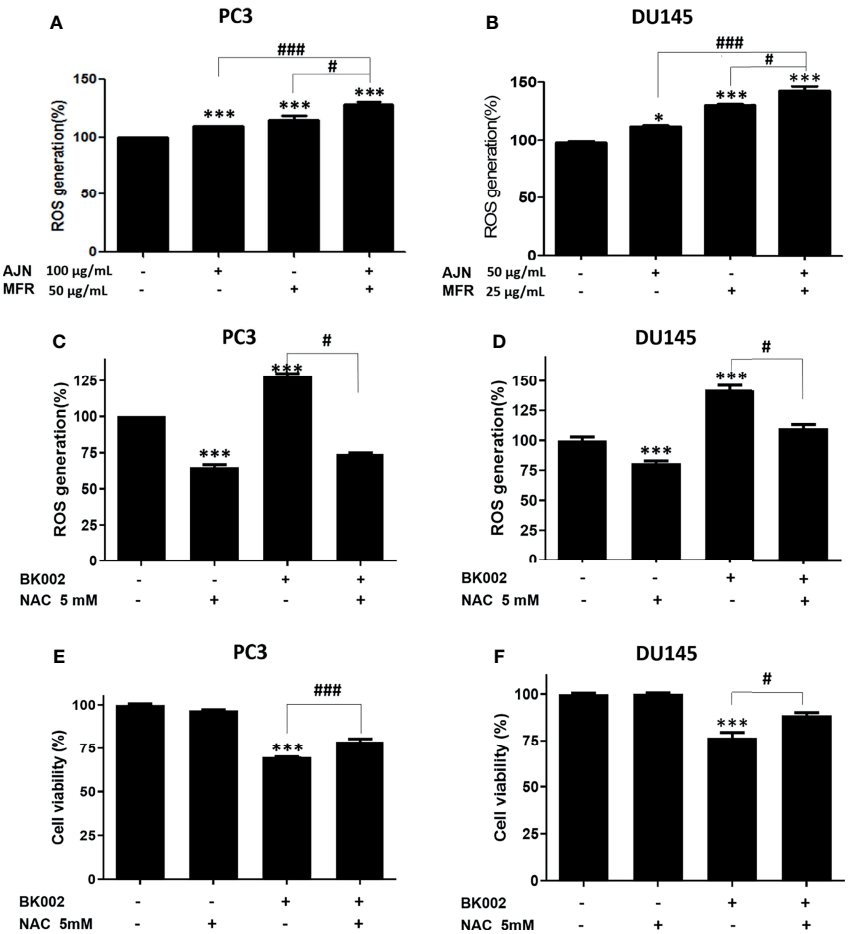

FIGURE 5 | BK002 increased ROS generation and NAC pretreatment reduced the cytotoxic effect of BK002 in PC3 and DU145 cells. Cells were subjected to a permeable fluorescent-based and chemiluminescent probe with 20 μM of DCFDA for 45 min at 37 °C in the dark. Cells were treated with AJN (100 μg/ml) and MFR (50 μg/ml) in **(A)** PC3 cells or AJN (50 μg/ml) and MFR (25 μg/ml) in **(B)** DU145 cells for 24 h. ROS generation was measured by using a microplate reader. **(C, D)** NAC was pretreated, and the cytotoxic effect of BK002 was studied in PC and DU145 cells. **(E, F)** A cell viability assay was conducted using EZ-Cytox by an absorbance measurement *via* an optical spectrometer. (Ex/Em=485/535). The values above represent the means of three experiments. Means ± SD; $^{*}p<0.05$, $^{***}p<0.001$ compared to untreated control, $^{\#}p<0.05$, $^{\#\#\#}p<0.001$ between two groups.

upon binding to DNA (68). Consistently, BK002 promoted effective apoptosis in DU145 cells as well as resistant PC cells, contributing to deepen the biological understanding under the live cell condition.

While studying whether the anticancer effect of BK002 is due to ER stress-related apoptosis, we found that BK002 significantly induced expression of ER-related apoptotic proteins such as CHOP and caspase activation (**Figures 3**, **4**).

Under normal conditions, ROS are responsible for stimulation of a second messenger in the Ca^{2+}-mediated cascade due to mitochondrial oxidative respiration. Meanwhile, ER stress caused by the upsurge of ROS generation in cancer cells persists in ROS-mediated cancer cell death. Several natural products have been found to induce apoptosis-mediated cell death *via* modulation of ROS generation. For example, the antiproliferation effect of natural products from *Withania somnifera* encourages ROS generation in addition to mitochondria-induced apoptosis in HL-60 myeloid leukemia cells (69). BK002 triggered an upsurge of ROS generation compared to control and single AJN and MFR treatment. These results have been identified as similar in ROS mediated-apoptosis induced by natural compounds (70, 71). Furthermore, ROS generation is reduced by ROS inhibitor NAC, implying the anticancer effect in DU145 cells or PC3 cells in accordance with ROS-mediated apoptosis against CRPC (**Figure 5**). Therefore, the current study suggests that BK002-mediated apoptosis is required to generate ROS production.

It has been extensively investigated whether miRNAs function as oncogene silencers or tumor suppressor gene enhancers depending on the target mRNA in various cancers including colon, prostate, pancreatic, lung, breast, bladder, and kidney (72). Recently, herbal medicine has been identified as having a potential anti-cancer effect *via* regulation of the miRNA network (73). Several studies have revealed the anti-cancer effect

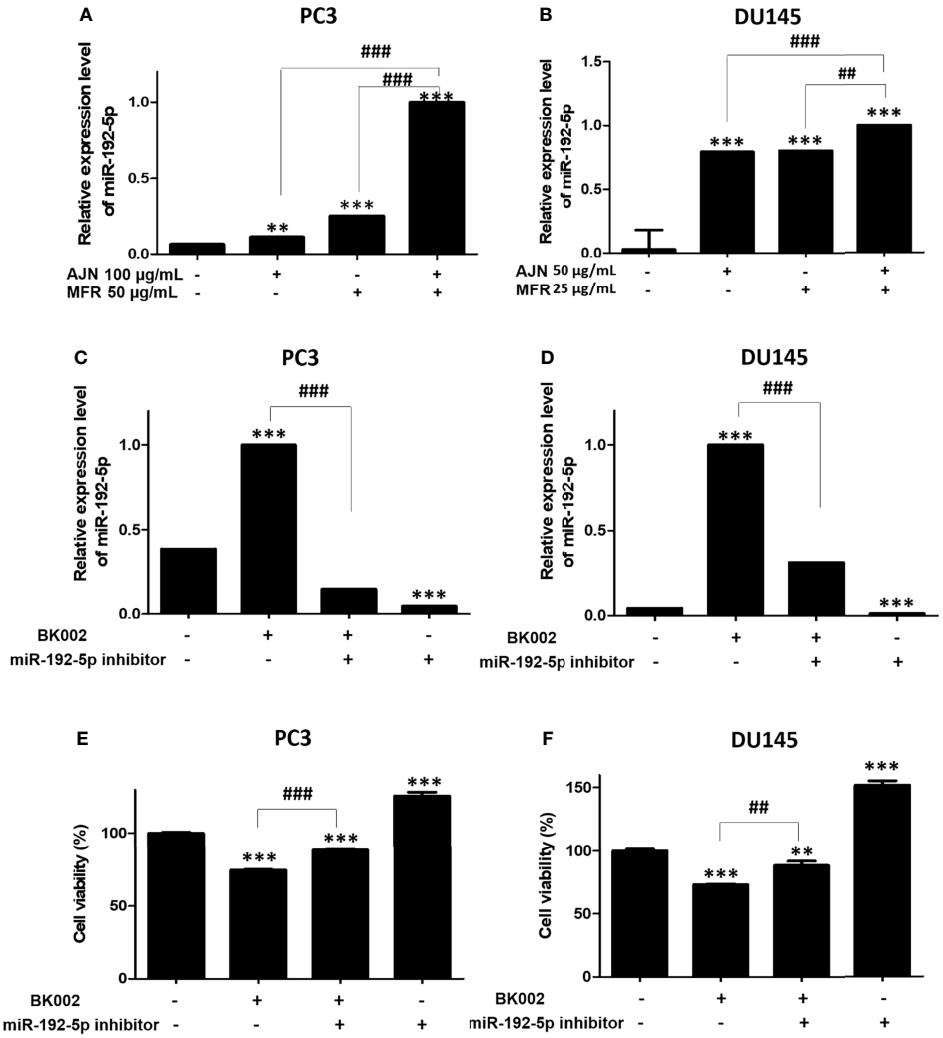

FIGURE 6 | Treatment of BK002 significantly increased miR-192-5p expression in PC3 and DU145 cells. Cells were treated with AJN (100 μg/ml) and MFR (50 μg/ml) in **(A)** PC3 cells or AJN (50 μg/ml) and MFR (25 μg/ml) in **(B)** DU145 cells for 24 h and the expression of miR-192-5p was measured by qRT-PCR in PC3 and DU145 cells. **(C, D)** Cells were transfected with miR-192-5p inhibitor for 48 h using a transfection reagent and the expression of miR-192-5p was calculated. **(E, F)** The effect of BK002 on cell viability in miR-192-5p inhibitor-transfected PC3 and DU145 cells was determined by an EZ-CYTOX cell viability assay kit. The values above represent the means of three experiments. Means ± SD; $^{**}p<0.01$, $^{***}p<0.001$ compared to untreated control, $^{\#\#}p<0.01$, $^{\#\#\#}p<0.001$ between two groups.

of a Sophorae Flos and *Lonicerae japonicae* Flos-regulated miR-let-7/f-CCR7 network (74), SSD-regulated miR-657/ATF2 network (16), *SM*-regulated miR-216b/c-Jun network (32), COM extract-regulated miR-211/CHOP network (31), and *Panax ginseng* C.A. Meyer (Rg3)-regulated miR-21/PI3K/AKT network (75). Accumulated evidence has shown that the herbal medicine-derived component inhibited oncogenes or enhanced tumor suppressor genes (76). In the present investigation, we found that transfection of miR-192-5p inhibitor significantly repressed miR-192-5p and increased cell viability *via* co-treatment with BK002 (**Figure 6**). In addition, our investigation also demonstrated that the mature sequence containing hsa-miR-192-5p within miR-192 was a significantly repressed oncogene and induced CHOP-mediated ER stress-related apoptosis (**Figure 7**). MiR-192-5p has been identified as a poor prognostic factor in metastatic colon cancer (77, 78). Here, our results suggested that BK002 increased miR-192-5p which implied the potential regulation of apoptosis *via* the miR-192-5p/PI3K pathway.

CONCLUSIONS

BK002 has been shown to have a significant effect on prostate cancer in PC3 cells and DU145 cells without affecting normal cells. Notably, BK002 treatment efficiently induced ROS-mediated endoplasmic reticulum-associated degradation (ERAD) in proteins such as CHOP along with caspase

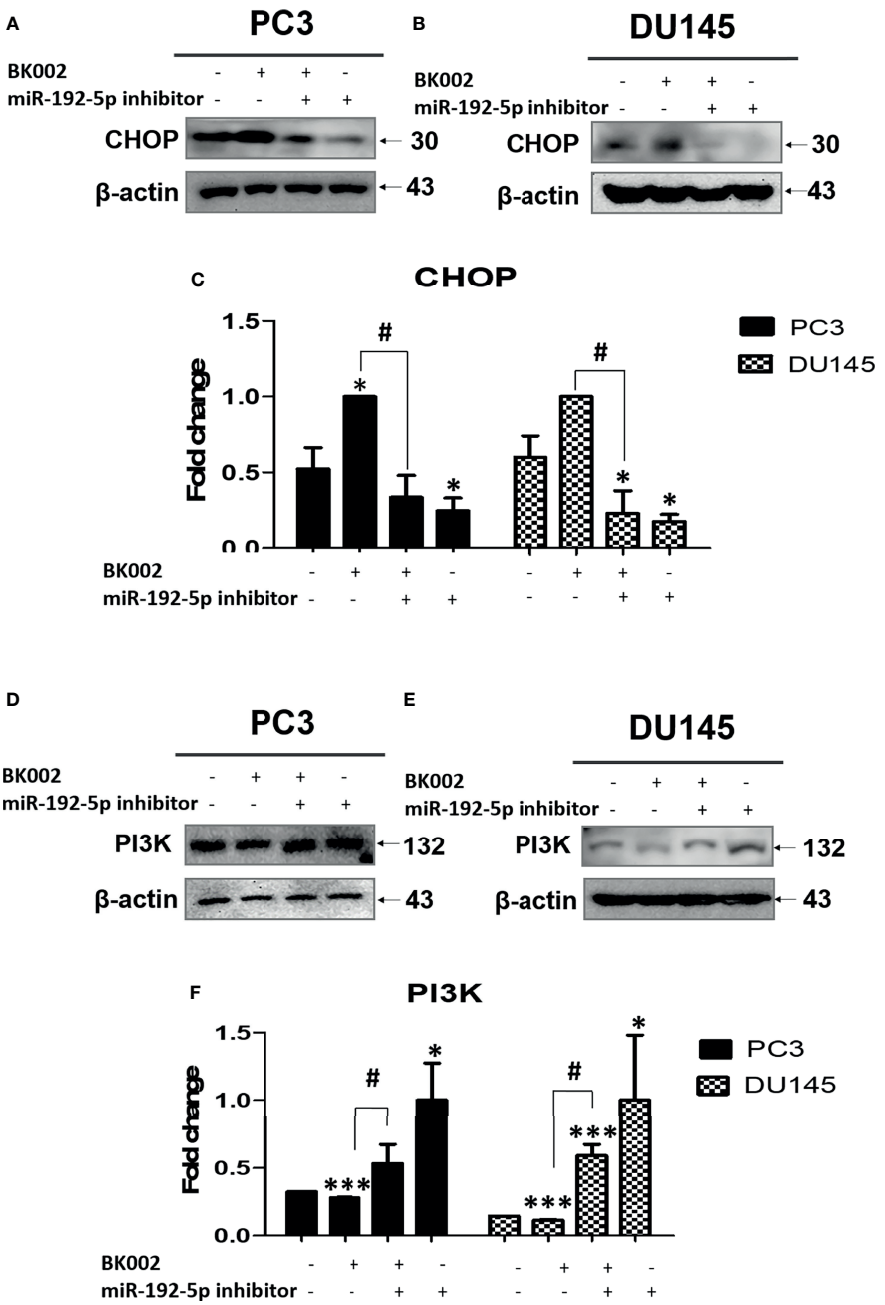

FIGURE 7 | The anti-cancer effect of BK002 was inhibited by miR-192-5p inhibition. Cells were transfected with miR-192-5p inhibitor for 48 h using a transfection reagent, and the expression of miR-192-5p was calculated. Cells were treated with AJN (100 μg/ml) and MFR (50 μg/ml) in **(A, D)** PC3 cells or AJN (50 μg/ml) and MFR (25 μg/ml) in **(B, E)** DU145 cells for 24 h. Western blotting was conducted for CHOP and PI3K in PC3 and DU145 cells. **(C, F)** The bar graph represents the fold change of protein expression above. The values above represent the means of three experiments. Means ± SD; *p<0.05, ***p<0.001 compared to untreated control, #p<0.05 between two groups.

activation and attenuated survivin or PI3K/AKT, leading to activation of p-γH2A.X. Moreover, BK002 treatment upregulated miR-192-5p, and inhibition of miR-192-5p modulated apoptosis signaling through regulation of CHOP and PI3K. BK002-mediated apoptosis induction has been presented in our proposed model in **Figure 8**. Therefore, the present study suggests that BK002 synergistic treatment might be useful as a potential therapeutic approach in CRPC control compared to single treatment of *Achyranthes japonica* Nakai and *Melandrium firmum* Rohrbach.

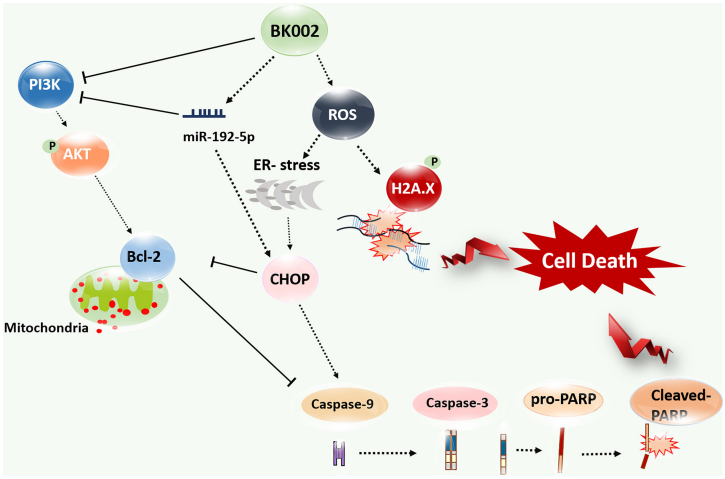

FIGURE 8 | Model of BK002-mediated apoptosis induction in castration-resistant prostate cancer (CRPC) cells and prostate cancer cells. BK002 efficiently encouraged ROS generation which activated ER stress and CHOP in conjunction with apoptotic cascade caspase activation and activation of p-γH2A.X leading to apoptosis. PI3K, p-AKT, and survivin were subsequently downregulated by BK002 treatment in CRPC cells and prostate cancer cells to induce apoptosis. Moreover, BK002 increased miR-192-5p expression and miR 192-5p regulated apoptosis.

DATA AVAILABILITY STATEMENT

The datasets presented in this study can be found in online repositories. The names of the repository/repositories and accession number(s) can be found in the article/supplementary material.

AUTHOR CONTRIBUTIONS

Conceptualization and writing—original draft preparation: MP, and HP. Formal analysis: CC, S-RS, and DJ. Data curation: JK, SP, YC, MR, and JC. Writing—review and editing: MP, HP, S-GK, B-SS, S-HK, MR, and BK. Visualization: MP and MR. Supervision: B-SS, S-HK, and BK. Project administration: BK. Funding acquisition: S-GK and BK. All authors have read and agreed to the published version of the manuscript.

FUNDING

This research was supported by the Basic Science Research Program through the National Research Foundation of Korea (NRF) funded by the Ministry of Education (NRF-2020R1I1A2066868), the National Research Foundation of Korea (NRF) grant funded by the Korea government (MSIT) (No. 2020R1A5A2019413), a grant from the Korea Health Technology R&D Project through the Korea Health Industry Development Institute (KHIDI), funded by the Ministry of Health & Welfare, Republic of Korea (grant number: HF20C0116), and a grant from the Korea Health Technology R&D Project through the Korea Health Industry Development Institute (KHIDI), funded by the Ministry of Health & Welfare, Republic of Korea (grant number: HF20C0038).

REFERENCES

1. Krušlin B, Ulamec M, Tomas D. Prostate Cancer Stroma: An Important Factor in Cancer Growth and Progression. *Bosn J Basic Med Sci* (2015) 15:1–8. doi: 10.17305/bjbms.2015.449
2. Siegel RL, Miller KD, Jemal A. Cancer Statistic. *CA Cancer J Clin* (2019) 69:7–34. doi: 10.3322/caac.21551
3. Heinlein CA, Chang C. Androgen Receptor in Prostate Cancer. *Endocr Rev* (2004) 25:276–308. doi: 10.1210/er.2002-0032
4. Saad F, Hotte SJ. Guidelines for the Management of Castrate-Resistant Prostate Cancer. *Can Urol Assoc J = J l'Assoc Des Urologues du Canada* (2010) 4:380–4. doi: 10.5489/cuaj.10167
5. Scher HI, Solo K, Valant J, Todd MB, Mehra M. Prevalence of Prostate Cancer Clinical States and Mortality in the United States: Estimates Using a Dynamic Progression Model. *PloS One* (2015) 10:e0139440. doi: 10.1371/journal.pone.0139440
6. Ingrosso G, Detti B, Scartoni D, Lancia A, Giacomelli I, Baki M, et al. Current Therapeutic Options in Metastatic Castration-Resistant Prostate Cancer. *Semin Oncol* (2018) 45:303–15. doi: 10.1053/j.seminoncol.2018.10.001
7. Kirby M, Hirst C, Crawford ED. Characterising the Castration-Resistant Prostate Cancer Population: A Systematic Review. *Int J Clin Pract* (2011) 65:1180–92. doi: 10.1111/j.1742-1241.2011.02799.x
8. Pal SK, Patel J, He M, Foulk B, Kraft K, Smirnov DA, et al. Identification of Mechanisms of Resistance to Treatment With Abiraterone Acetate or Enzalutamide in Patients With Castration-Resistant Prostate Cancer (CRPC). *Cancer* (2018) 124:1216–24. doi: 10.1002/cncr.31161
9. Taylor BS, Schultz N, Hieronymus H, Gopalan A, Xiao Y, Carver BS, et al. Integrative Genomic Profiling of Human Prostate Cancer. *Cancer Cell* (2010) 18:11–22. doi: 10.1016/j.ccr.2010.05.026
10. Araki K, Miyoshi Y. Mechanism of Resistance to Endocrine Therapy in Breast Cancer: The Important Role of PI3K/Akt/mTOR in Estrogen Receptor-Positive, HER2-Negative Breast Cancer. *Breast Cancer* (2018) 25:392–401. doi: 10.1007/s12282-017-0812-x
11. Luo J, Yao JF, Deng XF, Zheng XD, Jia M, Wang YQ, et al. 14, 15-EET Induces Breast Cancer Cell EMT and Cisplatin Resistance by Up-Regulating Integrin αvβ3 and Activating FAK/PI3K/AKT Signaling. *J Exp Clin Cancer Res* (2018) 37:23. doi: 10.1186/s13046-018-0694-6

12. Panda M, Biswal BK. Cell Signaling and Cancer: A Mechanistic Insight Into Drug Resistance. *Mol Biol Rep* (2019) 46:5645–59. doi: 10.1007/s11033-019-04958-6
13. Ramapriyan R, Caetano MS, Barsoumian HB, Mafra ACP, Zambalde EP, Menon H, et al. Altered Cancer Metabolism in Mechanisms of Immunotherapy Resistance. *Pharmacol Ther* (2019) 195:162–71. doi: 10.1016/j.pharmthera.2018.11.004
14. Ulianich L, Insabato L. Endoplasmic Reticulum Stress in Endometrial Cancer. *Front Med (Lausanne)* (2014) 1:55. doi: 10.3389/fmed.2014.00055
15. Rodvold JJ, Chiu KT, Hiramatsu N, Nussbacher JK, Galimberti V, Mahadevan NR, et al. Intercellular Transmission of the Unfolded Protein Response Promotes Survival and Drug Resistance in Cancer Cells. *Sci Signal* (2017) 10. doi: 10.1126/scisignal.aah7177
16. Lim HJ, Park MN, Kim C, Kang B, Song H-S, Lee H, et al. MiR-657/ATF2 Signaling Pathway Has a Critical Role in Spatholobus Suberectus Dunn Extract-Induced Apoptosis in U266 and U937 Cells. *Cancers* (2019) 11:150. doi: 10.3390/cancers11020150
17. Zhou W, Fang H, Wu Q, Wang X, Liu R, Li F, et al. Ilamycin E, a Natural Product of Marine Actinomycete, Inhibits Triple-Negative Breast Cancer Partially Through ER Stress-CHOP-Bcl-2. *Int J Biol Sci* (2019) 15:1723–32. doi: 10.7150/ijbs.35284
18. Ranganathan AC, Zhang L, Adam AP, Aguirre-Ghiso JA. Functional Coupling of P38-Induced Up-Regulation of BiP and Activation of RNA-Dependent Protein Kinase-Like Endoplasmic Reticulum Kinase to Drug Resistance of Dormant Carcinoma Cells. *Cancer Res* (2006) 66:1702–11. doi: 10.1158/0008-5472.CAN-05-3092
19. Misra UK, Deedwania R, Pizzo SV. Activation and Cross-Talk Between Akt, NF-Kappab, and Unfolded Protein Response Signaling in 1-LN Prostate Cancer Cells Consequent to Ligation of Cell Surface-Associated GRP78. *J Biol Chem* (2006) 281:13694–707. doi: 10.1074/jbc.M511694200
20. Zhang Y, Tseng CC, Tsai YL, Fu X, Schiff R, Lee AS. Cancer Cells Resistant to Therapy Promote Cell Surface Relocalization of GRP78 Which Complexes With PI3K and Enhances PI(3,4,5)P3 Production. *PloS One* (2013) 8:e80071. doi: 10.1371/journal.pone.0080071
21. Maimon Y, Samuels N, Cohen Z, Berger R, Rosenthal DS. Botanical Formula LCS101: A Multi-Targeted Approach to Cancer Care. *Integr Cancer Ther* (2018) 17:1020–6. doi: 10.1177/1534735418801528
22. Majumder R, Adhikari L, Dhara M. Olax Psittacorum (Lam.) Vahl. (Olacaceae): Current Status and Future Prospects as an Herbal Plant. *Adv Traditional Med* (2020). doi: 10.1007/s13596-020-00493-z
23. Soignet SL, Frankel SR, Douer D, Tallman MS, Kantarjian H, Calleja E, et al. United States Multicenter Study of Arsenic Trioxide in Relapsed Acute Promyelocytic Leukemia. *J Clin Oncol* (2001) 19:3852–60. doi: 10.1200/JCO.2001.19.18.3852
24. Wang X, Fang G, Pang Y. Chinese Medicines in the Treatment of Prostate Cancer: From Formulas to Extracts and Compounds. *Nutrients* (2018) 10. doi: 10.3390/nu10030283
25. Martins A, Tóth N, Ványolós A, Béni Z, Zupkó I, Molnár J, et al. Significant Activity of Ecdysteroids on the Resistance to Doxorubicin in Mammalian Cancer Cells Expressing the Human ABCB1 Transporter. *J Med Chem* (2012) 55:5034–43. doi: 10.1021/jm300424n
26. Martins A, Sipos P, Dér K, Csábi J, Miklos W, Berger W, et al. Ecdysteroids Sensitize MDR and Non-MDR Cancer Cell Lines to Doxorubicin, Paclitaxel, and Vincristine But Tend to Protect Them From Cisplatin. *BioMed Res Int* (2015) 2015:895360. doi: 10.1155/2015/895360
27. Fumagalli G, Giorgi G, Vágvölgyi M, Colombo E, Christodoulou MS, Collico V, et al. Heteronanoparticles by Self-Assembly of Ecdysteroid and Doxorubicin Conjugates To Overcome Cancer Resistance. *ACS Med Chem Lett* (2018) 9:468–71. doi: 10.1021/acsmedchemlett.8b00078
28. Vágvölgyi M, Martins A, Kulmány Ã., Zupkó I, Gáti T, Simon A, et al. Nitrogen-Containing Ecdysteroid Derivatives vs. Multi-Drug Resistance in Cancer: Preparation and Antitumor Activity of Oximes, Oxime Ethers and a Lactam. *Eur J Med Chem* (2018) 144:730–9. doi: 10.1016/j.ejmech.2017.12.032
29. Bortolozzi R, Luraghi A, Mattiuzzo E, Sacchetti A, Silvani A, Viola G. Ecdysteroid Derivatives That Reverse P-Glycoprotein-Mediated Drug Resistance. *J Nat Prod* (2020) 83:2434–46. doi: 10.1021/acs.jnatprod.0c00334
30. Lee YS, Dutta A. MicroRNAs in Cancer. *Annu Rev Pathol* (2009) 4:199–227. doi: 10.1146/annurev.pathol.4.110807.092222
31. Cha JA, Song H-S, Kang B, Park MN, Park KS, Kim S-H, et al. miR-211 Plays a Critical Role in Cnidium Officinale Makino Extract-Induced, ROS/ER Stress-Mediated Apoptosis in U937 and U266 Cells. *Int J Mol Sci* (2018) 19:865. doi: 10.3390/ijms19030865
32. Kim C, Song H-S, Park H, Kim B. Activation of ER Stress-Dependent miR-216b Has a Critical Role in Salviamiltiorrhiza Ethanol-Extract-Induced Apoptosis in U266 and U937 Cells. *Int J Mol Sci* (2018) 19:1240. doi: 10.3390/ijms19041240
33. Pan Y, Sun Y, Liu Z, Zhang C. Mir−192−5p Upregulation Mediates the Suppression of Curcumin in Human NSCLC Cell Proliferation, Migration and Invasion by Targeting C−Myc and Inactivating the Wnt/β−Catenin Signaling Pathway. *Mol Med Rep* (2020) 22:1594–604. doi: 10.3892/mmr.2020.11213
34. Kwon OS, Jeong MS, Kim B, Kim SH. Antiangiogenic Effect of Ethanol Extract of Vigna Angularis via Inhibition of Phosphorylation of VEGFR2, Erk, and Akt. *Evid Based Complement Alternat Med* (2015) 2015:371368. doi: 10.1155/2015/371368
35. Kim B, Woo MJ, Park CS, Lee SH, Kim JS, Kim B, et al. Hovenia Dulcis Extract Reduces Lipid Accumulation in Oleic Acid-Induced Steatosis of Hep G2 Cells via Activation of AMPK and PPARalpha/CPT-1 Pathway and in Acute Hyperlipidemia Mouse Model. *Phytother Res* (2017) 31:132–9. doi: 10.1002/ptr.5741
36. Zou Y, Wang R, Guo H, Dong M. Phytoestrogen β-Ecdysterone Protects PC12 Cells Against MPP+-Induced Neurotoxicity In Vitro: Involvement of PI3K-Nrf2-Regulated Pathway. *Toxicol Sci* (2015) 147:28–38. doi: 10.1093/toxsci/kfv111
37. Xu T, Niu C, Zhang X, Dong M. β-Ecdysterone Protects SH-SY5Y Cells Against β-Amyloid-Induced Apoptosis via C-Jun N-Terminal Kinase- and Akt-Associated Complementary Pathways. *Lab Invest* (2018) 98:489–99. doi: 10.1038/s41374-017-0009-0
38. Jian J, Li S, Liu LZ, Zhen L, Yao L, Gan LH, et al. XPD Inhibits Cell Growth and Invasion and Enhances Chemosensitivity in Esophageal Squamous Cell Carcinoma by Regulating the PI3K/AKT Signaling Pathway. *Int J Mol Med* (2020) 46:201–10. doi: 10.3892/ijmm.2020.4593
39. Wu LM, Liao XZ, Zhang Y, He ZR, Nie SQ, Ke B, et al. Parthenolide Augments the Chemosensitivity of Non-Small-Cell Lung Cancer to Cisplatin via the PI3K/AKT Signaling Pathway. *Front Cell Dev Biol* (2020) 8:610097. doi: 10.3389/fcell.2020.610097
40. Matsumoto M, Minami M, Takeda K, Sakao Y, Akira S. Ectopic Expression of CHOP (GADD153) Induces Apoptosis in M1 Myeloblastic Leukemia Cells. *FEBS Lett* (1996) 395:143–7. doi: 10.1016/0014-5793(96)01016-2
41. Boulares AH, Yakovlev AG, Ivanova V, Stoica BA, Wang G, Iyer S, et al. Role of Poly(ADP-Ribose) Polymerase (PARP) Cleavage in Apoptosis. Caspase 3-Resistant PARP Mutant Increases Rates of Apoptosis in Transfected Cells. *J Biol Chem* (1999) 274:22932–40. doi: 10.1074/jbc.274.33.22932
42. Branco PC, Pontes CA, Rezende-Teixeira P, Amengual-Rigo P, Alves-Fernandes DK, Maria-Engler SS, et al. Survivin Modulation in the Antimelanoma Activity of Prodiginines. *Eur J Pharmacol* (2020) 888:173465. doi: 10.1016/j.ejphar.2020.173465
43. Halasi M, Wang M, Chavan TS, Gaponenko V, Hay N, Gartel AL. ROS Inhibitor N-Acetyl-L-Cysteine Antagonizes the Activity of Proteasome Inhibitors. *Biochem J* (2013) 454:201–8. doi: 10.1042/BJ20130282
44. Ren FJ, Yao Y, Cai XY, Fang GY. Emerging Role of MiR-192-5p in Human Diseases. *Front Pharmacol* (2021) 12:614068. doi: 10.3389/fphar.2021.614068
45. Jin H, Qiao F, Wang Y, Xu Y, Shang Y. Curcumin Inhibits Cell Proliferation and Induces Apoptosis of Human Non-Small Cell Lung Cancer Cells Through the Upregulation of miR-192-5p and Suppression of PI3K/Akt Signaling Pathway. *Oncol Rep* (2015) 34:2782–9. doi: 10.3892/or.2015.4258
46. Huang W-C, Chang M-S, Huang S-Y, Tsai C-J, Kuo P-H, Chang H-W, et al. Chinese Herbal Medicine Ganoderma Tsugae Displays Potential Anti-Cancer Efficacy on Metastatic Prostate Cancer Cells. *Int J Mol Sci* (2019) 20:4418. doi: 10.3390/ijms20184418
47. Noh S, Choi E, Hwang CH, Jung JH, Kim SH, Kim B. Dietary Compounds for Targeting Prostate Cancer. *Nutrients* (2019) 11. doi: 10.3390/nu11102401
48. Fontana F, Raimondi M, Marzagalli M, Di Domizio A, Limonta P. Natural Compounds in Prostate Cancer Prevention and Treatment: Mechanisms of Action and Molecular Targets. *Cells* (2020) 9. doi: 10.3390/cells9020460
49. Culig Z, Santer FR. Androgen Receptor Signaling in Prostate Cancer. *Cancer Metastasis Rev* (2014) 33:413–27. doi: 10.1007/s10555-013-9474-0

50. Bellmunt J, Oh WK. Castration-Resistant Prostate Cancer: New Science and Therapeutic Prospects. *Ther Adv Med Oncol* (2010) 2:189–207. doi: 10.1177/1758834009359769
51. Ross RW, Kantoff PW. Hormone-Refractory Prostate Cancer: Choosing the Appropriate Treatment Option. *Oncol (Williston Park)* (2007) 21:185–93.
52. Md Ataur Rahman M, Dash R, Rahman MdH, Islam R, Uddin MdJ, Sohag A AlM, et al. Phytochemicals as a Complement to Cancer Chemotherapy: Pharmacological Modulation of the Autophagy-Apoptosis Pathway. *Front Pharmacol* (2021) 12:639628. doi: 10.3389/fphar.2021.639628
53. Shi J, Chen Q, Xu M, Xia Q, Zheng T, Teng J, et al. Recent Updates and Future Perspectives About Amygdalin as a Potential Anticancer Agent: A Review. *Cancer Med* (2019) 8:3004–11. doi: 10.1002/cam4.2197
54. Shan Q-Y, Sang X-N, Hui H, Shou Q-Y, Fu H-Y, Hao M, et al. Processing and Polyherbal Formulation of Tetradium Ruticarpum (A. Juss.) Hartley: Phytochemistry, Pharmacokinetics, and Toxicity. *Front Pharmacol* (2020) 11:133–3. doi: 10.3389/fphar.2020.00133
55. Shuvalov O, Fedorova O, Tananykina E, Gnennaya Y, Daks A, Petukhov A, et al. An Arthropod Hormone, Ecdysterone, Inhibits the Growth of Breast Cancer Cells via Different Mechanisms. *Front Pharmacol* (2020) 11:561537. doi: 10.3389/fphar.2020.561537
56. Li G, Petiwala SM, Pierce DR, Nonn L, Johnson JJ. Selective Modulation of Endoplasmic Reticulum Stress Markers in Prostate Cancer Cells by a Standardized Mangosteen Fruit Extract. *PloS One* (2013) 8:e81572. doi: 10.1371/journal.pone.0081572
57. Kim C, Kim B. Anti-Cancer Natural Products and Their Bioactive Compounds Inducing ER Stress-Mediated Apoptosis: A Review. *Nutrients* (2018) 10. doi: 10.3390/nu10081021
58. Mitsiades N. A Road Map to Comprehensive Androgen Receptor Axis Targeting for Castration-Resistant Prostate Cancer. *Cancer Res* (2013) 73:4599–605. doi: 10.1158/0008-5472.CAN-12-4414
59. Lapuk AV, Volik SV, Wang Y, Collins CC. The Role of mRNA Splicing in Prostate Cancer. *Asian J androl* (2014) 16:515–21. doi: 10.4103/1008-682X.127825
60. Delma MI. Three May Be Better Than Two: A Proposal for Metformin Addition to PI3K/Akt Inhibitor-Antiandrogen Combination in Castration-Resistant Prostate Cancer. *Cureus* (2018) 10:e3403. doi: 10.7759/cureus.3403
61. George DJ, Halabi S, Healy P, Jonasch D, Anand M, Rasmussen J, et al. Phase 2 Clinical Trial of TORC1 Inhibition With Everolimus in Men With Metastatic Castration-Resistant Prostate Cancer. *Urol Oncol* (2020) 38:79.e15–22. doi: 10.1016/j.urolonc.2019.08.015
62. Shim SY, Lee M, Lee KD. Achyranthes Japonica Nakai Water Extract Suppresses Binding of IgE Antibody to Cell Surface FcεRI. *Prev Nutr Food Sci* (2016) 21:323–9. doi: 10.3746/pnf.2016.21.4.323
63. Schröder M, Kaufman RJ. The Mammalian Unfolded Protein Response. *Annu Rev Biochem* (2005) 74:739–89. doi: 10.1146/annurev.biochem.73.011303.074134
64. George VC, Dellaire G, Rupasinghe HPV. Plant Flavonoids in Cancer Chemoprevention: Role in Genome Stability. *J Nutr Biochem* (2017) 45:1–14. doi: 10.1016/j.jnutbio.2016.11.007
65. Yenkejeh RA, Sam MR, Esmaeillou M. Targeting Survivin With Prodigiosin Isolated From Cell Wall of Serratia Marcescens Induces Apoptosis in Hepatocellular Carcinoma Cells. *Hum Exp Toxicol* (2017) 36:402–11. doi: 10.1177/0960327116651122
66. Parrish AB, Freel CD, Kornbluth S. Cellular Mechanisms Controlling Caspase Activation and Function. *Cold Spring Harb Perspect Biol* (2013) 5. doi: 10.1101/cshperspect.a008672
67. Sharma A, Singh K, Almasan A. Histone H2AX Phosphorylation: A Marker for DNA Damage. *Methods Mol Biol* (2012) 920:613–26. doi: 10.1007/978-1-61779-998-3_40
68. Jiménez-Hernández ME, Orellana G, Montero F, Portolés MT. A Ruthenium Probe for Cell Viability Measurement Using Flow Cytometry, Confocal Microscopy and Time-Resolved Luminescence. *Photochem Photobiol* (2000) 72:28–34. doi: 10.1562/0031-8655(2000)072<0028:ARPFCV>2.0.CO;2
69. Malik F, Kumar A, Bhushan S, Khan S, Bhatia A, Suri KA, et al. Reactive Oxygen Species Generation and Mitochondrial Dysfunction in the Apoptotic Cell Death of Human Myeloid Leukemia HL-60 Cells by a Dietary Compound Withaferin A With Concomitant Protection by N-Acetyl Cysteine. *Apoptosis* (2007) 12:2115–33. doi: 10.1007/s10495-007-0129-x
70. Rahman MA, Bishayee K, Habib K, Sadra A, Huh SO. 18alpha-Glycyrrhetinic Acid Lethality for Neuroblastoma Cells via De-Regulating the Beclin-1/Bcl-2 Complex and Inducing Apoptosis. *Biochem Pharmacol* (2016) 117:97–112. doi: 10.1016/j.bcp.2016.08.006
71. Rahman MA, Bishayee K, Sadra A, Huh SO. Oxyresveratrol Activates Parallel Apoptotic and Autophagic Cell Death Pathways in Neuroblastoma Cells. *Biochim Biophys Acta Gen Subj* (2017) 1861:23–36. doi: 10.1016/j.bbagen.2016.10.025
72. Tutar Y. miRNA and Cancer; Computational and Experimental Approaches. *Curr Pharm Biotechnol* (2014) 15:429. doi: 10.2174/1389201015051408281613335
73. Mohammadi A, Mansoori B, Baradaran B. Regulation of miRNAs by Herbal Medicine: An Emerging Field in Cancer Therapies. *BioMed Pharmacother* (2017) 86:262–70. doi: 10.1016/j.biopha.2016.12.023
74. Liu YX, Bai JX, Li T, Fu XQ, Chen YJ, Zhu PL, et al. MiR-Let-7a/F-CCR7 Signaling Is Involved in the Anti-Metastatic Effects of an Herbal Formula Comprising Sophorae Flos and Lonicerae Japonicae Flos in Melanoma. *Phytomedicine* (2019) 64:153084. doi: 10.1016/j.phymed.2019.153084
75. Liu W, Pan HF, Yang LJ, Zhao ZM, Yuan DS, Liu YL, et al. Panax Ginseng C.A. Meyer (Rg3) Ameliorates Gastric Precancerous Lesions in Atp4a(-/-) Mice via Inhibition of Glycolysis Through PI3K/AKT/miRNA-21 Pathway. *Evid Based Complement Alternat Med* (2020) 2020:2672648. doi: 10.1155/2020/2672648
76. Kitagishi Y, Kobayashi M, Matsuda S. Protection Against Cancer With Medicinal Herbs via Activation of Tumor Suppressor. *J Oncol* (2012) 2012:236530. doi: 10.1155/2012/236530
77. Geng L, Chaudhuri A, Talmon G, Wisecarver JL, Are C, Brattain M, et al. MicroRNA-192 Suppresses Liver Metastasis of Colon Cancer. *Oncogene* (2014) 33:5332–40. doi: 10.1038/onc.2013.478
78. Li P, Ou Q, Braciak TA, Chen G, Oduncu FS. MicroRNA-192-5p Is a Predictive Biomarker of Survival for Stage IIIB Colon Cancer Patients. *Jpn J Clin Oncol* (2018) 48:619–24. doi: 10.1093/jjco/hyy019

Conflict of Interest: The authors declare that the research was conducted in the absence of any commercial or financial relationships that could be construed as a potential conflict of interest.

frontiers in Oncology

ORIGINAL RESEARCH
published: 23 March 2022
doi: 10.3389/fonc.2022.759791

Urine- and Blood-Based Molecular Profiling of Human Prostate Cancer

Gang Chen[1†], Guojin Jia[1], Fan Chao[1], Feng Xie[2], Yue Zhang[2], Chuansheng Hou[1], Yong Huang[2], Haoran Tang[2], Jianjun Yu[2], Jihong Zhang[3], Shidong Jia[2] and Guoxiong Xu[3*†]*

[1] Department of Urology, Jinshan Hospital, Fudan University, Shanghai, China, [2] Huidu Shanghai Medical Sciences Ltd, Shanghai, China, [3] Research Center for Clinical Research, Jinshan Hospital, Fudan University, Shanghai, China

Objective: Prostate cancer (PCa) is one of the most common malignant tumors, accounting for 20% of total tumors ranked first in males. PCa is usually asymptomatic at the early stage and the specificity of the current biomarkers for the detection of PCa is low. The present study evaluates circulating tumor DNA (ctDNA) in blood or urine, which can be used as biomarkers of PCa and the combination of these markers may increase the sensitivity and specificity of the detection of PCa.

Methods: Tissue, blood, and urine samples were collected from patients with PCa. All prostate tissue specimens underwent pathological examination. A hybrid-capture-based next-generation sequencing assay was used for plasma and urinary ctDNA profiling. Sequencing data were analyzed by an in-house pipeline for mutation calling. Mutational profiles of PCa and BPH were compared in both plasma and urine samples. Associations of detected mutations and clinical characteristics were statistically analyzed.

Results: A significant association of mutation allele frequencies (MAFs) in the blood samples with patients with metastatic PCa rather than patients with primary PCa, and MAFs are changed after treatment in patients with PCa. Further, the number of mutations in urine is not associated with clinical characteristics of PCa patients, but the frequencies of mutation alleles in the urine are associated with patient age. Comparison of cfDNA aberration profiles between urine and blood reveals more alterations in urine than in blood, including *TP53*, *AR*, *ATM*, *MYC*, and *SPOP* mutations.

Conclusion: This work provides the potential clinical application of urine, in addition to blood, as a powerful and convenient non-invasive approach in personalized medicine for patients with PCa.

Keywords: biomarker, circulating tumor DNA, liquid biopsy, mutation allele frequency, prostate cancer

OPEN ACCESS

Edited by:
Hua Li,
Henry M Jackson Foundation for the Advancement of Military Medicine (HJF), United States

Reviewed by:
Gilda Alves Brown,
Rio de Janeiro State University, Brazil
Maolake Aerken,
University at Buffalo, United States

***Correspondence:**
Gang Chen
chgan365@126.com
Guoxiong Xu
guoxiong.xu@fudan.edu.cn

†ORCID:
Gang Chen
orcid.org/0000-0002-9989-2381
Guoxiong Xu
orcid.org/0000-0002-9074-8754

Specialty section:
This article was submitted to Genitourinary Oncology, a section of the journal Frontiers in Oncology

Received: *17 August 2021*
Accepted: *02 March 2022*
Published: *23 March 2022*

Citation:
Chen G, Jia G, Chao F, Xie F, Zhang Y, Hou C, Huang Y, Tang H, Yu J, Zhang J, Jia S and Xu G (2022) Urine- and Blood-Based Molecular Profiling of Human Prostate Cancer. Front. Oncol. 12:759791. doi: 10.3389/fonc.2022.759791

INTRODUCTION

Prostate cancer (PCa) is one of the most common malignant tumors in males. The American Cancer Society estimated 191,930 newly diagnosed PCa cases that account for 20% of male tumors ranked first in male cancers and 33,330 deaths ranked second in male cancers in 2020 (1). PCa is usually asymptomatic at the early stage and mostly diagnosed through the blood test of prostate-specific

antigen (PSA), a biomarker widely used for over 20 years (2), combined with magnetic resonance imaging (MRI) and digital rectal examination. However, serum PSA is organ-specific rather than cancer-specific, and PSA levels also increase in association with benign prostatic hyperplasia (BPH) and prostatitis. It has been reported that the specificity for the detection of PCa is only about 30% (3). Therefore, alternative biomarkers for the early diagnosis, prevention, and treatment of PCa are eagerly required (4).

Tissue biopsy for the analysis of primary and metastatic lesions is efficient but invasive and is limited by the heterogeneity of individual lesions. As an alternative to a tissue biopsy, the liquid biopsy is minimally invasive and can be easily acquired, thus often being used in clinical practice when a tumor sample is unavailable or difficult to obtain. The detection of circulating nucleic acids in human plasma was first described in 1948 (5). In recent years, liquid biopsy has achieved clinical utility for predicting the responsiveness of treatment, drug resistance, and disease recurrence through analyzing circulating tumor DNA (ctDNA) in blood samples. Generally, tumor cells are constantly shed in the patient's body, releasing cellular components such as DNA and proteins, which may enter into the blood circulation. Therefore, the peripheral blood from tumor patients may contain ctDNA, extracellular vesicles, and circulating tumor cells (CTCs) carrying tumor genomic information which might reflect tumor burden and progression (6).

A previous study showed that primary tissue and ctDNA share relevant somatic alterations, suggesting that ctDNA can be used for molecular subtyping in metastatic castration-sensitive PCa (7). Moreover, it has been reported that a ctDNA assay is sufficient to identify all driver DNA alterations presented in matched tissue in most metastatic castration-resistant PCa (mCRPC) cases, indicating that the management of patients with mCRPC could be based on ctDNA profiling alone (8). In general practice, liquid biopsy analysis can guide the use of androgen receptor (AR)-targeted therapy (9). Most interestingly, DNA fragments can also be detected in urine. The detection of the Y-chromosome SRY gene fragment in the urine supernatant was reported in 1999 (10), indicating the potential use of urine-based DNA biomarkers. Ten years later, transrenal DNA (tr-DNA) filtered by the kidney from the blood was detected in the urine and confirmed to be cell-free DNA (cfDNA) (11). Urine is also an effective source of tumor DNA and is more patient-friendly due to its non-invasive collection methods (12).

Liquid biopsy has been increasingly used in clinical applications. However, the diagnostic value of blood-based ctDNA and urinary ctDNA has not been fully validated. In the present study, we determined whether these circulating nucleic acids could be used as biomarkers of PCa and if the combination of these markers could increase the sensitivity and specificity of the early detection of PCa.

MATERIALS AND METHODS

Patient and Study Design

A total of 54 plasma samples and 20 urine samples were collected from patients with PCa (33 cases) and BPH (15 cases) at Jinshan Hospital, Fudan University from March 2017 to November 2018. The follow-up of patients was from March 2017 to December 2020. Written informed consent was obtained from each participant. The study was approved by the Ethics Committee of Jinshan Hospital (approval # IEC-2020-S27).

Tissue Sample Preparation and Pathological Assessment

The clinical diagnosis was based on the PSA level, a transrectal needle biopsy of the prostate gland, and histopathological examination. After surgery or biopsy, tissues from patients without neoadjuvant therapies such as hormonal therapy, chemotherapy, or radiotherapy were immediately frozen in liquid nitrogen and stored at -80°C for subsequent use. Fresh normal, BPH, and PCa tissues were used in this study. All tissues from patients without neoadjuvant therapies such as hormonal therapy, chemotherapy, or radiotherapy were immediately frozen in liquid nitrogen after surgery or biopsy and stored at -80°C for subsequent use.

All prostate tissue specimens underwent pathological examination after surgery in the Department of Pathology, Jinshan Hospital. The clinical diagnosis including histological grade and TNM stage were made by experienced pathologists and urologists according to the World Health Organization (WHO) classification and the American Joint Committee on Cancer (AJCC) Manual (eighth edition).

Liquid Sample Preparation and Cell-Free DNA Extraction

Peripheral blood was collected in EDTA vacutainer tubes and processed within 2 hours. The blood samples were allowed to clot for 30 min before centrifugation for 15 minutes at 1000 x *g* and the plasma was collected and stored at -80°C prior to cfDNA extraction. For urine sample collection, an in-house urine collection kit was developed to maintain the integrity of urinary cfDNA and to facilitate the transportation of urine samples. Morning urine was obtained through the urine collection cup and transferred into four vacuum tubes, where the urine samples were mixed thoroughly with prefilled preservation buffer.

Next-Generation Sequencing (NGS)-Based Liquid Biopsy

ctDNA sequencing and bioinformatic analysis were conducted based on previously published methods (13, 14). Briefly, plasma and urinary cfDNAs were extracted using the QIAamp circulating nucleic acid kit (Qiagen) from plasma and urine samples, respectively. Up to 30 ng of extracted cfDNA were used for library construction and then the amplified libraries were subjected to hydrid-based target panel (PredicineCARE) capture. The library was loaded to an Illumina HiSeqX Ten for 2 x 150 bp pair-end sequencing. Lastly, the sequencing data were analyzed by an in-house developed pipeline to identify point mutation, insertions, or deletions. For plasma samples, mutations with allele frequencies greater than 0.1% and with at least 4 unique supporting reads were called. For urine samples, mutations with

allele frequencies greater than 0.5% and with at least 4 unique supporting reads were called.

MSK-IMPACT Dataset

Publicly available prostate cancer mutation data were downloaded from MSK-IMPACT (15), in which 504 prostate cancer patients were reported in this study.

Blood Tests for PSA, Hemoglobin, Creatin, Albumin, Glucose

Serum PSA levels were tested using the Access Hybritech PSA kit (Beckman Coulter, Brea, CA, USA). The normal concentration of PSA ranged from 0 to 4 ng/mL. Hemoglobin levels were determined using the sodium lauryl sulfate – hemoglobin (SLS-Hb) method. Creatin levels were tested using the enzyme-linked immunosorbent assay (ELISA). Albumin levels were tested using bromocresol green. Glucose levels were tested using hexokinase ultraviolet colorimetry.

Microscopic Hematuria

Microscopic hematuria was diagnosed when there was no obvious change in the appearance of urine, but following centrifugation, there were more than 3 red blood cells per high-power field of view of the pelleted cell sample during microscopic examination.

Computed Tomography (CT) Scanning

CT scans were conducted using a 64-detector row scanner (Brilliance, Philips, Cleveland, OH, USA). The thickness of a section was 1 mm.

Statistical Analysis

Statistical analyses were conducted using the R language software (version 4.0) (https://www.r-project.org/) and Prism 8 (GraphPad Software, San Diego, CA, USA). Differences in gene mutation allele frequency (MAF) between patient groups were detected using a Mann-Whitney U test. The association of MAF or the number of mutations and categorized clinicopathological characteristics of the PCa patients was analyzed using a Mann-Whitney U test for two categories and a Kruskal-Wallis test for categories greater than two. The Association of MAF and continuous clinical features were evaluated by Spearman's correlation. Differences in the number of mutations between PCa and BPH patients were detected using a Mann-Whitney U test. A *P*-value of less than 0.05 was considered statistically significant.

RESULTS

PCa Patient Clinicopathological Characteristics

A total of 33 PCa patients and 15 BPH patients were enrolled in the present study. Compared to BPH, PCa was positively correlated with age and PSA concentration. We found that patients with PCa were older (P = 0.016) and the level of PSA was higher (P = 0.002) (**Supplementary Table 1**). Next, we compared the number of variants (< 2 *vs.* ≥ 2) among PCa patients. 19 PCa patients had variants < 2 and 14 PCa patients had variants ≥ 2. PCa patients with variants ≥ 2 were more advanced for M stage (P = 0.035) (**Table 1**).

Mutation Allele Frequencies Are Significantly Higher in The Plasma of Patients With PCa and Are Related to Metastasis

Next, we compared MAFs between PCa and BPH in plasma DNA sequencing. We observed a trend that patients with PCa have higher MAFs detected (**Figures 1A, B**), although it does not reach statistical significance (P = 0.10). Further, statistical analysis showed that there was no difference in MAF (P = 0.27; **Figure 1C**) between PCa and BPH.

Further analysis demonstrated that the MAF was associated with metastasis status. MAFs were significantly higher in metastatic PCa (P = 0.02) and lower in treatment naïve PCa patients (P = 0.03; **Supplementary Figures 1A, B**). MAF was not associated with Gleason score (P = 0.40), tumor stage (P = 0.17), PSA (P = 0.18), or age (P = 0.32) (**Supplementary Figures 1C-F**). Patients with PCa at stage IV tended to have higher MAFs (**Supplementary Figure 1D**).

Furthermore, we found that the number of mutations was associated with metastatic status and tumor stage. The number of mutations was significantly higher in metastatic PCa (P < 0.01; **Figure 1D**). Furthermore, the number of mutations was significantly associated with the tumor stage (P < 0.05; **Figure 1E**), being the highest frequent in patients with PCa at stage IV. However, the number of mutations was not associated with treatment naïve status (P = 0.53), PSA (P = 0.16), Gleason score (P = 0.61), or age (P = 0.32; **Figures 1F–I**).

PSA Levels Are Not Associated With Metastatic Status

We found that PCa patients had higher plasma PSA levels compared to BPH patients (**Figure 2A**). The serum PSA was significantly higher in PCa than in BPH patients (P < 0.01). However, there was no association of PSA concentration with MAF (P = 0.18; **Supplementary Figure 1E**), number of variants (P = 0.16; **Figure 1G**), metastatic status (P = 0.14; **Figure 2B**), treatment naïve status (P = 1.00; **Figure 2C**), Gleason score (P = 0.33; **Figure 2D**), tumor stage (P = 0.48; **Figure 2E**), or age (P = 0.49; **Figure 2F**).

Plasma cfDNA Genomic Alterations Across Samples

Alterations in some genes were detected in PCa patients, including *TP53*, *AR*, *ATM*, *MYC*, *APC*, *CTNNB1*, and *SPOP*, etc. (**Figures 1A**, **3**). In BPH, several genes were altered, including *TP53*, *PIK3CA*, *GNAS*, *VHL*, *CDK4*, *EGFR*, *NF1*, *RB1*, and *SMAD4* (**Figure 1A**). One patient harbored a *PIK3CA* p.Arg108His hotspot mutation. The spectrum of alterations in our study was almost identical and correlated with the clinical sequence cohort in the MSK-IMPACT

TABLE 1 | Correlation between No. of mutations and clinicopathological characteristics of the PCa patients.

Characteristic	No. of variants< 2 (n=19)	No. of variants≥ 2 (n=14)	*P*-value
Age at diagnosis, mean ± SD	77.14 ± 6.70	78.00 ± 6.62	0.7249
PSA, median (range)	56.0 (5.04-3327.0)	103.1 (10.37-6132.0)	0.4160
History of radiotherapy			0.8230
Yes, n (%)	1 (5.3)	1 (7.1)	
No, n (%)	18 (94.7)	13 (92.9)	
Castration-resistant			0.4791
Yes, n (%)	2 (10.5)	1 (7.1)	
No, n (%)	17 (89.5)	12 (85.7)	
Unknown, n (%)	0 (0.0)	1 (7.1)	
Grade group, n (%)			0.9136
1, n (%)	2 (10.5)	1 (7.1)	
2, n (%)	2 (10.5)	2 (14.3)	
3, n (%)	2 (10.5)	2 (14.3)	
4, n (%)	2 (10.5)	3 (21.4)	
5, n (%)	6 (31.6)	4 (28.6)	
Unknown, n (%)	5 (26.3)	2 (14.3)	
T stage, n (%)			0.6693
cT1, n (%)	6 (31.6)	2 (14.3)	
cT2, n (%)	7 (36.8)	5 (35.7)	
cT3, n (%)	2 (10.5)	3 (21.4)	
cT4, n (%)	3 (15.8)	2 (14.3)	
cTx, n (%)	1 (5.3)	2 (14.3)	
N stage, n (%)			0.9162
N0, n (%)	12 (63.2)	9 (64.3)	
N1, n (%)	2 (10.5)	2 (14.3)	
Nx, n (%)	5 (26.3)	3 (21.4)	
M stage, n (%)			**0.0346**
M0, n (%)	16 (84.2)	7 (50.0)	
M1, n (%)	3 (15.8)	7 (50.0)	
Stage group, n (%)			0.3035
I, n (%)	1 (5.3)	0 (0.0)	
II, n (%)	2 (10.5)	2 (14.3)	
III, n (%)	8 (42.1)	2 (14.3)	
IV, n (%)	5 (26.3)	8 (57.1)	
Unknown, n (%)	3 (15.8)	2 (14.3)	
Treatment naïve, n (%)			0.3174
Yes, n (%)	7 (36.8)	7 (50.0)	
No, n (%)	12 (63.2)	6 (42.9)	
Unknown, n (%)	0 (0.0)	1 (7.1)	

Contingency tables were analyzed using the chi-square test. Numerous data chosen from the normal population were analyzed using Student's t-test. Numerous data that were not chosen from the normal population were analyzed using the Mann-Whitney test. The bold value indicates a statistical significance. T, primary tumor; N, regional lymph node metastasis; M, distant metastasis.

database (37 *vs.* 504 samples; **Figure 3**). The mutation prevalence of SPOP and APC is lower in our dataset, which may be due to the limited sample size.

Mutation Allele Frequencies Are Changed After Treatment in Patients With PCa

Dynamic changes in MAFs in plasma samples during treatment were observed. For instance, in the case #1 patient, we observed changes of MAFs in *SPOP*, *BRAF*, *ATM*, *ESR1*, and *AR* after 6 or 12 months of treatment (**Figure 4A**). This patient was a 66-year-old man whose prostate biopsy revealed prostate adenocarcinoma with a Gleason score of 7 (3 in major + 4 in minor). At the time of diagnosis, the CT scan did not show bone metastasis (**Supplementary Figure 2A**), and the liquid biopsy revealed *BRAF* and *SPOP* mutations (**Figure 4A**). After oral treatment with bicalutamide and leuprolide for 4 months, the CT scan indicated multiple bone metastasis (**Supplementary Figure 2A**). After continuous treatment for 6 months, the liquid biopsy revealed the presence of *ATM* and *ESR1* mutations and the disappearance of *BRAF* and *SPOP* mutations. After treatment for 12 months, the liquid biopsy revealed *ATM*, *ESR1*, and *AR* mutations (**Figure 4A**). After treatment for 41 months with follow-up to August 2020, a CT scan still indicated multiple bone metastases (**Supplementary Figure 2A**). The case #2 patient was an 83-year-old man whose prostate biopsy revealed prostate adenocarcinoma with a Gleason score of 10 (5 in major + 5 in minor). At the time of diagnosis, the CT scan did not show metastasis (**Supplementary Figure 2B**) and the liquid biopsy did not reveal any gene mutations (**Figure 4B**). Subsequently, case #2 patient underwent bilateral orchiectomy and received oral bicalutamide treatment. After treatment for 5 months, the liquid biopsy revealed a *CDH1* mutation (**Figure 4B**). After treatment for 25 months and follow-up to April 2019, CT scans

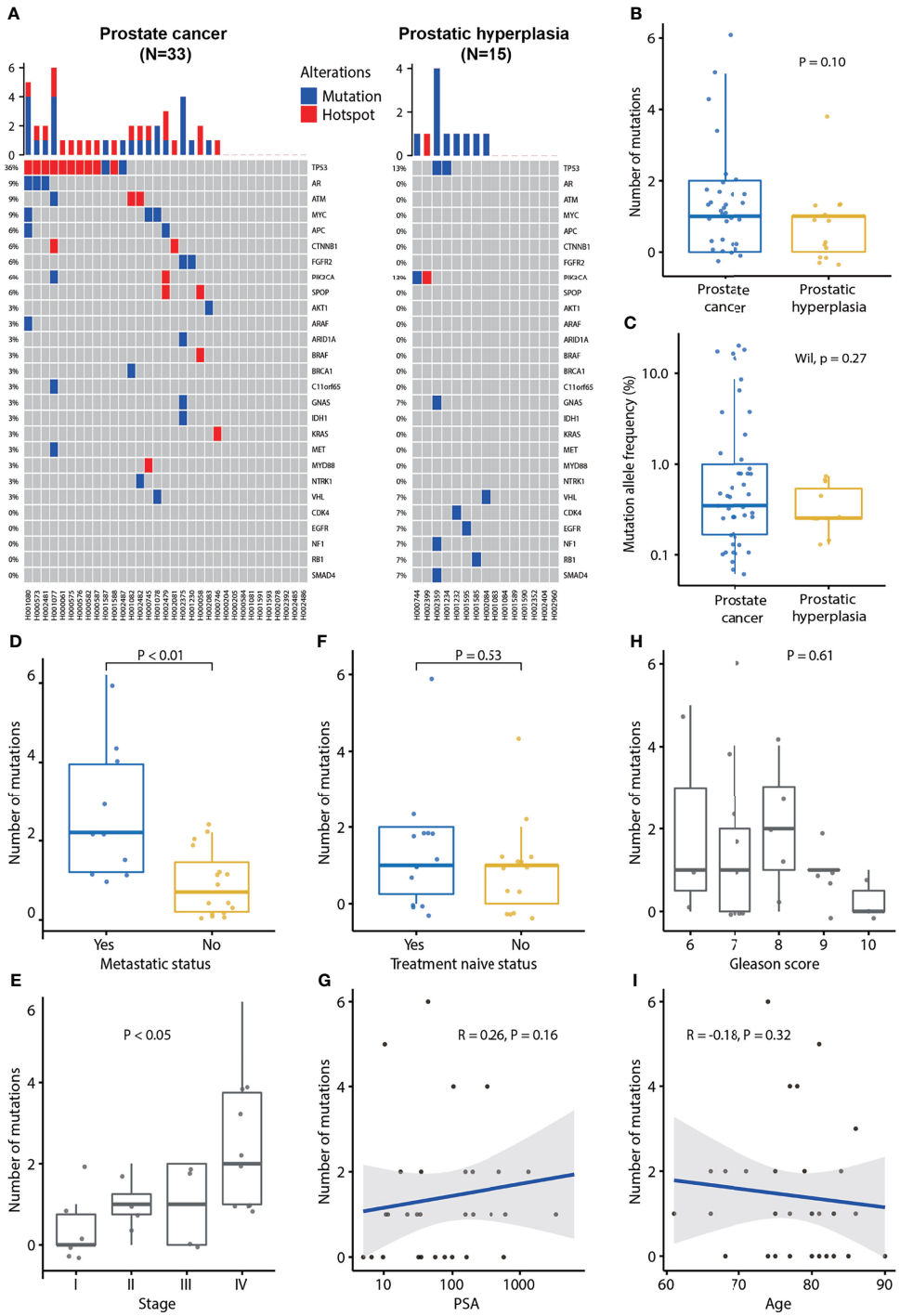

FIGURE 1 | Plasma cfDNA mutation profiles and association of the number of mutations detected in plasma cfDNA and clinical characteristics of prostate cancer. **(A)** cfDNA mutation profile of prostate cancer and prostatic hyperplasia. Blue color indicates mutation and red color indicates hotspot mutation which is defined as a mutation with occurrence greater than 20 in the COSMIC database. **(B)** The number of mutations in prostate cancer and prostatic hyperplasia. **(C)** Mutation allele frequencies in prostate cancer and hyperplasia. **(D)** Association of the number of mutation and metastatic status. p-value was calculated by the Mann-Whitney U test. **(E)** Association of the number of mutations and tumor stage. P-value was calculated by the Kruskal-Wallis test. **(F)** Association of the number of mutations and treatment naïve status. P-value was calculated by the Mann-Whitney U test. **(G)** Association of the number of mutations and PSA. Spearman's rank correlation coefficient and the corresponding P-value are shown. **(H)** Association of the number of mutations and Gleason score. P-value was calculated by the Kruskal-Wallis test. **(I)** Association of the number of mutations and age. Spearman's rank correlation coefficient and the corresponding p-value are shown. Each dot indicates one sample.

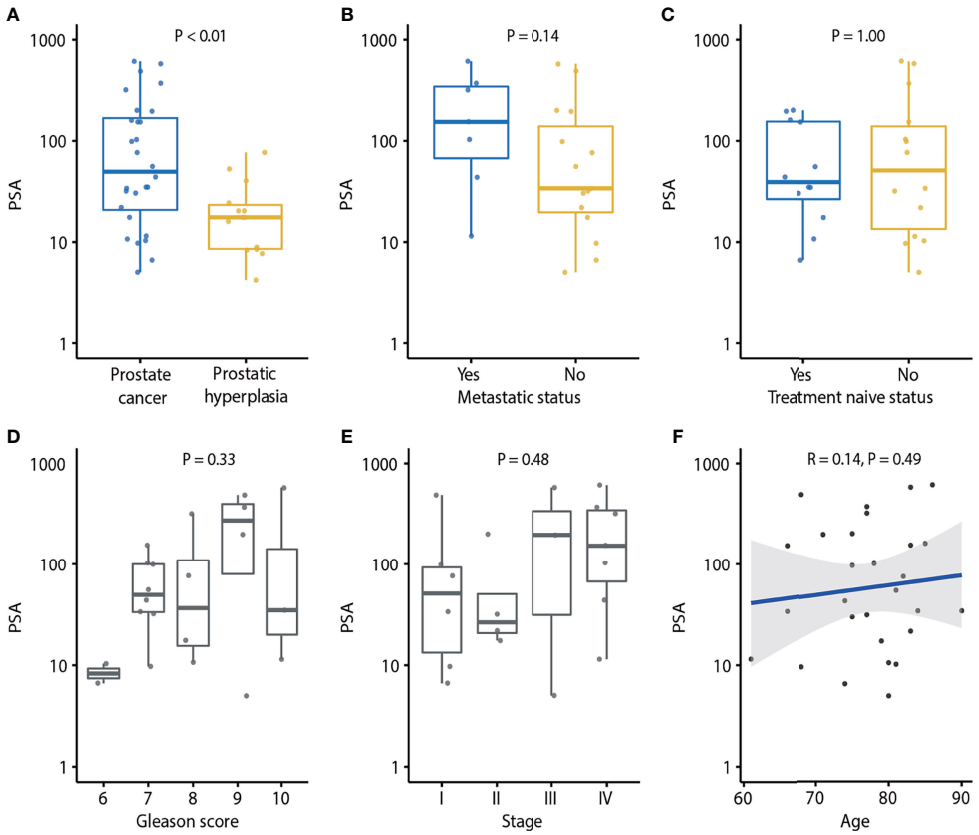

FIGURE 2 | Association of PSA and clinical characteristics of prostate cancer. **(A)** PSA in prostate cancer and prostatic hyperplasia. P-value was calculated by the Mann-Whitney U test. **(B)** Association of PSA and metastatic status. P-value was calculated by the Mann-Whitney U test. **(C)** Association of PSA and treatment naïve status. p-value was calculated by Mann-Whitney U test. **(D)** Association of PSA and Gleason score. P-value was calculated by the Kruskal-Wallis test. **(E)** Association of PSA and tumor stage. P-value was calculated by the Kruskal-Wallis test. **(F)** Association of PSA and age. Spearman's rank correlation coefficient and the corresponding P-value are shown. Each dot indicates one sample.

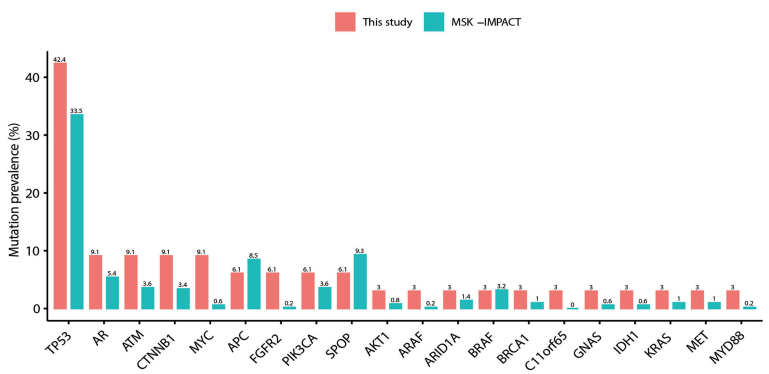

FIGURE 3 | Detection of gene mutation prevalence in plasma cfDNA samples. The plasma spectrum of alterations in this study was almost identical and correlated with tissue samples in the MSK-IMPACT Clinical Sequence Cohort of prostate cancer (37 vs. 504 samples).

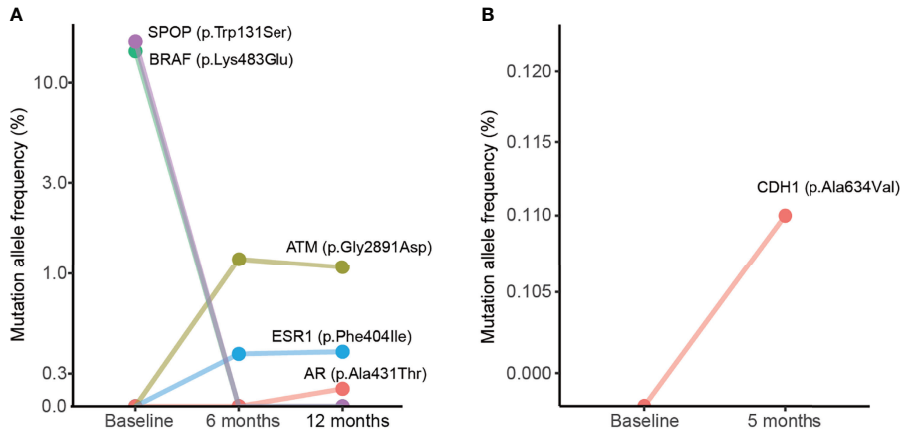

FIGURE 4 | Dynamic changes of mutation allele frequencies in plasma samples during treatment. **(A)** Plasma samples from the case #1 patient. **(B)** Plasma samples from the case #2 patient. The baseline indicates plasma samples collected from the patient before treatment.

indicated cancer recurrence and pelvic lymph node metastases (**Supplementary Figure 2B**). These data suggest that dynamic changes of MAFs may relate to metastases.

Number of Mutations and Mutation Allele Frequencies Detected in Urine From PCa Patients

In the urinary cfDNAs study, the number of mutations and the frequency of mutation alleles tended to be higher in PCa than in BPH (P = 0.25 and P = 0.06; **Supplementary Figures 3A, B**), indicating that urine may represent an alternative source for the diagnosis of PCa. The number of mutations in urine was not associated with clinical features such as metastatic status (P = 0.74). treatment naïve status (P = 0.95), Gleason score (P = 0.31), stage (P = 0.39), PSA level (P = 0.44), or age (P = 0.66) (**Supplementary Figure 4**). MAF was positively correlated with age (P = 0.03) but not associated with metastatic status (P = 0.80), treatment naïve status (P = 0.42), Gleason score (P = 0.23), tumor stage (P = 0.43), or PSA level (P = 0.69) (**Figure 5**).

cfDNA Genomic Alterations Across Urine Samples and Matched MSK-IMPACT

There were several altered genes in urine samples (n = 15) in our detection that were almost identical and correlated with the clinical sequence cohort (n = 504 samples) in the MSK-IMPACT database (**Supplementary Figure 5**).

Comparison of cfDNA Between Urine and Plasma

Next, we compared the sequencing results using urinary cfDNA to plasma cfDNA. 15 patients with paired urine and plasma samples were compared. Interestingly, the mutation profiles in plasma and urine are largely different. The prevalence rates are higher in urine than it in plasma, including *TP53* (27% *vs.* 20%), *APC* (33% *vs.* 7%), *KMT2D* (33% *vs.* 0%), *SPOP* (20% *vs.* 13%), *AR* (20% *vs.* 7%), *FGFR2* (20% *vs.* 7%), *ARID1A* (20% *vs.* 7%), *PIK3CA* (13% *vs.* 7%) and *ARAF* (20% *vs.* 0%) (**Figure 6A**). The average mutations per sample were higher in urine than it in plasma (5.2 *vs.* 1.3, P = 0.002). Interestingly, the MAFs were detected to be significantly higher in plasma than in urine by using the same variant calling cut-off 0.5% (P < 0.01; **Figures 6B, C**). From the comparison of the mutation landscape, we detected more mutations in PCa samples than BPH samples as well as more mutations in urine samples than plasma samples (**Figure 6D**).

DISCUSSION

The mechanism underlying the shift from an indolent castration-sensitive phenotype to a lethal castration-resistant PCa (CRPC) is not clear. Patients with PCa, compared with patients with BPH, had more genetic mutations in *TP53*, *AR*, *ATM*, *MYC*, *ESR1*, and *SPOP* genes and most of them were hotspot mutations. Mutations were also found in BPH samples which, as a group, harbored more *NF1*, *RB1*, and *SMAD4* mutations. In addition, *TP53*, *ATM*, *SPOP*, and *AR* gene mutations were more common in metastatic patients, which was consistent with the previous studies (16).

The *TP53* gene is a tumor suppressor gene and its inactivation plays an important role in tumorigenesis. The present study detected *TP53* mutation in the plasma and urine of patients with PCa. Indeed, *TP53* is the most frequently mutated gene in human cancers, and its mutations can cause cell cycle disorders, leading to abnormal proliferation and malignant transformation (17). About 3-47% of PCa specimens have *TP53* mutations and 2-15% contain homozygous deletions (18, 19). Previous studies have shown that a TP53R270H mutation was sufficient to induce PCa in mice (20). Mutations or deletions of *TP53* are also associated with an increased risk of the recurrence of PCa (21). The inactivation of p53 protein, encoded by the *TP53* gene, in the primary PCa may be predictive of inferior outcomes in response to novel hormonal therapies in CRPC (22).

The current study also detected mutations in the *AR* gene, which functions as a steroid hormone-activated transcription

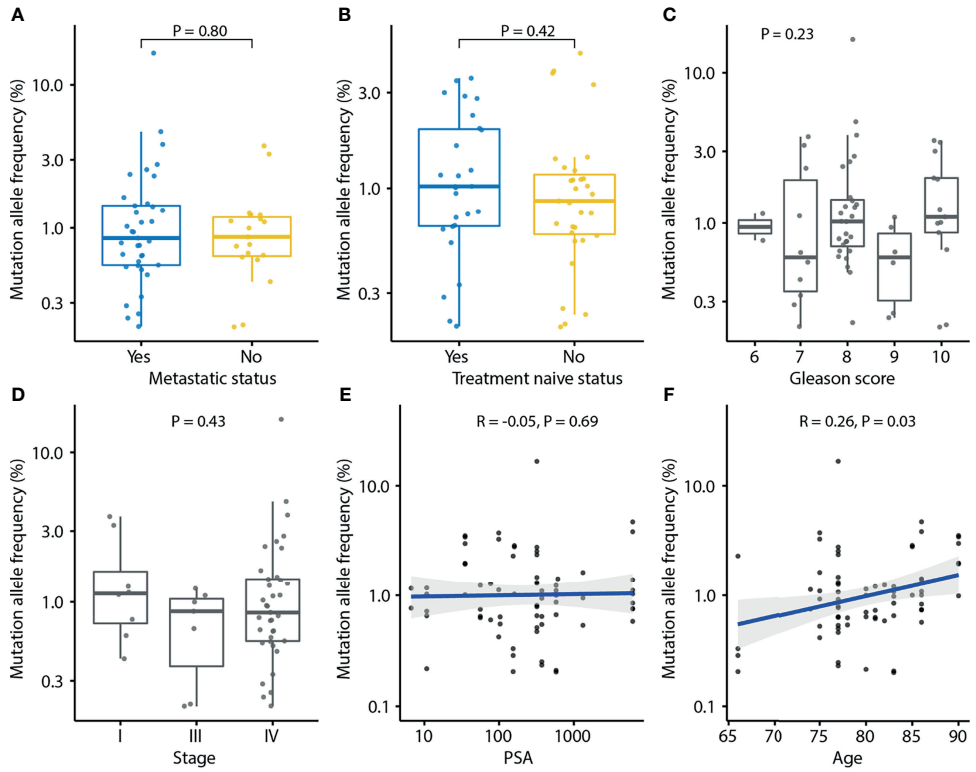

FIGURE 5 | Association of mutation allele frequency (MAF) detected in urine cfDNA and clinical characteristics of prostate cancer. Each dot indicates one sample. **(A)** Association of MAF and metastasis status. P-value was calculated by the Mann-Whitney U test. **(B)** Association of MAF and treatment naïve status. P-value was calculated by the Mann-Whitney U test. **(C)** Association of MAF and Gleason score. P-value was calculated by the Kruskal-Wallis test. **(D)** Association of MAF and tumor stage. P-value was calculated by the Kruskal-Wallis test. **(E)** Association of MAF and PSA. Spearman's rank correlation coefficient and the corresponding P-value are shown. **(F)** Association of MAF and age. Spearman's rank correlation coefficient and the corresponding P-value are shown. Each dot indicates one sample.

factor. *AR* gene aberrations are rare in prostate cancer before primary hormone treatment but emerge with castration resistance. Several studies reported the association between *AR* copy number gain in serum and abiraterone resistance (23–25). RNA in urine-derived extracellular vesicles is available for androgen receptor splice variant 7 (AR-V7) expression analysis, which is higher in patients with advanced PCa (26). Thus, liquid biopsy has detected *AR* gene mutations during late-stage PCa and in association with resistance to androgen deprivation therapy. We observed AR variants in 3/33 PCa patients.

The *ATM* gene is a DNA-damage response gene that is commonly mutated in cancer. The mutation status of *ATM* distinguishes lethal *vs.* indolent PCa and is associated with earlier age at death and shorter survival time (27). In addition, the mutation status of *ATM* is associated with grade reclassification among men undergoing active surveillance (28). Therefore, detecting the mutation status of *ATM* by liquid biopsy may aid decision-making for PCa screening and treatment.

The *MYC* gene is a proto-oncogene and encodes a nuclear phosphoprotein that plays a role in cell cycle progression, apoptosis, and cellular transformation. The *MYC* gene is overexpressed and contributes to the tumorigenesis and progression of PCa (29). A previous study reported that amplification of *MYC* ctDNA in serum was associated with worse failure-free survival and/or overall survival (OS), which remained significant after multivariable analysis (30).

SPOP gene mutation is common in solid tumors, especially in PCa (31–33). T speckle-type POZ protein, encoded by the *SPOP* gene, is a substrate adaptor of the cullin3-RING ubiquitin ligase and localizes to nuclear speckles. Recent genomic studies reported a decreased frequency of *SPOP* mutations in mCRPC when compared to localized disease (16, 34). Detection of *SPOP* mutations in serum is expected to become a new biomarker for PCa.

In the current study, liquid biopsy profiling of the case #1 patient detected *BRAF* and *SPOP* mutations after the pathological diagnosis and before treatment. Following androgen deprivation treatment, the liquid biopsy revealed the presence of *ATM*, *ESR1*, and *AR* mutations, but not *BRAF* or *SPOP* mutations. Previous studies discovered that *ESR1* mutation was associated with bone metastasis of breast cancer (35, 36). However, the role of *ESR1* mutation in PCa has not been investigated. The *CDH1* gene encodes E-cadherin protein, which mediates calcium cell-cell adhesion. *CDH1* mutations are associated with metastatic progression in various malignant

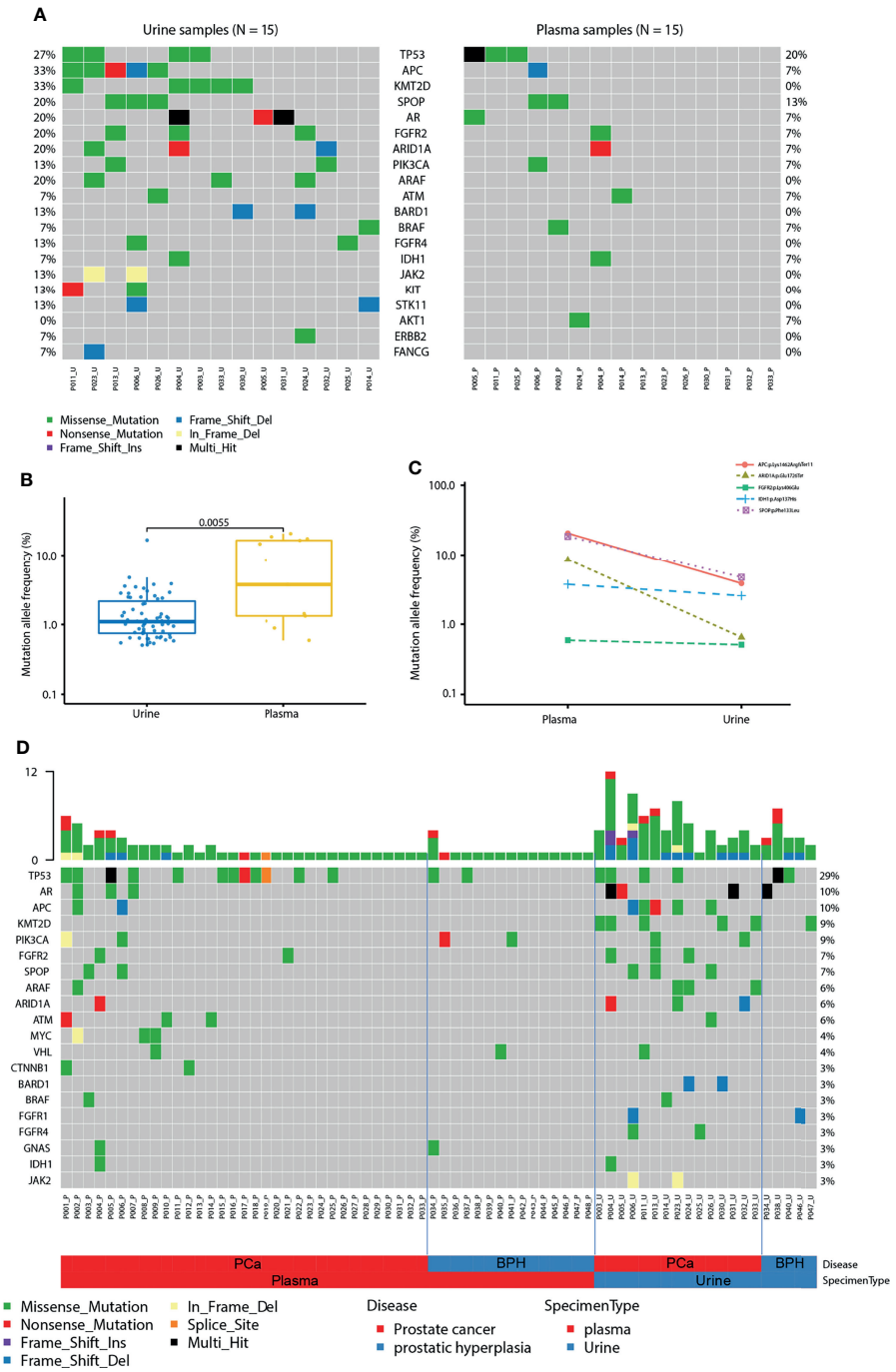

FIGURE 6 | Comparison of cfDNA between urine and plasma. **(A)** Mutation landscape of urine (left) and plasma (right) samples from patients with prostate cancer. Some genes with only one mutation were not shown in the figure. **(B)** Mutation allele frequencies detected in paired urine and plasma samples from patients with prostate cancer. **(C)** Mutation allele frequencies of matched mutations detected in paired urine and plasma samples. **(D)** The landscape of mutations in urine and plasma samples from patients with prostate cancer (PCa) and benign prostatic hyperplasia (BPH).

tumors (37–40). Our liquid biopsy detected a *CDH1* mutation in the case #2 patient after 7 months of treatment before the CT scan, which revealed cancer recurrence and pelvic lymph node metastases, indicating that liquid biopsy may have the ability to find clues of cancer recurrence and metastasis before traditional imaging examinations.

By profiling the genomic alterations in plasma and urine, we detected frequently mutated genes in PCa patients that have been

reported in previous studies. Mutations were detected in both plasma and urine samples, suggesting that the liquid biopsy technology, including both plasma- and urine-based NGS tests, may have great potential to impact PCa diagnosis, treatment selection, and disease monitoring. Interestingly, by comparing the mutations detected in plasma and urine samples from the same patients, we found more mutations were detected from urine, but higher mutation frequencies were detected in plasma. These findings suggest that the ctDNA in plasma and urine samples may come from different tumor sources. ctDNA in plasma samples are more likely from metastatic lesions, whereas ctDNA-based alterations in urine are more likely from the primary lesions. This observation suggests different clinical application scenarios of plasma- and urine-based NGS tests.

Although we recruited clinical cases and tried to focus on the evaluation of ctDNA in the blood and urine of PCa patients, there were some limitations in the current study. First, due to the short patients-recruiting period (one year and nine months), we had collected a total of 54 plasma samples and 20 urine samples. Therefore, the sample size seems to be relatively small. Second, samples of plasma and urine were not all paired from patients. Third, the follow-up timeframe was also short (three years and ten months). In the future study, we would continue to collect more samples and to follow up for five years even to ten years. Nevertheless, we thought that ctDNA can be used as biomarkers to increase the sensitivity and specificity of the detection for PCa.

In conclusion, we have used NGS-based liquid biopsy to detect alterations in several genes, including *TP53*, *AR*, *ATM*, *MYC*, and *SPOP* in PCa patients, which may be utilized for monitoring tumorigenesis. Thus, liquid biopsy is a powerful approach for analyzing tumor DNA sourced from blood and urine samples; the latter is the most convenient source for a patient and has great potential for clinical application.

DATA AVAILABILITY STATEMENT

The data presented in this study can be found in the article/**Supplementary Material**. Requests to access the datasets should be directed to Gang Chen, chgan365@126.com; Guoxiong Xu, guoxiong.xu@fudan.edu.cn.

ETHICS STATEMENT

The studies involving human participants were received and approved by The Ethics Committee of Jinshan Hospital (approval # IEC-2020-S27). Written informed consent was obtained from each participant. The patients/participants provided their written informed consent to participate in this study.

AUTHOR CONTRIBUTIONS

Conception and design: GC and GX. Development of methodology: GC, GX, GJ, FC, FX, YZ, CH, YH, and SJ. Acquisition of data (acquired and managed patients, provided facilities, sample collection, etc.): GC, GX, GJ, FC, CH, and JZ. Analysis and interpretation of data (statistical analysis, biostatistics, computational analysis, etc.): GC, GX, FX, YZ, FC, CH, YH, HT, JY, and SJ. Writing-review and editing the manuscript: GC, GX, FX, FC, JY, and SJ. Project administration and study supervision: GC, SJ, and GX. All authors contributed to the article and approved the submitted version.

FUNDING

This work was supported by a grant from the Nature Science Foundation of Shanghai (No. 18ZR1405800).

SUPPLEMENTARY MATERIAL

The Supplementary Material for this article can be found online at: https://www.frontiersin.org/articles/10.3389/fonc.2022.759791/full#supplementary-material

REFERENCES

1. Siegel RL, Miller KD, Jemal A. Cancer Statistics, 2020. *CA Cancer J Clin* (2020) 70(1):7–30. doi: 10.3322/caac.21590
2. Saini S. PSA And Beyond: Alternative Prostate Cancer Biomarkers. *Cell Oncol* (2016) 39(2):97–106. doi: 10.1007/s13402-016-0268-6
3. Jung K, Meyer A, Lein M, Rudolph B, Schnorr D, Loening SA. Ratio of Free-to-Total Prostate Specific Antigen in Serum Cannot Distinguish Patients With Prostate Cancer From Those With Chronic Inflammation of the Prostate. *J Urol* (1998) 159(5):1595–8. doi: 10.1097/00005392-199805000-00050
4. Garrido MM, Bernardino RM, Marta JC, Holdenrieder S, Guimaraes JT. Tumour Markers in Prostate Cancer: The Post-Prostate-Specific Antigen Era. *Ann Clin Biochem* (2022) 59(1):46–58. doi: 10.1177/00045632211041890
5. Alves G, Chantre M, Delmonico L. The Contribution of the 20th Century Discoveries on the Circulating DNA as Biomarkers for Cancer Screening. *Acad Bras Cienc* (2020) 92(4):e20200919. doi: 10.1590/0001-3765202020200919
6. Di Meo A, Bartlett J, Cheng Y, Pasic MD, Yousef GM. Liquid Biopsy: A Step Forward Towards Precision Medicine in Urologic Malignancies. *Mol Cancer* (2017) 16(1):80. doi: 10.1186/s12943-017-0644-5
7. Vandekerkhove G, Struss WJ, Annala M, Kallio HML, Khalaf D, Warner EW, et al. Circulating Tumor DNA Abundance and Potential Utility in *De Novo* Metastatic Prostate Cancer. *Eur Urol* (2019) 75(4):667–75. doi: 10.1016/j.eururo.2018.12.042
8. Wyatt AW, Annala M, Aggarwal R, Beja K, Feng F, Youngren J, et al. Concordance of Circulating Tumor DNA and Matched Metastatic Tissue Biopsy in Prostate Cancer. *J Natl Cancer Inst* (2017) 109(12):djx118. doi: 10.1093/jnci/djx118
9. Annala M, Vandekerkhove G, Khalaf D, Taavitsainen S, Beja K, Warner EW, et al. Circulating Tumor DNA Genomics Correlate With Resistance to Abiraterone and Enzalutamide in Prostate Cancer. *Cancer Discov* (2018) 8(4):444–57. doi: 10.1158/2159-8290.CD-17-0937
10. Zhang J, Tong KL, Li PK, Chan AY, Yeung CK, Pang CC, et al. Presence of Donor- and Recipient-Derived DNA in Cell-Free Urine Samples of Renal

Transplantation Recipients: Urinary DNA Chimerism. *Clin Chem* (1999) 45 (10):1741–6. doi: 10.1093/clinchem/45.10.1741
11. Siravegna G, Marsoni S, Siena S, Bardelli A. Integrating Liquid Biopsies Into the Management of Cancer. *Nat Rev Clin Oncol* (2017) 14(9):531–48. doi: 10.1038/nrclinonc.2017.14
12. Hatano K, Fujita K. Extracellular Vesicles in Prostate Cancer: A Narrative Review. *Transl Androl Urol* (2021) 10(4):1890–907. doi: 10.21037/tau-20-1210
13. Fettke H, Kwan EM, Docanto MM, Bukczynska P, Ng N, Graham LK, et al. Combined Cell-Free DNA and RNA Profiling of the Androgen Receptor: Clinical Utility of a Novel Multianalyte Liquid Biopsy Assay for Metastatic Prostate Cancer. *Eur Urol* (2020) 78(2):173–80. doi: 10.1016/j.eururo.2020.03.044
14. Kohli M, Tan W, Zheng T, Wang A, Montesinos C, Wong C, et al. Clinical and Genomic Insights Into Circulating Tumor DNA-Based Alterations Across the Spectrum of Metastatic Hormone-Sensitive and Castrate-Resistant Prostate Cancer. *EBioMedicine* (2020) 54:102728. doi: 10.1016/j.ebiom.2020.102728
15. Zehir A, Benayed R, Shah RH, Syed A, Middha S, Kim HR, et al. Mutational Landscape of Metastatic Cancer Revealed From Prospective Clinical Sequencing of 10,000 Patients. *Nat Med* (2017) 23(6):703–13. doi: 10.1038/nm.4333
16. Robinson D, Van Allen EM, Wu YM, Schultz N, Lonigro RJ, Mosquera JM, et al. Integrative Clinical Genomics of Advanced Prostate Cancer. *Cell* (2015) 161(5):1215–28. doi: 10.1016/j.cell.2015.05.001
17. Meek DW. Regulation of the P53 Response and Its Relationship to Cancer. *Biochem J* (2015) 469(3):325–46. doi: 10.1042/BJ20150517
18. Grasso CS, Wu YM, Robinson DR, Cao X, Dhanasekaran SM, Khan AP, et al. The Mutational Landscape of Lethal Castration-Resistant Prostate Cancer. *Nature* (2012) 487(7406):239–43. doi: 10.1038/nature11125
19. Taylor BS, Schultz N, Hieronymus H, Gopalan A, Xiao Y, Carver BS, et al. Integrative Genomic Profiling of Human Prostate Cancer. *Cancer Cell* (2010) 18(1):11–22. doi: 10.1016/j.ccr.2010.05.026
20. Vinall RL, Chen JQ, Hubbard NE, Sulaimon SS, Shen MM, Devere White RW, et al. Initiation of Prostate Cancer in Mice by Tp53R270H: Evidence for an Alternative Molecular Progression. *Dis Model Mech* (2012) 5(6):914–20. doi: 10.1242/dmm.008995
21. Kluth M, Harasimowicz S, Burkhardt L, Grupp K, Krohn A, Prien K, et al. Clinical Significance of Different Types of P53 Gene Alteration in Surgically Treated Prostate Cancer. *Int J Cancer* (2014) 135(6):1369–80. doi: 10.1002/ijc.28784
22. Maughan BL, Guedes LB, Boucher K, Rajoria G, Liu Z, Klimek S, et al. P53 Status in the Primary Tumor Predicts Efficacy of Subsequent Abiraterone and Enzalutamide in Castration-Resistant Prostate Cancer. *Prostate Cancer Prostatic Dis* (2018) 21(2):260–8. doi: 10.1038/s41391-017-0027-4
23. Romanel A, Gasi Tandefelt D, Conteduca V, Jayaram A, Casiraghi N, Wetterskog D, et al. Plasma AR and Abiraterone-Resistant Prostate Cancer. *Sci Transl Med* (2015) 7(312):312re10. doi: 10.1126/scitranslmed.aac9511
24. Salvi S, Casadio V, Conteduca V, Burgio SL, Menna C, Bianchi E, et al. Circulating Cell-Free AR and CYP17A1 Copy Number Variations May Associate With Outcome of Metastatic Castration-Resistant Prostate Cancer Patients Treated With Abiraterone. *Br J Cancer* (2015) 112(10):1717–24. doi: 10.1038/bjc.2015.128
25. Carreira S, Romanel A, Goodall J, Grist E, Ferraldeschi R, Miranda S, et al. Tumor Clone Dynamics in Lethal Prostate Cancer. *Sci Transl Med* (2014) 6 (254):254ra125. doi: 10.1126/scitranslmed.3009448
26. Woo HK, Park J, Ku JY, Lee CH, Sunkara V, Ha HK, et al. Urine-Based Liquid Biopsy: Non-Invasive and Sensitive AR-V7 Detection in Urinary EVs From Patients With Prostate Cancer. *Lab Chip* (2018) 19(1):87–97. doi: 10.1039/c8lc01185k
27. Na R, Zheng SL, Han M, Yu H, Jiang D, Shah S, et al. Germline Mutations in ATM and BRCA1/2 Distinguish Risk for Lethal and Indolent Prostate Cancer and Are Associated With Early Age at Death. *Eur Urol* (2017) 71(5):740–7. doi: 10.1016/j.eururo.2016.11.033
28. Carter HB, Helfand B, Mamawala M, Wu Y, Landis P, Yu H, et al. Germline Mutations in ATM and BRCA1/2 Are Associated With Grade Reclassification in Men on Active Surveillance for Prostate Cancer. *Eur Urol* (2019) 75(5):743–9. doi: 10.1016/j.eururo.2018.09.021
29. Koh CM, Bieberich CJ, Dang CV, Nelson WG, Yegnasubramanian S, De Marzo AM. MYC and Prostate Cancer. *Genes Cancer* (2010) 1(6):617–28. doi: 10.1177/1947601910379132
30. Sonpavde G, Agarwal N, Pond GR, Nagy RJ, Nussenzveig RH, Hahn AW, et al. Circulating Tumor DNA Alterations in Patients With Metastatic Castration-Resistant Prostate Cancer. *Cancer* (2019) 125(9):1459–69. doi: 10.1002/cncr.31959
31. Lawrence MS, Stojanov P, Mermel CH, Robinson JT, Garraway LA, Golub TR, et al. Discovery and Saturation Analysis of Cancer Genes Across 21 Tumour Types. *Nature* (2014) 505(7484):495–501. doi: 10.1038/nature12912
32. Kim MS, Je EM, Oh JE, Yoo NJ, Lee SH. Mutational and Expressional Analyses of SPOP, a Candidate Tumor Suppressor Gene, in Prostate, Gastric and Colorectal Cancers. *APMIS Acta Pathologica Microbiologica Immunologica Scandinavica* (2013) 121(7):626–33. doi: 10.1111/apm.12030
33. Cerami E, Gao J, Dogrusoz U, Gross BE, Sumer SO, Aksoy BA, et al. The Cbio Cancer Genomics Portal: An Open Platform for Exploring Multidimensional Cancer Genomics Data. *Cancer Discov* (2012) 2(5):401–4. doi: 10.1158/2159-8290.CD-12-0095
34. Cancer Genome Atlas Research N. The Molecular Taxonomy of Primary Prostate Cancer. *Cell* (2015) 163(4):1011–25. doi: 10.1016/j.cell.2015.10.025
35. Bartels S, Christgen M, Luft A, Persing S, Jodecke K, Lehmann U, et al. Estrogen Receptor (ESR1) Mutation in Bone Metastases From Breast Cancer. *Modern Pathol an Off J United States Can Acad Pathology Inc* (2018) 31(1):56–61. doi: 10.1038/modpathol.2017.95
36. Bertucci F, Ng CKY, Patsouris A, Droin N, Piscuoglio S, Carbuccia N, et al. Genomic Characterization of Metastatic Breast Cancers. *Nature* (2019) 569 (7757):560–4. doi: 10.1038/s41586-019-1056-z
37. Shenoy S. CDH1 (E-Cadherin) Mutation and Gastric Cancer: Genetics, Molecular Mechanisms and Guidelines for Management. *Cancer Manag Res* (2019) 11:10477–86. doi: 10.2147/CMAR.S208818
38. Corso G, Intra M, Trentin C, Veronesi P, Galimberti V. CDH1 Germline Mutations and Hereditary Lobular Breast Cancer. *Familial Cancer* (2016) 15 (2):215–9. doi: 10.1007/s10689-016-9869-5
39. Oliveira C, Pinheiro H, Figueiredo J, Seruca R, Carneiro F. Familial Gastric Cancer: Genetic Susceptibility, Pathology, and Implications for Management. *Lancet Oncol* (2015) 16(2):e60–70. doi: 10.1016/S1470-2045(14)71016-2
40. Luo W, Fedda F, Lynch P, Tan D. CDH1 Gene and Hereditary Diffuse Gastric Cancer Syndrome: Molecular and Histological Alterations and Implications for Diagnosis And Treatment. *Front Pharmacol* (2018) 9:1421. doi: 10.3389/fphar.2018.01421

Conflict of Interest: FX, YZ, YH, and HT are the employees of Huidu Shanghai Medical Sciences Ltd. JY and SJ are the employees and leaders of Huidu Shanghai Medical Sciences Ltd and Predicine. JY and SJ have the stock and other ownership interests of Huidu Shanghai Medical Sciences Ltd and Predicine.

The remaining authors declare that the research was conducted in the absence of any commercial or financial relationships that could be construed as a potential conflict of interest.

Publisher's Note: All claims expressed in this article are solely those of the authors and do not necessarily represent those of their affiliated organizations, or those of the publisher, the editors and the reviewers. Any product that may be evaluated in this article, or claim that may be made by its manufacturer, is not guaranteed or endorsed by the publisher.

frontiers | Frontiers in Oncology

ORIGINAL RESEARCH
published: 05 April 2022
doi: 10.3389/fonc.2022.784183

Overexpression of CDCA8 Predicts Poor Prognosis and Promotes Tumor Cell Growth in Prostate Cancer

Shun Wan†, *Yang He*†, *Bin Zhang*, *Zhi Yang*, *Fang-Ming Du*, *Chun-Peng Zhang*, *Yu-Qiang Fu* and *Jun Mi**

Department of Urology, Lanzhou University Second Hospital, Lanzhou, China

Human cell division cycle-related protein 8 (CDCA8) is an essential component of the vertebrate chromosomal passenger complex (CPC). CDCA8 was confirmed to play a role in promoting malignant tumor progression. However, the exact function of CDCA8 in the development and progression of prostate cancer (PCa) remains unclear. In this study, the database GSE69223 was downloaded by the gene expression omnibus (GEO) database, as well as CDCA8 expression differences in multiple tumor tissues and normal tissues were detected by The Cancer Genome Atlas (TCGA), TIMER, Oncomine, and Ualcan databases. Kaplan-Meier and Cox regression methods were used to analyze the correlation between CDCA8 expression and prognosis in PCa. We confirmed the expression of CDCA8 in PCa tissues by HPA. We also analyzed the association of CDCA8 expression with PCa clinical characteristics in the TCGA database. To further understand the role of CDCA8 in PCa, we assessed the effects of CDCA8 on PCa cell growth, proliferation, and migration *in vitro* studies. As a result, CDCA8 was significantly overexpressed in PCa cells compared with normal prostate cells. High CDCA8 expression predicts poor prognosis in PCa patients, and CDCA8 expression was higher in high-grade PCa. In addition, silencing of CDCA8 significantly inhibited PCa cell proliferation and migration. In summary, CDCA8 promoted the proliferation and migration of PCa cells.

Keywords: prostate cancer, CDCA8, proliferation, immune infiltration, molecular mechanism

OPEN ACCESS

Edited by:
Hua Li,
Henry M Jackson Foundation for the Advancement of Military Medicine (HJF), United States

Reviewed by:
Binil Eldhose,
Uniformed Services University, United States
Xian-Tao Zeng,
Wuhan University, China

****Correspondence:***
Jun Mi
mj7690@163.com

†These authors have contributed equally to this work

Specialty section:
This article was submitted to Genitourinary Oncology, a section of the journal Frontiers in Oncology

Received: *27 September 2021*
Accepted: *07 March 2022*
Published: *05 April 2022*

Citation:
Wan S, He Y, Zhang B, Yang Z, Du F-M, Zhang C-P, Fu Y-Q and Mi J (2022) Overexpression of CDCA8 Predicts Poor Prognosis and Promotes Tumor Cell Growth in Prostate Cancer. Front. Oncol. 12:784183. doi: 10.3389/fonc.2022.784183

INTRODUCTION

Prostate cancer (PCa) is the second leading cause of cancer death in men worldwide, with nearly 1.28 million new cases and 3.59 million deaths worldwide, according to epidemiological statistics in 2018 (1). Genetic testing plays an increasingly important role in treating patients with PCa. Studies now recommend that all patients with pancreatic or metastatic PCa and those with a family history of a high incidence of Gleason high-grade PCa should undergo genetic testing. Identifying genetic mutations can guide patients to assess the risk of other cancers and identify and manage diseases in relatives (2). The human cell division cycle-associated 8 (CDCA8) protein is a chromosomal complex essential for genome transmission during cell division (3). It has been shown that the CDCA8 gene is highly expressed in breast cancer cells and that CDCA8 gene knockdown can inhibit the survival and growth of cancer cells. Another interesting phenomenon is that higher CDCA8 gene expression is positively

correlated with the poor prognosis of which cancers. CDCA8 is, therefore, a key mediator of estrogen-stimulated breast cancer cell growth and survival (4). Studies have confirmed that CDCA8 plays a crucial role in mitosis, chromosome segregation, and cancer cell division (5). A study showed that CDCA8 was overexpressed in colorectal cancer. At the same time, loss of CDCA8 inhibited the growth of cancer cells and induced apoptosis (6). In addition, it has been reported that high expression of CDCA8 is significantly associated with lymph node metastasis in melanoma (7). This study aimed to evaluate the prognostic significance of CDCA8 gene expression in PCa by bioinformatics analysis of clinical features and survival information from The Cancer Genome Atlas (TCGA). We also performed *in vitro* experiments to investigate the effect of CDCA8 expression on PCa cell proliferation and invasion. Our results suggest that CDCA8 can be used to predict the prognosis of PCa patients and that high expression of CDCA8 is associated with poor prognosis in these patients.

MATERIALS AND METHODS

Dataset and Sample Extraction

From TCGA data (https://portal.gdc.cancer.gov/), RNA sequencing (RNA-seq) data on PCa and related cancers were obtained. The data were RNA-seq data in transcripts per million reads format of TCGA and GTEx uniformly processed by the Toil process (8). Ethics committee approval was not required as the data involved in this study were obtained from the TCGA database and adhered strictly to TCGA publication guidelines.

Screening of DEGs and Hub Genes

There were 15 PCa samples and 15 standard samples in this study. GSE69223 was downloaded from the Gene expression omnibus (GEO) database through the GEO query package to remove probes with a probe corresponding to multiple molecules. DEGs were identified by the GEO2R online analysis tool using adjusted $P < 0.05$ and $|\log FC| \geq 1$ as cut-off criteria. The GEO query package was used for data collection and download. A complex heatmap package was used to visualize the heat map. The target DEGs were imported into the Gene MANIA online database to construct a PPI network. The top 30 genes in the PPI network were selected as central genes. The cluster profile package was used for GO and KEGG enrichment analysis. The ggplot2 package was used for visualization. When the data satisfies p studies were included when p adj < 0.05 & q value < 0.2.

Epigenetic Inheritance of CDCA8 in Urinary Tumors

We used the UCSC Xena database (http://xena.ucsc.edu/) to analyze the gene copy number, methylation, somatic mutations, gene expression of CDCA8 in urinary tumors (PCa, ACC, KIRP, and KIRC).

Correlation Between CDCA8 and Human Immune Cells and Infiltration Level

Investigating the correlation between CDCA8 and human immune cells, the TISIDB database was used to explore CDCA8 expression in human cancer with human immune cells and chemokines. The TIMER algorithm was used to determine the possible link between CDCA8 expression and immune cell infiltration.

Expression of CDCA8 in Pantothenic Carcinoma and Its Expression in PCa

The GSE69223 dataset downloaded from the GEO database was analyzed for CDCA8 expression using R language visualization. The expression of CDCA8 in pan-cancer was obtained using the TCGA database. Immunohistochemical pictures of CDCA8 in normal prostate and PCa were obtained from the HPA online database.

CDCA8-Associated Signaling Pathways

To gain more insight into the function of CDCA8, GSEA was used to map the KEGG pathway and GO analysis databases. We performed GSEA using low and high CDCA8 expression datasets to identify signaling pathways differentially activated in PCa. The relevant gene pathways were selected based on the cut-off criteria FDR < 0.05 and gene size≥100.

Cell Line and Cell Transfection

RWPE-1, a normal prostate epithelial cell line, was cultured in DMEM (G4510; Servicebio, Wuhan, China) and PCa cell lines (LNCaP, DU-145, and PC3) were cultured in RPMI-1640 (G4530; Servicebio, Wuhan, China). All cell lines were obtained from the Second Hospital of Lanzhou University and incubated at 37°C and 5% CO_2 in a humidified incubator. All mediums were supplemented with 10% fetal bovine serum (FBS; 1276-025; Gibic, Beijing, China). Transfection was performed using Homo-CDCA8 (shRNA-CDCA8) and shRNA-negative control (shRNA-NC) lentivirus (GebePharma; Shanghai, China). LNCaP and DU-145 were cultured in six-well plates and transfected with lentivirus and Polybrene enhancer for 16 h. After 72 h, 2 μl 0.1 μg/μl puromycin was added to select stable cell lines. The shRNA single-strand sequences were as follows: Sh-CDCA8: 5'-TTGACTCAAGGGTCTTCAA-3'; Sh-NC: 5'-ACTACCGTTGTTATAGGTG-3'.

Real-Time PCR

Total RNA was extracted from cultured cells using TRIzol (AG21101; Hunan, China) reagent following the manufacturer's instructions and reverse transcription. Real-time quantitative PCR was performed as Yang et al. (9) described. All results for gene expression were normalized to those for β-actin. Relative quantification was performed using the $2^{-\Delta\Delta CT}$ method. Primers used for qRT-PCR were as follows: CDCA8: forward primer, 5'-CCAGAGGCCTTGGGAAACAT-3'; reverse primer, 5'-AGGAACATGGCTCCTTGC-3'; GAPDH: forward primer, 5 '-GGAAGCTTGTCATCAATGGAAATC-3' and reverse primer, 5 '-TGATGACCCTTTTGGCTCCC-3'.

Western Blotting

Total protein samples were extracted from tissues and cultured cells. Then, samples were separated using 10% SDS-PAGE and transferred to polyvinylidene fluoride membranes. After blocking with 5% skimmed milk in Tri-buffered water for 1 h,

membranes were incubated overnight at 4°C with target antibodies against the following proteins: anti-CDCA8 (1:1000, DF6115; Affinity, USA), anti-β-actin (1:2000; SA0000-1-Ig; Proteintech, Beijing, China), IRDye 800CW secondary antibody (1:20000; 926-32211; licor, Shanghai, China). β-actin was used as a reference. After three TBST washes, IRDye 800CW secondary antibody was added for 1 h at room temperature. Next, the bands were visualized by an Odyssey CLX dual-color infrared laser imaging system (CLX-0470, Genecompany, Shanghai, China). Finally, relative protein expression levels were assessed using Image J software.

Cell Proliferation Assay

For cell proliferation analysis, selected stable transplants of sh-CDCA8 and sh-NC from LNCaP and DU-145 cells were seeded in 96-well plates (2000 cells/well). CCK-8 reagent (100 μL/well) was then added to each well and cultured at 37°C for 2 h. Cell growth at 0, 24, 48, and 72 h were analyzed with Cell Counting Kit-8 (CCK-8; Apexbio, USA). The absorbance was measured at 450 nm.

Clonogenic Assay

Transfected LNCaP cells and DU-145 cells (shRNA-CDCA8, shRNA-NC) were seeded onto six-well plates with 700 cells per well and incubated for 14 days. They were fixed in 10% formaldehyde for 15 minutes, stained with 4% crystal violet for 30 minutes, and counted. Image J was used to calculate the number of colonies per well.

Wound-Healing Assay

Transfected LNCaP cells and DU-145 cells (shRNA-CDCA8, shRNA-NC) were seeded into six-well plates at 400,000 cells per well and cultured in an incubator for 24 h. Take out the 6-well plate use a ruler to draw a horizontal line on the bottom of the six-hole plate with a marking pen. The distance between each horizontal line and each horizontal line is 0.5 cm. The next day, use a 200 μl tip perpendicular to the surface of the six-hole plate and draw three vertical lines from the top perpendicular to the bottom. The culture medium was sucked off, the subcultured cells were washed off with PBS, and a serum-free medium was added for culture. The last scratch widths were collected under an inverted microscope for 0 and 24 hours.

Statistical Analysis

R (version 3.6.0), SPSS Statistics25.0 (IBM, Inc., Chicago), and ImageJ software performed all statistical analyses. To compare survival curves, we used the log-rank test to calculate HR and log-rank P values in Kaplan-Meier Plotter and GEPIA. Univariate Cox regression models were used to calculate HR and Cox P values in Progno Scan. R software and ggplot2 were used to visualize these cancers associated with CDCA8 and the poor prognosis of PCa. Differences in quantitative data between two groups were analyzed using paired or unpaired Student's t-test, Mann-Whitney U test, or Dunnett's test as appropriate. Two-way ANOVA with Sidak's multiple comparisons was applied for multiple comparisons. We considered $P < 0.05$ as statistically significant (*$P < 0.05$, **$P < 0.01$, ***$P < 0.001$).

RESULTS

Screening of DEGs and Hub Genes in TCGA and GEO

After filtering the GSE69223 data set, the samples were homogeneous and normalized by box plots (**Figure 1A**). Group1 (normal) and group2 (cancer) sample groups were quite different by PCa analysis (**Figure 1B**), and **Figure 1C** shows the expression of the top 20 up-regulated and 20 down-regulated DEGs with fold change 2. A total of 1203 DEGs were detected after analysis of GSE69223, of which 380 up-regulated genes and 823 were down-regulated (**Figure 1D**). Moreover, most of these genes were up-or down-regulated in metastatic PCa. We successfully constructed the PPI network based on the degree of correlation from high to low. Finally, We selected the top 12 central genes: CDCA8, HOXC6, CRISP3, ZIC2, FEY, PTK6, NKX2-3, GCNT1, KCNC2, STX19, ALDH3B2, GPR158 (**Supplementary Figure 1**). The results indicated that CDCA8 had a significant correlation with these Hub genes. In order to better study the mechanism and immunity of a single gene, we selected CDCA8 for further study.

Gene Methylation, Mutation, and CNV With CDCA8-Related in PCa

To analyze the potential mutation sites and methylation modifications of CDCA8 at the genetic level in urinary tumors. We used the UCSC Xena database to analyze the epigenetic inheritance of CDCA8 in PCa, ACC, KIRP, and KIRC. The results indicated that CDCA8 expression was significantly elevated in PCa, ACC, KIRP, and KIRC. Then we assessed the cause of the elevated CDCA8 levels. The heatmap indicated that CDCA8 mRNA expression correlated with CNV and DNA methylation in PCa (**Figure 2A**), ACC (**Figure 2B**), KIRP (**Figure 2C**), and KIRC (**Figure 2D**), but not with somatic mutations in PCa, ACC, and KIRC. As a result, DNA methylation, gene mutation, and CNV are closely related to genetic and epigenetic regulation and are associated with cancer progression. Therefore, we suggest that CNV and DNA methylation may cause elevated CDCA8 levels in PCa, ACC, KIRP, and KIRC.

CDCA8 Correlates With Immune Cell Infiltration and Chemokines in PCa

We used the TISIDB online database to analyze the link between CDCA8 expression and immune cell infiltration in cancers. The results indicated that CDCA8 expression was significantly positively correlated with tumor purity, infiltration levels of B cells, CD8+T cells, CD4+T cells, and macrophages in PCa (**Figure 3**). In analyzing the association of human cancers with immune cells and chemokines, we found that CDCA8 expression was positively correlated with human immune cells Act-CD4 ($rho = 0.465$, $p < 0.01$), Th2, MeM-B and chemokines CCL in PCa (**Supplementary Figure 2**). A separate analysis of the correlation between CDCA8 and immune cell infiltration in PCa revealed that CDCA8 was positively correlated with cellular infiltration such as Th2 and Tcm.

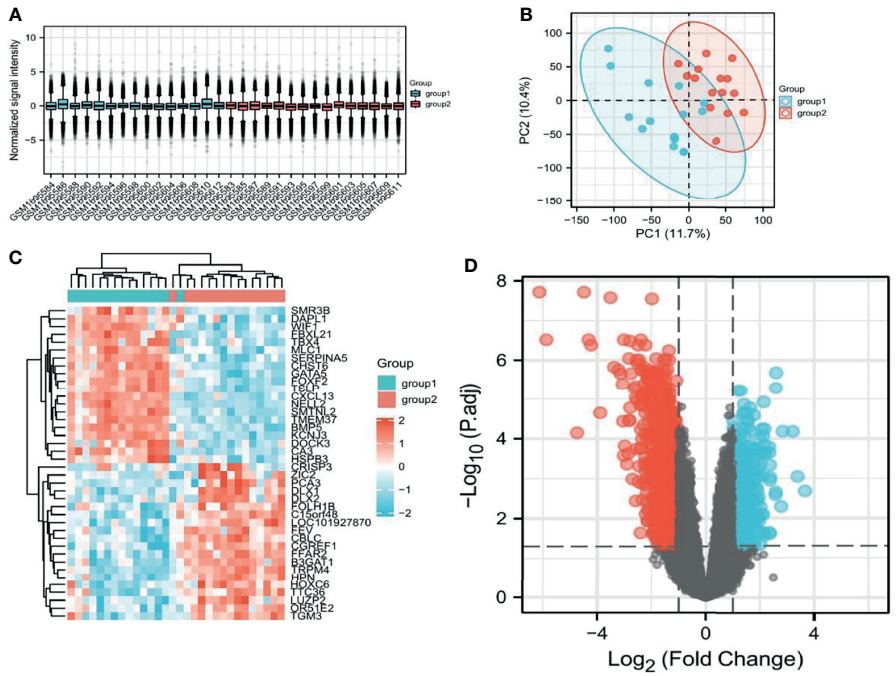

FIGURE 1 | Screening of relevant PCa genes in TCGA and GEO databases. **(A)** Sample homogeneous representation in the GSE69223 dataset. **(B)**, PCA indicates that the selected samples have good heterogeneity. **(C)** Differentially expressed genes between tumors and non-tumors. **(D)** Distribution of differentially expressed genes.

Expression of CDCA8 in Pantothenic Carcinoma Including PCa

Investigating the differential expression of CDCA8 between human tumors and normal tissues, the expression levels of CDCA8 in pan-cancer were analyzed using the TCGA database. The results showed that CDCA8 was highly expressed in ACC, BLCA, BRCA, ESCA, PRAD, and UCS cancer compared with each normal tissue (**Figure 4A**). Visual analysis showed that the expression of CDCA8 in PCa was significantly higher than that in normal tissues (**Figure 4B**), and analysis after another pairing to remove heterogeneity revealed the same results (**Figure 4C**). Receiver operating characteristic curve (ROC) was used to analyze the sensitivity and specificity of CDCA8 in the diagnosis of PCa (**Figure 4D**), and the result showed that the cut-off value of CDCA8 in the diagnosis of PCa was exact (AUC = 0.843). We then validated in GSE69223 that CDCA8 expression is significantly higher in PCa than in normal tissues (**Supplementary Figure 3B**); the above results were significantly different ($P < 0.05$). We obtained immunohistochemical pictures of normal prostate tissue and prostate cancer from HPA (**Supplementary Figures 3C, D**).

High CDCA8 Expression Is Associated With Poor Prognosis in PCa

This study analyzed the association between CDCA8 expression with OS and DFS in PCa, ACC, KIRP, KIRC, KICH, and LUAD patients by Kaplan-Meier analysis. The results showed that high expression of CDCA8 was associated with poor OS (HR = 5.08, 95% confidence interval (CI) = 1.21-21.28, P = 0.026) and poor DFS (HR = 2.31, 95% CI = 1.49-3.58, P < 0.001) in PCa patients. Similar high CDCA8 expression was associated with worse OS and DFS in patients with ACC, KIRP, KIRC, KICH, and LUAD (**Figures 5A–L**). After Cox regression analysis by collating OS, PFI, and DSS data of human cancers associated with CDCA8, human cancer was expressed using a deep forest plot. As a result, the expression of CDCA8 is correlated with OS, PFI, and DFS in PCa (**Supplementary Figure 4**). When analyzing the correlation between CDCA8 expression and clinical characteristics of PCa patients. 499 prostate samples were downloaded from the TCGA database, including the low CDCA8 expression group (n = 249) and the high CDCA8 expression group (n = 250). The high CDCA8 expression was positively correlated with PSA > = 4 and Gleason score > 7 (**Table 1**). Further visualization findings that high CDCA8 expression might be associated with poor clinical outcomes (**Figure 6**). Univariate analysis using logistic regression indicated that high expression of CDCA8 was significantly associated with Gleason score (8&9&10 vs. 6&7, OR= 3.53, 95% CI= 2.43–5.16, p < 0.001), T classification (T3&T4 vs. T2, OR = 3.09, 95%CI= 2.12–4.54, p < 0.001), and N classification (OR = 2.73, 95%CI = 1.62–4.74, p < 0.001) (**Table 2**).

The above results indicate that CDCA8 expression is significantly higher in PCa than in normal tissues. ROC curves indicate that CDCA8 can more accurately predict PCa. On the other hand, the higher the expression of CDCA8 is expressed, the worse the prognosis of PCa. Therefore, ultimately we chose the association of CDCA8 with PCa for further analysis.

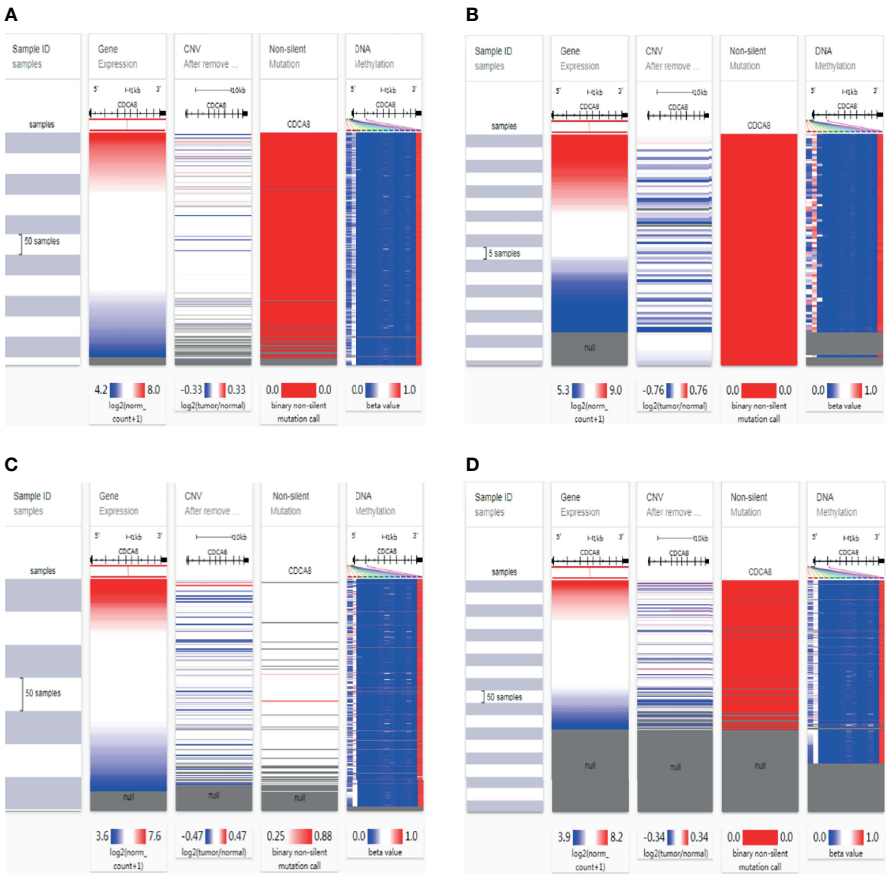

FIGURE 2 | Mutation, Copy Number Variation, and Methylation Analysis of CDCA8. CNV, DNA methylation and somatic mutations in PCa **(A)**, ACC **(B)**, KIRP **(C)** and KIRC **(D)**.

Enrichment Analysis of CDCA8 Co-Expressed Genes in PCa

To understand the signaling function of CDCA8 in PCa, GSEA was used to map KEGG pathways and GO analysis. GSEA was performed using low and high CDCA8 expression datasets to identify signaling pathways differentially activated in PCa. According to the selection criteria, the results showed four functional gene sets related to metastasis or oncogene pathways. This result indicated that high expression of CDCA8 was enriched in TP53 (ES=2.26, p=0.04, FDR=0.03), interleukins (ES=1.52, p=0.04, FDR=0.03), NOTCH (ES=1.54, p=0.04, FDR=0.03), and metabolism (ES=1.47, p=0.04, FDR=0.03) (**Figures 7A–D**). These results indicate that high CDCA8 expression shows differential enrichment in interleukin, metabolic function, TP53, NOTCH pathways.

CDCA8 Is Significantly Expressed in PCa Cells and Silencing of CDCA8 Inhibits PCa Cell Proliferation

We performed cell experiments to explore whether CDCA8 promotes PCa progression *in vitro* experiments. We first examined CDCA8 expression in prostate normal epithelial cells RWPE-1 versus PCa cell lines (LNCaP, DU-145, and PC-3). The results showed that CDCA8 was overexpressed in LNCaP, DU-145, and PC-3 cells compared with RWPE-1 (**Figures 8A, B**). For the following experiments, we selected LNCaP cells with the highest CDCA8 expression and DU-145 cells for subsequent experiments.

In order to investigate the effect of CDCA8 on the growth of PCa cells. A CCK-8 assay was performed to detect cell proliferation using stable transfer LNCaP and DU-145 cells obtained by sh-CDCA8 and sh-NC knockdown. LNCaP and DU-145 cells were transfected using shRNA-CDCA8 and shRNA-NC. The transfection efficiency was observed at 80% using an inverted fluorescence microscope after 72 h (**Figures 8C, D**). The knockdown efficiency was further verified using RT-PCR and Western blot experiments (**Figures 8E–H**). Our results indicated that down-regulation of CDCA8 significantly inhibited the proliferation of LNCaP and DU-145 cells (**Figures 9A, B**). In the colony formation assay, knockdown of CDCA8 also significantly reduced the number of cell colonies compared with sh-NC-transfected cells (**Figures 9C–F**). Both CCK8 cell proliferation and colony formation assays indicated that the decrease in CDCA8 expression inhibited the proliferation of PCa cells.

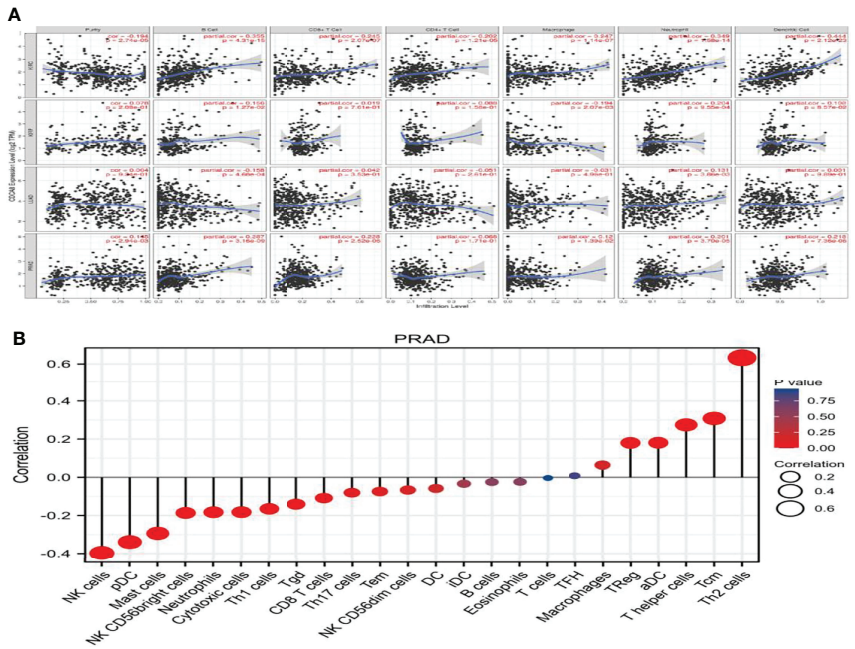

FIGURE 3 | **(A)** The correlation between PCa, KIRP, KIRC, LUAD, and immune cell infiltration. **(B)** The correlation between PCa and immune factor infiltration.

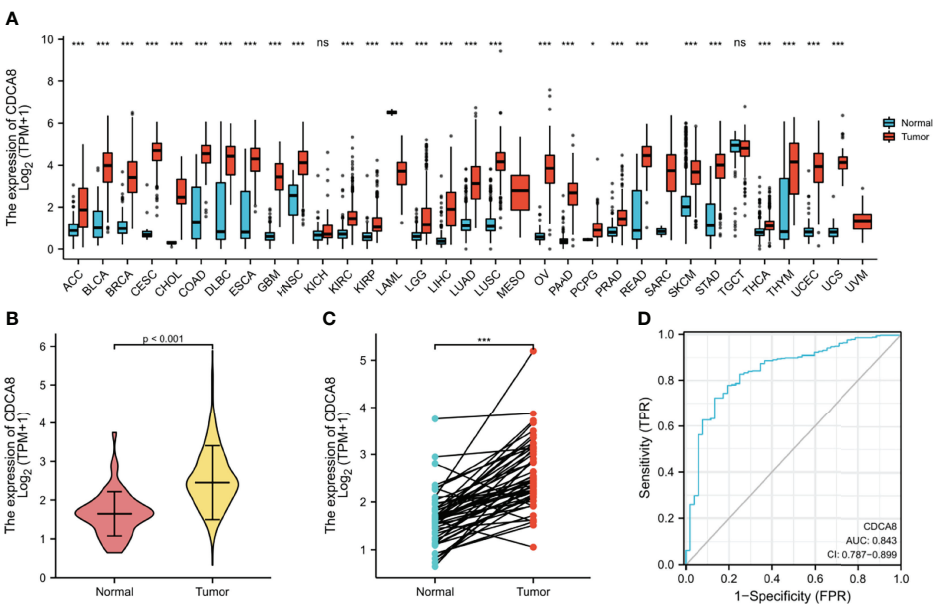

FIGURE 4 | **(A)** Expression of CDCA8 in pan-cancer. **(B, C)** Differential expression analysis of CDCA8 between prostate cancer and normal tissues in TCGA database; **(D)** Sensitivity and specificity of CDCA8 in the diagnosis of PCa. $^{ns}P > 0.05$; $^{*}P < 0.05$; $^{**}P < 0.01$; $^{***}P < 0.001$.

CDCA8 Silencing Reduces the Migratory Capacity of PCa Cells

We performed a wound-healing assay to investigate whether CDCA8 silencing affects PCa cell migration. The results showed that in LNCaP and DU-145 cells, wound healing was inhibited in sh-CDCA8-transfected cells compared with sh-NC-transfected cells for LNCaP (**Figures 10A, B**), DU-145 (**Figures 10C, D**) at 0 h and 24 h. The relative migration distances were analyzed in

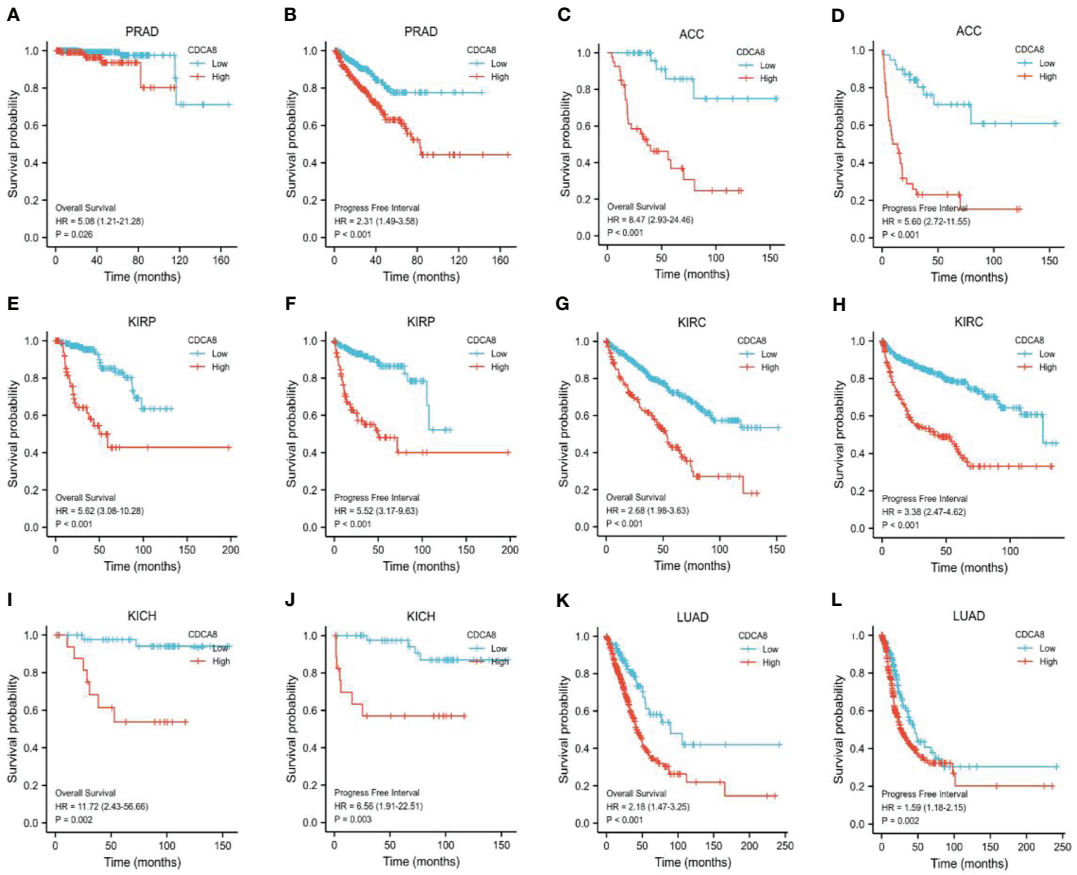

FIGURE 5 | Survival analysis of CDCA8-Associated Cancers. OS and DFS in patients with PCa **(A, B)**, ACC **(C, D)**, KIRP **(E, F)**, KIRC **(G, H)**, KICH **(I, J)**, and LUAD **(K, L)**.

TABLE 1 | Clinical features of PCa associated with CDCA8.

Characteristic	Low expression of CDCA8	High expression of CDCA8	p
n	249	250	
T stage, n (%)			<0.001
T2	124 (25.2%)	65 (13.2%)	
T3	119 (24.2%)	173 (35.2%)	
T4	3 (0.6%)	8 (1.6%)	
N stage, n (%)			0.004
N0	174 (40.8%)	173 (40.6%)	
N1	25 (5.9%)	54 (12.7%)	
M stage, n (%)			1.000
M0	221 (48.3%)	234 (51.1%)	
M1	1 (0.2%)	2 (0.4%)	
PSA(ng/ml), n (%)			0.016
<4	215 (48.6%)	200 (45.2%)	
>=4	7 (1.6%)	20 (4.5%)	
Gleason score, n (%)			<0.001
6	32 (6.4%)	14 (2.8%)	
7	145 (29.1%)	102 (20.4%)	
8	30 (6%)	34 (6.8%)	
9	41 (8.2%)	97 (19.4%)	
10	1 (0.2%)	3 (0.6%)	

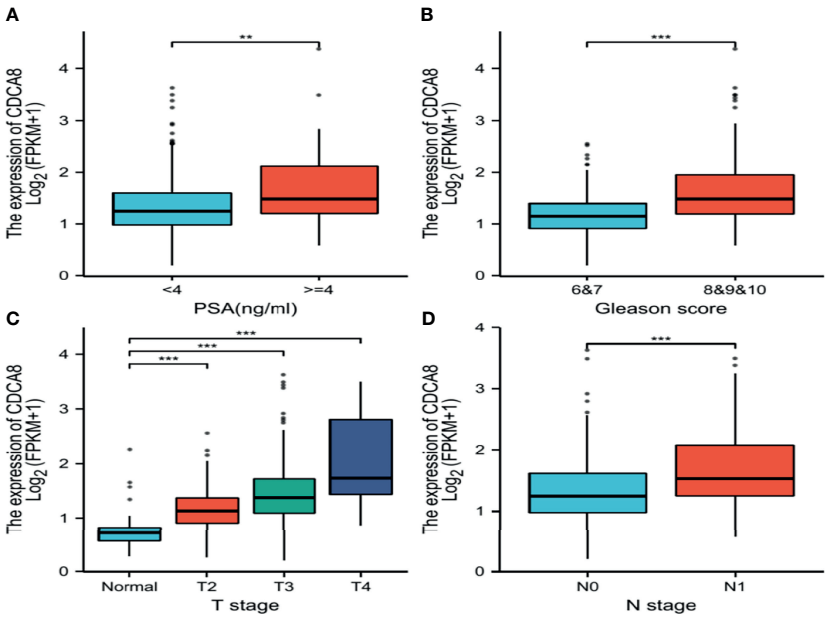

FIGURE 6 | Box plot evaluating CDCA8 expression of patients with lung adenocarcinoma according to different clinical characteristics. **(A)** PSA; **(B)** Gleason score; **(C)** T classification; **(D)** N classification, (**P < 0.01, ***P < 0.001).

TABLE 2 | Univariate regression analysis associated with high CDCA8 expression.

Characteristics	Total (N)	Odds Ratio (OR)	P value
Age (>60 vs. <=60)	499	1.306 (0.917-1.862)	0.139
PSA(ng/ml) (>=4 vs. <4)	442	1.827 (0.831-4.230)	0.142
Gleason score (8&9&10 vs. 6&7)	499	3.529 (2.431-5.163)	<0.001
T stage (T3&T4 vs. T2)	492	3.092 (2.122-4.543)	<0.001
N stage (N1 vs. N0)	426	2.729 (1.619-4.742)	<0.001

LNCaP and DU-145 cells, respectively. The results indicated that the cell migration rate of the sh-CDCA8 phase was lower than that of the sh-NC group, and the difference between the two groups was statistically significant (P < 0.01). These results indicate that CDCA8 promotes the migration of PCa cells and that the knockdown of CDCA8 inhibits their migration.

DISCUSSION

As stated in an epidemiological survey study that the incidence of PCa increased by 169.11% in 2019 compared with 1990 (10). Prostate specific antigen (PSA) is of great value in diagnosing of PCa. It is an FDA-approved biomarker for PCa (11). However, unnecessary biopsies and overtreatment in clinical practice are rising due to the low specificity of PSA in diagnosis (12). After the normal epithelium of the prostate developed into a tumor, the expression of PSA increased significantly. In people over 60 years of age, PSA production also increases, thereby reducing the sensitivity of PSA detection (13). Also, there was no significant correlation between PSA levels and PCa severity (14). Current target therapy is challenging in diagnosing and treating PCa (15). Therefore, exploring new PCa diagnostic and therapeutic targets has important clinical significance. Recent studies of high-throughput gene chips for analysis of patient average and tumor tissue samples have provided us with an opportunity to discover and explore the entire molecular landscape of tumors at various levels, from copy number changes and somatic mutations at the genomic level to altered gene expression at the transcriptional level (16–18). Microarrays currently have very few clinical applications. This limitation is broken when the advent of detecting many genes by gene profiling. However, there is still a lack of independent reliability, reproducibility, and complex statistical analysis for clinical application. At the same time, experimental identification of critical genes on a genome-wide scale is very time-consuming and laborious. An optimal method that can be processed by routine analysis needs to be developed to put these expression profiles into clinical practice as soon as possible. In addition, there is a clear need to improve our ability to enhance PCa patients at high risk of metastasis and recurrence after radical prostatectomy for PCa. The challenge of accurately predicting PCa metastasis and recurrence may be

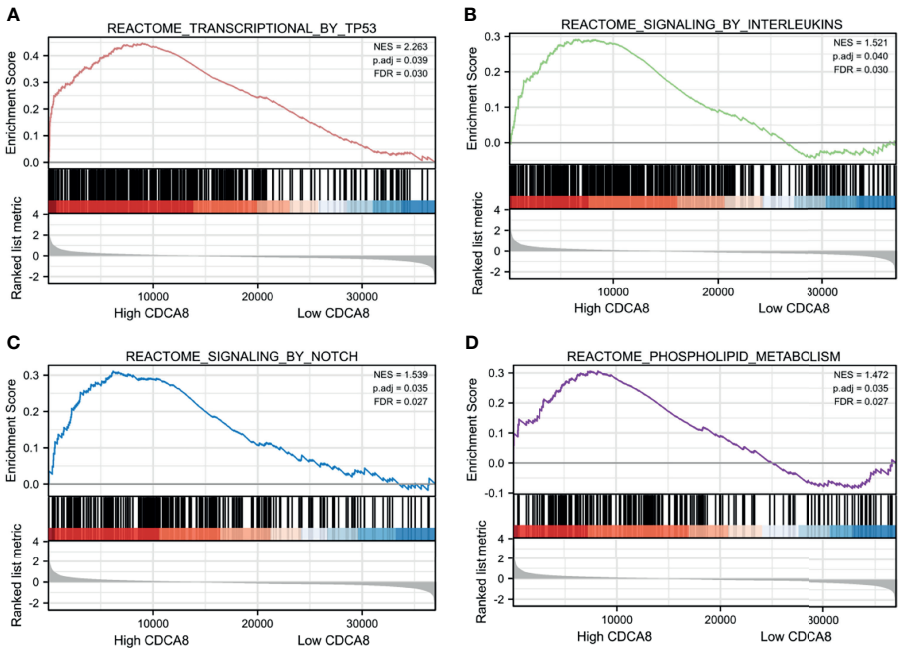

FIGURE 7 | GSEA analysis of CDCA8 co-expressed genes. High CDCA8 expression showed differential enrichment in TP53 **(A)**, interleukin **(B)**, NOTCH **(C)**, and metabolic function **(D)** pathways.

partially attributed to the complex pathways that promote disease development (19). CDCA8 plays a vital role in various tumor-related processes. In pancreatic ductal adenocarcinoma, CDCA8 promotes tumor cell proliferation (20). Consumption of CDCA8 leads to cell cycle arrest in the G2/M phase, increased DNA damage and apoptosis, and enhanced sensitivity of ovarian cancer cells to cisplatin and olaparib (21). Through the ROCK signaling pathway, CDCA8 knockdown may inhibit cancer cell proliferation and invasion (22). However, the importance of CDCA8 in PCa has not been fully elucidated. In a bioinformatics article, Songz et al. (23) built a PPI network through the KEGG database to analyze the interactions of visualized central genes. The discovery of CENPA, KIF20A, and CDCA8 may promote the development and progression of PCa, which may be new therapeutic targets and biomarkers for PCa diagnosis and prognosis. Some essential genes (including CDCA8) were validated and found to be associated with tumor stage, metastasis, biochemical recurrence, and survival. They suggested that these central genes can control cellular processes and have high clinical value. This study is the first to report that they are upregulated in PCa and correlate with survival in PCa patients. However, the authors only stated that high CDCA8 expression was associated with poor prognosis in PCa patients in this study. Nevertheless, not studied the epigenetic, genetic mutation role of CDCA8 in PCa patients and *in vitro* studies. Therefore, in our study, we further investigated the epigenetic, genetic mutation role of CDCA8 in PCa patients and further validated the role of CDCA8 in PCa patients with *in vitro* experiments. Although some prominent pathways involving AR, SPOP, MYC, RB1, and PTEN-related pathways also play a crucial role in PCa. In these complex and comprehensive processes, these central genes are involved in almost all critical cellular pathways, given that they can interact with many proteins (24–27). In another study, the authors analyzed a total of 367 PCa cases through the Cancer Genome Atlas database and performed weighted gene co-expression network analysis. The selected four central genes were CKAP2L, CDCA8, ERCC6L, and ARPC1A. The results indicate that these four central genes can distinguish tumor from normal tissue and are promising biomarkers for lymph node metastasis of PCa (28). This study provides novel insights that explain the mechanism of lymph node metastasis of PCa at the molecular level. The identified central genes may become potential biomarkers and therapeutic targets for precise diagnosis and treatment in the future. The above studies provide a more detailed molecular mechanism for lymph node metastasis with biochemical recurrence in PCa patients and provide clues for potential biomarkers and therapeutic targets. To get a reliable conclusion, we first explored CDCA8-promoted PCa progression in the TCGA and GSE69223 databases and then validated this conclusion in our experiments. In 15 pairs of PCa and prostate normal tissues from the TCGA database, CDCA8 expression was significantly higher in cancer than in normal controls. Similarly, in cell experiments, the content of CDCA8 was significantly higher in PCa cell lines than in normal prostate cells. High CDCA8 expression was associated with advanced N stage and lymphovascular invasion. In addition, CDCA8 expression gradually increased from stage I to stage III in the TCGA and GSE69223 databases.

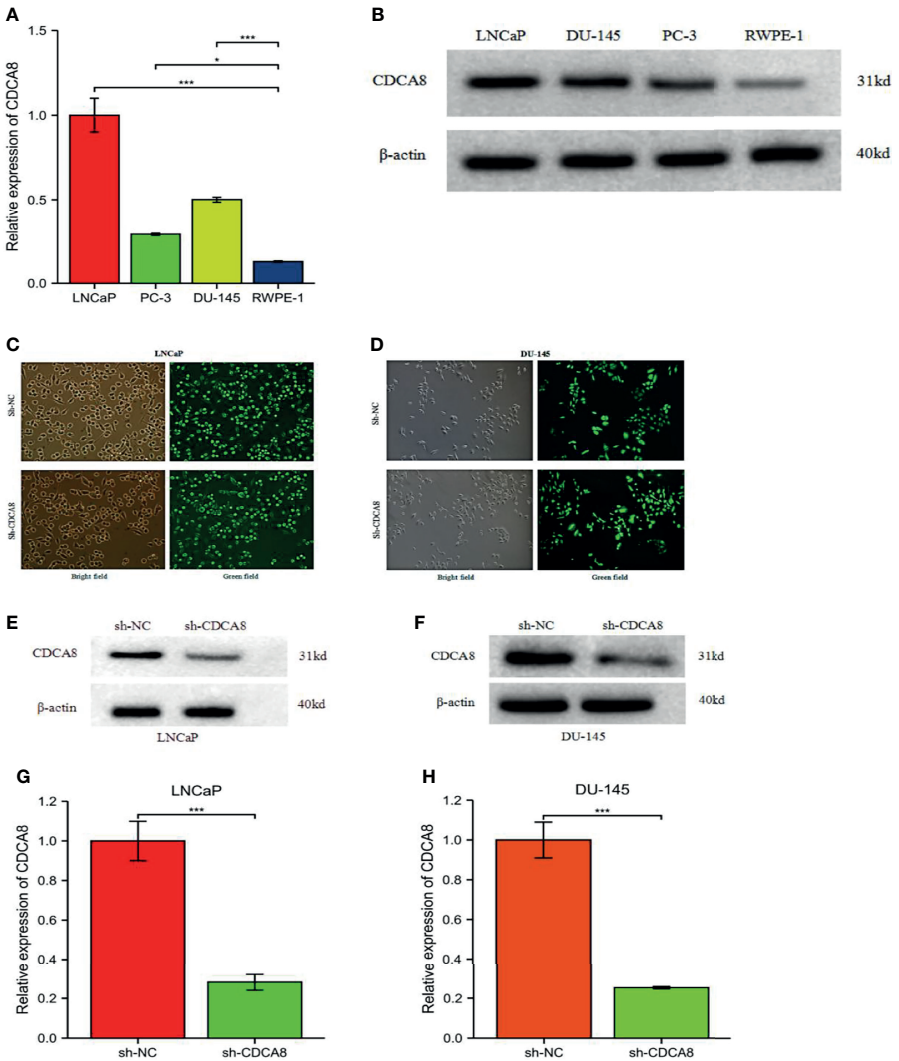

FIGURE 8 | The mRNA expression levels of CDCA8 in RWPE-1 and PCa cells. Sh-NC, negative control. CDCA8 expression levels were higher in PCa cells **(A, B)**. The knockdown efficiency of LNCaP and DU-145 cells was observed by inverted fluorescence microscopy **(C, D)**. After sh-CDCA8 and sh-NC were transfected into LNCaP and DU-145 cells, the expression levels of CDCA8 were detected by qRT-PCR and Western blotting **(E-H)**, *P < 0.5; ***P < 0.001; two-tailed t-test.

Therefore, we hypothesize that CDCA8 may be a cancer-promoting biomarker for PCa. We first validated our hypothesis in a public database. The high expression of CDCA8 in the TCGA database showed poor OS, DSS, and PFI, which confirmed the poor prognosis of the high expression of CDCA8 in PCa. All these findings indicate that CDCA8 plays a vital role in the carcinogenesis and progression of PCa. It has been stated that CDCA8 is highly expressed in LUAD cells, while miR-133b is lowly expressed, and that the promoting effect of CDCA8 on LUAD cell proliferation, migration, and invasion can be regulated by miR-133b (29). Future studies could further investigate how CDCA8 promotes prostate cancer proliferation and metastasis. Genetic testing has an extensive range of applications. Over the past few decades, this technology has made significant progress, and genetic defects in humans can be confirmed by genetic testing (30). Moreover, genetic testing can determine the appropriate targeted drug for cancer patients, which significantly improve the survival rate of cancer patients and avoid overtreatment to achieve precise treatment, thereby improving the quality of life and improving the prognosis (31, 32). It is not a problem to obtain 99% accurate DNA sequences based on the current technology. The main problem is what the ATCG combination in these DNA sequences represents and how much association is with human health remains to be solved. Monogenic diseases are relatively simple, and the corresponding relationship is also relatively easy to study. However, monogenic diseases are rare, so people often pay attention to highly prevalent complex diseases. Such as

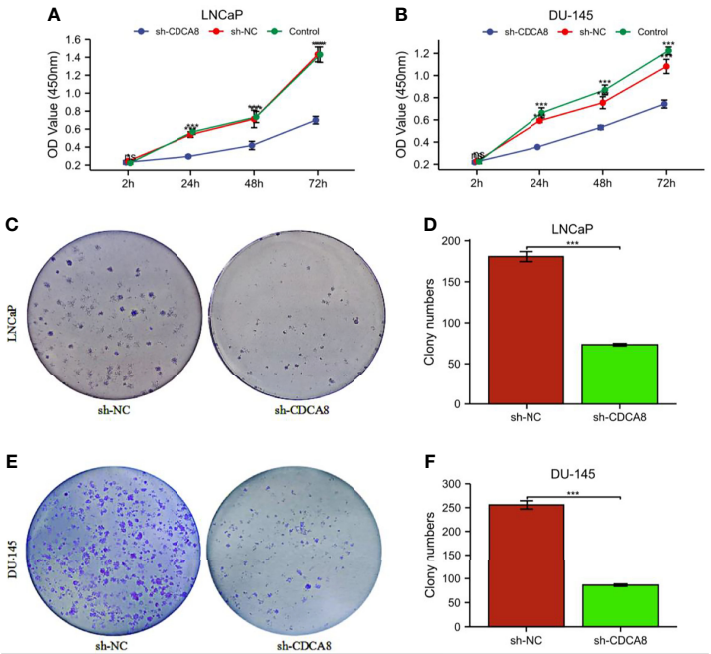

FIGURE 9 | The proliferation ability of PCa cells was significantly attenuated after the knockdown of CDCA8. **(A, B)** Cellcountingkit-8 (CCK8) analysis showed that down-regulation of CDCA8 inhibited the growth of LNCaP and DU-145 cells ($^{ns}P > 0.05$; $^{*}P < 0.05$; $^{***}P < 0.001$. two-way ANOVA). **(C-F)** In a colony formation assay, silencing of CDCA8 reduced the number of colonies in LNCaP and DU-145 cells ($^{***}P < 0.001$ versus sh-NC; two-tailed t-test). NC, negative control.

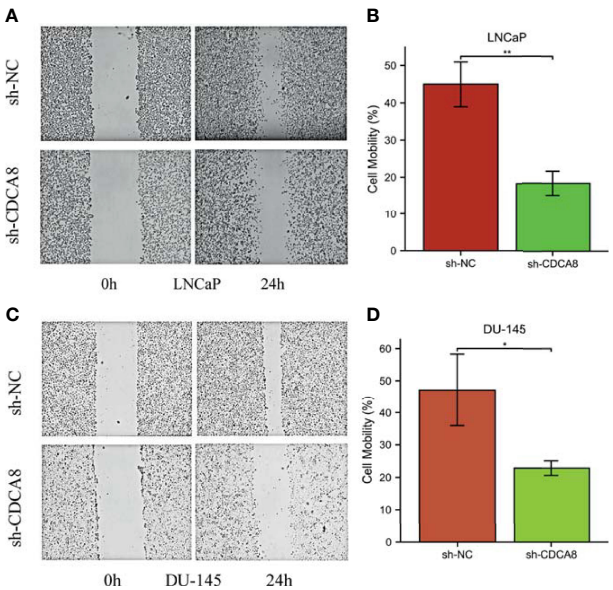

FIGURE 10 | Knockdown of CDCA8 inhibited the migration of PCa cells in vitro. **(A, C)** Wound healing assay, LNCaP and DU-145 at 0 and 24 h, respectively. **(B, D)** Relative migration distance was analyzed in LnCap and DU-145 cells, respectively. $^{*}P < 0.05$; $^{**}P < 0.01$; two-tailedt-test.

tumors, diabetes, and cardiovascular diseases are usually many opportunities to interact and participate in environmental factors (33, 34). Therefore, the limitations of genetic testing applications in risk inference for complex diseases are more pronounced. Moreover, the basic research of the CDCA8 gene in PCa needs further study. Alternatively, our study lacks clinical samples from our hospital, and future work will be needed to investigate the effects of CDCA8 *in vivo*.

CONCLUSION

In conclusion, our findings suggest that CDCA8 is significantly upregulated in PCa cell lines. High expression of CDCA8 correlates with tumor histological grade of PCa and predicts poor prognosis. Knockdown of CDCA8 inhibits PCa cell proliferation. Therefore, CDCA8 can serve as a promising diagnostic and prognostic biomarker and a new therapeutic target in PCa.

DATA AVAILABILITY STATEMENT

The original contributions presented in the study are included in the article/**Supplementary Material**. Further inquiries can be directed to the corresponding author.

AUTHOR CONTRIBUTIONS

SW wrote and edited the manuscript. YH edited the manuscript. BZ performed the statistical analyses and generated the figures. ZY, F-MD, C-PZ, and Y-QF collected the public data. JM revised and reviewed the manuscript. All authors contributed to the article and approved the submitted version.

SUPPLEMENTARY MATERIAL

The Supplementary Material for this article can be found online at: https://www.frontiersin.org/articles/10.3389/fonc.2022.784183/full#supplementary-material

REFERENCES

1. Pilarski R. The Role of BRCA Testing in Hereditary Pancreatic and Prostate Cancer Families. *Am Soc Clin Oncol Educ Book* (2019) 39:79–86. doi: 10.1200/EDBK_238977
2. Bu Y, Shi L, Yu D, Liang Z, Li W. CDCA8 Is a Key Mediator of Estrogen-Stimulated Cell Proliferation in Breast Cancer Cells. *Gene* (2019) 703:1–6. doi: 10.1016/j.gene.2019.04.006
3. Abad MA, Ruppert JG, Buzuk L, Wear M, Zou J, Webb KM, et al. Borealin-Nucleosome Interaction Secures Chromosome Association of the Chromosomal Passenger Complex. *J Cell Biol* (2019) 218(12):3912–25. doi: 10.1083/jcb.201905040
4. Bray F, Ferlay J, Soerjomataram I, Siegel RL, Torre LA, Jemal A, et al. Global Cancer Statistics 2018: GLOBOCAN Estimates of Incidence and Mortality Worldwide for 36 Cancers in 185 Countries. *CA Cancer J Clin* (2018) 68 (6):394–424. doi: 10.3322/caac.21492
5. Hindriksen S, Meppelink A, Lens SM. Functionality of the Chromosomal Passenger Complex in Cancer. *Biochem Soc Trans* (2015) 43(1):23–32. doi: 10.1042/BST20140275
6. Wang Y, Zhao Z, Bao X, Fang Y, Ni P, Chen Q, et al. Borealin/Dasra B is Overexpressed in Colorectal Cancers and Contributes to Proliferation of Cancer Cells. *Med Oncol* (2014) 31(11):248. doi: 10.1007/s12032-014-0248-5
7. Ci C, Tang B, Lyu D, Liu W, Qiang D, Ji X, et al. Overexpression of CDCA8 Promotes the Malignant Progression of Cutaneous Melanoma and Leads to Poor Prognosis. *Int J Mol Med* (2019) 43(1):404–12. doi: 10.3892/ijmm.2018.3985
8. Vivian J, Rao AA, Nothaft FA, Ketchum C, Armstrong J, Novak A, et al. Toil Enables Reproducible, Open Source, Big Biomedical Data Analyses. *Nat Biotechnol* (2017) 35(4):314–6. doi: 10.1038/nbt.3772
9. Yang Q, Tian S, Liu Z, Dong W. Knockdown of RIPK2 Inhibits Proliferation and Migration, and Induces Apoptosis *via* the NF-kappaB Signaling Pathway in Gastric Cancer. *Front Genet* (2021) 12:627464. doi: 10.3389/fgene.2021.627464
10. Zi H, He SH, Leng XY, Xu XF, Huang Q, Weng H, et al. Global, Regional, and National Burden of Kidney, Bladder, and Prostate Cancers and Their Attributable Risk Factors, 1990-2019. *Mil Med Res* (2021) 8(1):60. doi: 10.1186/s40779-021-00354-z
11. Rittenhouse HG, Finlay JA, Mikolajczyk SD, Partin AW. Human Kallikrein 2 (Hk2) and Prostate-Specific Antigen (PSA): Two Closely Related, But Distinct, Kallikreins in the Prostate. *Crit Rev Clin Lab Sci* (1998) 35(4):275–368. doi: 10.1080/10408369891234219
12. Shteynshlyuger A, Andriole GL. Cost-Effectiveness of Prostate Specific Antigen Screening in the United States: Extrapolating From the European Study of Screening for Prostate Cancer. *J Urol* (2011) 185(3):828–32. doi: 10.1016/j.juro.2010.10.079
13. Bassler TJ, Orozco R, Bassler IC, O'Dowd GJ, Stamey TA. Most Prostate Cancers Missed by Raising the Upper Limit of Normal Prostate-Specific Antigen for Men in Their Sixties Are Clinically Significant. *Urology* (1998) 52 (6):1064–9. doi: 10.1016/S0090-4295(98)00366-5
14. Cooperberg MR, Broering JM, Carroll PR. Time Trends and Local Variation in Primary Treatment of Localized Prostate Cancer. *J Clin Oncol* (2010) 28 (7):1117–23. doi: 10.1200/JCO.2009.26.0133
15. Vietri MT, D'Elia G, Caliendo G, Resse M, Casamassimi A, Passariello L, et al. Hereditary Prostate Cancer: Genes Related, Target Therapy and Prevention. *Int J Mol Sci* (2021) 22(7):3753. doi: 10.3390/ijms22073753
16. Liu M, Xu Z, Du Z, Wu B, Jin T, Xu K, et al. The Identification of Key Genes and Pathways in Glioma by Bioinformatics Analysis. *J Immunol Res* (2017) 2017:1278081. doi: 10.1155/2017/1278081
17. Sun C, Yuan Q, Wu D, Meng X, Wang B. Identification of Core Genes and Outcome in Gastric Cancer Using Bioinformatics Analysis. *Oncotarget* (2017) 8(41):70271–80. doi: 10.18632/oncotarget.20082
18. Chen L, Yuan L, Wang Y, Wang G, Zhu Y, Cao R, et al. Co-Expression Network Analysis Identified FCER1G in Association With Progression and Prognosis in Human Clear Cell Renal Cell Carcinoma. *Int J Biol Sci* (2017) 13 (11):1361–72. doi: 10.7150/ijbs.21657
19. Mazzone E, Gandaglia G, Ploussard G, Marra G, Valerio M, Campi R, et al. Risk Stratification of Patients Candidate to Radical Prostatectomy Based on Clinical and Multiparametric Magnetic Resonance Imaging Parameters: Development and External Validation of Novel Risk Groups. *Eur Urol* (2021) S0302-2838(21):01930–8. doi: 10.1016/j.eururo.2021.07.027
20. Li B, Liu B, Zhang X, Liu H, He L. KIF18B Promotes the Proliferation of Pancreatic Ductal Adenocarcinoma *via* Activating the Expression of CDCA8. *J Cell Physiol* (2020) 235(5):4227–38. doi: 10.1002/jcp.29201
21. Qi G, Zhang C, Ma H, Li Y, Peng J, Chen J, et al. CDCA8, Targeted by MYBL2, Promotes Malignant Progression and Olaparib Insensitivity in Ovarian Cancer. *Am J Cancer Res* (2021) 11(2):389–415.
22. Cui XH, Peng QJ, Li RZ, Lyu XJ, Zhu CF, Qin XH, et al. Cell Division Cycle Associated 8: A Novel Diagnostic Andprognostic Biomarker for Hepatocellular Carcinoma. *J Cell Mol Med* (2021) 25(24):11097–112. doi: 10.1111/jcmm.17032
23. Song Z, Huang Y, Zhao Y, Ruan H, Yang Y, Cao Q, et al. The Identification of Potential Biomarkers and Biological Pathways in Prostate Cancer. *J Cancer* (2019) 10(6):1398–408. doi: 10.7150/jca.29571
24. Huang H, Tang Y, Li P, Ye X, Chen W, Xie H, et al. Significance of TP53 and Immune-Related Genes to Prostate Cancer. *Transl Androl Urol* (2021) 10 (4):1754–68. doi: 10.21037/tau-21-179
25. Zhang B, Li Y, Wu Q, Xie L, Barwick B, Fu C, et al. Acetylation of KLF5 Maintains EMT and Tumorigenicity to Cause Chemoresistant Bone

Metastasis in Prostate Cancer. *Nat Commun* (2021) 12(1):1714. doi: 10.1038/s41467-021-21976-w
26. Vatapalli R, Sagar V, Rodriguez Y, Zhao JC, Unno K, Pamarthy S, et al. Histone Methyltransferase DOT1L Coordinates AR and MYC Stability in Prostate Cancer. *Nat Commun* (2020) 11(1):4153. doi: 10.1038/s41467-020-18013-7
27. Liu H, Wu Z, Zhou H, Cai W, Li X, Hu J, et al. The SOX4/miR-17-92/RB1 Axis Promotes Prostate Cancer Progression. *Neoplasia* (2019) 21(8):765–76. doi: 10.1016/j.neo.2019.05.007
28. Xu N, Chen SH, Lin TT, Cai H, Ke ZB, Dong RN, et al. Development and Validation of Hub Genes for Lymph Node Metastasis in Patients With Prostate Cancer. *J Cell Mol Med* (2020) 24(8):4402–14. doi: 10.1111/jcmm.15098
29. Hu C, Wu J, Wang L, Liu X, Da B, Liu Y, et al. miR-133b Inhibits Cell Proliferation, Migration, and Invasion of Lung Adenocarcinoma by Targeting CDCA8. *Pathol Res Pract* (2021) 223:153459. doi: 10.1016/j.prp.2021.153459
30. Lyu C, Huang M, Liu N, Chen Z, Lupo PJ, Tycko B, et al. Detecting Methylation Quantitative Trait Loci Using a Methylation Random Field Method. *Brief Bioinform* (2021) 22(6):bbab323. doi: 10.1093/bib/bbab323
31. Cheung NYC, Fung JLF, Ng YNC, Wong WHS, Chung CCY, Mak CCY, et al. Perception of Personalized Medicine, Pharmacogenomics, and Genetic Testing Among Undergraduates in Hong Kong. *Hum Genomics* (2021) 15(1):54. doi: 10.1186/s40246-021-00353-0
32. David V, Fylan B, Bryant E, Smith H, Sagoo GS, Rattray M, et al. An Analysis of Pharmacogenomic-Guided Pathways and Their Effect on Medication Changes and Hospital Admissions: A Systematic Review and Meta-Analysis. *Front Genet* (2021) 12:698148. doi: 10.3389/fgene.2021.698148
33. Abraham G, Rutten-Jacobs L, Inouye M. Risk Prediction Using Polygenic Risk Scores for Prevention of Stroke and Other Cardiovascular Diseases. *Stroke* (2021) 52(9):2983–91. doi: 10.1161/STROKEAHA.120.032619
34. Bhanji Y, Isaacs WB, Xu J, Cooney KA. Prostate Cancer Predisposition. *Urol Clin North Am* (2021) 48(3):283–96. doi: 10.1016/j.ucl.2021.03.001

Conflict of Interest: The authors declare that the research was conducted in the absence of any commercial or financial relationships that could be construed as a potential conflict of interest.

Publisher's Note: All claims expressed in this article are solely those of the authors and do not necessarily represent those of their affiliated organizations, or those of the publisher, the editors and the reviewers. Any product that may be evaluated in this article, or claim that may be made by its manufacturer, is not guaranteed or endorsed by the publisher.

frontiers | Frontiers in Oncology

MINI REVIEW
published: 25 April 2022
doi: 10.3389/fonc.2022.854151

Transcription Factors as Novel Therapeutic Targets and Drivers of Prostate Cancer Progression

*Kangzhe Xie, Keely Tan and Matthew J. Naylor**

Charles Perkins Centre, School of Medical Sciences, Faculty of Medicine & Health, University of Sydney, Sydney, NSW, Australia

Prostate cancer is the second most diagnosed cancer among men worldwide. Androgen deprivation therapy, the most common targeted therapeutic option, is circumvented as prostate cancer progresses from androgen dependent to castrate-resistant disease. Whilst the nuclear receptor transcription factor, androgen receptor, drives the growth of prostate tumor during initial stage of the disease, androgen resistance is associated with poorly differentiated prostate cancer. In the recent years, increased research has highlighted the aberrant transcriptional activities of a small number of transcription factors. Along with androgen receptors, dysregulation of these transcription factors contributes to both the poorly differentiated phenotypes of prostate cancer cells and the initiation and progression of prostate carcinoma. As master regulators of cell fate decisions, these transcription factors may provide opportunity for the development of novel therapeutic targets for the management of prostate cancer. Whilst some transcriptional regulators have previously been notoriously difficult to directly target, technological advances offer potential for the indirect therapeutic targeting of these transcription factors and the capacity to reprogram cancer cell phenotype. This mini review will discuss how recent advances in our understanding of transcriptional regulators and material science pave the way to utilize these regulatory molecules as therapeutic targets in prostate cancer.

Keywords: prostate cancer, transcription factor, epigenetic, ubiquitin-proteasome system, protein-protein interactions, targeting approaches

OPEN ACCESS

Edited by:
Shashwat Sharad, Center for Prostate Disease Research (CPDR), United States

Reviewed by:
Andrew C. B. Cato, Karlsruhe Institute of Technology (KIT), Germany
Renea A Taylor, Monash University, Australia

***Correspondence:**
Matthew J. Naylor
matthew.naylor@sydney.edu.au

Specialty section:
This article was submitted to Genitourinary Oncology, a section of the journal Frontiers in Oncology

Received: *13 January 2022*
Accepted: *23 March 2022*
Published: *25 April 2022*

Citation:
Xie K, Tan K and Naylor MJ (2022) Transcription Factors as Novel Therapeutic Targets and Drivers of Prostate Cancer Progression. Front. Oncol. 12:854151. doi: 10.3389/fonc.2022.854151

INTRODUCTION

Prostate cancer is the second most diagnosed cancer in men worldwide, with approximately 1.4 million cases in 2020 alone (1). Prostatic intraepithelial neoplasia (PIN) is a premalignant lesion characterized by the uncontrollable cell growth within the prostate gland (2). This unchecked proliferation precedes the development of localized prostate adenocarcinoma, whereby the tumor increases in volume and cells begin to infiltrate through the basement membrane. The initial pathogenesis of this disease is largely dependent on the activity of the transcriptional factor, androgen receptor (AR) (3). However, once the disease progresses to a more aggressive phenotype, the tumor becomes androgen resistant, evolving into castrate-resistant prostate carcinoma (CRPC) (4).

Metastatic CRPC (mCRPC) is the advanced/final stage of the disease, with cancer cells undergoing metastasis to distal organs such as bone, liver and lungs (5). In addition to androgen resistance, phenotypic changes such as alteration to chromatin structure and nucleus enlargement also occur during the malignant transformation in prostate cells (6, 7).

AR is a ligand activated transcription factor and it functions through the binding of androgens, such as testosterone and 5-α-dihydrotestosterone, which releases AR from its chaperone heat shock protein (HSP) 90. Similar to many steroid hormone nuclear receptors, this results in translocation of AR to the nucleus to regulate the expression of genes associated with growth and maintenance of the prostate epithelium (8). AR, along with a small number of other transcription factors, have been well established as regulatory molecules that govern prostate cell phenotype and are implicated in the initiation and progression of prostate cancer (**Table 1**, also see reviews (2, 36). As the same transcription factor has the ability to bind to regulatory regions of different genes (37), targeting transcription factors provides a direct target in developing effective treatments for prostate cancer and allows for the coordinated inhibition of various oncogenic genes and

TABLE 1 | Identified transcription factor targets and their implications in prostate cancer.

Target Types	Transcription Factors/Proteins	Biological Functions & Implications in Prostate Cancer	References
Nuclear hormone receptors	AR	Drives prostate cancer cell proliferation; maintain prostate cancer cell survival; mutation and amplification of AR in prostate cancer contributes to androgen deprivation therapy resistance.	(3)
	ERs	ERα stimulates prostate cancer cell proliferation and promotes the development of prostate malignancy; ERβ downregulates AR signaling and acts as tumour suppressor.	(9)
	Glucocorticoid receptor	Promotes prostate cancer cell proliferation; contributes to androgen deprivation therapy resistance.	(10)
	Progesterone receptor	Prevents prostate cancer cell migration and invasion.	(10)
	Vitamin D receptor	Promotes cell differentiation and apoptosis; inhibits cell growth, prostate cancer cell migration and angiogenesis.	(10)
	Retinoic acid receptors	Suppresses AR signaling; reduces prostate cancer cell proliferation.	(10)
	ERRα	Regulates energy homeostasis in prostate cells; regulates prostate cancer cell proliferation	(11)
Tumour protein p53	p53	Responds to cellular stress; regulates the expression of genes that are involved in DNA repair, cell arrests and apoptosis; inactivation of p53 is associated with poor clinical outcome.	(12)
ETS fusions	TMPRSS2-ERG fusion	Common chromosomal translocation observed in prostate cancer; increases incidence of prostatic intraepithelial neoplasia development.	(13–15)
Histone methyltransferase	EZH2	Acts as transcription regulators for genes such as PD-1; often overly expressed in advanced stage of prostate cancer.	(16)
MYC	c-Myc	Remodels chromatin structures to stimulate prostate cancer cell growth; promotes oncogenic signaling *via* hyperacetylation.	(17, 18)
	n-Myc	Maintains prostate tumour cell survival; promotes poorly differentiated aggressive prostate cancer phenotype; drives the development of neuroendocrine prostate cancer.	(19)
BET proteins	BRD2	Regulates by androgen; interacts with YY1 to co-activate downstream oncogenic genes; promotes prostate cancer cell growth.	(20)
	BRD4	Regulates the expression of oncogenic transcription factor MYC; regulates prostate cancer cell proliferation; drives ETM transition in CRPC.	(21, 22)
Ubiquitin-proteasome system	MDM2	Regulates prostate cancer cell growth, apoptosis, and the expression of tumour suppressor p53.	(23–25)
	USP2a	Regulates the expression of p53 indirectly by deubiquitinating MDM2.	(26)
	USP5	Acts as a DUB for p53; regulates the expression of p53.	(27)
	USP9X	Acts as DUB for ERG; regulates the expression of transcription factor ERG.	(28)
Core binding factor transcription complex	RUNX proteins	Promotes prostate cancer cell growth and increases metastatic potential *via* matrix metalloproteinase signaling.	(24)
Molecular chaperone	HSP90	Interacts with oncogenic transcription factors include AR, p53 and HIF-1α	(29, 30)
Hypoxia inducible factor transcription complex	HIF-1α	Induces angiogenesis; promotes cancer cell proliferation and survival; facilitates the development of CRPC and metastasis	(31)
Tumour suppressing phosphatase	PTEN	Regulates the PI3K-Akt signaling pathway; loss of PTEN increases the aggressiveness of prostate cancer.	(32)
Prostate specific homeobox gene	NKX3.1	Regulates prostate epithelial cells differentiation and growth; reduced level of NKX3.1 increases the aggressiveness of prostate cancer.	(33)
NF- κB	NF- κB	Promotes prostate tumour invasion; increases metastatic potential; inhibits prostate cancer cell death; contributes to chemotherapy resistance.	(34)
FOX protein family	FOXA1	Drives prostate cancer cell proliferation; maintain prostate cancer cell survival; regulates ETM transition.	(35)

AR, androgen receptors; ER, estrogen receptor; ERRα, estrogen related receptor alpha ETS, E-twenty-six; TMPRSS2, transmembrane-protease-serine 2; ERG, ETS related gene; EZH2, enhancer of zeste homolog 2; PD-1, programmed cell death protein 1; BET, bromodomain extra-terminal enhancer; BRD, bromodomain-containing protein; YY1, transcription factor Ying Yang 1; ETM, epithelial to mesenchymal; CRPC, castrate resistant prostate cancer; DUB, deubiquitinase; MDM2, murine double minute 2; USP, ubiquitin-specific peptidase; RUNX, runt-related transcription factor; HSP, heat shock protein; HIF-1α, hypoxia inducible factor 1 alpha; PTEN, phosphatase and tensin homolog; PI3K, phosphoinositide-3-kinase; Akt, protein kinase B; NF- κB, nuclear factor kappa B; FOX, Forkhead box.

signaling pathways. Whilst several direct approaches to alter transcription factor expression such as siRNA loaded nanoparticles and lentiviruses are under development, this mini review will focus on indirect approaches such as modulation of epigenetic mechanisms, manipulation of the ubiquitin-proteasome system, targeting the molecular chaperone network and exploitation of proteins in transcriptional complexes, with the discussion of some recent successful attempts (**Figure 1**).

THERAPEUTIC TARGETING OF TRANSCRIPTION FACTORS

Historically, many transcription factors have been considered as 'undruggable' targets, owing to their 'intrinsically disordered' interaction network formed with their functional partners (38, 39). In cells, transcription factors regulate gene expression through protein-protein interactions (PPIs) with their co-activators and co-repressors as well as *via* direct sequence specific DNA binding (40). As a result, the lack of enzymatic activities and catalytic sites presents a major blockade in the development of transcription factor inhibitors and modulators (41). In addition, the transcription factor-DNA binding interfaces are often positively charged and structurally convex, whereas the sites for transcription factor-co-regulator interactions are much flatter than the typical enzyme ligand binding pockets (42, 43). Together, these properties further exacerbate the challenges in developing small molecule inhibitors and modulators with desirable ADME (Absorption, Distribution, Metabolism and Excretion) indices (42, 43). In recent years, a plethora of studies have demonstrated success in targeting transcription factors in prostate cancer, showcasing the feasibility of this approach, and challenging previous dogma. In particular, chemical inhibitors targeting the AR ligand binding domains such as bicalutamide and enzalutamide, have been developed (44, 45). Whilst the use of AR inhibitors are now amongst the primary options for androgen-targeted therapies in early-stage prostate cancers (45, 46), these options become ineffective once the tumor becomes castrate-resistant, as they are able to circumvent androgen targeted treatments *via* various mechanisms which include AR amplification, point mutation, splicing variants and replacing AR functions with glucocorticoid receptors (4, 47, 48). As there is a profound paucity of effective treatments for mCRPC patients (49), research into methods of targeting non-AR transcription factors in prostate cancer is critical.

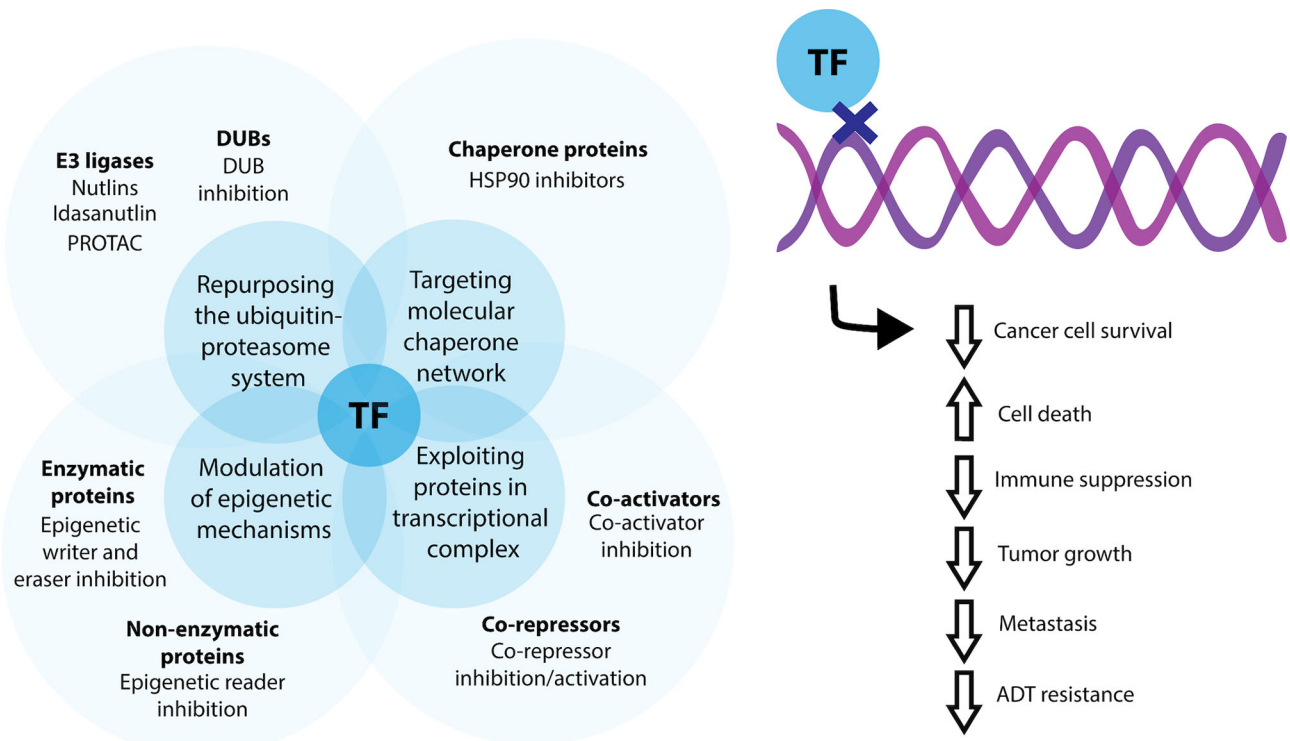

FIGURE 1 | Current indirect methods for targeting transcription factors for prostate cancer therapy. Transcription factor (TF) activity may be indirectly modulated by targeting enzymatic and non-enzymatic proteins involved in epigenetic signaling, through repurposing and manipulating aspects of the ubiquitin-proteasomal system for control of transcription factor degradation, by targeting the molecular chaperone network and by exploiting co-activator and co-repressors associated with a transcriptional complex. Using these methods, transcription factor activity can be favorable modified to decrease cancer cell survival, overall tumour growth and the potential for metastatic dissemination.

MODULATION OF EPIGENETIC MECHANISMS

Modulating epigenetic signaling pathways is one approach used to target oncogenic transcription factors within prostate cancer. As enzymes are druggable targets with relatively high tractability, epigenetic writers and erasers such as acetyl transferase, methyltransferase, deacetylases and demethylases provide a direct target for inhibitor development (50). Enhancer of zeste homolog 2 (EZH2) is an important epigenetic regulator and in prostate cancer, it was found that EZH2 negatively regulates the expression of interferon stimulated genes (ISGs) such as programmed cell death protein 1 (PD-1) and major histocompatibility complex, creating an immunosuppressive tumor microenvironment and increasing resistance to immune checkpoint blockade (ICB) therapies (16). In a recent study by Morel and colleagues, inhibition of EZH2 restored the expression of ISGs and reversed the resistance to ICB treatments, highlighting the therapeutic potential of EZH2 inhibitors in prostate cancer (51). The clinical applicability of EZH2 inhibitors was reinforced by Bai and colleagues, where EZH2 inhibition with GSK126 prevented prostate specific antigen expression and overcame enzalutamide resistance in CRPC (52). Furthermore, the development of neuroendocrine prostate cancer (NEPC), an aggressive subtype of CRPC, was also found to be associated with dysfunctional EZH2 activity (53). Using GSK126, Dardenne and colleagues showed that NEPC cells were more sensitive to EZH2 inhibition than androgen sensitive LNCaP cells (54), however, the clinical efficacy of EZH2 inhibitors against NEPC warrants further investigation. Whilst EZH2 represents a major target for prostate cancer, alternative targets include histone acetyl transferase E1A binding protein (p300) and CREB binding protein (CBP). In prostate cancer, p300 and CBP interact with numerous oncogenic transcription factors, including p53, MYC and AR, to drive tumour progression (55). These epigenetic enzymes can be inhibited by a CellCentric developed compound, CCS1477, where administration of CCS1477 was shown to downregulate the expression of AR and MYC, resulting in decreased tumor growth in a 22Rv1 xenograft model of CRPC (56, 57).

Alternatively, targeting regulators that do not possess enzymatic activities in the epigenetic signaling pathway have also proven successful. MYC is one of the most dysregulated transcription factors in human cancers (17). In prostate cancer, MYC remodels the chromatin structure to stimulate cell growth and promote oncogenic signaling *via* hyperacetylation (17, 18) and it has been shown that these oncogenic effects are partly mediated by the epigenetic reader protein, bromodomain extra-terminal (BET) (58). As a result, targeting the BET family of proteins provides a potential avenue to indirectly regulate the expression of MYC, ultimately regressing prostate tumor progression. Indeed, I-BET762, a BET inhibitor, has been shown to reduce MYC expression. This was associated with decreased prostate cancer cell proliferation, increased programmed cell death and reduced *in vivo* prostate tumour burden, highlighting the possibility of targeting BET proteins as a treatment for prostate cancer (59). The therapeutic potential of BET inhibition is further accentuated by JQ1, an inhibitor that targets bromodomain containing protein (BRD) 4 (60). BRD4 is a member of the BET family of proteins, and it has been shown to interact with transcription factors such as AR and MYC to mediate oncogenic effects (21). More recently, it has been suggested that BRD4 also plays a role in regulating tumor immune microenvironments. This is supported by Mao and colleagues, where BRD4 inhibition with JQ1 reduced PD-1 expression and promoted CD8-mediated lysis of prostate tumor cells both *in vitro* and *in vivo* (61). In addition, JQ1 was found to mediate anticancer effect by downregulating the expression of Achaete-scute homolog 1 (ASCL1) in small-cell lung cancer (62). With recent evidence suggesting that ASCL1 as a key driver for NEPC (63), JQ1 along with other BET inhibitors may have potential as NEPC therapeutics. The BET inhibitors, BMS-986158 and RO6870810 are now also in various phases of multicancer clinical trials, with the pan-BET inhibitor ZEN-3694, showcasing therapeutic efficacy in a Phase Ib/IIa mCRPC study (64–66).

MANIPULATION OF THE UBIQUITIN-PROTEASOME SYSTEM

Another way to target transcription factor in prostate cancer is utilizing the ubiquitin-proteasome system (UPS). Appropriate levels of transcription factor expression in cells is key in maintaining cellular homeostasis (67). Aberrant transcription factor expression or failure in the expression of regulatory circuits may lead to catastrophic effects and result in pathophysiological states. Ubiquitin ligases (E3 ligases) are enzymes in the UPS that catalyze the cellular process of ubiquitylation, in which ubiquitin covalently attaches to the substrate protein for proteasomal degradation as a method to regulate transcription factor expression (68, 69). This unique degradation pathway provides a potential platform for controlling transcription factor expression in prostate cancer.

In several human cancers, including prostate cancer, the expression of transcription factor and tumor suppressor p53, is known to be highly dysregulated (70). This dysregulation can arise from the increased activity of murine double minute 2 (MDM2), an E3 ligase, which decreases the expression of p53 and ultimately results in poor clinical outcomes for the patient (12, 23). Thus Nutlins, a novel class of MDM2 inhibitors, were developed by Vassilev and colleagues. The use of these inhibitors increased cellular expression of p53 and its target gene p21 (71), whilst further research using *in vivo* mouse xenograft models with androgen dependent LNCaP and androgen independent 22Rv1 cell lines, demonstrated increased apoptosis and reduced tumor burden in both cell types following Nutlins treatment (72, 73). To further improve the potency and selectivity of these Nutlins, a second-generation compound Idasanutlin (RG7738/RO5503781), was developed (74). Research shows that use of this compound induces cell death *via* a combined mechanism of cell cycle arrest and cytotoxic insult in LNCaP cells (75). The clinical applicability of E3 ligase inhibition has recently been assessed in

a Phase I clinical trial for prostate cancer patients who have not received docetaxel treatment previously (76). Whilst the trial was terminated due to safety concerns and financial withdrawal from Roche, promising preliminary results highlight the potential for this class of compound, and E3 ligases in general, to be further investigated as a prostate cancer therapy.

The utilization of the UPS (more specifically E3 ligase) to target transcription factors within prostate cancer was taken further with the discovery of proteolysis targeting chimeras (PROTACs). PROTACs are bifunctional molecules comprised of a protein interacting ligand, as well as an E3 ligase recruiting ligand (77). The two ligands in PROTACs are linked in a covalent manner, with protein interacting ligand binding with the protein of interest such as a transcription factor, whereas E3 ligase recruiting ligand facilitates the process of ubiquitylation and subsequent protein degradation (78). PROTACs generate a 'knocked-down' effect in cells, abrogating the cellular function of the protein of interest (79). Furthermore, it was discovered that this process is highly catalytic, where a single PROTAC molecule can eliminate multiple protein of interest (80). As discussed above, BET proteins regulate the expression of many pro-oncogenic transcription factors such as AR and MYC, and pharmacological inhibition of these regulatory molecules results in an anticancer effect. Therefore, the use of PROTACs could represent another avenue of pharmacological modification on dysregulated transcription factor expression in prostate cancer. WWL0245 is a highly selective and potent PROTAC-based degrader of BRD4 and has been shown to function by inducing cell cycle arrest of the androgen sensitive prostate cancer cell lines, LNCaP and VCaP, *in vitro*. This was simultaneously associated with the downregulation of oncogenic transcription factors AR and c-Myc, which highlights the therapeutic potential and clinical feasibility of this approach in prostate cancer (81). Such notion was further supported by Raina and colleagues, where they demonstrated that pan-BET PROTAC, ARV-771, induced cell apoptosis and tumour regression in a mouse xenograft model of CRPC (82). Excluding BET, most of the current research is focused on the PROTAC-based approached on targeting AR (83–85), whereas attempts to target other dysregulated transcription factors in prostate cancer *via* PROTACs is limited. Thus, identifying a wider variety of protein interacting ligands should be the topic of prospective research.

Another way to alter transcription factor expression is to inhibit the activities of deubiquitinases (DUBs). DUBs are enzymes that remove ubiquitin proteins in the UPS, terminating the ubiquitin-mediated proteasomal degradation process (86). Ubiquitin-specific peptidase (USP) 2a act as a DUB for MDM2, in which it positively regulates the expression of MDM2 (26). Since MDM2 is an E3 ligase for transcription factor p53, inhibition of USP2a would promote the proteasomal degradation of MDM2 and indirectly regulate the expression of p53 (23, 86). This was supported by Stevenson and colleagues, where siRNA inhibition of USP2a led to the accumulation of p53 protein *in vivo*, highlighting the therapeutic potential to inhibit DUBs in prostate cancer (87). Inhibition of DUBs in the context of prostate cancer is not limited to the p53 signaling pathway. The gene fusion product transmembrane-protease-serine-2 (TMPRSS2)-ETS-related gene (ERG) as a result of chromosomal translocation is observed in 20 to 50% of prostate cancer patients with different ethnicities (13, 14). The TMPRSS2-ERG fusion protein was showed to mediate prostate cancer cell invasion and activation of transcriptional programs for invasion-associated genes (15). The expression of ERG is regulated by E3 ligase tripartite-motif-containing-25 (TRIM25), whereas USP9X acts as DUB for ERG deubiquitylation (28, 88). Thus, target inhibition of ERG or TMPRSS2 may be beneficial in prostate cancer. WP1130 is a small molecule inhibitor comprised of two protein reactive moieties, a 2-bromo-pyridine functional group as well as an α,β-unsaturated amide moiety that is able to undergo Michael addition reactions (89). This enables WP1130 to interact with proteins in a partly selective manner and exerts inhibitory effects on multiple DUBs such as USP5, USP9X and USP14 (90). It has been shown that WP1130 reduces the level of ERG *in vitro* by inhibiting the enzymatic function of USP9X. This was associated with a decrease in tumour volume in murine xenografts with VCaP cells, highlighting the clinical feasibility to target DUBs in prostate cancer (28).

TARGETING THE MOLECULAR CHAPERONE NETWORK

The molecular chaperone network is responsible for various biological processes such as appropriate protein folding, intracellular localization, and degradation, thus maintaining protein homeostasis in cells (29). Chaperone protein such as HSP90 exert these functions by interacting with a diverse range of client proteins, and amongst them, many are oncogenic transcription factors. They include AR, p53 and hypoxia inducible factor (HIF)-1α (29, 30). As a result, disrupting HSP90-transcription factor interactions *via* small molecule inhibitors provide a potential pathway to rectify the dysregulated mechanisms that cause prostate malignancy. 17-AAG is the first-in-class HSP90 inhibitor developed by Schnur and colleagues. However, the weak potency and poor bioavailability of this compound has sparked further optimization (30). Ganetespib is a second-generation HSP90 inhibitor with improved potency. It has been shown that Ganetespib induced cell cycle arrest in LNCaP and LAPC4 cells and resulted in tumor regression in a PDX model of CRPC (91), highlighting the feasibility and clinical applicability of HSP90 inhibition as an anticancer treatment. This notion was reinforced recently by SU086, another novel HSP90 inhibitor that was found to reduce the proliferation of PC3 and DU145 prostate cancer cells *in vitro* and inhibit tumor growth in a preclinical murine model of prostate cancer (92). In addition to HSP90, other emerging targets from the molecular chaperone network include HSP70 and HSP90 co-chaperone CDC37, however, drug-like inhibitors targeting these two proteins are yet to be developed (93). Whilst targeting chaperone proteins other than HSP90 in prostate cancer are not well understood and requires further investigation, it represents a novel strategy for prostate cancer treatment.

EXPLOITING OTHER PROTEINS IN A TRANSCRIPTIONAL COMPLEX

Another approach to modulate transcription factor expressions can be achieved *via* the exploitation of proteins in a transcriptional complex. HIF is a transcriptional complex that plays a key role in inducing angiogenesis, an essential requirement for prostate tumour growth and the CRPC development. Prior to sufficient vascular development by the prostate tumour, cancer cells must adapt to the low oxygen concentration to fulfil their large energy expenditure (31). Estrogen related receptor alpha (ERRα) is involved in the regulation of prostate energy homeostasis (11). It has been shown that ERRα can interact with hypoxia inducible factor 1 (HIF) transcription factor complex to prevent HIF-1α from undergoing proteasomal degradation and augments the cellular adaptive response to hypoxia generated by the prostate tumour cells (94, 95). As a result, interference of this indispensable PPI is a lucrative approach to develop prostate cancer therapeutics. XCT790 is an inverse agonist of ERRα (94). It was demonstrated that administration of XCT790 attenuated ERRα-HIF-1 interactions and reduced the expressions of HIF-1 (95). This was associated with a decrease in LNCaP prostate cancer cell proliferation *in vitro* (95), outlining the clinical applicability of this approach to disrupt transcription factor interactions.

The heterodimeric transcription factor complex core binding factor (CBF) is another emerging target. CBF consists of two proteins: DNA binding runt-related transcription factor (RUNX) and its non-DNA binding beta subunit (CBFβ) (96). The CBFβ functions as a co-activator to RUNX, resulting in RUNX being relieved from its autoinhibited state, facilitating the CBF complex binding to DNA and regulation of target gene expression (97). In recent years, there has been growing recognition of RUNX transcription factors in promoting cell growth and metastatic potential of prostate cancer *via* matrix metalloproteinase signaling (24). Therefore, targeting such essential PPIs may disrupt the transcription process of oncogenic genes, resulting the anticarcinogenic effects. Successful targeting of this modality was achieved using a monovalent derivative of the AI-10-49 scaffolds, a bivalent inhibitor that was originally developed to target CBFβ-smooth muscle myosin heavy chain interactions (98). This novel monovalent inhibitor interferes the binding between wildtype CBFβ and the RUNX1 protein by altering their conformational dynamics (99). In a study on triple negative breast cancer, CBFβ-RUNX1 inhibition was shown to abolish colony formation and alter the expression of epithelial-mesenchymal transition genes, a characteristic cancer hallmark associated with metastasis (99). With regards to prostate cancer, this finding highlights the therapeutic potential to disrupt RUNX interaction circuity, which may be applicable for developing prostate malignancy therapeutics.

CONCLUSION

This mini review briefly summarized the recent success in targeting non-AR transcription factors. However, it is worth noting that possible approaches to modulate non-AR transcription factors are not restricted to the ones mentioned above, and these successful discoveries only mark the starting point of further transcription factor research. Nevertheless, the newly discovered inhibitors and modulators represent an encouraging potential to develop effective treatment options for mCRPC by targeting non-AR transcription factor.

AUTHOR CONTRIBUTIONS

KX designed the study, was responsible for writing the article and the creation of the table. KT was responsible for writing the article and the creation of the figure. MN designed the study and was responsible for writing and revising the manuscript. All authors contributed to the generation of the concepts and ideas provided. All authors contributed to the article and approved the submitted version.

FUNDING

This work was supported by Cancer Council NSW Research Project Grant (RG 20-08) and Priority-driven Collaborative Cancer Research Scheme (Grant #1130499), funded by the National Breast Cancer Foundation Australia with the assistance of Cancer Australia awarded to MN.

REFERENCES

1. Sung H, Ferlay J, Siegel RL, Laversanne M, Soerjomataram I, Jemal A, et al. Global Cancer Statistics 2020: GLOBOCAN Estimates of Incidence and Mortality Worldwide for 36 Cancers in 185 Countries. *CA Cancer J Clin* (2021) 71(3):209–49. doi: 10.3322/caac.21660
2. Abate-Shen C, Shen MM. Molecular Genetics of Prostate Cancer. *Genes Dev* (2000) 14(19):2410–34. doi: 10.1101/gad.819500
3. Lonergan PE, Tindall DJ. Androgen Receptor Signaling in Prostate Cancer Development and Progression. *J Carcinog* (2011) 10:20. doi: 10.4103/1477-3163.83937
4. Sharma NL, Massie CE, Ramos-Montoya A, Zecchini V, Scott HE, Lamb AD, et al. The Androgen Receptor Induces a Distinct Transcriptional Program in Castration-Resistant Prostate Cancer in Man. *Cancer Cell* (2013) 23(1):35–47. doi: 10.1016/j.ccr.2012.11.010
5. Shen MM, Abate-Shen C. Molecular Genetics of Prostate Cancer: New Prospects for Old Challenges. *Genes Dev* (2010) 24(18):1967–2000. doi: 10.1101/gad.1965810
6. Epstein JI. Precursor Lesions to Prostatic Adenocarcinoma. *Virchows Arch* (2009) 454(1):1–16. doi: 10.1007/s00428-008-0707-5
7. Koh CM, Bieberich CJ, Dang CV, Nelson WG, Yegnasubramanian S, De Marzo AM. MYC and Prostate Cancer. *Genes Cancer* (2010) 1(6):617–28. doi: 10.1177/1947601910379132
8. Dai C, Heemers H, Sharifi N. Androgen Signaling in Prostate Cancer. *Cold Spring Harb Perspect Med* (2017) 7(9):a030452. doi: 10.1101/cshperspect.a030452

9. Yeh C-R, Da J, Song W, Fazili A, Yeh S. Estrogen Receptors in Prostate Development and Cancer. *Am J Clin Exp urology* (2014) 2(2):161.
10. Shiota M, Fujimoto N, Kashiwagi E, Eto M. The Role of Nuclear Receptors in Prostate Cancer. *Cells* (2019) 8(6):602. doi: 10.3390/cells8060602
11. Cheung CP, Yu S, Wong KB, Chan LW, Lai FM, Wang X, et al. Expression and Functional Study of Estrogen Receptor-Related Receptors in Human Prostatic Cells and Tissues. *J Clin Endocrinol Metab* (2005) 90(3):1830–44. doi: 10.1210/jc.2004-1421
12. Kluth M, Harasimowicz S, Burkhardt L, Grupp K, Krohn A, Prien K, et al. Clinical Significance of Different Types of P53 Gene Alteration in Surgically Treated Prostate Cancer. *Int J Cancer* (2014) 135(6):1369–80. doi: 10.1002/ijc.28784
13. Ren S, Peng Z, Mao JH, Yu Y, Yin C, Gao X, et al. RNA-Seq Analysis of Prostate Cancer in the Chinese Population Identifies Recurrent Gene Fusions, Cancer-Associated Long Noncoding RNAs and Aberrant Alternative Splicings. *Cell Res* (2012) 22(5):806–21. doi: 10.1038/cr.2012.30
14. Magi-Galluzzi C, Tsusuki T, Elson P, Simmerman K, LaFargue C, Esgueva R, et al. TMPRSS2-ERG Gene Fusion Prevalence and Class Are Significantly Different in Prostate Cancer of Caucasian, African-American and Japanese Patients. *Prostate* (2011) 71(5):489–97. doi: 10.1002/pros.21265
15. Tomlins SA, Laxman B, Varambally S, Cao X, Yu J, Helgeson BE, et al. Role of the TMPRSS2-ERG Gene Fusion in Prostate Cancer. *Neoplasia* (2008) 10 (2):177–88. doi: 10.1593/neo.07822
16. Peng D, Kryczek I, Nagarsheth N, Zhao L, Wei S, Wang W, et al. Epigenetic Silencing of TH1-Type Chemokines Shapes Tumour Immunity and Immunotherapy. *Nature* (2015) 527(7577):249–53. doi: 10.1038/nature15520
17. Rebello RJ, Pearson RB, Hannan RD, Furic L. Therapeutic Approaches Targeting MYC-Driven Prostate Cancer. *Genes (Basel)* (2017) 8(2):71. doi: 10.3390/genes8020071
18. Grandori C, Gomez-Roman N, Felton-Edkins ZA, Ngouenet C, Galloway DA, Eisenman RN, et al. C-Myc Binds to Human Ribosomal DNA and Stimulates Transcription of rRNA Genes by RNA Polymerase I. *Nat Cell Biol* (2005) 7 (3):311–8. doi: 10.1038/ncb1224
19. Lee JK, Phillips JW, Smith BA, Park JW, Stoyanova T, McCaffrey EF, et al. N-Myc Drives Neuroendocrine Prostate Cancer Initiated From Human Prostate Epithelial Cells. *Cancer Cell* (2016) 29(4):536–47. doi: 10.1016/j.ccell.2016.03.001
20. Xu C, Tsai YH, Galbo PM, Gong W, Storey AJ, Xu Y, et al. Cistrome Analysis of YY1 Uncovers a Regulatory Axis of YY1:BRD2/4-PFKP During Tumorigenesis of Advanced Prostate Cancer. *Nucleic Acids Res* (2021) 49 (9):4971–88. doi: 10.1093/nar/gkab252
21. Delmore JE, Issa GC, Lemieux ME, Rahl PB, Shi J, Jacobs HM, et al. BET Bromodomain Inhibition as a Therapeutic Strategy to Target C-Myc. *Cell* (2011) 146(6):904–17. doi: 10.1016/j.cell.2011.08.017
22. Shafran JS, Jafari N, Casey AN, Gyorffy B, Denis GV. BRD4 Regulates Key Transcription Factors That Drive Epithelial-Mesenchymal Transition in Castration-Resistant Prostate Cancer. *Prostate Cancer Prostatic Dis* (2021) 24(1):268–77. doi: 10.1038/s41391-020-0246-y
23. Honda R, Tanaka H, Yasuda H. Oncoprotein MDM2 Is a Ubiquitin Ligase E3 for Tumor Suppressor P53. *FEBS Lett* (1997) 420(1):25–7. doi: 10.1016/S0014-5793(97)01480-4
24. Ashe H, Krakowiak P, Hasterok S, Sleppy R, Roller DG, Gioeli D. Role of the Runt-Related Transcription Factor (RUNX) Family in Prostate Cancer. *FEBS J* (2021) 288(21):6112–26. doi: 10.1111/febs.15804
25. Freedman DA, Wu L, Levine AJ. Functions of the MDM2 Oncoprotein. *Cell Mol Life Sci* (1999) 55(1):96–107. doi: 10.1007/s000180050273
26. Kwon SK, Saindane M, Baek KH. P53 Stability Is Regulated by Diverse Deubiquitinating Enzymes. *Biochim Biophys Acta Rev Cancer* (2017) 1868 (2):404–11. doi: 10.1016/j.bbcan.2017.08.001
27. Dayal S, Sparks A, Jacob J, Allende-Vega N, Lane DP, Saville MK. Suppression of the Deubiquitinating Enzyme USP5 Causes the Accumulation of Unanchored Polyubiquitin and the Activation of P53. *J Biol Chem* (2009) 284(8):5030–41. doi: 10.1074/jbc.M805871200
28. Wang S, Kollipara RK, Srivastava N, Li R, Ravindranathan P, Hernandez E, et al. Ablation of the Oncogenic Transcription Factor ERG by Deubiquitinase Inhibition in Prostate Cancer. *Proc Natl Acad Sci USA* (2014) 111(11):4251–6. doi: 10.1073/pnas.1322198111
29. Hong DS, Banerji U, Tavana B, George GC, Aaron J, Kurzrock R. Targeting the Molecular Chaperone Heat Shock Protein 90 (HSP90): Lessons Learned and Future Directions. *Cancer Treat Rev* (2013) 39(4):375–87. doi: 10.1016/j.ctrv.2012.10.001
30. Powers MV, Workman P. Targeting of Multiple Signalling Pathways by Heat Shock Protein 90 Molecular Chaperone Inhibitors. *Endocr Relat Cancer* (2006) 13 Suppl 1:S125–35. doi: 10.1677/erc.1.01324
31. Ranasinghe WK, Sengupta S, Williams S, Chang M, Shulkes A, Bolton DM, et al. The Effects of Nonspecific HIF1alpha Inhibitors on Development of Castrate Resistance and Metastases in Prostate Cancer. *Cancer Med* (2014) 3 (2):245–51. doi: 10.1002/cam4.189
32. Turnham DJ, Bullock N, Dass MS, Staffurth JN, Pearson HB. The PTEN Conundrum: How to Target PTEN-Deficient Prostate Cancer. *Cells* (2020) 9 (11):2342. doi: 10.3390/cells9112342
33. Gurel B, Ali TZ, Montgomery EA, Begum S, Hicks J, Goggins M, et al. NKX3.1 as a Marker of Prostatic Origin in Metastatic Tumors. *Am J Surg Pathol* (2010) 34(8):1097–105. doi: 10.1097/PAS.0b013e3181e6cbf3
34. Verzella D, Fischietti M, Capece D, Vecchiotti D, Del Vecchio F, Cicciarelli G, et al. Targeting the NF-kappaB Pathway in Prostate Cancer: A Promising Therapeutic Approach? *Curr Drug Targets* (2016) 17(3):311–20. doi: 10.2174/1389450116666150907100715
35. Teng M, Zhou S, Cai C, Lupien M, He HH. Pioneer of Prostate Cancer: Past, Present and the Future of FOXA1. *Protein Cell* (2021) 12(1):29–38. doi: 10.1007/s13238-020-00786-8
36. Wang G, Zhao D, Spring DJ, DePinho RA. Genetics and Biology of Prostate Cancer. *Genes Dev* (2018) 32(17-18):1105–40. doi: 10.1101/gad.315739.118
37. Marco A, Konikoff C, Karr TL, Kumar S. Relationship Between Gene Co-Expression and Sharing of Transcription Factor Binding Sites in Drosophila Melanogaster. *Bioinformatics* (2009) 25(19):2473–7. doi: 10.1093/bioinformatics/btp462
38. Henley MJ, Koehler AN. Advances in Targeting 'Undruggable' Transcription Factors With Small Molecules. *Nat Rev Drug Discov* (2021) 20(9):669–88. doi: 10.1038/s41573-021-00199-0
39. Liu J, Perumal NB, Oldfield CJ, Su EW, Uversky VN, Dunker AK. Intrinsic Disorder in Transcription Factors. *Biochemistry* (2006) 45(22):6873–88. doi: 10.1021/bi0602718
40. Lambert SA, Jolma A, Campitelli LF, Das PK, Yin Y, Albu M, et al. The Human Transcription Factors. *Cell* (2018) 172(4):650–65. doi: 10.1016/j.cell.2018.01.029
41. Inamoto I, Shin JA. Peptide Therapeutics That Directly Target Transcription Factors. *Pept Science* (2019) 111(1):e24048. doi: 10.1002/pep2.24048
42. Arkin MR, Tang Y, Wells JA. Small-Molecule Inhibitors of Protein-Protein Interactions: Progressing Toward the Reality. *Chem Biol* (2014) 21(9):1102–14. doi: 10.1016/j.chembiol.2014.09.001
43. Bushweller JH. Targeting Transcription Factors in Cancer - From Undruggable to Reality. *Nat Rev Cancer* (2019) 19(11):611–24. doi: 10.1038/s41568-019-0196-7
44. Masiello D, Cheng S, Bubley GJ, Lu ML, Balk SP. Bicalutamide Functions as an Androgen Receptor Antagonist by Assembly of a Transcriptionally Inactive Receptor. *J Biol Chem* (2002) 277(29):26321–6. doi: 10.1074/jbc.M203310200
45. Ito Y, Sadar MD. Enzalutamide and Blocking Androgen Receptor in Advanced Prostate Cancer: Lessons Learnt From the History of Drug Development of Antiandrogens. *Res Rep Urol* (2018) 10:23–32. doi: 10.2147/RRU.S157116
46. Nevedomskaya E, Baumgart SJ, Haendler B. Recent Advances in Prostate Cancer Treatment and Drug Discovery. *Int J Mol Sci* (2018) 19(5):1359. doi: 10.3390/ijms19051359
47. Arora VK, Schenkein E, Murali R, Subudhi SK, Wongvipat J, Balbas MD, et al. Glucocorticoid Receptor Confers Resistance to Antiandrogens by Bypassing Androgen Receptor Blockade. *Cell* (2013) 155(6):1309–22. doi: 10.1016/j.cell.2013.11.012
48. Fujita K, Nonomura N. Role of Androgen Receptor in Prostate Cancer: A Review. *World J Mens Health* (2019) 37(3):288–95. doi: 10.5534/wjmh.180040
49. Moussa M, Papatsoris A, Abou Chakra M, Sryropoulou D, Dellis A. Pharmacotherapeutic Strategies for Castrate-Resistant Prostate Cancer. *Expert Opin Pharmacother* (2020) 21(12):1431–48. doi: 10.1080/14656566.2020.1767069

50. Mohammad HP, Barbash O, Creasy CL. Targeting Epigenetic Modifications in Cancer Therapy: Erasing the Roadmap to Cancer. *Nat Med* (2019) 25 (3):403–18. doi: 10.1038/s41591-019-0376-8
51. Morel KL, Sheahan AV, Burkhart DL, Baca SC, Boufaied N, Liu Y, et al. EZH2 Inhibition Activates a dsRNA-STING-Interferon Stress Axis That Potentiates Response to PD-1 Checkpoint Blockade in Prostate Cancer. *Nat Cancer* (2021) 2(4):444–56. doi: 10.1038/s43018-021-00185-w
52. Bai Y, Zhang Z, Cheng L, Wang R, Chen X, Kong Y, et al. Inhibition of Enhancer of Zeste Homolog 2 (EZH2) Overcomes Enzalutamide Resistance in Castration-Resistant Prostate Cancer. *J Biol Chem* (2019) 294(25):9911–23. doi: 10.1074/jbc.RA119.008152
53. Luo J, Wang K, Yeh S, Sun Y, Liang L, Xiao Y, et al. LncRNA-P21 Alters the Antiandrogen Enzalutamide-Induced Prostate Cancer Neuroendocrine Differentiation *via* Modulating the EZH2/STAT3 Signaling. *Nat Commun* (2019) 10(1):2571. doi: 10.1038/s41467-019-09784-9
54. Dardenne E, Beltran H, Benelli M, Gayvert K, Berger A, Puca L, et al. N-Myc Induces an EZH2-Mediated Transcriptional Program Driving Neuroendocrine Prostate Cancer. *Cancer Cell* (2016) 30(4):563–77. doi: 10.1016/j.ccell.2016.09.005
55. Welti J, Sharp A, Brooks N, Yuan W, McNair C, Chand SN, et al. Targeting the P300/CBP Axis in Lethal Prostate Cancer. *Cancer Discov* (2021) 11 (5):1118–37. doi: 10.1158/2159-8290.CD-20-0751
56. Pegg N, Brooks N, Worthington J, Young B, Prosser A, Lane J, et al. Characterisation of CCS1477: A Novel Small Molecule Inhibitor of P300/CBP for the Treatment of Castration Resistant Prostate Cancer. *J Clin Oncol* (2017) 35:11590. doi: 10.1200/JCO.2017.35.15_suppl.11590
57. Brooks N, Prosser A, Young B, Gaughan L, Elvin P, Pegg N. CCS1477, a Potent and Selective P300/CBP Bromodomain Inhibitor, Is Targeted & Differentiated From BET Inhibitors in Prostate Cancer Cell Lines *In Vitro*. *AACR* (2019) 79(13_Supplement):3826. doi: 10.1158/1538-7445.AM2019-3826
58. Mertz JA, Conery AR, Bryant BM, Sandy P, Balasubramanian S, Mele DA, et al. Targeting MYC Dependence in Cancer by Inhibiting BET Bromodomains. *Proc Natl Acad Sci USA* (2011) 108(40):16669–74. doi: 10.1073/pnas.1108190108
59. Wyce A, Degenhardt Y, Bai Y, Le B, Korenchuk S, Crouthame MC, et al. Inhibition of BET Bromodomain Proteins as a Therapeutic Approach in Prostate Cancer. *Oncotarget* (2013) 4(12):2419–29. doi: 10.18632/oncotarget.1572
60. Coleman DJ, Gao L, Schwartzman J, Korkola JE, Sampson D, Derrick DS, et al. Maintenance of MYC Expression Promotes *De Novo* Resistance to BET Bromodomain Inhibition in Castration-Resistant Prostate Cancer. *Sci Rep* (2019) 9(1):3823. doi: 10.1038/s41598-019-40518-5
61. Mao W, Ghasemzadeh A, Freeman ZT, Obradovic A, Chaimowitz MG, Nirschl TR, et al. Immunogenicity of Prostate Cancer Is Augmented by BET Bromodomain Inhibition. *J Immunother Cancer* (2019) 7(1):277. doi: 10.1186/s40425-019-0758-y
62. Lenhart R, Kirov S, Desilva H, Cao J, Lei M, Johnston K, et al. Sensitivity of Small Cell Lung Cancer to BET Inhibition Is Mediated by Regulation of ASCL1 Gene Expression. *Mol Cancer Ther* (2015) 14(10):2167–74. doi: 10.1158/1535-7163.MCT-15-0037
63. Fraser JA, Sutton JE, Tazayoni S, Bruce I, Poole AV. Hash1 Nuclear Localization Persists in Neuroendocrine Transdifferentiated Prostate Cancer Cells, Even Upon Reintroduction of Androgen. *Sci Rep* (2019) 9(1):19076. doi: 10.1038/s41598-019-55665-y
64. Shapiro GI, LoRusso P, Dowlati A, T Do K, Jacobson CA, Vaishampayan U, et al. A Phase 1 Study of RO6870810, a Novel Bromodomain and Extra-Terminal Protein Inhibitor, in Patients With NUT Carcinoma, Other Solid Tumours, or Diffuse Large B-Cell Lymphoma. *Br J Cancer* (2021) 124(4):744–53. doi: 10.1038/s41416-020-01180-1
65. US National Library of Medicine. *Study of BMS-986158 in Subjects With Select Advanced Cancers (BET)*. ClinicalTrials.gov (2015). Available at: https://clinicaltrials.gov/ct2/show/NCT02419417.
66. Aggarwal RR, Schweizer MT, Nanus DM, Pantuck AJ, Heath EI, Campeau E, et al. A Phase Ib/IIa Study of the Pan-BET Inhibitor ZEN-3694 in Combination With Enzalutamide in Patients With Metastatic Castration-Resistant Prostate Cancer. *Clin Cancer Res* (2020) 26(20):5338–47. doi: 10.1158/1078-0432.CCR-20-1707
67. Seth A, Watson DK. ETS Transcription Factors and Their Emerging Roles in Human Cancer. *Eur J Cancer* (2005) 41(16):2462–78. doi: 10.1016/j.ejca.2005.08.013
68. Geng F, Wenzel S, Tansey WP. Ubiquitin and Proteasomes in Transcription. *Annu Rev Biochem* (2012) 81:177–201. doi: 10.1146/annurev-biochem-052110-120012
69. Yang Q, Zhao J, Chen D, Wang Y. E3 Ubiquitin Ligases: Styles, Structures and Functions. *Mol Biomedicine* (2021) 2(1):1–17. doi: 10.1186/s43556-021-00043-2
70. Meek DW. Tumour Suppression by P53: A Role for the DNA Damage Response? *Nat Rev Cancer* (2009) 9(10):714–23. doi: 10.1038/nrc2716
71. Vassilev LT, Vu BT, Graves B, Carvajal D, Podlaski F, Filipovic Z, et al. *In Vivo* Activation of the P53 Pathway by Small-Molecule Antagonists of MDM2. *Science* (2004) 303(5659):844–8. doi: 10.1126/science.1092472
72. Tovar C, Graves B, Packman K, Filipovic Z, Higgins B, Xia M, et al. MDM2 Small-Molecule Antagonist RG7112 Activates P53 Signaling and Regresses Human Tumors in Preclinical Cancer Models. *Cancer Res* (2013) 73(8):2587–97. doi: 10.1158/0008-5472.CAN-12-2807
73. Tovar C, Higgins B, Kolinsky K, Xia M, Packman K, Heimbrook DC, et al. MDM2 Antagonists Boost Antitumor Effect of Androgen Withdrawal: Implications for Therapy of Prostate Cancer. *Mol Cancer* (2011) 10:49. doi: 10.1186/1476-4598-10-49
74. Ding Q, Zhang Z, Liu JJ, Jiang N, Zhang J, Ross TM, et al. Discovery of RG7388, a Potent and Selective P53-MDM2 Inhibitor in Clinical Development. *J Med Chem* (2013) 56(14):5979–83. doi: 10.1021/jm400487c
75. Natarajan U, Venkatesan T, Radhakrishnan V, Samuel S, Rasappan P, Rathinavelu A. Cell Cycle Arrest and Cytotoxic Effects of SAHA and RG7388 Mediated Through P21(WAF1/CIP1) and P27(KIP1) in Cancer Cells. *Medicina (Kaunas)* (2019) 55(2):30. doi: 10.3390/medicina55020030
76. EU Clinical Trials Register. *A Phase I/randomised Phase II Trial of Abiraterone Acetate or Enzalutamide With or Without Idasanutlin (RO5503781) in Patients With Metastatic Castration Resistant Prostate Cancer Who Have Not Previously Received Docetaxel*. EU Clinical Trials Register (2013). Available at: https://www.clinicaltrialsregister.eu/ctr-search/trial/2013-002014-13/results.
77. Sun X, Gao H, Yang Y, He M, Wu Y, Song Y, et al. PROTACs: Great Opportunities for Academia and Industry. *Signal Transduct Target Ther* (2019) 4:64. doi: 10.1038/s41392-019-0101-6
78. Sakamoto KM, Kim KB, Kumagai A, Mercurio F, Crews CM, Deshaies RJ. Protacs: Chimeric Molecules That Target Proteins to the Skp1-Cullin-F Box Complex for Ubiquitination and Degradation. *Proc Natl Acad Sci USA* (2001) 98(15):8554–9. doi: 10.1073/pnas.141230798
79. Neklesa TK, Winkler JD, Crews CM. Targeted Protein Degradation by PROTACs. *Pharmacol Ther* (2017) 174:138–44. doi: 10.1016/j.pharmthera.2017.02.027
80. Bondeson DP, Mares A, Smith IE, Ko E, Campos S, Miah AH, et al. Catalytic *In Vivo* Protein Knockdown by Small-Molecule PROTACs. *Nat Chem Biol* (2015) 11(8):611–7. doi: 10.1038/nchembio.1858
81. Hu R, Wang WL, Yang YY, Hu XT, Wang QW, Zuo WQ, et al. Identification of a Selective BRD4 PROTAC With Potent Antiproliferative Effects in AR-Positive Prostate Cancer Based on a Dual BET/PLK1 Inhibitor. *Eur J Med Chem* (2022) 227:113922. doi: 10.1016/j.ejmech.2021.113922
82. Raina K, Lu J, Qian Y, Altieri M, Gordon D, Rossi AM, et al. PROTAC-Induced BET Protein Degradation as a Therapy for Castration-Resistant Prostate Cancer. *Proc Natl Acad Sci USA* (2016) 113(26):7124–9. doi: 10.1073/pnas.1521738113
83. Han X, Wang C, Qin C, Xiang W, Fernandez-Salas E, Yang CY, et al. Discovery of ARD-69 as a Highly Potent Proteolysis Targeting Chimera (PROTAC) Degrader of Androgen Receptor (AR) for the Treatment of Prostate Cancer. *J Med Chem* (2019) 62(2):941–64. doi: 10.1021/acs.jmedchem.8b01631
84. Liang JJ, Xie H, Yang RH, Wang N, Zheng ZJ, Zhou C, et al. Designed, Synthesized and Biological Evaluation of Proteolysis Targeting Chimeras (PROTACs) as AR Degraders for Prostate Cancer Treatment. *Bioorg Med Chem* (2021) 45:116331. doi: 10.1016/j.bmc.2021.116331
85. Neklesa T, Snyder LB, Willard RR, Vitale N, Pizzano J, Gordon DA, et al. ARV-110: An Oral Androgen Receptor PROTAC Degrader for Prostate Cancer. *J Clin Oncol* (2019) 37(259.10):1200. doi: 10.1200/JCO.2019.37.7_suppl.259

86. Antao AM, Tyagi A, Kim KS, Ramakrishna S. Advances in Deubiquitinating Enzyme Inhibition and Applications in Cancer Therapeutics. *Cancers (Basel)* (2020) 12(6):1579. doi: 10.3390/cancers12061579
87. Stevenson LF, Sparks A, Allende-Vega N, Xirodimas DP, Lane DP, Saville MK. The Deubiquitinating Enzyme USP2a Regulates the P53 Pathway by Targeting Mdm2. *EMBO J* (2007) 26(4):976–86. doi: 10.1038/sj.emboj.7601567
88. Wang S, Kollipara RK, Humphries CG, Ma SH, Hutchinson R, Li R, et al. The Ubiquitin Ligase TRIM25 Targets ERG for Degradation in Prostate Cancer. *Oncotarget* (2016) 7(40):64921–31. doi: 10.18632/oncotarget.11915
89. Kapuria V, Levitzki A, Bornmann WG, Maxwell D, Priebe W, Sorenson RJ, et al. A Novel Small Molecule Deubiquitinase Inhibitor Blocks Jak2 Signaling Through Jak2 Ubiquitination. *Cell Signal* (2011) 23(12):2076–85. doi: 10.1016/j.cellsig.2011.08.002
90. Kapuria V, Peterson LF, Fang D, Bornmann WG, Talpaz M, Donato NJ. Deubiquitinase Inhibition by Small-Molecule WP1130 Triggers Aggresome Formation and Tumor Cell Apoptosis. *Cancer Res* (2010) 70(22):9265–76. doi: 10.1158/0008-5472.CAN-10-1530
91. Jansson KH, Tucker JB, Stahl LE, Simmons JK, Fuller C, Beshiri ML, et al. High-Throughput Screens Identify HSP90 Inhibitors as Potent Therapeutics That Target Inter-Related Growth and Survival Pathways in Advanced Prostate Cancer. *Sci Rep* (2018) 8(1):17239. doi: 10.1038/s41598-018-35417-0
92. Rice MA, Kumar V, Tailor D, Garcia-Marques FJ, Hsu E-C, Liu S, et al. SU086, an Inhibitor of HSP90, Impairs Glycolysis and Represents a Treatment Strategy for Advanced Prostate Cancer. *Cell Rep Med* (2022) 3(2):100502. doi: 10.1016/j.xcrm.2021.100502
93. Wang L, Xu X, Jiang Z, You Q. Modulation of Protein Fate Decision by Small Molecules: Targeting Molecular Chaperone Machinery. *Acta Pharm Sin B* (2020) 10(10):1904–25. doi: 10.1016/j.apsb.2020.01.018
94. Matos B, Howl J, Jeronimo C, Fardilha M. The Disruption of Protein-Protein Interactions as a Therapeutic Strategy for Prostate Cancer. *Pharmacol Res* (2020) 161:105145. doi: 10.1016/j.phrs.2020.105145
95. Zou C, Yu S, Xu Z, Wu D, Ng CF, Yao X, et al. ERRalpha Augments HIF-1 Signalling by Directly Interacting With HIF-1alpha in Normoxic and Hypoxic Prostate Cancer Cells. *J Pathol* (2014) 233(1):61–73. doi: 10.1002/path.4329
96. Tahirov TH, Inoue-Bungo T, Morii H, Fujikawa A, Sasaki M, Kimura K, et al. Structural Analyses of DNA Recognition by the AML1/Runx-1 Runt Domain and Its Allosteric Control by CBFbeta. *Cell* (2001) 104(5):755–67. doi: 10.1016/S0092-8674(01)00271-9
97. Gu TL, Goetz TL, Graves BJ, Speck NA. Auto-Inhibition and Partner Proteins, Core-Binding Factor Beta (CBFbeta) and Ets-1, Modulate DNA Binding by CBFalpha2 (Aml1). *Mol Cell Biol* (2000) 20(1):91–103. doi: 10.1128/MCB.20.1.91-103.2000
98. Illendula A, Pulikkan JA, Zong H, Grembecka J, Xue L, Sen S, et al. Chemical Biology. A Small-Molecule Inhibitor of the Aberrant Transcription Factor CBFbeta-SMMHC Delays Leukemia in Mice. *Science* (2015) 347(6223):779–84. doi: 10.1126/science.aaa0314
99. Illendula A, Gilmour J, Grembecka J, Tirumala VSS, Boulton A, Kuntimaddi A, et al. Small Molecule Inhibitor of CBFbeta-RUNX Binding for RUNX Transcription Factor Driven Cancers. *EBioMedicine* (2016) 8:117–31. doi: 10.1016/j.ebiom.2016.04.032

Conflict of Interest: The authors declare that the research was conducted in the absence of any commercial or financial relationships that could be construed as a potential conflict of interest.

Publisher's Note: All claims expressed in this article are solely those of the authors and do not necessarily represent those of their affiliated organizations, or those of the publisher, the editors and the reviewers. Any product that may be evaluated in this article, or claim that may be made by its manufacturer, is not guaranteed or endorsed by the publisher.

frontiers | Frontiers in Oncology

ORIGINAL RESEARCH
published: 20 May 2022
doi: 10.3389/fonc.2022.814912

Identification of Novel Pyroptosis-Related Gene Signatures to Predict Prostate Cancer Recurrence

Chun Li[1,2,3,4†], *Jie Zhu*[5†], *Hexi Du*[1,3,4*] *and Chaozhao Liang*[1,3,4*]

[1] Department of Urology, The First Affiliated Hospital of Anhui Medical University, Hefei, China, [2] Department of General Surgery, The First Affiliated Hospital of Anhui Medical University, Hefei, China, [3] Institute of Urology, Anhui Medical University, Hefei, China, [4] Anhui Province Key Laboratory of Genitourinary Diseases, Anhui Medical University, Hefei, China, [5] Central Hospital Affiliated to Shandong First Medical University, Jinan, China

OPEN ACCESS

Edited by:
Hua Li,
Henry M. Jackson Foundation for the Advancement of Military Medicine (HJF), United States

Reviewed by:
Jun Pang,
Sun Yat-sen University, China
Svetlana Khaiboullina,
University of Nevada, Reno, United States

***Correspondence:**
Chaozhao Liang
liang_chaozhao@ahmu.edu.cn
Hexi Du
duhexi1989@163.com

[†]*These authors have contributed equally to this work*

Specialty section:
This article was submitted to Genitourinary Oncology, a section of the journal Frontiers in Oncology

Received: *14 November 2021*
Accepted: *12 April 2022*
Published: *20 May 2022*

Citation:
Li C, Zhu J, Du H and Liang C (2022) Identification of Novel Pyroptosis-Related Gene Signatures to Predict Prostate Cancer Recurrence. Front. Oncol. 12:814912. doi: 10.3389/fonc.2022.814912

Prostate cancer (PCa) is a common malignant type of urogenital tract tumor with poor prognosis. Despite therapeutic advances, the recurrence and mortality rates of PCa have continued to increase with poor prognoses. Pyroptosis, also known as inflammatory cell necrosis, is a recently identified type of programmed cell death that can regulate the invasiveness, differentiation, proliferation, and metastasis of tumor cells; thus, it has a profound effect on the prognosis of patients with tumors. However, the relationship between pyroptosis and PCa remains unclear. We first identified 25 pyroptosis-related genes (PRGs) that were differentially expressed between PCa tissues and matched normal tissues in The Cancer Genome Atlas (TCGA) cohort. Based on the expression levels of 25 PRGs, PCa patients were clearly divided into two clusters and 17 PRGs were found to be significantly different between the two clusters, suggesting probable roles for these genes in the progression and recurrence of PCa. Therefore, the GSE40272 dataset with recurrence follow-up information was used to verify their value. Univariate analysis suggested that 5/17 genes were associated with recurrence, the number of genes did not decrease after least absolute shrinkage and selection operator (LASSO) regression analysis, and 5 PRGs constituted the risk score formula. Low-risk and high-risk subgroups identified using the recurrence model showed different disease-free survival (DFS) times ($P<0.001$) and the risk score of five PRGs was a factor of independence for recurrence in patients with PCa. In addition, Gene Ontology (GO) and Kyoto Encyclopedia of Genes and Genomes (KEGG) analyses suggested that these pathways, and comprising PRGs might be closely related to carcinogenesis and invasion of tumors, tumor microenvironment, and immune response. In conclusion, the expression signatures of PRGs play an important role in predicting PCa recurrence.

Keywords: pyroptosis, prostate cancer, recurrence, immunity, prognosis

INTRODUCTION

Prostate cancer (PCa) is the most malignant tumor of the male genitourinary tract, with approximately 1,276,106 new cases of PCa worldwide and a total of 358,989 deaths in 2018, ranking second in the incidence of male malignant tumors and posing a serious threat to the health of elderly men (1). With the spread of awareness regarding prostate-specific antigen (PSA) screening and health examination, more patients have access to radical local treatment but 30–40% of patients with PSA still show recurrence after local treatment or transfer. In medium–high risk patients, the biochemical recurrence rate within 5 years after radical prostatectomy is more than 50%, suggesting the need for attention to residual tumors after treatment, metastasis before treatment, or new therapeutic strategies to compensate for the lack of local treatment (2–4). Genetic biomarkers have shown potential for predicting PCa recurrence; however, these have not yet been used in medical practice and are only in the molecular research stage. Therefore, it would be of great significance to discover the prognostic or genetic characteristics associated with the recurrence of PCa.

In 2001, scientists proposed the concept of pyroptosis, describing it as a new type of programmed inflammatory cell death that triggers certain inflammatory bodies by activating inactive factors and lysing gasdermin D, leading to a variety of diseases, such as heart disease, stroke, microbial infections, and tumors (5–7). The relationship between pyroptosis and cancer is extremely complex. Although pyroptosis inhibits tumorigenesis and tumor progression, it also creates a microenvironment that delivers nutrients to the tumor and accelerates its growth (8). Studies have increasingly shown that pyroptosis affects the invasiveness, differentiation, proliferation, and metastasis of tumor cells, thereby affecting the prognosis of tumors (9–11). In addition, several studies have suggested that pyroptosis may be associated with regulation of the tumor immune microenvironment (12, 13).

In this study, pyroptosis likely had both positive and negative effects on PCa development. To date, the function of PRG expression in the prognosis of PCa is still unclear and none of the previous publications comprehensively evaluated PRGs in PCa. Moreover, the prognostic value of pyroptosis in PCa has not been reported. Therefore, studying the effect of pyroptosis on tumorigenesis and the development of PCa can facilitate: the evaluation of prognosis and recurrence in patients, a better understanding of the progression and metastasis of PCa, along with better guidance for the identification of new therapeutic targets. In the present study, we performed a comprehensive evaluation of differentially expressed PRGs in PCa and identified PRG-based differences to predict the recurrence of PCa, which may provide a new approach for its diagnosis and treatment.

MATERIALS AND METHODS

Datasets

The design process and grouping are illustrated in **Figure 1**. The RNA sequencing (RNA-Seq) data of PCa patient samples, matched normal samples, and corresponding clinical features were obtained from the TCGA database (https://portal.gdc.cancer.gov/, **Table 1**). Validation cohort of RNA-seq data and clinical information were from the GEO database on August 16, 2021 (https://ncbi.nlm.nih.gov/geo/, ID: GSE40272, **Table 1**).

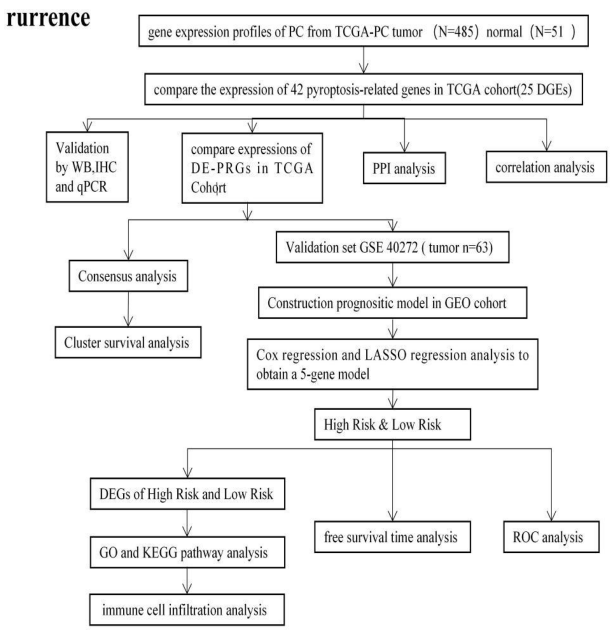

FIGURE 1 | The flowchart of the overall procedures. This flowchart illustrates the process of data collection and analysis for prognostic study.

TABLE 1 | Clinical characteristic of patients with prostate cancer.

	TCGA	GEO
	Number of patients	
Age		
<60	283	25
≥60	202	38
Stage		
T TI-T2	187	–
T3-T4	296	
unknown	7	
N N0	340	–
NI	78	
Unknown	72	
M	unknown	–
Disease state		
Dlive	476	–
Dead	9	
Disease free survival	–	63
Treatment		
Operation	–	62
Operation and hormone	–	1
	Time	
Median disease free survival time	–	35.82 months
Median follow-up survival time	1092.89 days	–

Identification of DE-PRGs Between PCa and Matched Normal Control Groups

From the Reactome database (https://reactome.org/) and Molecular Signatures Database (https://www.gsea-msigdb.org/), 42 PRGs were obtained and verified in several reviews (13–20). TCGA expression data were uniformly standardized to fragments per kilobase per million (FPKM) prior to comparison. The 25 DE-PRGs were identified using the "limma" package, and the P value threshold was less than 0.05. The 25 DE-PRGs were annotated as follows: * $P < 0.05$, ** $P < 0.01$, and *** $P < 0.001$. A protein–protein interaction (PPI) network was modelled using the Search Tool for the Retrieval of Interacting Genes/Proteins (STRING) version 11.0.

Cell Lines and Cell Culture

PCa cell lines PC3, C4-2, 22RV1 and human prostatic epithelial cells (RWPE-1) were purchased from ATCC (American Type Culture Collection, Manassas, VA, USA). All PC cell lines were cultured in RP1640 medium (RP1640, Gibco) supplemented with 10% foetal bovine serum (FBS, Gibco), 100 U/mL penicillin, and 100 μg/mL streptomycin at 37°C in 5% CO2.

Reagents and Antibodies

Reagents and antibodies used were: Cytochrome C antibody (AF0146) (Affinity Biosciences,USA); anti-GSDMB antibody (ab235540) and anti-caspase-8 antibody (Abcam, USA); and Bak (BAK1) antibody (AB016), BAX antibody, and TP53 antibody (AF1270) (Beyotime, China).

Western Blotting

Cells were lysed in cold RIPA buffer (Beyotime, China) in the presence of 1 × protease inhibitor cocktail and 1 × PhosStop (Roche, Isere, France) after two washes with phosphate-buffered saline (PBS). The lysate was removed by sonication, and the protein concentration was determined using a Pierce bicinchoninic acid (BCA) protein assay kit (Thermo Fisher Scientific, MA, USA). Equal amounts of proteins were loaded onto polyacrylamide gels.

Immunohistochemistry

Prostate tissue blocks were cut into 5-μm-thick sections, dewaxed in xylene, and rehydrated in an ethanol gradient. Antigen was retrieved by boiling the tissue sections for 20 minutes in retrieval buffer. Sections were later immersed in a 3% hydrogen peroxide solution for 15 minutes to block endogenous peroxidase activity. Next, the slides were rinsed with PBS 3 times, blocked with 3% BSA at room temperature for 30 minutes, and then incubated with purified rabbit anti-human primary antibody (1:300 dilution) at 4°C overnight. After incubation, the slides were incubated with diluted goat anti-rabbit secondary antibody for 1 hour at room temperature. They were then rinsed twice with PBS. The detection reagent DAB was added and the slides were incubated in the dark at room temperature for 10 minutes. After DAB staining, the slides were rinsed in running tap water for 3 minutes. Finally, they were incubated with haematoxylin to counterstain the nucleus. All slides were independently examined by two authorized pathologists who were not informed of the patients' clinical statuses or outcomes.

RNA Extraction and Quantitative Analysis

Real-Time PCR (qRT–PCR)

Total RNA was extracted from cell lines with TRIzol Reagent (Invitrogen, USA). Total RNA was reverse-transcribed into cDNA with PrimeScript RT Master Mix (Takara, USA) and then used to perform quantitative real-time PCR (qRT–PCR) with SYBR qPCR Master Mix (Vazyme, China). GAPDH was used as an internal control for gene quantification. The 2−ΔCT was calculated for every sample and normalised to GAPDH. The primer sequences used are shown in **Table 2**.

Ethics Approval and Consent to Participate

Fifteen cases of cancer tissues and eleven cases of paracancerous tissues were extracted at the Pathology Department of the First Affiliated Hospital of Anhui Medical University and all patients were clinically diagnosed with prostate cancer from February 25, 2022 to March 26, 2022. The project was approved by the Ethics Committee of the hospital and written informed consent was obtained from each patient who enrolled in the study (Reference number: Quick-PJ 20220320).

Consensus Clustering Analysis of PRGs

Consensus clustering, a technique for combining multiple clusters into a more stable single cluster, was used to distinguish different pyroptosis correlation patterns associated with pyroptosis regulation using the k-means method. The quantity and stability of the clusters were determined using the consensus clustering algorithm in the ConsensusClusterPlus package. The chi-square test and R package "survival" were used to analyse the correlation between clusters and overall survival (OS), showing the results by Kaplan–Meier curves. The differential expression analysis of PRGs among different

TABLE 2 | Primer Sequences Used in the qRT-PCR Assay.

Primer	Sequence (5'-3'))
BAK-For	GTTTTCCGCAGCTACGTTTTT
BAK-Rev	GCAGAGGTAAGGTGACCATCTC
BAX-For	CCCGAGAGGTCTTTTTCCGAG
BAX-Rev	CCAGCCCATGATGGTTCTGAT
CASP8-For	TTTCTGCCTACAGGGTCATGC
CASP8-Rev	GCTGCTTCTCTCTTTGCTGAA
CYCS-For	CTTTGGGCGGAAGACAGGTC
CYCS-Rev	TTATTGGCGGCTGTGTAAGAG
GSDMB-For	TGATTGCCGTTAGAAGCCTTG
GSDMB-Rev	TCCCGTTGAGTCTACATTATCCA
TP53-For	CAGCACATGACGGAGGTTGT
TPS3-Rev	TCATCCAAATACTCCACACGC
GAPDH-For	GGAGCGAGATCCCTCCAAAAT
GAPDH-REv	GGCTGTTGTCATACTTCTCATGG

clusters was performed again, and 17 DE-PRGs were displayed in the form of heatmaps.

Establishment and Validation of the PRG Model of Recurrence and Prognosis

Seventeen PRGs were found to be related to PCa progression. Since very few patients died in the TCGA cohort, it was difficult to select PRGs closely related to OS. Therefore, the GSE40272 dataset with disease-free survival (DFS) traits was used to construct a prognostic model. First, univariate Cox regression analysis was used to assess the association between DFS status and 17 PRGs to evaluate their prognostic value. With 0.05 as the cut-off value, 5/17 genes involved in recurrence were identified for further analysis. Subsequently, the LASSO Cox regression model (R package "glmnet") was used to construct a refined recurrence prediction model. Finally, the 5 PRGs and their coefficients were reserved to determine the penalty parameter λ using the minimum standard. The risk scoring formula was as follows: PCa recurrence risk score (PRRS) = $\sum_{(n=1)}^{i} Coefi * Xi$ expression level (*Coefi* indicates the coefficients, and *Xi* represents the standardised levels of gene expression). Patients with PCa from the GSE40272 cohort were divided into low- and high-risk groups according to the median risk score, and the DFS time of the two groups was compared using Kaplan–Meier analysis. On the basis of the 5-gene signature, principal component analysis (PCA) was used to assess the separability of the two groups according to the "prcomp" function. A three-year ROC curve was analysed using the "survival", "survminer", and "time ROC" R packages.

GO and KEGG (Gene Set Enrichment) Analysis of the DEGs

Patients with PCa from the GEO cohort were classified into two groups based on the median risk score. According to the specific standard (|log2FC| ≥ 1 and P value < 0.05), the DEGs between the low- and high-risk groups were extracted. Based on these DEGs, the "cluster profiler" package was applied to enrich GO and KEGG pathways and the "GO plot" package was used to visualize the results.

Immune Infiltration Analysis

Single-sample gene set enrichment analysis (ssGSEA) was performed using the "gsva" package to calculate the immune cell infiltration score and to assess the activity of immune-related pathways.

Statistical Analysis

Univariate analysis of variance was used to compare the gene expression levels between matched normal prostate tissues and PCa tissues, while the Pearson chi-square test was applied to compare the categorical variables. The Kaplan–Meier method was used to perform a bilateral log-rank test to assess the DFS of patients in the two subgroups. In addition, a univariate Cox regression model was used to evaluate the recurrence value of this risk model. The infiltration of immune cells and activation of immune pathways were compared between the two groups and the Mann–Whitney test was performed. R software (v4.0.2) was used to perform all statistical analyses.

RESULTS

Identified DEGs From Matched Normal and Cancer Tissues in the TCGA Cohort

The expression levels of 42 PRGs were detected in 485 tumor tissues and matched normal tissues from the TCGA database and 25 DE-PRGs were identified (P < 0.05). Among them, 10 genes (*BAK*, *BAX*, *CASP8*, *CHMP2A*, *CHMP4C*, *CSCY*, *GSDMA*, *GSDMB*, *TP53*, and *ZBP1*) were upregulated, whereas 15 genes (*CASP1*, *CHMP2B*, *CHMP3*, *CHMP7*, *ELANE*, *GSDMD*, *GSDME*, *HMGB1*, *IL18, ILα, ILβ*, *IRF2*, *NLRP1*, *NLRP9*, and *TP63*) were downregulated in the cancer tissues. The RNA expression profile of the DEGs is shown in **Figure 2A** (red and blue colors indicate higher and lower expression levels, respectively). **Figures 2B, C** shows the PPIs and related network of DE-PRGs in TCGA data, where the interaction score was 0.9 (the highest confidence). The results showed that *BAK1*, *BAX*, *CASP8*, *CASP1*, *IL18*, *IL1β*, *CYCS*, *GSDMB, GSDMD and TP53* are hub genes.

Validation of the Hub DE-PRGs by Western Blotting and Immunohistochemical Staining

Western blotting was used to validate the expression levels of differentially expressed pyroptosis-related genes, including *CASP8, BAK, BAX, CYCS, TP53, and GSDMB* in three castration-resistant prostate cancer (CRPC) cell lines (PC3, C4-2, and 22RV1) and one normal human prostatic epithelial cell line (RWPE-1). The results showed that the protein expression levels of *CASP8, BAK, BAX, CYCS, TP53, and GSDMB* were higher in the three CRPC cell lines than in the control cell line (RWPE-1). Subsequently, immunohistochemical validation of human tissues was performed. This finding was consistent with our prediction (**Figures 3**, **4**). The results showed that the expression of glandular epithelium (cytoplasm, cell membrane) in the tumor group was significantly higher than that in the normal group (clearly deepened yellowish brown compared to normal groups).

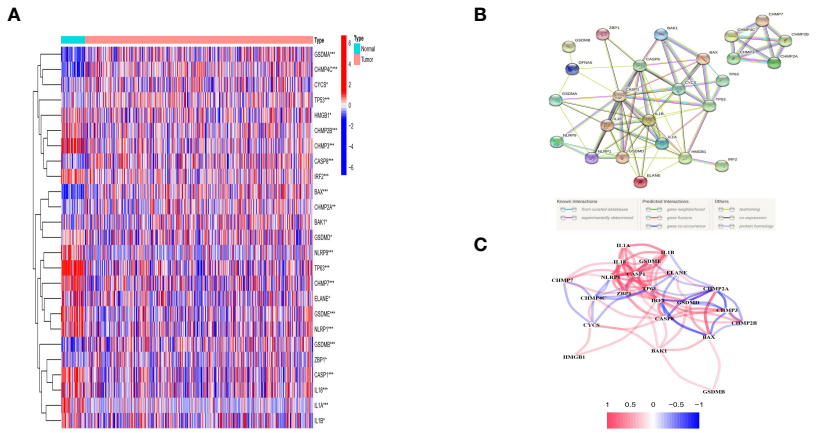

FIGURE 2 | Expressions of the 25 differentially expressed pyroptosis-related genes between tumor and normal and the interactions among them. **(A)** Heatmap (green: low expression level; red; high expression level) of the pyroptosis-related genes between the normal (N, brilliant blue) and the tumour tissues (T.red). P values were showed as: *P < 0.05; **P < 0.01; ***P < 0 001. **(B)** PPI network showing the interactions of DEPRGs (interaction score= 0.9). **(C)** The correlation network of DEPRGs (red line: positive correlation: blue line negative correlation. The depth of the colours reflects the strength of the relevance).

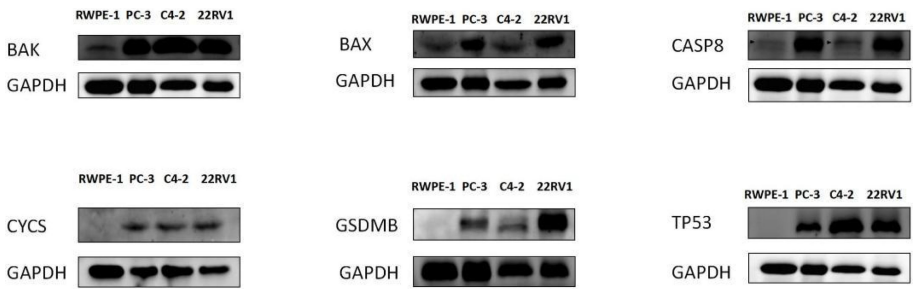

FIGURE 3 | WESTERN-BLOT validation of hub DE-PRGs expressions in normal and tumor tissues, the results showed that protein expression levels of CASP8, BAK, BAX, CYCS, TP53, and GSDMB genes were highly expressed in three CRPC (Castration Resistant Prostate Cancer) cell lines compared to the control normal cell line (RWPE- I). CRPC cell lines (PC-3, C4-2, 22RVI), Control cell line (normal human prostatic epithelial cell, RWPE-1).

All pathological tissues and immunohistochemical sections were confirmed by two senior pathologists.

Validation of the Hub DE-PRGs Genes by qRT-PCR

qRT–PCR was used to validate the expression of the hub DE-PRG genes, including *CASP8, BAK, BAX, CYCS, TP53, and GSDMB* in human prostate cancer tissues and matched normal prostate tissues. The results show that the *CASP8, BAK, BAX, CYCS, TP53, and GSDMB* genes were highly expressed in human prostate cancer tissues compared to matched normal prostate tissues. This is consistent with our predictions. The results are shown in **Figure 5**.

Tumor Classification Based on the DE-PRGs in the TCGA Cohort

Consensus clustering analysis was performed on all 485 patients with PCa in the TCGA cohort to study the relationship between the expression of 25 DE-PRGs and PCa subtypes. An unsupervised clustering method was used to identify two different regulatory patterns by increasing the clustering variate k from 2 to 10. When k was equal to 2, the intragroup and intergroup correlations were the highest and lowest, respectively, which could be well classified into two clusters (**Figure 6A**). The heatmap shows the DE-PRGs between the two clusters (**Figure 6B**). Subsequently, the OS time between the two clusters was compared and no significant differences were found (P = 0.058, **Figure 6C**).

Construction of the Prognostic Model Based on DE-PRGs in a GEO Cohort

Information on 63 patients with PCa was obtained from the GEO database (GSE40272), and the data were randomized. Five out of seventeen genes (*BAK*, *BAX*, *CHMP7*, *GSDMB*, and *NLRP1*) met the standard of P value < 0.05 by univariate Cox regression analysis. Among these, three genes (*BAK1*, *BAX*, and

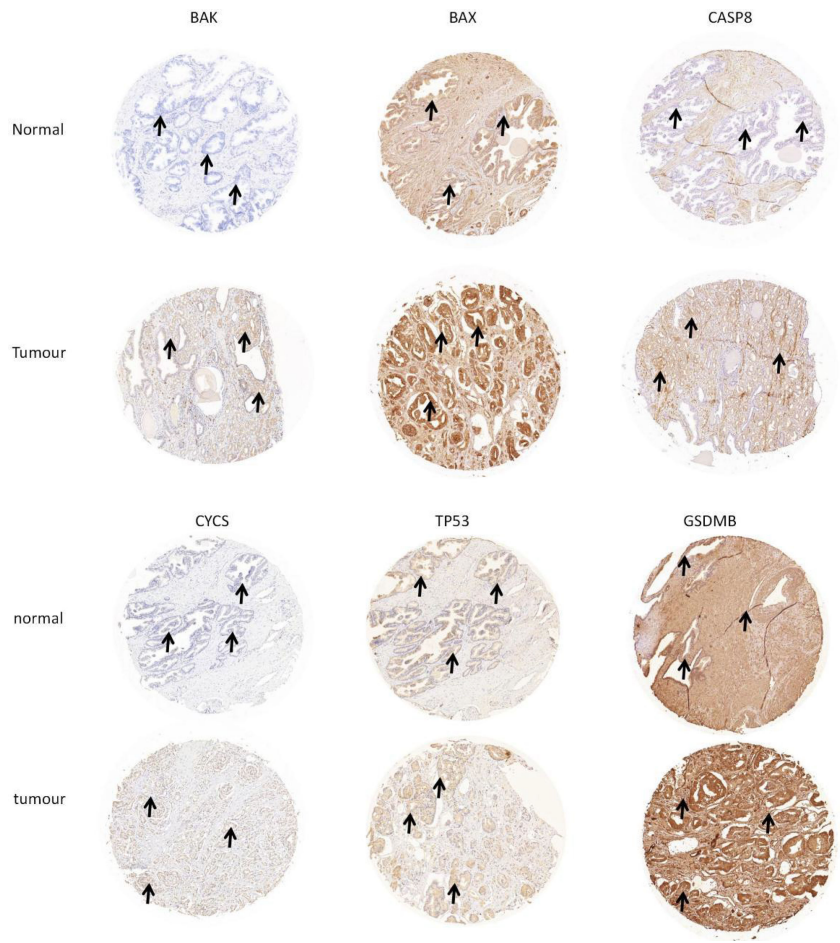

FIGURE 4 | Verification of hub DE-PROs expressions in normal and tumour tissue with Immunohistochemistry (IHC), the expression of glandular epithelium (cytoplasm, cell membrane) in tumour group was significantly higher than that in normal group (obviously deepened in yellowish brown compared to normal groups. " →").

CHMP7) were related to increased risk in HR>1, while the other two genes (*GSDMB* and *NLRP1*) were associated with lower risk in HR<1 (**Figure 7A**). LASSO Cox regression analysis did not reduce the genes; thus, a 5-gene signature was constructed based on the optimum λ value (**Figures 7B, C**) and subsequently, a pyroptosis-related signature risk score known as the "PRRS" was built. The PRRS was calculated as PRRS = (0.598**BAK* exp.) + (0.223**BAX* exp.) + (0.800**CHMP7* exp.) + (-0.863**GSDMB* exp.) + (-0.155**NLRP1* exp.). The high-risk group of 31 patients with PCa and the low-risk group of 32 patients with PCa were divided according to the GEO cohort median risk score (**Figure 7D**). The PCA indicated the separation of satisfaction between the two groups (**Figure 7E**). Furthermore, a clear distinction in DFS was observed in the Kaplan–Meier analysis between these two groups (P value <0.001, **Figure 7F**). ROC analysis in the GEO cohort had a significant predictive effect on PCa recurrence (1-year AUC = 0.793, 2-year AUC = 0.757, and 3-year AUC = 0.772) (**Figure 7G**).

Functional Enrichment Analysis of DEGs

To identify other pathways that may be closely related to pyroptosis-related pathways, all DEGs (**Table S1**) of the two risk groups were analyzed for GO and KEGG enrichment. These significant DEGs were found in the major positive regulation of cell junction assembly, protein targeting, protein maturation, peroxisome organization, ficolin-1-rich granule lumen, neuron-to-neuron synapse, recycling endosome, and cadherin binding in GO analysis. Moreover, KEGG analysis showed that these DEGs were mainly involved in the regulation of Fc gamma R-mediated phagocytosis, peroxisomes, chemical carcinogenesis, ECM-receptor interaction, and focal adhesion (**Figures 8A, B**).

Association between the Immune Status of Patients and PCa Risk in the GEO Cohort

We further explored the changes in immune cell infiltration between the low- and high-risk groups. Based on functional analysis, the activity of 13 immune-related pathways and the

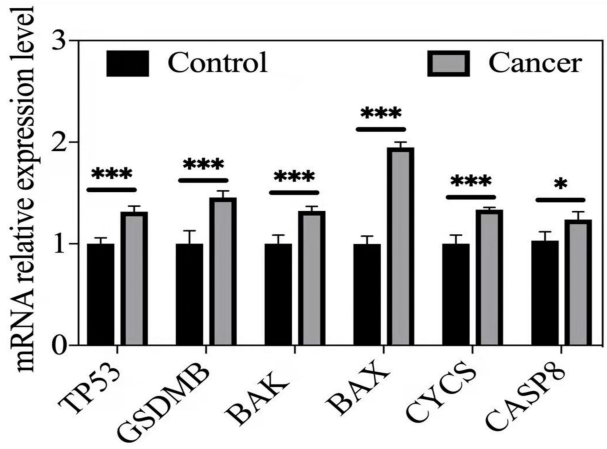

FIGURE 5 | qRT-PCR validation or hub DE-PRGs in human prostate cancer tissues compared to control tissues. *p < 0.05; ***p < 0.001. Cancer (n = 5-6), human prostate cancer tissues. Control (n = 5-6), matched human normal prostate tissues.

enrichment fractions of 16 types of immune cells were compared in the two risk groups and the results were compared using ssGSEA in the GEO cohort. The results showed that, the level of immune cell infiltration was generally lower in the high-risk subgroup, especially in Tfh and Th1 cells. Conversely, CCR and the inflammatory-promoting activity of immune pathways were lower in the high-risk group (**Figures 9A, B**).

DISCUSSION

Pyroptosis, mediated by the gasdermin family and associated with inflammatory and immune responses, is a recently discovered form of programmed cell death. The early stage of pyroptosis has always been considered an apoptotic process and the downstream pathway of pyroptosis activation by infection or injury has been elucidated. Recent evidence suggests that pyroptosis is related to cancer and the dual effects of pyroptosis have aroused the interest of researchers. However, the relationship between pyroptosis and PCa has not been elucidated. Pyroptosis may have two sides in cancer patients, acting as a double-edged sword. The most direct way to better understand pyroptosis and its importance is to establish a prognostic model.

In this study, we first clarified the expression and prognostic value of PRGs in PCa, studied the mRNA expression levels of 42 PRGs in PCa and matched normal tissues, and found 25 differentially expressed genes. To explore the relationship between the expression of these PRGs and PCa subtypes, we identified 17 pyroptosis-related DEGs associated with survival.

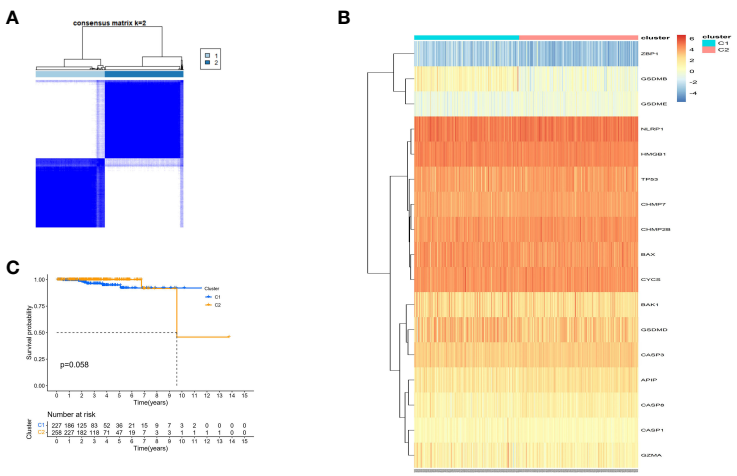

FIGURE 6 | Tumour classification based on the pyroptosis-related DEGs. **(A)** 485 PC patients were grouped into two clusters according to the consensus clustering matrix (k=2). **(B)** Heatmap and the clinicopathologic characters of the two clusters classified by these DEPRGs. **(C)** Kaplan-Meier OS curves for the two clusters.

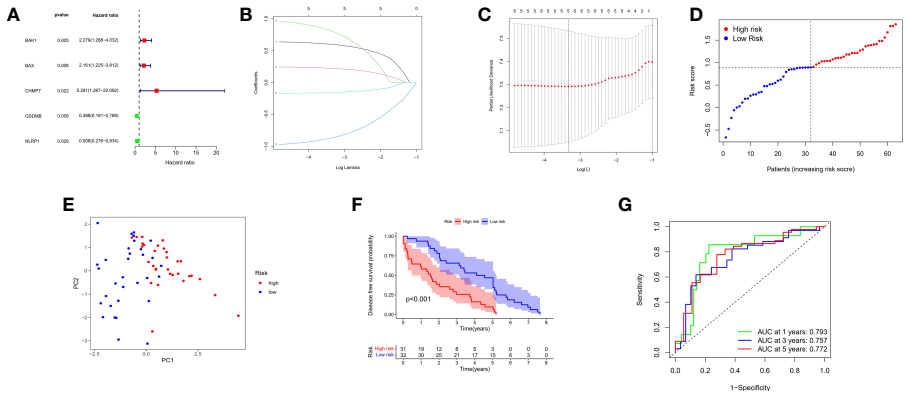

FIGURE 7 | Construction of risk signature in the GEO cohort. **(A)** Univariate cox regression analysis of DFS for each pyroptosis-related gene, and genes with P < 0.05. **(B)** LASSO regression of the 5 DFS-related genes. **(C)** Cross-validation for tuning the parameter selection in the LASSO regression. **(D)** Distribution of patients based on the risk score. **(E)** PCA plot for PCs based on the risk score. **(F)** Kaplan-Meier curves for the DFS of patients in the high- and low-risk groups. **(G)** ROC curves demonstrated the predictive sensitivity of the risk score.

Our findings suggested that these genes play an important role both in the pathogenesis of cancer and in the heterogeneity of cancer patients and we inferred that differential expression of these genes was related to a reduced death rate in the TCGA database. Therefore, to further evaluate the relationship of these PRGs with PCa survival, we searched the GEO database and other related databases and found insufficient follow-up survival data on PCa; however, a set of follow-up data of recurrence (DFS) rate caught our attention. Although not significant in the survival analysis, the high recurrence rate of primary PCa may be valuable. Therefore, we aimed to verify the relationship between these PRGs and recurrence. In addition, we evaluated the prognostic value of these pyroptosis-related regulatory factors and obtained the risk profile of five genes using univariate Cox and LASSO Cox regression analyses with the GEO cohort. The results showed that these pyroptosis-related risk genes constitute a risk formula to predict the recurrence of patients, which is similar to a biomarker: the higher the risk score is, the worse the recurrence.

In our study, ten hub genes were identified in the PPI network. However, how these PRGs interact and whether they are relevant to patient prognostic outcomes remain unclear. For example, Casp1 encodes *CASP1*, a member of the caspase family that is activated by inflammasomes and induces pyroptosis (21). Casp1 is underexpressed in a variety of tumor tissues when it acts as a tumor suppressor (22). Based on our differential gene sorting analysis, it was observed to be poorly expressed in tumors, which is consistent with previous reports. Casp8 can cause pyroptosis by cleaving GSDMD into its active form when TAK1 is suppressed, and TAK1 inhibition also leads to GSDME cleavage (23). In addition, activation of Casp8 can drive inflammasome-independent IL-1β and exogenous cell death receptor signaling downstream of GSDMD to convert apoptotic signals into GSDMD-dependent pyroptosis-like cell

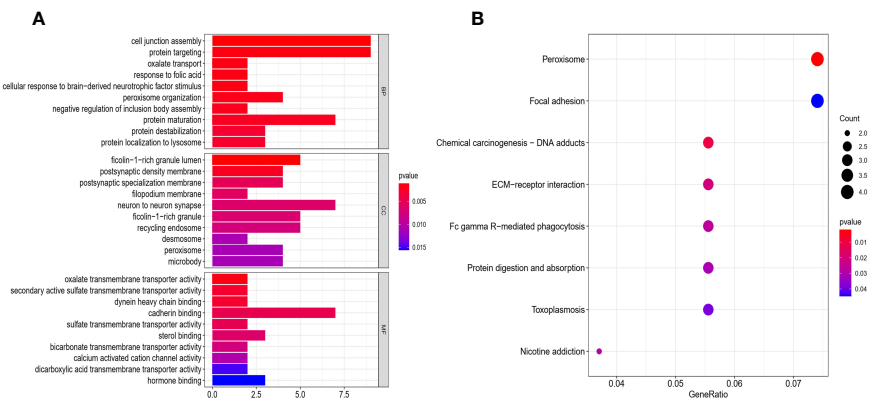

FIGURE 8 | Functional analysis based on the DEGs between the two-risk groups in the GEO cohort. **(A)** Barplot graph for GO enrichment (the longer bar means the more genes enriched, and the increasing depth of red mans the differences were more obvious). **(B)** Bubble graph for KEGG pathways (the bigger bubble means the more genes enriched, and the increasing depth of red means the differences were more obvious; q-value: the adjusted p-value).

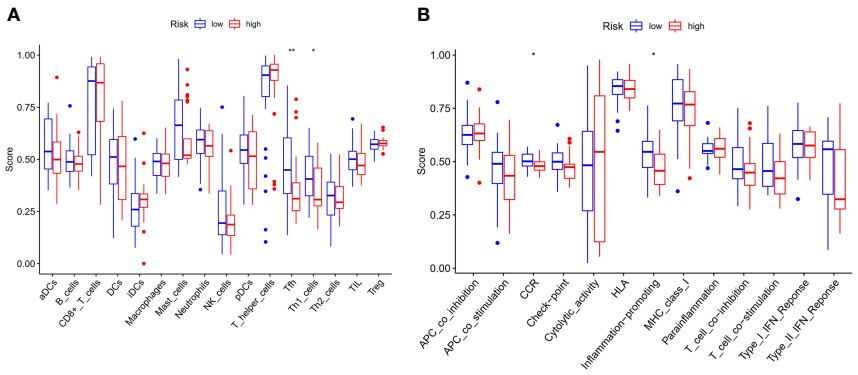

FIGURE 9 | Comparison of the ssGSEA scores for immune cells and immune pathways. **(A)** Comparison of the enrichment score s of 16 types of immune cells between low- (blue box) and high-risk (red box) group in the GEO cohort. **(B)** Comparison of the and 13 immune-related pathways between low- (blue box) and high-risk (red box) group in the GEO cohort. P values were showed as: ns not significant; *P < 0.05; **P < 0.01.

death (24). Both our prediction and experimental validation showed that Casp8 was elevated, suggesting that we can treat PCa by activating the Casp8 pathway to trigger cell death in the future. There is an opportunity to further verify this. BAK and BAX are well-known regulators of the apoptosis pathway and have been found to play a role in the pyroptotic pathway. As tumors grow and progress, these pathways inevitably interact. Studies have shown that the Bak/Bax-Caspase-3-GSDME pathway can enhance the antitumor effect (25). Similar to CASP8, BAK and BAX were elevated in our prediction and validation and were important components of the prediction formula. We hypothesized that BAK and BAX could be used to treat high-risk recurrent PCa by coactivating upstream and downstream genes to promote pyroptosis and kill tumors. Furthermore, interleukin IL1β, a proinflammatory factor that induces pyroptosis (26), has a tumorigenic effect, and its main role is to promote proliferation, migration, and metastasis (27). GSDMB belongs to the GSDM family and is more widely expressed than other members of the GSDM family. Pyroptosis is induced by the cleavage of GSDMB by lymphocytic granzyme A (28). This study demonstrates that activation of GSDMB induces pyroptosis and promotes tumor clearance, supporting an important regulation of reactivation in our predicted formula with a high-risk factor. NLRP1 is an NLR family protein that can also induce apoptosis and pyroptosis, which can impact cancer pathogenesis by modulating congenital immune responses, dysregulation of NLR family members, and results in various inflammatory diseases and autoimmune disorders. Studies have shown that the mRNA and protein levels of NLRP1 are reduced in colorectal cancer cells compared to normal cells and the anticancer drug DAC increases the expression of NLRP1 to inhibit the progression of colorectal cancer (29, 30). In our differential pyroptosis gene expression and prediction formula, NLRP1 was identified as a low-risk factor, which was consistent with literature reports. Immunohistochemistry showed that NLRP1 expression was lower in the high-grade PCa group than in the low-grade PCa group. According to our results, some of these PRGs appear to be cancer suppressor genes because they are downregulated threefold in cancer tissues, Nevertheless, they also help prolong patients' DFS because they are enriched in the low-risk group. Additionally, five genes were identified as promoters of pyroptosis in the prognostic model. However, not all of these promoters were related to better PCa prognosis in our study, indicating that these five genes are in the same formula and their sensitivity and specificity are mutually restricted to achieve the optimal ROC. Therefore, it was not possible to determine the expression level of one gene separately to evaluate high or low risk. We will further study how these genes interact with each other during pyroptosis.

To identify other pathways that might be closely related to pyroptosis-related pathways, all DEGs (**Table S1**) in the two risk groups were analyzed for GO and KEGG enrichment. The results showed that these genes were mainly involved in regulatory protein targeting, cadherin binding, chemical carcinogenesis, ECM-receptor interaction, and focal adhesion. Studies have shown that cadherin-11 affects the invasiveness and migration of PCa cells (31–34). These functions or pathways suggest that PRGs might play an important role in the oncogenesis, recurrence, and metastasis of PCa and may be related to the intensity of pyroptosis or counter-regulation.

Another important finding of our study was that PRGs were correlated with immune infiltration, and 13 of 16 important antitumor immune cells were increased in the low-risk group compared to the high-risk group. However, some comparisons were not significantly different, probably because of the limited number of samples in the two cohorts. In the GEO cohort, the accumulation of cancer-promoting immune cells in the tumor microenvironment was generally observed in the high-risk group. Tfh and Th1 cells were statistically significant in our study. Relevant studies have shown that blood Th1 levels are negatively correlated with PCa and can reduce the occurrence of prostate bone metastasis and improve survival. Notably, Th1 levels in the high-risk group were lower than those in the low-risk group and exhibited a potential immunotherapeutic effect, which is consistent with our findings (35–37). Based on these results, poor DFS in high-risk PCa patients might be related to

the suppressed levels of antitumor immunity and changes in the tumor microenvironment.

The advantage of our study lies in the systemic analysis based on TCGA and GEO cohorts and the evaluation of PRGs in PCa. Our study has several limitations. Owing to the nature of publicly available datasets, the number of deaths among patients with PCa was very limited. The specific mechanism by which PRGs regulate PCa occurrence and progression remains to be explored. Large and well-designed clinical or *in vivo* experiments are required to validate our predictive model. Despite these limitations, our experiments achieved some consistency with the predictions. In summary, we conducted a comprehensive and systematic bioinformatics analysis and identified PRG signatures that were significantly associated with DFS in patients with PCa and some relevant experiments were performed to verify our results. Furthermore, the risk score based on the prognostic model of five PRGs was an independent risk factor for PCa recurrence and was found to be related to the immune microenvironment, which should be verified in future studies.

DATA AVAILABILITY STATEMENT

The datasets presented in this study can be found in online repositories. The names of the repository/repositories and accession number(s) can be found in the article/**Supplementary Material**.

ETHICS STATEMENT

The studies involving human participants were reviewed and approved by Clinical Medical Research Ethics Committee of the First Affiliated Hospital of Anhui Medical University. The patients/participants provided their written informed consent to participate in this study.

AUTHOR CONTRIBUTIONS

CL and JZ conceived the study. CL and JZ designed the study and analyzed the data. CL wrote the manuscript, which was reviewed by CZL and HXD. All authors contributed to the article and approved the submitted version.

FUNDING

This work is supported by the National Natural Science Foundation of China (31800834, 81773299, 82072055, 82072040, 82100815), and Anhui Natural Science Foundation of China (2108085QH315).

ACKNOWLEDGMENTS

We would like to acknowledge the TCGA, and the GEO (GSE40272) database network for providing data.

SUPPLEMENTARY MATERIAL

The Supplementary Material for this article can be found online at: https://www.frontiersin.org/articles/10.3389/fonc.2022.814912/full#supplementary-material

REFERENCES

1. Bray F, Ferlay J, Soerjomataram I, Siegel RL, Torre LA, Jemal A. Global Cancer Statistics 2018: GLOBOCAN Estimates of Incidence and Mortality World-Wide for 36 Cancers in 185 Countries. *CA Cancer J Clin* (2018) 68:394–424. doi: 10.3322/caac.21492
2. Leao R, Domingos C, Figueiredo A, Hamilton R, Tabori U, Castelo-Branco P. Cancer Stem Cells in Prostate Cancer: Implication for Targeted Therapy. *Urol Int* (2017) 99:125–36. doi: 10.1159/000455160
3. Kirby M, Hirst C, Crawford ED. Characterising the Castration-Resistant Prostate Cancer Population: A Systematic Review. *Int J Clin Pract* (2011) 65:1180–92. doi: 10.1111/j.1742-1241.2011.02799.x
4. Sartor O, de Bono JS. Metastatic Prostate Cancer. *N Engl J Med* (2018) 378:645–57. doi: 10.1056/NEJMra1701695
5. Cookson BT, Brennan MA. Pro-Inflammoatory Programmed Cell Death. *Trends Microbiol* (2001) 9:113–4. doi: 10.1016/s0966-842x(00)01936-3
6. Schneider KS, Groß CJ, Dreier RF, Saller BS, Mishra R, Gorka O, et al. The Inflammasome Drives GSDMD-Independent Secondary Pyroptosis and IL-1release in the Absence of Caspase-1 Protease Activity. *Cell Rep* (2017) 21:3846–59. doi: 10.1016/j.celrep.2017.12.018
7. Yu P, Zhang X, Liu N, Tang L, Peng C, Chen X, et al. Pyroptosis: Mechanisms and Diseases. *Signal Transduct Target Ther* (2021) 6:128. doi: 10.1038/s41392-021-00507-5
8. Xia XJ, Wang X, Cheng Z, Qin WH, Lei LC, Jiang JQ, et al. The Role of Pyroptosis in Cancer: Pro-Cancer or Pro- "Host"? *Cell Death Dis* (2019) 10:650. doi: 10.1038/s41419-019-1883-8
9. Fang Y, Tian S, Pan Y, Li W, Wang Q, Tang Y, et al. Pyroptosis: A New Frontier in Cancer. *BioMed Pharmacother* (2020) 121:109595. doi: 10.1016/j.biopha.2019.109595
10. Tan YF, Wang M, Chen ZY, Wang L, Liu XH. Inhibition of BRD4 Prevents Proliferation and Epithelial-Mesenchymal Transition in Renal Cell Carcinoma *Via* NLRP3 Inflammasome-Induced Pyroptosis. *Cell Death Dis* (2020) 11:239. doi: 10.1038/s41419-020-2431-2
11. Dupaul-Chicoine J, Yeretssian G, Doiron K, Bergstrom KSB, Mclntire CR, LeBlanc PM, et al. Control of Intestinal Homeostasis, Colitis, and Colitis-Associated Colorectal Cancer by the Inflammatory Caspases. *Immunity* (2010) 32:367–78. doi: 10.1016/j.immuni.2010.02.012
12. Xi G, Gao JW, Wan B, Zhan P, Xu WJ, Lv TF, et al. GSDMD is Required for Effector $CD8^+$T Cell Responses to Lung Cancer Cells. *Int Immunopharmacol* (2019) 74:105713. doi: 10.1016/j.intimp.2019.105713
13. Zhang Z, Zhang Y, Xia SY, Kong Q, Li Sy, Liu X, et al. Gasdermin E Suppresses Tumour Growth by Activating Anti-Tumour Immunity. *Nature* (2020) 579:415–20. doi: 10.1038/s41586-020-2071-9
14. Karki R, Kanneganti TD. Diverging Inflammasome Signals in Tumorigenesis and Potential Targeting. *Nat Rev Cancer* (2019) 19:197–214. doi: 10.1038/s41568-019-0123-y
15. Wang B, Yin Q. AIM2 Inflammasome Activation and Regulation: A Structural Perspective. *J Struct Biol* (2017) 200:279–82. doi: 10.1016/j.jsb.2017.08.001
16. Man SM, Kanneganti TD. Regulation of Inflammasome Activation. *Immunol Rev* (2015) 265:6–21. doi: 10.1111/imr.12296
17. Latz E, Xiao TS, Stutz A. Activation and Regulation of the Inflammasomes. *Nat Rev Immunol* (2013) 13:397–411. doi: 10.1038/nri3452

18. Hartman ML. Non-Apoptotic Cell Death Signaling Pathways in Melanoma. *Int J Mol Sci* (2020) 21:2980. doi: 10.3390/ijms21082980
19. Shi J, Gao W, Shao F. Pyroptosis: Gasdermin-Mediated Programmed Necrotic. *Cell Death Trends Biochem Sci* (2017) 42:245–54. doi: 10.1016/j.tibs.2016.10.004
20. Schroder K, Tschopp J. The Inflammasomes. *Cell* (2010) 140:821–32. doi: 10.116/j
21. Miao EA, Rajan JV, Aderem A. Caspase-1-induced Pyroptotic Cell Death. *Immunol Rev* (2011) 243:206–14. doi: 10.1111/j.1600-065X.2011.01044.x
22. Shalini S, Dorstyn L, Dawar S, Kumar S. Old, New and Emerging Functions of Caspases. *Cell Death Dif* (2015) 22:526–39. doi: 10.1038/cdd.2014.216
23. Sarhan J, Liu BC, Muendlein H, Li P, Nilson R, Tang AY, et al. Caspase-8 Induces Cleavage of Gasdermin D to Elicit Pyroptosis During Yersinia Infection. *Proc Natl Acad Sci USA* (2018) 115:E10888–97. doi: 10.1073/pnas.1809548115
24. Donado CA, Cao AB, Simmons DP, Croker BA, Brennan PJ, Brenner MB, et al. A Two-Cell Model for IL-1β Release Mediated by Death-Receptor Signaling. *Cell Rep* (2020) 31:107466. doi: 10.1016/j.celrep.2020.03.030
25. Hu L, Chen M, Chen XR, Zhao CG, Fang ZY, Wang HZ, et al. Chemotherapy-Induced Pyroptosis is Mediated by BAK/BAX-caspase-3-GSDME Pathway and Inhibited by 2- Bromopalmitate. *Cell Death Dis* (2020) 11:281. doi: 10.1038/s41419-020-2476-2
26. Man SM, Karki R, Kanneganti TD. Molecular Mechanisms and Functions of Pyroptosis, Inflammatory Caspases and Inflammasomes in Infectious Diseases. *Immunol Rev* (2017) 277:61–75. doi: 10.1111/imr.12534
27. Rébé C, Ghiringhelli F. Interleukin-1β and Cancer. *Cancers (Basel)* (2020) 12:1791. doi: 10.3390/cancers12071791
28. Zhou ZW, He HB, Wang K, Shi XY, Wang YP, Su Y, et al. Granzyme A From Cytotoxic Lymphocytes Cleaves GSDMB to Trigger Pyroptosis in Target Cells. *Science* (2020) 368:eaaz7548. doi: 10.1126/science.aaz7548
29. Shen E, Han Y, Cai C, Liu P, Chen YH, Gao L, et al. Low Expression of NLRP1 is Associated With a Poor Prognosis and Immune Infiltration in Lung Adenocarcinoma Patients. *Aging (Albany NY)* (2021) 13:7570–88. doi: 10.18632/aging.202620
30. Chen C, Wang B, Sun J, Na H, Chen Z, Yan L, Ren S, et al. DAC can Restore Expression of NALP1 to Suppress Tumor Growth in Colon Cancer. *Cell Death Dis* (2015) 6(1):e1602. doi: 10.1038/cddis.2014.532
31. Satcher R, Pan T, Bilen MA, Li XX, Lee YC, Ortiz A, et al. Cadherin-11 Endocytosis Through Binding to Clathrin Promotes cadherin-11-mediated Migration in Prostate Cancer Cells. *J Cell Sci* (2015) 128:4629–41. doi: 10.1242/jcs.176081
32. Huang CF, Lira C, Chu K, Bilen MA, Lee YC, Ye XC, et al. Cadherin-11 Increases Migration and Invasion of Prostate Cancer Cells and Enhances Their Interaction With Osteoblasts. *Cancer Res* (2010) 70(11):4580–9. doi: 10.1158/0008-5472.CAN-09-3016
33. Spans L, Helsen C, Clinckemalie L, Broeck TVD, Prekovic S, Joniau S, et al. Comparative Genomic and Transcriptomic Analyses of LNCaP and C4-2B Prostate Cancer Cell Lines. *PloS One* (2014) 9:e90002. doi: 10.1371/journal.pone.0090002
34. Bono JS, Guo C, Gurel B, Marzo AMD, Sfanos KS, Mani RS, et al. Prostate Carcinogenesis: Inflammatory Storms. *Nat Rev Cancer* (2020) 20:455–69. doi: 10.1038/s41568-020-0267-9
35. Bhavsar NA, Bream JH, Meeker AK, Drake CG, Peskoe SB, Dabitao D, et al. A Peripheral Circulating TH1 Cytokine Profile is Inversely Associated With Prostate Cancer Risk in CLUE Ii. *Cancer Epidemiol Biomarkers Prev* (2014) 23:2561–7. doi: 10.1158/1055-9965.EPI-14-0010
36. Jiao SJ, Subudhi SK, Aparicio A, Ge ZQ, Guan BX, Miura YJ, et al. Differences in Tumor Microenvironment Dictate T Helper Lineage Polarization and Response to Immune Checkpoint Therapy. *Cell* (2019) 179:1177–90.e13. doi: 10.1016/j.cell.2019.10.029
37. Tan JF, Jin XF, Zhao R, Wei X, Liu Y, Kong XB, et al. Beneficial Effect of T Follicular Helper Cells on Antibody Class Switching of B Cells in Prostate Cancer. *Oncol Rep* (2015) 33:1512–8. doi: 10.3892/or.2014.3684

Conflict of Interest: The authors declare that the research was conducted in the absence of any commercial or financial relationships that could be construed as a potential conflict of interest.

Publisher's Note: All claims expressed in this article are solely those of the authors and do not necessarily represent those of their affiliated organizations, or those of the publisher, the editors and the reviewers. Any product that may be evaluated in this article, or claim that may be made by its manufacturer, is not guaranteed or endorsed by the publisher.

frontiers | Frontiers in Oncology

ORIGINAL RESEARCH
published: 25 May 2022
doi: 10.3389/fonc.2022.873516

Heterogeneous Expression and Subcellular Localization of Pyruvate Dehydrogenase Complex in Prostate Cancer

Caroline E. Nunes-Xavier[1,2], Janire Mingo[1], Maite Emaldi[1], Karine Flem-Karlsen[2], Gunhild M. Mælandsmo[2], Øystein Fodstad[2], Roberto Llarena[3], José I. López[1,4] and Rafael Pulido[1,5]*

[1] Biomarkers in Cancer, Biocruces Bizkaia Health Research Institute, Barakaldo, Spain, [2] Department of Tumor Biology, Institute for Cancer Research, Oslo University Hospital Radiumhospitalet, Oslo, Norway, [3] Department of Urology, Cruces University Hospital, Barakaldo, Spain, [4] Department of Pathology, Cruces University Hospital, Barakaldo, Spain, [5] Ikerbasque, Basque Foundation for Science, Bilbao, Spain

OPEN ACCESS

Edited by:
Alagarsamy Srinivasan, NanoBio Diagnostics, United States

Reviewed by:
Zhenbang Chen, Meharry Medical College, United States
Humberto De Vitto, University of Minnesota Twin Cities, United States

***Correspondence:**
Caroline E. Nunes-Xavier
carolinenunesxavier@gmail.com

Specialty section:
This article was submitted to Genitourinary Oncology, a section of the journal Frontiers in Oncology

Received: *10 February 2022*
Accepted: *31 March 2022*
Published: *25 May 2022*

Citation:
Nunes-Xavier CE, Mingo J, Emaldi M, Flem-Karlsen K, Mælandsmo GM, Fodstad Ø, Llarena R, López JI and Pulido R (2022) Heterogeneous Expression and Subcellular Localization of Pyruvate Dehydrogenase Complex in Prostate Cancer. Front. Oncol. 12:873516. doi: 10.3389/fonc.2022.873516

Background: Pyruvate dehydrogenase (PDH) complex converts pyruvate into acetyl-CoA by pyruvate decarboxylation, which drives energy metabolism during cell growth, including prostate cancer (PCa) cell growth. The major catalytic subunit of PDH, PDHA1, is regulated by phosphorylation/dephosphorylation by pyruvate dehydrogenase kinases (PDKs) and pyruvate dehydrogenase phosphatases (PDPs). There are four kinases, PDK1, PDK2, PDK3 and PDK4, which can phosphorylate and inactivate PDH; and two phosphatases, PDP1 and PDP2, that dephosphorylate and activate PDH.

Methods: We have analyzed by immunohistochemistry the expression and clinicopathological correlations of PDHA1, PDP1, PDP2, PDK1, PDK2, PDK3, and PDK4, as well as of androgen receptor (AR), in a retrospective PCa cohort of patients. A total of 120 PCa samples of representative tumor areas from all patients were included in tissue microarray (TMA) blocks for analysis. In addition, we studied the subcellular localization of PDK2 and PDK3, and the effects of the PDK inhibitor dichloroacetate (DCA) in the growth, proliferation, and mitochondrial respiration of PCa cells.

Results: We found heterogeneous expression of the PDH complex components in PCa tumors. PDHA1, PDP1, PDK1, PDK2, and PDK4 expression correlated positively with AR expression. A significant correlation of PDK2 immunostaining with biochemical recurrence and disease-free survival was revealed. In PCa tissue specimens, PDK2 displayed cytoplasmic and nuclear immunostaining, whereas PDK1, PDK3 and PDK4 showed mostly cytoplasmic staining. In cells, ectopically expressed PDK2 and PDK3 were mainly localized in mitochondria compartments. An increase in maximal mitochondrial respiration was observed in PCa cells upon PDK inhibition by DCA, in parallel with less proliferative capacity.

Conclusion: Our findings support the notion that expression of specific PDH complex components is related with AR signaling in PCa tumors. Furthermore, PDK2 expression associated with poor PCa prognosis. This highlights a potential for PDH complex components as targets for intervention in PCa.

Keywords: prostate cancer (PCa), pyruvate dehydrogenase (PDH), pyruvate dehydrogenase kinase (PDK), androgen receptor (AR), dichloroacetate (DCA)

INTRODUCTION

PCa is a long-latency cancer, evolving from low malignancy early stages (prostatic intraepithelial neoplasia) to high-grade and metastatic adenocarcinomas, which frequently do not respond to anti-androgen hormone therapies (castrate-resistant prostate cancer, CRPC) (1–3). The androgen pathway is the central signaling pathway in PCa, together with the retinoblastoma (RB), PI3K/PTEN/AKT/mTOR, and RAS/RAF/MAPK pathways (4–7). Frequent alterations in PCa include gene amplification of MYC transcription factor and androgen receptor (AR), the gene deletion of NKX3.1 homeobox, RB1, and PTEN phosphatase, and the gene reorganization of the ETS family of transcription factors (8–12). Currently, the identification of early tumor markers, including metabolic biomarkers, and molecular targets for effective PCa treatment is a research priority (13–17).

PCa presents a high extent of metabolic modifications, mainly related with increase in aerobic glycolysis and protein and fatty acid synthesis (18, 19). As in other cancer types, this metabolic switch facilitates the synthesis of biomolecules required by the tumor cell to support its rapid growth and division (20). PCa cells display high levels of aerobic glycolysis in the more advanced tumor stages, while primary PCa cells show higher oxidative respiration than non-transformed prostatic cells. This is mainly due to a decrease in Zn accumulation in primary PCa cells, which allows citrate oxidation through the Krebs cycle. High *de novo* fatty acid synthesis is characteristic of PCa progression towards CRPC, which is facilitated by high expression of fatty acid synthase (FASN) and other lipogenic enzymes (21, 22). PCa progression and metastasis has been recently linked to glycolytic enzymes such as pyruvate kinase isoform M2 (PKM2) (23). Together, these observations suggest that specific interference with key metabolic reactions could be useful to improve the current therapies for advanced PCa.

The enzyme pyruvate dehydrogenase (PDH) is essential in the glycolytic and Krebs cycle metabolism, and play important roles in carcinogenesis, making this enzyme a feasible therapeutic target in cancer (24–27). PDH exists as a multi-enzyme complex formed by three catalytic (E1 [two genes: *PDHA1-2*], E2 [*DLAT*], and E3 [*DLD*]) and three regulatory subunits (E3BP [*PDHX*], PDKs [four genes: *PDK1-4*], and PDPs [two genes: *PDP1-2*). The mRNA expression patterns of these genes in prostate tissues and prostate tumors are distinct, as shown in databases GTEx (Genotype-Tissue Expression; https://gtexportal.org) and TCGA (The Cancer Genome Atlas; https://www.proteinatlas.org), but comprehensive comparative studies on the expression at the protein level of these enzymes in PCa are lacking. The association of PDKs expression with poor prognosis and resistance to anti-cancer therapies is widely documented, and PDKs inhibition (which results in PDH activation) constitutes a potential therapeutic possibility in several cancer types, including PCa (28–34). In addition, differing results have been reported on the association of other PDH components, such as PDHA1 and PDP1, with PCa prognosis (35, 36). Together, this makes relevant to investigate comparatively the individual expression and function of the distinct components of the PDH complex in relation with PCa progression and malignancy.

In this study, we have evaluated the expression and subcellular localization of components of the PDH complex in PCa, including PDHA1, PDP1, PDP2, PDK1, PDK2, PDK3 and PDK4. We have found specific correlations between the expression of some of these PDH complex components and AR expression in PCa tumors. Furthermore, a significant correlation of PDK2 PCa tumor immunostaining with patient biochemical recurrence and disease-free survival has been revealed. We discuss the potential of PDH complex components as targets for intervention in PCa.

MATERIAL AND METHODS

Cell Lines

Simian kidney COS-7 cells were cultured in DMEM (Dulbecco's Modified Eagle's Medium) (Lonza, Basel, Switzerland) medium supplemented with 5% FBS (Fetal Bovine Serum) (Sigma Aldrich, St. Louis, MO, USA). Human prostate carcinoma LNCaP cells were cultured in RPMI-1640 (Lonza) medium supplemented with 10% FBS. Human prostate carcinoma DU-145 cells were cultured in EMEM (Eagle's Minimal Essential Medium) (Lonza) medium supplemented with 10% FBS. All media were supplemented with 1% L-Glutamine and 1% penicillin/streptomycin (Lonza). Cells were incubated at 37°C and 5% CO2.

Plasmids, Transfection, and Immunoblot

Human PDK2 (NM_002611.4) and PDK3 (NM_001142386) cDNAs, cloned in pcDNA3.1+/C-DYK mammalian expression plasmids (C-terminal Flag fusion), were purchased from GeneScript (Piscataway, NJ, USA). pRK5 Flag-PTEN was made by PCR incorporation of an N-terminal Flag sequence to human PTEN (NM_000314) from pRK5 PTEN (37). Cells were transiently transfected with empty vector, pRK5 Flag-PTEN, pCDNA3.1 PDK2-Flag, or pCDNA3.1 PDK3-Flag using GenJet reagent (SignaGen, Frederick, MD, USA). Cells were lysed in M-PER extraction reagent (ThermoFisher, Waltham, MA, USA) and processed for immunoblot as described (38). Primary antibody used was mouse anti-Flag (1:500, MAB3118, Sigma Aldrich). Secondary antibody was IRDye 680RD Goat

anti-Mouse (LI-COR, Lincoln, NE, USA). Blots were processed with Odyssey CLx Imaging system (LI-COR).

Metabolism/Seahorse

Oxygen Consumption Rate Assay Kit (Cayman Chemical, Ann Arbor, MI, USA) was used to measure extracellular oxygen consumption levels according to manufacturer's instructions. XF96 Mitochondrial stress test was performed using Seahorse Extracellular Flux Analyzer XF96e (Agilent Technologies, Santa Clara, CA, USA) to measure the oxygen consumption rate (OCR) of cells according to manufacturer's instructions. Seahorse assays were performed in at least triplicate wells in three independent experiments for each condition.

Cell Proliferation and Confluence

Cell proliferation/viability of LNCaP and DU-145 cells was assessed as described (39). $5x10^3$ cells/well were plated in 96-well culture plates. A day after plating the cells, different concentrations of dichloroacetate (DCA; Sigma Aldrich) or vehicle were added. Cell proliferation was measured with the CellTiter 96®AQ_{ueous} One Solution Cell Proliferation Assay Kit (MTS Assay, Promega, Madison, WI, USA) in 96-well plates, and luminescence was measured at 490 nm using Victor3 microplate reader (PerkinElmer, Waltham MA, USA). To assess cell confluence, $5x10^3$ cells/well were seeded on 96-well plates and the cell confluence was measured every three hours by the IncuCyte FLR imaging microscopes (Essen Biosciences, Ann Arbor, MI, USA), as described (40). The cells were treated with the indicated DCA concentrations 21 h post-plating and were scanned for 72 h after adding the drug.

Immunofluorescence

$3x10^4$ COS-7 cells per well were plated in 8-well chamber slides for immunofluorescence (Ibidi, Gräfelfing, Germany). Transient transfection was performed as described above. Cells were washed and mitochondria were stained with Mitotracker™ Red CMXRos following manufacturer's instructions (250 nM, 20 min) (ThermoFisher). before they were fixed in methanol for 5 min at -20°C and blocked in blocking solution (Phosphate Buffered Saline (PBS) containing 3% Bovine Serum Albumin (BSA). Mouse anti-Flag primary antibody (1/100 in blocking solution) was incubated overnight at 4°C in a wet chamber. Subsequently, cells were washed three times with PBS-BSA for 10 min prior to incubation with anti-mouse FITC secondary antibody (1/100) for 1 h in a wet chamber and darkness at room temperature. Cells were washed and mounted in Mounting Medium with DAPI (4'6-diamidino-2-phenylindole) (Abcam) and visualized by standard [NIKON ECLIPSE TE2000 (Nikon, Tokyo, Japan)] or confocal microscopy [ZEISS LSM880 AIRYSCAN (Zeiss, Jena, Germany)].

Clinical Data and Tumor Samples

The PCa cohort has been previously described (41). Briefly, it consisted of 120 PCa patients treated with radical prostatectomy at Cruces University Hospital (Barakaldo, Spain) between 2000 and 2005. An experienced pathologist (JIL) selected tumor areas with well-preserved tissue, representative of the whole tumor, from formalin-fixed and paraffin-embedded (FFPE) tumor tissue blocks, and TMA blocks were made from these areas. 4 µm sections were made from the TMA blocks, one of which was stained with hematoxylin and eosin (H&E) to verify the presence of tumor content. Biochemical recurrence (BR) was defined as a Prostate-Specific Antigen (PSA) measurement equal to or greater than 0.4 ng/ml after surgery. Follow-up has been recorded until October 1, 2016. Cancer of the Prostate Risk Assessment Postsurgical (CAPRA-S) score was calculated according to its definition (42), that is, by combining preoperative PSA, Gleason grade, surgical margins, extracapsular extension, seminal vesicle invasion, and lymph node invasion.

Immunohistochemistry and Scoring

Immunohistochemistry (IHC) was carried out using the following primary antibodies: PDHA1 (Sigma Aldrich, HPA047864, dilution: 1:10), PDP1 (Sigma Aldrich, HPA019081, dilution 1:10), PDP2 (Sigma Aldrich, HPA019950, dilution 1:65), PDK1 (Cell Signaling, Danvers, MA, USA, HPA027376, dilution: 1:120), PDK2 (Sigma Aldrich, HPA008287, dilution 1:25), PDK3 (Sigma Aldrich, HPA046583, dilution 1:50), PDK4 (Sigma Aldrich, HPA056731, dilution 1:100), and AR (SP107 ready to use, Ventana, Roche, Basel, Switzerland) antibodies. Antigen retrieval was performed at pH 6 and pH 9 using PT link system (Agilent Technologies). IHC immunostainings were performed in automated immunostainers (EnVision FLEX, Dako Autostainer Plus; Dako, Glostrup, Denmark and BenchMark Ultra, Ventana Medical Systems, Tucson, AZ, USA). Antibodies were incubated for 30 min, followed by secondary antibody incubation for 15 min using Goat Anti Mouse and Anti-rabbit Ig/HRP secondary antibodies (Dako), FLEX/HPR for 20 min, FLEX DAB/Sub Chromo for 10 min, and finally counterstaining with hematoxylin. Immunostainings were evaluated in tumor cells as negative (weak/no staining) or positive (medium/high staining). The analysis was performed using a Nikon Eclipse 80i microscope (Nikon, Tokyo, Japan).

Statistical Analysis

Error bars in results represent ± standard deviation (S.D.). Cell data was analyzed by GraphPad Prism t Test Calculator (San Diego, CA, USA), where significance was calculated using two-tailed student t-test. p values smaller than 0.05 were considered significant and are indicated with an asterisk (*). All experiments were performed at least twice, and results shown are from one representative experiment. The SPSS version 23 software (SPSS Inc., Chicago, IL, USA) was used for statistical calculations of the clinical material. For all the experiments, any p value below 0.05 was considered statistically significant.

RESULTS

PDH complex components, including the negative regulators of PDH activity, PDKs, have been involved in PCa carcinogenesis (27). We analyzed the role of PDKs in the growth, proliferation,

and mitochondrial respiration of PCa cells, using the PDK inhibitor dichloroacetate (DCA), which selectively shifts the cancer cell metabolism from glycolysis to oxidative phosphorylation (29). As expected, DCA treatment inhibited in a dose-response manner the growth/viability of LNCaP and DU-145 PCa cells, as shown by MTS assay and cell confluence measurements (**Figures 1A–C**). In addition, an increase in maximal oxygen consumption rate (OCR) was observed in LNCaP PCa cells upon PDK inhibition by DCA, in parallel with less proliferative capacity and cell viability (**Figure 1D**). These results suggest a role for PDKs in the regulation of cell growth and viability of PCa cells.

This prompted us to investigate the expression of PDKs and other PHD complex components in PCa patient tumor samples. The expression of PDHA1, PDP1, PDP2, PDK1, PDK2, PDK3, and PDK4, as well as the expression of AR was evaluated by IHC in a retrospective cohort of 120 PCa patients (**Tables 1**–**3**). FFPE samples from representative tumor areas were included in TMAs for analysis, and expression was scored as negative or positive. We observed heterogeneous expression of PDHA1, PDP1, PDP2, PDK1, PDK2, PDK3, and PDK4 in PCa specimens, and examples of different patterns of staining for the different PDKs are shown in **Figure 2**. PDK2 expression in tumors displayed a nuclear/cytoplasmic pattern, whereas PDK1, PDK3, and PDK4 expression was mostly cytoplasmic (**Figure 2**). PDP1 expression positively correlated with stage ($p = 0.037$) and extracapsular extension ($p = 0.027$) (**Table 1**). Importantly, we found a significant positive correlation of PDK2 immunostaining with biochemical recurrence ($p = 0.033$), and negative correlation with disease-free survival ($p = 0.045$), suggesting a negative prognostic role for PDK2 expression in PCa (**Table 2**). Significant positive correlations were found with respect to AR expression for PDHA1 ($p = 0.035$), PDP1 ($p = 0.046$), PDK1 ($p = 0.003$), PDK2 ($p = 0.001$), and PDK4 ($p = 0.031$) expression (**Table 3** and **Figure 3**). PDP2 and PDK3 did not show any significant correlation. Together, these findings show a heterogeneous expression pattern of PDH complex components in PCa related with AR and suggest an association between PDK2 expression and PCa progression.

PDH complex components are found at the mitochondria, but they have also been found in the nucleus, which has been proposed to have clinical implications (36, 43). Next, we investigated by immunoblot and immunofluorescence the expression and subcellular localization of PDK2 and PDK3 (tagged with a Flag epitope at the C-terminus) ectopically expressed in COS-7 (as a suitable cell model for ectopic protein expression) and LNCaP PCa cells (**Figures 4A–D**). The expression of the phosphatase PTEN was monitored as a control. PDK2-Flag and PDK3-Flag proteins displayed a predominant punctate pattern of expression that overlapped with Mitotracker marker staining, indicating a major mitochondrial localization in cells (**Figures 4B–D**). This is in accordance with the mitochondrial subcellular localization reported for PDH components in other human cancer cell lines (43). In contrast, Flag-PTEN displayed cytoplasmic/nuclear localization (**Figure 4B**). Together, these results illustrate differential subcellular localization of PDKs in cells and in PCa tissues. In the case of PDK2, which showed predominant nuclear localization in PCa tissues, further studies are required to

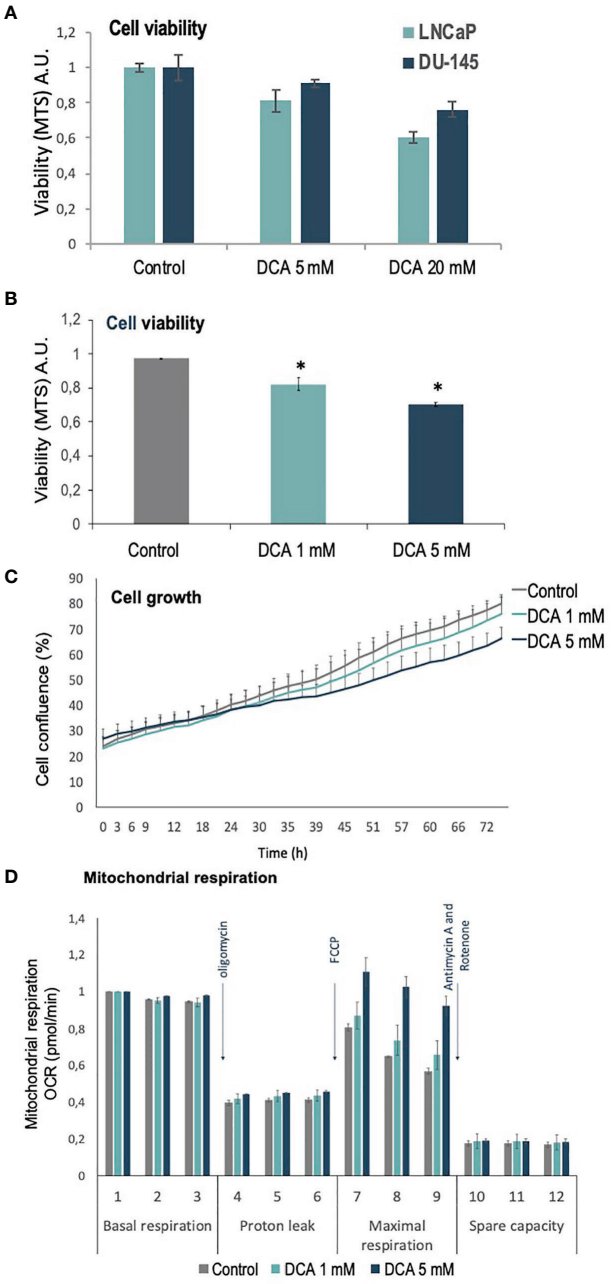

FIGURE 1 | Viability, proliferation and mitochondrial function of PCa cells treated with DCA. **(A)** Cell viability is shown for LNCaP and DU-145 PCa cells, as determined by MTS analysis, after 72 h in the presence of DCA (5 mM and 20 mM). **(B)** Cell viability is shown for LNCaP cells, as determined by MTS analysis, after 72 h in the presence of DCA (1 mM and 5 mM). **(C)** Cell growth is shown for LNCaP cells, as determined by Incucyte live-cell analysis, after 72 h in the presence of DCA (1 mM and 5 mM). **(D)** Mitochondrial respiration is shown for LNCaP cells, as determined by Seahorse extracellular flux analysis, after 48 h in the presence of DCA (1 mM and 5 mM). p value below 0.05 are indicated with *.

TABLE 1 | Correlation between clinical and pathological variables and PDHA1, PDP1 and PDP2 protein expression in prostate cancer.

Patients – no.	N = 120	PDHA1 negative (N = 91)	PDHA1 positive (N = 28)	PDP1 negative (N = 106)	PDP1 positive (N = 13)	PDP2 negative (N = 88)	PDP2 positive (N = 31)
Median follow-up time (IQR) – year	120	ρ = -0.182 / P = 0.720		ρ = -0.124 / P = 0.745		ρ = -0.086 / P = 0.564	
	10.5 (9.8-12.4)	10.9 (1-16)	9.9 (5.9-15)	10.6 (1-16)	9.9 (5.9-15)	10.7 (1-16)	10 (5.9-15)
Median age at surgery (IQR) – year		ρ = 0.057 / P = 0.739		ρ = 0.041 / P = 0.615		ρ = 0.011 / P = 0.970	
	63 (59-68)	63 (48-71)	63.5 (52-73)	63 (48-73)	64 (53-69)	63 (48-73)	63 (50-70)
Age at surgery – no. (%)		ρ = 0.015 / P = 0.872		ρ = -0.027 / P = 0.767		ρ = 0.013 / P = 0.888	
< 65 year	78 (65)	60 (66)	18 (64)	69 (65)	9 (69)	58 (66)	20 (64.5)
> 65 year	42 (35)	31 (34)	10 (36)	37 (35)	4 (31)	30 (34)	11 (35.5)
Preoperative PSA – no. (%)		ρ = -0.100 / P = 0.440		ρ = -0.082 / P = 0.819		ρ = -0.168 / P = 0.311	
≤ 6 ng/ml	36 (30)	25 (27.5)	11 (39.5)	31 (29)	5 (38.5)	23 (26)	13 (42)
> 6 ng/ml and ≤ 10 ng/ml	43 (35)	34 (37.5)	8 (28.5)	37 (35)	5 (38.5)	32 (36.5)	11 (35.5)
> 10 ng/ml and ≤ 20 ng/ml	33 (27.5)	25 (27.5)	8 (28.5)	30 (28)	3 (23)	26 (29.5)	7 (22.5)
> 20 ng/ml	4 (3.3)	4 (4.5)	0 (0)	4 (4)	0 (0)	4 (4.5)	0 (0)
Missing	4 (3.3)	3 (3)	1 (3.5)	4 (4)	0 (0)	3 (3.5)	0 (0)
Gleason grade – no. (%)		ρ = -0.051 / P = 0.389		ρ = -0.004 / P = 0.545		ρ = 0.065 / P = 0.480	
≤ 6	72 (60)	55 (60.5)	16 (57)	64 (60)	7 (54)	55 (62.5)	16 (52)
3+4	22 (18)	14 (15.5)	8 (28.5)	18 (17)	4 (31)	14 (16)	8 (26)
4+3	7 (6)	6 (6.5)	1 (3.5)	7 (7)	0 (0)	6 (7)	1 (3)
≥ 8	19 (16)	16 (17.5)	3 (11)	17 (16)	2 (15)	13 (14.5)	6 (19)
Stage - no. (%)		ρ = 0.107 / P = 0.243		ρ = 0.191 / P = 0.037		ρ = - 0.024 / P = 0.797	
T2	99 (82.5)	77 (84.5)	21 (75)	90 (85)	8 (61.5)	72 (82)	26 (84)
T3	21 (17.5)	14 (15.5)	7 (25)	16 (15)	5 (38.5)	16 (18)	5 (16)
Surgical margins – no. (%)		ρ = -0.069 / P = 0.454		ρ = -0.084 / P = 0.360		ρ = -0.1 08 / P = 0.239	
Negative	78 (65)	58 (64)	20 (71.5)	68 (64)	10 (77)	55 (62.5)	23 (74)
Positive	42 (35)	33 (36)	8 (28.5)	38 (36)	3 (23)	33 (37.5)	8 (26)
Extracapsular extension– no. (%)		ρ = 0.122 / P = 0.185		ρ = 0.203 / P = 0.027		ρ = -0.011 / P = 0.907	
No	100 (83)	78 (86)	21 (75)	91 (86)	8 (61.5)	73 (83)	26 (84)
Yes	20 (17)	13 (14)	7 (25)	15 (14)	5 (38.5)	15 (17)	5 (16)
Seminal vesicle invasion – no. (%)		ρ = -0.017 / P = 0.849		ρ = 0.061 / P = 0.506		ρ = -0.124 / P = 0.175	
No	20 (17)	87 (96)	27 (96.5)	102 (96)	12 (92)	83 (94.5)	31 (100)
Yes	100 (83)	4 (4)	1 (3.5)	4 (4)	1 (8)	5 (5.5)	0 (0)
CAPRA-S risk group – no. (%)*		ρ = -0.111 / P = 0.529		ρ = -0.005 / P = 0.388		ρ = -0.1 45 / P = 0.240	
Low	48 (40)	35 (38.5)	13 (46.5)	44 (41.5)	4 (31)	36 (41)	12 (39)
Intermediate	44 (37)	34 (37)	9 (32)	37 (35)	6 (46)	34 (39)	9 (29)
High	9 (8)	8 (9)	1 (3.5)	9 (8.5)	0 (0)	9 (10)	0 (0)
Missing	19 (15)	14 (25.5)	5 (18)	16 (15)	3 (23)	9 (10)	10 (32)
Biochemical recurrence – no. (%)		ρ = -0.027 / P = 0.769		ρ = -0.084 / P = 0.360		ρ = 0.013 / P = 0.888	
Negative	78 (65)	59 (65)	19 (68)	68 (64)	10 (77)	58 (66)	20 (64.5)
Positve	42 (35)	32 (35)	9 (32)	38 (36)	3 (23)	30 (34)	11 (35.5)
Disease-free survival – no. (%)		ρ = 0.105 / P = 0.299		ρ = 0.074 / P = 0.463		ρ = -0.046 / P = 0.652	
Yes	41 (34)	32 (35)	8 (28)	37 (35)	3 (23)	28 (32)	12 (39)
No	58 (48)	41 (45)	17 (61)	51 (48)	7 (54)	43 (49)	15 (48)
Missing	21 (18)	18 (20)	5 (11)	18 (17)	3 (23)	17 (19)	4 (13)

**The CAPRA-S scores were categorized to give the three risk groups: Low risk if sscore 0-2; Intermediate risk if score 3 to 5; High risk if score 6 to 12.*

Spearsman´s correlation ρ (95% CI) / P value.

IQR, interquartile range; PSA, prostate-specific antigen; AR, androgen receptor.

TABLE 2 | Correlation between clinical and pathological variables and PDK1, PDK2, PDK3 and PDK4 protein expression in prostate cancer.

Patients – no.	N = 120	PDK1 negative (N = 26)	PDK1 positive (N = 89)	PDK2 negative (N = 17)	PDK2 positive (N = 102)	PDK3 negative (N = 13)	PDK3 positive (N = 100)	PDK4 negative (N = 14)	PDK4 positive (N = 96)
Median follow-up time (IQR) – year	120	ρ = -0.180 / P = 0.295		ρ = 0.080 / P = 0.580		ρ = 0.006 / P = 0.592		ρ = -0.315 / P = 0.016	
	10.5 (9.8-12.4)	12 (8.4-14.9)	10.3 (1-16)	10 (2-14)	10.5 (1-16)	10.2 (9.4-13.9)	10.5 (1-16)	13.2 (1-15)	10.3 (2.1-16)
Median age at surgery (IQR) – year		ρ = 0.097 / P = 0.632		ρ = -0.112 / P = 0.603		ρ = 0.035 / P = 0.065		ρ = 0.019 / P = 0.834	
	63 (59-68)	62 (50-73)	63 (48-71)	64 (54-73)	63 (48-71)	61 (52-73)	63 (48-71)	62 (52-71)	63 (48-73)
Age at surgery – no. (%)		ρ = 0.046 / P = 0.625		ρ = -0.108 / P = 0.237		ρ = 0.022 / P = 0.817		ρ = 0.041 / P = 0.668	
< 65 year	78 (65)	18 (69)	57 (64)	9 (53)	69 (68)	9 (69)	66 (66)	10 (71)	63 (66)
> 65 year	42 (35)	8 (31)	32 (36)	8 (47)	33 (32)	4 (31)	34 (34)	4 (29)	33 (34)
Preoperative PSA – no. (%)		ρ = 0047 / P = 0.305		ρ = 0.020 / P = 0.875		ρ = -0.056 / P = 0.715		ρ = 0.109 / P = 0.280	
≤ 6 ng/ml	36 (30)	10 (38.5)	26 (29)	5 (29.5)	31 (30.5)	4 (31)	32 (32)	7 (50)	29 (30)
> 6 ng/ml and ≤ 10 ng/ml	43 (35)	6 (23)	34 (38)	6 (35)	36 (35)	3 (23)	36 (36)	2 (14)	34 (36)
> 10 ng/ml and ≤ 20 ng/ml	33 (27.5)	9 (34.5)	23(26)	5 (29.5)	28 (27.5)	4 (31)	27 (27)	4 (29)	27 (28)
> 20 ng/ml	4 (3.3)	0 (0)	4 (5)	0 (0)	4 (4)	1 (7.5)	3 (3)	0 (0)	4 (4)
Missing	4 (3.3)	1 (4)	2 (2)	1 (6)	3 (3)	1 (7.5)	2 (2)	1 (7)	2 (2)
Gleason grade – no. (%)		ρ = 0.179 / P = 0.056		ρ = 0.092 / P = 0.617		ρ = 0.042 / P = 0.839		ρ = 0.075 / P = 0.199	
≤ 6	72 (60)	19 (73)	51 (57)	12 (70)	59 (58)	8 (62)	61 (61)	8 (57)	60 (62.5)
3+4	22 (18)	4 (15.5)	17 (19)	3 (18)	19 (18)	3 (23)	18 (18)	5 (36)	16 (16.5)
4+3	7 (6)	3 (11.5)	4 (5)	0 (0)	7 (7)	1 (7.5)	5 (5)	1 (7)	5 (5)
≥ 8	19 (16)	0 (0)	17 (19)	2 (12)	17 (17)	1 (7.5)	16 (16)	0 (0)	15 (16)
Stage - no. (%)		ρ = 0.083 / P = 0.371		ρ = 0.000 / P = 1		ρ = 0.095 / P = 0.315		ρ = 0.107 / P = 0.243	
T2	99 (82.5)	23 (88.5)	72 (81)	14 (82)	84 (82)	12 (92)	81 (81)	14 (100)	77 (80)
T3	21 (17.5)	3 (11.5)	17 (19)	3 (18)	18 (18)	1 (8)	19 (19)	0 (0)	19 (20)
Surgical margins – no. (%)		ρ = -0.042 / P = 0.654		ρ = -0.007 / P = 0.937		ρ = 0.022 / P = 0.817		ρ = -0.132 / P = 0.165	
Negative	78 (65)	16 (61.5)	59 (66)	11 (65)	67 (66)	9 (69)	66 (66)	7 (50)	66 (69)
Positive	42 (35)	10 (38.5)	30 (34)	6 (35)	35 (34)	4 (31)	34 (34)	7 (50)	30 (31)
Extracapsular extension– no. (%)		ρ = 0.073 / P = 0.437		ρ = -0.009 / P = 0.921		ρ = 0.088 / P = 0.350		ρ = 0.169 / P = 0.076	
No	100 (83)	23 (88)	73 (82)	14 (82)	85 (83)	12 (92)	82 (82)	14 (100)	78 (81)
Yes	20 (17)	3 (12)	16 (18)	3 (18)	17 (17)	1 (8)	18 (18)	0 (0)	18 (19)
Seminal vesicle invasion – no. (%)		ρ = -0.011 / P = 0.907		ρ = 0.085 / P = 0.351		ρ = -0.081 / P = 0.389		ρ = 0.074 / P = 0.437	
No	20 (17)	25 (96)	86 (96)	17 (100)	97 (95)	12 (92)	97 (97)	14 (100)	92 (96)
Yes	100 (83)	1 (4)	3 (4)	0 (0)	5 (5)	1 (8)	3 (3)	0 (0)	4 (4)
CAPRA-S risk group – no. (%)*		ρ = 0.085 / P = 0.492		ρ = 0.180 / P = 0.197		ρ = 0.032 / P = 0.817		ρ = 0.032 / P = 0.544	
Low	48 (40)	13 (50)	32 (36)	10 (59)	38 (37)	6 (46)	39 (39)	6 (43)	38 (40)
Intermediate	44 (37)	8 (31)	36 (40)	5 (29)	38 (37)	4 (31)	39 (39)	7 (50)	35 (36)
High	9 (8)	2 (7.5)	6 (7)	0 (0)	9 (9)	1 (7.5)	6 (6)	0 (0)	6 (6)
Missing	19 (15)	3 (11.5)	15 (17)	2 (12)	17 (17)	2 (15.5)	16 (16)	1 (7)	17 (18)
Biochemical recurrence – no. (%)		ρ = 0.142 / P = 0.128		ρ = 0.195 / P = 0.033		ρ = 0.028 / P = 0.763		ρ = 0.163 / P = 0.088	
Negative	78 (65)	20 (77)	54 (61)	15 (88)	63 (62)	9 (69)	65 (65)	12 (86)	60 (62.5)
Positve	42 (35)	6 (23)	35 (39)	2 (12)	39 (38)	4 (31)	35 (35)	2 (14)	36 (37.5)
Disease-free survival – no. (%)		ρ = -0.141 / P = 0.168		ρ = -0.202 / P = 0.045		ρ = -0.030 / P = 0.770		ρ = -0.170 / P = 0.106	
Yes	41 (34)	6 (23)	34 (38)	2 (12)	38 (37)	4 (31)	34 (34)	2 (14)	35 (36)
No	58 (48)	15 (58)	42 (47)	11 (65)	47 (46)	7 (53.5)	39 (39)	9 (64)	45 (47)
Missing	21 (18)	5 (19)	13 (15)	4 (23)	17 (17)	2 (15.5)	27 (27)	3 (22)	16 (17)

**The CAPRA-S scores were categorized to give the three risk groups: Low risk if sscore 0-2; Intermediate risk if score 3 to 5; High risk if score 6 to 12.*

Spearsman´s correlation ρ (95% CI) / P value.

IQR, interquartile range; PSA, prostate-specific antigen; AR, androgen receptor.

TABLE 3 | Correlation between PDHA complex components and androgen receptor protein expression in prostate cancer.

Patients - no.	N = 120	AR negative (N = 26)	AR positive (N = 92)
Missing	2		
PDHA1- no. (%)		p = 0.195 / P = 0.035	
Negative	89 (75)	23 (88)	66 (72)
Positive	28 (24)	2 (8)	26 (28)
Missing	1 (1)	1 (4)	0 (0)
PDP1 - no. (%)		p = 0.184 / P = 0.046	
Negative	104 (88)	25 (96)	79 (86)
Positive	13 (11)	0 (0)	13 (14)
Missing	1 (1)	1 (4)	0 (0)
PDP2 - no. (%)		p = 0.124 / P = 0.180	
Negative	86 (73)	21 (80)	65 (70)
Positive	31 (26)	4 (15)	27 (30)
Missing	1 (1)	1 (4)	0 (0)
PDK1 - no. (%)		p = 0.282 / P = 0.003	
Negative	26 (22)	11 (42)	15 (16)
Positive	87 (74)	13 (50)	74 (81)
Missing	5 (4)	2 (8)	3 (3)
PDK2 - no. (%)		p = 0.299 / P = 0.001	
Negative	15 (13)	8 (30)	7 (7)
Positive	102 (86)	17 (65)	85 (93)
Missing	1 (1)	1 (4)	0 (0)
PDK3 - no. (%)		p = -0.046 / P = 0.625	
Negative	13 (11)	2 (8)	11 (12)
Positive	99 (84)	21 (80)	78 (85)
Missing	6 (5)	3 (12)	3 (3)
PDK4 - no. (%)		p = 0.206 / P = 0.031	
Negative	14 (12)	6 (23)	8 (9)
Positive	96 (81)	17 (65)	79 (86)
Missing	8 (7)	3 (12)	5 (5)

Spearsman's correlation p (95% CI) / P value; AR, Androgen receptor.

elucidate how its localization at specific subcellular compartments in PCa tumors may affect PCa progression.

DISCUSSION

PCa cells show a unique metabolic reprogramming process during their progression towards malignancy, in which signaling through AR plays an essential role. Primary PCa tumor cells display unusual high oxidative respiration levels, which switch in CRPC cells to high aerobic glycolysis upon androgen-independent AR signaling (44). PDH enzymatic activity is a major universal driver of the energy metabolism in cells, coordinating the energy flux through the glycolytic and the mitochondrial TCA-oxidative pathways. Accordingly, PDH complex plays an important role in cancer-associated metabolic reprograming (27). Here, we have analyzed by IHC the expression of PDH components in PCa tumor samples. We have found a positive correlation of AR expression with PDHA1, PDP1, PDK1, PDK2, and PDK4 expression, which sustains the involvement of AR signaling in the control of PDH activity in PCa cells. In this regard, PDHA1 and PDK2 have been reported in a meta-analysis study as common androgen-regulated genes (45). In concordance, PDH/PDHA1 protein and its activator phosphatase PDP1 have been found to be overexpressed in PCa, in association with high Gleason score (36, 46), although low PDHA1 protein expression in PCa tumors has also been associated with poor prognosis (35). In our study, we found significant correlation of PDP1 expression, but not PDHA1, with stage and extracapsular extension. Prostate conditional *Pten*-null mice, knocked-out for PDHA1 expression in the prostate, displayed growth inhibition of prostate cells, and pharmacological inhibition of PDH activity in prostate *Pten*-null mice and in human PCa cells caused tumor and cell growth inhibition (36). Similarly, diminished cell growth was observed in PDHA1 knock-out LNCaP PCa cells (35, 47). Overall, these findings suggest a potential therapeutic benefit of PDH inhibition in advanced PCa tumors.

PDKs are physiologic negative regulators of PDH. In a variety of cancer types, PDK1-3 have been proposed to play oncogenic roles, whereas PDK4 has been proposed to play both oncogenic and tumor suppressive functions depending on the tumor type (33). In PCa, PDK1 has been found to be upregulated in correlation with disease progression, and PDK1 knock-down using siRNAs increased PCa cell migration and invasion, without significantly affecting cell proliferation (48). On the other hand, low PDK4 expression has been associated with biochemical recurrence in PCa datasets (49). PDK4 mRNA, followed by PDK2, are the more abundant PDK mRNAs detected in prostate and PCa (**Supplementary Figure 1**), and our IHC analysis revealed expression of all PDK proteins in PCa tumors. Notably, we detected correlation of PDK2 high expression with higher biochemical recurrence and lower disease-free survival, suggesting a pro-oncogenic role for PDK2 in PCa. This is in line with the proposed oncogenicity of PDK2 overexpression in other cancer types (50, 51). The tumor suppressor p53 negatively regulates PDK2 transcription (52), making of interest the analysis of the participation of p53 in the regulation of PDK2 expression in PCa cells. PDK2 showed a marked nuclear localization in PCa tumors, but not in PCa cell lines, which displayed PDK2 mitochondrial localization. Additional experiments are necessary to uncover the functional activities of nuclear PDK2 in PCa tissue.

The inhibition of PDKs by DCA, alone or in combination with other drugs, has been proposed as an alternative therapeutic anti-cancer approach, especially in chemoresistant tumors (34, 53–56). In our study, treatment of LNCaP and DU-145 PCa cells with DCA resulted in diminished cell proliferation, suggesting the feasibility of DCA, or DCA-related drugs, in the treatment of PCa. However, the clinical use of DCA in cancer therapy is limited, mainly due to undesired side effects, including peripheral neurotoxicity (32, 57). Kailavasan et al. reported metabolite ratios alterations in highly metastatic LNCaP-LN3 cells upon DCA treatment, which were not detected in poorly metastatic LNCaP cells (28). It has also been reported the sensitization to radiation of PCa cells by DCA (58), as well as PDK isozyme-specific effects of DCA on PCa cells (34). Interestingly, early studies on PDKs enzymatic activity revealed PDK2 as the PDK more

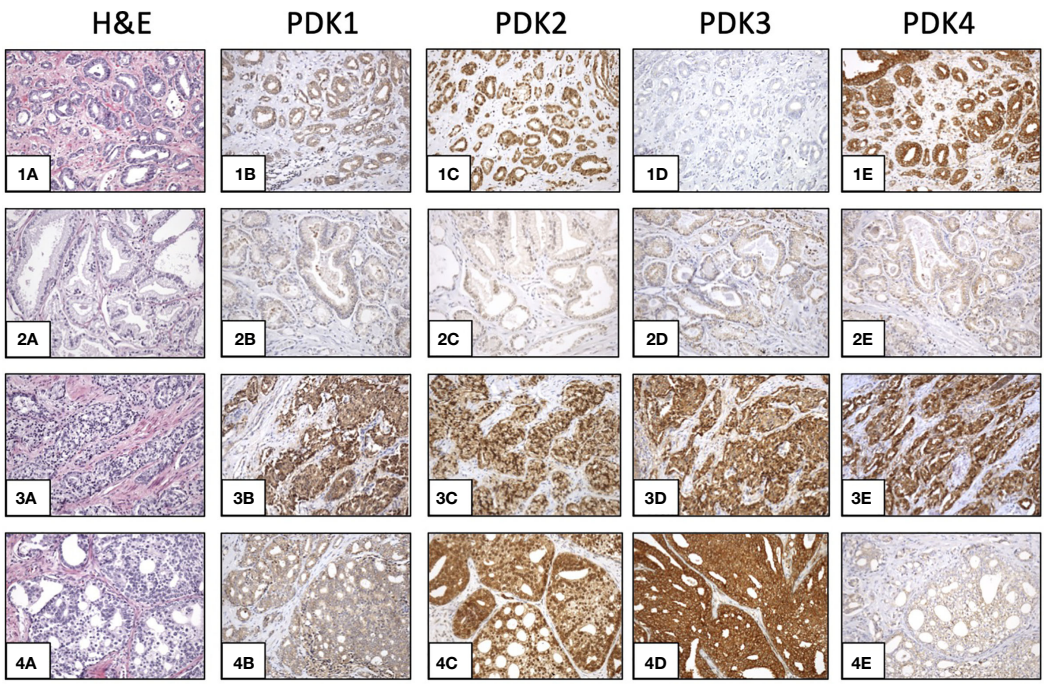

FIGURE 2 | Expression of PDKs in PCa specimens. Immunohistochemical staining of expression of PDKs in four representative prostate carcinoma patient samples (1-4). Hematoxylin and eosin (H&E) staining (1A, 2A, 3A, 4A). High expression of all PDKs (case 3: 3B, 3C, 3D, 3E). Low expression of all PDKs (case 2: 2B, 2C, 2D, 2E). High expression of PDK2 and PDK4 (case 1: 1C, 1E), and low expression of PDK1 and PDK3 (case 1: 1B, 1D). High expression of PDK2 and PDK3 (case 4: 4C, 4D), and low expression of PDK1 and PDK4 (case 4: 4B, 4E). Magnification: X100.

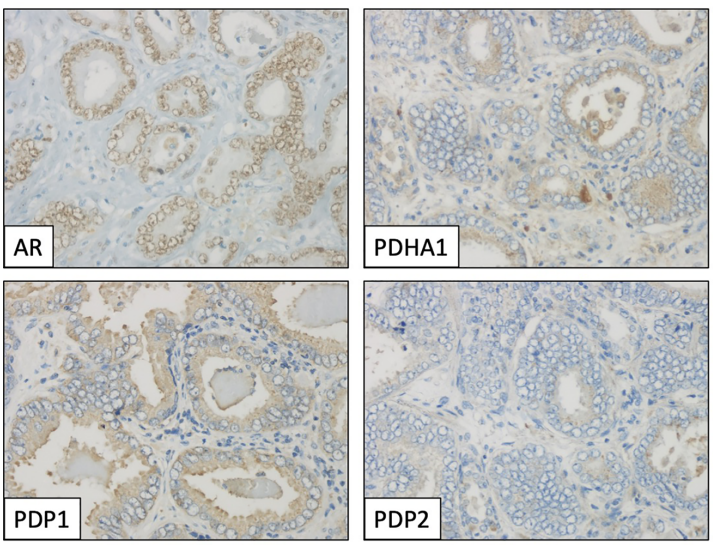

FIGURE 3 | Immunohistochemical profile of a prostate adenocarcinoma specimen, showing positive staining for androgen receptor (AR, nuclear), PDHA1 and PDP1 (cytoplasmic), and negative for PDP2. Magnification: X400.

efficiently inhibited by DCA (59). Whether DCA selectively targets PDK2 in PCa cells needs to be tested. It cannot be ruled out a DCA antiproliferative effect in PCa cells mediated by other PDKs. Dedicated studies are required to ascertain the involvement of inhibition of specific PDKs in the sensitivity to current anti-PCa therapies.

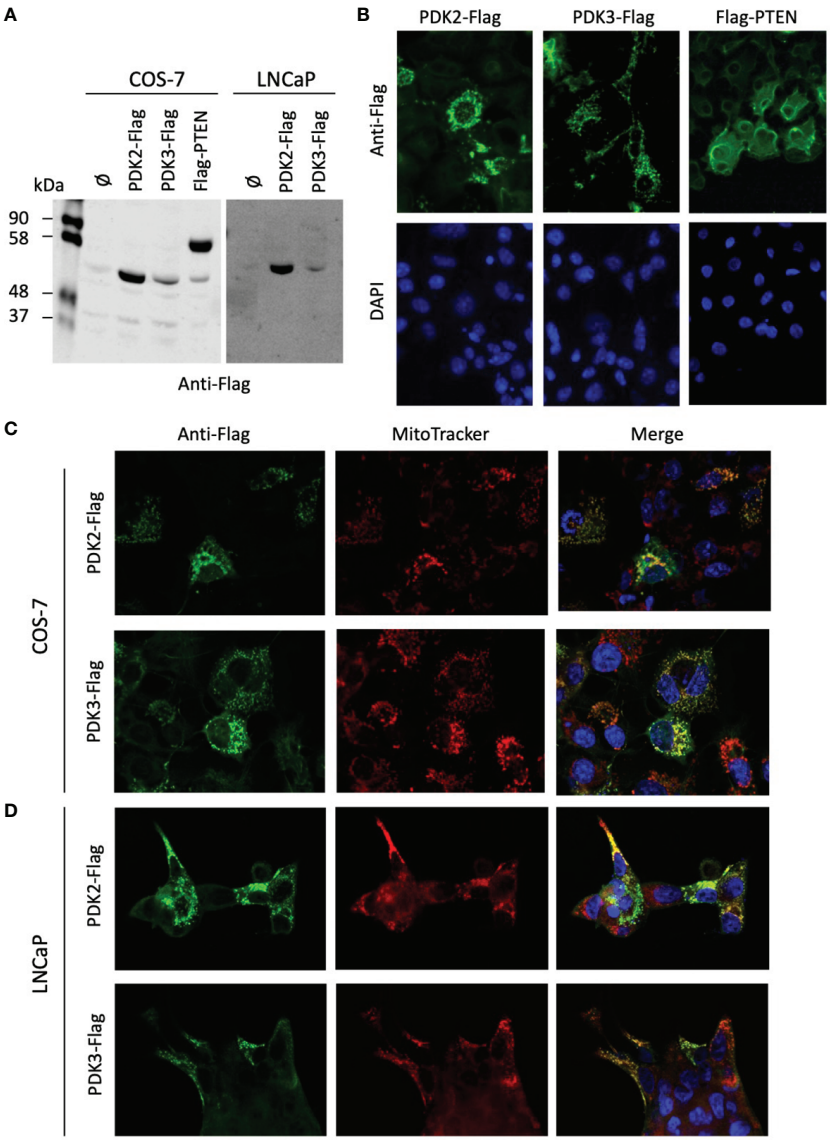

FIGURE 4 | Expression and subcellular localization of PDK2 and PDK3 in PCa cells. **(A)** Immunoblot of ectopically expressed PDK2-Flag, PDK3-Flag, and Flag-PTEN (as a control) in COS-7 and LNCaP cells using anti-Flag antibody. **(B)** Immunofluorescence of PDK2-Flag, PDK3-Flag, and Flag-PTEN in COS-7 cells, using anti-Flag antibody (green). **(C)** Immunofluorescence of PDK2-Flag and PDK3-Flag (green) as in B, with Mitotracker as a mitochondria marker (red). **(D)** Immunofluorescence of PDK2-Flag and PDK3-Flag (green) in LNCaP cells, with Mitotracker as a mitochondria marker (red). In **(B–D)** nuclei were stained with DAPI (blue). Note the punctuated and mitochondrial localization of PDK2 and PDK3, as compared to the cytoplasmic PTEN localization.

DATA AVAILABILITY STATEMENT

The original contributions presented in the study are included in the article/**Supplementary Material**. Further inquiries can be directed to the corresponding author.

ETHICS STATEMENT

The studies involving human participants were reviewed and approved by Comité Ético de Investigación Clínica, Hospital Universitario Cruces, Barakaldo, Spain. The patients/participants provided their written informed consent to participate in this study.

AUTHOR CONTRIBUTIONS

CN-X, JL, and RP contributed to conception and design of the study. CN-X, JM, ME, KF-K, JL, and RP performed experiments, collected and analyzed data. CN-X and KF-K performed the statistical analysis. RL and JL provided tumor samples, data acquisition and clinical details of patients. CN-X and RP wrote

the first draft of the manuscript. CN-X, JM, KF-K, GM, ØF, RL, JL, and RP contributed to manuscript revision, read, and approved the submitted version.

FUNDING

This study was funded by Instituto de Salud Carlos III (ISCIII; Spain and The European Social Fund+ ("Investing in your future"; Grant number CP20/00008), and The Research Council of Norway (Grant number 239813) and Marie Skłodowska-Curie Actions, UNIFORFRIMED Legacy (2020, Norway) to CN-X; and by Ministerio de Economía y Competitividad (Spain and The European Regional Development Fund; Grant number SAF2016-79847-R) to RP and JL. CN-X is the recipient of a Miguel Servet Research Contract from ISCIII; Grant number CP20/00008).

ACKNOWLEDGMENTS

The authors would like to thank Håkon Ramberg and Kristin A. Taskén (Oslo University Hospital) for providing LNCaP cells, and Arantza Perez Dobaran (University of the Basque Country, UPV/EHU, Leioa, Bizkaia, Spain) and Javier Diez García (Microscope Core facility at the Biocruces Bizkaia Health Research Institute) for expert technical support.

SUPPLEMENTARY MATERIAL

The Supplementary Material for this article can be found online at: https://www.frontiersin.org/articles/10.3389/fonc.2022.873516/full#supplementary-material

REFERENCES

1. Knudsen BS, Vasioukhin V. Mechanisms of Prostate Cancer Initiation and Progression. *Adv Cancer Res* (2010) 109:1–50. doi: 10.1016/B978-0-12-380890-5.00001-6
2. Schrecengost R, Knudsen KE. Molecular Pathogenesis and Progression of Prostate Cancer. *Semin Oncol* (2013) 40:244–58. doi: 10.1053/j.seminoncol.2013.04.001
3. Attard G, Parker C, Eeles RA, Schroder F, Tomlins SA, Tannock I, et al. Prostate Cancer. *Lancet* (2016) 387:70–82. doi: 10.1016/S0140-6736(14)61947-4
4. Bluemn EG, Nelson PS. The Androgen/Androgen Receptor Axis in Prostate Cancer. *Curr Opin Oncol* (2012) 24:251–7. doi: 10.1097/CCO.0b013e32835105b3
5. Ramalingam S, Ramamurthy VP, Njar VCO. Dissecting Major Signaling Pathways in Prostate Cancer Development and Progression: Mechanisms and Novel Therapeutic Targets. *J Steroid Biochem Mol Biol* (2017) 166:16–27. doi: 10.1016/j.jsbmb.2016.07.006
6. Nunes-Xavier CE, Mingo J, Lopez JI, Pulido R. The Role of Protein Tyrosine Phosphatases in Prostate Cancer Biology. *Biochim Biophys Acta Mol Cell Res* (2019) 1866:102–13. doi: 10.1016/j.bbamcr.2018.06.016
7. Formaggio N, Rubin MA, Theurillat JP. Loss and Revival of Androgen Receptor Signaling in Advanced Prostate Cancer. *Oncogene* (2021) 40:1205–16. doi: 10.1038/s41388-020-01598-0
8. Baca SC, Garraway LA. The Genomic Landscape of Prostate Cancer. *Front Endocrinol (Lausanne)* (2012) 3:69. doi: 10.3389/fendo.2012.00069
9. Barbieri CE, Bangma CH, Bjartell A, Catto JW, Culig Z, Gronberg H, et al. The Mutational Landscape of Prostate Cancer. *Eur Urol* (2013) 64:567–76. doi: 10.1016/j.eururo.2013.05.029
10. Spans L, Clinckemalie L, Helsen C, Vanderschueren D, Boonen S, Lerut E, et al. The Genomic Landscape of Prostate Cancer. *Int J Mol Sci* (2013) 14:10822–51. doi: 10.3390/ijms140610822
11. Mitchell T, Neal DE. The Genomic Evolution of Human Prostate Cancer. *Br J Cancer* (2015) 113:193–8. doi: 10.1038/bjc.2015.234
12. Spratt DE, Zumsteg ZS, Feng FY, Tomlins SA. Translational and Clinical Implications of the Genetic Landscape of Prostate Cancer. *Nat Rev Clin Oncol* (2016) 13:597–610. doi: 10.1038/nrclinonc.2016.76
13. Crawford ED, Higano CS, Shore ND, Hussain M, Petrylak DP. Treating Patients With Metastatic Castration Resistant Prostate Cancer: A Comprehensive Review of Available Therapies. *J Urol* (2015) 194:1537–47. doi: 10.1016/j.juro.2015.06.106
14. Kelly RS, Vander Heiden MG, Giovannucci E, Mucci LA. Metabolomic Biomarkers of Prostate Cancer: Prediction, Diagnosis, Progression, Prognosis, and Recurrence. *Cancer Epidemiol Biomark Prev* (2016) 25:887–906. doi: 10.1158/1055-9965.EPI-15-1223
15. Baciarello G, Gizzi M, Fizazi K. Advancing Therapies in Metastatic Castration-Resistant Prostate Cancer. *Expert Opin Pharmacother* (2018) 19:1797–804. doi: 10.1080/14656566.2018.1527312
16. Lima AR, Pinto J, Bastos ML, Carvalho M, Guedes De Pinho P. NMR-Based Metabolomics Studies of Human Prostate Cancer Tissue. *Metabolomics* (2018) 14:88. doi: 10.1007/s11306-018-1384-2
17. Meehan J, Gray M, Martinez-Perez C, Kay C, Mclaren D, Turnbull AK. Tissue- and Liquid-Based Biomarkers in Prostate Cancer Precision Medicine. *J Pers Med* (2021) 11:664. doi: 10.3390/jpm11070664
18. Flavin R, Zadra G, Loda M. Metabolic Alterations and Targeted Therapies in Prostate Cancer. *J Pathol* (2011) 223:283–94. doi: 10.1002/path.2809
19. Giunchi F, Fiorentino M, Loda M. The Metabolic Landscape of Prostate Cancer. *Eur Urol Oncol* (2019) 2:28–36. doi: 10.1016/j.euo.2018.06.010
20. Ngo DC, Ververis K, Tortorella SM, Karagiannis TC. Introduction to the Molecular Basis of Cancer Metabolism and the Warburg Effect. *Mol Biol Rep* (2015) 42:819–23. doi: 10.1007/s11033-015-3857-y
21. Ciccarese C, Santoni M, Massari F, Modena A, Piva F, Conti A, et al. Metabolic Alterations in Renal and Prostate Cancer. *Curr Drug Metab* (2016) 17:150–5. doi: 10.2174/1389200216666151015112356
22. Zadra G, Loda M. Metabolic Vulnerabilities of Prostate Cancer: Diagnostic and Therapeutic Opportunities. *Cold Spring Harb Perspect Med* (2018) 8:a030569. doi: 10.1101/cshperspect.a030569
23. Guo W, Zhang Z, Li G, Lai X, Gu R, Xu W, et al. Pyruvate Kinase M2 Promotes Prostate Cancer Metastasis Through Regulating ERK1/2-COX-2 Signaling. *Front Oncol* (2020) 10:544288. doi: 10.3389/fonc.2020.544288
24. Stacpoole PW. Therapeutic Targeting of the Pyruvate Dehydrogenase Complex/Pyruvate Dehydrogenase Kinase (PDC/PDK) Axis in Cancer. *J Natl Cancer Inst* (2017) 109:djx071. doi: 10.1093/jnci/djx071
25. Feng Y, Xiong Y, Qiao T, Li X, Jia L, Han Y. Lactate Dehydrogenase A: A Key Player in Carcinogenesis and Potential Target in Cancer Therapy. *Cancer Med* (2018) 7:6124–36. doi: 10.1002/cam4.1820
26. Sradhanjali S, Reddy MM. Inhibition of Pyruvate Dehydrogenase Kinase as a Therapeutic Strategy Against Cancer. *Curr Top Med Chem* (2018) 18:444–53. doi: 10.2174/1568026618666180523105756
27. Woolbright BL, Rajendran G, Harris RA, Taylor JA3rd. Metabolic Flexibility in Cancer: Targeting the Pyruvate Dehydrogenase Kinase: Pyruvate Dehydrogenase Axis. *Mol Cancer Ther* (2019) 18:1673–81. doi: 10.1158/1535-7163.MCT-19-0079
28. Kailavasan M, Rehman I, Reynolds S, Bucur A, Tozer G, Paley M. NMR-Based Evaluation of the Metabolic Profile and Response to Dichloroacetate of Human Prostate Cancer Cells. *NMR BioMed* (2014) 27:610–6. doi: 10.1002/nbm.3101
29. Kankotia S, Stacpoole PW. Dichloroacetate and Cancer: New Home for an Orphan Drug? *Biochim Biophys Acta* (2014) 1846:617–29. doi: 10.1016/j.bbcan.2014.08.005
30. Harting T, Stubbendorff M, Willenbrock S, Wagner S, Schadzek P, Ngezahayo A, et al. The Effect of Dichloroacetate in Canine Prostate Adenocarcinomas and Transitional Cell Carcinomas *In Vitro*. *Int J Oncol* (2016) 49:2341–50. doi: 10.3892/ijo.2016.3720
31. Kinnaird A, Dromparis P, Saleme B, Gurtu V, Watson K, Paulin R, et al. Metabolic Modulation of Clear-Cell Renal Cell Carcinoma With

Dichloroacetate, an Inhibitor of Pyruvate Dehydrogenase Kinase. *Eur Urol* (2016) 69:734–44. doi: 10.1016/j.eururo.2015.09.014
32. Tataranni T, Piccoli C. Dichloroacetate (DCA) and Cancer: An Overview Towards Clinical Applications. *Oxid Med Cell Longev* (2019) 2019:8201079. doi: 10.1155/2019/8201079
33. Atas E, Oberhuber M, Kenner L. The Implications of PDK1-4 on Tumor Energy Metabolism, Aggressiveness and Therapy Resistance. *Front Oncol* (2020) 10:583217. doi: 10.3389/fonc.2020.583217
34. Skorja Milic N, Dolinar K, Mis K, Matkovic U, Bizjak M, Pavlin M, et al. Suppression of Pyruvate Dehydrogenase Kinase by Dichloroacetate in Cancer and Skeletal Muscle Cells Is Isoform Specific and Partially Independent of HIF-1alpha. *Int J Mol Sci* (2021) 22:8610. doi: 10.3390/ijms22168610
35. Zhong Y, Li X, Ji Y, Li X, Li Y, Yu D, et al. Pyruvate Dehydrogenase Expression is Negatively Associated With Cell Stemness and Worse Clinical Outcome in Prostate Cancers. *Oncotarget* (2017) 8:13344–56. doi: 10.18632/oncotarget.14527
36. Chen J, Guccini I, Di Mitri D, Brina D, Revandkar A, Sarti M, et al. Compartmentalized Activities of the Pyruvate Dehydrogenase Complex Sustain Lipogenesis in Prostate Cancer. *Nat Genet* (2018) 50:219–28. doi: 10.1038/s41588-017-0026-3
37. Torres J, Navarro S, Rogla I, Ripoll F, Lluch A, Garcia-Conde J, et al. Heterogeneous Lack of Expression of the Tumour Suppressor PTEN Protein in Human Neoplastic Tissues. *Eur J Cancer* (2001) 37:114–21. doi: 10.1016/S0959-8049(00)00366-X
38. Mingo J, Luna S, Gaafar A, Nunes-Xavier CE, Torices L, Mosteiro L, et al. Precise Definition of PTEN C-Terminal Epitopes and Its Implications in Clinical Oncology. *NPJ Precis Oncol* (2019) 3:11. doi: 10.1038/s41698-019-0083-4
39. Nunes-Xavier CE, Aurtenetxe O, Zaldumbide L, Lopez-Almaraz R, Erramuzpe A, Cortes JM, et al. Protein Tyrosine Phosphatase PTPN1 Modulates Cell Growth and Associates With Poor Outcome in Human Neuroblastoma. *Diagn Pathol* (2019) 14:134. doi: 10.1186/s13000-019-0919-9
40. Flem-Karlsen K, Tekle C, Oyjord T, Florenes VA, Maelandsmo GM, Fodstad O, et al. P38 MAPK Activation Through B7-H3-Mediated DUSP10 Repression Promotes Chemoresistance. *Sci Rep* (2019) 9:5839. doi: 10.1038/s41598-019-42303-w
41. Nunes-Xavier CE, Kildal W, Kleppe A, Danielsen HE, Waehre H, Llarena R, et al. Immune Checkpoint B7-H3 Protein Expression Is Associated With Poor Outcome and Androgen Receptor Status in Prostate Cancer. *Prostate* (2021) 81:838–48. doi: 10.1002/pros.24180
42. Cooperberg MR, Hilton JF, Carroll PR. The CAPRA-S Score: A Straightforward Tool for Improved Prediction of Outcomes After Radical Prostatectomy. *Cancer* (2011) 117:5039–46. doi: 10.1002/cncr.26169
43. Sutendra G, Kinnaird A, Dromparis P, Paulin R, Stenson TH, Haromy A, et al. A Nuclear Pyruvate Dehydrogenase Complex Is Important for the Generation of Acetyl-CoA and Histone Acetylation. *Cell* (2014) 158:84–97. doi: 10.1016/j.cell.2014.04.046
44. Uo T, Sprenger CC, Plymate SR. Androgen Receptor Signaling and Metabolic and Cellular Plasticity During Progression to Castration Resistant Prostate Cancer. *Front Oncol* (2020) 10:580617. doi: 10.3389/fonc.2020.580617
45. Jin HJ, Kim J, Yu J. Androgen Receptor Genomic Regulation. *Transl Androl Urol* (2013) 2:157–77. doi: 10.3978/j.issn.2223-4683.2013.09.01
46. Lexander H, Palmberg C, Auer G, Hellstrom M, Franzen B, Jornvall H, et al. Proteomic Analysis of Protein Expression in Prostate Cancer. *Anal Quant Cytol Histol* (2005) 27:263–72.
47. Li Y, Li X, Li X, Zhong Y, Ji Y, Yu D, et al. PDHA1 Gene Knockout in Prostate Cancer Cells Results in Metabolic Reprogramming Towards Greater Glutamine Dependence. *Oncotarget* (2016) 7:53837–52. doi: 10.18632/oncotarget.10782
48. Subramaniam S, Jeet V, Gunter JH, Clements JA, Batra J. Allele-Specific MicroRNA-Mediated Regulation of a Glycolysis Gatekeeper PDK1 in Cancer Metabolism. *Cancers (Basel)* (2021) 13:3582. doi: 10.3390/cancers13143582
49. Oberhuber M, Pecoraro M, Rusz M, Oberhuber G, Wieselberg M, Haslinger P, et al. STAT3-Dependent Analysis Reveals PDK4 as Independent Predictor of Recurrence in Prostate Cancer. *Mol Syst Biol* (2020) 16:e9247. doi: 10.15252/msb.20199247
50. Cui L, Cheng Z, Liu Y, Dai Y, Pang Y, Jiao Y, et al. Overexpression of PDK2 and PDK3 Reflects Poor Prognosis in Acute Myeloid Leukemia. *Cancer Gene Ther* (2020) 27:15–21. doi: 10.1038/s41417-018-0071-9
51. Kitamura S, Yamaguchi K, Murakami R, Furutake Y, Higasa K, Abiko K, et al. PDK2 Leads to Cisplatin Resistance Through Suppression of Mitochondrial Function in Ovarian Clear Cell Carcinoma. *Cancer Sci* (2021) 112:4627–40. doi: 10.1111/cas.15125
52. Contractor T, Harris CR. P53 Negatively Regulates Transcription of the Pyruvate Dehydrogenase Kinase Pdk2. *Cancer Res* (2012) 72:560–7. doi: 10.1158/0008-5472.CAN-11-1215
53. Ferriero R, Iannuzzi C, Manco G, Brunetti-Pierri N. Differential Inhibition of PDKs by Phenylbutyrate and Enhancement of Pyruvate Dehydrogenase Complex Activity by Combination With Dichloroacetate. *J Inherit Metab Dis* (2015) 38:895–904. doi: 10.1007/s10545-014-9808-2
54. Roh JL, Park JY, Kim EH, Jang HJ, Kwon M. Activation of Mitochondrial Oxidation by PDK2 Inhibition Reverses Cisplatin Resistance in Head and Neck Cancer. *Cancer Lett* (2016) 371:20–9. doi: 10.1016/j.canlet.2015.11.023
55. Sun H, Zhu A, Zhou X, Wang F. Suppression of Pyruvate Dehydrogenase Kinase-2 Re-Sensitizes Paclitaxel-Resistant Human Lung Cancer Cells to Paclitaxel. *Oncotarget* (2017) 8:52642–50. doi: 10.18632/oncotarget.16991
56. Klose K, Packeiser EM, Muller P, Granados-Soler JL, Schille JT, Goericke-Pesch S, et al. Metformin and Sodium Dichloroacetate Effects on Proliferation, Apoptosis, and Metabolic Activity Tested Alone and in Combination in a Canine Prostate and a Bladder Cancer Cell Line. *PloS One* (2021) 16:e0257403. doi: 10.1371/journal.pone.0257403
57. Stacpoole PW, Martyniuk CJ, James MO, Calcutt NA. Dichloroacetate-Induced Peripheral Neuropathy. *Int Rev Neurobiol* (2019) 145:211–38. doi: 10.1016/bs.irn.2019.05.003
58. Cao W, Yacoub S, Shiverick KT, Namiki K, Sakai Y, Porvasnik S, et al. Dichloroacetate (DCA) Sensitizes Both Wild-Type and Over Expressing Bcl-2 Prostate Cancer Cells *In Vitro* to Radiation. *Prostate* (2008) 68:1223–31. doi: 10.1002/pros.20788
59. Bowker-Kinley MM, Davis WI, Wu P, Harris RA, Popov KM. Evidence for Existence of Tissue-Specific Regulation of the Mammalian Pyruvate Dehydrogenase Complex. *Biochem J* (1998) 329:191–6. doi: 10.1042/bj3290191

Conflict of Interest: The authors declare that the research was conducted in the absence of any commercial or financial relationships that could be construed as a potential conflict of interest.

Publisher's Note: All claims expressed in this article are solely those of the authors and do not necessarily represent those of their affiliated organizations, or those of the publisher, the editors and the reviewers. Any product that may be evaluated in this article, or claim that may be made by its manufacturer, is not guaranteed or endorsed by the publisher.

frontiers | Frontiers in Oncology

REVIEW
published: 07 June 2022
doi: 10.3389/fonc.2022.873296

The Potential Role of Exosomal Proteins in Prostate Cancer

Shangzhi Feng[1,2†], *Kecheng Lou*[1,2†], *Xiaofeng Zou*[2,3,4], *Junrong Zou*[2,3,4*] *and Guoxi Zhang*[2,3,4*]

[1] The First Clinical College, Gannan Medical University, Ganzhou, Jiangxi, China, [2] Department of Urology, The First Affiliated hospital of Gannan Medical University, Ganzhou, China, [3] Institute of Urology, The First Affiliated Hospital of Ganna Medical University, Ganzhou, China, [4] Department of Jiangxi Engineering Technology Research Center of Calculi Prevention, Gannan Medical University, Ganzhou, Jiangxi, China

Prostate cancer is the most prevalent malignant tumor in men across developed countries. Traditional diagnostic and therapeutic methods for this tumor have become increasingly difficult to adapt to today's medical philosophy, thus compromising early detection, diagnosis, and treatment. Prospecting for new diagnostic markers and therapeutic targets has become a hot topic in today's research. Notably, exosomes, small vesicles characterized by a phospholipid bilayer structure released by cells that is capable of delivering different types of cargo that target specific cells to regulate biological properties, have been extensively studied. Exosomes composition, coupled with their interactions with cells make them multifaceted regulators in cancer development. Numerous studies have described the role of prostate cancer-derived exosomal proteins in diagnosis and treatment of prostate cancer. However, so far, there is no relevant literature to systematically summarize its role in tumors, which brings obstacles to the later research of related proteins. In this review, we summarize exosomal proteins derived from prostate cancer from different sources and summarize their roles in tumor development and drug resistance.

Keywords: chemoresistance, exosomal proteins, prostate cancer, tumor markers, cancer treatment

OPEN ACCESS

Edited by:
Alagarsamy Srinivasan, NanoBio Diagnostics, United States

Reviewed by:
Luciana N. S. Andrade, University of São Paulo, Brazil
Nagaraja Sethuraman Balakathiresan, National Institute on Alcohol Abuse and Alcoholism (NIH), United States

***Correspondence:**
Junrong Zou
ydzjr@gmu.edu.cn
Guoxi Zhang
gyfyurology@yeah.net

†These authors have contributed equally to this work and share first authorship

Specialty section:
This article was submitted to Genitourinary Oncology, a section of the journal Frontiers in Oncology

Received: *10 February 2022*
Accepted: *16 May 2022*
Published: *07 June 2022*

Citation:
Feng S, Lou K, Zou X, Zou J and Zhang G (2022) The Potential Role of Exosomal Proteins in Prostate Cancer. Front. Oncol. 12:873296. doi: 10.3389/fonc.2022.873296

INTRODUCTION

Prostate cancer (PCa) is a highly prevalent and the second highest cause of cancer-related mortalities in men. Although PCa incidence is lower in Asia, relative to that in Europe and the United States, there is a continuous increasing trend (1). Currently, clinical treatment of PCa faces numerous challenges, due to its progression to Castration-resistant prostate cancer (CRPC)and a high rate of bone metastasis. Therefore, prospecting for new diagnostic and therapeutic targets is imperative to effective management of the malignancy. Previous studies have shown that novel diagnostic and therapeutic pathways, represented by exosomes, have potential for solving such problems. For example, miR-21 in PCa-derived exosomes (PCaDE) was found to inhibit apoptosis thereby promoting survival of cancer cells (2), whereas miR-423-5p was differentially expressed in PCa bone metastases a phenomenon that provided a basis for diagnosis of potential bone metastases (3). On the other hand, long non-coding RNA (lncRNA)was associated with vascular regeneration, tumor survival and metastasis, as well as tumor microenvironment (TME) establishment (4). Apart from RNA, prostate cancer-derived exosomal proteins (PCaDEPr), such as Exportin1(XPO1) which

is present in all PCa cell lines exosomes, have been studied. Notably, this nuclear protein which is involved in nucleoplasmic exportation of the carry signal protein, not only plays a crucial role in the tumorigenic signaling pathway but also increases with the Gleason score (5, 6). This may be a new avenue for diagnosis and treatment of advanced PCa.

Exosomes are small membranous vesicles with a diameter of 30-150 nm that are formed by cells budding inward to form early endosomes that subsequently evolve into multi-vesicular bodies, which then fuse with the plasma membrane and are eventually released into the extracellular matrix. They participate in intercellular signaling by carrying various biomolecules such as proteins and nucleic acids, and regulate the pathophysiological processes of the organism (7). Exosomal proteins include endosomal proteins, plasma proteins and nuclear proteins. In PCa, these proteins have been shown to have a higher level of glycosylation than cellular ones (1). In addition, exosomes carry both membrane transport and fusion proteins, such as RabGTPases, Annexin, flotillins1(Flot), microvesicle-forming proteins Alix and Tsg101, as well as lipid-associated protein families including CD9, CD81, CD82and CD63 integrin proteins (8–11). Notably, the four transmembrane proteins play an important role in exosome-mediated regulation of cellular homeostasis components (**Figure 1**).

Although several studies have described the role of exosomal proteins in PCa, precise markers for PCa development have not been elucidated. Therefore, identification of the main types of PCaDEPr, coupled with elucidating the precise roles and underlying mechanisms of action for these proteins in cancer are imperative to guiding future developmental studies. Recent studies have demonstrated that exosomes proteins derived from PCa cell lines, plasma, tissues and urine are closely associated with tumor development (**Figure 2**). Therefore, understanding the roles played by these proteins, coupled with elucidating their underlying mechanisms of action in tumors will enable better targeting of these proteins for clinical treatment and improve the quality of survival of PCa patients (**Figure 3**).

PCADEPR FROM DIFFERENT SOURCES

PCaDEPr in the Cell Line

Findings from several exosomal proteomics and subsequent functional validation in PCa cell lines have shown that exosomal proteins secreted by the cell lines play an important role in both tumorigenesis and development (**Table 1**). The exosomal proteins secreted by PCa cell lines are relatively high in tetraspanins such as CD9, CD82, CD61, heat shock protein (HSP) family HSP90, HSP70, and integrin proteins ITGA3, ITGB1, etc., and previous studies have confirmed these Proteins may play a role in the occurrence and development of tumors. Kurozumi et al. found that knocking down ITGA3 and ITGB1 significantly downregulated phosphorylation of FAK, SRC, AKT and ERK1/2 proteins, thereby markedly inhibiting migration and invasion of PCa cells (16). Similarly, Ramteke et al. extracted exosomes from LNCaP and PC3 cells exposed to hypoxic (1% O2) and normoxic (21% O2) media and found that CD63, CD81, HSP90, HSP70, Annexin II were expressed at higher levels in the hypoxic environment and that hypoxia enhanced the invasiveness and motility of LNCaP and PC3 cells as confirmed by cell invasion assays. Further research found that this may be related to the above-mentioned proteins promoting the formation of pre-metastatic niche in cancer cells and inducing stem cell proliferation and epithelial–mesenchymal transition (EMT) transformation (38). Furthermore, an exosomal protein study by Jinlu et al. found that the exosomal protein PKM2 secreted by C4-2B cells can be transported to bone marrow stromal cells (BMSC) *via* exosomes and upregulate CXCL12 production in BMSC in a HIF-1α-dependent manner to promote bone metastasis of PCa (45).

PCaDEPr in Plasma

Studies evaluating the clinical value of exosomal proteins in PCa have confirmed that plasma-derived exosomal proteins play a key role in tumor survival and metastasis, among others (**Table 2**). Notably, PCa patients exhibit significantly higher levels of proteins involved in substance metabolism (P-gp), bioactive enzymes (NEU3, C1r), and cell survival (Survivin, PIF1) in their plasma exosomes, relative to cell lines, and have reportedly been associated with a variety of tumor survival and metastasis. Bergelson et al. found that NEU3 is highly expressed in various cancers such as colon cancer and renal cancer, and significantly inhibits the apoptosis of cancer cells. Another study found that NEU3, as an enzyme that specifically hydrolyzes gangliosides, can reduce the ganglioside-mediated immune activation process (54). This result suggests that NEU3 may act as an immunosuppressant in tumors. Kishi et al. detected the expression of Survivin in the tissues of 82 PCa patients and found that its expression was positively correlated with the pathological stage, Gleason score (ranges from 1-5 and describes how much the cancer from a biopsy looks like healthy tissue (lower score) or abnormal tissue (higher score)) and cell proliferation activity of PCa, and could inhibit cell apoptosis (58). Additional research evidences have shown that plasma exosomal proteins may also have bidirectional effects on tumors. For example, P-gp in exosomes was reportedly elevated in doxorubicin-resistant PCa (18), while another study showed that it enhanced the anti-cancer ability of anti-cancer cytokines, such as $CD4^+$ T cells, in ovarian cancer (84). Conversely P-gp was also found to activate expression of pro-tumor progressive M2 type macrophages (85). Collectively, these findings suggest that plasma exosomeal protein P-gp may be a potential therapeutic target for tumors.

PCaDEPr in Urine

Numerous studies have shown that urinary exosomal proteins from PCa patients play a non-negligible role in tumors (**Table 3**). The urine exosomes are more abundant in substance synthesis (Sepiapterin), signaling (Ras GTPase, Flot-2), tight junction (Claudin-3, δ-catenin) and other proteins compared to the plasma exosomes. Wu et al. compared SMMC-7721 containing epiapterin reductase (SPR) with SMMC-7721(human hepatocarcinoma cells) containing this mutant and concluded that SPR might be a tumor promoter in HCC (hepatocellular

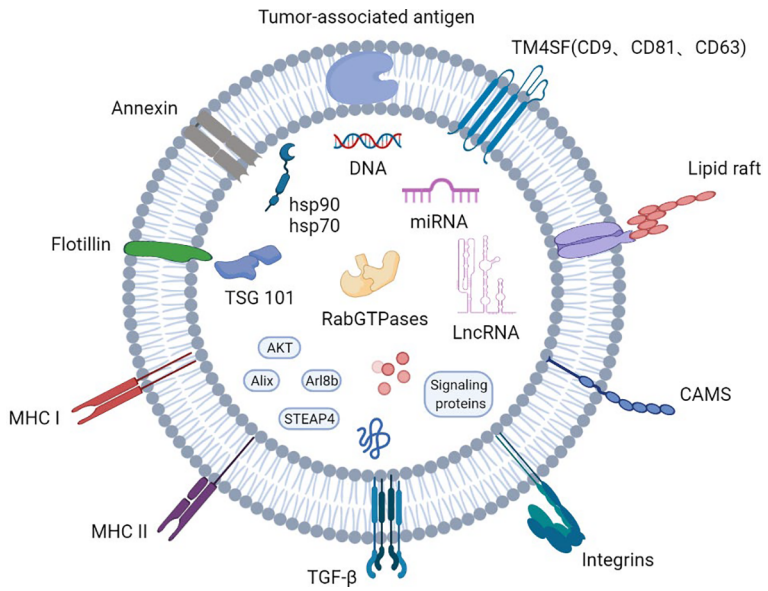

FIGURE 1 | Profile of the basic structure of exosomes.

carcinoma). Results from further cellular experiments, as well as analysis of a nude mouse xenograft model, revealed that SPR depletion inhibited HCC cell proliferation and promoted apoptosis, affirming that SPR may regulate hepatocellular carcinoma progression *via* the FoxO3a/Bim pathway (a transcriptional target in apoptosis regulation *in vivo* and *in vitro*) (99). On the other hand, Hazarika et al. performed immunohistochemical staining of Flot-2 and found significantly higher intensities in metastatic melanoma from lymph nodes or visceral sites relative to those in nevi and primary melanoma and their results indicated that overexpression of Flot-2 promoted tumor cell proliferation and vascular regeneration (124). In addition, Flot-2 reportedly plays a role in promoting tumor metastasis, such as and has been shown to induce metastasis in nasopharyngeal carcinoma by activating the NF-κB and PI3K/Akt3 signaling pathways (125). This factor has also been shown to regulate the cell cycle and induce EMT, thereby promoting growth and metastasis of HCC (126). Lin et al. found that knocking down the expression of Claudin 3 (CLDN3) resulted in significant changes in the phenotype of ovarian cancer cells, and further studies found that this would significantly downregulate the expression level of E-cadherin and upregulate the expression of N-cadherin. Therefore, CLDN3 may be involved in regulation of the EMT to promote metastasis in ovarian cancer (47). Exploration of the value of urinary exosomal proteins during early diagnosis of PCa is of great importance for subsequent clinical use, owing to the ease of obtaining urine samples. Results from differential protein analysis between healthy men and PCa patients revealed that 246 proteins were differentially expressed, 221 of which were significantly upregulated in exosomes of PCa patients (86). Taken together, these findings suggest that exosomal proteins may have potential as diagnostic and therapeutic markers in PCa.

PCaDEPr in Tissues

Apart from plasma and urine exosomal proteins from PCa patients, exosomal proteins from PCa tissues have also been extensively studied (**Table 4**). For example, results from mass spectrometry analysis revealed that PCa tissue exosomal protein types are mainly involved in vesicle transport and composition (Annexin A5, Annexin A3), biotransformation enzymes (such as Glutathione synthetase, and D-3-phosphoglycerate dehydrogenase), cytoskeletal molecules (Syntenin-1) and other related proteins. Moreover, previous studies have confirmed that these proteins play a role in tumor initiation and progression. Tang et al. demonstrated that Annexin A5 could activate the PI3K/Akt/mTOR signaling pathway to regulate the EMT process and matrix metalloproteinase (MMP) expression thereby significantly promoting proliferation, migration and invasion of renal cancer cells both *in vitro* and *in vivo* (145). Kennedy et al. reported that Glutathione plays a role as an intracellular antioxidant in cancer, a where it regulates reactive oxygen species (ROS)-mediated signaling pathways, including NF-kB and MAPK/ERK, to maintain tumor survival and induce tumorigenesis (128). ROS, which are closely related to Glutathione, were found to regulate Cav-1 expression in human lung cancer H460 cells, thereby modulating their migration and invasion. However, different ROS exert different effects in tumors. Superoxide anion and hydrogen peroxide were found to significantly downregulate Cav-1 expression and inhibit both cell migration and invasion, while hydroxyl radicals reportedly upregulated Cav-1 expression and also promoted cell migration and invasion (163). With regards to chemoresistance, Iwamoto et al. reported that Syntenin-1 was upregulated in rectal cancer (CRC) tumor tissues, while its downregulation mediated a significant downregulation of prostaglandin E2 receptor (PTGER2). On the

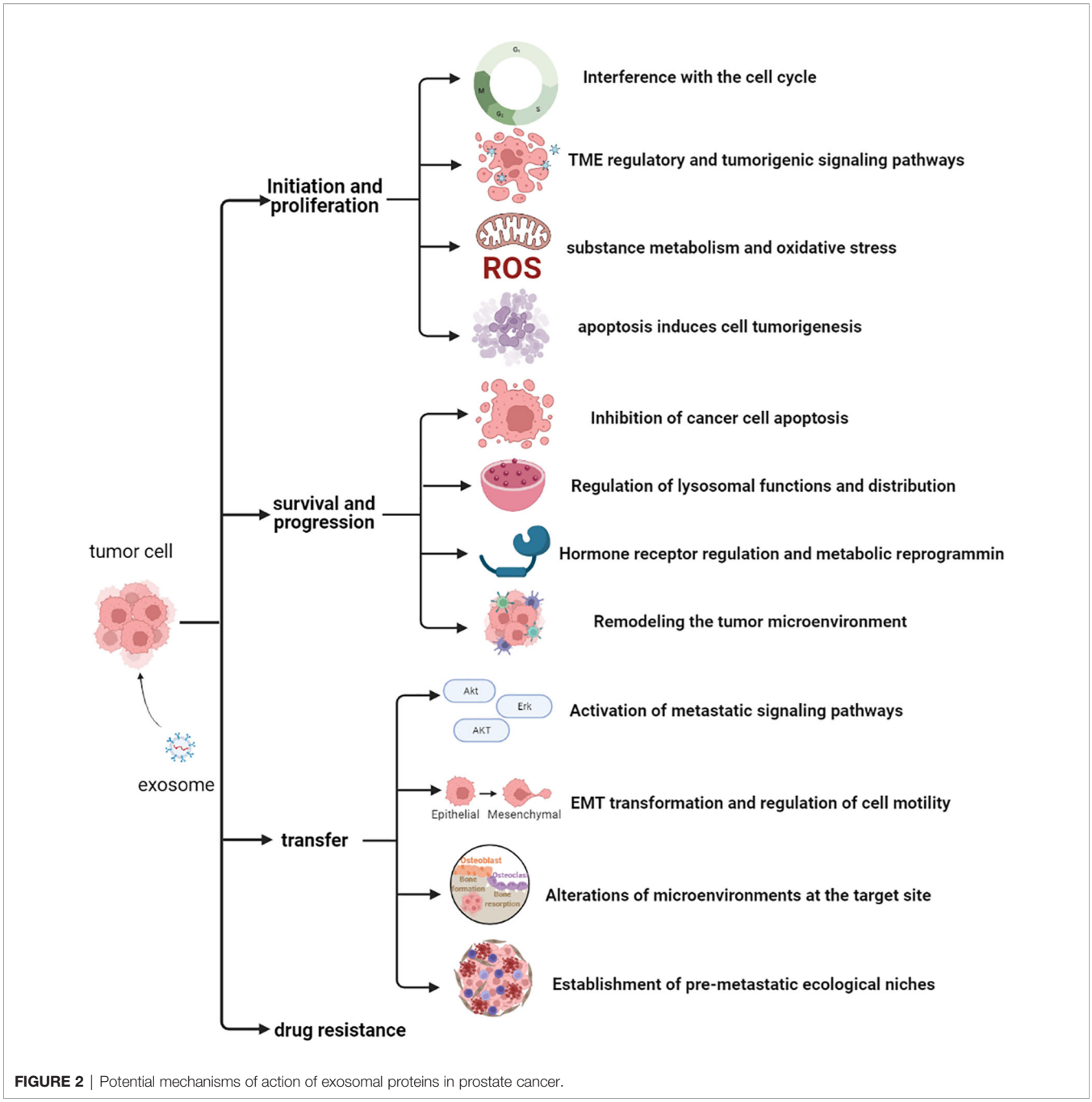

FIGURE 2 | Potential mechanisms of action of exosomal proteins in prostate cancer.

other hand, silencing PTGER2 decreased chemoresistance of cancer stem cells to oxaliplatin. Taken together, these results indicated that Syntenin-1 may promote chemoresistance in cancer cells (147).

PCADEPR IN TUMOR CELL INITIATION AND PROLIFERATION

The basic understanding of tumorigenesis is uncontrolled cell proliferation or uncontrolled apoptosis. In addition to changes in tumor cells, changes also occur in the tumor microenvironment, including variations in structure and function of stromal cells such as fibroblasts, lymphocytes, epithelial cells, and matrix molecules, like growth factors and cytokines. Previous studies have shown that PCaDEPr can induce tumor cell initiation and proliferation processes by regulating metabolic, apoptotic, and TME pathways.

Inhibition of Apoptosis Induces Cell Tumorigenesis

Apoptosis is an orderly and coordinated process of cell death that occurs under physiological and pathological conditions. In

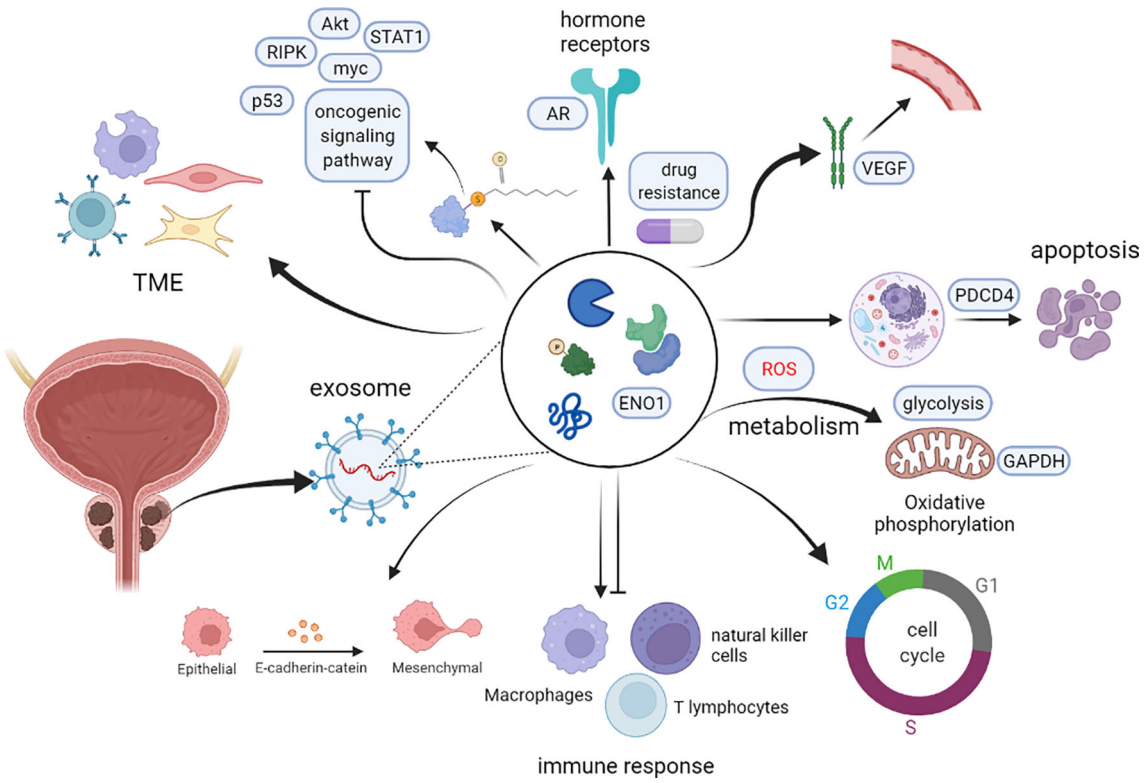

FIGURE 3 | The potential role of PCaDEPrs in cancer. Exosomes originating from the tumor cell play a crucial role in tumor development. During tumor initiation, they mediate apoptosis, lipid metabolism, TME, and tumorigenic signaling, and also interfere with the cell cycle to induce cancer development. During tumor survival and progression, they regulate remodeling the tumor microenvironment, hormonal regulation and metabolic alterations, as well as lysosomal function and distribution, and inhibition of cancer cell apoptosis. During tumor metastasis, PCaDEPrs can contribute to EMT transformation, trigger microenvironment alteration, and establishment of a pre-metastatic ecological niche. Finally, they can also regulate tumor resistance to chemotherapeutic agents.

cancer, dying cells do not receive apoptotic signals, due to an imbalance between cell division and cell death, a phenomenon that causes normal cells to tumorize. Apoptosis can induce development of cancer cells through intrinsic and extrinsic pathways, which involve action of many proteins that regulate apoptosis and these proteins are also present in prostate cancer-derived exosomes. For example, Sepiapterin reductase (SPR), an important regulator of tetrahydrobiopterin (BH4) biosynthesis, has been shown to be a promoter of various tumors. Zhang et al. found that ROS-mediated apoptosis could be induced by knocking down SPR expression to inhibit progression of breast cancer cells (100). Similarly, Basu et al. found a strong association between S100 Calcium Binding Protein P (S100P) expression and prostate tumorigenesis, with S100P expression mediating basal apoptosis and impeding camptothecin-induced apoptosis. Moreover, silencing of S100P significantly inhibited growth of 22Rv1 cells, while overexpressing S100P in PC3 cells resulted in increased proliferation of tumor cells (164). In addition, other exosomal proteins interact with apoptosis-related proteins to induce tumorigenesis. Ingo et al. found that ornithine decarboxylase (ODC) and Sepiapterin reductase (SPR) proteins interacted to elevate ODC activity, thereby inhibiting apoptosis and inducing neuroblastoma cell genesis (165). Exosomal protein phosphatase and tensin homolog (PTEN) was shown to negatively regulate expression of the cyclin-dependent kinase (CDK) inhibitor p27 (KIP1), thereby inhibiting apoptosis (166). Previous studies have shown that S100 calcium-binding protein A6 (S100A6) interacts with p53 to affect oligomerization and activity of p53, thereby reducing its ability to promote apoptosis (167, 168). Moreover, tumor cells can also induce cancer by secreting exosomes to eliminate proteins that initiate apoptosis. Diederick et al. showed that cancer cells can remove PDCD6IP, a protein involved in programmed cell death, by exosome secretion to inhibit apoptosis, explained by high PDCD6IP abundance in PCa-derived exosomes and low abundance in autologous tumor cells this possibility (6). Collectively, these studies indicate that exosomal proteins can induce tumorigenesis and proliferation by inhibiting the apoptotic process both directly and indirectly.

Involvement in Substance Metabolism and Oxidative Stress

Alteration of pathways regulating cellular substance metabolism is more common in cancer, compared to normal tissue cells. In fact, alterations in normal cellular substance metabolism have been implicated in convergence of cells to a tumor state. Previous

TABLE 1 | Exosomal protein derived from prostate cancer cell line.

protein	Prostate cancer source	Role in tumors	references
PDCD6IP, FASN, XPO1, ENO1	PNT2C2, RWPE-1, PC346C, and VCaP	Inhibition of apoptosis Involved in lipid metabolism and oncogenic signaling pathways	(6, 12–15)
ITGA3, ITGB1	LNCaP and PC3	Activate oncogenic signaling pathway.	(2, 16, 17)
p-glycoprotein	docetaxel-resistant PC3、PC3	Chemotherapy resistance	(2, 18)
Ets-1	PC3 and DU145	Enhance osteoblast differentiation	(2, 19)
Integrin beta4, vinculin	taxane-resistant PC3	Interacts with proteins to promote tumor metastasis	(20, 21)
ANXA2, CLSTN1, FLNC, FOLH1, GDF15	PC3, DU145, VCaP, LNCaP, C4-2, and RWPE-1	Involved in fat metabolism, cell proliferation, migration and drug resistance, remodeling of cytoskeleton, Angiogenesis, oncogenic signaling pathways	(22–26)
CD9, CD82	LNCaP and PC3	Inhibit the movement of tumor cells, chemoresistance	(27, 28)
CML28	DU145, LNCaP	Activate immunity	(28, 29)
Integrin alphavbeta6	PC3, DU145, C4-2B, RWPE-1	Activating MMP2 promotes the autonomous osteolysis process of cells	(30)
Trop-2	PC3	Activate the metastasis signaling pathway FAK	(31)
CD61, CD81, HSP90, HSP70, Annexin II	PC3, LNCaP	cellular activation、cell motility、tumor cell metastasis、Metabolic reprogramming, mediating immune microenvironment, tumor resistance	(32–38)
TGF-beta	PC stem cells	Proliferation, apoptosis, differentiation, epithelial -mesenchymal transition (EMT) and migration	(38, 39)
Rab1a, Rab1b, Rab11a	C4-2B	Tumor reprogramming of patient-derived adipose stem cells promotes tumor proliferation	(40)
CD276	DU145, 22Rv1, and LNCaP	Acts as a T cell inhibitor to promote tumor proliferation and invasion	(41)
δ-catenin	PC3	Interacts with E-cadherin to inhibit tumor migration	(42, 43)
LDHA	VCaP, LNCaP, C4-2B	Cell metabolism	(22, 44)
CLU, FN1, KRT8, LAMA5, NPM1, PRDX1, TFRC	DU145, PC3 cells	Regulate cell death and intercellular signaling	(22)
PKM2	LNCaP, DU145, and PC3	Promote the expression of CXCL12 in stromal cells	(45)
Claudin 3	DU145	Increase cell motility and survival by activating MMP -2/Suppression of EMT	(46, 47)
MDR-1、MDR-3、Endophilin-A2 、PABP4、PACSIN2	U145 Tax-Res	Chemotherapy resistance	(48)
Caveolin-1	PC3	suppresses tumor formation through the inhibition of the unfolded protein response	(49)
CD147 、CD44	U145 Tax-Res	Activation of PI3K and MAPK pathways mediate tumor me -tastasis and chemotherapy resistance	(50, 51)
ACTN4	DU145	Promote the movement and proliferation of tumor cells	(52, 53)

studies have shown that alterations in tumor metabolism include glycolysis, lipid hydrolysis, increased nutrient utilization, and increased production of biosynthetic intermediates required for cell growth and proliferation. Liu et al. found that Fatty acid synthase (FASN) protein was upregulated in exosomes derived from Vertebral-Cancer of the Prostate (VCaP) cells. Additional studies have demonstrated that FASN catalyzes formation of long-chain fatty acids from acetyl coenzyme A, malonyl coenzyme A and NADPH, to promote proliferation of VCaP cells, and that inhibition of FASN effectively and selectively kills cancer cells (166). Qin et al. demonstrated that ADP-ribosylation factor-like 8b (Arl8b) Arl8b depletion reduced the ability of PCa cells to establish subcutaneous xenografts in mice. Under a low nutrient environment, Arl8b maintained efficient metabolism in PCa cells thereby allowing them maintain their excessive proliferative capacity by promoting lipid hydrolysis. Metabolic defects in the proliferation of cells with low Arl8b expression inhibit tumor growth initiation *in vivo*. The phenomenon may be attributed to the fact that Arl8b depletion impairs intracellular neutral lipid hydrolysis, thereby shifting the metabolic profile to an abnormal lipogenic phenotype, which subsequently impairs glucose utilization and limits the propensity for cytokinesis (169). In addition, Webber et al. demonstrated that the exosomal protein TGFβ1 secreted by cancer-associated fibroblasts enhanced proliferation of PCa cells under both hypoxic and low nutrient environments by inhibiting mitochondrial oxidative phosphorylation and elevating anaerobic glycolysis (170).

Oxidative stress, a series of adaptive responses caused by an imbalance between ROS and the body's antioxidant system, plays a key role in cancer development and progression. Previous studies have shown that by interfering with the normal redox state of cells, oxidative stress causes generation of peroxides and free radicals that subsequently damage cellular proteins, lipids and DNA, thereby causing tumor development. For example, ROS can either initiate or stimulate tumorigenesis and support the transformation and proliferation of cancer cells. Over-proliferation of tumor cells is often accompanied by high ROS production, and thrives under such oxidative load conditions. At the same time, tumor cells can optimize the ROS-driven cell proliferation process by increasing their antioxidant capacity, to avoid the ROS threshold that triggers senescence, apoptosis and iron-induced cell death (171). Previous studies have shown that some proteins in exosomes can influence ROS expression during oxidative stress in cells, thereby affecting the tumor initiation process. For example, Qin et al. reported that ectopic expression of six transmembrane epithelial antigen of prostate 4 (STEAP4) in PCa cells significantly increased tumor cell proliferation and colony formation, suggesting that STEAP4 may be playing a role in tumor growth. This phenomenon may be explained by the fact

TABLE 2 | Exosomal proteins in the blood of prostate cancer patients.

protein	Role in tumors	references
NEU3	Immunosuppressive	(2, 54, 55)
p-glycoprotein	Chemotherapy resistance	(18)
CYP17A1、CYP17	Activate AR	(56)
HSP72	Activate immunity	(57)
Survivin	Inhibit apoptosis	(58, 59)
CML28	Promote cell proliferation	(28, 29)
αvβ3 integrin	Participate in cell migration	(60)
Claudin 3	Tumor metastasis	(61)
DNA Helicase Homolog PIF1	suppresses Apoptosis	(62)
Four and a Half LIM Domain 3	Protein interaction	(63)
Glutathione S Transferase Omega 2	Participate in cell metabolism	(64)
Maternal Embryonic Leucine Zipper Kinase	Chemotherapy resistance	(65)
Iroquois Homeobox Protein 5	Promote cell proliferation	(66)
Leucine Rich Zipper Containing 4	Enhance cell migration	(67)
Minichromosome Maintenance complex Component 5	Enhance cell migration	(68)
Mitochondrial Tumor Suppressor 1 Isoform 4	Increase cell proliferation and invasion	(69)
Nasopharyngeal epithelium Specific Protein	Interfering oncogenes	(70)
Ubiquitin-like with PHD and ring finger domains	Interfering oncogenes	(71)
Trinucleotide repeat containing 6B Isoform 3	Promote cell proliferation	(72)
Apolipoprotein E (isoform E2)	Protein interaction	(73, 74)
C3a anaphylatoxin des Arginine	Inhibit T cell toxicity	(74, 75)
Complement C1q subcomponent	Promote angiogenesis、Promote immune suppression	(74, 76)
Complement C1r subcomponent	Inhibit apoptosis、Promote angiogenesis	(74, 77)
D-dimer	Promote angiogenesis	(74, 78)
Fibrinogen	Changes in the tumor microenvironment	(74, 79)
Fibrinogen gamma chain	Interaction with FGF-2 promotes cancer growth	(74, 79)
Fibronectin	Interacts with proteins to promote tumor progression or inhibit tumor survival	(74, 80)
Properdin	Activate the complement system to inhibit tumor survival	(74, 81)
von Willebrand factor	mediate multiple cell–cell interactions	(74, 82)
PTEN	Tumor suppression	(83)
ACTN4	Promote the movement and proliferation of tumor cells	(52, 53)

that high STEAP4 expression not only downregulates IRS-1, PI3K and AKT phosphorylation but also impairs insulin-mediated GLUT4 translocation, thereby resulting in ROS-associated mitochondrial dysfunction (169). In another study, silencing of STEAP4 significantly inhibited growth of mouse PCa xenografts in a mouse model. Furthermore, STEAP4 expression was found to mediate elevation of ROS levels probably by increasing levels of ferrous iron in cells after using it as a redox intermediate (electron donor) to generate free radicals. In addition, STEAP4 expression reportedly depleted production of NADPH (172), an inhibitor of ROS production, thereby resulting elevated ROS production. Notably, persistently high ROS levels were found to promote cancer development, owing to is oncogenic nature (113).

Activation of TME Regulatory and Tumorigenic Signaling Pathways

The tumor microenvironment refers to the surrounding microenvironment where tumor cells exist, including surrounding blood vessels, immune cells, fibroblasts, bone marrow-derived inflammatory cells, adipose stem cells and various signaling molecules and the extracellular matrix (ECM). During early stages of cancer development, tumor cells appropriately regulate the microenvironment. For example, various microenvironmental changes, such as adjustment of the ECM, immune response, stromal stem cell transformation and induction of angiogenesis, can be triggered during tumor initiation (173). Recent studies have shown that PCaDEPr may promote production of tumor cells through this pathway. Zakaria et al. found that the PCa cell microenvironment disrupts adipose-derived stem cells in PCa patients to induce tumor transformation, but unlike normal stem cells, the use of PCa cell-conditioned medium effectively triggers conversion of adipose-derived stem cells into prostate-like tumor lesions *in vivo*. Furthermore, exosomal proteins, namely Rab1a, Rab1b, and Rab11a, in PCa were found to recapitulate the formation of prostate tumorigenic mimics generated by adipose-derived stem cells triggered by PCa cell conditioned medium. In fact, the use of PCa cell-derived conditioned medium (CM) or exosomes was found to effectively trigger adipose stem cells to undergo genetic instability, mesenchymal-to-epithelial transformation (MET), and oncogenic transformation, thereby inducing PCa *in vivo*. This may be explained by the fact that exosomes deliver oncogenic factors, such as Rab proteins (Rab1a, Rab1b, and Rab11a) translocated to pASCs to inhibit large tumor suppressor kinase 2 (LATS2) and programmed downregulation of cell death protein 4 (PDCD4), thereby promoting tumor growth (40). In the tumor vascular microenvironment, Dominique et al. showed that HSP27 interacted with CD283, thereby inducing NF-κB activation, which subsequently led to vascular endothelial growth factor (VEGF)-mediated angiogenesis in the tumor microenvironment (174).

In addition, PCaDEPrs have also been shown to induce tumorigenesis by modulating alterations in tumorigenic signaling pathways. For example, flotillins that are also present in tumor-

TABLE 3 | Exosomal protein in urine of prostate cancer patients.

protein (86)	Role in tumors	references
PPP2CA	Reverse EMT transformation to inhibit prostate tumor growth and metastasis	(87)
Rab-35	Induced EMT、intracellular signaling、apico-basal polarity、cytokinesis and cell migration Promote the differentiation and proliferation of tumor cells	(88)
S100-A6	S100A6 interacts with annexin 2 promotes cancer cell motility	(89)
P2X purinoceptor 4	Induction of immunosuppression and angiogenesis, Activate anti-tumor response	(90)
Galectin-3	These include inhibition of apoptosis, promotion of cell growth, and regulation of TCR signal transduction, promotes angiogenesis	(91–94)
flotillin-2	Molecules involved in signal transduction, adhesion, and extracellular matrix remodeling	(95)
Calmodulin	The interaction of CaM and AR promotes the proliferation of LNCaP cells	(96)
3-hydroxybutyrate dehydrogenase type 2	Induce apoptosis	(97)
Thioredoxin domain-containing protein 17	Induces autophagy to promote chemotherapy resistance	(98)
Sepiapterin reductase	Regulate FoxO3a、Bim signal to promote tumor progression、Induce ROS-mediated apoptosis and inhibit tumor cell proliferation	(99, 100)
Melanophilin	Accelerate EMT to promote tumor metastasis	(101)
MFSD12	Promote G1 phase	(102)
LIMP-2(Lysosome membrane protein 2)	Transport lysosome	(103)
Glucosamine-6-phosphate isomerase 1	Promote metabolism and inhibit apoptosis	(104)
GDP-mannose 4.6 dehydratase	Regulate TRAIL-induced apoptosis and increase NK cell-mediated tumor surveillance	(105)
Claudin-3	Increase cell motility and survival by activating MMP-2/Suppression of EMT	(46, 47)
Claudin-2	Epithelial-mesenchymal transition (EMT), tumor initiation, and chemotherapy resistance	(61)
Claudin-10	Transforming growth factor-β (TGF-β)- or WNT/β-catenin-induced EMT affects the progress of OC	(106)
Tetraspanin-6	Regulate EGFR-dependent signaling	(107)
Proton myo-inositol cotransporter	Regulate Hif-1α to promote tumor cell hypoxia	(108)
ADP-ribosylation factor-like protein 8B	Lysosomal transport	(109)
Synaptotagmin-like protein 4	Chemotherapy resistance	(110)
Protein S100-P	Chemotherapy resistance	(86, 111)
Protein DJ-1	Inhibit PTEN tumor suppressor	(112)
Metalloreductase STEAP4	Involved in the metabolism of cell iron and copper	(113)
ATP6V0C	Enhance the function of V-ATPase to promote the migration and invasion of cancer cells	(114)
Ras-related protein Rab-7a	Prevent HGF-induced lysosomal trafficking, cathepsin B secretion and cell invasion	(115)
Ras-related protein Rab-3D	Induces cytoskeleton remodeling, enhances cancer cell movement, induces EMT, regulates Hsp90α secretion and promotes tumor cell invasion	(116)
Ras-related protein Rab-3B	Inhibit apoptosis and maintain cancer cell survival	(117)
Ras-related protein Rab-2A	Activate Erk signal to promote breast cancer stem cells and tumorigenesis	(118)
Plastin-2	Regulate integrin-mediated tumor cell adhesion	(119)
Ragulator complex protein LAMTOR1	Affect lysosomal localization	(120)
ADIRF	Induce PPARG expression to promote adipocyte differentiation	(121)
PSA, PSMA	Related to angiogenesis	(2, 122)
δ-catenin	Interacts with E-cadherin to inhibit tumor migration	(42, 43)
ITGA3, ITGB1	Activate oncogenic signaling pathway	(16)
Transmembrane Protein 256	Induce tumor formation	(123)

derived exosomes. Jang et al. showed that palmitoylation of Flot-1 could regulate proliferation of PCa cells by activating the IGF-1R signaling pathway. Moreover, palmitoylation (S-palmitoylation) modification of Flot-1 was found to regulate intracellular signaling proteins p53, STAT1 (signal transducer and activator of transcription 1) and IκBα (nuclear factor of kappa light polypeptide gene enhancer in B-cells inhibitor, alpha), thereby inducing oncogenic effects (175). Furthermore, Takahashi-Niki et al. found that Parkinson disease protein 7 (DJ-1) binds to Topors/p53BP3 (176), both *in vitro* and *in vivo*, thereby releasing the monoglycosylated form of p53 and helping to restore the transcriptional activity of p53. Recent research evidence showed that DJ-1 directly binds to Sirtuin1 (Sirt1), to stimulate Sirt1 deacetylase activity. Furthermore, DJ-1 downregulated the transcriptional activity of sirt1-suppressed sirt1 target p53 (177). Taken together, these results indicated that p53 is closely associated with DJ-1, suggesting presence of a finely regulated circuit between both proteins during tumorigenesis and apoptosis. Previous studies have also shown that major facilitator superfamily domain containing 12 (MFSD12), which is highly expressed in melanoma, induces proliferation of melanoma cells *via* the PI3K- AKT signaling pathway (102).

Interference With the Cell Cycle

Continued unregulated growth of cancer cells is a fundamental abnormality during cancer development and progression. In fact, the first step in the process, tumor initiation, is believed to be the basis for initiation of abnormal proliferation of individual cells.

TABLE 4 | Exosomal proteins in prostate cancer tissue.

protein (127)	Role in tumors	references
Glutathione synthetase	Inhibit oxidative stress, tumor progression and chemotherapy resistance	(128)
D-3-phosphoglycerate dehydrogenase	Up-regulation of cancer-promoting genes, regulation of metabolism, chemotherapy resistance	(129)
Cytosol aminopeptidase	Affects MHC class I mediated antigen presentation	(130)
Alpha-enolase	Protein-protein interactions that regulate glycolysis, activation of signaling pathways, and resistance to chemotherapy	(131)
Keratin, type I cytoskeletal 10	Inhibit cell cycle progression	(132)
Actin, cytoplasmic 1	Causes cytoskeletal changes to promote tumor progression	(133)
Isocitrate dehydrogenase 1 (NADP+), soluble	Control lipid metabolism and inhibit apoptosis	(134)
Alcohol dehydrogenase [NADP+]	Activate the carcinogenic effects of acetaldehyde	(135)
Sorbitol dehydrogenase	Inhibit cell hypoxia	(136)
F-Actin-capping protein subunit alpha-1	Remodeling the cytoskeleton inhibits EMT, thereby inhibiting cancer migration and invasion	(137)
N(G), N(G)-Dimethylarginine dimethylaminohydrolase 1	Inhibit angiogenesis	(138)
Annexin A1	Induces apoptosis, activates immunity, mediates cancer pathways, and protein interactions	(139–143)
14-3-3 Protein sigma	Induces cell cycle arrest and apoptosis of cancer cells, affects transcription factors and cell signal transduction in cancer cells, and resists oxidative stress	(144)
Annexin A5	Annexin A5 can activate the PI3K/Akt/mTOR signaling pathway to promote epithelial-mesenchymal transition (EMT) and the expression of MMP2 and MMP9	(145)
Annexin A3	Participate in cell signal transduction and promote tumor development	(146)
Syntenin-1	Regulating PTGER2 expression enhances CSC amplification, oxaliplatin chemoresistance and migration	(147)
Heat-shock protein beta-1	Inhibit cell apoptosis in various malignant tumors, up-regulate the expression of MMP-9, promote the invasion of breast cancer cells, and increase VEGF) to induce angiogenesis	(148–151)
Peroxiredoxin-6	Regulate the expression of uPAR, Ets-1, MMP-9, RhoC and TIMP-2 to increase the invasion and metastasis of breast cancer	(152)
Triosephosphate isomerase	Regulate glycolysis and metabolism, as an oncogene	(153)
Phosphatidylethanolamine-binding protein 1	Inhibit most of the kinase functions in the signal cascade, metastasis inhibitors, participate in cell proliferation, inhibit metastasis, and promote apoptosis	(154)
Semenogelin-1	Activate androgen receptor	(155)
Superoxide dismutase [Cu-Zn]	Inhibit the oxidative stress response of cells	(156)
Ubiquitin-conjugating enzyme E2 N	Involved in DNA repair, cell cycle progression, cell apoptosis and carcinogenic signals	(157)
Prolactin-inducible protein	Enhance anti-tumor immunity and promote tumor metastasis	(158)
Protein S100-A9	Regulate tumor immune microenvironment	(159)
Histidine triad nucleotide-binding protein 1	Inhibition of oncogene transcriptional control pathways	(160)
Acyl-CoA-binding protein	Maintain fatty acid oxidation to induce tumorigenesis	(161)
Protein S100-A11	Regulate cell cycle, promote cell proliferatio n, migration, invasion and EMT, activate Wnt, β-catenin signaling pathway to induce cancer	(162)

Subsequent cell proliferation causes growth of clonally derived tumor cell populations. Numerous studies have identified a number of proteins that regulate proliferation of the cell cycle, to subsequently trigger tumorigenesis. For example, one study showed that estrogen stimulates the proliferative cycle of endometrial cells, while exposure to excess estrogen significantly increases the risk of endometrial cancer in women (178). PCaDE also contains similar proteins that interfere with cell cycle processes, to promote tumor cell development. For instance, Bosch et al. demonstrated that Ca^{2+} and calmodulin (CaM) play a key role in proliferation and viability of a variety of cells, including PCa. This phenomenon may be attributed to the fact that CaM interacts with various proteins that regulate the cell cycle, including p21Cip1, D1-Cdk4 and CaM kinase II, to control their activities and nuclear localization, thereby influencing proliferation of tumor cells (179). Moreover, cell cycle protein A in LNCaP cellular extracts was found to directly or indirectly bind to CaM, indicating that its expression is sensitive to the inhibitory effect of the anti-CaM drug W-7. Notably, this indicates that CaM regulates expression of cell cycle protein A in PCa cells to induce over-proliferation of LNCaP cells (96). In addition, previous studies have shown that expression of MFSD12, a novel suppressor gene in lung cancer, and its protein, can control cell cycle distribution, matrix attachment and cell motility, thereby regulating tumor growth and development. MFSD12 was significantly upregulated in melanoma tissues, with interreference in its expression in A2058 and M14 melanoma cells found to significantly suppress tumor cell proliferation. Results from flow cytometry analysis confirmed that silencing MFSD12 expression mediated increase and decrease in the proportion of cells in the G1and S phases, respectively, suggesting that MFSD12-induced proliferation is associated with promotion of the G1 phase (102).

PCADEPR IN CANCER SURVIVAL AND PROGRESSION

Evasion of death is imperative to cancer cells' persistence and their subsequent progression. Several tumor survival proteins are

present in the tumor survival microenvironment, where they play a key role in regulatory processes including apoptosis (180), metabolism (181), immune escape, nutrient transport, hypoxic environment and drug resistance, that promote tumor cell survival. Proteins related to apoptosis and also present in PCa exosomes, such as Bcl-2, inhibitor of apoptosis (IAP) and heat shock protein (HSP) and proteins related to cell metabolism, such as glucose transporter 1 (GLUT1) and Ras, etc. Considered a family of survivin proteins of tumor cells (180). Abnormal expression of these proteins is associated with a series of biological regulatory processes that promote cancer cell survival, proliferation, and treatment resistance (181). In addition, cancer cells employ progression as a means for tumors to maintain survival, thus tumor survival is closely associated with progression. Tumor progression is characterized by rapid changes in the tumor phenotype, a phenomenon that has made tumors to become more aggressive. Exosomal proteins are thought to play various roles in progression of various tumor types, including remodeling of the tumor microenvironment, promoting epithelial mesenchymal transition (EMT), angiogenesis induction, promoting migration, invasion and immune escape of cancer cells, as well as regulating the corresponding signaling pathways (182).

Remodeling the Tumor Microenvironment

Immune escape is an important aspect in tumor survival, as tumor cells can only proliferate, migrate and invade tissues if they escape killing by immune cells, such as phagocytes, T cells, and NK cells. The exosomal proteins, which are secreted by cancer cells support immune escape to promote tumor cell survival. For instance, exosomal proteins support immune cell migration (such as neutrophils, macrophages and regulatory T cells) to secondary sites, suppress immune responses to tumors by inhibiting the efficacies of antigen-presenting cells, such as dendritic cells. They can also impair immune functions of T and NK cells by activating apoptosis (183, 184). Moriwaki et al. demonstrates that tumor cells lacking GDP-mannose-4,6-dehydratase (GMDS) can evade NK cell-mediated tumor immune surveillance by acquiring resistance to tumor necrosis factor-related apoptosis-inducing ligand (TRAIL)-induced apoptosis (105). Aled et al. found that TGF-β-positive exosomes downregulated natural-killer group 2, member D (NKG2D) expressions in NK and CD8+ T cells, which in turn impaired immune effector functions (185). TGF-β-rich exosome inhibits lymphocyte responses to IL-2, thereby altering the tumor microenvironment to promote immune escape functions of tumor cells (186). In addition, documented those expressions of some purinergic receptors directly or indirectly inhibit T cells and NK cells effects, thereby suppressing immune responses to primary tumors. For instance, oncogenic exosomes with elevated CD39 and CD73 levels can promote adenosine production, thereby enhancing regulatory T cell and myeloid cell proliferation to suppress immune functions (187). Interestingly, exsomeal proteins have also been shown to promote tumor progression by activating tumor-associated immune cells. Wang et al. found that LAMP 2a contributes to tumor progression by degrading PRDX1 (peroxiredoxin 1) and CRTC1 (CREB-regulated transcriptional coactivator 1), which enhances tumor-associated macrophage activation (188). These studies confirm that cancer-derived exosomal proteins can mediate the escape of tumor cells from immune surveillance to promote their survivability.

In addition to regulation of immune microenvironments, exosomal proteins are involved in construction of other tumor microenvironments to maintain tumor survival. For example, tumor cell over proliferation leads to the development of hypoxic environments, therefore, the ability to regulate tumor cell tolerance to hypoxic environments is necessary for tumor cell survival, and some proteins in exosome can play this function. Hypoxia-inducible factor-1α (HIF-1α), a master transcription factor, is stable under hypoxic conditions. It regulates the expressions of several target genes and enhances the adaptability of tumor cells to hypoxia (189). Zhong et al. found that under hypoxic conditions, DJ-1 is involved in regulation of HIF-1α transcriptional activities, promoting PCa adaptation to hypoxic environments (190). Inflammatory microenvironments can also affect tumor survival and progression. For instance, DJ-1 is involved in creation of inflammatory tumor microenvironments. In their study, Chien et al. found elevated levels of IL-1β in cultured macrophages from DJ-1 DJ-1 Knockdown mice and DJ-1 knockdown mice (191). It was also confirmed that the inflammatory microenvironment generated by DJ-1 dysregulation sustained melanoma survival at the point of lung metastasis. Another study found that adipose-derived stem cells (ADSCs) induced by exosomal proteins exhibited typical characteristics of tumor-associated myofibroblasts, and could induce the phenotype and function of myofibroblasts in ADSCs by activating intracellular signaling pathways. Increased expression of smooth muscle actin (α-SMA) and tumor-promoting factors such as the stromal cell-derived factor 1 (SDF-1) and TGF-β. These outcomes are associated with increased expressions of TGF-β receptors I and II in exosomes (189). Therefore, exosomal proteins contribute to the generation of tumor-associated myofibroblasts in the tumor stroma to construct an extracellular matrix environment suitable for tumor survival.

Hormone Receptor Regulation and Metabolic Reprogramming

Although the emergence of castration-resistant PCa poses difficulties for androgen deprivation therapy (ADT), androgen depletion and hormonal regulation have been the mainstay of advanced disease treatment since the landmark discovery of Huggins and Hodges (192). The PCaDEPr that are associated with hormone receptor regulation, including adhesion spot protein (VCL), play an important role in cancer progression. Kawakami et al. reported that the VCL, through which integrins associate with the actin cytoskeleton, promotes paclitaxel resistance-associated PCa invasion. They found that VCL levels were highest in CRPC, negative or very low in BPH and non-CRPC, and confirmed that VCL overexpressions promotes PCa progression by altering androgen receptor (AR) levels (21). Iwamoto et al. found that Syntenin-1 levels are positively correlated with prostaglandin E2 receptor (PTGER2) levels and

promotes rectal cancer cell progression (147). In addition to regulation of hormone receptors, these proteins mediate hormone levels, thereby activating hormone receptors. Abiraterone acetate (CYP17A1), an integrase involved in adrenal steroid conversion and *de novo* synthesis of androgens, is involved in CRPC production. Attard et al. used an inhibitor of CYP17A1 synthesis to treat 21 desmoresistant PCa patients. They reported a decrease in serum androstenedione, dehydroepiandrosterone (DHEA) and testosterone levels *in vivo*, and in CRPC patients. The antifungal drug, ketoconazole, is similar to CYP17A1 inhibitors and suppresses testosterone synthesis (193). Therefore, CYP17A1 promotes androgen expressions, which have a significant role in AR activation. Therefore, PCaDEPr mediated regulation of hormone receptors may be one of the pathways in cancer progression.

Metabolic processes are crucial for cell survival, especially tumor cells. The exosomal proteins have the ability to regulate substance metabolism-related proteins to induce metabolic reprogramming and provide energy as well as biosynthetic pathways to tumor cells. For example, glucose transporter protein 1 (GLUT1) regulates cellular glucose uptake and responds to suppressed intracytoplasmic glucose levels. Cheng et al. found that Rab25 (member RAS oncogene family) regulates GLUT1 transport to cell surfaces to enhance glucose uptake and ultimately increases glycogen reserves as well as ATP levels in ovarian cancer cells (194). Even though dysregulated glucose metabolism is important for metabolic reprogramming in tumor cells, metabolic reprogramming in tumor cells also involves lipid storage and mobilization. Walther et al. found that Rab GTPases regulates GLUT (glucose transporter protein) transport and lipid droplet (LD) formation during glucose and lipid metabolism in cancer cells. Lipid droplets (LD) have a role in intracellular lipid storage and maintenance of intracellular levels of free lipids and energy homeostasis (195). Wu et al. reported that Rab8a regulates lipid droplet fusion and cancer cell growth in hepatocellular carcinoma (196), thereby maintaining hepatocellular carcinoma cell survival.

Regulation of Lysosomal Functions and Distribution

Lysosomes are important components of the endosomal system. They are involved in various biological processes, including macromolecular degradation, antigen presentation, intracellular pathogen destruction, plasma membrane repair, exosomesrelease, cell adhesion/migration, and apoptosis. Functional states and spatial distributions of lysosomes are closely associated with cancer cell proliferation, energy metabolism, invasion and metastasis, as well as immune escape. Invasiveness of radiation-surviving cancer cells is associated with altered lysosomal exocytosis induced by activation of Arl8b present in prostate cancer-derived exosomes. Ping-Hsiu Wu et al. found that after radiation, Arl8b, a small GTPase that regulates lysosomal transport, increased its binding to its effector-SifA and kinesin-interacting protein (SKIP) through the regulation of the BORC (Biogenesis of lysosome-related organelles complex) subunit. Knockdown of Arl8b or the BORC subunit suppressed lysosomal cytokinesis and invasiveness of radiation-surviving breast cancer tumor cells. *In vivo*, suppression of Arl8b levels inhibited radiation-induced invasive tumor growth and distant metastasis (109). Moreover, Arl8b is also a key regulator of lysosomal localization (197). The active form of Arl8b is mainly located in the lysosome, where it regulates lysosomal transport to the cell periphery (198). The cis-transport of lysosomes from the center of microtubule tissues to the cell periphery is regulated by the BORC/Arl8b/SKIP complex (199). Therefore, Arl8b regulates spatial distribution of lysosomes and protease release through lysosomal localization, leading to elevated tumor cell invasiveness. In addition, as a key protein in lysosomal functions, cathepsin D is widely found in PCa-derived exosomes and is associated with tumor progression. Yong et al. found that cathepsin D levels are positively correlated with colorectal cancer malignancy, and that patients with elevated cathepsin D levels have lower survival rates (200).

Inhibition of Cancer Cell Apoptosis

Homeostatic balance in an organism is maintained by programmed cell death or apoptosis. In addition to being associated with tumor survival, apoptosis is also closely associated late survival of tumor cells. In cancer patients, tumor cells also undergo their own apoptosis, leading to the death of cancer cells. However, some biomolecules such as proteins present in prostate cancer-derived exosomes inhibit this process to keep tumor cells alive. Hahm et al. reported that induction of lysosomal-associated membrane protein 2A (LAMP2A) expression inhibited the apoptotic abilities of prostate cells, thereby enhancing cancer cell survival. LAMP2A protein knockdown in PC-3 and 22Rv1 cells significantly increased the apoptotic rate in both cells, confirming that LAMP2A is involved in induction and activation of the apoptotic protein (Bcl-2) (201). Ding et al. documented that LAMP2A downregulation significantly increased positive apoptosis-staining of hepatocellular carcinoma cells, while decreasing Ki-67(a staining for lipid membranes) staining, confirming that LAMP2A contributes to cancer persistence by inhibiting apoptosis and promoting cell proliferation (202). Moreover, in primary breast cancer samples, DJ-1 levels were negatively correlated with PTEN immunoreactivity and positively correlated with PKB (Protein kinase B)/Akt hyperphosphorylation. Co-expressions of DJ-1 and PTEN completely rescued the apoptotic processes of PTEN-induced tumor cells (112).

Apoptosis affects tumorigenesis and has an important role in late tumor progression. Therefore, interference with apoptosis can promote cancer progression. *In vitro* and *in vivo*, elevated caveolin-1 expressions in metastatic mice and human PCa cells have been reported, suggesting that inhibition of apoptosis promotes tumor progression. Overexpressions of caveolin-1 in LNCaP) or upregulation of Cav-1 in androgen-insensitive LNCaP clones makes these cells resistant to apoptosis (203). Li et al. found a significant association between elevated glucosamine-6-Phosphate Deaminase 1 (GNPDA1) levels and advanced tumor stage, TNM (the TNM classification of malignant tumors) stage or grade, and the subsequent apoptotic staining analysis revealed that elevated GNPDA1 levels inhibited HCC cell apoptosis (104). Therefore, GNPDA1

promotes hepatocellular carcinoma progression by inhibiting HCC cell apoptosis.

PCADEPR IN CANCER TRANSFER

Approximately 90% of human cancer-associated deaths are attributed to metastases (204). One of the hallmarks of malignancy is a high degree of invasiveness and metastatic capacity. During development of most cancer types, sooner or later, the primary tumor mass produces free cells that invade adjacent tissues and migrate to distant sites, where they establish new tumor cell colonies. Presumably, the processes involved in invasion and metastasis are: separation from the primary tumor mass, reorganization/remodeling of the extracellular matrix, cell migration, recognition, movement through endothelial cells and vascular circulation, as well as colonization and proliferation within the ectopic stroma. The key and initial to all these processes is an increased ability of cancer cells to move themselves and escape the control of normal physiological regulation. Various biomolecules, including proteins, are involved in regulation of tumor cell invasion and metastasis. This could be because, proteins can influence the tumor microenvironment, EMT, target microenvironment, vascular regeneration, and metastatic signaling pathways to induce distant tumor cell metastasis.

Establishment of pre-Metastatic Ecological Niches

Tumor cells require a permissive environment in terms of nutrients, extracellular matrix and immune cells to successfully metastasize to distant organs. Therefore, tumor-adapted metastable environments are particularly important for tumor metastasis, and the process of constructing these microenvironments involve the establishment of pre-metastatic ecological niches. Studies on metabolic networks and seeding mechanisms of cancer cells in specific environments have revealed that some integrin proteins are involved in establishment of these ecological niches. During metastasis, tumor cells must acquire the ability to remodel the extracellular matrix (ECM) to achieve invasion and metastasis. Some exosomal proteins are involved in regulation of this process. Bijnsdorp et al. found that Integrin Subunit Alpha 3 (ITGA3) and Integrin beta-1 (ITGB1) were highly expressed in urinary esosomes of metastatic PCa patients, and that ITGA3 and ITGB1, as well as ITGA3 in exosomes, stimulated non-cancerous epithelial cell migration and invasion. This enables the progression and distant metastasis of cancer cells (205). Moreover, the immunosuppressive microenvironment is important in development of pre-metastatic niches, and some exosomal proteins in PCa are involved in establishment of immunosuppressive microenvironments. Allard et al. found that synergistic actions of two extracellular nucleotidases (CD39 and CD73), constituted the main source of extracellular adenosine in TME and were jointly involved in development of immunosuppressive TME, such as through tumor kinetics to redirect ATP to the immunosuppressive adenosine-rich tumor microenvironment (206).

Vascular regeneration of tumor cells enhances the migratory as well as metastatic capacities of tumor cells, in addition to providing them with a favorable nutritional environment (207). Some exosomal proteins promote distant tumor cell metastasis through this process. Gesierich et al. reported that quadruple transmembrane protein-8 (Tspan8)-positive exosomes promoted endothelial cell production and increased the expressions of vascular endothelial growth factors as well as growth factor receptors in fibroblasts, thereby promoting angiogenesis in pancreatic and gastric cancers (208). Chen et al. found that in patients with metastatic colon cancer, high serum Galectin-3 levels were associated with elevated serum G-CSF, IL-6 and sICAM1 levels, which interacts with the vascular endothelium to increase the expressions of vascular cell adhesion protein type I (VCAM-1) on endothelial cell surfaces, leading to increased cancer cell-endothelial adhesion and increased endothelial cell migration and small vessel formation (209). In addition, intramembrane cleavage mediated by γ-secretase, a large protease complex consisting of a catalytic subunit (presenilin-1 or presenilin-2) and auxiliary subunits (Pen-2, Aph1 and nicastrin), is an important link in the Notch signaling pathway. Zeng et al. documented that γ-secretase affects cancer metastasis after Notch activation cascade reactions, probably because γ-secretase promotes angiogenesis in solid tumors through Notch signaling (210).

In conclusion, the establishment of metastatic ecotone, including immunosuppression and angiogenesis suggests that PCaDEPr is involved in mediating the establishment of pre-metastatic ecotone in tumors, thereby inducing cancer metastasis.

Alterations of Microenvironments at the Target Site

Adaptive regulation of the microenvironment at tumor colonization sites prior to metastasis is important for tumor colonization. Recently, exosomal proteins have been shown to promote tumor cell colonization of tissues and organs by modulating the tumor metastasis target site microenvironments. In addition to alterations of tumor microenvironments at the target site, there are changes in bone colonization processes, such as the number and structures of outcomes and osteoclasts. Prior to the arrival of tumor cells, primary tumors actively regulate the nutritional, extracellular matrix and immune environments of distant organs by secreting regulatory factors, thus producing a permissive and supportive ecological niche for tumor survival at the metastatic site. In tumor bone cell metastasis, malignant communication between PCa cells and bone cells (osteoblasts and osteoclasts) is established. Casimiro et al. found that PCa cells provide osteoblasts with osteogenic cytokines [e.g. bone morphogenetic proteins (BMPs), platelet-derived growth factors (PDGF), endothelin-1 (ET1)] and osteolytic factors [e.g. MMPs and vascular endothelial growth factor (VEGF)], which enables these cells to make bone-derived cell growth factors (211). Itoh et al. identified the ETS Proto-Oncogene 1 (Ets1) protein in PCa-derived exosomes to be an osteoblast differentiation-related transcription factor and found it to be a candidate inducer of osteoblast differentiation (19). A standard exosomal protein study found that exosome-mediated translocation of pyruvate kinase M2 (PKM 2) from PCa cells into BMSCs promotes PCa bone metastasis. Moreover, the PKM2 protein upregulates hypoxia-inducible factor

1α (HIF-1α) in BMSCs to promote CXCL12 expressions in stromal cells. Biologically, exosome-mediated PKM2 transport of prostate tumor origin is a key mediator of PCa bone metastasis (45).

EMT Transformation and Regulation of Cell Motility

Prior to metastasis, tumor cells are detached from their original sites through loss of attachment and adhesion capacities and metastasize to their target sites with blood or lymphatic chemotaxis, eventually undergoing clonal growth at metastatic sites. Therefore, epithelial-mesenchymal transition processes of EMT formation are important in initiation of cancer metastasis. Various molecules, including exosomal proteins, are involved in EMT transformation in tumor cells. The loss of E-cadherin is associated with the loss of intercellular contacts, disruption of the E-cadherin-catenin complex, abnormal activation of β-catenin signaling as well as cytoskeletal changes. This is critical for cells to lose their epithelial polarity and acquire aggressive phenotypes. In primary PCa, suppressed E-cadherin levels and elevated nucleus β-catenin levels are strongly associated with metastasis and poor prognostic outcomes. Zhang et al. observed elevated E-cadherin levels and suppressed N-cadherin as well as wave protein levels in response to melanopsin depletion. Silencing of melanopsin was associated with suppressed total and activated β-catenin levels. In a subsequent study, it was noted that when melanopsin was downregulated, PCa cells exhibited decreased proliferation, migration and invasion abilities (101). In addition to melanopsin, Rab3D induces epithelial mesenchymal transformation. Tauro et al. found that Rab3D regulates EMT transformation of tumor cells by activating the Akt/GSK-3β/Snail signaling pathways (212). In addition, overexpressing cells with melanopsin-like Rab2A suppresses E-calmodulin while elevating N-calmodulin, wave protein, and fibronectin levels, which affects the EMT phenotype (118).

Cell motility is key in cancer invasion and metastasis. The loss of cell-cell adhesion and enhanced cell-matrix interactions are essential for enhanced tumor cell motility (213). Four-transmembrane proteins are associated with various processes, including signal transduction pathways, cell activation, proliferation, motility, adhesion, tissue differentiation, angiogenesis, tumor progression, and metastasis (214, 215)and are present in urinary exosomes of PCa patients. Even though most tetra-transmembrane proteins are downregulated in metastatic tumors, the CD151 glycoprotein was the first member of the tetra-transmembrane protein to be identified as a metastasis promoter. This shows that the tetra-transmembrane superfamily protein CD151 promotes cancer migration and metastasis (216). Detchokul et al. revealed that CD151 can regulate the redistribution of adhesion components required for cell migration as well as invasion and the process of targeted delivery of matrix degrading enzymes, confirming that CD151 promotes cell motility and tumor invasion (217). Gesierich et al. found that colocalization of integrin β4 with CD151 activates PKC to promote integrin internalization, thereby increasing tumor cell motility (218). Ang et al. found that CD151-transfected LNCaP cells had greater motility, compared to controls and that PC3 cells with CD151 knockdown showed reduced motility. However, the responsible mechanisms have not been elucidated (219). In conclusion, CD151 induces distant cancer cell metastasis by regulating tumor cell motility.

Activation of Metastatic Signaling Pathways

Tumor-associated exosomal proteins have the ability to mediate the activation of common signaling pathways to induce tumor cell metastasis. Hao et al. found that CD44 or CD147 knockdown downregulated p-Akt and p-Erk levels in PC3 cells and inhibited the activations of PI3K/Akt and MAPK/Erk signaling pathways. The administration of drugs that selectively target CD44/CD147 alone or in combination with docetaxel restricted CaP metastasis (50). Therefore, CD44 and CD147 enhances the metastatic abilities of CaP cells, possibly by activating PI3K and MAPK pathways. He et al. found that DJ-1 knockdown markedly suppressed invasive and migration abilities of pancreatic cancer cells, inhibited the expressions and activities of uPA and induced cytoskeletal disruption. These outcomes may have been because DJ-1 downregulation inhibited SRC and ERK1/2 phosphorylation, which suppressed SRC and ERK signaling pathways-mediated expressions of uPA (220). Yang et al. reported that the exosomal protein (Rab3D) was highly expressed in malignant breast cancer but not in normal tissues and benign breast tumors. The knockdown of Rab3D significantly inhibited the migration abilities of breast cancer cells, which was confirmed to be mediated by Rab3D activations of AKT/GSK-3β/Snail signaling pathways (116). In addition, exosoemal proteins are involved in intermediate pathways of metastatic signaling pathways to induce cancer metastasis. Boscher et al. found that EGF activations of downstream integrin signaling pathways in breast cancer adenocarcinoma epithelial cells induces tumor metastasis dependent on synergistic actions of Galectin 3 and p-Caveolin-1 (221). Thus, PCaDEPr activates multiple tumor metastasis signaling pathways to induce cancer metastasis.

PCADEPR IN CANCER DRUG RESISTANCE

Tumor cell sensitivity to chemotherapeutic agents is essential for cancer drug therapy. Many biological factors modulate the sensitivity as well as resistance of tumors to chemotherapeutic agents (222, 223). In patients with prostate tumors, exosomal proteins have been shown to be essential for the development of drug resistance. With increasing administrations of chemotherapeutic drugs, the rates of tumor drug resistance have been increasing year by year. Therefore, elucidation of the mechanisms involved in chemotherapeutic resistance to identify new therapeutic targets is the direction of today's oncology research. Previous exosomes studies found that PCaDEPr regulates tumor sensitivity to drugs through various pathways. For example, Survivin is expressed in PCa-derived exosomes and its downregulation sensitizes PCa cells to chemotherapeutic agents (59). Doxorubicin is a chemotherapeutic agent that usually becomes ineffective against tumor cells over time due to chemoresistance. Breast cancer cells lacking LAMP2A exhibit

increased sensitivity to this drug (224). In addition, LAMP2-mediated autophagy in PCa-derived exosomes modulates lung cancer cell resistance to temozolomide (225). Pedram et al. found that resistance of DU145 and PC-3 to docetaxel and paclitaxel was partly due to P-gp expressions and confirmed that P-gp protein levels in exosomes reflect P-gp levels in PCa cells (226).

In cisplatin-resistant ovarian cancer cells, claudin-4 was overexpressed 7.2-fold and was one of the most overexpressed proteins, suggesting that it may be associated with cisplatin resistance in ovarian cancer. Expressions of claudin, including claudin-3, -4 and -7, were markedly higher in chemoresistant ovarian cancer cells than in chemo-sensitive ovarian cancer cells. Their high expressions were positively correlated with ovarian cancer resistance to chemotherapy (227). Liu et al. found that elevated levels of synaptic binding protein-like 4 (SYTL4), a Rab effector in vesicular transport, are associated with poor prognostic outcomes in TNBC (triple negative breast cancer, referring to breast cancer lacking estrogen receptor (ESr or Er), progesterone receptor (Pr) expression with lack of epidermal growth factor receptor-2 gene (HER) expression), especially in paclitaxel treated TNBC. It has been postulated that SYTL4 confers resistance to paclitaxel in triple-negative breast cancer (110).

These findings demonstrate that PCaDEPr plays an important role in promoting drug resistance in tumor cells.

SUMMARY AND OUTLOOK

With further research on PCaDE, tumor-derived exosomal proteins have attracted special attention. In this review, we discuss recent advances in research related to PCaDEPrs from the perspective of promoting tumorigenesis and progression. The role of these exosomal proteins present in cells or other tumors is also highlighted, although this does not mean that they remain such in specific tumor exosomes. However, because of this, this may provide researchers who identify differential proteins by routine protein analysis for subsequent functional validation with new directions for these exosomal proteins in prostate cancer research.

Although PSA is of great value as a commonly used tumor marker in the diagnosis and prognosis of prostate cancer, it has undeniable limitations, especially for the early diagnosis of bone metastatic prostate cancer. Exosomes may have more potential than PSA for therapeutic purposes, with a number of publications reporting that interference with exosome production and expression of exosome-containing substances will significantly reduce tumor metastasis and aggressiveness. In addition, important progress has been made in the study of drug-loaded exosomes, modified exosomes, and MSC exosomes in disease therapy. However, several questions remain to be addressed in future studies:1. With the study of exosome proteomics, more and more different kinds of proteins have been discovered one after another. However, it is not possible to conclude that the extracted proteins are necessarily present in exosomes according to the current database, so a more rigorous and extensive study is still needed to clarify the types of substances contained in tumor-derived exosomes in order to exclude heterogeneous proteins. 2. Due to the limitations of current extraction techniques, it is difficult to extract exosomes with 100% purity, and exosomes themselves contain a variety of secretory proteins, so it is difficult to determine the exact source of secretory proteins in exosomes of somatic fluid origin: exosomal origin? Body fluids themselves contain? 3. We found that tumors can release some exosomes rich in protective proteins that can inhibit cancer progression, so extracting these exosomes for interfering with tumor progression may be a new avenue for tumor therapy. 4. A large number of studies have found that some proteins present in exosomes and with protective effects significantly decrease with cancer progression. it remains unclear whether the effect of exosomes derived from primary and bone metastatic PCa on the establishment of the target microenvironment is persistent or transient, and further studies of these exosomes are therefore still necessary.

Bone metastatic prostate cancer and the emergence of CRPC types pose great difficulties in the treatment of PCa. Recent literature has demonstrated that tumor-derived exosomal proteins can be transported to distant metastatic targets, creating "fertile ground" to promote cancer metastasis. This may offer hope for finding ways to diagnose and treat bone metastases from prostate cancer. Furthermore, exploring the role of tumor-derived exosomes in cancer development may be a way to address these challenges. The successful treatment of these complex cancers depends on our full understanding of the single actions or interactions and mechanisms of action of the various components of exocytosis. We elucidated on the various functions and possible mechanisms of exosomeal proteins in PCa body fluids or tissues during tumor development. The exosomeal proteins can influence tumor initiation, progression, and drug resistance processes through various complex mechanisms. Elucidation of the mechanisms through which biomolecules, such as proteins, act on these processes will make it possible for us to target these proteins for cancer treatment. However, the most suitable exosomes molecular target for the diagnosis and treatment of PCa has yet to be identified, and the clinical applications of exosomes are associated with some challenges. For instance, exosomes isolation and extraction methods are still limited to the laboratory, relatively harsh storage conditions for exosomes, and medical costs. With rapid advances in exosome-related technologies and in-depth research on PCaDEPr, applications of exosomal proteins in the diagnosis and treatment of PCa will soon be realized.

AUTHOR CONTRIBUTIONS

SF and KL searched for literature and wrote the first draft of this article. SF edited tables and figures. JZ and GZ reviewed the manuscript and polished the grammar. All authors approved the final version submitted and agree on its submission to this journal.

FUNDING

This work was supported by the National Natural Science Foundation of China (grant nos. 81760462 and 81860456).

REFERENCES

1. Lorenc T, Klimczyk K, Michalczewska I, Słomka M, Kubiak-Tomaszewska G, Olejarz W. Exosomes in Prostate Cancer Diagnosis, Prognosis and Therapy. *Int J Mol Sci* (2020) 21(6):2118. doi: 10.3390/ijms21062118
2. Liu CM, Hsieh CL, Shen CN, Lin CC, Shigemura K, Sung SY. Exosomes From the Tumor Microenvironment as Reciprocal Regulators That Enhance Prostate Cancer Progression. *Int J Urol* (2016) 23(9):734–44. doi: 10.1111/iju.13145
3. Guo T, Wang Y, Jia J, Mao X, Stankiewicz E, Scandura G, et al. The Identification of Plasma Exosomal miR-423-3p as a Potential Predictive Biomarker for Prostate Cancer Castration-Resistance Development by Plasma Exosomal miRNA Sequencing. *Front Cell Dev Biol* (2020) 8:602493. doi: 10.3389/fcell.2020.602493
4. Dragomir M, Chen B, Calin GA. Exosomal lncRNAs as New Players in Cell-to-Cell Communication. *Transl Cancer Res* (2018) 7(Suppl 2):S243–s252. doi: 10.21037/tcr.2017.10.46
5. Stade K, Ford CS, Guthrie C, Weis K. Exportin 1 (Crm1p) is an Essential Nuclear Export Factor. *Cell* (1997) 90(6):1041–50. doi: 10.1016/S0092-8674(00)80370-0
6. Duijvesz D, Burnum-Johnson KE, Gritsenko MA, Hoogland AM, Vredenbregt-van den Berg MS, Willemsen R, et al. Proteomic Profiling of Exosomes Leads to the Identification of Novel Biomarkers for Prostate Cancer. *PloS One* (2013) 8(12):e82589. doi: 10.1371/journal.pone.0082589
7. Kowal J, Tkach M, Théry C. Biogenesis and Secretion of Exosomes. *Curr Opin Cell Biol* (2014) 29:116–25. doi: 10.1016/j.ceb.2014.05.004
8. Kowal J, Arras G, Colombo M, Jouve M, Morath JP, Primdal-Bengtson B, et al. Proteomic Comparison Defines Novel Markers to Characterize Heterogeneous Populations of Extracellular Vesicle Subtypes. *Proc Natl Acad Sci USA* (2016) 113(8):E968–77. doi: 10.1073/pnas.1521230113
9. Andreu Z, Yáñez-Mó M. Tetraspanins in Extracellular Vesicle Formation and Function. *Front Immunol* (2014) 5:442. doi: 10.3389/fimmu.2014.00442
10. Shahir M, Mahmoud Hashemi S, Asadirad A, Varahram M, Kazempour-Dizaji M, Folkerts G, et al. Effect of Mesenchymal Stem Cell-Derived Exosomes on the Induction of Mouse Tolerogenic Dendritic Cells. *J Cell Physiol* (2020) 235(10):7043–55. doi: 10.1002/jcp.29601
11. Huang D, Chen J, Hu D, Xie F, Yang T, Li Z, et al. Advances in Biological Function and Clinical Application of Small Extracellular Vesicle Membrane Proteins. *Front Oncol* (2021) 11:675940. doi: 10.3389/fonc.2021.675940
12. Fhu CW, Ali A. Fatty Acid Synthase: An Emerging Target in Cancer. *Mol (Basel Switzerland)* (2020) 25(17):3935. doi: 10.3390/molecules25173935
13. Azizian NG, Li Y. XPO1-Dependent Nuclear Export as a Target for Cancer Therapy. *J Hematol Oncol* (2020) 13(1):61. doi: 10.1186/s13045-020-00903-4
14. Li HJ, Ke FY, Lin CC, Lu MY, Kuo YH, Wang YP, et al. ENO1 Promotes Lung Cancer Metastasis *via* HGFR and WNT Signaling-Driven Epithelial-To-Mesenchymal Transition. *Cancer Res* (2021) 81(15):4094–109. doi: 10.1158/0008-5472.CAN-20-3543
15. Husi H, Skipworth RJ, Cronshaw A, Stephens NA, Wackerhage H, Greig C, et al. Programmed Cell Death 6 Interacting Protein (PDCD6IP) and Rabenosyn-5 (ZFYVE20) are Potential Urinary Biomarkers for Upper Gastrointestinal Cancer. *Proteomics Clin Appl* (2015) 9(5-6):586–96. doi: 10.1002/prca.201400111
16. Kurozumi A, Goto Y, Matsushita R, Fukumoto I, Kato M, Nishikawa R, et al. Tumor-Suppressive microRNA-223 Inhibits Cancer Cell Migration and Invasion by Targeting ITGA3/ITGB1 Signaling in Prostate Cancer. *Cancer Sci* (2016) 107(1):84–94. doi: 10.1111/cas.12842
17. Pellinen T, Blom S, Sánchez S, Välimäki K, Mpindi JP, Azegrouz H, et al. ITGB1-Dependent Upregulation of Caveolin-1 Switches Tgfβ Signalling From Tumour-Suppressive to Oncogenic in Prostate Cancer. *Sci Rep* (2018) 8(1):2338. doi: 10.1038/s41598-018-20161-2
18. Kato T, Mizutani K, Kameyama K, Kawakami K, Fujita Y, Nakane K, et al. Serum Exosomal P-Glycoprotein is a Potential Marker to Diagnose Docetaxel Resistance and Select a Taxoid for Patients With Prostate Cancer. *Urol Oncol* (2015) 33(9):385.e15–20. doi: 10.1016/j.urolonc.2015.04.019
19. Itoh T, Ito Y, Ohtsuki Y, Ando M, Tsukamasa Y, Yamada N, et al. Microvesicles Released From Hormone-Refractory Prostate Cancer Cells Facilitate Mouse Pre-Osteoblast Differentiation. *J Mol Histol* (2012) 43(5):509–15. doi: 10.1007/s10735-012-9415-1
20. Wan X, Kim SY, Guenther LM, Mendoza A, Briggs J, Yeung C, et al. Beta4 Integrin Promotes Osteosarcoma Metastasis and Interacts With Ezrin. *Oncogene* (2009) 28(38):3401–11. doi: 10.1038/onc.2009.206
21. Kawakami K, Fujita Y, Kato T, Mizutani K, Kameyama K, Tsumoto H, et al. Integrin β4 and Vinculin Contained in Exosomes are Potential Markers for Progression of Prostate Cancer Associated With Taxane-Resistance. *Int J Oncol* (2015) 47(1):384–90. doi: 10.3892/ijo.2015.3011
22. Hosseini-Beheshti E, Pham S, Adomat H, Li N, Tomlinson Guns ES. Exosomes as Biomarker Enriched Microvesicles: Characterization of Exosomal Proteins Derived From a Panel of Prostate Cell Lines With Distinct AR Phenotypes. *Mol Cell Proteomics* (2012) 11(10):863–85. doi: 10.1074/mcp.M111.014845
23. Chen CY, Lin YS, Chen CH, Chen YJ. Annexin A2-Mediated Cancer Progression and Therapeutic Resistance in Nasopharyngeal Carcinoma. *J Biomed Sci* (2018) 25(1):30. doi: 10.1186/s12929-018-0430-8
24. Chu Y, Lai YH, Lee MC, Yeh YJ, Wu YK, Tsao W, et al. Calsyntenin-1, Clusterin and Neutrophil Gelatinase-Associated Lipocalin are Candidate Serological Biomarkers for Lung Adenocarcinoma. *Oncotarget* (2017) 8(64):107964–76. doi: 10.18632/oncotarget.22438
25. Watt F, Martorana A, Brookes DE, Ho T, Kingsley E, O'Keefe DS, et al. A Tissue-Specific Enhancer of the Prostate-Specific Membrane Antigen Gene, FOLH1. *Genomics* (2001) 73(3):243–54. doi: 10.1006/geno.2000.6446
26. Li S, Ma YM, Zheng PS, Zhang P. GDF15 Promotes the Proliferation of Cervical Cancer Cells by Phosphorylating AKT1 and Erk1/2 Through the Receptor Erbb2. *J Exp Clin Cancer Res CR* (2018) 37(1):80. doi: 10.1186/s13046-018-0744-0
27. Kwon HJ, Min SY, Park MJ, Lee C, Park JH, Chae JY, et al. Expression of CD9 and CD82 in Clear Cell Renal Cell Carcinoma and its Clinical Significance. *Pathol Res Pract* (2014) 210(5):285–90. doi: 10.1016/j.prp.2014.01.004
28. Mizutani K, Terazawa R, Kameyama K, Kato T, Horie K, Tsuchiya T, et al. Isolation of Prostate Cancer-Related Exosomes. *Anticancer Res* (2014) 34(7):3419–23.
29. Yang XF, Wu CJ, Chen L, Alyea EP, Canning C, Kantoff P, et al. CML28 is a Broadly Immunogenic Antigen, Which is Overexpressed In Tumor Cells. *Cancer Res* (2002) 62(19):5517–22.
30. Fedele C, Singh A, Zerlanko BJ, Iozzo RV, Languino LR. The αvβ6 Integrin is Transferred Intercellularly *via* Exosomes. *J Biol Chem* (2015) 290(8):4545–51. doi: 10.1074/jbc.C114.617662
31. Trerotola M, Ganguly KK, Fazli L, Fedele C, Lu H, Dutta A, et al. Trop-2 is Up-Regulated in Invasive Prostate Cancer and Displaces FAK From Focal Contacts. *Oncotarget* (2015) 6(16):14318–28. doi: 10.18632/oncotarget.3960
32. Kumar D, Gupta D, Shankar S, Srivastava RK. Biomolecular Characterization of Exosomes Released From Cancer Stem Cells: Possible Implications for Biomarker and Treatment of Cancer. *Oncotarget* (2015) 6(5):3280–91. doi: 10.18632/oncotarget.2462
33. Zhu C, Kong Z, Wang B, Cheng W, Wu A, Meng X. ITGB3/CD61: A Hub Modulator and Target in the Tumor Microenvironment. *Am J Trans Res* (2019) 11(12):7195–208.
34. Vences-Catalán F, Duault C, Kuo CC, Rajapaksa R, Levy R, Levy S. CD81 as a Tumor Target. *Biochem Soc Trans* (2017) 45(2):531–5. doi: 10.1042/BST20160478
35. Miyata Y, Nakamoto H, Neckers L. The Therapeutic Target Hsp90 and Cancer Hallmarks. *Curr Pharm Design* (2013) 19(3):347–65. doi: 10.2174/138161213804143725
36. Albakova Z, Armeev GA, Kanevskiy LM, Kovalenko EI, Sapozhnikov AM. HSP70 Multi-Functionality in Cancer. *Cells* (2020) 9(3):587. doi: 10.3390/cells9030587
37. Wang T, Wang Z, Niu R, Wang L. Crucial Role of Anxa2 in Cancer Progression: Highlights on its Novel Regulatory Mechanism. *Cancer Biol Med* (2019) 16(4):671–87. doi: 10.20892/j.issn.2095-3941.2019.0228
38. Ramteke A, Ting H, Agarwal C, Mateen S, Somasagara R, Hussain A, et al. Exosomes Secreted Under Hypoxia Enhance Invasiveness and Stemness of Prostate Cancer Cells by Targeting Adherens Junction Molecules. *Mol Carcinog* (2015) 54(7):554–65. doi: 10.1002/mc.22124
39. Colak S, Ten Dijke P. Targeting TGF-β Signaling in Cancer. *Trends Cancer* (2017) 3(1):56–71. doi: 10.1016/j.trecan.2016.11.008

40. Abd Elmageed ZY, Yang Y, Thomas R, Ranjan M, Mondal D, Moroz K, et al. Neoplastic Reprogramming of Patient-Derived Adipose Stem Cells by Prostate Cancer Cell-Associated Exosomes. *Stem Cells* (2014) 32(4):983–97. doi: 10.1002/stem.1619
41. Liu S, Liang J, Liu Z, Zhang C, Wang Y, Watson AH, et al. The Role of CD276 in Cancers. *Front Oncol* (2021) 11:654684. doi: 10.3389/fonc.2021.654684
42. Lu Q. δ-Catenin Dysregulation in Cancer: Interactions With E-Cadherin and Beyond. *J Pathol* (2010) 222(2):119–23. doi: 10.1002/path.2755
43. Lu Q, Zhang J, Allison R, Gay H, Yang WX, Bhowmick NA, et al. Identification of Extracellular Delta-Catenin Accumulation for Prostate Cancer Detection. *Prostate* (2009) 69(4):411–8. doi: 10.1002/pros.20902
44. Feng Y, Xiong Y, Qiao T, Li X, Jia L, Han Y, et al. A Key Player in Carcinogenesis and Potential Target in Cancer Therapy. *Cancer Med* (2018) 7(12):6124–36. doi: 10.1002/cam4.1820
45. Dai J, Escara-Wilke J, Keller JM, Jung Y, Taichman RS, Pienta KJ, et al. Primary Prostate Cancer Educates Bone Stroma Through Exosomal Pyruvate Kinase M2 to Promote Bone Metastasis. *J Exp Med* (2019) 216 (12):2883–99. doi: 10.1084/jem.20190158
46. Agarwal R, D'Souza T, Morin PJ. Claudin-3 and Claudin-4 Expression in Ovarian Epithelial Cells Enhances Invasion and is Associated With Increased Matrix Metalloproteinase-2 Activity. *Cancer Res* (2005) 65 (16):7378–85. doi: 10.1158/0008-5472.CAN-05-1036
47. Lin X, Shang X, Manorek G, Howell SB. Regulation of the Epithelial-Mesenchymal Transition by Claudin-3 and Claudin-4. *PLoS One* (2013) 8 (6):e67496. doi: 10.1371/journal.pone.0067496
48. Kharaziha P, Chioureas D, Rutishauser D, Baltatzis G, Lennartsson L, Fonseca P, et al. Molecular Profiling of Prostate Cancer Derived Exosomes may Reveal a Predictive Signature for Response to Docetaxel. *Oncotarget* (2015) 6(25):21740–54. doi: 10.18632/oncotarget.3226
49. Díaz MI, Díaz P, Bennett JC, Urra H, Ortiz R, Orellana PC, et al. Caveolin-1 Suppresses Tumor Formation Through the Inhibition of the Unfolded Protein Response. *Cell Death Dis* (2020) 11(8):648. doi: 10.1038/s41419-020-02792-4
50. Hao J, Madigan MC, Khatri A, Power CA, Hung TT, Beretov J, et al. *In Vitro* and *In Vivo* Prostate Cancer Metastasis and Chemoresistance can be Modulated by Expression of Either CD44 or CD147. *PLoS One* (2012) 7 (8):e40716. doi: 10.1371/journal.pone.0040716
51. Xiao Y, Zhong J, Zhong B, Huang J, Jiang L, Jiang Y, et al. Exosomes as Potential Sources of Biomarkers in Colorectal Cancer. *Cancer Lett* (2020) 476:13–22. doi: 10.1016/j.canlet.2020.01.033
52. Ishizuya Y, Uemura M, Narumi R, Tomiyama E, Koh Y, Matsushita M, et al. The Role of Actinin-4 (ACTN4) in Exosomes as a Potential Novel Therapeutic Target in Castration-Resistant Prostate Cancer. *Biochem Biophys Res Commun* (2020) 523(3):588–94. doi: 10.1016/j.bbrc.2019.12.084
53. Khurana S, Chakraborty S, Lam M, Liu Y, Su YT, Zhao X, et al. Familial Focal Segmental Glomerulosclerosis (FSGS)-Linked α-Actinin 4 (ACTN4) Protein Mutants Lose Ability to Activate Transcription by Nuclear Hormone Receptors. *J Biol Chem* (2012) 287(15):12027–35. doi: 10.1074/jbc.M112.345421
54. Bergelson LD. Serum Gangliosides as Endogenous Immunomodulators. *Immunol Today* (1995) 16(10):483–6. doi: 10.1016/0167-5699(95)80032-8
55. Hata K, Tochigi T, Sato I, Kawamura S, Shiozaki K, Wada T, et al. Increased Sialidase Activity in Serum of Cancer Patients: Identification of Sialidase and Inhibitor Activities in Human Serum. *Cancer Sci* (2015) 106(4):383–9. doi: 10.1111/cas.12627
56. Locke JA, Fazli L, Adomat H, Smyl J, Weins K, Lubik AA, et al. A Novel Communication Role for CYP17A1 in the Progression of Castration-Resistant Prostate Cancer. *Prostate* (2009) 69(9):928–37. doi: 10.1002/pros.20940
57. Hurwitz MD, Kaur P, Nagaraja GM, Bausero MA, Manola J, Asea A. Radiation Therapy Induces Circulating Serum Hsp72 in Patients With Prostate Cancer. *Radiother Oncol* (2010) 95(3):350–8. doi: 10.1016/j.radonc.2010.03.024
58. Kishi H, Igawa M, Kikuno N, Yoshino T, Urakami S, Shiina H. Expression of the Survivin Gene in Prostate Cancer: Correlation With Clinicopathological Characteristics, Proliferative Activity and Apoptosis. *J Urol* (2004) 171 (5):1855–60. doi: 10.1097/01.ju.0000120317.88372.03
59. Khan S, Jutzy JM, Valenzuela MM, Turay D, Aspe JR, Ashok A, et al. Plasma-Derived Exosomal Survivin, A Plausible Biomarker for Early Detection of Prostate Cancer. *PLoS One* (2012) 7(10):e46737. doi: 10.1371/journal.pone.0046737
60. Krishn SR, Singh A, Bowler N, Duffy AN, Friedman A, Fedele C, et al. Prostate Cancer Sheds the αvβ3 Integrin *In Vivo* Through Exosomes. *Matrix Biol* (2019) 77:41–57. doi: 10.1016/j.matbio.2018.08.004
61. Kwon MJ. Emerging Roles of Claudins in Human Cancer. *Int J Mol Sci* (2013) 14(9):18148–80. doi: 10.3390/ijms140918148
62. Gagou ME, Ganesh A, Thompson R, Phear G, Sanders C, Meuth M. Suppression of Apoptosis by PIF1 Helicase in Human Tumor Cells. *Cancer Res* (2011) 71(14):4998–5008. doi: 10.1158/0008-5472.CAN-10-4404
63. Ding L, Wang Z, Yan J, Yang X, Liu A, Qiu W, et al. Human Four-and-a-Half LIM Family Members Suppress Tumor Cell Growth Through a TGF-Beta-Like Signaling Pathway. *J Clin Invest* (2009) 119(2):349–61. doi: 10.1172/JCI35930
64. Terayama M, Yamada K, Hagiwara T, Inazuka F, Sezaki T, Igari T, et al. Glutathione S-Transferase Omega 2 Regulates Cell Growth and the Expression of E-Cadherin *via* Post-Transcriptional Down-Regulation of β-Catenin in Human Esophageal Squamous Cells. *Carcinogenesis* (2020) 41 (7):875–86. doi: 10.1093/carcin/bgz189
65. Bolomsky A, Heusschen R, Schlangen K, Stangelberger K, Muller J, Schreiner W, et al. Maternal Embryonic Leucine Zipper Kinase is a Novel Target for Proliferation-Associated High-Risk Myeloma. *Haematologica* (2018) 103(2):325–35. doi: 10.3324/haematol.2017.172973
66. Barrios N, González-Pérez E, Hernández R, Campuzano S. The Homeodomain Iroquois Proteins Control Cell Cycle Progression and Regulate the Size of Developmental Fields. *PLoS Genet* (2015) 11(8): e1005463. doi: 10.1371/journal.pgen.1005463
67. Berezovsky AD, Poisson LM, Cherba D, Webb CP, Transou AD, Lemke NW, et al. Sox2 Promotes Malignancy in Glioblastoma by Regulating Plasticity and Astrocytic Differentiation. *Neoplasia (New York N.Y.)* (2014) 16(3):193–206, 206.e19-25. doi: 10.1016/j.neo.2014.03.006
68. Lei M. The MCM Complex: Its Role in DNA Replication and Implications for Cancer Therapy. *Curr Cancer Drug Targets* (2005) 5(5):365–80. doi: 10.2174/1568009054629654
69. Sim EU, Lee CW, Narayanan K. The Roles of Ribosomal Proteins in Nasopharyngeal Cancer: Culprits, Sentinels or Both. *biomark Res* (2021) 9 (1):51. doi: 10.1186/s40364-021-00311-x
70. Patnaik D, Estève PO, Pradhan S. Targeting the SET and RING-Associated (SRA) Domain of Ubiquitin-Like, PHD and Ring Finger-Containing 1 (UHRF1) for Anti-Cancer Drug Development. *Oncotarget* (2018) 9 (40):26243–58. doi: 10.18632/oncotarget.25425
71. Walsh PC. Heterogeneity of Genetic Alterations in Prostate Cancer: Evidence of the Complex Nature of the Disease. *J Urol* (2002) 168(4 Pt 1):1635–6.
72. Liu Z, Johnson ST, Zhang Z, Corey DR. Expression of TNRC6 (GW182) Proteins Is Not Necessary for Gene Silencing by Fully Complementary RNA Duplexes. *Nucleic Acid Ther* (2019) 29(6):323–34. doi: 10.1089/nat.2019.0815
73. Anand R, Prakash SS, Veeramanikandan R, Kirubakaran R. Association Between Apolipoprotein E Genotype and Cancer Susceptibility: A Meta-Analysis. *J Cancer Res Clin Oncol* (2014) 140(7):1075–85. doi: 10.1007/s00432-014-1634-2
74. Welton JL, Brennan P, Gurney M, Webber JP, Spary LK, Carton DG, et al. Proteomics Analysis of Vesicles Isolated From Plasma and Urine of Prostate Cancer Patients Using a Multiplex, Aptamer-Based Protein Array. *J Extracell Vesicles* (2016) 5:31209. doi: 10.3402/jev.v5.31209
75. Afshar-Kharghan V. The Role of the Complement System in Cancer. *J Clin Invest* (2017) 127(3):780–9. doi: 10.1172/JCI90962
76. Mangogna A, Belmonte B, Agostinis C, Zacchi P, Iacopino DG, Martorana A, et al. Prognostic Implications of the Complement Protein C1q in Gliomas. *Front Immunol* (2019) 10:2366. doi: 10.3389/fimmu.2019.02366
77. Riihilä P, Viiklepp K, Nissinen L, Farshchian M, Kallajoki M, Kivisaari A, et al. Tumour-Cell-Derived Complement Components C1r and C1s Promote Growth of Cutaneous Squamous Cell Carcinoma. *Br J Dermatol* (2020) 182(3):658–70. doi: 10.1111/bjd.18095

78. Dirix LY, Salgado R, Weytjens R, Colpaert C, Benoy I, Huget P, et al. Plasma Fibrin D-Dimer Levels Correlate With Tumour Volume, Progression Rate and Survival in Patients With Metastatic Breast Cancer. *Br J Cancer* (2002) 86(3):389–95. doi: 10.1038/sj.bjc.6600069
79. Simpson-Haidaris PJ, Rybarczyk B. Tumors and Fibrinogen. The Role of Fibrinogen as an Extracellular Matrix Protein. *Ann New York Acad Sci* (2001) 936:406–25. doi: 10.1111/j.1749-6632.2001.tb03525.x
80. Lin TC, Yang CH, Cheng LH, Chang WT, Lin YR, Cheng HC. Fibronectin in Cancer: Friend or Foe. *Cells* (2019) 9(1):27. doi: 10.3390/cells9010027
81. Mangogna A, Varghese PM, Agostinis C, Alrokayan SH, Khan HA, Stover CM, et al. Prognostic Value of Complement Properdin in Cancer. *Front Immunol* (2020) 11:614980. doi: 10.3389/fimmu.2020.614980
82. Yang AJ, Wang M, Wang Y, Cai W, Li Q, Zhao TT, et al. Cancer Cell-Derived Von Willebrand Factor Enhanced Metastasis of Gastric Adenocarcinoma. *Oncogenesis* (2018) 7(1):12. doi: 10.1038/s41389-017-0023-5
83. Gabriel K, Ingram A, Austin R, Kapoor A, Tang D, Majeed F, et al. Regulation of the Tumor Suppressor PTEN Through Exosomes: A Diagnostic Potential for Prostate Cancer. *PloS One* (2013) 8(7):e70047. doi: 10.1371/journal.pone.0070047
84. Frank MH, Denton MD, Alexander SI, Khoury SJ, Sayegh MH, Briscoe DM. Specific MDR1 P-Glycoprotein Blockade Inhibits Human Alloimmune T Cell Activation *In Vitro*. *J Immunol (Baltimore Md. 1950)* (2001) 166 (4):2451–9. doi: 10.4049/jimmunol.166.4.2451
85. Cory TJ, He H, Winchester LC, Kumar S, Fletcher CV. Alterations in P-Glycoprotein Expression and Function Between Macrophage Subsets. *Pharm Res* (2016) 33(11):2713–21. doi: 10.1007/s11095-016-1998-x
86. Øverbye A, Skotland T, Koehler CJ, Thiede B, Seierstad T, Berge V, et al. Identification of Prostate Cancer Biomarkers in Urinary Exosomes. *Oncotarget* (2015) 6(30):30357–76. doi: 10.18632/oncotarget.4851
87. Bhardwaj A, Singh S, Srivastava SK, Arora S, Hyde SJ, Andrews J, et al. Restoration of PPP2CA Expression Reverses Epithelial-to-Mesenchymal Transition and Suppresses Prostate Tumour Growth and Metastasis in an Orthotopic Mouse Model. *Br J Cancer* (2014) 110(8):2000–10. doi: 10.1038/bjc.2014.141
88. Shaughnessy R, Echard A. Rab35 GTPase and Cancer: Linking Membrane Trafficking to Tumorigenesis. *Traffic (Copenhagen Denmark)* (2018) 19 (4):247–52. doi: 10.1111/tra.12546
89. Nedjadi T, Kitteringham N, Campbell F, Jenkins RE, Park BK, Navarro P, et al. S100A6 Binds to Annexin 2 in Pancreatic Cancer Cells and Promotes Pancreatic Cancer Cell Motility. *Br J Cancer* (2009) 101(7):1145–54. doi: 10.1038/sj.bjc.6605289
90. Di Virgilio F. Purines, Purinergic Receptors, and Cancer. *Cancer Res* (2012) 72(21):5441–7. doi: 10.1158/0008-5472.CAN-12-1600
91. Hsu DK, Chen HY, Liu FT. Galectin-3 Regulates T-Cell Functions. *Immunol Rev* (2009) 230(1):114–27. doi: 10.1111/j.1600-065X.2009.00798.x
92. Nakahara S, Oka N, Raz A. On the Role of Galectin-3 in Cancer Apoptosis. *Apoptosis an Int J Programmed Cell Death* (2005) 10(2):267–75. doi: 10.1007/s10495-005-0801-y
93. Funasaka T, Raz A, Nangia-Makker P. Galectin-3 in Angiogenesis and Metastasis. *Glycobiology* (2014) 24(10):886–91. doi: 10.1093/glycob/cwu086
94. Merseburger AS, Kramer MW, Hennenlotter J, Simon P, Knapp J, Hartmann JT, et al. Involvement of Decreased Galectin-3 Expression in the Pathogenesis and Progression of Prostate Cancer. *Prostate* (2008) 68 (1):72–7. doi: 10.1002/pros.20688
95. Gauthier-Rouvière C, Bodin S, Comunale F, Planchon D. Flotillin Membrane Domains in Cancer. *Cancer Metastasis Rev* (2020) 39(2):361–74. doi: 10.1007/s10555-020-09873-y
96. Cifuentes E, Mataraza JM, Yoshida BA, Menon M, Sacks DB, Barrack ER, et al. Physical and Functional Interaction of Androgen Receptor With Calmodulin in Prostate Cancer Cells. *Proc Natl Acad Sci USA* (2004) 101 (2):464–9. doi: 10.1073/pnas.0307161101
97. Liang H, Xiong Z, Li R, Hu K, Cao M, Yang J, et al. BDH2 is Downregulated in Hepatocellular Carcinoma and Acts as a Tumor Suppressor Regulating Cell Apoptosis and Autophagy. *J Cancer* (2019) 10(16):3735–45. doi: 10.7150/jca.32022
98. Zhang SF, Wang XY, Fu ZQ, Peng QH, Zhang JY, Ye F, et al. TXNDC17 Promotes Paclitaxel Resistance *via* Inducing Autophagy in Ovarian Cancer. *Autophagy* (2015) 11(2):225–38. doi: 10.1080/15548627.2014.998931
99. Wu Y, Du H, Zhan M, Wang H, Chen P, Du D, et al. Sepiapterin Reductase Promotes Hepatocellular Carcinoma Progression *via* FoxO3a/Bim Signaling in a Nonenzymatic Manner. *Cell Death Dis* (2020) 11(4):248. doi: 10.1038/s41419-020-2471-7
100. Zhang X, Chen Y, Wang K, Tang J, Chen Y, Jin G, et al. The Knockdown of the Sepiapterin Reductase Gene Suppresses the Proliferation of Breast Cancer by Inducing ROS-Mediated Apoptosis. *Int J Clin Exp Pathol* (2020) 13(9):2228–39.
101. Zhang T, Sun Y, Zheng T, Wang R, Jia D, Zhang W. MLPH Accelerates the Epithelial-Mesenchymal Transition in Prostate Cancer. *Onco Targets Ther* (2020) 13:701–8. doi: 10.2147/OTT.S225023
102. Wei CY, Zhu MX, Lu NH, Peng R, Yang X, Zhang PF, et al. Bioinformatics-Based Analysis Reveals Elevated MFSD12 as a Key Promoter of Cell Proliferation and a Potential Therapeutic Target in Melanoma. *Oncogene* (2019) 38(11):1876–91. doi: 10.1038/s41388-018-0531-6
103. Gonzalez A, Valeiras M, Sidransky E, Tayebi N. Lysosomal Integral Membrane Protein-2: A New Player in Lysosome-Related Pathology. *Mol Genet Metab* (2014) 111(2):84–91. doi: 10.1016/j.ymgme.2013.12.005
104. Li D, Cheng X, Zheng W, Chen J. Glucosamine-6-Phosphate Isomerase 1 Promotes Tumor Progression and Indicates Poor Prognosis in Hepatocellular Carcinoma. *Cancer Manag Res* (2020) 12:4923–35. doi: 10.2147/CMAR.S250094
105. Moriwaki K, Shinzaki S, Miyoshi E. GDP-Mannose-4,6-Dehydratase (GMDS) Deficiency Renders Colon Cancer Cells Resistant to Tumor Necrosis Factor-Related Apoptosis-Inducing Ligand (TRAIL) Receptor- and CD95-Mediated Apoptosis by Inhibiting Complex II Formation. *J Biol Chem* (2011) 286(50):43123–33. doi: 10.1074/jbc.M111.262741
106. Li Z, Xuan W, Huang L, Chen N, Hou Z, Lu B, et al. Claudin 10 Acts as a Novel Biomarker for the Prognosis of Patients With Ovarian Cancer. *Oncol Lett* (2020) 20(1):373–81. doi: 10.3892/ol.2020.11557
107. Andrijes R, Hejmadi RK, Pugh M, Rajesh S, Novitskaya V, Ibrahim M, et al. Tetraspanin 6 is a Regulator of Carcinogenesis in Colorectal Cancer. *Proc Natl Acad Sci USA* (2021) 118(39):e2011411118. doi: 10.1073/pnas.2011411118
108. Shih Ie M, Wang TL. Notch Signaling, Gamma-Secretase Inhibitors, and Cancer Therapy. *Cancer Res* (2007) 67(5):1879–82. doi: 10.1158/0008-5472.CAN-06-3958
109. Wu PH, Onodera Y, Giaccia AJ, Le QT, Shimizu S, Shirato H, et al. Lysosomal Trafficking Mediated by Arl8b and BORC Promotes Invasion of Cancer Cells That Survive Radiation. *Commun Biol* (2020) 3(1):620. doi: 10.1038/s42003-020-01339-9
110. Liu XY, Jiang W, Ma D, Ge LP, Yang YS, Gou ZC, et al. SYTL4 Downregulates Microtubule Stability and Confers Paclitaxel Resistance in Triple-Negative Breast Cancer. *Theranostics* (2020) 10(24):10940–56. doi: 10.7150/thno.45207
111. Arumugam T, Logsdon CD. S100P: A Novel Therapeutic Target for Cancer. *Amino Acids* (2011) 41(4):893–9. doi: 10.1007/s00726-010-0496-4
112. Kim RH, Peters M, Jang Y, Shi W, Pintilie M, Fletcher GC, et al. DJ-1, a Novel Regulator of the Tumor Suppressor PTEN. *Cancer Cell* (2005) 7 (3):263–73. doi: 10.1016/j.ccr.2005.02.010
113. Scarl RT, Lawrence CM, Gordon HM, Nunemaker CS. STEAP4: Its Emerging Role in Metabolism and Homeostasis of Cellular Iron and Copper. *J Endocrinol* (2017) 234(3):R123–r134. doi: 10.1530/JOE-16-0594
114. Zou P, Yang Y, Xu X, Liu B, Mei F, You J, et al. Silencing of Vacuolar ATPase C Subunit ATP6V0C Inhibits the Invasion of Prostate Cancer Cells Through a LASS2/TMSG1-Independent Manner. *Oncol Rep* (2018) 39(1):298–306. doi: 10.3892/or.2017.6092
115. Steffan JJ, Dykes SS, Coleman DT, Adams LK, Rogers D, Carroll JL, et al. Supporting a Role for the GTPase Rab7 in Prostate Cancer Progression. *PLoS One* (2014) 9(2):e87882. doi: 10.1371/journal.pone.0087882
116. Yang J, Liu W, Lu X, Fu Y, Li L, Luo Y. High Expression of Small GTPase Rab3D Promotes Cancer Progression and Metastasis. *Oncotarget* (2015) 6 (13):11125–38. doi: 10.18632/oncotarget.3575
117. Tan PY, Chang CW, Chng KR, Wansa KD, Sung WK, Cheung E. Integration of Regulatory Networks by NKX3-1 Promotes Androgen-Dependent Prostate Cancer Survival. *Mol Cell Biol* (2012) 32(2):399–414. doi: 10.1128/MCB.05958-11
118. Luo ML, Gong C, Chen CH, Hu H, Huang P, Zheng M, et al. The Rab2A GTPase Promotes Breast Cancer Stem Cells and Tumorigenesis *via* Erk

Signaling Activation. *Cell Rep* (2015) 11(1):111–24. doi: 10.1016/j.celrep.2015.03.002
119. Riplinger SM, Wabnitz GH, Kirchgessner H, Jahraus B, Lasitschka F, Schulte B, et al. Metastasis of Prostate Cancer and Melanoma Cells in a Preclinical *In Vivo* Mouse Model is Enhanced by L-Plastin Expression and Phosphorylation. *Mol Cancer* (2014) 13:10. doi: 10.1186/1476-4598-13-10
120. Colaço A, Jäättelä M. Ragulator-A Multifaceted Regulator of Lysosomal Signaling and Trafficking. *J Cell Biol* (2017) 216(12):3895–8. doi: 10.1083/jcb.201710039
121. Eriksson P, Aine M, Veerla S, Liedberg F, Sjödahl G, Höglund M. Molecular Subtypes of Urothelial Carcinoma are Defined by Specific Gene Regulatory Systems. *BMC Med Genomics* (2015) 8:25. doi: 10.1186/s12920-015-0101-5
122. Chang SS. Overview of Prostate-Specific Membrane Antigen. *Rev Urol* (2004) 6 Suppl 10:S13–8.
123. Gu TL, Cherry J, Tucker M, Wu J, Reeves C, Polakiewicz RD. Identification of Activated Tnk1 Kinase in Hodgkin's Lymphoma. *Leukemia* (2010) 24 (4):861–5. doi: 10.1038/leu.2009.293
124. Hazarika P, McCarty MF, Prieto VG, George S, Babu D, Koul D, et al. Up-Regulation of Flotillin-2 is Associated With Melanoma Progression and Modulates Expression of the Thrombin Receptor Protease Activated Receptor 1. *Cancer Res* (2004) 64(20):7361–9. doi: 10.1158/0008-5472.CAN-04-0823
125. Liu J, Huang W, Ren C, Wen Q, Liu W, Yang X, et al. Flotillin-2 Promotes Metastasis of Nasopharyngeal Carcinoma by Activating NF-κb and PI3K/Akt3 Signaling Pathways. *Sci Rep* (2015) 5:11614. doi: 10.1038/srep11614
126. Wang CH, Zhu XD, Ma DN, Sun HC, Gao DM, Zhang N, et al. Flot2 Promotes Tumor Growth and Metastasis Through Modulating Cell Cycle and Inducing Epithelial-Mesenchymal Transition of Hepatocellular Carcinoma. *Am J Cancer Res* (2017) 7(5):1068–83.
127. Ronquist KG, Ronquist G, Larsson A, Carlsson L. Proteomic Analysis of Prostate Cancer Metastasis-Derived Prostasomes. *Anticancer Res* (2010) 30 (2):285–90.
128. Kennedy L, Sandhu JK, Harper ME, Cuperlovic-Culf M. Role of Glutathione in Cancer: From Mechanisms to Therapies. *Biomolecules* (2020) 10(10):1429. doi: 10.3390/biom10101429
129. Zhao X, Fu J, Du J, Xu W. The Role of D-3-Phosphoglycerate Dehydrogenase in Cancer. *Int J Biol Sci* (2020) 16(9):1495–506. doi: 10.7150/ijbs.41051
130. Kim E, Kwak H, Ahn K. Cytosolic Aminopeptidases Influence MHC Class I-Mediated Antigen Presentation in an Allele-Dependent Manner. *J Immunol (Baltimore Md. 1950)* (2009) 183(11):7379–87. doi: 10.4049/jimmunol.0901489
131. Almaguel FA, Sanchez TW, Ortiz-Hernandez GL, Casiano CA. Alpha-Enolase: Emerging Tumor-Associated Antigen, Cancer Biomarker, and Oncotherapeutic Target. *Front Genet* (2020) 11:614726. doi: 10.3389/fgene.2020.614726
132. Chen J, Cheng X, Merched-Sauvage M, Caulin C, Roop DR, Koch PJ. An Unexpected Role for Keratin 10 End Domains in Susceptibility to Skin Cancer. *J Cell Sci* (2006) 119(Pt 24):5067–76. doi: 10.1242/jcs.03298
133. Guo C, Liu S, Wang J, Sun MZ, Greenaway FT. ACTB in Cancer. *Clin Chim acta; Int J Clin Chem* (2013) 417:39–44. doi: 10.1016/j.cca.2012.12.012
134. Calvert AE, Chalastanis A, Wu Y, Hurley LA, Kouri FM, Bi Y, et al. Cancer-Associated IDH1 Promotes Growth and Resistance to Targeted Therapies in the Absence of Mutation. *Cell Rep* (2017) 19(9):1858–73. doi: 10.1016/j.celrep.2017.05.014
135. Jelski W, Szmitkowski M. Alcohol Dehydrogenase (ADH) and Aldehyde Dehydrogenase (ALDH) in the Cancer Diseases. *Clin Chim acta; Int J Clin Chem* (2008) 395(1-2):1–5. doi: 10.1016/j.cca.2008.05.001
136. Bardella C, Pollard PJ, Tomlinson I. SDH Mutations in Cancer. *Biochim Biophys Acta* (2011) 1807(11):1432–43. doi: 10.1016/j.bbabio.2011.07.003
137. Huang D, Cao L, Zheng S. CAPZA1 Modulates EMT by Regulating Actin Cytoskeleton Remodelling in Hepatocellular Carcinoma. *J Exp Clin Cancer Res CR* (2017) 36(1):13. doi: 10.1186/s13046-016-0474-0
138. Hulin JA, Tommasi S, Elliot D, Mangoni AA. Small Molecule Inhibition of DDAH1 Significantly Attenuates Triple Negative Breast Cancer Cell Vasculogenic Mimicry *In Vitro*. *Biomed Pharmacother* (2019) 111:602–12. doi: 10.1016/j.biopha.2018.12.117
139. Scannell M, Flanagan MB, deStefani A, Wynne KJ, Cagney G, Godson C, et al. Annexin-1 and Peptide Derivatives are Released by Apoptotic Cells and Stimulate Phagocytosis of Apoptotic Neutrophils by Macrophages. *J Immunol (Baltimore Md. 1950)* (2007) 178(7):4595–605. doi: 10.4049/jimmunol.178.7.4595
140. Blume KE, Soeroes S, Waibel M, Keppeler H, Wesselborg S, Herrmann M, et al. Cell Surface Externalization of Annexin A1 as a Failsafe Mechanism Preventing Inflammatory Responses During Secondary Necrosis. *J Immunol (Baltimore Md. 1950)* (2009) 183(12):8138–47. doi: 10.4049/jimmunol.0902250
141. Huggins A, Paschalidis N, Flower RJ, Perretti M, D'Acquisto F. Annexin-1-Deficient Dendritic Cells Acquire a Mature Phenotype During Differentiation. *FASEB J Off Publ Fed Am Soc Exp Biol* (2009) 23(4):985–96. doi: 10.1096/fj.08-119040
142. Bist P, Shu S, Lee H, Arora S, Nair S, Lim JY, et al. Annexin-A1 Regulates TLR-Mediated IFN-β Production Through an Interaction With TANK-Binding Kinase 1. *J Immunol (Baltimore Md. 1950)* (2013) 191(8):4375–82. doi: 10.4049/jimmunol.1301504
143. Jorge YC, Mataruco MM, Araújo LP, Rossi AF, de Oliveira JG, Valsechi MC, et al. Expression of Annexin-A1 and Galectin-1 Anti-Inflammatory Proteins and mRNA in Chronic Gastritis and Gastric Cancer. *Mediators Inflammation* (2013) 2013:152860. doi: 10.1155/2013/152860
144. Ullah MF. Sulforaphane (SFN): An Isothiocyanate in a Cancer Chemoprevention Paradigm. *Medicines (Basel Switzerland)* (2015) 2 (3):141–56. doi: 10.3390/medicines2030141
145. Tang J, Qin Z, Han P, Wang W, Yang C, Xu Z, et al. High Annexin A5 Expression Promotes Tumor Progression and Poor Prognosis in Renal Cell Carcinoma. *Int J Oncol* (2017) 50(5):1839–47. doi: 10.3892/ijo.2017.3942
146. Yang L, Lu P, Yang X, Li K, Qu S. Annexin A3, A Calcium-Dependent Phospholipid-Binding Protein: Implication in Cancer. *Front Mol Biosci* (2021) 8:716415. doi: 10.3389/fmolb.2021.716415
147. Iwamoto K, Takahashi H, Okuzaki D, Osawa H, Ogino T, Miyoshi N, et al. Syntenin-1 Promotes Colorectal Cancer Stem Cell Expansion and Chemoresistance by Regulating Prostaglandin E2 Receptor. *Br J Cancer* (2020) 123(6):955–64. doi: 10.1038/s41416-020-0965-9
148. van Ommeren R, Staudt MD, Xu H, Hebb MO. Advances in HSP27 and HSP90-Targeting Strategies for Glioblastoma. *J Neuro-oncol* (2016) 127 (2):209–19. doi: 10.1007/s11060-016-2070-8
149. Hansen RK, Parra I, Hilsenbeck SG, Himelstein B, Fuqua SA. Hsp27-Induced MMP-9 Expression is Influenced by the Src Tyrosine Protein Kinase Yes. *Biochem Biophys Res Commun* (2001) 282(1):186–93. doi: 10.1006/bbrc.2001.4548
150. Lemieux P, Oesterreich S, Lawrence JA, Steeg PS, Hilsenbeck SG, Harvey JM, et al. The Small Heat Shock Protein Hsp27 Increases Invasiveness But Decreases Motility of Breast Cancer Cells. *Invasion Metastasis* (1997) 17 (3):113–23.
151. Liang HH, Huang CY, Chou CW, Makondi PT, Huang MT, Wei PL, et al. Heat Shock Protein 27 Influences the Anti-Cancer Effect of Curcumin in Colon Cancer Cells Through ROS Production and Autophagy Activation. *Life Sci* (2018) 209:43–51. doi: 10.1016/j.lfs.2018.07.047
152. Chang X-Z, Li D-Q, Hou Y-F, Wu J, Lu J-S, Di G-H, et al. Identification of the Functional Role of Peroxiredoxin 6 in the Progression of Breast Cancer. *Breast Cancer Res* (2007) 9(6):1–15. doi: 10.1186/bcr1789
153. Chen T, Huang Z, Tian Y, Lin B, He R, Wang H, et al. Clinical Significance and Prognostic Value of Triosephosphate Isomerase Expression in Gastric Cancer. *Medicine* (2017) 96(19):e6865. doi: 10.1097/MD.0000000000006865
154. Schoentgen F, Jonic SJAPA. PEBP1/RKIP: From Multiple Functions to a Common Role in Cellular Processes. (2018) arXiv:1802.02378. doi: doi: 10.48550/arXiv.1802.02378
155. Ishiguro H, Izumi K, Kashiwagi E, Zheng Y, Li Y, Kawahara T, et al. Semenogelin I Promotes Prostate Cancer Cell Growth *via* Functioning as an Androgen Receptor Coactivator and Protecting Against Zinc Cytotoxicity. *Am J Cancer Res* (2015) 5(2):738–47.
156. Hileman EA, Achanta G, Huang P. Superoxide Dismutase: An Emerging Target for Cancer Therapeutics. *Expert Opin Ther Targets* (2001) 5(6):697–710. doi: 10.1517/14728222.5.6.697
157. Hosseini SM, Okoye I, Chaleshtari MG, Hazhirkarzar B, Mohamadnejad J, Azizi G, et al. E2 Ubiquitin-Conjugating Enzymes in Cancer: Implications for Immunotherapeutic Interventions. *Clin Chim acta; Int J Clin Chem* (2019) 498:126–34. doi: 10.1016/j.cca.2019.08.020

158. Edechi CA, Ikeogu NM, Akaluka GN, Terceiro LEL, Machado M, Salako ES, et al. The Prolactin Inducible Protein Modulates Antitumor Immune Responses and Metastasis in a Mouse Model of Triple Negative Breast Cancer. *Front Oncol* (2021) 11:639859. doi: 10.3389/fonc.2021.639859
159. Markowitz J, Carson WE. 3rd, Review of S100A9 Biology and its Role in Cancer. *Biochim Biophys Acta* (2013) 1835(1):100–9. doi: 10.1016/j.bbcan.2012.10.003
160. Wei X, Zhou J, Hong L, Xu Z, Zhao H, Wu X, et al. Hint1 Expression Inhibits Proliferation and Promotes Radiosensitivity of Human SGC7901 Gastric Cancer Cells. *Oncol Lett* (2018) 16(2):2135–42. doi: 10.3892/ol.2018.8900
161. Duman C, Yaqubi K, Hoffmann A, Acikgöz AA, Korshunov A, Bendszus M, et al. Acyl-CoA-Binding Protein Drives Glioblastoma Tumorigenesis by Sustaining Fatty Acid Oxidation. *Cell Metab* (2019) 30(2):274–89.e5. doi: 10.1016/j.cmet.2019.04.004
162. Meng M, Sang L, Wang X. S100 Calcium Binding Protein A11 (S100A11) Promotes The Proliferation, Migration And Invasion Of Cervical Cancer Cells, And Activates Wnt/β-Catenin Signaling. *Onco Targets Ther* (2019) 12:8675–85. doi: 10.2147/OTT.S225248
163. Luanpitpong S, Talbott SJ, Rojanasakul Y, Nimmannit U, Pongrakhananon V, Wang L, et al. Regulation of Lung Cancer Cell Migration and Invasion by Reactive Oxygen Species and Caveolin-1. *J Biol Chem* (2010) 285(50):38832–40. doi: 10.1074/jbc.M110.124958
164. Basu GD, Azorsa DO, Kiefer JA, Rojas AM, Tuzmen S, Barrett MT, et al. Functional Evidence Implicating S100P in Prostate Cancer Progression. *Int J Cancer* (2008) 123(2):330–9. doi: 10.1002/ijc.23447
165. Lange I, Geerts D, Feith DJ, Mocz G, Koster J, Bachmann AS. Novel Interaction of Ornithine Decarboxylase With Sepiapterin Reductase Regulates Neuroblastoma Cell Proliferation. *J Mol Biol* (2014) 426(2):332–46. doi: 10.1016/j.jmb.2013.09.037
166. Liu H, Liu JY, Wu X, Zhang JT. Biochemistry, Molecular Biology, and Pharmacology of Fatty Acid Synthase, an Emerging Therapeutic Target and Diagnosis/Prognosis Marker. *Int J Biochem Mol Biol* (2010) 1(1):69–89.
167. Słomnicki ŁP, Nawrot B, Leśniak W. S100A6 Binds P53 and Affects its Activity. *Int J Biochem Cell Biol* (2009) 41(4):784–90. doi: 10.1016/j.biocel.2008.08.007
168. van Dieck J, Brandt T, Teufel DP, Veprintsev DB, Joerger AC, Fersht AR. Molecular Basis of S100 Proteins Interacting With the P53 Homologs P63 and P73. *Oncogene* (2010) 29(14):2024–35. doi: 10.1038/onc.2009.490
169. Qin DN, Zhu JG, Ji CB, Chunmei S, Kou CZ, Zhu GZ, et al. Monoclonal Antibody to Six Transmembrane Epithelial Antigen of Prostate-4 Influences Insulin Sensitivity by Attenuating Phosphorylation of P13K (P85) and Akt: Possible Mitochondrial Mechanism. *J Bioenerg Biomembr* (2011) 43(3):247–55. doi: 10.1007/s10863-011-9360-9
170. Webber JP, Spary LK, Sanders AJ, Chowdhury R, Jiang WG, Steadman R, et al. Differentiation of Tumour-Promoting Stromal Myofibroblasts by Cancer Exosomes. *Oncogene* (2015) 34(3):290–302. doi: 10.1038/onc.2013.560
171. Hayes JD, Dinkova-Kostova AT, Tew KD. Oxidative Stress in Cancer. *Cancer Cell* (2020) 38(2):167–97. doi: 10.1016/j.ccell.2020.06.001
172. Ying W. NAD+/NADH and NADP+/NADPH in Cellular Functions and Cell Death: Regulation and Biological Consequences. *Antioxid Redox Signaling* (2008) 10(2):179–206. doi: 10.1089/ars.2007.1672
173. Neophytou CM, Panagi M, Stylianopoulos T, Papageorgis P. The Role of Tumor Microenvironment in Cancer Metastasis: Molecular Mechanisms and Therapeutic Opportunities. *Cancers* (2021) 13(9):2053. doi: 10.3390/cancers13092053
174. Thuringer D, Jego G, Wettstein G, Terrier O, Cronier L, Yousfi N, et al. Extracellular HSP27 Mediates Angiogenesis Through Toll-Like Receptor 3. *FASEB J Off Publ Fed Am Soc Exp Biol* (2013) 27(10):4169–83. doi: 10.1096/fj.12-226977
175. Jang D, Kwon H, Jeong K, Lee J, Pak Y. Essential Role of Flotillin-1 Palmitoylation in the Intracellular Localization and Signaling Function of IGF-1 Receptor. *J Cell Sci* (2015) 128(11):2179–90. doi: 10.1242/jcs.169409
176. Shinbo Y, Taira T, Niki T, Iguchi-Ariga SM, Ariga H. DJ-1 Restores P53 Transcription Activity Inhibited by Topors/P53bp3. *Int J Oncol* (2005) 26 (3):641–8. doi: 10.3892/ijo.26.3.641
177. Takahashi-Niki K, Ganaha Y, Niki T, Nakagawa S, Kato-Ose I, Iguchi-Ariga SMM, et al. DJ-1 Activates SIRT1 Through its Direct Binding to SIRT1. *Biochem Biophys Res Commun* (2016) 474(1):131–6. doi: 10.1016/j.bbrc.2016.04.084
178. Watanabe J, Kamata Y, Seo N, Okayasu I, Kuramoto H. Stimulatory Effect of Estrogen on the Growth of Endometrial Cancer Cells is Regulated by Cell-Cycle Regulators. *J Steroid Biochem Mol Biol* (2007) 107(3-5):163–71. doi: 10.1016/j.jsbmb.2007.03.045
179. Bosch M, Gil J, Bachs O, Agell N. Calmodulin Inhibitor W13 Induces Sustained Activation of ERK2 and Expression of P21(Cip1). *J Biol Chem* (1998) 273(34):22145–50. doi: 10.1074/jbc.273.34.22145
180. Pandey MK, Prasad S, Tyagi AK, Deb L, Huang J, Karelia DN, et al. Targeting Cell Survival Proteins for Cancer Cell Death. *Pharmaceut (Basel Switzerland)* (2016) 9(1):11. doi: 10.3390/ph9010011
181. Boroughs LK, DeBerardinis RJ. Metabolic Pathways Promoting Cancer Cell Survival and Growth. *Nat Cell Biol* (2015) 17(4):351–9. doi: 10.1038/ncb3124
182. Liu Y, Shi K, Chen Y, Wu X, Chen Z, Cao K, et al. Exosomes and Their Role in Cancer Progression. *Front Oncol* (2021) 11:639159. doi: 10.3389/fonc.2021.639159
183. Gordon SR, Maute RL, Dulken BW, Hutter G, George BM, McCracken MN, et al. PD-1 Expression by Tumour-Associated Macrophages Inhibits Phagocytosis and Tumour Immunity. *Nature* (2017) 545(7655):495–9. doi: 10.1038/nature22396
184. Dong H, Strome SE, Salomao DR, Tamura H, Hirano F, Flies DB, et al. Tumor-Associated B7-H1 Promotes T-Cell Apoptosis: A Potential Mechanism of Immune Evasion. *Nat Med* (2002) 8(8):793–800. doi: 10.1038/nm730
185. Clayton A, Mitchell JP, Court J, Linnane S, Mason MD, Tabi Z. Human Tumor-Derived Exosomes Down-Modulate NKG2D Expression. *J Immunol (Baltimore Md. 1950)* (2008) 180(11):7249–58. doi: 10.4049/jimmunol.180.11.7249
186. Clayton A, Mitchell JP, Court J, Mason MD, Tabi Z. Human Tumor-Derived Exosomes Selectively Impair Lymphocyte Responses to Interleukin-2. *Cancer Res* (2007) 67(15):7458–66. doi: 10.1158/0008-5472.CAN-06-3456
187. Novitskiy SV, Ryzhov S, Zaynagetdinov R, Goldstein AE, Huang Y, Tikhomirov OY, et al. Adenosine Receptors in Regulation of Dendritic Cell Differentiation and Function. *Blood* (2008) 112(5):1822–31. doi: 10.1182/blood-2008-02-136325
188. Wang R, Liu Y, Liu L, Chen M, Wang X, Yang J, et al. Tumor Cells Induce LAMP2a Expression in Tumor-Associated Macrophage for Cancer Progression. *EBioMedicine* (2019) 40:118–34. doi: 10.1016/j.ebiom.2019.01.045
189. Cho JA, Park H, Lim EH, Lee KW. Exosomes From Breast Cancer Cells can Convert Adipose Tissue-Derived Mesenchymal Stem Cells Into Myofibroblast-Like Cells. *Int J Oncol* (2012) 40(1):130–8. doi: 10.3892/ijo.2011.1193
190. Zhong H, Chiles K, Feldser D, Laughner E, Hanrahan C, Georgescu MM, et al. Modulation of Hypoxia-Inducible Factor 1alpha Expression by the Epidermal Growth Factor/Phosphatidylinositol 3-Kinase/PTEN/AKT/FRAP Pathway in Human Prostate Cancer Cells: Implications for Tumor Angiogenesis and Therapeutics. *Cancer Res* (2000) 60(6):1541–5.
191. Chien CH, Lee MJ, Liou HC, Liou HH, Fu WM. Local Immunosuppressive Microenvironment Enhances Migration of Melanoma Cells to Lungs in DJ-1 Knockout Mice. *PLoS One* (2015) 10(2):e0115827. doi: 10.1371/journal.pone.0115827
192. Huggins C, Hodges CV. Studies on Prostatic Cancer. I. The Effect of Castration, of Estrogen and Androgen Injection on Serum Phosphatases in Metastatic Carcinoma of the Prostate. *CA: Cancer J Clin* (1972) 22(4):232–40. doi: 10.3322/canjclin.22.4.232
193. Attard G, Reid AH, Auchus RJ, Hughes BA, Cassidy AM, Thompson E, et al. Clinical and Biochemical Consequences of CYP17A1 Inhibition With Abiraterone Given With and Without Exogenous Glucocorticoids in Castrate Men With Advanced Prostate Cancer. *J Clin Endocrinol Metab* (2012) 97(2):507–16. doi: 10.1210/jc.2011-2189
194. Cheng KW, Agarwal R, Mitra S, Lee JS, Carey M, Gray JW, et al. Rab25 Increases Cellular ATP and Glycogen Stores Protecting Cancer Cells From Bioenergetic Stress. *EMBO Mol Med* (2012) 4(2):125–41. doi: 10.1002/emmm.201100193
195. Walther TC, Chung J, Farese RVJrs. Lipid Droplet Biogenesis. *Annu Rev Cell Dev Biol* (2017) 33:491–510. doi: 10.1146/annurev-cellbio-100616-060608

196. Wu L, Xu D, Zhou L, Xie B, Yu L, Yang H, et al. Rab8a-AS160-MSS4 Regulatory Circuit Controls Lipid Droplet Fusion and Growth. *Dev Cell* (2014) 30(4):378–93. doi: 10.1016/j.devcel.2014.07.005
197. Raposo G, Stoorvogel W. Extracellular Vesicles: Exosomes, Microvesicles, and Friends. *J Cell Biol* (2013) 200(4):373–83. doi: 10.1083/jcb.201211138
198. Schiefermeier N, Scheffler JM, de Araujo ME, Stasyk T, Yordanov T, Ebner HL, et al. The Late Endosomal P14-MP1 (LAMTOR2/3) Complex Regulates Focal Adhesion Dynamics During Cell Migration. *J Cell Biol* (2014) 205 (4):525–40. doi: 10.1083/jcb.201310043
199. Tuli A, Thiery J, James AM, Michelet X, Sharma M, Garg S, et al. Arf-Like GTPase Arl8b Regulates Lytic Granule Polarization and Natural Killer Cell-Mediated Cytotoxicity. *Mol Biol Cell* (2013) 24(23):3721–35. doi: 10.1091/mbc.e13-05-0259
200. Shin IY, Sung NY, Lee YS, Kwon TS, Si Y, Lee YS, et al. The Expression of Multiple Proteins as Prognostic Factors in Colorectal Cancer: Cathepsin D, P53, COX-2, Epidermal Growth Factor Receptor, C-erbB-2, and Ki-67. *Gut Liver* (2014) 8(1):13–23. doi: 10.5009/gnl.2014.8.1.13
201. Hahm ER, Singh KB, Kim SH, Powolny AA, Singh SV. The Role of Lysosome-Associated Membrane Protein 2 in Prostate Cancer Chemopreventive Mechanisms of Sulforaphane. *Cancer Prev Res (Phila)* (2020) 13(8):661–72. doi: 10.1158/1940-6207.CAPR-20-0054
202. Ding ZB, Fu XT, Shi YH, Zhou J, Peng YF, Liu WR, et al. Lamp2a is Required for Tumor Growth and Promotes Tumor Recurrence of Hepatocellular Carcinoma. *Int J Oncol* (2016) 49(6):2367–76. doi: 10.3892/ijo.2016.3754
203. Timme TL, Goltsov A, Tahir S, Li L, Wang J, Ren C, et al. Caveolin-1 is Regulated by C-Myc and Suppresses C-Myc-Induced Apoptosis. *Oncogene* (2000) 19(29):3256–65. doi: 10.1038/sj.onc.1203654
204. Sporn MB. The War on Cancer. *Lancet (London England)* (1996) 347 (9012):1377–81. doi: 10.1016/S0140-6736(96)91015-6
205. Bijnsdorp IV, Geldof AA, Lavaei M, Piersma SR, van Moorselaar RJ, Jimenez CR. Exosomal ITGA3 Interferes With non-Cancerous Prostate Cell Functions and is Increased in Urine Exosomes of Metastatic Prostate Cancer Patients. *J Extracell Vesicles* (2013) 2:22079. doi: 10.3402/jev.v2i0.22097
206. Allard D, Chrobak P, Allard B, Messaoudi N, Stagg J. Targeting the CD73-Adenosine Axis in Immuno-Oncology. *Immunol Lett* (2019) 205:31–9. doi: 10.1016/j.imlet.2018.05.001
207. Ebos JM, Lee CR, Cruz-Munoz W, Bjarnason GA, Christensen JG, Kerbel RS. Accelerated Metastasis After Short-Term Treatment With a Potent Inhibitor of Tumor Angiogenesis. *Cancer Cell* (2009) 15(3):232–9. doi: 10.1016/j.ccr.2009.01.021
208. Gesierich S, Berezovskiy I, Ryschich E, Zöller M. Systemic Induction of the Angiogenesis Switch by the Tetraspanin D6.1A/CO-029. *Cancer Res* (2006) 66(14):7083–94. doi: 10.1158/0008-5472.CAN-06-0391
209. Chen C, Duckworth CA, Zhao Q, Pritchard DM, Rhodes JM, Yu LG. Increased Circulation of Galectin-3 in Cancer Induces Secretion of Metastasis-Promoting Cytokines From Blood Vascular Endothelium. *Clin Cancer Res an Off J Am Assoc Cancer Res* (2013) 19(7):1693–704. doi: 10.1158/1078-0432.CCR-12-2940
210. Zeng Q, Li S, Chepeha DB, Giordano TJ, Li J, Zhang H, et al. Crosstalk Between Tumor and Endothelial Cells Promotes Tumor Angiogenesis by MAPK Activation of Notch Signaling. *Cancer Cell* (2005) 8(1):13–23. doi: 10.1016/j.ccr.2005.06.004
211. Casimiro S, Guise TA, Chirgwin J. The Critical Role of the Bone Microenvironment in Cancer Metastases. *Mol Cell Endocrinol* (2009) 310 (1-2):71–81. doi: 10.1016/j.mce.2009.07.004
212. Tauro BJ, Mathias RA, Greening DW, Gopal SK, Ji H, Kapp EA, et al. Oncogenic H-Ras Reprograms Madin-Darby Canine Kidney (MDCK) Cell-Derived Exosomal Proteins Following Epithelial-Mesenchymal Transition. *Mol Cell Proteomics* (2013) 12(8):2148–59. doi: 10.1074/mcp.M112.027086
213. Stuelten CH, Parent CA, Montell DJ. Cell Motility in Cancer Invasion and Metastasis: Insights From Simple Model Organisms. *Nat Rev Cancer* (2018) 18(5):296–312. doi: 10.1038/nrc.2018.15
214. Berditchevski F. Complexes of Tetraspanins With Integrins: More Than Meets the Eye. *J Cell Sci* (2001) 114(Pt 23):4143–51. doi: 10.1242/jcs.114.23.4143
215. Yánez-Mó M, Mittelbrunn M, Sánchez-Madrid F. Tetraspanins and Intercellular Interactions. *Microcirc (New York N.Y 1994)* (2001) 8(3):153–68. doi: 10.1111/j.1549-8719.2001.tb00166.x
216. Ang J, Lijovic M, Ashman LK, Kan K, Frauman AG. CD151 Protein Expression Predicts the Clinical Outcome of Low-Grade Primary Prostate Cancer Better Than Histologic Grading: A New Prognostic Indicator? *Cancer Epidemiol Biomarkers Prev Publ Am Assoc Cancer Res Cosponsored by Am Soc Prev Oncol* (2004) 13(11 Pt 1):1717–21.
217. Detchokul S, Williams ED, Parker MW, Frauman AG. Tetraspanins as Regulators of the Tumour Microenvironment: Implications for Metastasis and Therapeutic Strategies. *Br J Pharmacol* (2014) 171(24):5462–90. doi: 10.1111/bph.12260
218. Gesierich S, Paret C, Hildebrand D, Weitz J, Zgraggen K, Schmitz-Winnenthal FH, et al. Colocalization of the Tetraspanins, CO-029 and CD151, With Integrins in Human Pancreatic Adenocarcinoma: Impact on Cell Motility. *Clin Cancer Res an Off J Am Assoc Cancer Res* (2005) 11 (8):2840–52. doi: 10.1158/1078-0432.CCR-04-1935
219. Ang J, Fang BL, Ashman LK, Frauman AG. The Migration and Invasion of Human Prostate Cancer Cell Lines Involves CD151 Expression. *Oncol Rep* (2010) 24(6):1593–7. doi: 10.3892/or_00001022
220. He X, Zheng Z, Li J, Ben Q, Liu J, Zhang J, et al. DJ-1 Promotes Invasion and Metastasis of Pancreatic Cancer Cells by Activating SRC/ERK/uPA. *Carcinogenesis* (2012) 33(3):555–62. doi: 10.1093/carcin/bgs002
221. Boscher C, Nabi IR. Galectin-3- and Phospho-Caveolin-1-Dependent Outside-in Integrin Signaling Mediates the EGF Motogenic Response in Mammary Cancer Cells. *Mol Biol Cell* (2013) 24(13):2134–45. doi: 10.1091/mbc.e13-02-0095
222. Espinosa-Sánchez A, Suárez-Martínez E, Sánchez-Díaz L, Carnero A. Therapeutic Targeting of Signaling Pathways Related to Cancer Stemness. *Front Oncol* (2020) 10:1533. doi: 10.3389/fonc.2020.01533
223. McCubrey JA, Abrams SL, Fitzgerald TL, Cocco L, Martelli AM, Montalto G, et al. Roles of Signaling Pathways in Drug Resistance, Cancer Initiating Cells and Cancer Progression and Metastasis. *Adv Biol Regul* (2015) 57:75–101. doi: 10.1016/j.jbior.2014.09.016
224. Saha T. LAMP2A Overexpression in Breast Tumors Promotes Cancer Cell Survival *via* Chaperone-Mediated Autophagy. *Autophagy* (2012) 8 (11):1643–56. doi: 10.4161/auto.21654
225. Bao L, Lv L, Feng J, Chen Y, Wang X, Han S, et al. miR-487b-5p Regulates Temozolomide Resistance of Lung Cancer Cells Through LAMP2-Medicated Autophagy. *DNA Cell Biol* (2016) 35(8):385–92. doi: 10.1089/dna.2016.3259
226. Xu H, Hong FZ, Li S, Zhang P, Zhu L. Short Hairpin RNA-Mediated MDR1 Gene Silencing Increases Apoptosis of Human Ovarian Cancer Cell Line A2780/Taxol. *Chin J Cancer Res* (2012) 24(2):138–42. doi: 10.1007/s11670-012-0138-3
227. Stewart JJ, White JT, Yan X, Collins S, Drescher CW, Urban ND, et al. Proteins Associated With Cisplatin Resistance in Ovarian Cancer Cells Identified by Quantitative Proteomic Technology and Integrated With mRNA Expression Levels. *Mol Cell Proteomics* (2006) 5(3):433–43. doi: 10.1074/mcp.M500140-MCP200

Conflict of Interest: The authors declare that the research was conducted in the absence of any commercial or financial relationships that could be construed as a potential conflict of interest.

frontiers | Frontiers in Oncology

MINI REVIEW
published: 04 July 2022
doi: 10.3389/fonc.2022.862416

Myeloid-Derived Suppressor Cells as Key Players and Promising Therapy Targets in Prostate Cancer

Izabela Siemińska[1,2] *and Jarek Baran*[1*]

[1] Department of Clinical Immunology, Jagiellonian University Medical College, Cracow, Poland, [2] University Centre of Veterinary Medicine, Jagiellonian University - University of Agriculture, Cracow, Poland

Prostate cancer (PC) is the second most often diagnosed malignancy in men and one of the major causes of cancer death worldwide. Despite genetic predispositions, environmental factors, including a high-fat diet, obesity, a sedentary lifestyle, infections of the prostate, and exposure to chemicals or ionizing radiation, play a crucial role in PC development. Moreover, due to a lack of, or insufficient T-cell infiltration and its immunosuppressive microenvironment, PC is frequently classified as a "cold" tumor. This is related to the absence of tumor-associated antigens, the lack of T-cell activation and their homing into the tumor bed, and the presence of immunological cells with regulatory functions, including myeloid-derived suppressor cells (MDSCs), regulatory T cells (Treg), and tumor-associated macrophages (TAMs). All of them, by a variety of means, hamper anti-tumor immune response in the tumor microenvironment (TME), stimulating tumor growth and the formation of metastases. Therefore, they emerge as potential anti-cancer therapy targets. This article is focused on the function and role of MDSCs in the initiation and progression of PC. Clinical trials directly targeting this cell population or affecting its biological functions, thus limiting its pro-tumorigenic activity, are also presented.

Keywords: prostate cancer, myeloid-derived suppressor cells, immunosuppression, immunotherapy, anti-tumor immune response

OPEN ACCESS

Edited by:
Hua Li,
Henry M. Jackson Foundation for the Advancement of Military Medicine (HJF), United States

Reviewed by:
Suman Kapur,
Birla Institute of Technology and Science, India
Nader Bagheri,
Shahrekord University of Medical Sciences, Iran

***Correspondence:**
Jarek Baran
mibaran@cyf-kr.edu.pl

Specialty section:
This article was submitted to Genitourinary Oncology, a section of the journal Frontiers in Oncology

Received: *25 January 2022*
Accepted: *06 June 2022*
Published: *04 July 2022*

Citation:
Siemińska I and Baran J (2022) Myeloid-Derived Suppressor Cells as Key Players and Promising Therapy Targets in Prostate Cancer. Front. Oncol. 12:862416. doi: 10.3389/fonc.2022.862416

PROSTATE CANCER—EPIDEMIOLOGY

Prostate cancer (PC) is the most common, after lung cancer, malignancy in men—in 2020, more than 1.4 million new cases of PC were diagnosed worldwide (1, 2). Advanced age, race, and ethnicities such as African descent and family history are well-established risk factors of PC (3–6). Additionally, a higher incidence of PC has been associated with a diet rich in saturated animal fat and red meat, low intake of fruits/vegetables, obesity, hyperglycemia, lack of physical activity, prostate inflammation, as well as exposure to chemicals or ionizing radiation (6–8). The most common genetic predispositions for PC development are related to aberrations of the *PTEN* tumor suppressor gene. Inactivation of *PTEN* by deletion or mutations is identified in ~20% of primary PC and as many as 50% of advanced castration-resistant tumors (9). The role of the immune system and prostatitis in PC development was also confirmed, indicating that inflammatory mediators may promote prostatic carcinogenesis *via* inhibition of apoptosis, promotion of cell proliferation, and

even loss of the tumor suppressor genes (10). Importantly, not only the local, prostate inflammation, but also systemic reaction associated with chronic inflammatory diseases, including asthma and allergies, are associated with the higher risk of PC (11).

Most of the patients develop a low-risk neoplasm (12); however, approximately 15% of men with localized PC present with high-risk tumors, which will progress, metastasize, and finally result in death (13). In men with advanced metastatic prostate cancer (mPC), hormonal–androgen deprivation therapy is a method of choice with a good response rate. In some patients, however, the mPC will evolve into metastatic castration-resistant prostate cancer (mCRPC) (14). While a radical prostatectomy may be beneficial for patients with high-risk PC (15), only multimodal treatment, including surgery, radiation, and systemic therapy, gives the best chance for a long-term progression-free outcome (13). Nowadays, immunotherapy options, including anti-PC vaccines, e.g., Sipuleucel-T (Provenge), and the use of immune checkpoint inhibitors (anti-CTLA-4 and anti-PD-1/PD-L1 monoclonal antibodies or antagonists) further improve the effectiveness of the PC treatment (16).

PC is often considered a "cold" tumor, meaning that due to the reduced or complete lack of T-cell infiltration, e.g., because of the missing tumor-associated antigens, lack of T-cell activation and their homing into the tumor bed, and local immunosuppression, it does not trigger a strong immune response. This term emphasizes the role of the immune system in PC progression (16, 17). Studies indicate that regulatory T cells (Tregs) and other cell populations, namely, myeloid-derived suppressor cells (MDSCs; attracted to TME by low-grade chronic inflammatory signals) and tumor-associated macrophages (TAMs) (17), are mainly responsible for the immunosuppression observed in PC (18). Among them, MDSCs emerge as potential therapeutic targets (19).

MYELOID-DERIVED SUPPRESSOR CELLS —THEIR ORIGIN AND ACTIVITY

The term "myeloid-derived suppressor cells" has been used in the literature since 2007; however, the history of these cells dates back to the early 20th century, when it was shown that cancer is often accompanied by extra-medullary hematopoiesis (EMH) and neutrophilia (20, 21). These immature leukocytes were further characterized by their suppressive activity and called myeloid suppressor cells (MSC) (22). This term was further changed to MDSCs (22), and although current, the progress in resolution techniques, including a high-dimensional single-cell analysis, has raised concerns regarding the development and activation state of MDSCs (23); it is still accepted that MDSCs represent a heterogeneous population of immature myeloid cells, promptly expanding during pathological conditions, including infection, inflammation, and cancer (24). With respect to their origin, MDSCs have been divided into two main subsets—monocytic (Mo-MDSCs) and granulocytic or polymorphonuclear (PMN-MDSCs). Recently, a third population of the so-called early-stage MDSCs (e-MDSCs) was also described (25). In cancer, the accumulation of MDCSs is inseparably related to the production of pro-inflammatory mediators by the tumor microenvironment (TME), which activate and drive their suppressive activity (26). The immunosuppressive mechanisms developed by MDSCs are diverse and may include arginase-1 (ARG1) and inducible nitric oxide synthase (iNOS) activity; secretion of TGFβ, IL-10, and cyclooxygenase-2 (COX-2); and depletion of tryptophan by indoleamine 2,3-dioxygenase (IDO) (27). Although the immunosuppressive nature and the induction of antigen-specific T-cell tolerance is common for all the MDSCs subsets (28), they differ in the mechanism of action. In this context, Mo-MDSCs suppress T-cell response in both an antigen-specific and an unspecific manner, utilizing the mechanisms associated with iNOS activity and production of nitric oxide (NO) (29, 30). In contrast, PMN-MDSCs suppress immune response primarily in an antigen-specific manner, using the STAT3-mediated mechanisms of NADPH-oxidase and ARG1 activities (31). PMN-MDSCs store ARG1 in the granules and release it to the extracellular milieu, leading to the local depletion of L-arginine, affecting T-cell functionality. Both MDSCs subsets release ROS, which are essential for their immunosuppressive activity, and for retaining their undifferentiated status. Numerous studies confirmed the interplay between chronic inflammatory factors and expansion of MDSCs (24, 32). The transcription factor STAT3 plays a central role in the generation and functioning of MDSCs (33–35). Various cytokines, including IL-6, IL-1β, IL-10, GM-CSF, and VEGF, secreted mainly in the TME by tumor cells (26), are involved in the activation of pSTAT3. Conversely, chronic inflammation is associated with the initiation and progression of the tumor (10). In this context, chemokines and their receptors, e.g., CCL2/CCL12-CCR2, CXCL5/2/1-CXCR2, CCL3/4/5-CCR5, CCL15-CCR1, and CXCL8-CXCR1/2, are relevant for a rapid progression of PC and the recruitment of MDSCs (36, 37). PC patients were shown to have higher MDSCs infiltration than those with a benign prostate hyperplasia (38). Therefore, the role of inflammation in the development and expansion of MDSCs, and hence in PC progression, is unquestionable.

EXPANSION OF MDSCs IN PC

Studies with the use of *PTEN* KO murine PC model documented that lack of this gene was associated with upregulated inflammatory response (enhanced production of CSF-1 and IL-1β), and an extensive MDSCs tumor infiltration (39). Another mechanism involved in the recruitment of MDSCs in PC could be linked to the Hippo–YAP signaling. This pathway, relevant for the regulation of cell proliferation and apoptosis, is often deregulated in human solid tumors and associated with enhanced cancer cell proliferation (40). In PC, the hyperactivated Hippo–YAP signaling causes the upregulation of CXCL5 in cancer cells, which promotes the MDSCs recruitment *via* the CXCL5–CXCR2 axis (41, 42). The

recruitment of MDSCs to the tumor mass may also benefit from the tumor-related hypoxia. This is supported by the observation that the hypoxia-targeted therapy may lead to a long-lasting decrease in the accumulation of MDSCs in the tumor (43). A significant role in the recruitment of MDSCs to PC has also been assigned to chromodomain helicase DNA-binding protein 1 (CHD1), an essential tumor suppressor (44). Its depletion was found in 29.7% of cases in African Americans, and 11.0% of European PC patients (45). It has been shown that CHD1 deficiency may recruit MDSCs *via* an IL-6-dependent mechanism (46). Interestingly, a positive correlation between CHD1 and CD15 expression (a surface marker of PMN-MDSCs) in PC was also documented (46).

A growing list of evidence suggests that miRNA carried by tumor-derived extracellular vesicles (TEVs) may also play a role in the generation of MDSCs in many types of cancer (47–49). Although there are no data confirming such a role of EV miRNA in PC, some miRNAs already shown as relevant in the induction of MDSCs in other cancers have also been considered for PC (50).

The crosstalk between MDSCs and the TME in PC is schematically presented in **Figure 1**.

ROLE OF MDSCs IN PC DEVELOPMENT AND PROGRESSION

In various cancers, the level of tumor-infiltrating MDSCs has been proposed as a prognostic marker (51, 52). In PC, however, such data are scarce and refer mainly to the *PTEN* mouse model (39). In contrast, there are observations that the MDSCs' blood level could be a useful parameter for monitoring the disease burden in PC, allowing researchers to distinguish between metastatic cancer, localized PC, and cancer-free men (53). Additionally, circulating MDSCs correlate well with PSA level and metastasis (33, 54). The pivotal role of MDSCs in the development and progression of PC was further confirmed in randomized clinical studies showing that the increased level of MDSCs after the treatment is associated with the overall worse patients' survival (55, 56). Moreover, in a mouse model of PC, the lung infiltration by MDSCs was associated with the formation of lung metastases (57). However, what type of MDSCs subpopulation is pivotal and prevalent in PC remains controversial, mainly due to the lack of reproducibility and standardization of such research. The work showing MDSCs as a negative prognostic marker in mCRPC indicates only blood Mo-MDSCs as relevant (58). Furthermore, in patients with mCRPC, a positive correlation between Mo-MDSCs and Treg cells has been described (58), suggesting a mutual positive feedback loop (59). Generally, most of the studies in PC have focused on Mo-MDSCs rather than on PMN-MDSCs (55, 58, 60). Even early reports on circulating immunosuppressive cells in patients with PC were concentrated on CD14+HLA-DR$^{low/-}$ monocytes (54). This may result from the fact that Mo-MDSCs are more frequent in peripheral blood than PMN-MDSCs (61, 62). Another reason could be the fact that, in many studies, a cryopreserved material was used (63), affecting the recovery of PMN-MDSCs (64). Recently, Wen et al. documented infiltration of the primary prostate tumor by cells referred to as PMN-MDSCs (65); however, the markers used for their identification did not allow researchers to distinguish them from the population of tumor-associated neutrophils (TANs) (25). In this context, the phenotype definition of circulating blood PMN-MDSCs seems to be more reliable, but still, this should be further confirmed by functional tests that document the immunosuppressive nature of these cells (25).

Studies in PC showed that Mo-MDSCs and PMN-MDSCs are transcriptomically different (61), pointing out the ARG1 as typical for PMN-MDSCs (66) and iNOS or IDO for Mo-MDSCs (58, 60). Moreover, PMN-MDSCs can exert their immunosuppressive action also by the release of neutrophil elastase (NE), which was shown to stimulate the proliferation,

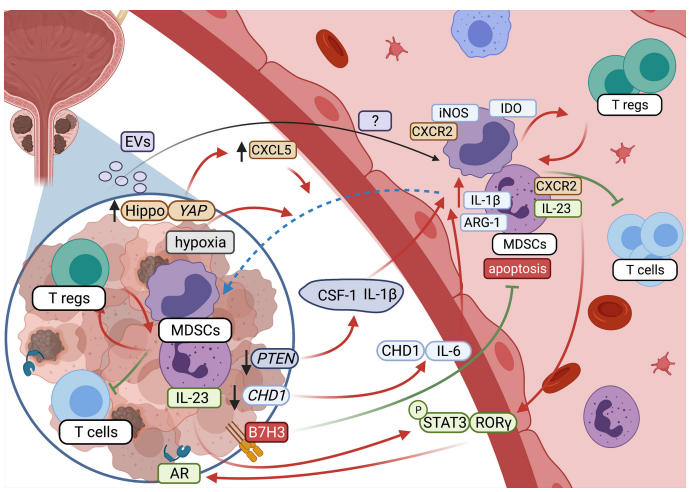

FIGURE 1 | Crosstalk between MDSCs and tumor microenvironment in prostate cancer (created with BioRender.com).

migration, and invasion of cancer cells both *in vitro* and *in vivo* in a mouse model of PC (67, 68).

It is proposed that, in PC, the tumor-infiltrating PMN-MDSCs express upregulated IL-1β and IL-23a (66). Although the IL-1β-restrained antitumor immunity was described before for other tumors (69), the secretion of IL-23 by PMN-MDSCs so far has been documented only for PC. In this context, it was shown that IL-23 preserves the androgen receptor's (AR) functionality, enabling survival and proliferation of PC in the androgen-deprived environment. The same mechanism is postulated as a driving force in the development of castration resistance (40). However, castration resistance may also be related to the secretion of IL-8 and subsequent tumor infiltration by PMN-MDSCs (66).

TARGETING MDSCs IN PC

Due to a lack of, or insufficient T-cell infiltration and immunosuppressive microenvironment in PC, there is a need to design new therapies that could "turn up the heat on the cold immune microenvironment" (17), to enhance the local anti-tumor immune response (16). Radiation *per se* has been found to activate the immune response (70); however, studies using the animal models of PC revealed that radiotherapy induces a rapid increase in the tumor-infiltrating MDSCs (71). Our previous studies showed that surgery or hormonal therapy alone did not reduce the level of circulating Mo-MDSCs in PC patients (62). In this context, in addition to the standard treatment, immunotherapy (72) or dietary strategies (73) are implemented, targeting cells with immunosuppressive potential, including MDSCs. One of the major challenges in targeting human MDSCs is their heterogeneous nature, e.g., differences in phenotype and mechanisms of suppression. A type of "universal" approach, covering the above aspects, may be the use of gemtuzumab ozogamicin, a calicheamicin-conjugated anti-CD33 humanized monoclonal antibody, already approved to treat a subset of patients with acute myeloid leukemia, which has also been highly effective against MDSCs in many solid tumors, including PC *in vitro* (61).

Clinically, MDSCs may be targeted by different approaches, including, e.g., inhibition of MDSCs expansion, MDSCs depletion, induction of their differentiation, functional inhibition, or multifactorial treatment. The clinical trials concerning all these potentially therapeutic strategies in PC have been described below **Table 1**.

Inhibition of MDSCs Expansion

Currently, there are three registered clinical trials, aiming at the inhibition of MDSCs expansion in PC. As mentioned, chemokines and their receptors are pivotal for the recruitment of MDSCs and the rapid progression of PC (36, 37); therefore, targeting the chemokine receptors or the use of chemokine inhibitors seems to be a promising form of immunotherapy in PC (74). One of the ongoing clinical trials (NCT03177187) seems to verify this hypothesis by using the CXCR2 antagonist AZD5069 in combination with enzalutamide—the androgen receptor's antagonist in patients with mCRPC (75). An important additional factor associated with MDSCs expansion is VEGF (26); thus, administration of cabozantinib (a small-molecule inhibitor of tyrosine kinase receptor, including the VEFG pathway) followed by radical prostatectomy vs. prostatectomy alone (NCT03964337) is being tested in men with high-risk PC. Moreover, cabozantinib has already shown inhibitory effects on MDSCs (76). Another trial concerning dietary intervention, NCT03654638, is focused on soy bread, containing isoflavones, which were shown to reduce the level of pro-inflammatory cytokines and MDSCs (77).

MDSCs Depletion

MDSCs isolated from both mice and humans display elevated levels of STAT3, while inhibition of its pathway resulted in enhanced antitumor activity (28, 78). Circulating Mo-MDSCs maintain high levels of STAT3 until they reach the tumor, where hypoxia induces its rapid downregulation, causing differentiation of MDSCs to TAMs (79). STAT3 regulates the expression of the main factors of MDSCs activity, e.g., IDO, ARG1, IL-6, IL-10, IL-1β, and VEGF, among others, suggesting this pathway as an attractive therapeutic option (26). In this context, a fungal-derived pSTAT3 inhibitor, galiellalactone, was recently assessed for its ability to prevent PC-induced generation of MDSCs *in vitro* (53). In keeping with this, the clinical trial NCT03709550, aiming at testing decitabine (5-aza-2′-deoxycytidine), a hypomethylating agent with the ability to selectively deplete Mo-MDSCs, in mCRPC patients was implemented (80).

Inhibition of MDSCs Differentiation

Another therapeutic option involves a controlled differentiation of MDSCs towards the M1 anti-tumor macrophages with the use of curcumin (81). This approach will be considered in the recruiting clinical trial (NCT03769766). A similar approach will be used in the phase I clinical study in patients with biochemically recurrent PC, testing the effectiveness of the white button mushroom (WBM) extract containing β-glucan (NCT04519879). β-glucans, the most abundant carbohydrates found in yeast and mushrooms (82), may induce MDSCs differentiation to antigen-presenting cells, eliminating their suppressive abilities (83). The rationale for this concept was additionally grounded on the preclinical data showing that dietary WBM powder reduced not only the frequency of circulating MDSCs but also the level of prostate-specific antigen (PSA) (84).

Inhibition of MDSCs Induced Suppressive Circuits

There is also a possibility to inhibit some of the MDSCs-induced suppressive mechanisms operating in PC. One of such approaches is represented by a combination of abiraterone, a novel hormone therapy available for CRPC (85), and tildrakizumab (anti-IL-23 mAb) (NCT04458311), altering the production of IL-23 and therefore having a potential to target the MDSCs function specific for PC (41). In another clinical trial, a

TABLE 1 | Clinical trials targeting MDSCs in PC patients.

No.	Title	Condition or disease	Interventions	Mechanism of action	Trial number	Status
Inhibition of MDSC expansion						
1	Combination Study of AZD5069 and Enzalutamide. (ACE)	Metastatic Castration-Resistant Prostate Cancer	CXCR2 antagonist + enzalutamide	CXCR2 antagonist may block recruitment of MDSCs to the tumor (41)	NCT03177187	Recruiting
2	Immediate Prostatectomy vs. Cabozantinib Followed by Prostatectomy in Men with High-Risk Prostate Cancer (SPARC)	Prostate Cancer Prostate Cancer Adenocarcinoma Non-Metastatic	Cabozantinib (small molecule inhibitor of tyrosine kinase receptor) + Radical prostatectomy	Cabozantinib may reduce the tumor infiltration by MDSCs (76)	NCT03964337	Recruiting
3	Soy Bread Diet in Improving Immune Function in Participants With Prostate Cancer	Prostate Adenocarcinoma	Dietary intervention	Soy bread isoflavones may reduce pro-inflammatory cytokines and MDSCs level (77)	NCT03654638	Recruiting
MDSC depletion						
4	Enzalutamide and Decitabine in Treating Patients with Metastatic Castration Resistant Prostate Cancer	Metastatic Castration-Resistant Prostate Cancer	Decitabine (nucleic acid synthesis inhibitor)	Decitabine (5-aza-2′-deoxycytidine), a hypomethylating agent with the ability to selectively deplete Mo-MDSCs (80)	NCT03709550	Withdrawn
Stimulation of MDSC differentiation						
5	Trial of Curcumin to Prevent Progression of Low-risk Prostate Cancer Under Active Surveillance	Prostate Cancer	Curcumin	Curcumin may promote the differentiation of MDSCs (81)	NCT03769766	Recruiting
6	White Button Mushroom Soup for the Reduction of PSA in Patients with Biochemically Rec or Therapy Naive Fav Risk Prostate CA	Prostate Adenocarcinoma PSA Failure PSA Progression Recurrent Prostate Carcinoma Stage I Prostate Cancer stage IIA–C, III A, C	White Button Mushroom (WBM) Extract	WBM powder as a source of β-glucan may induce MDSC differentiation to antigen-presenting cells (83) and reduce the number of circulating MDSCs (84)	NCT04519879	Recruiting
Inhibition of MDSCs induced suppressive mechanisms						
7	Abiraterone Acetate in Combination with Tildrakizumab (ACTIon)	Metastatic Castration-Resistant Prostate Cancer	Abiraterone Acetate (selective inhibitor of CYP17) + Tildrakizumab (anti-IL-23)	Tildrakizumab (anti-IL-23 mAb), alters the production of IL-23 in PC, has the potential to affect castration resistance caused by MDSCs (41)	NCT04458311/ 2019-003485-40	Recruiting
8	A Trial of Ipatasertib in Combination with Atezolizumab (IceCAP)	Solid Tumor Glioblastoma Multiforme Prostate Cancer Metastatic	Ipatasertib (inhibitor of all three isoforms of protein kinase AKT) + Atezolizumab (anti-PD-L1)	Atezolizumab (anti-PD-L1 monoclonal antibodies)—a checkpoint inhibitor on MDSCs (86)	NCT03673787	Recruiting

(Continued)

TABLE 1 | Continued

No.	Title	Condition or disease	Interventions	Mechanism of action	Trial number	Status
9	A phase I/II basket trial evaluating a combination of Metronomic Oral Vinorelbine plus anti-PD-L1/anti-CTLA4 Immunotherapy in patients with advanced solid tumors.	Patients with locally advanced or metastatic solid tumors	Vinorelbine (cytostatic) Durvalumab (anti-PD-L1) + Tremelimumab (anti-CTLA-4)	Anti-PD-L1 and anti-CTLA-4 checkpoint inhibitors on MDSCs (86)	2017-001857-14	Ongoing
Multifactorial action: inhibition of MDSC expansion and blocking their suppressive activity						
10	A Phase 1b/2, Open-Label, Multicenter Study Assessing the Safety, Tolerability, Pharmacokinetics, and Preliminary Anti-tumor Activity of MEDI4736 in Combination with AZD9150 or AZD5069 in Patients with Advanced Solid Malignancies and Subsequently Comparing AZD9150 and AZD5069 Both as Monotherapy and in Combination with MEDI4736 as Second-Line Treatment in Patients with Recurrent and/or Metastatic Squamous Cell Carcinoma of the Head and Neck.	Part A: Advanced solid tumor Part B: Recurrent and/or spreading tumor of Head and Neck	MEDI4736 (Durvalumab- anti-PD-L1) + AZD9150 (Danvatirsen-STAT3 inhibitor) + AZD5069 (CXCR2 antagonist)	Combination of STAT3 inhibitor, selective CXCR2 antagonist, and PD-L1 inhibitor, where each of them has the potential to inhibit MDSCs activity (41, 60, 86)	2015-002525-19	Restarted or completed depending on the country
11	Phase II Trial of EP4 Receptor Antagonist in Advanced Solid Tumors	Prostate Cancer Non-Small Cell Lung Cancer Breast Cancer	Grapiprant + Gemcitabine	Gemcitabine may reduce the level of MDSCs (87), whereas grapiprant, a PGE2-receptor inhibitor, may block induction of MDSCs (88) and their suppressive effect (26)	NCT02538432	Withdrawn

combination of ipatasertib (inhibitor of all three isoforms of protein kinase AKT, which blocks the PI3K/AKT signaling pathway—a key driver of cancer cell growth and proliferation in PC), atezolizumab (anti-PD-L1 monoclonal antibodies)—a checkpoint inhibitor on MDSCs (86), and docetaxel (NCT03673787) will be tested in patients with mCRPC. Currently, in Europe, there is one registered clinical trial focused on blocking the MDSCs function in PC patients (no. 2017-001857-14). It tests the combination of vinorelbine, a cytostatic drug, and two checkpoint inhibitors, durvalumab and tremelimumab, which are anti-PD-L1 and anti-CTLA-4 mAb, respectively.

Multifactorial Intervention: Inhibition of MDSCs Expansion and Blocking Their Suppressive Activity

Combinations of both the inhibition of MDSCs expansion and blocking their suppressive activity provide the opportunity for multifactorial interventions with potential better therapeutic effectiveness. One of such trials tests the combination of STAT3 inhibitor (AZD9150), a selective CXCR2 antagonist (AZD5069), and the PD-L1 inhibitor (MEDI4736) (no. 2015-002525-19), where each can inhibit either MDSCs expansion or function. Another drug combination that is being tested is gemcitabine and RQ-00000007 (grapiprant), where gemcitabine inhibits MDSCs expansion (87), while grapiprant —an inhibitor of PGE2-receptor—reduces the differentiation, expansion, and suppressive activities of Mo-MDSCs (88), confirming its role in MDSCs functioning (26).

Potential New Targets

Despite a wide scope of the ongoing clinical research, there are other available potential therapeutic options targeting MDSCs in PC. One, yet unexplored route, concerns the angiotensin-converting enzyme (ACE)–angiotensin pathway, where the overexpression of ACE in monocytic cells was shown to reduce the generation of MDSCs (89), while angiotensin was able to reduce the tumor malignancy in PC (90). Nowadays, during the SARS-CoV-2 pandemic, this pathway, however, takes on a quite different significance. However, other forms of angiotensin may impact the biological properties of PC cells by modulating inflammatory reaction, or even genes, including downregulation of HIF1a and upregulation of CDH-1 (91) expression, both associated with MDSCs recruitment. Another potential approach involves estrogen, used previously in PC therapy (92). The combined therapy, linking activation of estrogen receptor β (ERβ) and the checkpoint inhibitor anti-PD-1 mAb, diminishes MDSCs infiltration in mouse models of colorectal and breast cancer (93). Interestingly, apoptosis and/or differentiation of PC cells may be promoted during the ERβ activation (94). Additionally, studies confirmed the benefits of ERβ activation in androgen-dependent CRPC, decreasing the viability of the tumor cells (95). Also, ARG1 is a potential therapeutic target in PC, and its inactivation through STAT3 inhibition was already confirmed (34). The ongoing clinical trials aiming at targeting MDSCs may be a trigger for more frequent

use of immunotherapy in combination with other forms of PC treatment.

CONCLUSION

Although the first observations reporting the negative role of MDSCs in antitumor responses in PC date back from the beginning of the 21st century, the last decade saw an upsurge of studies indicating their mechanisms of action and clinical relevance (96). Although several questions remain unanswered, the role of MDSCs in the development and progression of PC seems unquestionable, suggesting their potential as a therapeutic target. Hence, the implementation of the combination therapy, e.g., radiotherapy and immunotherapy, targeting both the tumor and MDSCs in PC seems crucial. Such therapy may increase the frequency of the abscopal response, which is a phenomenon associated with tumor shrinkage, occurring not only locally at the site of the treatment but also in other locations, where the tumor has already spread (97).

AUTHOR CONTRIBUTIONS

IS wrote the draft version of the manuscript. JB revised and edited the final version of the manuscript. All authors contributed to the article and approved the submitted version.

FUNDING

The authors declare and acknowledge financial support from EU H2020-MSCA-RISE-2017 program - grant "CANCER" (GA 777682).

ACKNOWLEDGMENTS

Figure created with BioRender.com.

REFERENCES

1. Sung H, Ferlay J, Siegel RL, Laversanne M, Soerjomataram I, Jemal A, et al. Global Cancer Statistics 2020: GLOBOCAN Estimates of Incidence and Mortality Worldwide for 36 Cancers in 185 Countries. *CA: A Cancer J Clin* (2021) 71:209–49. doi: 10.3322/caac.21660
2. Rawla P. Epidemiology of Prostate Cancer. *World J Oncol* (2019) 10:63. doi: 10.14740/WJON1191
3. Rebbeck TR. Prostate Cancer Genetics: Variation by Race, Ethnicity, and Geography. *Semin Radiat Oncol* (2017) 27:3. doi: 10.1016/J.SEMRADONC.2016.08.002
4. Pienta KJ, Esper PS. Risk Factors for Prostate Cancer. *Ann Internal Med* (1993) 118:793–803. doi: 10.7326/0003-4819-118-10-199305150-00007
5. Bostwick DG, Burke HB, Djakiew D, Euling S, Ho SM, Landolph J, et al. Human Prostate Cancer Risk Factors. *Cancer* (2004) 101:2371–490. doi: 10.1002/CNCR.20408
6. Dagnelie PC, Schuurman AG, Goldbohm RA, van den Brandt PA. Diet, Anthropometric Measures and Prostate Cancer Risk: A Review of Prospective Cohort and Intervention Studies. *BJU Int* (2004) 93:1139–50. doi: 10.1111/J.1464-410X.2004.04795.X
7. Kolonel LN. Fat, Meat, and Prostate Cancer. *Epidemiol Rev* (2001) 23:72–81. doi: 10.1093/OXFORDJOURNALS.EPIREV.A000798
8. Wolk A. Diet, Lifestyle and Risk of Prostate Cancer. *Acta Oncol (Stockholm Sweden)* (2005) 44:277–81. doi: 10.1080/02841860510029572
9. Jamaspishvili T, Berman DM, Ross AE, Scher HI, de Marzo AM, Squire JA, et al. Clinical Implications of PTEN Loss in Prostate Cancer. *Nat Rev Urol* (2018) 15:222–34. doi: 10.1038/NRUROL.2018.9
10. Jiang J, Li J, Zhang Y, Zhu H, Liu J, Pumill C. The Role of Prostatitis in Prostate Cancer: Meta-Analysis. *PLos One* (2013) 8:85179. doi: 10.1371/JOURNAL.PONE.0085179
11. Beckmann K, Russell B, Josephs D, Garmo H, Haggstrom C, Holmberg L, et al. Chronic Inflammatory Diseases, Anti-Inflammatory Medications and Risk of Prostate Cancer: A Population-Based Case-Control Study. *BMC Cancer* (2019) 19:1–9. doi: 10.1186/S12885-019-5846-3/TABLES/5
12. Punnen S, Cooperberg MR. The Epidemiology of High-Risk Prostate Cancer. *Curr Opin Urol* (2013) 23:331–6. doi: 10.1097/MOU.0B013E328361D48
13. McKay RR, Feng FY, Wang AY, Wallis CJD, Moses KA. Recent Advances in the Management of High-Risk Localized Prostate Cancer: Local Therapy, Systemic Therapy, and Biomarkers to Guide Treatment Decisions. *ASCO Educ Book* (2020) 40:241–52. doi: 10.1200/EDBK_279459
14. Shelley M, Harrison C, Coles B, Stafforth J, Wilt T, Mason M. Chemotherapy for Hormone-Refractory Prostate Cancer. *Cochrane Database Syst Rev* (2006) 4. doi: 10.1002/14651858.CD005247.PUB2
15. Ghodoussipour S, Cacciamani GE, Luis A, Abreu C. Radical Prostatectomy for High-Risk Prostate Cancer | Opinion: No. *Int Braz J Urol* (2019) 45(3):428–34. doi: 10.1590/S1677-5538.IBJU.2019.03.03
16. Fay EK, Graff JN. Immunotherapy in Prostate Cancer. *Cancers* (2020) 12:1–17. doi: 10.3390/CANCERS12071752
17. Stultz J, Fong L. How to Turn Up the Heat on the Cold Immune Microenvironment of Metastatic Prostate Cancer. *Prostate Cancer Prostatic Dis* (2021) 24:697–717. doi: 10.1038/s41391-021-00340-5
18. Sfanos KS, Bruno TC, Maris CH, Xu L, Thoburn CJ, Demarzo AM, et al. Phenotypic Analysis of Prostate-Infiltrating Lymphocytes Reveals TH17 and Treg Skewing. *Clin Cancer Res* (2008) 14:3254–61. doi: 10.1158/1078-0432.CCR-07-5164
19. Li X, Zhong J, Deng X, Guo X, Lu Y, Lin J, et al. Targeting Myeloid-Derived Suppressor Cells to Enhance the Antitumor Efficacy of Immune Checkpoint Blockade Therapy. *Front Immunol* (2021) 0:754196. doi: 10.3389/FIMMU.2021.754196
20. Sonnenfeld A. Leukamische Reaktiones Bei Carcinoma. *Z f Klin Med* 1929) 111:108.
21. Talmadge JE, Gabrilovich DI. History of Myeloid Derived Suppressor Cells (MDSCs) in the Macro-and Micro-Environment of Tumour-Bearing Hosts. *Nat Rev Cancer* (2013) 13:739–52. doi: 10.1038/nrc3581
22. Gabrilovich DI, Bronte V, Chen S-H, Colombo MP, Ochoa A, Ostrand-Rosenberg S, et al. The Terminology Issue for Myeloid-Derived Suppressor Cells. *Cancer Res* (2007) 67:425–5. doi: 10.1158/0008-5472.CAN-06-3037
23. Hegde S, Leader AM, Merad M. MDSCs: Markers, Development, States, and Unaddressed Complexity. *Immunity* (2021) 54:875–84. doi: 10.1016/J.IMMUNI.2021.04.004
24. Sinha P, Chornoguz O, Clements VK, Artemenko KA, Zubarev RA, Ostrand-Rosenberg S. Myeloid-Derived Suppressor Cells Express the Death Receptor Fas and Apoptose in Response to T Cell-Expressed FasL. *Blood* (2011) 117:5381–90. doi: 10.1182/blood-2010-11-321752
25. Bronte V, Brandau S, Chen S, Colombo MP, Frey AB, Greten TF, et al. Recommendations for Myeloid-Derived Suppressor Cell Nomenclature and Characterization Standards. *Nat Commun* (2016) 7:1–10. doi: 10.1038/ncomms12150
26. Parker KH, Beury DW, Ostrand-Rosenberg S. Myeloid-Derived Suppressor Cells: Critical Cells Driving Immune Suppression in the Tumor Microenvironment. *Adv Cancer Res* (2015) 128:95–139. doi: 10.1016/bs.acr.2015.04.002
27. Shackleton EG, Ali HY, Khan M, Pockley GA, McArdle SE. Novel Combinatorial Approaches to Tackle the Immunosuppressive Microenvironment of Prostate Cancer. (2021) 13:1145. doi: 10.3390/CANCERS13051145

28. Marigo I, Bosio E, Solito S, Mesa C, Fernandez A, Dolcetti L, et al. Tumor-Induced Tolerance and Immune Suppression Depend on the C/Ebpβ Transcription Factor. *Immunity* (2010) 32:790–802. doi: 10.1016/j.immuni.2010.05.010
29. Kumar V, Patel S, Tcyganov E, Gabrilovich DI. The Nature of Myeloid-Derived Suppressor Cells in the Tumor Microenvironment. *Trends Immunol* (2016) 37:1–13. doi: 10.1016/j.it.2016.01.004
30. Gabrilovich DI. Myeloid-Derived Suppressor Cells. *Cancer Immunol Res* (2017) 5:3–8. doi: 10.1158/2326-6066.CIR-16-0297
31. Grzywa TM, Sosnowska A, Matryba P, Rydzynska Z, Jasinski M, Nowis D, et al. Myeloid Cell-Derived Arginase in Cancer Immune Response. *Front Immunol* (2020) 11:938. doi: 10.3389/fimmu.2020.00938
32. Gabrilovich DI, Ostrand-Rosenberg S, Bronte V. Coordinated Regulation of Myeloid Cells by Tumours. *Nat Rev Immunol* (2012) 12:253–68. doi: 10.1038/nri3175
33. Hossain DMS, Pal SK, Moreira D, Duttagupta P, Zhang Q, Won H, et al. TLR9-Targeted STAT3 Silencing Abrogates Immunosuppressive Activity of Myeloid-Derived Suppressor Cells From Prostate Cancer Patients. *Clin Cancer Res* (2015) 21:3771–82. doi: 10.1158/1078-0432.CCR-14-3145
34. Rébé C, Végran F, Berger H, Ghiringhelli F. STAT3 Activation: A Key Factor in Tumor Immunoescape. *JAK-STAT* (2013) 2:e23010. doi: 10.4161/JKST.23010
35. de Haas N, de Koning C, Spilgies L, de Vries IJM, Hato S V. Improving Cancer Immunotherapy by Targeting the STATe of MDSCs. *Oncoimmunology* (2016) 5. doi: 10.1080/2162402X.2016.1196312
36. Li BH, Garstka MA, Li ZF. Chemokines and Their Receptors Promoting the Recruitment of Myeloid-Derived Suppressor Cells Into the Tumor. *Mol Immunol* (2020) 117:201–15. doi: 10.1016/J.MOLIMM.2019.11.014
37. Maynard JP, Ertunc O, Kulac I, Valle JAB-D, de Marzo AM, Sfanos KS. IL8 Expression Is Associated With Prostate Cancer Aggressiveness and Androgen Receptor Loss in Primary and Metastatic Prostate Cancer. *Mol Cancer Res* (2020) 18:153–65. doi: 10.1158/1541-7786.MCR-19-0595
38. Sanaei MJ, Taheri F, Heshmati M, Bashash D, Nazmabadi R, Mohammad-Alibeigi F, et al. Comparing the Frequency of CD33 + Pstat3 + Myeloid-Derived Suppressor Cells and IL-17 + Lymphocytes in Patients With Prostate Cancer and Benign Prostatic Hyperplasia. *Cell Biol Int* (2021) 45:2086–95. doi: 10.1002/CBIN.11651
39. Garcia AJ, Ruscetti M, Arenzana TL, Tran LM, Bianci-Frias D, Sybert E, et al. Pten Null Prostate Epithelium Promotes Localized Myeloid-Derived Suppressor Cell Expansion and Immune Suppression During Tumor Initiation and Progression. *Mol Cell Biol* (2014) 34:2017. doi: 10.1128/MCB.00090-14
40. Johnson R, Halder G. The Two Faces of Hippo: Targeting the Hippo Pathway for Regenerative Medicine and Cancer Treatment. *Nat Rev Drug Discovery* (2014) 13:63. doi: 10.1038/NRD4161
41. Calcinotto A, Spataro C, Zagato E, di Mitri D, Gil V, Crespo M, et al. IL-23 Secreted by Myeloid Cells Drives Castration-Resistant Prostate Cancer. (2018) 559:363–9. doi: 10.1038/s41586-018-0266-0
42. Wang G, Lu X, Dey P, Deng P, Wu CC, Jiang S, et al. Targeting YAP-Dependent MDSCs Infiltration Impairs Tumor Progression. *Cancer Discovery* (2016) 6:80–95. doi: 10.1158/2159-8290.CD-15-0224
43. Jayaprakash P, Ai M, Liu A, Budhani P, Bartkowiak T, Sheng J, et al. Targeted Hypoxia Reduction Restores T Cell Infiltration and Sensitizes Prostate Cancer to Immunotherapy. *J Clin Invest* (2018) 128:5137–49. doi: 10.1172/JCI96268
44. Burkhardt L, Fuchs S, Krohn A, Masser S, Mader M, Kluth M, et al. CHD1 Is a 5q21 Tumor Suppressor Required for ERG Rearrangement in Prostate Cancer. *Cancer Res* (2013) 73:2795–805. doi: 10.1158/0008-5472.CAN-12-1342
45. Diossy M, Tisza V, Li H, Zhou J, Sztupinszki Z, Young D, et al. Increased Frequency of CHD1 Deletions in Prostate Cancers of African American Men is Associated With Distinct Homologous Recombination Deficiency Associated DNA Aberration Profiles. *medRxiv* (2021) 21251199. doi: 10.1101/2021.02.08.21251199
46. Zhao D, Cai L, Lu X, Liang X, Li J, Chen P, et al. Chromatin Regulator CHD1 Remodels the Immunosuppressive Tumor Microenvironment in PTEN-Deficient Prostate Cancer. *Cancer Discov* (2020) 10:1374–87. doi: 10.1158/2159-8290.CD-19-1352
47. Ren W, Zhang X, Li W, Feng Q, Feng H, Tong Y, et al. Exosomal miRNA-107 Induces Myeloid-Derived Suppressor Cell Expansion in Gastric Cancer. *Cancer Manage Res* (2019) 11:4023. doi: 10.2147/CMAR.S198886
48. Huber V, Vallacchi V, Fleming V, Hu X, Cova A, Dugo M, et al. Tumor-Derived microRNAs Induce Myeloid Suppressor Cells and Predict Immunotherapy Resistance in Melanoma. *J Clin Invest* (2018) 128:5517–30. doi: 10.1172/JCI98060
49. Daveri E, Vergani E, Shahaj E, Bergamaschi L, la Magra S, Dosi M, et al. microRNAs Shape Myeloid Cell-Mediated Resistance to Cancer Immunotherapy. *Front Immunol* (2020) 0:1214. doi: 10.3389/FIMMU.2020.01214
50. Cochetti G, Poli G, Guelfi G, Boni A, Egidi MG, Mearini E. Different Levels of Serum microRNAs in Prostate Cancer and Benign Prostatic Hyperplasia: Evaluation of Potential Diagnostic and Prognostic Role. *OncoTargets Ther* (2016) 9:7545–53. doi: 10.2147/OTT.S119027
51. Ai L, Mu S, Wang Y, Wang H, Cai L, Li W, et al. Prognostic Role of Myeloid-Derived Suppressor Cells in Cancers: A Systematic Review and Meta-Analysis. *BMC Cancer* (2018) 18:1–9. doi: 10.1186/s12885-018-5086-y
52. Zhang X, Fu X, Li T, Yan H. The Prognostic Value of Myeloid Derived Suppressor Cell Level in Hepatocellular Carcinoma: A Systematic Review and Meta-Analysis. *PLos One* (2019) 14:12:e0225327. doi: 10.1371/journal.pone.0225327
53. Chang G, Kang I, Shahabi A, Nadadur M, Athreya K, Suer D, et al. MDSCs Clinical Assay for Disease Surveillance in Prostate Cancer. *J Clin Oncol* (2015) 33:e16091–1. doi: 10.1200/jco.2015.33.15_suppl.e16091
54. Vuk-Pavlović S, Bulur PA, Lin Y, Qin R, Szumlanski CL, Zhao X, et al. Immunosuppressive CD14+HLA-DRlow/– Monocytes in Prostate Cancer. *Prostate* (2010) 70:443–55. doi: 10.1002/PROS.21078
55. Santegoets SJ, Stam AG, Lougheed SM, Gall H, Jooss K, Sacks N, et al. Myeloid Derived Suppressor and Dendritic Cell Subsets are Related to Clinical Outcome in Prostate Cancer Patients Treated With Prostate GVAX and Ipilimumab. *J ImmunoTher Cancer* (2014) 2:31. doi: 10.1186/S40425-014-0031-3
56. Takahashi R, Amano H, Ito Y, Eshima K, Satoh T, Iwamura M, et al. Microsomal Prostaglandin E Synthase-1 Promotes Lung Metastasis *via* SDF-1/CXCR4-Mediated Recruitment of CD11b+Gr1+MDSCs From Bone Marrow. *Biomed Pharmacother* (2020) 121:109581. doi: 10.1016/J.BIOPHA.2019.109581
57. Koga N, Moriya F, Waki K, Yamada A, Itoh K, Noguchi M. Immunological Efficacy of Herbal Medicines in Prostate Cancer Patients Treated by Personalized Peptide Vaccine. *Cancer Sci* (2017) 108:2326. doi: 10.1111/CAS.13397
58. Idorn M, Køllgaard T, Kongsted P, Sengeløv L, thor Straten P. Correlation Between Frequencies of Blood Monocytic Myeloid-Derived Suppressor Cells, Regulatory T Cells and Negative Prognostic Markers in Patients With Castration-Resistant Metastatic Prostate Cancer. *Cancer Immunol Immunother* (2014) 63:1177–87. doi: 10.1007/S00262-014-1591-2
59. Lee C-R, Kwak Y, Yang T, Han JH, Park S-H, Ye MB, et al. Myeloid-Derived Suppressor Cells Are Controlled by Regulatory T Cells *via* TGF-β During Murine Colitis. *Cell Rep* (2016) 17:3219–32. doi: 10.1016/j.celrep.2016.11.062
60. Hellsten R, Lilljebjörn L, Johansson M, Leandersson K, Bjartell A. The STAT3 Inhibitor Galiellalactone Inhibits the Generation of MDSCs-Like Monocytes by Prostate Cancer Cells and Decreases Immunosuppressive and Tumorigenic Factors. *Prostate* (2019) 79:1611–21. doi: 10.1002/PROS.23885
61. Fultang L, Panetti S, Ng M, Collins P, Graef S, Rizkalla N, et al. MDSCs Targeting With Gemtuzumab Ozogamicin Restores T Cell Immunity and Immunotherapy Against Cancers. *EBioMedicine* (2019) 47:235–46. doi: 10.1016/j.ebiom.2019.08.025
62. Siemińska I, Rychlicka-Buniowska E, Jaszczyński J, Palaczyński M, Bukowska-Strakova K, Ryś J, et al. The Level of Myeloid Derived-Suppressor Cells in Peripheral Blood of Patients With Prostate Cancerafter Various Types of Therapy. *Polish J Pathol* (2020) 71:46–54. doi: 10.5114/PJP.2020.95415
63. Trellakis S, Bruderek K, Hü J, Elian M, Hoffmann TK, Lang S, et al. Granulocytic Myeloid-Derived Suppressor Cells are Cryosensitive and Their Frequency Does Not Correlate With Serum Concentrations of Colony-Stimulating Factors in Head and Neck Cancer. *Innate Immun* (2013) 19:328–36 doi: 10.1177/1753425912463618
64. Grützner E, Stirner R, Arenz L, Athanasoulia AP, Schrödl K, Berking C, et al. Kinetics of Human Myeloid-Derived Suppressor Cells After Blood Draw. *J Trans Med* (2016) 14. doi: 10.1186/S12967-015-0755-Y
65. Wen J, Huang G, Liu S, Wan J, Wang X, Zhu Y, et al. Polymorphonuclear MDSCs are Enriched in the Stroma and Expanded in Metastases of Prostate Cancer. *J Pathol: Clin Res* (2020) 6:171. doi: 10.1002/CJP2.160
66. Lopez-Bujanda ZA, Haffner MC, Chaimowitz MG, Chowdhury N, Venturini NJ, Obradovic A, et al. Castration-Mediated IL-8 Promotes Myeloid

Infiltration and Prostate Cancer Progression. *bioRxiv* (2019) 651083. doi: 10.1101/651083
67. Zhiguang X, Lerman I, Hammes SR. SAT-138 Neutrophil Elastase Promotes Proliferative Signals in Prostate Cells Through EGFR and DDR1. *J Endocr Soc* (2020) 4:1. doi: 10.1210/jendso/bvaa046.140
68. Lerman I, de la Luz Garcia-Hernandez M, Rangel-Moreno J, Chiriboga L, Pan C, Nastiuk KL, et al. Infiltrating Myeloid Cells Exert Protumorigenic Actions *via* Neutrophil Elastase. *Mol Cancer Res* (2017) 15:1138–52. doi: 10.1158/1541-7786.MCR-17-0003
69. Bruchard M, Mignot G, Derangère V, Chalmin F, Chevriaux A, Végran F, et al. Chemotherapy-Triggered Cathepsin B Release in Myeloid-Derived Suppressor Cells Activates the Nlrp3 Inflammasome and Promotes Tumor Growth. *Nat Med* (2012) 19:57–64. doi: 10.1038/nm.2999
70. Kaur P, Asea A. Radiation-Induced Effects and the Immune System in Cancer. *Front Oncol* (2012) 0:191. doi: 10.3389/FONC.2012.00191
71. Lin L, Kane N, Kobayashi N, Kono EA, Yamashiro JM, Nickols NG, et al. High-Dose Per Fraction Radiotherapy Induces Both Antitumor Immunity and Immunosuppressive Responses in Prostate Tumors. *Clin Cancer Res* (2021) 27:1505–15. doi: 10.1158/1078-0432.CCR-20-2293
72. May KFJr., Gulley JL, Drake CG, Dranoff G, Kantoff PW. Prostate Cancer Immunotherapy. *Clin Cancer Res* (2011) 17:5233. doi: 10.1158/1078-0432.CCR-10-3402
73. Chen F, Zhao X. Prostate Cancer: Current Treatment and Prevention Strategies. *Iranian Red Crescent Med J* (2013) 15:279. doi: 10.5812/IRCMJ.6499
74. Poeta VM, Massara M, Capucetti A, Bonecchi R. Chemokines and Chemokine Receptors: New Targets for Cancer Immunotherapy. *Front Immunol* (2019) 10:379. doi: 10.3389/FIMMU.2019.00379
75. Koivisto CS, Parrish M, Bonala SB, Ngoi S, Torres A, Gallagher J, et al. Evaluating the Efficacy of Enzalutamide and the Development of Resistance in a Preclinical Mouse Model of Type-I Endometrial Carcinoma. *bioRxiv* (2019). doi: 10.1101/2019.12.06.86818
76. Kwilas AR, Ardiani A, Donahue RN, Aftab DT, Hodge JW. Dual Effects of a Targeted Small-Molecule Inhibitor (Cabozantinib) on Immune-Mediated Killing of Tumor Cells and Immune Tumor Microenvironment Permissiveness When Combined With a Cancer Vaccine. *J Transl Med* (2014) 12:1–15. doi: 10.1186/s12967-014-0294-y
77. Lesinski GB, Reville PK, Mace TA, Young GS, Ahn-Jarvis J, Thomas-Ahner J, et al. Consumption of Soy Isoflavone Enriched Bread in Men With Prostate Cancer Is Associated With Reduced Proinflammatory Cytokines and Immunosuppressive Cells. *Cancer Prev Res (Phila)* (2015) 8:1036–44. doi: 10.1158/1940-6207.CAPR-14-0464
78. Moreira D, Adamus T, Zhao X, Su YL, Zhang Z, White SV, et al. STAT3 Inhibition Combined With CpG Immunostimulation Activates Antitumor Immunity to Eradicate Genetically Distinct Castration-Resistant Prostate Cancers. *Clin Cancer Res* (2018) 24:5948–62. doi: 10.1158/1078-0432.CCR-18-1277
79. Kumar V, Cheng P, Condamine T, Mony S, Languino LR, McCaffrey JC, et al. CD45 Phosphatase Inhibits STAT3 Transcription Factor Activity in Myeloid Cells and Promotes Tumor-Associated Macrophage Differentiation. *Immunity* (2016) 44:303. doi: 10.1016/J.IMMUNI.2016.01.014
80. Zhou J, Shen Q, Lin H, Hu L, Li G, Zhang X. Decitabine Shows Potent Anti-Myeloma Activity by Depleting Monocytic Myeloid-Derived Suppressor Cells in the Myeloma Microenvironment. *J Cancer Res Clin Oncol* (2019) 145:329–36. doi: 10.1007/s00432-018-2790-6
81. Tu SP, Jin H, Shi JD, Zhu LM, Suo Y, Lu G, et al. Curcumin Induces the Differentiation of Myeloid-Derived Suppressor Cells and Inhibits Their Interaction With Cancer Cells and Related Tumor Growth. *Cancer Prev Res* (2012) 5:205–15. doi: 10.1158/1940-6207.CAPR-11-0247
82. Murphy EJ, Rezoagli E, Major I, Rowan NJ, Laffey JG. β-Glucan Metabolic and Immunomodulatory Properties and Potential for Clinical Application. *J Fungi* (2020) 10:356. doi: 10.3390/jof6040356
83. Albeituni SH, Ding C, Liu M, Hu X, Luo F, Kloecker G, et al. Yeast-Derived Particulate β-Glucan Treatment Subverts the Suppression of Myeloid-Derived Suppressor Cells (MDSCs) by Inducing Polymorphonuclear MDSCs Apoptosis and Monocytic MDSCs Differentiation to APC in Cancer. *J Immunol* (2016) 196:2167–80. doi: 10.4049/jimmunol.1501853
84. Twardowski P, Kanaya N, Frankel P, Synold T, Ruel C, Pal SK, et al. A Phase I Trial of Mushroom Powder in Patients With Biochemically Recurrent Prostate Cancer: Roles of Cytokines and Myeloid-Derived Suppressor Cells for Agaricus Bisporus-Induced Prostate-Specific Antigen Responses. *Cancer* (2015) 121:2942–50. doi: 10.1002/cncr.29421
85. Tran C, Ouk S, Clegg NJ, Chen Y, Watson PA, Arora V, et al. Development of a Second-Generation Antiandrogen for Treatment of Advanced Prostate Cancer. *Science* (2009) 324:787–90. doi: 10.1126/SCIENCE.1168175
86. Weber R, Fleming V, Hu X, Nagibin V, Groth C, Altevogt P, et al. Myeloid-Derived Suppressor Cells Hinder the Anti-Cancer Activity of Immune Checkpoint Inhibitors. (2018) 9:1. doi: 10.3389/fimmu.2018.01310
87. Le HK, Graham L, Cha E, Morales JK, Manjili MH, Bear HD. Gemcitabine Directly Inhibits Myeloid Derived Suppressor Cells in BALB/c Mice Bearing 4T1 Mammary Carcinoma and Augments Expansion of T Cells From Tumor-Bearing Mice. *Int Immunopharmacol* (2009) 9:900–9. doi: 10.1016/J.INTIMP.2009.03.015
88. Lu W, Yu W, He J, Liu W, Yang J, Lin X, et al. Reprogramming Immunosuppressive Myeloid Cells Facilitates Immunotherapy for Colorectal Cancer. *EMBO Mol Med* (2021) 13:e12798. doi: 10.15252/EMMM.202012798
89. Shen XZ, Okwan-Duodu D, Blackwell WL, Ong FS, Janjulia T, Bernstein EA, et al. Myeloid Expression of Angiotensin-Converting Enzyme Facilitates Myeloid Maturation and Inhibits the Development of Myeloid-Derived Suppressor Cells. *Lab Invest* (2014) 94:536–44. doi: 10.1038/LABINVEST.2014.41
90. Domińska K, Okła P, Kowalska K, Habrowska-Górczyńska DE, Urbanek KA, Ochędalski T, et al. Angiotensin 1–7 Modulates Molecular and Cellular Processes Central to the Pathogenesis of Prostate Cancer. *Sci Rep* (2018) 8:1–12. doi: 10.1038/s41598-018-34049-8
91. Domińska K, Kowalska K, Anna Urbanek K, Ewa Habrowska-Górczy D, Och T, Wanda Piastowska Ciesielska A. The Impact of Ang-(1-9) and Ang-(3-7) on the Biological Properties of Prostate Cancer Cells by Modulation of Inflammatory and Steroidogenesis Pathway Genes. *Int J Mol Sci Article* (2020) 21:6227. doi: 10.3390/ijms21176227
92. Ockrim J, Lalani EN, Abel P. Therapy Insight: Parenteral Estrogen Treatment for Prostate Cancer - A New Dawn for an Old Therapy. *Nat Clin Pract Oncol* (2006) 3:552–63. doi: 10.1038/NCPONC060
93. Huang S, Zhou N, Zhao L, Gimple RC, Ahn YH, Zhang P, et al. Pharmacological Activation of Estrogen Receptor Beta Overcomes Tumor Resistance to Immune Checkpoint Blockade Therapy. *iScience* (2020) 23:101458. doi: 10.1016/J.ISCI.2020.101458
94. di Zazzo E, Galasso G, Giovannelli P, di Donato M, Castoria G. Estrogens and Their Receptors in Prostate Cancer: Therapeutic Implications. *Front Oncol* (2018) 8:2. doi: 10.3389/FONC.2018.00002
95. Gehrig J, Kaulfuß S, Jarry H, Bremmer F, Stettner M, Burfeind P, et al. Prospects of Estrogen Receptor β Activation in the Treatment of Castration-Resistant Prostate Cancer. *Oncotarget* (2017) 8:34971–9. doi: 10.18632/ONCOTARGET.16496
96. Sanaei MJ, Salimzadeh L, Bagheri N. Crosstalk Between Myeloid-Derived Suppressor Cells and the Immune System in Prostate Cancer: MDSCs and Immune System in Prostate Cancer. *J Leukoc Biol* (2020) 107:43–56. doi: 10.1002/JLB.4RU0819-150RR
97. Ollivier L, Labbé M, Fradin D, Potiron V, Supiot S. Interaction Between Modern Radiotherapy and Immunotherapy for Metastatic Prostate Cancer. *Front Oncol* (2021) 11:744679/BIBTEX. doi: 10.3389/FONC.2021.744679/BIBTEX

Conflict of Interest: The authors declare that the research was conducted in the absence of any commercial or financial relationships that could be construed as a potential conflict of interest.

frontiers | Frontiers in Oncology

TYPE Original Research
PUBLISHED 05 August 2022
DOI 10.3389/fonc.2022.856580

OPEN ACCESS

EDITED BY
Alagarsamy Srinivasan,
NanoBio Diagnostics, United States

REVIEWED BY
Tan Shyh-Han,
Uniformed Services University of the Health Sciences, United States
Shashwat Sharad,
Center for Prostate Disease Research (CPDR), United States

*CORRESPONDENCE
Yanbo Chen
fantasy_cyb@msn.com
Zhong Wang
zhongwang2000@sina.com

†These authors share first authorship

‡These authors have contributed equally to this work

SPECIALTY SECTION
This article was submitted to Genitourinary Oncology, a section of the journal Frontiers in Oncology

RECEIVED 24 January 2022
ACCEPTED 08 July 2022
PUBLISHED 05 August 2022

CITATION
Li P, Shi Y, Guo M, Xu H, Zhan M, Wang Z and Chen Y (2022) MAFG-AS1 is a prognostic biomarker and facilitates prostate cancer progression. *Front. Oncol.* 12:856580. doi: 10.3389/fonc.2022.856580

MAFG-AS1 is a prognostic biomarker and facilitates prostate cancer progression

Peizhang Li[1†], Yuanping Shi[2†], Miaomiao Guo[3,4], Huan Xu[1], Ming Zhan[1], Zhong Wang[1*‡] and Yanbo Chen[1*‡]

[1]Department of Urology, Shanghai Ninth People's Hospital Affiliated to Shanghai Jiaotong University School of Medicine, Shanghai, China, [2]Department of Endocrinology and Metabolism, Peking University People's Hospital, Beijing, China, [3]The Core Laboratory in Medical Center of Clinical Research, Department of Molecular Diagnostics and Endocrinology, Shanghai Ninth People's Hospital, Shanghai Jiaotong University School of Medicine, Shanghai, China, [4]Department of Molecular Diagnostics, Shanghai Ninth People's Hospital Affiliated to Shanghai Jiaotong University School of Medicine, Shanghai, China

Long Noncoding RNAs (LncRNAs) have recently been identified as key regulator in tumor progression. The LncRNA MAFG-AS1 has been reported to facilitate the progression of multiple cancers, however, its role in prostate cancer is still unknown. Here, we reported that MAFG-AS1 was upregulated in prostate cancer. Importantly, high expression of MAFG-AS1 indicated advanced stage prostate cancer. Univariate and Multivariate Cox regression analyses showed that high MAFG-AS1 expression was independently correlated with poor progression-free interval (PFI). According to the result of The Cancer Genome Atlas (TCGA) database and tissue microarray, high MAFG-AS1 expression indicated a poor prognosis in prostate cancer patients. In addition, gene functional enrichment analysis revealed that MAFG-AS1 may be involved in ribosome biogenesis, ribonucleoprotein complex subunit organization, ribonucleoprotein complex assembly, rRNA metabolic process, structural constituent of ribosome, and ribonucleoprotein complex binding. Furthermore, MAFG-AS1 knockdown by siRNA markedly impaired prostate cancer cell proliferation, migration, and invasion.

KEYWORDS

MAFG-AS1, lncRNAs, prostate cancer, prognosis, tumor-microarray

Introduction

Prostate cancer is one of the most common cancers in men worldwide. With regard to the cancer-related mortality of prostate cancer, it is currently ranked first in the US (1–3). According to the American Cancer Society (ACS), 161,360 new cases of prostate cancer accounted for the first incidence of malignant tumors in men (19%), and 26,730 new deaths from prostate cancer accounted for the third highest mortality rate among male malignant

tumors (8%) in 2017 (4). Androgen deprivation therapy (ADT) is the first-line therapy for prostate cancer patients, and it has been proven to improve the overall survival (OS) of men diagnosed with metastatic prostate cancer (5). However, the tumor will subsequently progress to resistance to ADT and inevitably develop into castration-resistant prostate cancer (CRPC). Metastasis has become a bottleneck restricting the long-term survival of prostate cancer patients and is also the key to overcoming prostate cancer. The molecular mechanisms underlying the progression of prostate cancer remain largely unknown. Therefore, there is an urgent need to elucidate the underlying mechanisms of prostate cancer and explore novel molecular targets that are crucial for the development of new diagnostic and therapeutic drugs for the treatment of prostate cancer.

Long non coding RNAs (lncRNAs) are a large class of no protein-coding capacity transcripts that are longer than 200 nucleotides (6). lncRNAs have been reported to be involved in different biological processes, such as cell proliferation, apoptosis, angiogenesis, migration, invasion, and drug resistance (7–11). Accumulating evidence has demonstrated that dysregulation of lncRNAs is strongly associated with the development and progression of cancer. Furthermore, many lncRNAs have been reported to regulate the pathogenesis of prostate cancer (12). Previous studies have suggested that lncRNA NEAT1-1 is involved in bone metastasis of prostate cancer and promotes the binding ability between CYCLINL1 and CDK19 in an N6-methyladenosine dependent manner (13). Luo et al. showed that lncRNA-p21 is upregulated in neuroendocrine prostate cancer (NEPC) and overexpressed lncRNA-p21 induces the neuroendocrine differentiation (NED) (14). Mechanistically, lncRNA-p21 can disrupt the PRC2 complex and promote the methylation of STAT3 to induce NED. Several studies have demonstrated that MALAT1 upregulation promotes prostate cancer cell growth, migration, and invasion (15). Furthermore, the lncRNA MAFG-AS1 was upregulated in breast cancer and facilitated breast carcinoma progression by regulating MMP15 expression (16). MAFG-AS1 also promoted cell proliferation, migration, and invasion of hepatocellular cancer *via* targeting miR-3196/OTX1 axis (17). Additionally, MAFG-AS1 regulated tumorigenesis of colorectal cancer by acting as a sponge of miR-149-3p (18). However, the role of MAFG-AS1 in prostate cancer progression remains largely unknown.

In the current study, we investigated the expression of MAFG-AS1 in prostate cancer according to the TCGA database and a tissue microarray, and determined its role as a prognostic biomarker in prostate cancer. In addition, we searched for the gene set most related to the expression of MAFG-AS1, then predicted the functions and pathways of MAFG-AS1 in prostate cancer through gene enrichment analysis. Furthermore, to investigate the role of MAFG-AS1 in cell proliferation, migration, and invasion in prostate cancer, we performed a series of *in vitro* experiments.

Methods and materials

RNA-sequencing data and bioinformatics analysis

A total of 495 cases containing both gene expression data (HTSeq-Counts) and clinical information from the PRAD database were obtained from The Cancer Genome Atlas (TCGA) for further analysis. HTSeq-Counts data were transformed into transcripts per million reads (TPM). Data of 495 cases were used for survival analysis. Next, the characteristics of patients consists of T stage, N stage, Gleason score of pathologic of surgical specimens, and progression-free interval (PFI) result. Pathological T and N stage were performed according to the extent of tumor invasion and the presence of lymphatic metastasis. This study satisfied the publication requirements stated by TCGA (http://cancergenome.nih.gov/publications-/publicationguidelines).

Cell lines and culture

The human prostate cancer cell line PC-3 originated from bone marrow metastases in a 62-year-old white male patient diagnosed with grade IV prostate cancer. Prostate cancer cells DU145 were established from a brain metastasis of a 69-year-old Caucasian patient with prostate cancer. The cells were obtained from the National Collection of Authenticated Cell Culture at the Chinese Academy of Science (Shanghai, China). PC-3 and DU145 cells were cultured in MEM supplemented with 10% fetal bovine serum (FBS) (Gibco, USA). Cell authentication was validated using STR profiling.

Small interfere RNA (siRNA) construction

Small interfering RNAs (siRNAs) targeting MAFG-AS1 were obtained from GenePharma (Shanghai, China), and the sequence information targeting MAFG-AS1 was as follows: siMAFG-AS1-1, GGAGTCAGGGCAATTCCAA; siMAFG-AS1-2, GGTAACATAGAGACCCTAT.

Total RNA isolation and real-time qPCR

Total RNA was extracted from prostate cancer cells using TRIzol reagent (Invitrogen, USA) according to the manufacturer's protocol. Total RNA was then reverse

transcribed to cDNA using random primers using a Revert Aid First Strand cDNA Synthesis kit (Thermo Fisher, USA). RT-qPCR was performed using TB Green Premix Ex Taq (Takara, Germany). GAPDH was used as an internal control. qPCR primers were synthesized from BioSune (Shanghai, China). The primers used were as follows: MAFG-AS1-F: CGGGAGG AAGATAAACGGGG, MAFG-AS1-R: TGACCACGGAAC ACCTTCAG, GAPDH-F: CTGGGCTACACTGAGCACC, GAPFH-R: AAGTGGTCGTTGAGGGCAATG.

Cell proliferation assay and colony formation assay

For the cell proliferation assay, a total of 3000 prostate cancer cells were seeded into 96-well plates and incubated in 10% CCK-8 medium for one hour at 0 hour, 24 hours, 48 hours, and 72 hours after seeding. The absorbance was measured at 450 nm with a spectrophotometer. For the colony formation assay, prostate cancer cells were seeded in 6-well plates at a density of 200 cells per well and cultured for 2 weeks. The cells were then fixed and subsequently examined by crystal violet staining.

Transwell migration assays and transwell invasion assay

For the transwell migration assay, 20000 cells were suspended in 200 µl of medium without FBS and were seeded in the upper chamber of transwell inserts (Corning, USA). 500 µl medium with 20% FBS were added into the lower chamber. The cells were then incubated for 18 h. For the transwell invasion assay, 30000 cells were suspended in 200 µl of medium without FBS and were seeded on the upper chamber of transwell inserts coated with Matrigel (BD Biosciences, USA). The cells were then cultured for 24 h. Cells were fixed with 4% PFA and stained with a crystal violet staining solution. Images were captured with a ×20 objective using a Leica DM LB light microscope and the number of cells was counted using ImageJ.

Statistical analysis

All statistical analyses were conducted using SPSS (22.0). Pearson's $\chi 2$ test was used to determine the correlation between MAFG-AS1 expression and clinicopathological variables. The t-test was used to determine statistically significant differences between the two groups. Kaplan–Meier analysis was performed to compare the survival time differences between the MAFG-AS1 high expression group and low expression group. The log-rank test $p < 0.05$ suggested the significance of survival time differences. The hazard risk of the individual indicators was estimated using hazard ratios (HRs) with 95% confidence intervals (CIs). All reported P-values were two-sided and P-values of less than 0.05 were considered to be significant. * represents $P < 0.05$, ** represents $P < 0.01$, and *** represents $P < 0.001$.

Result

MAFG-AS1 was highly expressed in prostate cancer

The data collected from TCGA in October 2019 contained 495 tumor samples with both clinical information and gene expression data (Table 1) and the clinical features of the patients included age, TNM stage, Gleason scores, and PFI events. To evaluate the expression of MAFG-AS1 in prostate cancer, we compared MAFG-AS1 expression in 495 prostate cancer and 50 adjacent normal tissues, and the results suggested that MAFG-AS1 was upregulated in prostate cancer (Figure 1A). Similarly, by comparing 50 pairs of prostate cancer tissues and adjacent normal tissues, we also found that MAFG-AS1 was highly expressed in prostate cancer (Figure 1B). In addition, we collected 18 pairs of prostate cancer tissues and adjacent normal tissues, and the results of RT-qPCR demonstrated that MAFG-AS1 expression was upregulated in prostate cancer (Figure 1C). Next, the results of RT-qPCR indicated that MAFG-AS1 expression in prostate cancer cell lines PC-3 and DU145 was higher than that in the normal prostate epithelial cell line RWPE-1 (Figure 1D). These results demonstrated that MAFG-AS1 expression is overexpressed in prostate cancer.

MAFG-AS1 was upregulated in advanced prostate cancer and indicated a poor prognosis in TCGA database

Logistic regression analysis demonstrated that higher MAFG-AS1 expression, regarded as an independent variable, was correlated with better prognostic characteristics (Table 2). High MAFG-AS1 expression in the PRAD cohort was significantly associated with T classification (OR = 1.952 for T3&T4 *vs.* T2, $P < 0.001$), N classification (OR = 2.005 for N1 *vs.* N0, $P = 0.008$), and Gleason score (OR = 2.074 for 8&9&10 *vs.* 6&7, $P < 0.001$). These results revealed that prostate cancer with high MAFG-AS1 expression is more likely to be in a primitive stage than those with low MAFG-AS1 expression. The expression level of MAFG-AS1 was higher in the T3&T4 stage than in the T2 stage (Figure 2A). Similarly, MAFG-AS1 expression was higher in advanced prostate cancer according to N stage, Gleason scores, and PFI events (Figures 2B–D). Consistently, MAFG-AS1 high expression was significantly correlated with poor prognosis in patients with prostate cancer patients (Figure 2E). Furthermore, univariate Cox regression analysis showed that high MAFG-AS1 expression was correlated

TABLE 1 Correlation between MAFG-AS1 expression and clinicopathological characteristics of prostate cancer.

Characteristic	Low expression of MAFG-AS1	High expression of MAFG-AS1	p
n	249	250	
T stage, n (%)			<0.001
T2	113 (23%)	76 (15.4%)	
T3	128 (26%)	164 (33.3%)	
T4	3 (0.6%)	8 (1.6%)	
N stage, n (%)			0.010
N0	177 (41.5%)	170 (39.9%)	
N1	27 (6.3%)	52 (12.2%)	
M stage, n (%)			1.000
M0	224 (48.9%)	231 (50.4%)	
M1	1 (0.2%)	2 (0.4%)	
Age, n (%)			0.226
<=60	119 (23.8%)	105 (21%)	
>60	130 (26.1%)	145 (29.1%)	
PSA(ng/ml), n (%)			0.923
<4	212 (48%)	203 (45.9%)	
>=4	13 (2.9%)	14 (3.2%)	
Gleason score, n (%)			<0.001
6	34 (6.8%)	12 (2.4%)	
7	134 (26.9%)	113 (22.6%)	
8	30 (6%)	34 (6.8%)	
9	50 (10%)	88 (17.6%)	
10	1 (0.2%)	3 (0.6%)	
PFI event, n (%)			0.002
Alive	216 (43.3%)	189 (37.9%)	
Dead	33 (6.6%)	61 (12.2%)	
Primary therapy outcome, n (%)			0.012
PD	13 (3%)	15 (3.4%)	
SD	9 (2.1%)	20 (4.6%)	
PR	14 (3.2%)	26 (5.9%)	
CR	187 (42.7%)	154 (35.2%)	
Age, meidan (IQR)	61 (56, 66)	62 (57, 66)	0.231

with a poor PFI (hazard ratio [HR]: 1.985; 95% confidence interval [CI]: 1.299- 3.035; P < 0.01), and other clinical variables, including advanced T stage, N stage, and Gleason score, remained associated with a poor prognosis (Table 3). Multivariate analysis suggested that high MAFG-AS1 expression was independently associated with poor PFI (HR = 1.78; CI: 1.121- 2.847; P = 0.015).

We then performed a stratified analysis based on the clinical information of prostate cancer patients. KM-plot analysis revealed that high MAFG-AS1 expression was associated with a poor prognosis in T3&T4 stage patients with prostate cancer; however, MAFG-AS1 expression was not associated with prognosis in T2 stage patients (Figures 2F, G). In patients with or without lymph node metastasis, MAFG-AS1 expression could be used as a prognostic marker, indicating poor PFI (Figures 2H, I). Similarly, in patients with high or low Gleason scores, high expression of MAFG-AS1 was correlated with poor prognosis (Figures 2J, K). In addition, high MAFG-AS1 expression was associated with a poor prognosis in prostate cancer patients with PSA levels more than 4 ng/ml or less than 4 ng/ml (Figures 2L, M).

MAFG-AS1 indicated a poor prognosis in tissue-microarray

To critically evaluate the prognostic value of MAFG-AS1 in prostate cancer, we performed a tissue microarray (Figure 3A; Figure S1), and the clinical information of TMA patient cohort was shown in Table 4. The ISH results demonstrated that MAFG-AS1 expression was higher in the T3&T4 stages than in the T2 stage (Figure 3B). Similarly, MAFG-AS1 was upregulated in the N1 stage compared to the N0 stage (Figure 3C). Furthermore, prostate cancer with a higher

10.3389/fonc.2022.856580

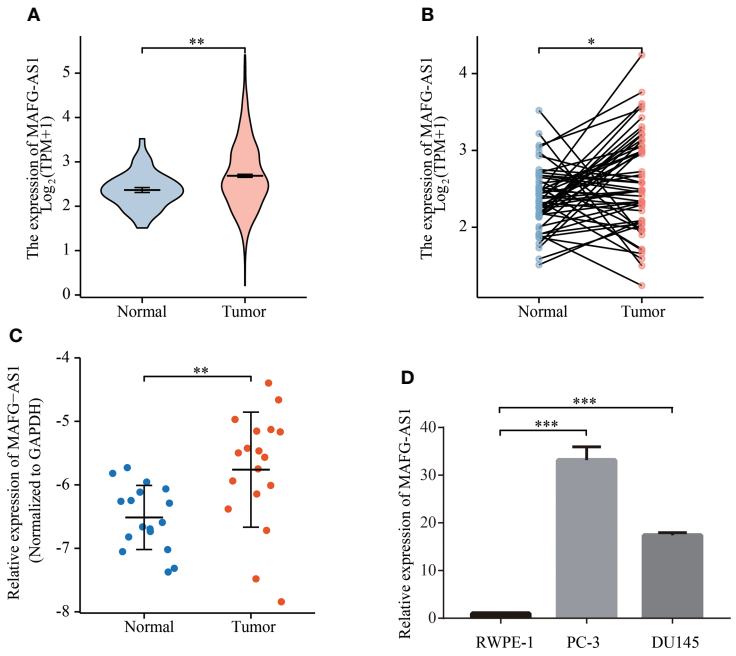

FIGURE 1
MAFG-AS1 was highly expressed in prostate cancer. **(A)** MAFG-AS1 expression in prostate cancer and adjacent normal tissue in TCGA database. **(B)** MAFG-AS1 expression in 50 pairs of prostate cancer and adjacent normal tissue in TCGA database. **(C)** MAFG-AS1 expression in prostate cancer and normal prostate tissue using RT-qPCR. **(D)** MAFG-AS1 expression in prostate cancer cell lines (PC-3, DU145) and normal prostate epithelial cell line (RWPE-1). Data were indicated as mean ± standard deviation, ns $P \geq 0.05$, * $P < 0.05$, ** $P < 0.01$, *** $P < 0.001$..

Gleason score showed higher MAFG-AS1 expression (Figure 3D). KM-plot analysis suggested that high expression of MAFG-AS1 indicated a poor overall survival (OS) in the TMA patient cohort (Figure 3E). These results demonstrate that MAFG-AS1 is correlated with prostate cancer clinical features, and high expression of MAFG-AS1 is associated with a poor prognosis in prostate cancer.

Functional enrichment analysis of MAFG-AS1 in prostate cancer

Next, we performed a functional gene enrichment analysis of MAFG-AS1. We searched for the top 500 genes related to MAFG-AS1 expression according to the TCGA-PRAD database. The results showed that these genes were enriched in ribosome biogenesis, ribonucleoprotein complex subunit organization, ribonucleoprotein complex assembly, and rRNA metabolic process in biological process (BP). Results also showed that these genes were enriched in ribosome and ribosomal subunit in cellular component (CC), and enriched in structural constituent of ribosome and ribonucleoprotein complex binding in molecular function (MF) (Figures 4A–C). Kyoto Encyclopedia of Genes and Genomes (KEGG) pathway analysis revealed that MAFG-AS1 related genes were enriched in the ribosome and DNA replication pathways (Figure 4D).

The correlation analysis between MAFG-AS1 and ribosome related genes

Since functional enrichment analysis revealed that MAFG-AS1 may be involved in ribosome biogenesis, we investigated the

TABLE 2 MAFG-AS1 expression associated with clinical pathological characteristics (logistic regression).

Characteristics	Total (N)	Odds Ratio (OR)	P value
T stage (T3&T4 *vs.* T2)	492	1.952 (1.352-2.831)	<0.001
N stage (N1 *vs.* N0)	426	2.005 (1.213-3.378)	0.008
M stage (M1 *vs.* M0)	458	1.939 (0.185-41.906)	0.590
Gleason score (8&9&10 *vs.* 6&7)	499	2.074 (1.445-2.989)	<0.001
PSA (ng/ml) (>=4 *vs.* <4)	442	1.125 (0.514-2.480)	0.768

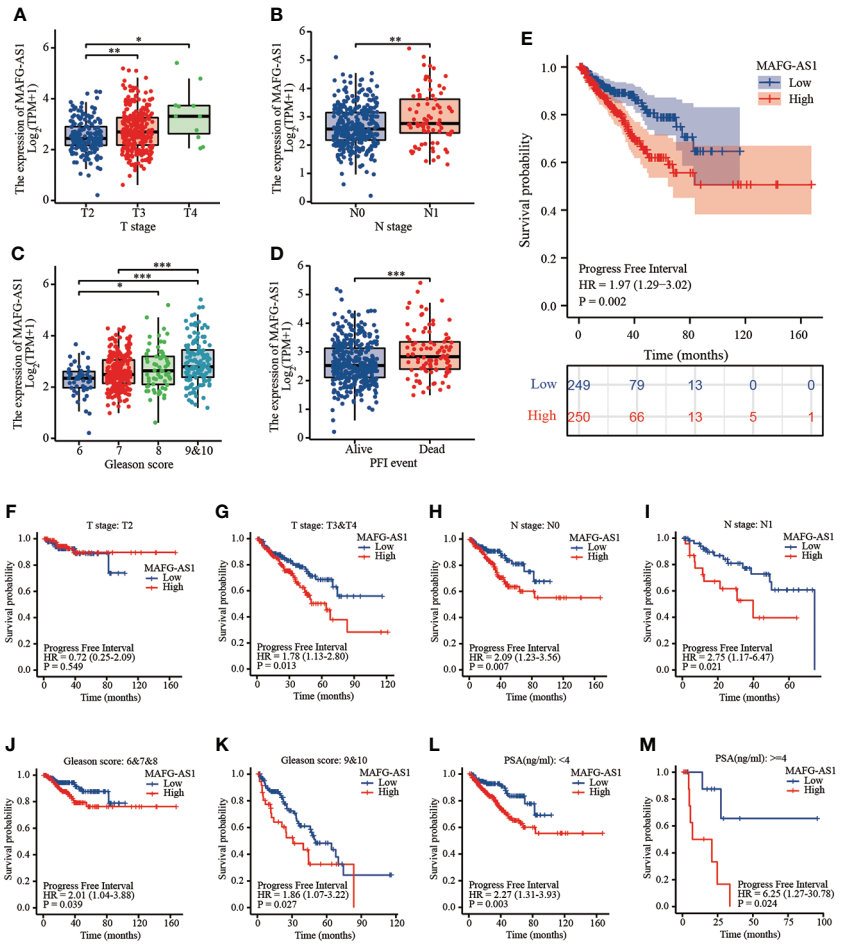

FIGURE 2
MAFG-AS1 was upregulated in advanced prostate cancer and indicated a poor prognosis. **(A)** MAFG-AS1 expression in prostate cancer with T3&T4 stage or T2 stage. **(B)** MAFG-AS1 expression in prostate cancer with N1 stage or N0 stage. **(C)** MAFG-AS1 expression in prostate cancer with Gleason score 6&7&8 or 9&10. **(D)** MAFG-AS1 expression in prostate cancer patients with different PFI. **(E)** Kaplan-Meier survival analysis revealed that prostate cancer patients with high MAFG-AS1 expression exhibited a shorter PFI. **(F, G)** Kaplan-Meier survival analysis of prostate cancer with different MAFG-AS1 level with T2 or T3&T4 stage. **(H, I)** Kaplan-Meier survival analysis of prostate cancer with different MAFG-AS1 level with N0 or N1 stage. **(J, K)** Kaplan-Meier survival analysis of prostate cancer with different MAFG-AS1 level with Gleason score 6&7&8 or 9&10. **(L, M)** Kaplan-Meier survival analysis of prostate cancer with different MAFG-AS1 level with PSA level < 4ng/ml or > 4ng/ml. Data were indicated as mean ± standard deviation, ns $P \geq 0.05$, * $P < 0.05$, ** $P < 0.01$, *** $P < 0.001$..

TABLE 3 Univariate and multivariate analysis of factors associated with PFI using Cox regression.

Characteristics	Total (N)	Univariate analysis		Multivariate analysis	
		Hazard ratio (95% CI)	P value	Hazard ratio (95% CI)	P value
T stage (T3&T4 *vs.* T2)	492	3.785 (2.140-6.693)	<0.001	3.386 (1.752-6.544)	<0.001
N stage (N1 *vs.* N0)	426	1.946 (1.202-3.150)	0.007	1.225 (0.732-2.051)	0.441
M stage (M1 *vs.* M0)	458	3.566 (0.494-25.753)	0.208		
PSA (ng/ml)	442	4.196 (2.095-8.405)	<0.001	2.616 (1.186-5.768)	0.017
MAFG-AS1 (High *vs.* Low)	495	1.985 (1.299-3.035)	0.002	1.787 (1.121-2.847)	0.015

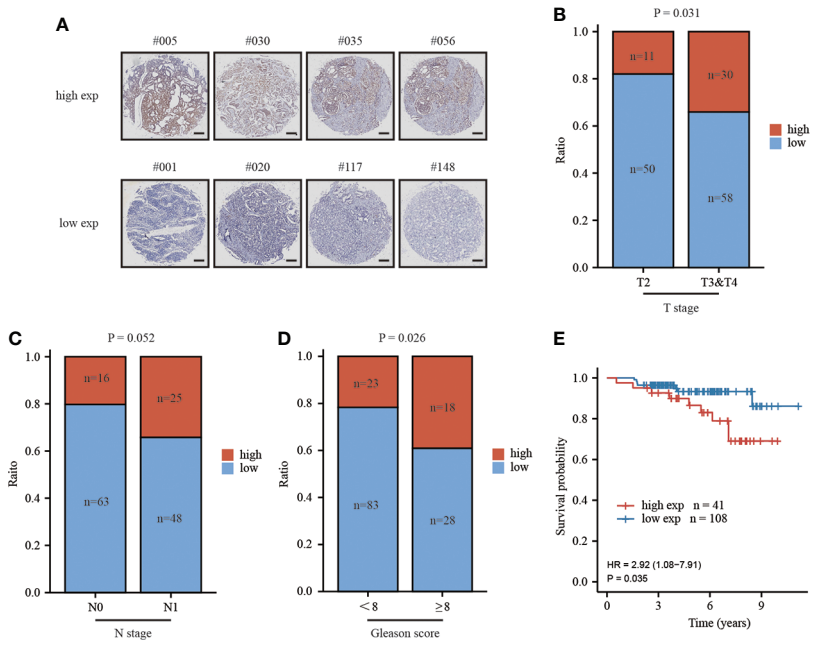

FIGURE 3
high expression of MAFG-AS1 indicated a poor prognosis. **(A)** Representative ISH results of prostate cancer patients in different groups (Scale bar: 200μm) **(B)** MAFG-AS1 expression in prostate cancer in T3&T4 or T2 stage by *in situ* hybridization (ISH). **(C)** MAFG-AS1 expression in prostate cancer in N1 or N0 stage by *in situ* hybridization (ISH). **(D)** MAFG-AS1 expression in prostate cancer in Gleason score<8 or ≥8. **(E)** High expression of MAFG-AS1 indicated a poor overall survival (OS) by Kaplan-Meier analysis.

correlation between MAFG-AS1 and ribosome-related genes. Among the top 500 genes most related to MAFG-AS1 expression, a number of genes were the components of ribosomes or involved in ribosome biosynthesis. For example, MAFG-AS1 expression was positively correlated with 60S ribosomal proteins (RPL6, RPL7, RPL7A, RPL8, etc.) and 40S ribosomal proteins (RPS2, RPS3, RPS3A, RPS7, etc.) (Figure 4E). Collectively, these results suggest that MAFG-AS1 may be involved in ribosome biogenesis to regulate prostate cancer tumorigenicity.

MAFG-AS1 knockdown significantly impaired prostate cancer cell proliferation, migration and invasion

To further elucidate the role of MAFG-AS1 expression in prostate cancer, we selected two prostate cancer cell lines (PC-3 and DU145) for subsequent research. RT-qPCR results showed that MAFG-AS1 expression was effectively downregulated in PC-3 and DU145 cells transfected with si-MAFG-AS1

TABLE 4 Clinicopathological characteristics of prostate cancer patients in TMA cohort.

Characteristic	high exp	low exp	p
n	41	108	
T stage, n (%)			0.031
T2	11 (7.4%)	50 (33.6%)	
T3&T4	30 (20.1%)	58 (38.9%)	
N stage, n (%)			0.052
N0	16 (10.7%)	63 (42.3%)	
N1	25 (16.8%)	45 (30.2%)	
Gleasion scores, n (%)			0.026
<8	23 (15.4%)	83 (55.7%)	
≥8	18 (12.1%)	25 (16.8%)	
ages (years), mean ± SD	66.98 ± 7.16	68.92 ± 5.89	0.093

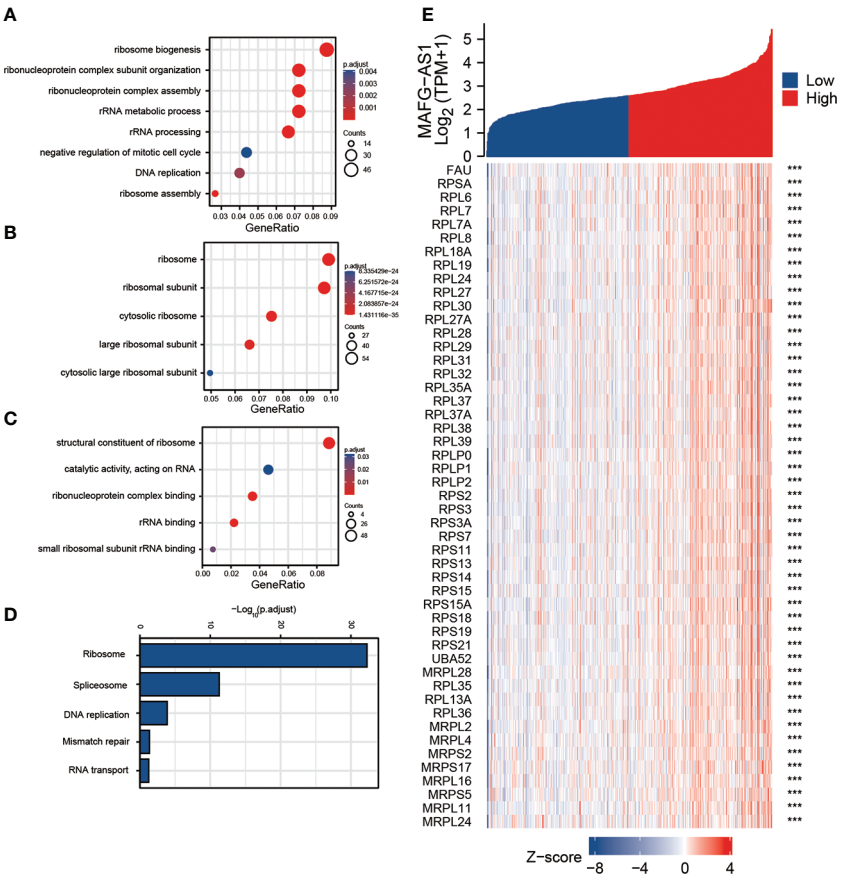

FIGURE 4
Gene functional enrichment analysis of the most relative genes with MAFG-AS1 expression. **(A)** Gene Ontology analysis of MAFG-AS1 related genes in biological process (BP). **(B)** Gene Ontology analysis of MAFG-AS1 related genes in cellular component (CC). **(C)** Gene Ontology analysis of MAFG-AS1 related genes in molecular function (MF). **(D)** Kyoto Encyclopedia of Genes and Genomes (KEGG) pathway analysis of MAFG-AS1 related genes. **(E)** The correlation analysis between MAFG-AS1 and ribosome related genes. ns $P \geq 0.05$, * $P < 0.05$, ** $P < 0.01$, *** $P < 0.001$.

(Figure 5A). The results of the CCK-8 assay demonstrated that MAFG-AS1 knockdown significantly inhibited prostate cancer cell viability (Figures 5B, C). The colony formation assay demonstrated that downregulation of MAFG-AS1 decreased the colony formation rate in prostate cancer cells (Figure 5D). For further studies, we conducted a transwell assay to clarify the role of MAFG-AS1 in prostate cancer migration and invasion. The results suggested that migration and invasion abilities were prominently impaired in MAFG-AS1 knockdown prostate cancer cells (Figures 5E, F). Taken together, we demonstrated that MAFG-AS1 knockdown significantly inhibited prostate cancer cell proliferation, migration, and invasion.

Discussion

Several studies have highlighted the potential of MAFG-AS1 as a therapeutic target for cancer treatment. Mechanistically, MAFG-AS1 acts as a microRNA sponge to regulate tumorigenesis (16–20). For example, MAFG-AS1 facilitates esophageal squamous cell cancer progression by regulating miR143/LASP1 (19). MAFG-AS1 promotes the progression of pancreatic cancer by acting as a sponge for miR-3196 (20). In addition, MAFG-AS1 inhibited the stability of P53 to support cancer cell survival and division. Mechanistically, MAFG-AS1 binds to P53 and competitively inhibits TRIML2-mediated P53 SUMOylation and promotes the degradation of P53 by polyubiquitination (21). However, the role of MAFG-AS1 in prostate cancer has not been clearly elucidated.

Bioinformatics analysis showed that MAFG-AS1 expression was elevated in prostate cancer compared with normal prostate tissue and was higher in more advanced prostate cancer, indicating that MAFG-AS1 is a diagnostic biomarker for prostate cancer. In addition, KM-plot analysis and Cox regression analysis suggested that high expression of MAFG-AS1 was associated with a poor prognosis, and a series of

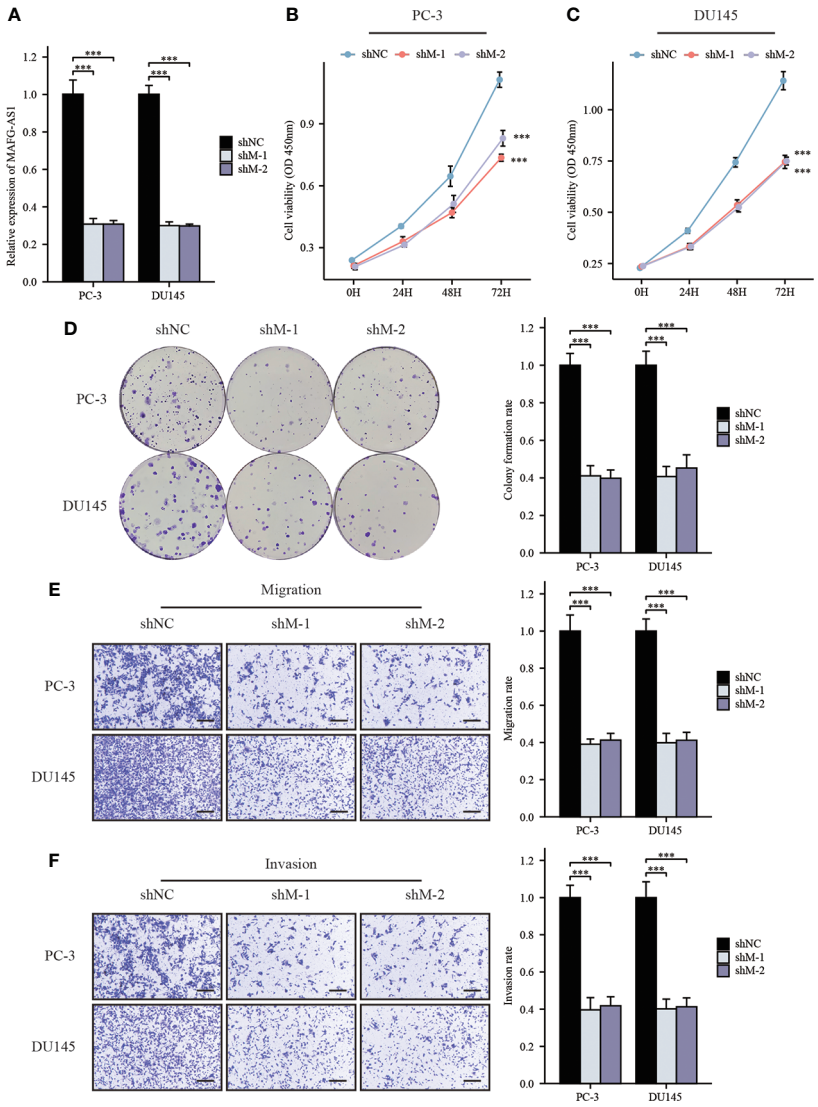

FIGURE 5
MAFG-AS1 knockdown significantly inhibited prostate cancer cell progression. **(A)** RT-qPCR analysis of MAFG-AS1 in MAFG-AS1 knockdown prostate cancer cells. **(B, C)** Downregulated MAFG-AS1 markedly inhibited cell viability of PC-3 and DU145 cells. **(D)** Knockdown of MAFG-AS1 impaired the ability of colony formation of PC-3 and DU145 cells. **(E, F)** The migration and invasion ability of PC-3 and DU145 cells were reduced following MAFG-AS1 knockdown (Scale bar: 50μm). Data were indicated as mean ± standard deviation, ns $P \geq 0.05$, * $P < 0.05$, ** $P < 0.01$, *** $P < 0.001$.

functional experiments demonstrated that MAFG-AS1 knockdown significantly impaired prostate cancer cell progression. This indicates that MAFG-AS1 is a potential therapeutic target in prostate cancer.

Ribosomes are intracellular organelles that are responsible for translation of messenger RNAs (mRNAs) into functional proteins. Eukaryotes have 80S ribosomal subunits composed of large (60S) and small (60S) subunits. The 60S subunit consists of 5S rRNA, 5.8S rRNA, 28S rRNA, and approximately 47 proteins (RPL). The 40S subunit consists of 18S rRNA and approximately 33 proteins (RPS) (22, 23). Ribosomes play a pivotal role in the maintenance of cell growth, proliferation, and differentiation. Ribosomal dysfunction can lead to various diseases (24–26). Additionally, a large amount of evidence has demonstrated that ribosomal proteins are involved in tumor progression (27–30). In this study, we discovered that MAFG-AS1 expression was related to a number of RPLs and RPSs, and the genes most closely related to MAFG-AS1 expression were enriched in ribonucleoprotein complex subunit organization and ribonucleoprotein complex assembly, suggesting that MAFG-AS1 may be involved in ribosome biogenesis. However, further experimental evidence is needed to prove our hypothesis.

Conclusion

In summary, MAFG-AS1 may play an important role in the occurrence and development of prostate cancer by regulating ribosome biogenesis. MAFG-AS1 may serve as a biomarker for the early diagnosis of prostate cancer and serve as a target for the treatment of prostate cancer.

Data availability statement

The raw data supporting the conclusions of this article will be made available by the authors, without undue reservation.

Ethics statement

The studies involving human participants were reviewed and approved by ethics committee of Shanghai Ninth People's Hospital. The patients/participants provided their written informed consent to participate in this study.

Author contributions

PL and YS conducted all the experiments. PL participated in the design of the study and drafted the manuscript. MG, HX, and MZ conducted the statistical analysis. YC and ZW designed the project and finalized the manuscript. All authors contributed to the article and approved the submitted version.

Funding

This study was supported by Scientific research project of Shanghai Municipal Health Commission (20214Y0408), multi-center clinical research project of Shanghai JiaoTong University School of Medicine (DLY201809), and Shanghai Huangpu District Industry Support Fund (XK2020011), and Technology Transfer Project of Shanghai Jiao Tong University School of Medicine (ZT202110).

Conflict of interest

The authors declare that the research was conducted in the absence of any commercial or financial relationships that could be construed as a potential conflict of interest.

Publisher's note

Supplementary material

The Supplementary Material for this article can be found online at: https://www.frontiersin.org/articles/10.3389/fonc.2022.856580/full#supplementary-material

References

1. Cooperberg MR. Prostate cancer: a new look at prostate cancer treatment complications. *Nat Rev Clin Oncol* (2014) 11(6):304–5. doi: 10.1038/nrclinonc.2014.58

2. Siegel RL, Miller KD, Jemal A. Cancer statistics, 2018. *CA Cancer J Clin* (2018) 68(1):7–30. doi: 10.3322/caac.21442

3. Roehl KA, Han M, Ramos CG, Antenor JA, Catalona WJ. Cancer progression and survival rates following anatomical radical retropubic prostatectomy in 3,478 consecutive patients: long-term results. *J Urol* (2004) 172(3):910–4. doi: 10.1097/01.ju.0000134888.22332.bb

4. Siegel RL, Miller KD, Jemal A. Cancer statistics, 2017. *CA Cancer J Clin* (2017) 67(1):7–30. doi: 10.3322/caac.21387

5. Thompson I, Thrasher JB, Aus G, Burnett AL, Canby-Hagino ED, Cookson MS, et al. Guideline for the management of clinically localized prostate cancer: 2007 update. *J Urol* (2007) 177(6):2106–31. doi: 10.1016/j.juro.2007.03.003

6. Ulitsky I, Bartel DP. lincRNAs: genomics, evolution, and mechanisms. *Cell* (2013) 154(1):26–46. doi: 10.1016/j.cell.2013.06.020

7. Prensner JR, Chinnaiyan AM. The emergence of lncRNAs in cancer biology. *Cancer Discovery* (2011) 1(5):391–407. doi: 10.1158/2159-8290.CD-11-0209

8. Hu Z, Mi S, Zhao T, Peng CA-OX, Peng Y, Chen L, et al. BGL3 lncRNA mediates retention of the BRCA1/BARD1 complex at DNA damage sites. *EMBO J* (2020) 9(12):e104133. doi: 10.15252/embj.2019104133

9. Chen C, Luo Y, He W, Zhao Y, Kong Y, Liu H, et al. Exosomal long noncoding RNA LNMAT2 promotes lymphatic metastasis in bladder cancer. *J Clin Invest* (2020) 130(1):404–21. doi: 10.1172/JCI130892

10. Tian H, Lian R, Li Y, Liu C, Liang S, Li W, et al. AKT-induced lncRNA VAL promotes EMT-independent metastasis through diminishing Trim16-dependent vimentin degradation. *Nat Commun* (2020) 11(1):5127. doi: 10.1038/s41467-020-18929-0

11. Sun CC, Zhu W, Li SJ, Hu W, Zhang J, Zhuo Y, et al. FOXC1-mediated LINC00301 facilitates tumor progression and triggers an immune-suppressing microenvironment in non-small cell lung cancer by regulating the HIF1α pathway. *Genome Med* (2020) 12(1):77. doi: 10.1186/s13073-020-00773-y

12. Hua JT, Chen S, He HH. Landscape of noncoding RNA in prostate cancer. *Trends Genet* (2019) 35(11):840–51. doi: 10.1016/j.tig.2019.08.004

13. Wen S, Wei Y, Zen C, Xiong W, Niu Y, Zhao Y. Long non-coding RNA NEAT1 promotes bone metastasis of prostate cancer through N6-methyladenosine. *Mol Cancer* (2020) 19(1):171. doi: 10.1186/s12943-020-01293-4

14. Luo J, Wang K, Yeh S, Sun Y, Liang L, Xiao Y, et al. LncRNA-p21 alters the antiandrogen enzalutamide-induced prostate cancer neuroendocrine differentiation *via* modulating the EZH2/STAT3 signaling. *Nat Commun* (2019) 10(1):2571. doi: 10.1038/s41467-019-09784-9

15. Hao T, Wang Z, Yang J, Zhang Y, Shang Y, Sun J. MALAT1 knockdown inhibits prostate cancer progression by regulating miR-140/BIRC6 axis. *BioMed Pharmacother* (2020) 123:109666. doi: 10.1016/j.biopha.2019.109666

16. Li H, Zhang GY, Pan CH, Zhang XY, Su XY. LncRNA MAFG-AS1 promotes the aggressiveness of breast carcinoma through regulating miR-339-5p/MMP15. *Eur Rev Med Pharmacol Sci* (2019) 23(7):2838–46. doi: 10.26355/eurrev_201904_17561

17. Hu ZQ, Li HC, Teng F, Chang QM, Wu XB, Feng JF, et al. Long noncoding RNA MAFG-AS1 facilitates the progression of hepatocellular carcinoma *via* targeting miR-3196/OTX1 axis. *Eur Rev Med Pharmacol Sci* (2020) 24 (23):12131–43. doi: 10.26355/eurrev_202012_24002

18. Ruan Z, Deng H, Liang M, Xu Z, Lai M, Ren H, et al. Downregulation of long non-coding RNA MAFG-AS1 represses tumorigenesis of colorectal cancer cells through the microRNA-149-3p-dependent inhibition of HOXB8. *Cancer Cell Int* (2020) 20:511. doi: 10.1186/s12935-020-01485-4

19. Qu Y, Liu J. lncRNA MAFG-AS1 contributes to esophageal squamous-cell carcinoma progression *via* regulating miR143/LASP1. *Onco Targets Ther* (2020) 13:8359–70. doi: 10.2147/OTT.S258157

20. Ye L, Feng W, Weng H, Yuan C, Liu J, Wang Z. MAFG-AS1 aggravates the progression of pancreatic cancer by sponging miR-3196 to boost NFIX. *Cancer Cell Int* (2020) 20(1):591. doi: 10.1186/s12935-020-01669-y

21. Feng YC, Liu XY, Teng L, Ji Q, Wu Y, Li JM, et al. C-myc inactivation of p53 through the pan-cancer lncRNA MILIP drives cancer pathogenesis. *Nat Commun* (2020) 11(1):4980. doi: 10.1038/s41467-020-18735-8

22. Ben-Shem A, Garreau de Loubresse N, Melnikov S, Jenner L, Yusupova G, Yusupov M. The structure of the eukaryotic ribosome at 3.0 Å resolution. *Science* (2011) 334(6062):1524–9. doi: 10.126/science.1212642

23. Khatter H, Myasnikov AG, Natchiar SK, Klaholz BP. Structure of the human 80S ribosome. *Nature* (2015) 520(7549):640–5. doi: 10.1038/nature14427

24. McCann KL, Baserga SJ. Genetics. *Mysterious ribosomopathies Science* (2013) 341(6148):849–50. doi: 10.1126/science.1244156

25. Narla A, Ebert BL. Ribosomopathies: human disorders of ribosome dysfunction. *Blood* (2010) 115(16):3196–205. doi: 10.1182/blood-2009-10-178129

26. Doudna JA, Rath VL. Structure and function of the eukaryotic ribosome: the next frontier. *Cell* (2002) 109(2):153–6. doi: 10.1016/s0092-8674(02)00725-0

27. Zhang Y, Wolf GW, Bhat K, Jin A, Allio T, Burkhart WA, et al. Ribosomal protein L11 negatively regulates oncoprotein MDM2 and mediates a p53-dependent ribosomal-stress checkpoint pathway. *Mol Cell Biol* (2003) 23 (23):8902–12. doi: 10.1128/MCB.23.23.8902-8912.2003

28. Fancello L, Kampen KR, Hofman IJ, Verbeeck J, De Keersmaecker K. The ribosomal protein gene RPL5 is a haploinsufficient tumor suppressor in multiple cancer types. *Oncotarget* (2017) 8(9):14462–78. doi: 10.18632/oncotarget.14895

29. Goudarzi KM, Lindström MS. Role of ribosomal protein mutations in tumor development (Review). *Int J Oncol* (2016) 48(4):1313–24. doi: 10.3892/ijo.2016.3387

30. Dong Z, Jiang H, Liang S, Wang Y, Jiang W, Zhu C. Ribosomal protein L15 is involved in colon carcinogenesis. *Int J Med Sci* (2019) 16(8):1132–41. doi: 10.7150/ijms.34386

Frontiers in Oncology

Advances knowledge of carcinogenesis and tumor progression for better treatment and management

The third most-cited oncology journal, which highlights research in carcinogenesis and tumor progression, bridging the gap between basic research and applications to imrpove diagnosis, therapeutics and management strategies.

Discover the latest Research Topics

See more →

Frontiers

Avenue du Tribunal-Fédéral 34
1005 Lausanne, Switzerland
frontiersin.org

Contact us

+41 (0)21 510 17 00
frontiersin.org/about/contact